

**MVMA TWO DIMENSIONAL
CRASH VICTIM SIMULATION
VERSION 4, TUTORIAL SECTION,
AND SELF STUDY GUIDE**

EDC Library Ref. No. 1023

DISCLAIMER

These materials are available in the public domain and are not copyrighted. Engineering Dynamics Corporation (EDC) copies and distributes these materials to provide a source of information to the accident investigation community. EDC makes no claims as to their accuracy and assume no liability for the contents or use thereof.

38136

Technical Report Documentation Page

1. Report No. UM-HSRI-77-18-1	2. Government Accession No.	3. Recipient's Catalog No.	
4. Title and Subtitle MVMA Two-Dimensional Crash Victim Simulation Tutorial System: Self-Study Guide		5. Report Date April 27, 1977	
		6. Performing Organization Code 361118	
7. Author(s) Bowman, Bruce M., Robbins, D. Hurley, and Bennett, Robert O.		8. Performing Organization Report No. UM-HSRI-77-18-1	
9. Performing Organization Name and Address Highway Safety Research Institute The University of Michigan Huron Parkway & Baxter Road Ann Arbor, Michigan 48109		10. Work Unit No. (TRAIS)	
		11. Contract or Grant No.	
12. Sponsoring Agency Name and Address Motor Vehicle Manufacturers Association 320 New Center Building Detroit, Michigan 48202		13. Type of Report and Period Covered Final Report	
14. Sponsoring Agency Code		15. Supplementary Notes	
16. Abstract <p>The MVMA Two-Dimensional Crash Victim Simulator is a mathematical model used for predicting occupant dynamics in a crash environment. The computer model is large and complex. Its many options and features provide the automotive safety engineer considerable flexibility in defining a crash event but at the same time impose considerable demands for specification of input data. As a means of facilitating learning to use the model, the Tutorial System combines a Self-Study Guide and an Audio-Visual Program. Both are divided into thirteen segments, called "modules," each of which deals with the data requirements of a set of related model features. Each audio-visual module consists of 35 mm slides and approximately twenty minutes of narration on a tape cassette.</p> <p>Tutorial System documentation is in two volumes. The Self-Study Guide consists of text, illustrations, and example problems. The Audio-Visual Program includes the narration text and figures used for the 35 mm slides. All documentation is loose-leaf.</p>			
17. Key Words Automotive Safety Design Crash Victim Simulation Occupant Dynamics Whole-Body Re- Self-Study Guide sponse		18. Distribution Statement UNLIMITED	
19. Security Classif. (of this report) Unclassified	20. Security Classif. (of this page) Unclassified	21. No. of Pages 397	22. Price

Form DOT F 1700.7 (8-72)

Reproduction of completed page authorized

MVMA Two-Dimensional Crash Victim Simulation:
Tutorial System Update

The Tutorial System for the MVMA Two-Dimensional Crash Victim Simulation (Version 3) was released April 27, 1977. There were twelve modules in the original Tutorial System. On August 3, 1977, a thirteenth module was released together with several replacement pages for the original twelve modules. The Tutorial System now consists of a 397-page Self-Study Guide and a 298-page Audio-Visual Program with 198 35 mm slides and nearly five hours of narration on tape cassettes.

This document is a Tutorial System Update which makes the Self-Study Guide and Audio-Visual Program current to June 1979. HSRI has recently completed Version 4 of the MVMA 2-D model. Versions 3 and 4 differ primarily in program organization and many associated modifications to the Tutorial System were required. In addition, several other modifications not related to Version 4 differences have been made. The Tutorial System Update consists of:

- a) 59 replacement pages for the Self-Study Guide;
- b) 5 insert pages for the Self-Study Guide;
- c) 41 replacement pages for the Audio-Visual Program;
- d) 17 replacement slides for the Audio-Visual Program.

The user of the Tutorial System should note that modifications have been made to the Audio-Visual text. None of these changes are of great significance, so re-taping of the affected Audio-Visual Program cassettes was not warranted. Also, seven of the replacement pages for the Audio-Visual Program are for modifications to figures that are so minor that associated replacement slides were felt unnecessary.

Listed on the next page are the pages and slides which should be replaced in existing copies of the Tutorial System. Each page is three-hole punched and each has "6/28/79", the release date for this document, in the lower right-corner.

Self-Study Guide: replacement pages

xix, 6, 23, 25-28, 30, 31, 32, 34, 54, 57-60, 62, 63, 168, 231-233, 237, 238,
240-243, 286-288, 301-307, 311, 314, 319, 326, 328, 330, 332, 334, 343,
346-348, 355, 367, 368, 370, 371, 378-380, 384

(59 pages total)

Self-Study Guide: insert pages

xx, 31.1, 366.1, 366.2, 366.3

(5 pages total)

Audio-Visual Program: replacement pages

3, 8-10, 33, 35, 36, 39, 47-49, 64, 66, 145, 194, 199, 202-204, 227, 228,
234, 240, 241, 243, 245, 248, 249, 251, 252, 255, 256, 260, 262, 266, 267,
271, 273, 284, 292, 295

(41 pages total)

Audio-Visual Program: replacement slides

Slides 1-4, 1-23, 1-24, 1-27, 2-12, 2-14, 8-5, 8-6, 8-7, 10-2, 12-2,
12-3, 12-5, 12-6, 12-9, 12-14, 13-2

(17 slides total)

TABLE OF CONTENTS

	Page
LIST OF FIGURES	ix
MODULES	
1.0 Introduction to the MVMA 2-D Crash Victim Simulation	1
1.1 Introduction	1
1.2 Computer Models	4
1.3 The Tutorial System	4
1.4 The MVMA 2-D Crash Victim Simulation	7
1.4.1 The Occupant	7
1.4.2 The Vehicle	13
1.4.3 Restraint Systems	13
1.4.4 The Impact Event	22
1.4.5 Post-Processing and Model Output	25
1.5 Data Set Structure	28
1.6 Using the Tutorial System	34
2.0 The Body Linkage	45
2.1 Body Linkage	45
2.2 Masses and Moments of Inertia	47
2.3 Joint Properties	50
2.3.1 Joint Stop Angles	50
2.3.2 Link Equilibrium Position	54
2.3.3 Example Angle Data for Joints	54
2.3.4 Linear and Nonlinear Spring Torques	57
2.3.5 Energy Absorption in Joints	60
2.3.6 The Neck Joints	63

TABLE OF CONTENTS (continued)

	Page
2.4 Muscle Tension	64
2.5 Scaling Relations	74
3.0 Neck and Shoulder Models	78
3.1 The Neck	78
3.1.1 The Anatomy of the Neck	78
3.1.2 The MVMA-2D Neck Model	83
3.1.3 Special Uses of the Neck Model	90
3.2 The Shoulder	96
3.2.1 The Anatomy of the Shoulder	96
3.2.2 The MVMA-2D Shoulder Model	100
4.0 Contact Surfaces Attached to the Occupant	106
4.1 Occupant Profiles: General	106
4.2 Occupant Profile for Interaction with Vehicle Surfaces	106
4.2.1 Specification of Unnecessary Ellipses	107
4.2.2 Incomplete Specification of Ellipses	109
4.2.3 Inhibition Switches	109
4.2.4 Spaces in Occupant Profile	109
4.2.5 Use of a Circle Instead of Ellipse	110
4.2.6 Use of Several Circles Instead of Ellipse	110
4.2.7 Compliance of the Occupant-Vehicle Interface	112
4.2.8 Specification of Data	116
4.3 Occupant Profile for Interaction Between Body Segments	120
4.4 Occupant Profile for Interaction with Airbag	127

TABLE OF CONTENTS (continued)

	Page
5.0 Contact Surfaces Attached to the Vehicle	131
5.1 The Occupant Compartment	131
5.2 Vehicle Interior Regions and Line Segments	133
5.2.1 Regions	133
5.2.2 Line Segments	135
5.3 Inhibition of Contact Interaction	143
5.4 Material Property Specifications	144
5.5 Contact Surface Friction	148
6.0 Generation of Contact Forces on the Occupant (Parts 1 and 2)	152
6.1 Generation of Contact Forces (beginning of Part 1)	152
6.2 Determination of Deflections	154
6.2.1 Ellipse Against Line Segment	154
6.2.2 Ellipse Against Ellipse	160
6.3 Material Properties	160
6.3.1 Loading: Static Curve	162
6.3.2 Loading: Inertial Spike Curve	164
6.3.3 Loading: Force Saturation	166
6.3.4 Unloading	166
6.3.5 Unloading: Permanent Deformation	169
6.3.6 Unloading: Hysteretic Energy Absorption	169
6.3.7 Unloading: Force Saturation	173
6.3.8 Rigid-Rigid Interactions	173
6.3.9 Material Property Data Cards	176
6.4 Shared Deflection (beginning of Part 2)	180
6.5 Edge Effects	182

TABLE OF CONTENTS (continued)

	Page
6.6 Contact Surface Friction	187
6.7 Special Contact Force Adjustment Features	192
6.8 Modeling Notes	195
7.0 Occupant Positioning with Respect to the Vehicle	204
7.1 Generalized Coordinates	204
7.2 Initial Positioning of Occupant - Data Cards	215
7.3 Initial Positioning of Occupant - Equilibrium Considerations	218
7.4 Initial Equilibrium -- Other Considerations	230
8.0 Crash Deceleration Profiles and Head Applied Forces	231
8.1 Vehicle Motions	231
8.1.1 Data Requirements	231
8.1.2 Example Data	233
8.1.3 Acceleration Components in Different Frames of Reference	237
8.2 Head Applied Forces	238
9.0 Belt Restraint Systems	245
9.1 Introduction	245
9.2 A Three-Belt Submodel	245
9.2.1 Anchors and Attachment Points	245
9.2.2 Deflection and Strain	248
9.2.3 Material Properties	250
9.2.4 Mutual Deformation of Body and Belt	250
9.2.5 Data Cards for the Three-Belt Submodel	251
9.3 An Advanced Belt-System Submodel	257
9.3.1 General Description	257
9.3.2 Deflection and Strain	259

TABLE OF CONTENTS (continued)

	Page
9.3.3 Material Properties	260
9.3.4 Force Equalization	260
9.3.5 Torso-Belt Interbelt Influence	261
9.3.5.1 Normal-Force Friction	261
9.3.5.2 Force Difference Saturation	262
9.3.5.3 Percentage Influence	262
9.3.6 Inertia Reels	263
9.3.7 Slip Points	263
9.3.8 Data Cards for the Advanced Belt-System Submodel	264
9.3.8.1 Anchor Types and Ring Types	264
9.3.8.2 Belt Segment Specifications	267
9.3.8.3 System Specifications	274
9.3.8.4 Inertia Reel Specifications	276
9.4 Modeling Considerations	276
9.4.1 Static Tests	276
9.4.2 Adjustment of Loading Properties	278
9.4.3 Special Uses of Loading Curves	280
9.4.4 Special Uses of Contact Surfaces	280
10.0 Airbag Restraint System	283
10.1 Airbag Submodel: General Description	283
10.2 Airbag Enclosure	283
10.3 Assumptions	285
10.4 Simulation Description	285
10.5 Input Data Cards	293
11.0 Energy-Absorbing Steering Column (See MVMA 2-D Technical Report)	

TABLE OF CONTENTS (continued)

	Page
12.0 Model Operation	301
12.1 Model Architecture	301
12.2 Output Categories	302
12.3 General Model Controls	306
12.4 Auxiliary Printed Output	308
12.5 Accelerometer Location	309
12.6 Generation of Page Titles	311
12.7 End of Input Processor Data Deck	311
12.8 Output Processor Control Cards	311
12.9 Output Comparisons	316
12.10 Stick Figure Output	322
12.11 End of Output Processor Data Deck	326
12.12 Example Input Cards	326
13.0 Example Crash Simulations	329
13.1 Introduction	329
13.2 Input Data for Example 1	329
13.2.1 Title Cards	332
13.2.2 General Controls for IN and GO	332
13.2.3 Vehicle Motion	334
13.2.4 Occupant Description	334
13.2.5 Occupant Position	338
13.2.6 Vehicle Interior	338
13.2.7 Friction Characteristics	341
13.2.8 Interaction "Inhibition" Cards	343

TABLE OF CONTENTS (continued)

	Page
13.2.9 Belt Restraint System	343
13.2.10 End of Data Deck for IN	343
13.2.11 Output Processor Controls	346
13.2.11.1 Output Categories for Printout	346
13.2.11.2 HIC, Femur Loads, and Filtering	346
13.2.11.3 Potential Injury Indicators	346
13.2.11.4 Printer-Plot Stick Figures	348
13.2.11.5 End of Data Deck for OUT	348
13.3 Selected Output from Simulation Example 1	348
13.3.1 Data Set Echo	348
13.3.2 Summary of Input Data	348
13.3.3 Printer-Plot Stick Figure Sequence	349
13.3.4 Printout of Numerical Results	349
13.4 Input Data for Example 2	375
13.4.1 Belt Restraint System	375
13.4.2 Auxiliary Debugging Printout	377
13.4.3 Output Variable Storage	377
13.4.4 Other "Example 2" Modifications	377
13.5 Selected Output from Simulation Example 2	379

LIST OF FIGURES

FIGURE	TITLE	PAGE
1-1	Computer Simulation of Occupant Dynamics	2
1-2	Relationship of Position Conditions and Interaction Forces Within the Framework of an Initial Value Problem	3
1-3	Modules of the MVMA 2-D Crash Victim Simulation Tutorial System	5
1-4	The MVMA 2-D Model	8
1-5	Articulated Body Schematic	9
1-6	Seated Occupant in Position of Approximate Equilibrium	10
1-7	Muscle Element	
1-8	Muscle Activity Moment as a Function of Time	12
1-9	MVMA-2D Extensible Neck Geometry	14
1-10	Maximum Range of Motion of the Glenoid Fossa (shoulder socket) in Shrugging Motions	15
1-11	Example Profile of Vehicle-Interior Surfaces	16
1-12	Unloading With Permanent Deformation From Deflections Greater Than δ_c	17
1-13	MVMA 2-D Airbag Model	18
1-14	Simple Belt System	20
1-15	Advanced Belt System	21
1-16	Vehicle Coordinates	23
1-17	Vehicle Acceleration Profiles	24
1-18	Schematic of Force Applied to Head	26
1-19	The Multiprocessor MVMA 2-D Model	27
1-20	Example of Printer Plot Output	29
1-21a	List of Output Categories	30
1-21b	List of Output Categories	31
1-22	Data Decks	32

LIST OF FIGURES (continued)

FIGURE	TITLE	PAGE
1-23	A Data Card	33
1-24	Example Card Layout from Volume 2 of MVMA 2-D Report Manuals	35
1-25	Data Cards Referenced By Modules	37
1-26	Data Card Fields Referencing Modules	38
2-1	Articulated Body Schematic	46
2-2	Example Data Cards for Body Link Lengths, Masses, and Moments of Inertia	49
2-3	Standing Position	51
2-4	Sitting Position	52
2-5	In-Line Orientation	53
2-6	Definition of Joint Stop Angles and Natural Link Po- sition	55
2-7	Joint Stop Positions for Knee	56
2-8	Joint Property Cards	58
2-9	Linear and Nonlinear Joint Torque	59
2-10	R-ratio for Energy Conserved at Joint Stop	61
2-11	Joint Friction at Joint "i"	62
2-12	Muscle Element	65
2-13	Muscle Activity Moment as a Function of Time	67
2-14	Muscle at a Joint	68
2-15	Muscle Element Parameters	70
2-16	Muscle Tension Parameter Cards	72
2-17	Cards for Time-Dependent Muscle Activity	73
2-18	Parameter Scaling Relations	75
2-19	Selected References for Anthropometric Data	77

LIST OF FIGURES (continued)

FIGURE	TITLE	PAGE
3-1	The Cervical Vertebrae	79
3-2	X-Rays of a Normal Human Neck in the Neutral Position and in Full Voluntary Flexion and Extension	81
3-3	Average Range of Flexion and Extension (in Degrees) at Each Vertebral Level in 20 Normal Adults	82
3-4	The Major Muscle Groups Controlling Head and Neck Movements	84
3-5	The MVMA 2-D Two-Joint, Extensible Neck	85
3-6	MVMA 2-D Extensible Neck Geometry	87
3-7	Lineal Viscoelastic Components in MVMA 2-D Extensible Neck	89
3-8	Example Data Cards for MVMA 2-D Neck	91
3-9	Effective Reduction of MVMA 2-D Two-Joint Extensible Neck to a Pin-Joint Neck	92
3-10	Maximum Stiffness and Damping Values for Numerical Stability with Integration Time Step Δt	93
3-11	Solution of $e^{-x} + (1+\epsilon)x - (1+\epsilon) = 0$ for x With ϵ As a Parameter	95
3-12	The Shoulder Complex and its Skeletal Parts	97
3-13	Joint Sinus of Sternoclavicular Joint	98
3-14	Maximum Range of Motion of the Glenoid Fossa (shoulder socket) in Shrugging Movements	99
3-15	Articulated Body Schematic Showing Three-Degree-of-Freedom Shoulder	101
3-16	Shoulder Joint	103
3-17	Example Data Cards for MVMA 2-D Shoulder	105
4-1	Example Occupant Profile of Contact Sensing Ellipses for Interaction with Vehicle Interior Surfaces	108
4-2	A Contact Sensing Ellipse and a Better Representation of the Body Segment Profile with Circles	111

LIST OF FIGURES (continued)

FIGURE	TITLE	PAGE
4-3	Example Force-Deflection Curves for the Chest and a Padded Panel	113
4-4	Chest Loads for Example Force-Deflection Curves	115
4-5	Example Data Cards for a Contact-Sensing Ellipse	117
4-6	Definition of Location and Dimensions of Contact-Sensing Ellipses	118
4-7	Ellipse Replacement Circles at Positions of Nearest Approach	123
4-8	Approximation of an Ellipse by a Replacement Circle of Fixed Position	124
4-9	Approximation of an Ellipse by a Replacement Circle of Varying Position	125
4-10	Example Data Cards for a Special Ellipse on the Upper Legs Link	126
4-11	MVMA 2-D Airbag Model	128
4-12	Airbag Contact Lines on Occupant	129
4-13	Example Cards for Airbag-Sensing Profile on Occupant	130
5-1	Example Profile of Vehicle-Interior Surfaces	132
5-2	Example Data Cards for a Region	134
5-3	Padded Panel Region Displacement for Example Data	138
5-4	A Line-Segment Endpoint Coordinate and its Velocity as a Function of Time	139
5-5	Line-Segment Direction Factors, Defined at $t = 0$	141
5-6	Selection of Value for Line-Segment Penetration Limit	142
5-7	Seven Occupant Ellipses and Eleven Line Segments for Potential Contact	145
5-8	Example Data Cards Specifying Allowed Contact Interactions	146

LIST OF FIGURES (continued)

FIGURE	TITLE	PAGE
5-9	Data Cards for Example Vehicle-Interior Region Material	147
5-10	Example Static Load-Deflection Curve for a Panel Region	149
5-11	Example Data Cards for Coefficients of Friction	151
6-1	Relationship of Position Conditions and Interaction Forces Within the Framework of an Initial Value Problem	153
6-2	Development of Interaction Forces	155
6-3	Deflection Between a Straight-Line Segment and an Ellipse	156
6-4	Constants and Variables Relevant to Evaluation of Ellipse-Line Deflection	157
6-5	Evaluation of Deflection Between a Straight-Line Segment and an Ellipse	158
6-6	Occupant Model Configuration with all Internal Link Angles Equal to Zero (NOT for Input or Output)	159
6-7	Deflection Between Ellipse Replacement Circles	161
6-8	Static Loading Curve	163
6-9	Inertial Spike Curve	165
6-10	Static Loading Curve with Force Saturation	167
6-11	Unloading From Deflections Greater Than δ_p	168
6-12	Unloading With Permanent Deformation from Deflections Greater Than δ_c	170
6-13	Permanent Deformation ω and G-ratio as Functions of Maximum Deflection	171
6-14	Unloading With Energy Loss from Deflections Greater Than δ_c	172
6-15	R-ratio as a Function of Maximum Deflection	174
6-16	Unloading from Force Saturation	175
6-17	Example Material Property Data Cards	177
6-18	Mutual Deformation of an Ellipse and a Line	181

LIST OF FIGURES (continued)

FIGURE	TITLE	PAGE
6-19	An Ellipse Which Misses a Line Segment to the Side	183
6-20	An Ellipse Contacting a Line Segment Near Its Edge	185
6-21	Effectiveness Factor E as a Function of s, the Position of the Contact Point with Respect to Line Segment, With Edge Constant λ as a Parameter	186
6-22	Effectiveness Factors for Edge Constant Values of 0. and .5	188
6-23	Resultant Interaction Force Vector For Friction Coefficient $\mu = .4$: Resultant = $1.08 F_{\text{normal}}$, Heading = 21.8°	190
6-24	Example Data Cards for Coefficients of Friction	191
6-25	Adjustment of Coefficient of Friction for Small Sliding Speeds	193
6-26	Example Cards with Data Relating To Contact Force Adjustment Options	194
6-27	Maximum-Energy Unloading for a G-Ratio Near to 1.	197
6-28	Determination of Compatibility of R-Ratio with a Specified G-Ratio	198
6-29	G-R Compatibility Constraint for Constant Stiffness Loading Curve	199
6-30	A Sudden, Large Deflection Near an Acute Angle	202
7-1	Computer Simulation of Occupant Dynamics	205
7-2	"n" Free Particles in an Inertial Coordinate Frame	206
7-3	A Rigid Body in 2-Space, with Three Degrees of Freedom	208
7-4	Occupant Model Generalized Coordinates for Input and Output (absolute coordinates defined with respect to vehicle axes)	209
7-5	Shoulder Joint	211
7-6	Occupant Model Configuration with all Body Link Angles Equal to Zero, for INPUT or OUTPUT	213

LIST OF FIGURES (continued)

FIGURE	TITLE	PAGE
9-10	Data Cards for Advanced Belt System Representation of the Three-Belt System Data Set in Figure 9-5.	269
9-11	Belt Index Specifications	270
9-12	Belt Attachment Point Coordinates for Advanced Belt-Restraint Submodel	271
9-13	A Belt System With One Inertia Reel, Two Slip Points, and One Ring Strap	272
9-14	Data for a Belt System with One Inertia Reel, Two Slip Points, and One Ring Strap	273
9-15	Belt Strength Test Device	277
9-16	An Example Simplification of a Restraint System	279
9-17	Modified Loading Curve for Modeling Belt Slip	281
9-18	Modeling of an Artificial Belt Segment	282
10-1	MVMA 2-D Airbag Model	284
10-2	Summary of Assumptions in Airbag Submodel Analysis	287
10-3	General Organization of the Airbag Simulation	289
10-4	Supply Cylinder and Bag	290
10-5	Incremental Force Generation	292
10-6	Airbag Input Data	294
10-7	Airbag Contact Lines on Occupant	300
12-1	Overall Model Information Flow	303
12-2a	List of Output Categories	304
12-2b	List of Output Categories	305
12-3	Metric/English System Conversion Constants	307
12-4	Hexadecimal Debug Switch Setting Generation	310
12-5	Layout of Automatic Title	312

LIST OF FIGURES (continued)

FIGURE	TITLE	PAGE
7-7	Occupant Model Configuration with all Internal Link Angles Equal to Zero (NOT for Input or Output)	214
7-8	Example Initial Position Data for Seated Driver	217
7-9	Seated Occupant in Position of Approximate Equilibrium	220
7-10	Force-Deflection Curves for Seat Cushion and Hip Circle	225
7-11	Constants and Variables Relevant to Evaluation of Ellipse-Line Deflection	228
7-12	Evaluation of Deflection Between a Straight-Line Segment and an Ellipse	229
8-1	Vehicle Coordinates	232
8-2	Deceleration Pulse Data Cards	235
8-3	Vehicle Acceleration Profiles	236
8-4	Vehicle Pitch Angle	239
8-5	Schematic of Force Applied to Head	241
8-6	Example of Data for Force Applied to Head	242
8-7	Head Applied Force Data Cards	243
9-1	Simple Belt System	246
9-2	Advanced Belt System	247
9-3	Definition of Belt Deflection	249
9-4	Three-Belt System Geometry	252
9-5a	Example Data Cards for the Three-Belt System	254
9-5b	Example Data Cards for the Three-Belt System	255
9-6	Advanced Belt System	258
9-7	Belt Anchor Type Designation for Anchor "i"	265
9-8	Designation of Ring-Belt Relationship for Slip-Point "i"	266
9-9	Simulation of a Three-Belt System Using the Advanced Belt-System Submodel	268

LIST OF FIGURES (continued)

FIGURE	TITLE	PAGE
9-10	Data Cards for Advanced Belt System Representation of the Three-Belt System Data Set in Figure 9-5.	269
9-11	Belt Index Specifications	270
9-12	Belt Attachment Point Coordinates for Advanced Belt-Restraint Submodel	271
9-13	A Belt System With One Inertia Reel, Two Slip Points, and One Ring Strap	272
9-14	Data for a Belt System with One Inertia Reel, Two Slip Points, and One Ring Strap	273
9-15	Belt Strength Test Device	277
9-16	An Example Simplification of a Restraint System	279
9-17	Modified Loading Curve for Modeling Belt Slip	281
9-18	Modeling of an Artificial Belt Segment	282
10-1	MVMA 2-D Airbag Model	284
10-2	Summary of Assumptions in Airbag Submodel Analysis	287
10-3	General Organization of the Airbag Simulation	289
10-4	Supply Cylinder and Bag	290
10-5	Incremental Force Generation	292
10-6	Airbag Input Data	294
10-7	Airbag Contact Lines on Occupant	300
12-1	Overall Model Information Flow	303
12-2a	List of Output Categories	304
12-2b	List of Output Categories	305
12-3	Metric/English System Conversion Constants	307
12-4	Hexadecimal Debug Switch Setting Generation	310
12-5	Layout of Automatic Title	312

LIST OF FIGURES (continued)

FIGURE	TITLE	PAGE
12-6	Characteristics of a Martin-Graham Digital Filter	314
12-7	Mirror and Polar Images	315
12-8	Relationship of Test Value Card ID Numbers to Joints	317
12-9	List of Injury Related Test Quantities	318
12-10	Category Four Column Numbers	320
12-11	Belt Identifier Names	321
12-12	Example of Printer Plot Output	323
12-13	Stick Figure Symbol Legend	324
12-14	Example Data Cards	328
13-1	Arbitrary Decomposition of MVMA 2-D Data Set into Sub-sets	330
13-2	Occupant and Vehicle Interior Configuration for Example 1	331
13-3	Title Cards for Example 1	333
13-4	General Controls for IN and GO for Example 1	333
13-5	Vehicle Motion Cards for Example 1	335
13-6	Horizontal Component of Vehicle Acceleration for Example 1	336
13-7	Occupant Parameter Cards for Example 1	337
13-8	Occupant Position Cards for Example 1	339
13-9	Vehicle Interior Profile for Example 1	340
13-10	Data Cards for Definition of Geometrical Profile and Material Properties for a Typical Region	342
13-11	Data Cards for Coefficients of Friction for Example 1	344
13-12	Interaction "Inhibition" Cards for Example 1	345
13-13	Output Processor Data Deck for Example 1	347
13-14	Complete Data Set for Simulation Example 1	350

LIST OF FIGURES (continued)

FIGURE		PAGE
13-15	Input Processor Data Deck Echo for Example 1 (example page)	356
13-16	Summary of Input Data (example page)	357
13-17	Printer-Plot Time Sequence for Example 1	358
13-18	Vehicle Motion for Example 1	366
13-18.1	Head Center of Mass Motion for Example 1	366.1
13-18.2	Chest Center of Mass Motion for Example 1	366.2
13-18.3	Hip Motion for Example 1	366.3
13-19	Body Link Angles for Example 1	367
13-20	Body Link Angle Accelerations for Example 1	368
13-21	Example Region Line Segment Movement from Example 1	369
13-22	Example (A) Ellipse-Line Contact Interaction from Example 1	370
13-23	Example (B) Ellipse-Line Contact Interaction from Example 1	371
13-24	Femur and Tibia Loads for Example 1	372
13-25	Unfiltered Head, Chest, and Hip Accelerations for Example 1	373
13-26	Severity Indices for Unfiltered Accelerations for Example 1	374
13-27	Belt Restraint System Cards for Example 2	376
13-28	Debugging Printout Specifications for Example 2	378
13-29	Specifications for Storage of Output Categories for Example 2	378
13-30	Complete Data Set for Simulation Example 2	380
13-31	Printer-Plot Time Sequence for Example 2	385
13-32	Example Debugging Printout from Example 2	393
13-33	Belt System Response for Example 2	394
13-34	Body Link Angle Accelerations for Example 2	395

LIST OF FIGURES (continued)

FIGURE		PAGE
13-35	Unfiltered Head, Chest and Hip Accelerations for Example 2	396
13-36	Severity Indices for Unfiltered Accelerations for Example 2	397

MODULE 1 -- INTRODUCTION TO THE MVMA 2-D CRASH VICTIM SIMULATION

1.1 Introduction

Since 1966, sophisticated analyses have been developed which can be used for estimating the dynamic response of a human or an anthropomorphic dummy in a crash environment. The use of such mathematical models as tools in automotive safety design has been made possible by modern large-storage, high-speed computers.

The problem of determining occupant dynamics in a crash environment can be simply stated (See Figure 1-1). A description of a mechanical or biomechanical system, the occupant, is given. A description of a potentially interacting mechanical system, the occupant compartment, is given. The occupant's position and orientation and their rates of change are specified for some single instant in time. And finally, the motion in space of the occupant compartment as a function of time is specified. It is required to determine the subsequent motion of the occupant and the forces which describe his interaction with the vehicle interior.

Figure 1-2 illustrates the relationship between the motion and the forces. From the initial position and velocity conditions of the occupant relative to a vehicle-fixed reference frame, the instantaneous state of displacements between body and vehicle elements, and hence the interaction forces, may be determined. Further, the instantaneous interaction forces thus found, together with the motion equations of classical mechanics, namely Newton's Laws, determine the instantaneous accelerations essentially as $a = F/m$, or $\{a\} = [M]^{-1} \{F\}$ in a vector formulation. Integration of the accelerations then yields the occupant velocities and positions at a new time, different from the time at which forces were determined by an arbitrarily small amount, dt or Δt . New position and velocity conditions having been determined, new deflections can be determined and so forth so that the entire time histories for motion and forces are established. This flow sequence is an appropriate description for all mathematical models which could be used for determining occupant dynamics.

**COMPUTER SIMULATION
OF OCCUPANT DYNAMICS
IN A CRASH ENVIRONMENT**

GIVEN (Input):

- 1) Description of a biomechanical system representing the occupant
- 2) Description of a mechanical system representing the occupant compartment
- 3) Time-history of occupant compartment motion
- 4) Occupant position at onset of crash

DETERMINED (Output):

- 1) Occupant motion
- 2) Forces on Occupant
- 3) Derived descriptions and measures of the crash dynamics

FIGURE 1-1 Computer Simulation of Occupant Dynamics

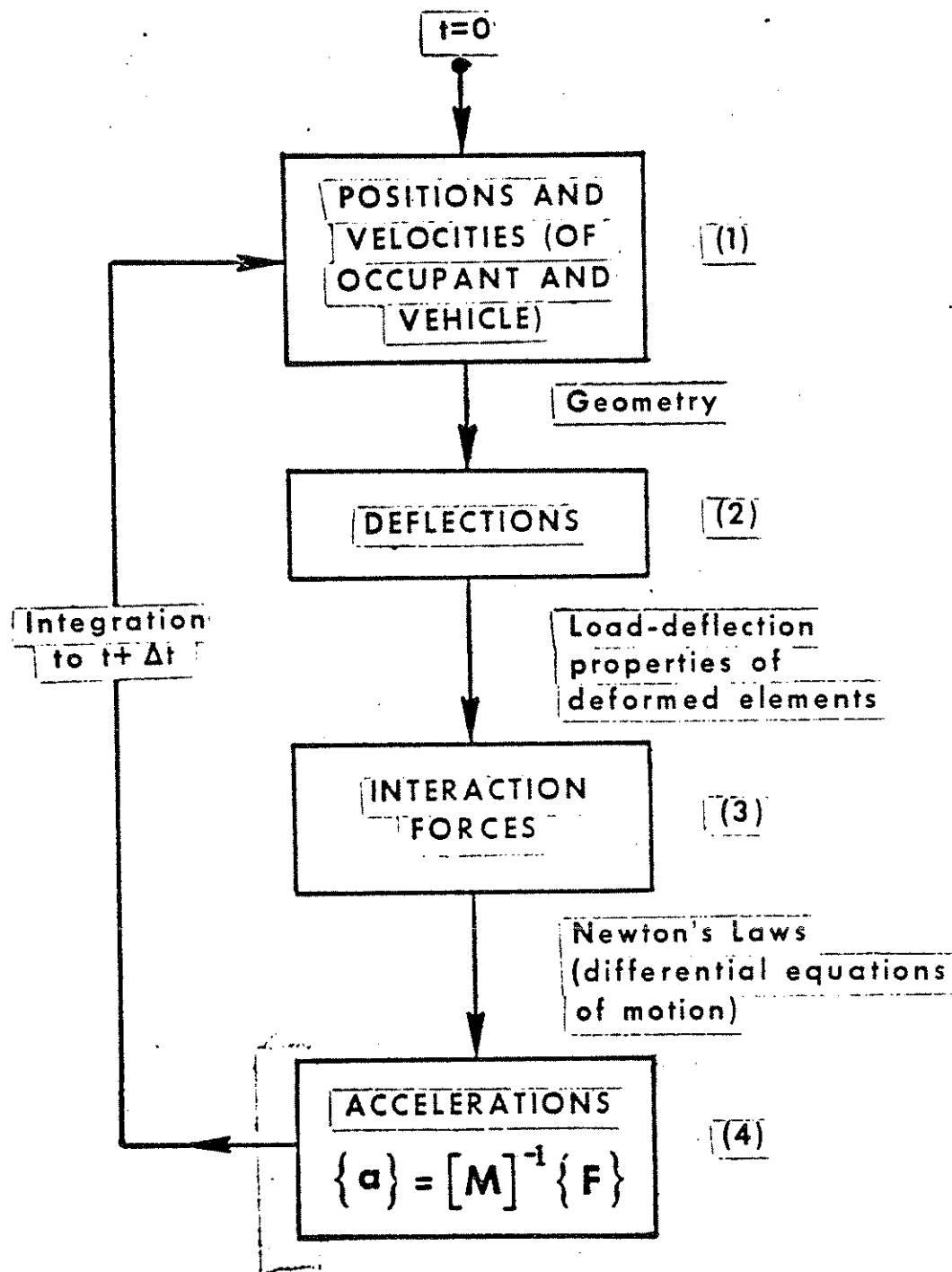


FIGURE 1-2 Relationship of Position Conditions and Interaction Forces Within the Framework of an Initial Value Problem

1.2 Computer Models

The embodiment of a mathematical model within a computer program is called a "computer model." Computer models which have been used to simulate occupant crash dynamics include both two-dimensional and three-dimensional motion simulators. The two-dimensional models are appropriately used for simulating crash events in which primary occupant motions may be expected to lie within a plane. Thus, two-dimensional models are most useful for simulating front-end and rear-end impacts. With care, however, they may be used for some oblique and side impacts as well. One such planar motion model, the "MVMA Two-Dimensional Crash Victim Simulator," is the subject of this Tutorial System.

1.3 The Tutorial System

The MVMA 2-D model is a large and complex computer program. Its many options and features provide the user considerable flexibility in defining a crash event but at the same time impose considerable demands for specification of input data. As a means of facilitating learning to use the model, the Tutorial System combines a self-study guide with an audio-visual program. Both the self-study manual and the audio-visual program are divided into thirteen segments called "modules." Each of the Modules 2 through 12 deals with the data requirements of a set of related model features. Data decks for two example simulations are described and assembled in Module 13. The titles of the modules are descriptive of their content and are listed in Figure 1-3. It should be noted that Module 6 is in two parts and that there is no Module 11.

The Tutorial System is intended for use by engineers. It is assumed that the user is familiar with basic engineering terms such as "acceleration," "force-deflection loading curve," and "moment of inertia." No mathematical skills are required for understanding most of the material presented in the Tutorial System modules, but any user of the computer model is expected to understand the basics of algebra and analytic geometry. These are required for some aspects of the task of input data preparation. Knowledge of calculus, differential equations, and Lagrangian mechanics is not a necessity for any user, but it is normally the case that a user with skills in these areas is better able to use the model effectively. But most

MODULES OF THE MVMA 2-D CRASH VICTIM SIMULATION TUTORIAL SYSTEM

MODULE

- 1 Introduction to the MVMA 2-D Crash Victim Simulation
- 2 The Body Linkage
- 3 Neck and Shoulder Models
- 4 Contact Surfaces Attached to the Occupant
- 5 Contact Surfaces Attached to the Vehicle
- 6 Generation of Contact Forces on the Occupant (Parts 1 and 2)
- 7 Occupant Positioning with Respect to the Vehicle
- 8 Crash Deceleration Profiles and Head Applied Forces
- 9 Belt Restraint Systems
- 10 Airbag Restraint System
- 11 (Module 11 is reserved for an energy absorbing steering column)
- 12 Model Operation
- 13 Example Crash Simulations

FIGURE 1-3 Modules of the MVMA 2-D Crash Victim
Simulation Tutorial System

important, and independent from a user's mathematical background, are good engineering judgment and an understanding of the fundamentals of Newtonian mechanics.

The focus of the Tutorial System is preparation of input data. It is here that design data, the mathematical model, and engineering judgment must be brought together. The mathematical model, like all mathematical models, will allow only imperfect representations of reality. In order to simulate physical phenomena as accurately as possible with the model, it is necessary for the user to understand the manner by which features of the occupant/vehicle system have been approximated analytically. Therefore, most of the material in the Tutorial System is explanation of the features of the mathematical model and the associated parameters for which the user must supply values. Engineering judgment is brought to bear in deciding, for simulation of a specific crash event, which features of the model are best used, how they are used, and what parameters are critical and therefore require special attention. Such "special attention" may be given to a critical parameter in two different ways. 1) First, it will sometimes be the case that it is entirely unfeasible to establish an experimental value for a parameter, e.g., a measure for hysteretic energy absorption for an impact to the head of a six-year-old child. Also, we might consider the case of a design parameter of the occupant compartment for which there are minimal non-safety related design constraints, e.g., the webbing stiffness for a component of a belt restraint system. For these two examples it may be necessary or appropriate to perform simulations for a range of values for the respective parameters. 2) Special attention can be given to a critical parameter in a second way. Its value might be measured. Any critical biomechanical parameter or any design parameter that is essentially fixed in value, or which at least has a nominal "baseline" value, should be measured experimentally if feasible and practical. It has been demonstrated time and again that for satisfactory performance of mathematical models, there is no substitute for good experimental data. Reality can be simulated only if reality is represented.

1.4 The MVMA 2-D Crash Victim Simulation

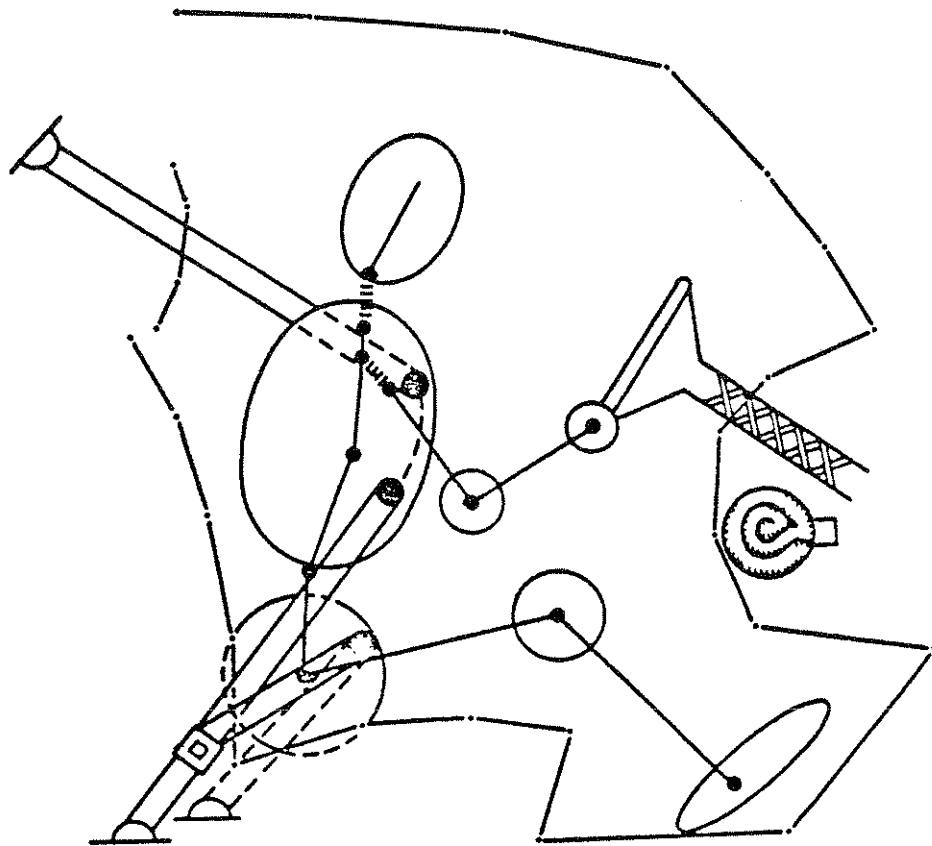
Figure 1-4 is a schematic of the occupant, vehicle interior, and restraint systems of the MVMA 2-D model. Listed with the schematic are some of the basic features of the model. Much of the remainder of this module is summary of these features. Modules 2 through 12 treat these subjects in detail.

1.4.1 The Occupant. The MVMA 2-D model includes the following features in its representation of the crash victim, which may be either a human or an anthropomorphic dummy:

1. A nine-mass, ten-segment body linkage;
2. An extensible, two-joint neck and a realistically-flexible shoulder complex;
3. Energy-absorbing joints;
4. Time-dependent muscle activity level;
5. Contact-sensing ellipses of arbitrary size, position, and number which define the body profile; and,
6. General and arbitrarily-definable nonlinear materials with energy-absorbing capability for all parts of the body.

Some of these features are illustrated in Figure 1-5, a schematic of the body linkage. Note that since this is a planar model, a single two-link leg represents right and left legs combined. Similarly, there are only two arm links. Angulations at joints are restricted by user specification of range-of-motion limits and viscoelastic parameters for hard-tissue resistance. Figure 1-6 illustrates a typical occupant profile defined by user-specified contact-sensing ellipses.

A feature that is unique to the MVMA 2-D Crash Victim Simulator is its muscle model. Moderate levels of muscle contraction generally have a significant effect on the crash dynamics, especially for low-g impacts, so analytical representation of the effect is of obvious value. Provision is made for calculation of muscle torques at the eight joints of the body linkage. The muscle model is shown in Figure 1-7. It does not include a contractile element, but the passive viscoelastic parameters k and c are functions of a user-prescribed, time-dependent muscle activity level. The typical curve shape is shown in Figure 1-8. t_R and t_C are reflex and contraction times for the muscle.



MVMA 2-D MODEL

1. Nine-Mass Occupant Model
2. Contact-Sensing Ellipses
3. Collapsing Vehicle Interior
4. Vehicle Exterior for Pedestrian Studies
5. Extensible Two-Joint Neck
6. Flexible Shoulder
7. Time-Dependent Muscle Contraction
8. Deployable Airbag
9. Energy-Absorbing Steering Column
10. Two Belt Restraint-System Submodels
11. Horizontal, Vertical, and Pitching Vehicle Motions

FIGURE 1-4 The MVMA 2-D Model

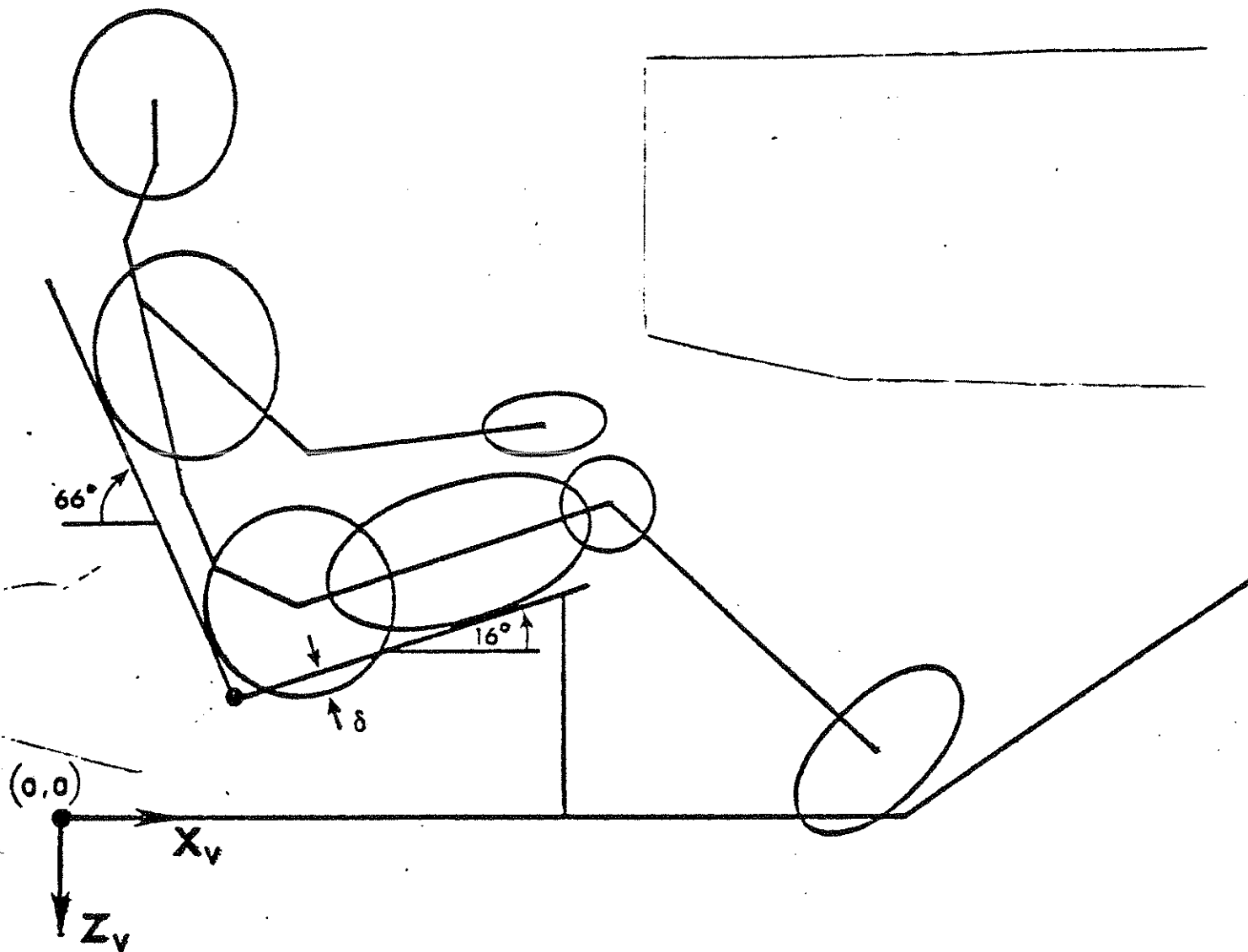
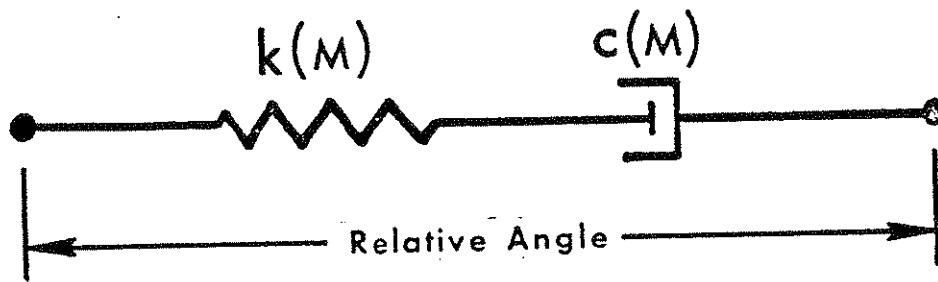


FIGURE 1-6 Seated Occupant in Position of Approximate Equilibrium



$$k = a_1 + a_2 |M|$$

$$c = a_3 |M|$$

$M = M(t)$, muscle activity level

FIGURE 1-7 Muscle element

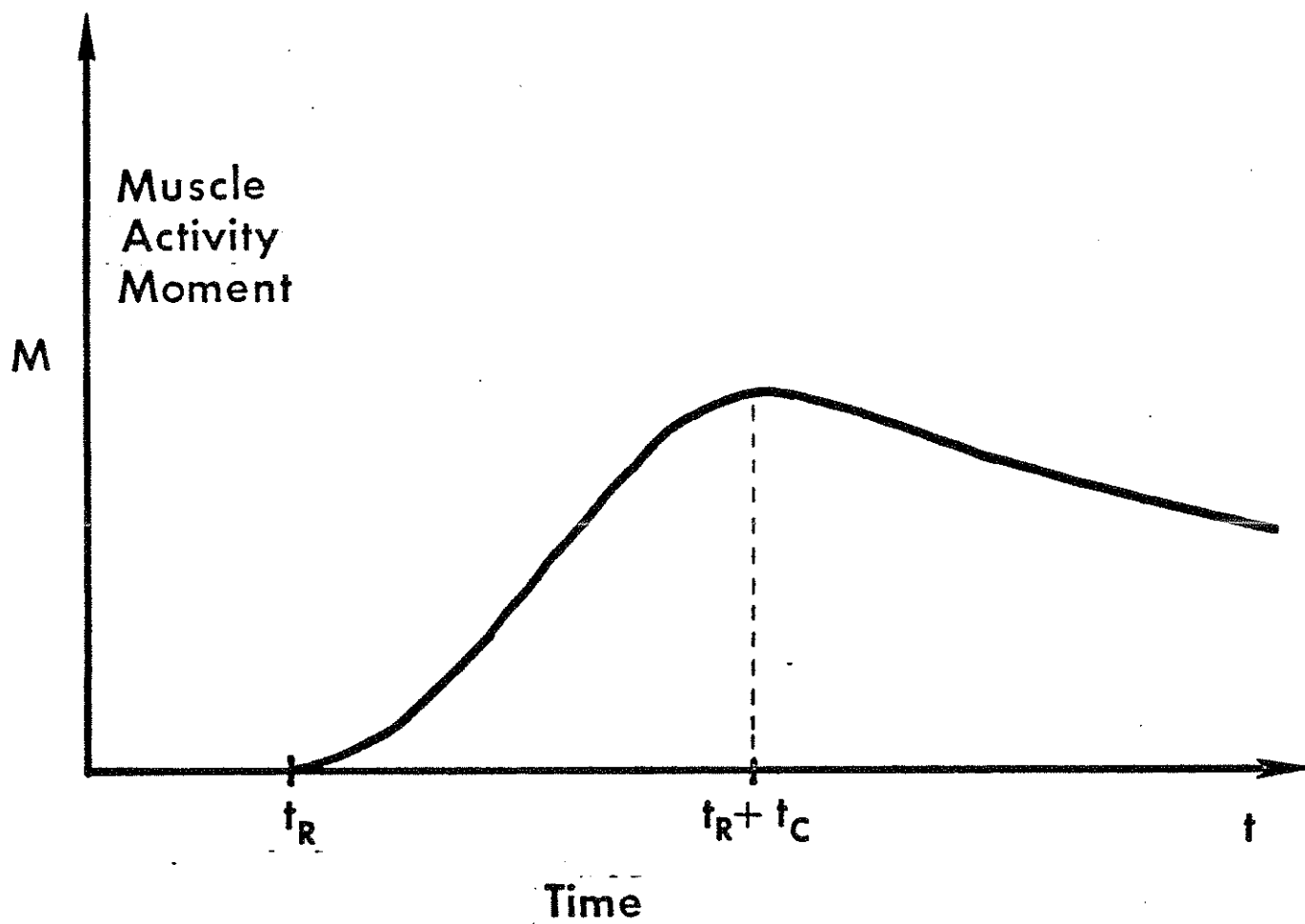


FIGURE 1-8 Muscle activity moment as a function of time

The extensible two-joint neck is illustrated in Figure 1-9. Visco-elastic elements are not shown. The joints are at either end of the cervical spine. The upper neck joint may be positioned arbitrarily with respect to the head center of mass.

Figure 1-10 shows shoulder "shrugging" motions that may be represented in simulations with the MVMA 2-D model. Angular articulations of the upper arm link are independent from the translatory motions of its proximal end.

1.4.2 The Vehicle. Forces between the occupant and the vehicle interior are generated by the model as a result of interaction of a profile of occupant ellipses with a user-defined vehicle-interior profile.* This profile is a set of connected or disconnected straight-line segments. The example profile illustrated in Figure 1-11 has eleven segments. However, any number of segments may be prescribed and their lengths and locations are arbitrary. Time-dependent positioning of the segments makes possible simulation of direct intrusions into the occupant compartment or secondary frontal interior displacements resulting from gross deformation of the engine compartment.

The line segments may be assigned material properties or they may be specified as rigid. Material properties for elements of the vehicle interior (and also for occupant ellipses) include the following:

1. Tabular or polynomial loading curves
2. Material yield point deflection
3. Force saturation level for plastic loading
4. Hysteretic unloading characteristics that depend on maximum deformation
5. Surface friction characteristics

Example loading and unloading curves are shown in Figure 1-12.

1.4.3 Restraint Systems. Three optional occupant restraint systems may be used in MVMA 2-D simulations. Two are belt systems and the third is an airbag model, which is illustrated in Figure 1-13.

*A pedestrian and a vehicle exterior may be represented just as easily.

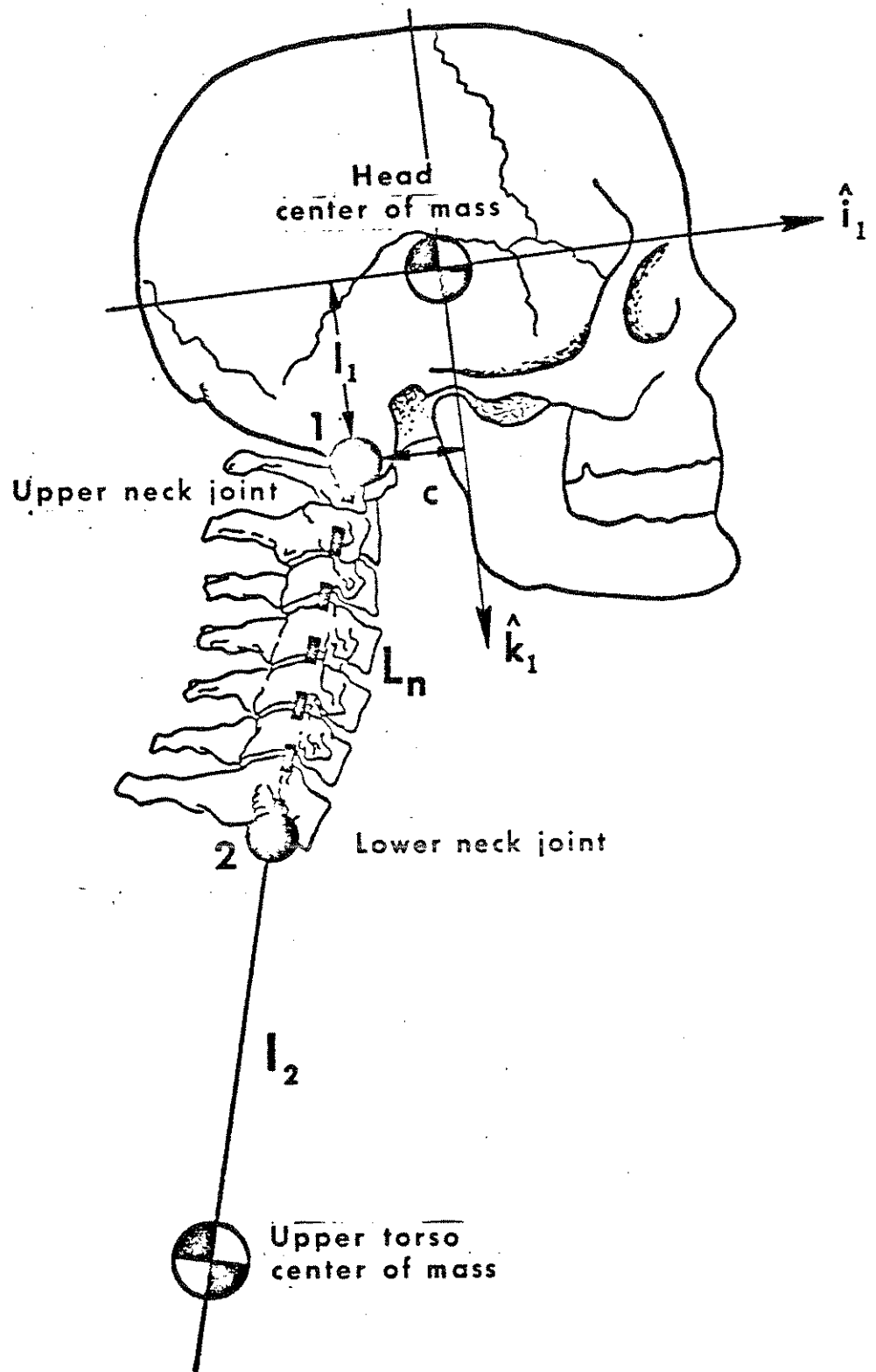


FIGURE 1-9 MVMA-2D extensible neck geometry

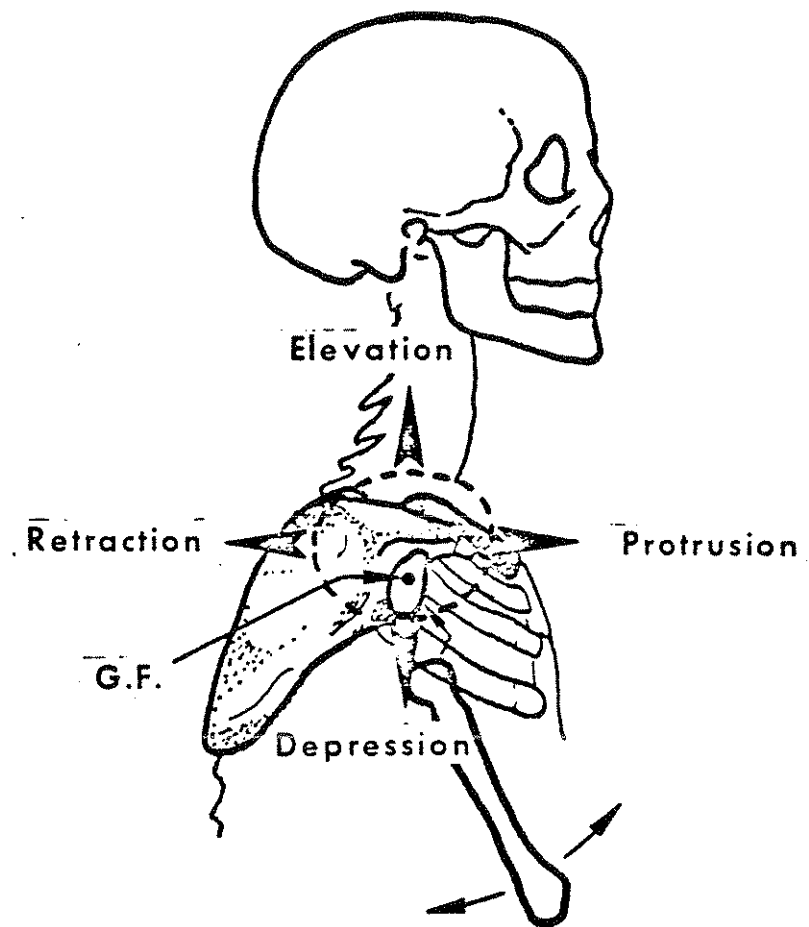


FIGURE 1-10 Maximum range of motion of the glenoid fossa (shoulder socket) in shrugging movements

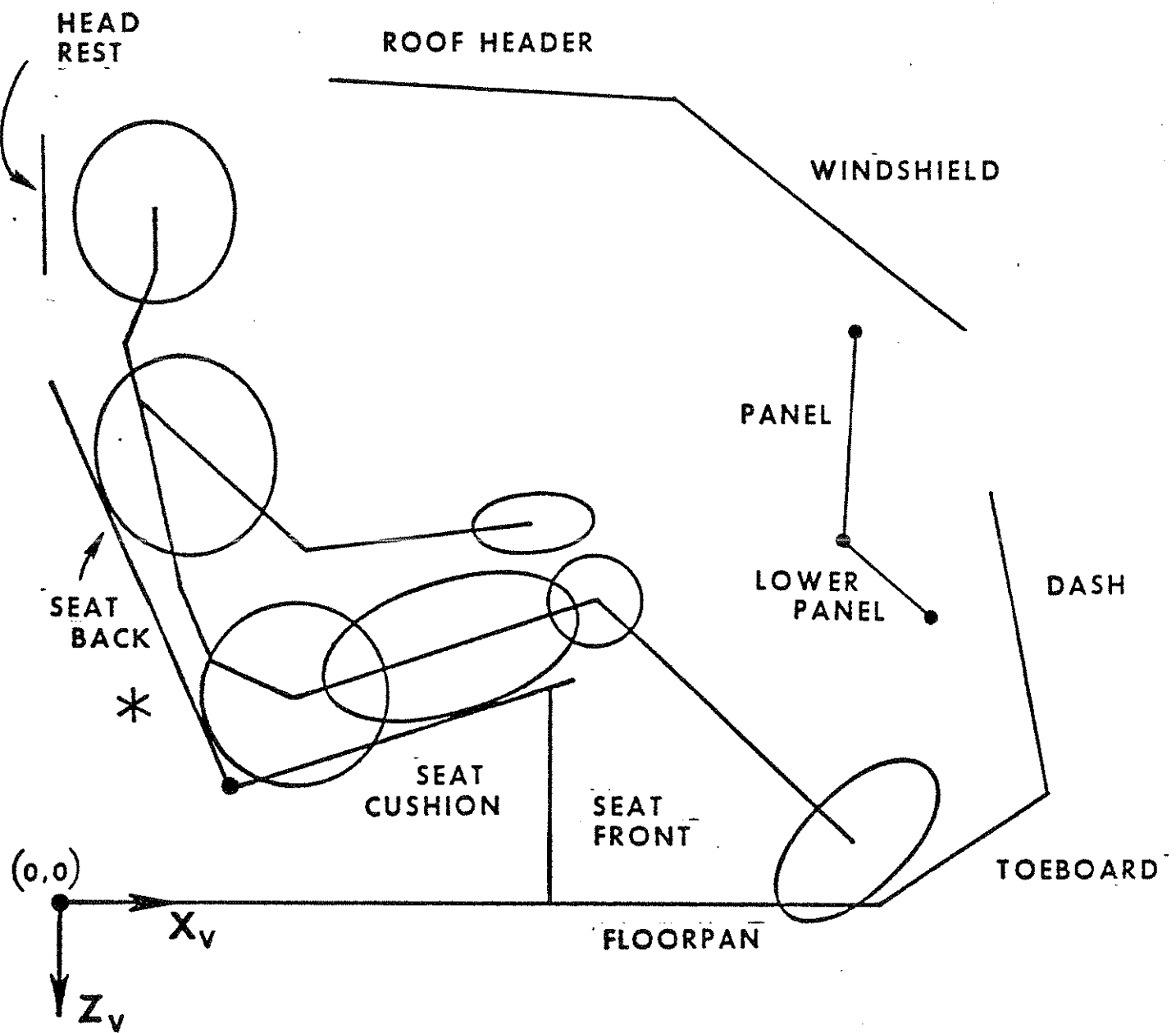


FIGURE 1-11 Example Profile of Vehicle-Interior Surfaces

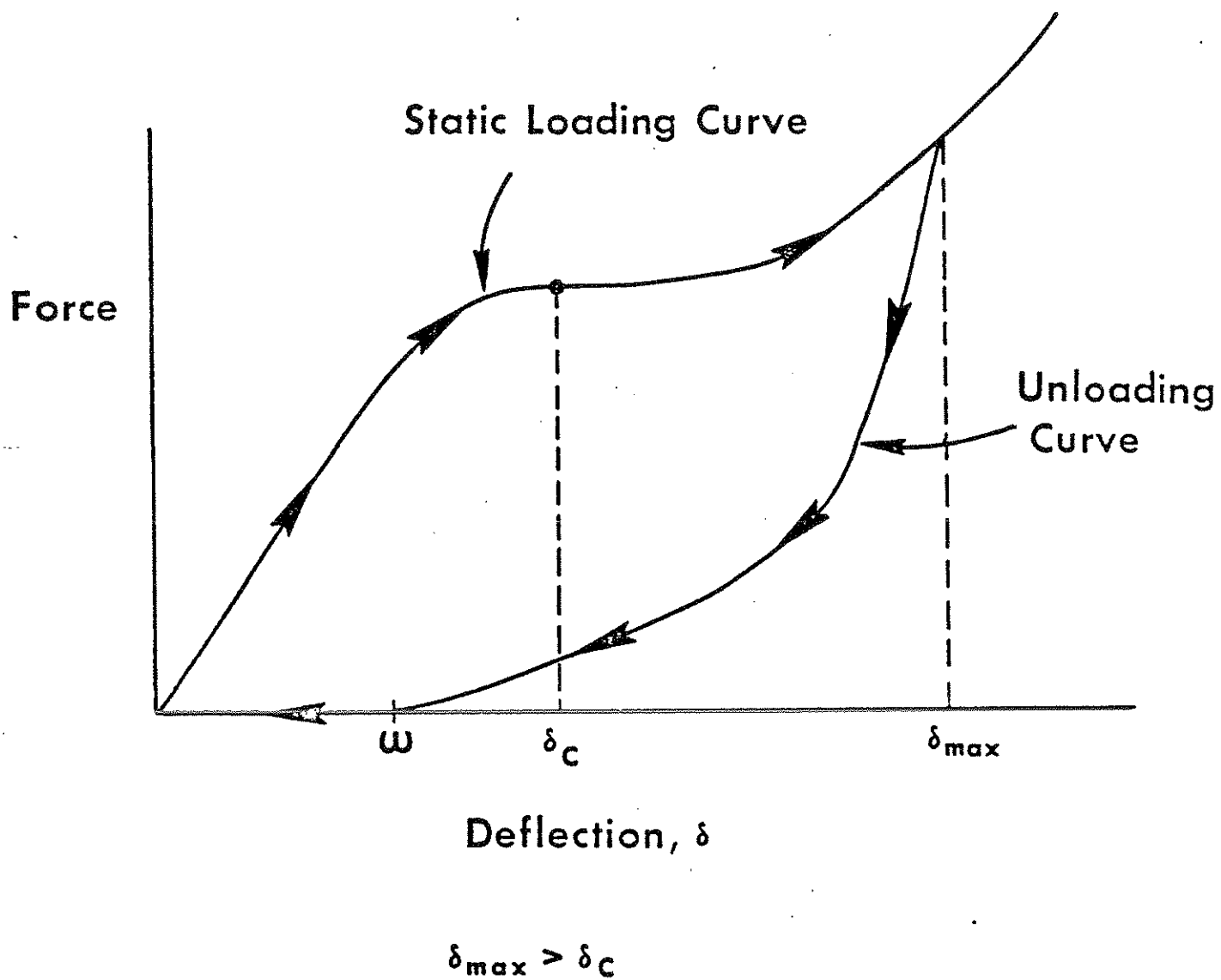


FIGURE 1-12 Unloading With Permanent Deformation from Deflections Greater Than δ_c

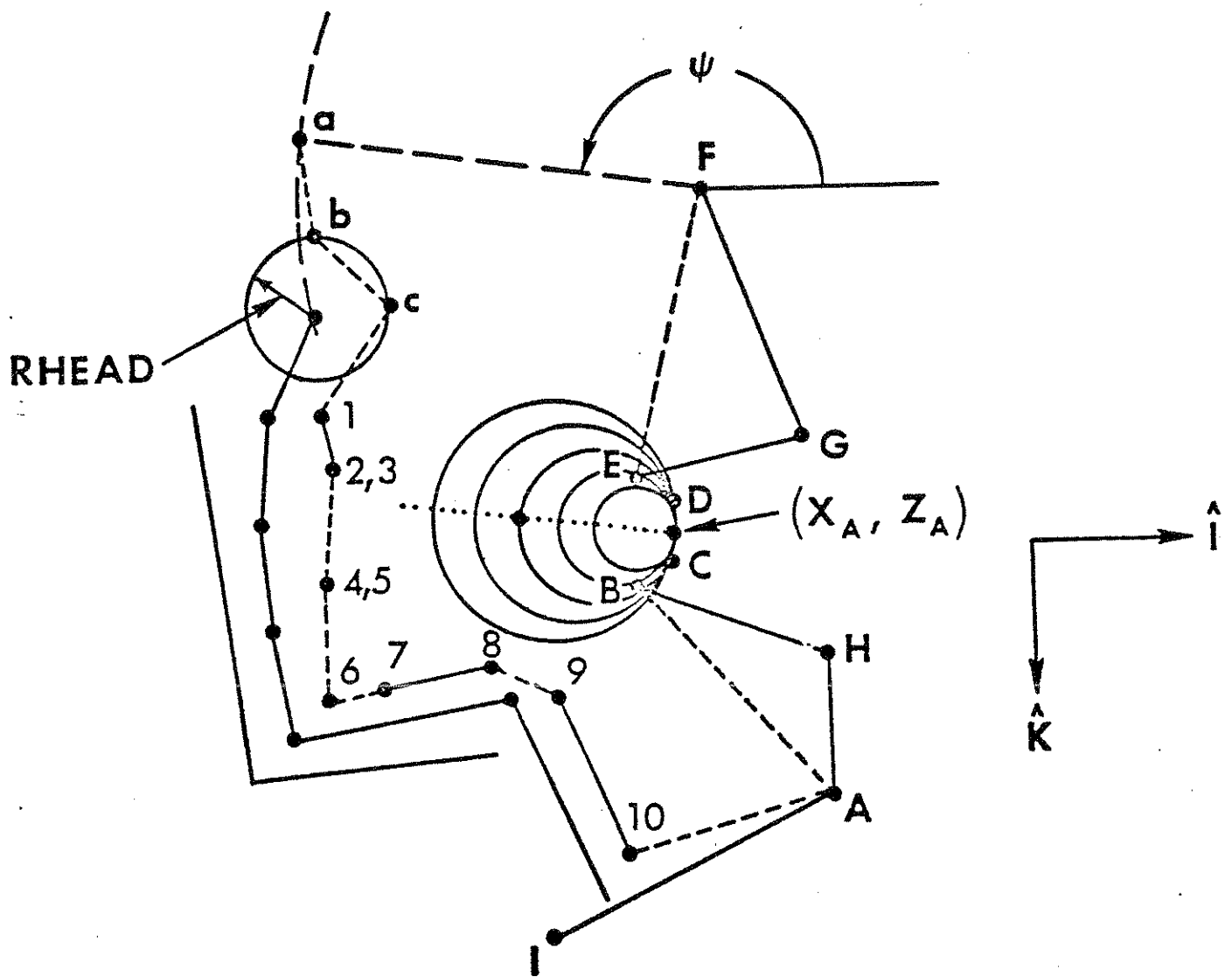


FIGURE 1-13 MVMA 2-D Airbag Model

The figure shows the bag expanding from its source toward the occupant, for which an airbag contact profile is defined with straight-line segments. Estimation of bag forces is based on solution of the differential equations of gas thermodynamics. The airbag is inflated at a time-dependent rate specified by the user; inlet mass flow rate is a tabular input to the simulation. When the bag is fully inflated, restraining forces due to internal pressure and skin tension are generated if the bag is in contact with the occupant. The shape of the bag is allowed to conform to that of the occupant and the vehicle interior with free sections of the perimeter defined as circular segments. When the pressure in the bag reaches a specified level, gas is allowed to flow out of the bag through defined orifices or through porous bag fabric.

The first optional belt system is illustrated in Figure 1-14. It consists of: 1) a one-piece lap belt attached to the lower torso element and anchored at each end to the vehicle; 2) an upper torso harness strap attached to the upper torso element and anchored to the vehicle; 3) a lower torso harness strap attached arbitrarily to any torso element and anchored to the vehicle. This belt-restraint submodel is effectively a three-belt system. The two-segment lap belt shown in the figure is treated by the computer model as a single piece of webbing that slides freely over the pelvis through a user-specified point on the lower-torso element. Thus, a lap-belt tension is determined from the elongation or strain of the total belt length, with no adjustment for possible friction effects, and the established tension is applied at the attachment point on the body through both the inboard and outboard segments. The lap belt anchor positions in the vehicle, as well as the attachment point on the lower-torso segment, can be specified arbitrarily by the user.

The torso harness restraint consists of two individual straps: an upper strap attached to a fixed point on the upper torso segment and a lower strap attached to a fixed point on the upper-, middle-, or lower-torso segment.

Figure 1-15 is a schematic of the second optional belt-restraint system. It includes the following features: 1) seven belt segments

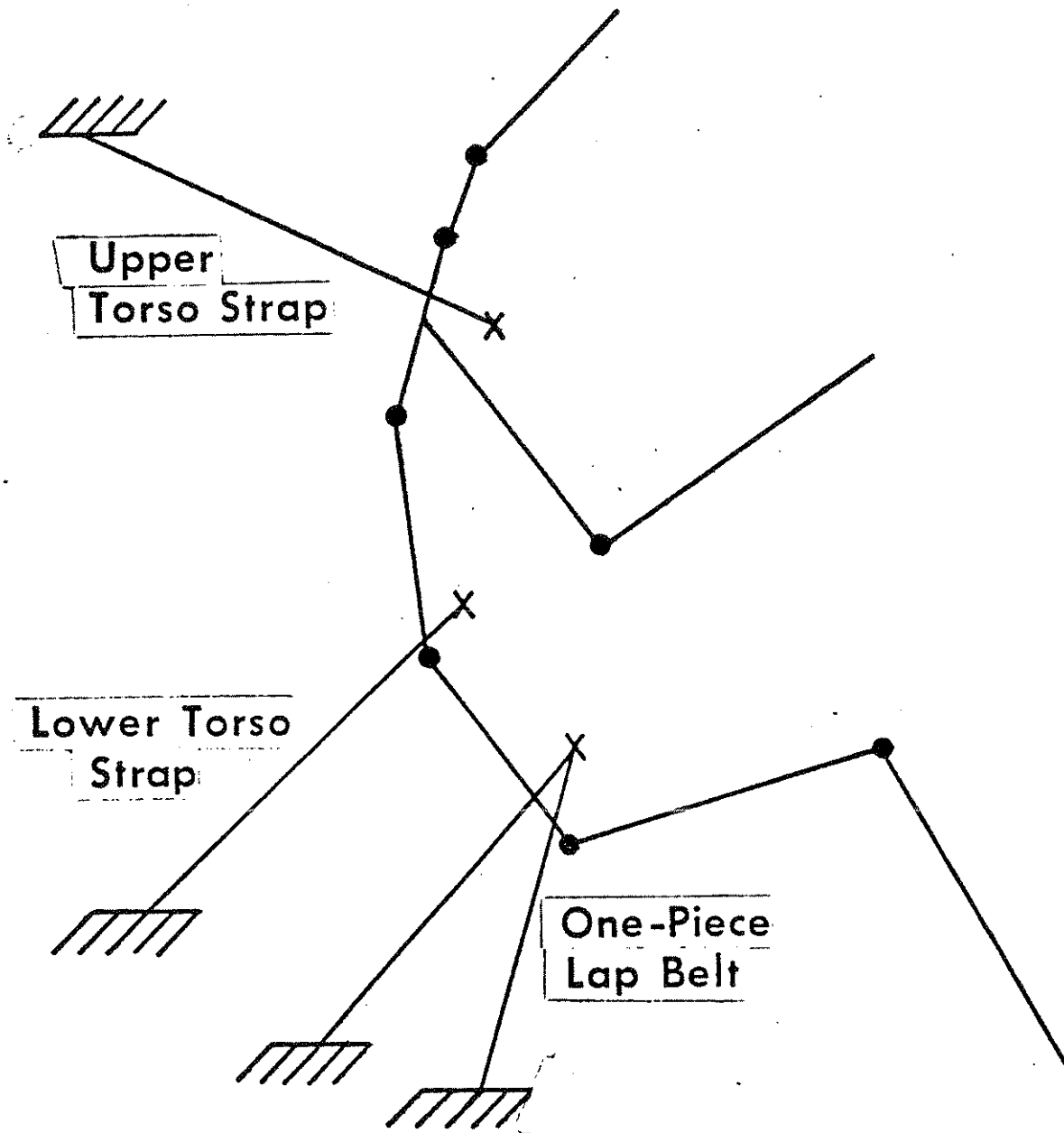


FIGURE 1-14 Simple Belt System

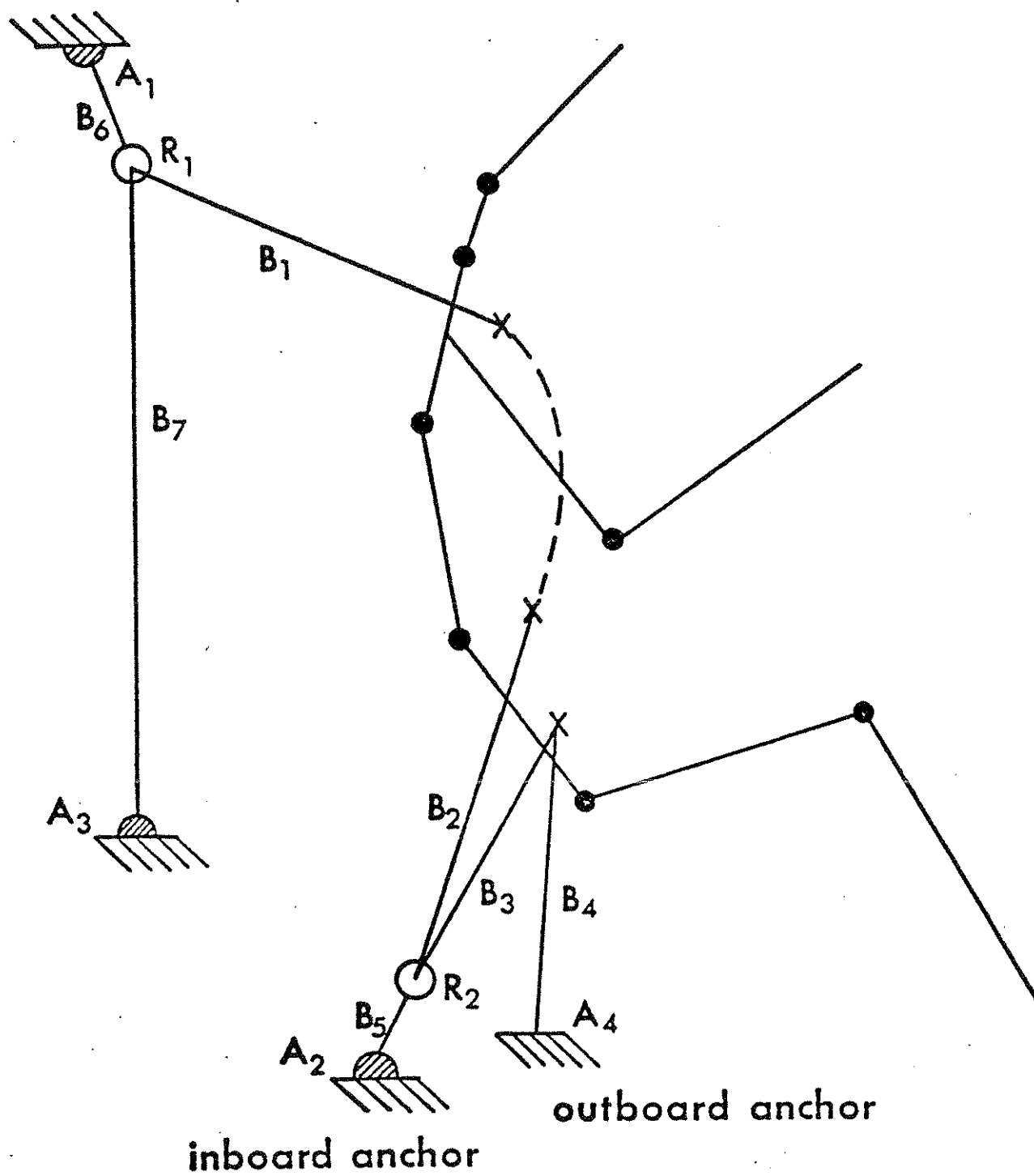


FIGURE 1-15 Advanced Belt System

which may be independent or, at option, may be paired in certain combinations to act as a lesser number or separate lengths of webbing by use of various free-slipping and friction elections at the torso and lap and at slip points; 2) a slip point in the three-belt upper harness system; 3) a slip point between the lower torso and lap sections; 4) optionally, inertia reels, either vehicle-sensitive or webbing-sensitive, at three of the four anchor locations. The slip points are shown as open circles, rings R_1 and R_2 . The rings may be fastened to ring straps, which lead to anchors A_1 and A_2 , or they may be fixed to the vehicle frame at anchor locations A_1 and A_2 , in which case the corresponding ring straps, B_6 and B_5 , are absent. The belt pairs B_1 - B_7 and B_2 - B_3 , may be considered common straps that may slip freely through their respective rings or with an amount of frictional resistance which depends on the resultant normal force at the ring. Three optional methods are available for simulating the effects of torso belt slippage and friction against the torso.

As for the simpler belt system, webbing properties for this system may be prescribed either in terms of force-deflection or force-strain characteristics.

1.4.4 The Impact Event. The crash victim's environment is made to be dynamic by specifying vehicle motion. Three independent motions are prescribed in tabular form as functions of time: 1) a horizontal acceleration; 2) a vertical acceleration; and 3) an angular "pitching" acceleration. The three degrees of freedom for vehicle motion are shown in Figure 1-16. Example piecewise-linear approximations of hypothetical crash profiles are shown in Figure 1-17.

For user convenience several options are available with regard to specification of vehicle accelerations. Horizontal and vertical components may be defined as the responses of a biaxial accelerometer mounted on a part of the frame that is fixed with respect to the occupant compartment. Alternatively, the accelerations may be prescribed as motion components within an inertial frame of reference. The accelerations may be entered in g's or in physical units. Pitching accelerations may be in either rad/sec^2 or deg/sec^2 .

Inertial reference frame

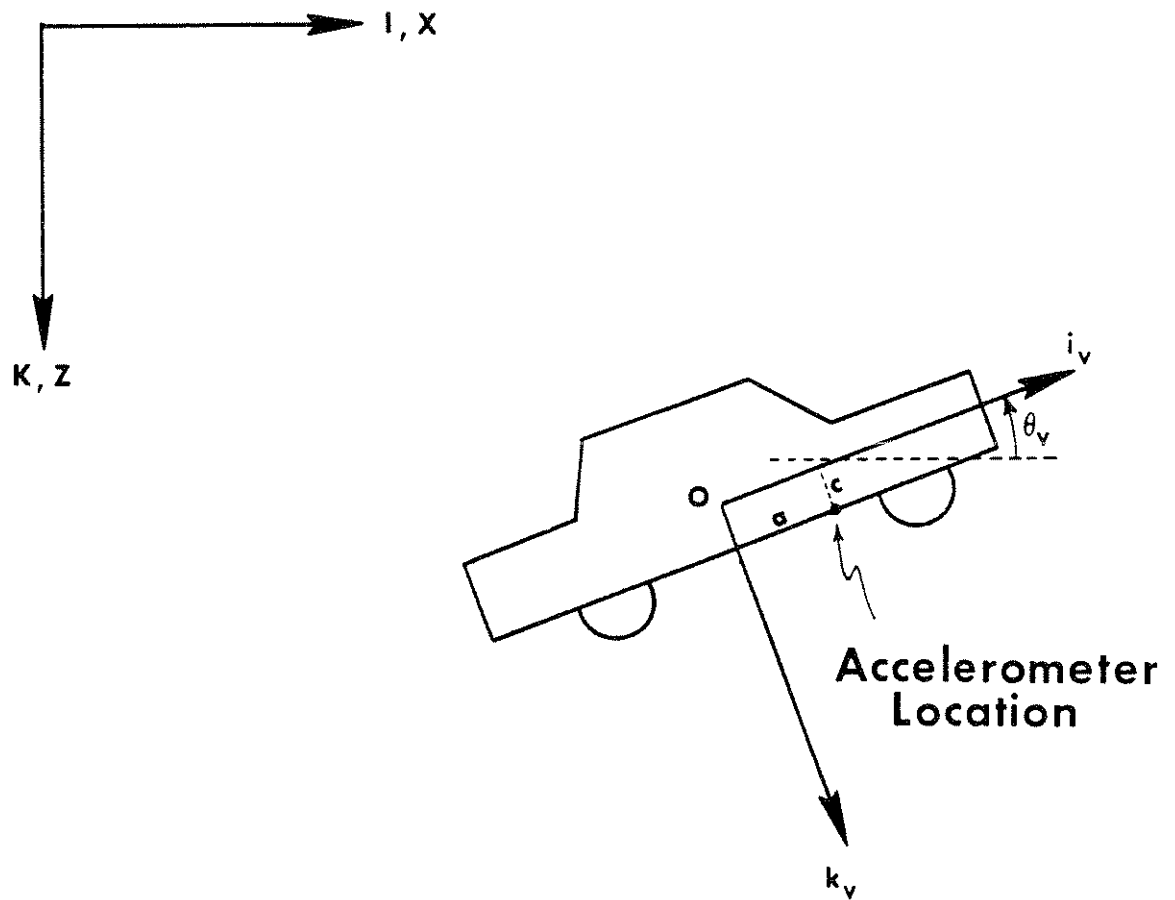


FIGURE 1-16 Vehicle Coordinates

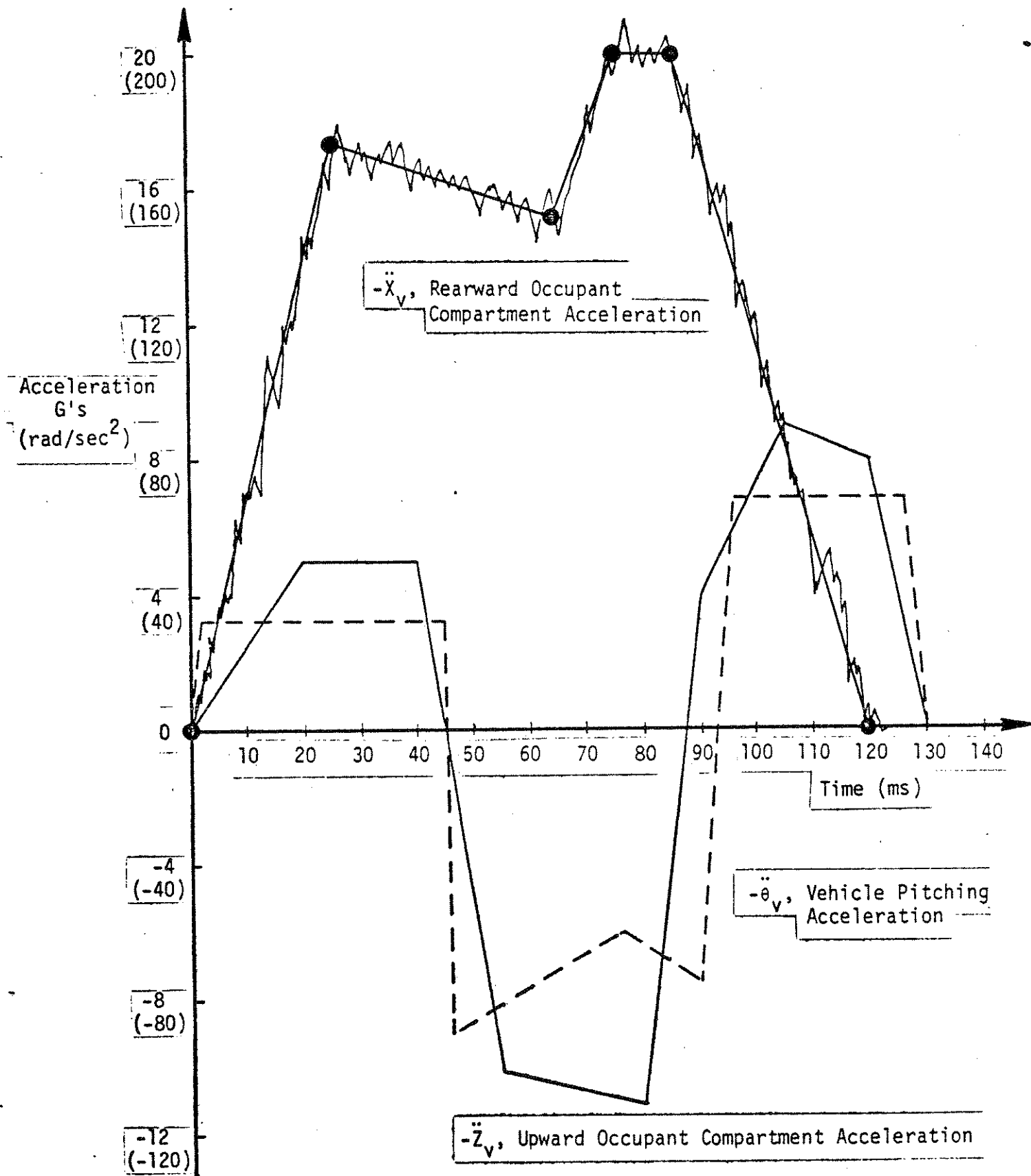


FIGURE 1-17 Vehicle Acceleration Profiles

In special applications of the MVMA 2-D model, it can be useful to be able to specify time-dependent forces for direct application to the occupant. Provision is made for applying such a force to any desired point on the head, as shown in Figure 1-18.

1.4.5 Post-Processing and Model Output. The MVMA 2-D computer model is organized as a multiprocessor in that it is divided into five parts which operate in turn. (See Figure 1-19.) The first processor is called the Input Pre-Processor, or INP. It reads data cards and writes the main program for the second processor. The second processor is called the Input Processor, or IN. It packs input data into binary tables and records those tables for use by subsequent processors. It also writes two programs needed by the third processor, including the main program. The third processor is called the Dynamics Solution Processor, or GO. It reads the binary tables, solves the equations of motion, and incorporates the computed results into the binary tables. The fourth processor is the Output Pre-Processor, or OUTP. It reads data cards and writes three programs needed by the fifth processor, including the main program. The fifth processor is called the Output Processor, or OUT. It reads the binary tables produced by the other processors and prints a comprehensive summary of all recorded information as the user specifies.

Discussion of the MVMA-2D model in preceding sections of this module is pertinent only to the functions of the first three processors, that is: 1) reading and interpreting the input data; 2) solving the equations of motion for the simulated crash; and 3) storing results. This section is pertinent to the output processors, particularly the last processor, OUT.

The Output Processor has two primary functions: 1) to process and analyze computed results with various so-called "post-processor" sub-routines, and 2) to produce printed output.

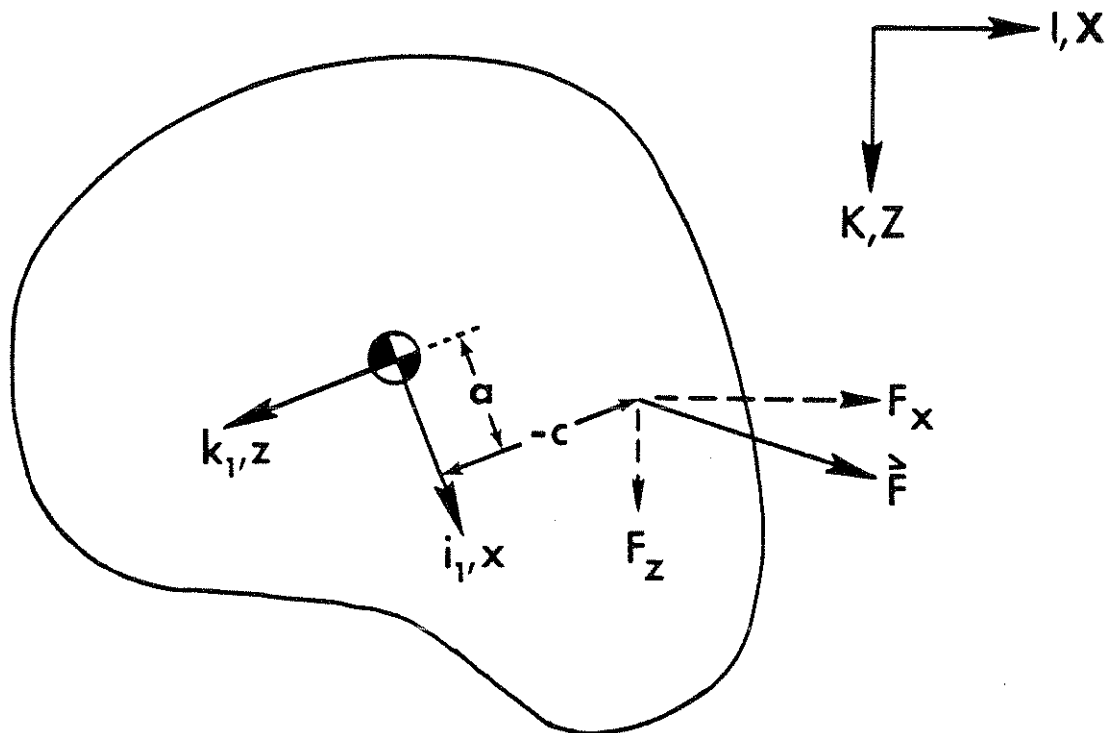


FIGURE 1-18 Schematic of Force Applied to Head

THE MULTIPROCESSOR MVMA 2-D MODEL

- INP = Input Pre-Processor
- IN = Input Processor
- GO = Dynamics Solution Processor, or Execution Processor
- OUTP = Output Pre-Processor
- OUT = Output Processor

FIGURE 1-19 The Multiprocessor MVMA 2-D Model

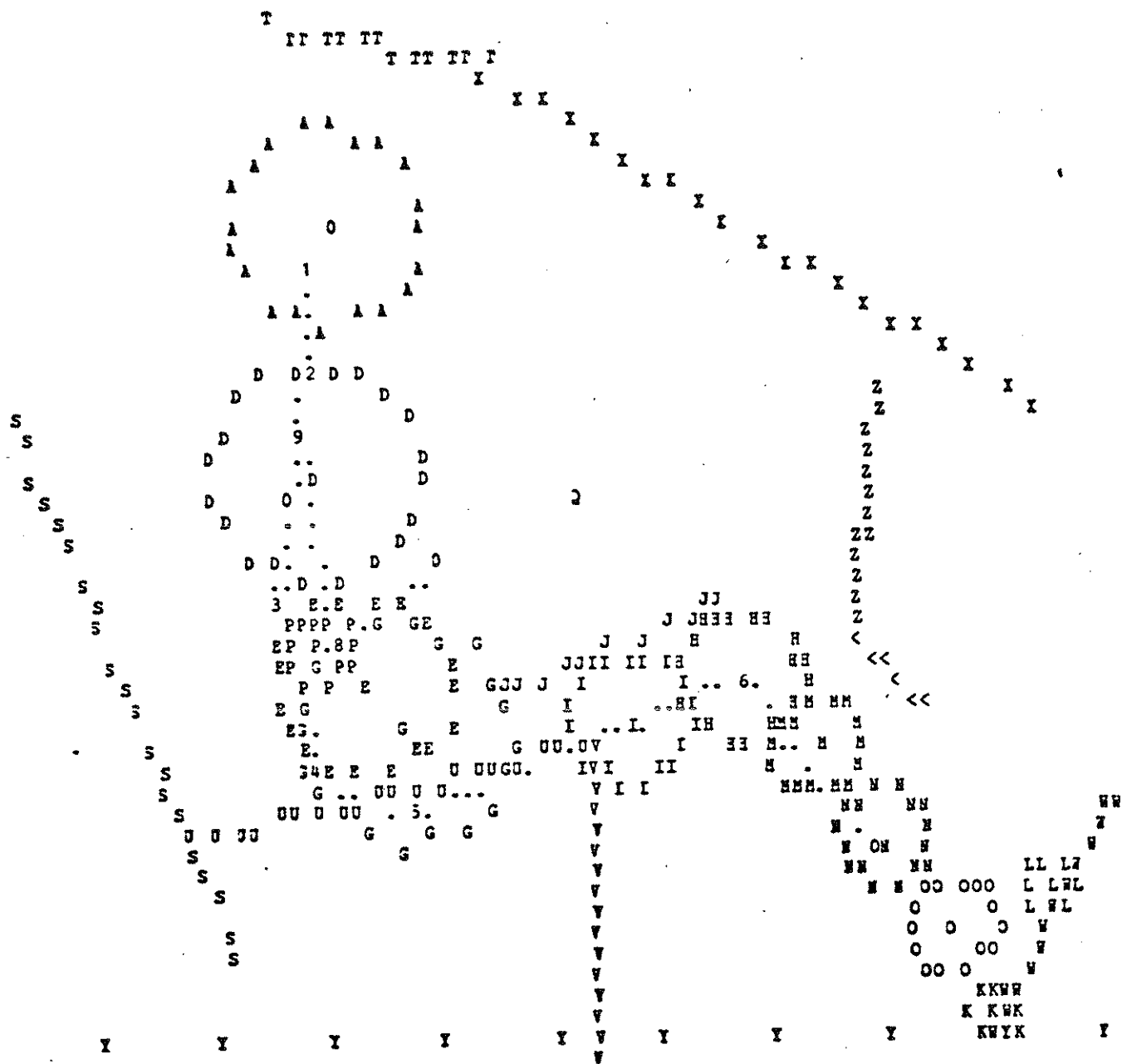
Post-processor subroutines make possible digital filtering of occupant accelerations. Either filtered or unfiltered accelerations may be used in determinations of the Head Injury Criterion, HIC, and head and chest Severity Indices. Also, axial and shear components of femur and tibia loads can be calculated. Up to eighteen standard potential injury indicators including accelerations, loads, HIC, and severity indices can be compared against user-specified test values. Joint relative angles can be similarly tested. In addition, it is possible to compare any recorded response variable against any other or against high and low test values. The final post-processor function is to produce printer-plot stick-figure representations of the occupant, the vehicle interior, and the restraint configuration. One stick figure from a time sequence of plots is shown in Figure 1-20.*

In its second function, printing time histories of response variables, the output processor deals with fifty different categories of computed results. These are categories 1-40 and 46-50 in Figure 1-21. They include information about vehicle motion, occupant motion, joint torques, and forces resulting from occupant interaction with elements of the vehicle interior and restraint systems. Any or all of these categories can be requested by the user for printout. In addition, it is possible to obtain formatted printout of input quantities.

* The Tutorial System does not deal with the use of VCL (Validation Command Language), a separate MVMA 2-D computer program which can perform most of the post-processing functions mentioned here. VCL has many other post-processing uses as well. It was developed to aid the automotive safety researcher in quantifying comparison between impact test results and predictions of mathematical simulations.

STICK FIGURE PRINTER PLOT FRAME FOR TIME=

60.00 MSSEC.



Coordinate ranges for plot are X = 0.0 (at left) to 64.00 (at right) and Z = 2.24 (at bottom) to -41.24 (at top). Scale factor is (in) = 4.923 (in), X and Z point resolution errors equal respectively 0.246 and 0.410 (in) in scale.

FIGURE 1-20 Example of Printer Plot Output

Category Number	Description
0	Formatted Printout of Input Quantities
1	Vehicle Response
2	Real Line Region Parameters
3	Real Line Region Individual Line Segment Movement
4	Contact Forces Including Occupant-Vehicle, Occupant-Belt, Occupant-Occupant
5	Neck Reaction Forces
6	Unfiltered Body Accelerations (Head, Chest, Pelvis)
7	Filtered Body Accelerations (Head, Chest, Pelvis)
8	Unfiltered Severity Indices
9	Filtered Severity Indices
10	Body Link Angles
11	Body Link Angular Velocities
12	Body Link Angular Accelerations
13	Body Joint Coordinates
14	Body Joint Velocities
15	Body Joint Torques
16	Body Joint Absorbed Energies
17	Body Kinetic Energies
18	Airbag Variables
19	Airbag Contact Forces
20	Airbag Center of Mass Forces and Moments
21	Neck Joint Coordinates
22	Shoulder Joint Coordinates
23	Joint Torque Elastic Components
24	Joint Torque Joint-Stop Components
25	Joint Torque Friction Components
26	Joint Torque Viscosity Components
27	Joint Absorbed Energy Joint Stop Components
28	Joint Absorbed Energy Friction Components
29	Joint Absorbed Energy Viscosity Components
30	Center of Mass X-Component Forces
31	Center of Mass Z-Component Forces

FIGURE 1-21a List of Output Categories

Category Number	Description
32	Center of Mass Resultant Moments
33	Steering Column Coordinates
34	Steering Column Generalized Coordinates
35	Steering Column Forces and Moments
36	Forces and Moments on Body Due to Steering Column
37	Neck and Shoulder Forces
38	Muscle Tension Forces
39	Muscle Tension Energy Absorption
40	Femur and Tibia Accelerations and Loads
41	Joint Relative Angle Comparisons Against Upper and Lower Test Values
42	Standard List of Quantities to be Compared Against Test Values
43	Individual Type A Comparisons
44	Individual Type B Comparisons
45	Printer-Plots of Stick Figures
46	Head Center-of-Gravity Motion
47	Chest Center-of-Gravity Motion
48	Hip Motion
49	Joint Relative Angles
50	Joint Relative Angle Velocities

FIGURE 1-21b List of Output Categories

1.5 Data Set Structure

Two data decks are required for computer simulations made with the MVMA 2-D model. (See Figure 1-22.) Each data deck consists of a series of eighty-character lines which will be called "cards" in this discussion. The first data deck is read by the input pre-processor, and the cards are identified by numbers 100 through 1000 in columns 78-80 or 77-80. Primarily, these cards contain data which describe the crash event, the occupant, the vehicle interior, and the restraint systems. The second data deck is read by the output pre-processor. Each card is identified by a number 1001 through 1600 in columns 77-80. These cards contain data which control printout and the use of post-processors discussed in the last section. In general, data cards can be in any order within a data deck. Cards which control model options not used for a particular simulation need not be present. Also, as explained in Volume 2 of the MVMA 2-D manuals, various quantities can be defaulted to constants stored within the program by omitting their cards from the data deck(s).

Each card consists of ten fields. (See Figure 1-23.) The tenth field is reserved for the previously mentioned card identification number. The first nine fields, consisting of eight columns each, are data fields. Thus, up to nine numbers may be required per card although most cards make use of a smaller number of fields. Numerical data must be specified in either F, E, or D format, examples of which are given with Figure 1-23. Blanks in numeric fields are treated as zeros by most computer systems, so E- and D-format numbers must be right-adjusted within data fields. Alphanumeric data are required on some cards; blanks within an alphanumeric field will not be ignored since a blank is a legitimate alphanumeric character.

DATA DECKS

Card Number

100	Cards read by INP. 100, 200,..., 900 content used for automatic titling of pages
101	
102	
⋮	
1000	1000 (blank) marks end of data deck
1001	Cards read by OUTP.
1002	
1003	
⋮	
1600	1600 (blank) marks end of data deck

FIGURE 1-22 Data Decks

1.6 Using the Tutorial System

The Tutorial System self-study guide and audio-visual program are intended to facilitate learning to use the MVMA Two-Dimensional Crash Victim Simulator. The point must be made, however, that the model user must have the MVMA 2-D report manuals, specifically Volume 2, in order to prepare data for a simulation. The Tutorial System self-study guide is not intended to be a replacement for the report manuals, but, rather, a detailed supplement.

Volume 2 of the MVMA 2-D report manuals includes a description of all data cards and their content, card by card and field by field. Figure 1-24 is a typical card layout from Volume 2. The table from which this example page is taken includes over 100 such card layouts. They must be referenced in the preparation of a data set, but they are not included with the Tutorial System. The table, in addition to collecting in one place a description of all required input data, includes information regarding default values for fields of cards omitted from the data deck(s) and also information regarding required units for data, field by field. The units required for running the model with metric-system or English-system data are indicated separately.*

As previously mentioned, Tutorial System Modules 2 through 12 deal with different groups of related model features. However, it is not possible to make the treatment of all subject matter in each module completely self-contained. For example, Module 9 describes the two optional

* All example data included in the Tutorial System self-study manual are in English system units.

TABLE 7. INPUT DATA

FRICTION COEFFICIENTS
(9 Fields of 8)

Fields	Name of Quantity	Units	Description	Defaults
1			Ellipse friction class (1. to 5.)	
2			Region friction class (1. to 10.)	
3	CMU (.,.,1), μ_k^0		Constant friction coefficient.	0.
4	CMU (.,.,2), μ_k^1	1/in (1/cm)	Linear friction coefficient.	0.
5	CMU (.,.,3), μ_k^2	1/in ² (1/cm ²)	Second order friction coefficient	0.

NOTES: 1. A non-linear friction coefficient is computed to simulate "plowing."

$$\mu = \mu_k^0 + \mu_k^1 \delta + \mu_k^2 \delta^2$$

2. There must be one 412 card for each combination of ellipse and region friction class indicated on Cards 215 and Cards 402.
3. See Section 2.6.6.

MVMA 2-D Model
Card 412

FIGURE 1-24 Example Card Layout from Volume 2 of MVMA 2-D Report Manuals

belt restraint systems in detail. But the description of general material property specifications, which are relevant to belt webbing, body parts, and elements of the vehicle interior, is in Module 6. Thus, reference to belt webbing material properties is made in more than one module. Figures 1-25 and 1-26 are included to aid the Tutorial System user in locating information within the self-study guide relevant to any input data parameter. Figure 1-25 shows all data cards referenced by each module, and Figure 1-26 indicates all modules which reference each field of each card.

Module 1 has served as an introduction to the MVMA Two-Dimensional Crash Victim Simulator and the Tutorial System. The Tutorial System should be used in either of two ways.

First, the thirteen audio-visual modules may all be run, sequentially, before the self-study manual is used. The audio-visual modules, each consisting of 35 mm slides and narration on a tape cassette, treat model features in much greater detail than they have been discussed in this introductory module. However, they cover their material in much less depth than the self-study manual; each includes only 15 to 25 minutes of narration. Therefore, they can be used together as a detailed, four and one-half hour audio-visual introduction to the model. They need not be viewed in one session, of course. In this method of using the Tutorial System, use of the self-study guide would follow viewing of all modules.

Alternatively, viewing of audio-visual modules and use of the self-study guide can alternate. In this method, the user of the Tutorial System would study the subject matter of a module in detail before proceeding to the next module.

Either method should be an effective way of preparing the user for applying the MVMA Two-Dimensional Crash Victim Simulator to problems of automotive safety design. After study of Module 13, the user should be ready to exercise the model. The MVMA 2-D model can be applied in various ways for the modeling of dynamical systems. A broad range of front, rear, and even side impacts for driver and

DATA CARDS REFERENCED BY MODULES

Module	Data Cards Referenced
2	201-217, 303, 227-238
3	201-203, 205-217, 227, 228, 233, 235-242, 303
4	102, 103, 106, 219-226, 402, 412, 903, 907-909
5	102, 103, 106, 219, 401-412
6-1	103, 219, 221-226, 401, 403-408, 702-716
6-2	102, 103, 219, 222, 401, 402, 404, 409, 410, 412, 605, 606, 705
7	205, 206, 215, 216, 301-304, 409, 1501, 1502
8	601-606
9	102, 218, 501, 701-723
10	102, 411, 901-909
11	-
12	101, 102, 104, 105, 107-111, 218, 1000-1004, 1100-1107, 1200-1202, 1300, 1400, 1401, 1500-1502, 1600

FIGURE 1-25 Data Cards Referenced By Modules

DATA CARD FIELDS
AND REFERENCING MODULES

Card	Field								
	1	2	3	4	5	6	7	8	9
101	12	12	12	12	12	12	12	12	12
102	9,12	10,12	12	4	4,5	4	6-2	12	12
103	6-2	6-2	6-1	6-1	6-2	5	5	4	4
104	12	12	12	12	12	12	12	12	12
105	12	12	12	12	12	12	12	12	12
106	4,5	4,5	4,5	4,5					
107	12	12	12	12	12	12	12	12	12
108	12	12	12	12	12	12	12	12	12
109	12	12	12	12	12	12	12	12	12
110	12	12	12	12	12	12	12	12	12
111	12	12	12	12					
201	2,3	2	2	2	2		2	3	3
202	2,3	2,3	2	2	2	2	2	2	3
203	2	2	2	2	2	2	2	2	2,3
204	2	2	2	2	2	2	2	2	
205	2,3	2,3	2,3	2,3	2,3	2,3	2,3	2,3,7	2,3
206	2,3	2,3	2,3	2,3	2,3	2,3	2,3	2,3,7	2,3
207	2	2	2	2	2	2	2	2	2
208	2	2	2	2	2	2	2	2	2
209	2	2	2	2	2	2	2	2	2
210	2	2	2	2	2	2	2	2	2
211	2,3	2,3	2,3	2,3	2,3	2,3	2,3	2,3	2,3
212	2	2	2	2	2	2	2	2	2

FIGURE 1-26 Data Card Fields Referencing Modules (Page 1 of 6)

Card	Field								
	1	2	3	4	5	6	7	8	9
213	3	3	3	3					
214	3	3	3	3			3		3
215	2,3	2,3	2,3	2,3	2,3	2,3	2,3,7	2,3	2,3
216	2,3	2,3	2,3	2,3	2,3	2,3	2,3,7	2,3	2,3
217	2	2	2	2	2	2	2,3	2	
218	12	12	12	9	9	9	9	9	9
219	4	4	4,6-1	4,6-1	4	4,5,6-2			
220	4	4	4	4	4	4			
221	4,6-1	4,6-1	4,6-1	4,6-1	4,6-1	4,6-1	4,6-1	4,6-1	4,6-1
222	4,6-1	4,6-1	4,6-2				4,6-1	4,6-1	4,6-1
223	4,6-1	4,6-1	4,6-1						
224	4,6-1	4,6-1	4,6-1						
225	4,6-1	4,6-1	4,6-1	4,6-1	4,6-1	4,6-1	4,6-1	4,6-1	
226	4,6-1	4,6-1	4,6-1	4,6-1	4,6-1	4,6-1	4,6-1	4,6-1	
227	2,3	2,3	2,3	2,3	2,3				
228	2,3	2,3	2,3	2,3	2,3				
229	2	2	2	2	2				
230	2	2	2	2	2				
231	2	2	2	2	2				
232	2	2	2	2	2				
233	2,3	2,3	2,3	2,3	2,3				
234	2	2	2	2	2				
235	2,3	2,3	2,3	2,3	2,3				

FIGURE 1-26 Data Card Fields Referencing Modules (page 2 of 6)

Card	Field								
	1	2	3	4	5	6	7	8	9
236	2,3	2,3	2,3	2,3	2,3				
237	2,3	2,3	2,3	2,3	2,3				
238	2,3	2,3	2,3						
239	3	3							
240	3	3							
241	3	3							
242	3	3	3	3					
301	7	7	7	7	7	7	7	7	7
302	7	7	7	7	7	7	7	7	7
303	7	7	7	7	2,3,7	3,7			
304	3,7	7	3,7	7					
401	5	5	5,6-1	5,6-1	5,6-2	5,6-2	5,6-2	5,6-2	
402	5	5	5	4,5,6-2	5,6-2	5	5		
403	5,6-1	5,6-1	5,6-1	5,6-1	5,6-1	5,6-1	5,6-1	5,6-1	5,6-1
404	5,6-1	5,6-1	5,6-2	6-2	6-2	6-2	5,6-1	5,6-1	5,6-1
405	6-1	6-1	6-1						
406	6-1	6-1	6-1						
407	6-1	6-1	6-1	6-1	6-1	6-1	6-1	6-1	
408	6-1	6-1	6-1	6-1	6-1	6-1	6-1	6-1	
409	5	5	5	5	5,6-2,7	6-2	5	5	
410	5	5	5	6-2	6-2	6-2	6-2		
411	5	5	5	5,10	5,10	5	5	10	
412	4,5,6-2	4,5,6-2	4,5,6-2	5,6-2	5,6-2				

FIGURE 1-26 Data Card Fields Referencing Modules (page 3 of 6)

Card	Field								
	1	2	3	4	5	6	7	8	9
501	9	9	9	9	9	9	9	9	
601	8	8	8	8	8	8	8	8	
602	8	8	8						
603	8	8	8						
604	8	8							
605	6-2,8	6-2,8	6-2,8	6-2,8	6-2,8				
606	6-2,8	6-2,8	6-2,8						
701	9	9	9	9	9	9	9		
702	6-1,9	6-1,9	9	9	9	9	9	9	
703	6-1,9	6-1,9	9	9	6-1,9	6-1,9	9	9	
704	6-1,9	6-1,9	6-1,9	6-1,9	6-1,9	6-1,9	6-1,9	6-1,9	6-1,9
705	6-1,9	6-1,9	6-2,9				6-1,9	6-1,9	6-1,9
706	6-1,9	6-1,9	6-1,9						
707	6-1,9	6-1,9	6-1,9						
708	6-1,9	6-1,9	6-1,9	6-1,9	6-1,9	6-1,9	6-1,9	6-1,9	
709	6-1,9	6-1,9	6-1,9	6-1,9	6-1,9	6-1,9	6-1,9	6-1,9	
710	9	9	9	9	9	6-1,9	6-1,9	9	9
711	9	9	9	9	9	6-1,9	6-1,9	9	9
712	9	9	9	9	9	6-1,9	6-1,9	9	9
713	9	9	9	9	9	6-1,9	6-1,9	9	9
714	9	9	9	9	9	6-1,9	6-1,9	9	9
715	9	9	9	9	9	6-1,9	6-1,9	9	9
716	9	9	9	9	9	6-1,9	6-1,9	9	9

FIGURE 1-26 Data Card Fields Referencing Modules (page 4 of 6)

Card	Field								
	1	2	3	4	5	6	7	8	9
717	9	9	9	9	9	9	9		
718		9	9						
719	9	9	9	9	9	9	9		
720	9	9	9	9	9	9	9	9	
721	9	9	9	9	9	9			
722	9	9	9	9	9	9			
723	9	9	9	9	9	9			
901	10	10	10	10	10	10	10	10	10
902	10	10	10	10	10	10	10		10
903	10	10	10		10	10	4,10		
904	10								
905	10								
906	10								
907	4,10	4,10	4,10	4,10			4,10	4,10	
908			4,10	4,10	4,10	4,10	4,10	4,10	
909	4,10	4,10	4,10	4,10					
1000	12								
1001	12								
1002	12								
1003	12	12	12	12	12				
1004	12	12	12	12	12	12	12	12	
1100	12	12							
1101	12	12							

FIGURE 1-26 Data Card Fields Referencing Modules (page 5 of 6)

[illegible]

passenger have been simulated. Applications have included simulating anthropomorphic dummy drops onto a hard surface and human fall victims striking yielding and unyielding surfaces. They have included simulating pedestrians struck by a vehicle. Simulations have been done of laboratory tests in which lateral neck response of human subjects was measured when the head was jerked to the side by a falling weight. But use of the MVMA 2-D model need not be restricted to simulating human or human-analog systems. Diverse applications are possible if the user is clever in utilizing the many features of the model.

MODULE 2--THE BODY LINKAGE

2.1 Body Linkage

The MVMA-2D crash victim is represented analytically as a "lumped mass" dynamical system. That is to say that we are approximating the body by a string of rigid links and that all viscoelastic elements affecting angulation of body parts relative to each other act at discrete points connecting the links. This approach to the analytical problem is common to all crash victim simulators developed to date.

Figure 2-1 illustrates the body linkage. The crash victim is treated as an eight-mass system in which ten physical links are represented. Since this is a planar model there would be no great purpose to including left and right legs separately. Consequently, a single two-link leg represents the two legs combined, as if bound together. Accordingly, the thigh and lower leg masses, M_5 and M_6 in Figure 2-1, should be assigned doubled values. The arms are similarly treated as only two links. The human spinal column is more or less continuously flexible since it is composed of thirty-three vertebrae and intervening fibrocartilaginous discs. The model simulates flexibility of the combined thoracic and lumbar spines by two articulations, which connect three torso masses. These are joints 3 and 4 in the figure. Flexibility of the cervical spine (neck) is accounted for by two articulations, one at the occipital condyles and one at the seventh-cervical/first-thoracic juncture, joints 1 and 2, respectively. The neck element itself is massless in this model, but neck mass can be apportioned however desired at the head and torso junctures. This element can undergo compression and elongation. A similar massless body link is found at the shoulder. It connects joints 7 and 9 in Figure 2-1. This element allows simulation of shoulder flexibility resulting

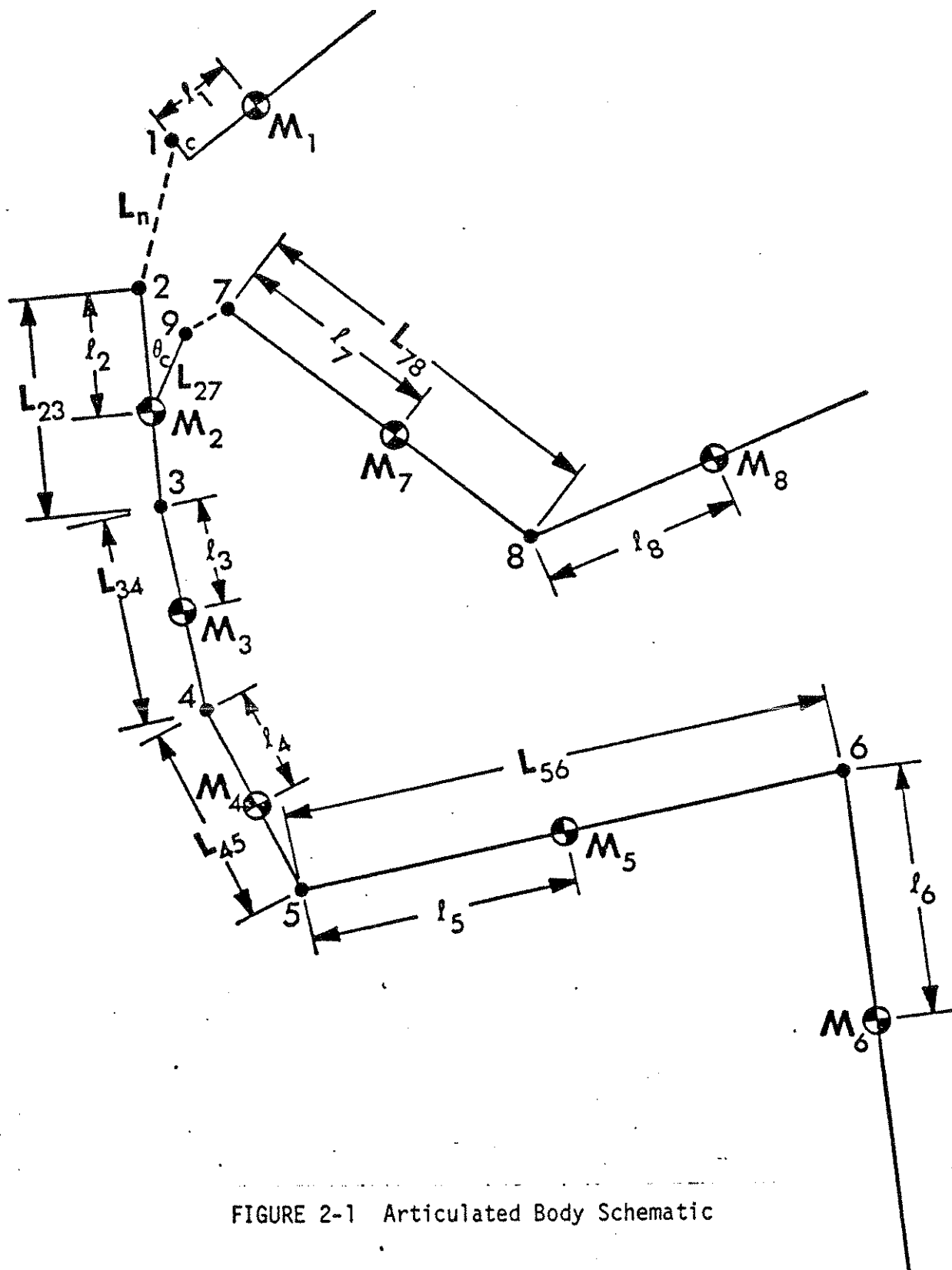


FIGURE 2-1 Articulated Body Schematic

from out-of-plane motion of the clavicle.* Neck and shoulder flexibility is discussed in detail in Module 3.

The length quantities shown in Figure 2-1 are inputted on 201- and 202-Cards. Body segment lengths are in fields 2 through 7 of Card 201. These are joint-to-joint lengths. For example, the upper arm length L_{78} is entered in field 7. Torso segment lengths are entered in fields 2, 3, and 4, and the hip-knee length is in field 5. Field 6 is unused. The initial value for neck length is in field 5 of Card 303. Body segment centers of mass are positioned with respect to joints by defining the length values ℓ_1 through ℓ_8 . These are entered in fields 1 through 8 of Card 202. Centers of mass must lie on body segment centerlines, that is, on joint-to-joint lines, since no offset terms are included in the analysis. The only exception to this is that the head center of mass can be assigned an offset from the upper neck joint at the occipital condyles. That is to say, the vertical head axis need not pass through the upper neck joint. In Figure 2-1 the condyles offset is the quantity "c" at joint 1. Its value is entered in field 1 of Card 201.

2.2 Masses and Moments of Inertia

Body segment masses are inputted on Card 203. Values for the masses M_1 through M_8 shown in Figure 2-1 are entered in fields 1 through 8, respectively. It has been previously noted that the arm and leg masses in fields 5 through 8 should be doubled values in order to represent both left and right limbs. Field 9 contains the neck mass, which is not shown in the figure. The total neck mass is distributed as lump masses at each end of the neck, at joints 1 and 2. The decimal proportion of this mass to be placed at the upper

*Joint 9 is fixed with respect to the upper torso link, i.e., θ_c and L_{27} are constants. See Module 3.

neck joint is indicated in field 9 of the 202-Card and the remainder will be lumped at joint 2. Moments of inertia for the body links about the centers of mass are entered on Card 204. Figure 2-2 shows example data cards with values for link lengths, masses, and moments of inertia. These data are for a 161 lb male of average stature.

The MVMA-2D linkage is sometimes used for modeling systems other than humans or human analogs. In such applications, it is occasionally useful to specify some mass and moment-of-inertia values as zero. Certain combinations of these parameters are not allowed to be zero, depending on which link lengths, if any, are set to zero. The only simply-stated guideline that can be given the user is that diagonal elements of the coefficient matrix for the generalized accelerations may not be zero. The analytical expressions for the matrix elements are given in Volume 1 of the MVMA-2D manuals.

.97	11.93	5.47	4.25	16.0		12.6	1.74	0.	201
1.64	4.00	3.46	1.65	7.28	11.3	5.28	12.3	.33	202
.0234	.1087	.0183	.0480	.1006	.0541	.0290	.0257	.0088	203
.146	2.603	.473	1.766	2.394	3.020	.547	1.644		204

FIGURE 2-2 Example data cards for body link lengths, masses, and moments of inertia

2.3 Joint Properties

The quantities on Cards 205 through 217 define the geometry and torsional strength properties of the various joint structures. Joint geometry will be described together with a discussion of joint torque components.

Figure 2-3 is a schematic of a human in a standing position. The body links approximate the skeletal structure and are shown here to illustrate that they are not necessarily in alignment even in an erect posture. Figure 2-4 is a similar schematic of a seated human. A so-called "in-line orientation" is defined as a reference orientation for several model input quantities. Figure 2-5 depicts the in-line orientation. Body joints are numbered here as in Figure 2-1.

2.3.1 Joint Stop Angles

Angulation at body joints is relatively free until hard-tissue resistance is encountered. Polynomial coefficients for nonlinear resistive torques are inputted and become effective when specified range-of-motion limits are reached. Values for the range-of-motion limits, the so-called joint stop angles, are normally taken as the extreme angulations voluntarily imposed by human subjects. Two joint stop angles are defined for each joint so that both clockwise and counterclockwise angulations can be properly limited. A relative angle is considered positive when the link nearer the head is positioned counterclockwise from its in-line orientation. This is illustrated in Figure 2-5. Joint stop angles are defined for those values of relative angles between which no hard-tissue resistance is encountered. For many joints these positions are on

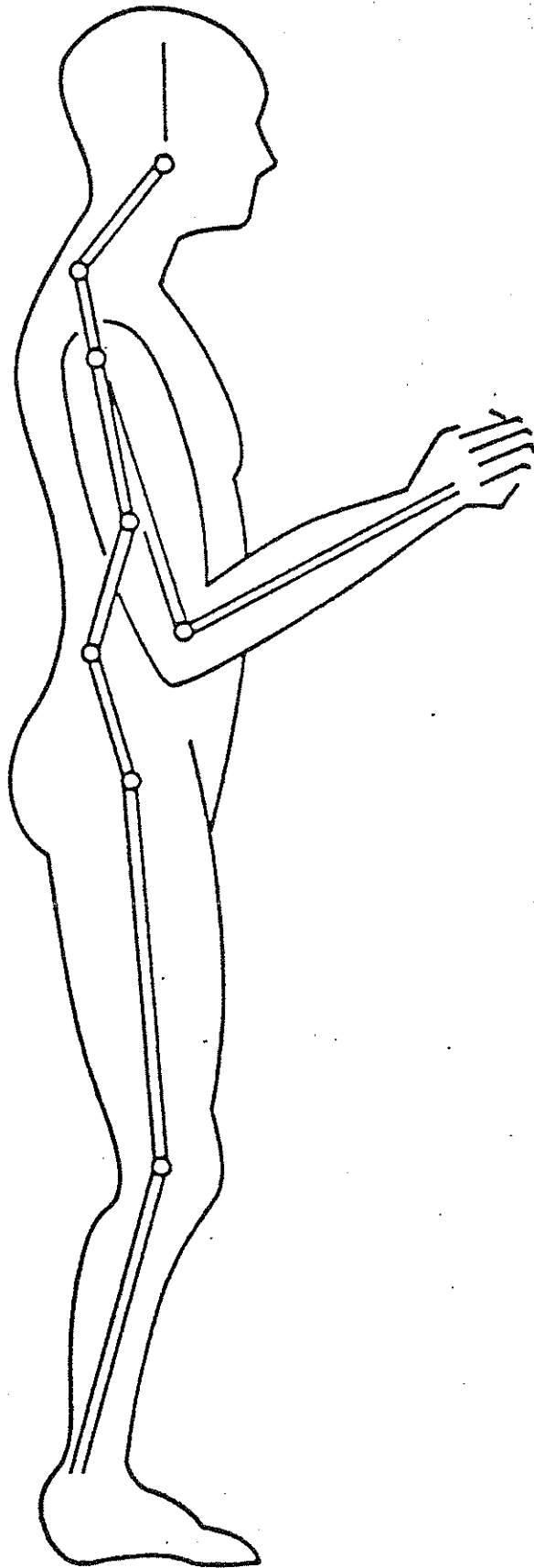


FIGURE 2-3 Standing Position

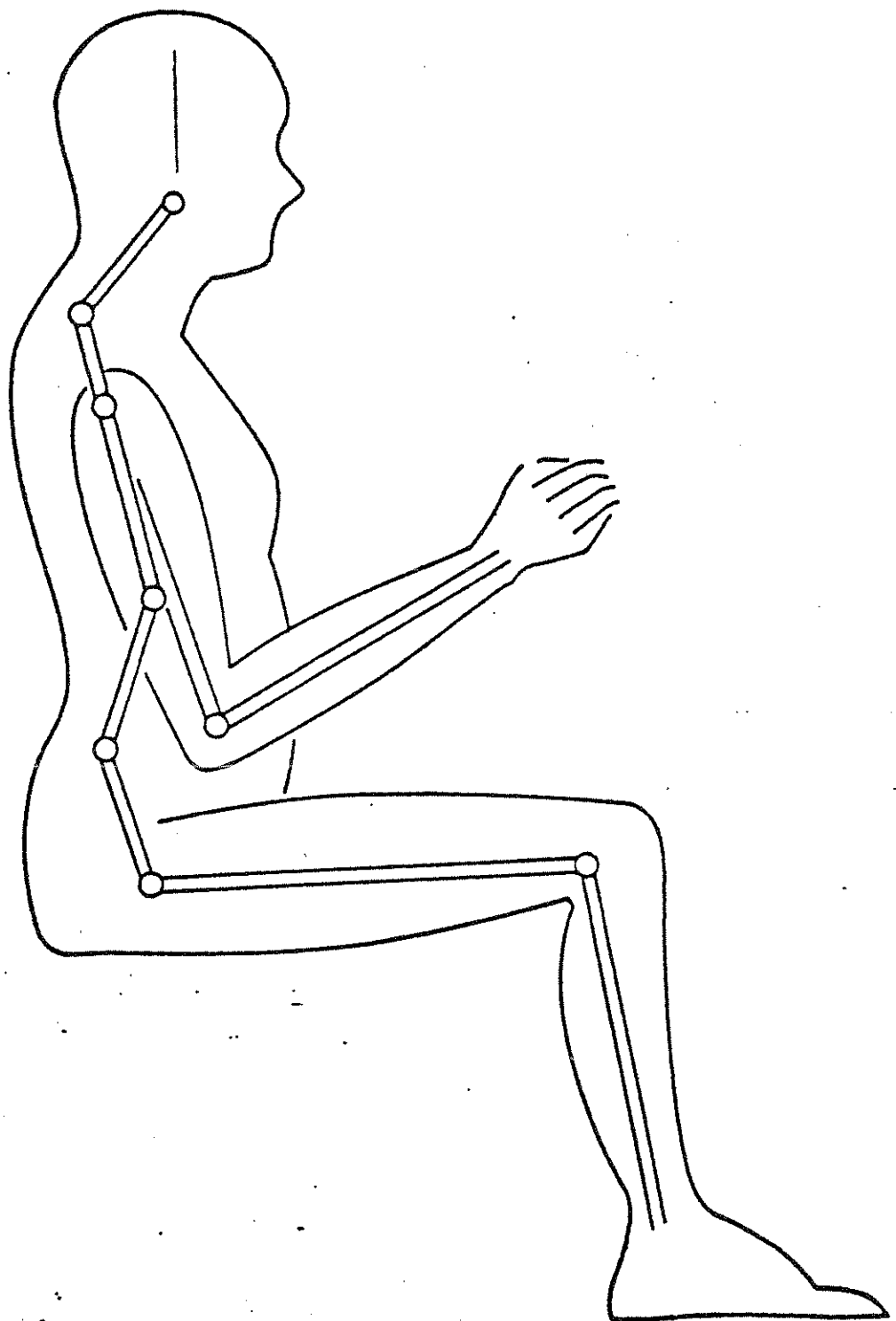
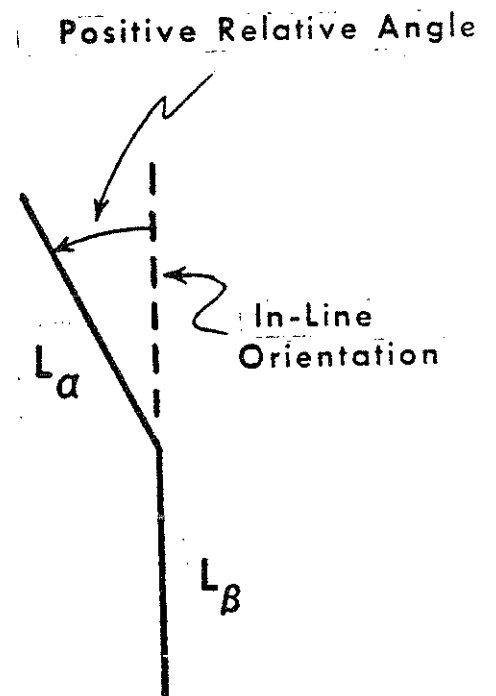
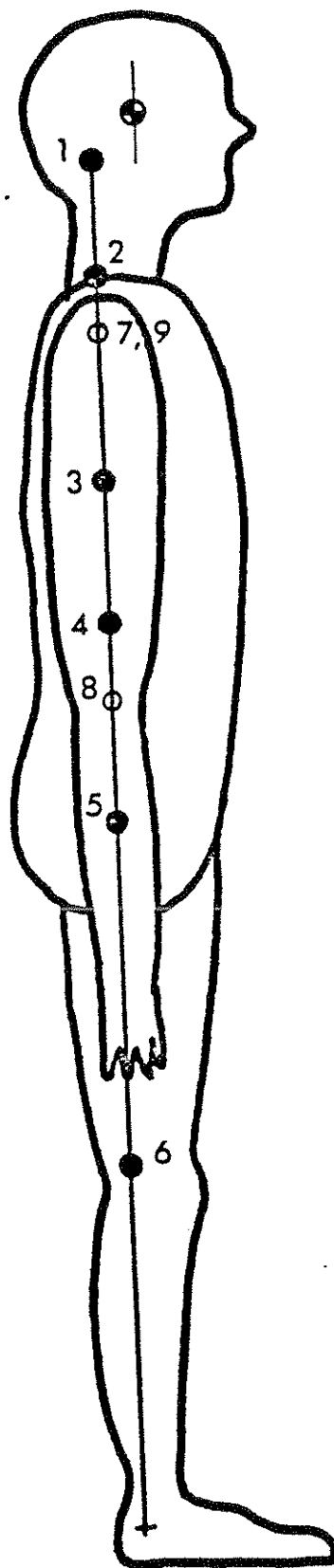


FIGURE 2-4 Sitting Position



L_α = body link nearer to head

L_β = body link nearer to feet

FIGURE 2-5 In-line Orientation

either side of the in-line orientation, i.e., one value is positive and one is negative. For this reason they are often called "positive" and "negative" joint stop angles. But since there is no general restriction on the stop values and since indeed the stops are not always on either side of the in-line orientation, they are best called "upper" and "lower" stop angles, the upper joint stop being the positive-most position. The stop angles are illustrated in Figure 2-6. Positions of L_α , the upper link, requiring clockwise rotation are described by negative angles.

2.3.2 Link Equilibrium Position

Another quantity illustrated by Figure 2-6 is the "natural link position." A better name for this quantity might be "link equilibrium position." It is the value of the relative angle at which no linear, elastic component of spring torque results. In contrast to the nonlinear joint-stop coefficients, the values normally used for elastic coefficients produce small torques except for large relative angulations. The natural link positions are most commonly set to coincide with the initial occupant configuration so that no joint torques exist at time zero. Resistance to small motion away from this configuration is normally considered to be due to soft-tissue deformation.

2.3.3 Example Angle Data for Joints

Figure 2-7 is a stick-figure representation of a seated occupant at time zero. Consider the knee as a typical joint. The figure

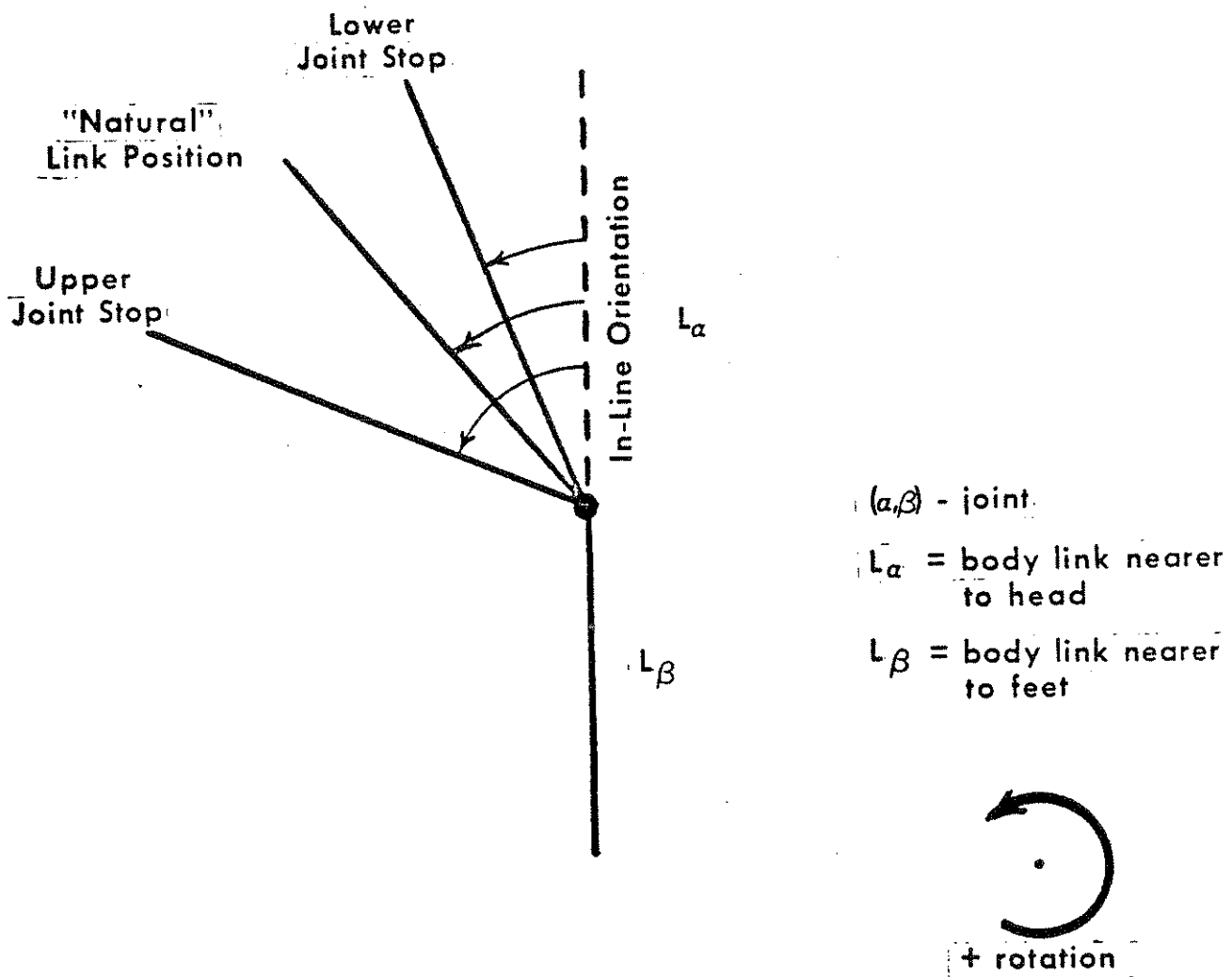


FIGURE 2-6 Definition of joint stop angles and natural link position

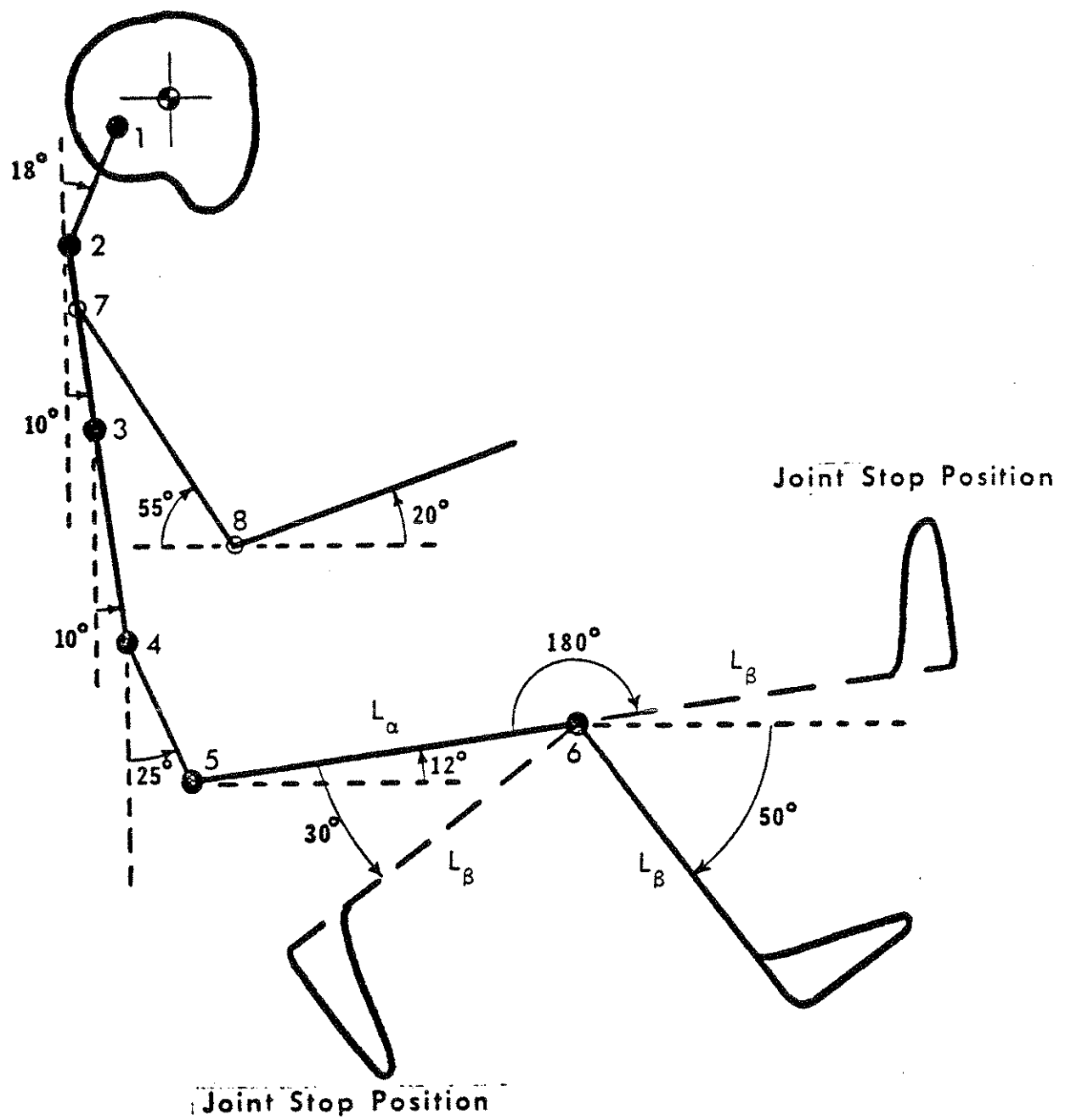


FIGURE 2-7 Joint Stop Positions for Knee

illustrates the range of motion of the lower leg. Thus far six quantities relating to joint geometry and torsional properties have been defined. Four primary quantities remain to be defined, but for the moment let us consider the input requirements for the six. Nine knee joint specifications are entered on the 210-Card and the tenth is entered on the 217-Card, which contains natural link angle values for all joints. The upper (or positive-most) and lower (or negative-most) joint stop angles for the knee are entered in fields 7 and 8 of Card 210. Figure 2-7 shows a bent-knee stop position for which the thigh element, L_α , is 150° counterclockwise from an in-line orientation with the lower leg element, L_β . The other stop is at 0° so the positive-most stop is at $+150^\circ$ and 0° (leg straight) is the negative-most stop. Suppose that it is desired to have the natural link angle of the knee coincide with the initial knee angle so that there will be no elastic torque component in this position. Again considering angulation of element α with respect to element β from the in-line orientation, we see that the natural link angle must be $+62^\circ$. These values are among the contents of Cards 210 and 217, which are shown in Figure 2-8. It is suggested that the user demonstrate, as an exercise, that the natural link angle values in fields 1 through 8 of Card 217 correspond to the relative angles in the initial configuration depicted in Figure 2-7.

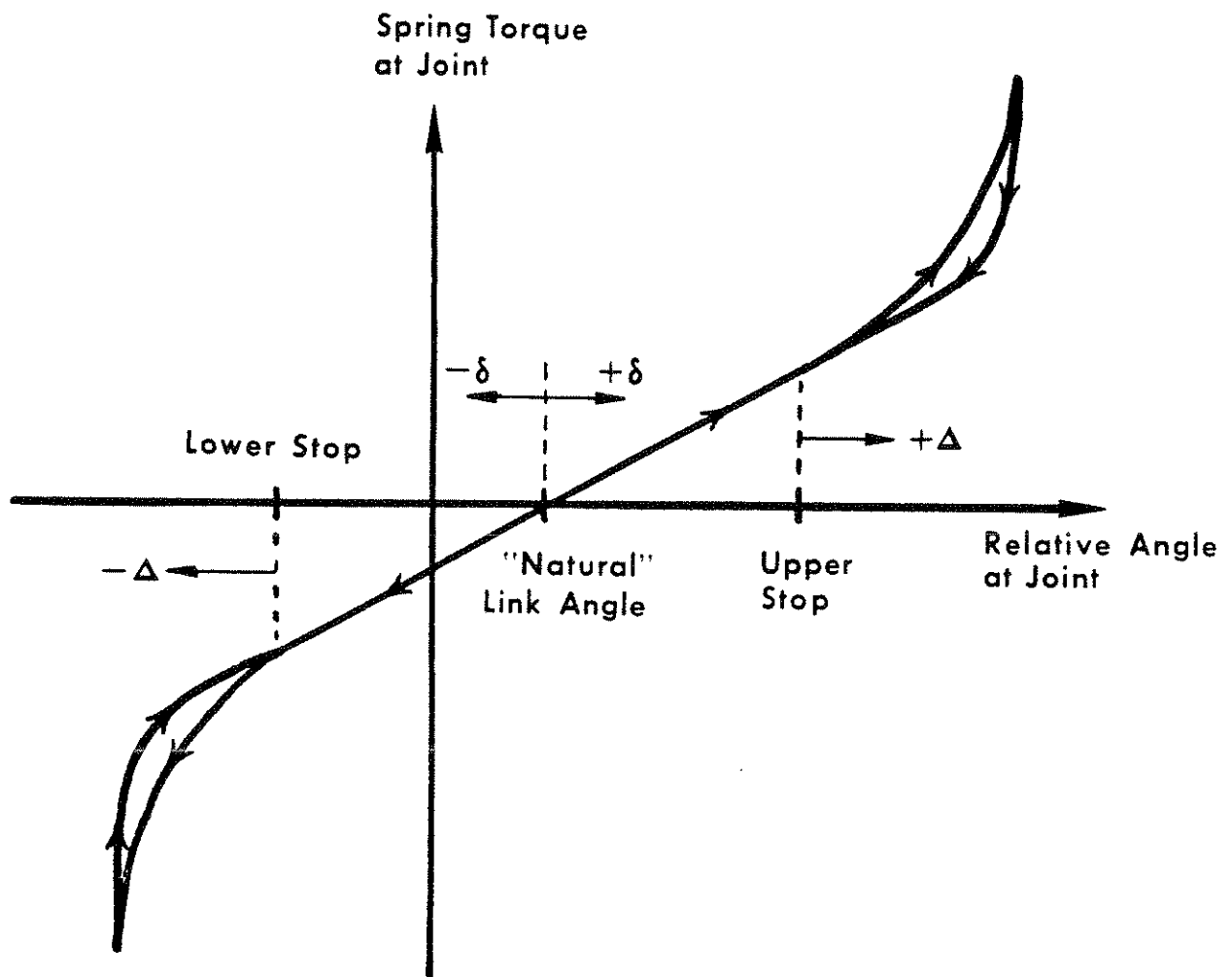
2.3.4 Linear and Nonlinear Spring Torques

Fields 1, 2, and 3 of the knee joint card, 210, contain values for quantities which have already been discussed -- namely, the polynomial coefficients for linear and nonlinear spring torque components. The equation with Figure 2-9 describes these components.

0.1	2.1	0.	.01	0.	400.	150.	0.	.3	210
18.	-28.	0.	-15.	-77.	62.	-25.	-75.		217

FIGURE 2-8 Joint property cards

6/28/79



$$\text{SPRING TORQUE} = -k_{ELASTIC} \delta - \left\{ K_{1,STOP} |\Delta| + K_{2,STOP} \Delta^2 + K_{3,STOP} |\Delta^3| \right\} \text{sgn } \Delta$$

Linear, elastic
component

Nonlinear, joint-stop component

FIGURE 2-9 Linear and nonlinear joint torques

$$\text{SPRING TORQUE} = \underbrace{-k_{\text{ELASTIC}} \delta}_{\text{linear, elastic component}} - \underbrace{\left\{ K_{1,\text{STOP}} |\Delta| + K_{2,\text{STOP}} \Delta^2 + K_{3,\text{STOP}} |\Delta^3| \right\} \text{sgn } \Delta}_{\text{nonlinear, joint-stop component}}$$

The linear elastic torque component is proportional to δ , the angular difference from the natural link position. The proportionality constant k_{ELASTIC} is in field 1. There can be three terms in the nonlinear, joint-stop component. The first term is proportional to Δ , the angular penetration into a motion-limiting stop. This linear joint-stop term can be used, however, only if the linear elastic component is not used, and conversely. The second term is proportional to the square of Δ , and the third term is cubic in the quantity Δ . The total joint-stop component is made positive or negative, depending on whether the upper stop or lower stop is active. Values for the linear, quadratic, and cubic joint-stop spring rate coefficients are in fields 1, 2, and 3 of the 210-Card. If the value in field 1 is negative, its magnitude is used for the linear joint-stop coefficient. If the value is positive, then it is used instead for the linear elastic coefficient.

2.3.5 Energy Absorption in Joints

The four primary joint quantities which have not yet been defined are in fields 4, 5, 6 and 9 of the joint parameters data card -- for the knee, Card 210. Field 9 contains the so-called "R-ratio" for the joint. This is the fraction of the energy stored in the nonlinear loading of a joint stop which will be conserved upon complete unloading of the stop. A typical loading-unloading loop for the nonlinear spring torque component is illustrated in Figure 2-10. The quadratic unloading curve is determined such that the area A is equal to $BR/(1-R)$ since the R-ratio is $A/(A+B)$. Field 4 contains a viscous friction coefficient. This is the proportionality constant for a velocity-dependent torque. The torque is directly proportional to the magnitude of the relative angle velocity and, of course, acts in a direction to resist motion. Fields 5 and 6 both relate to

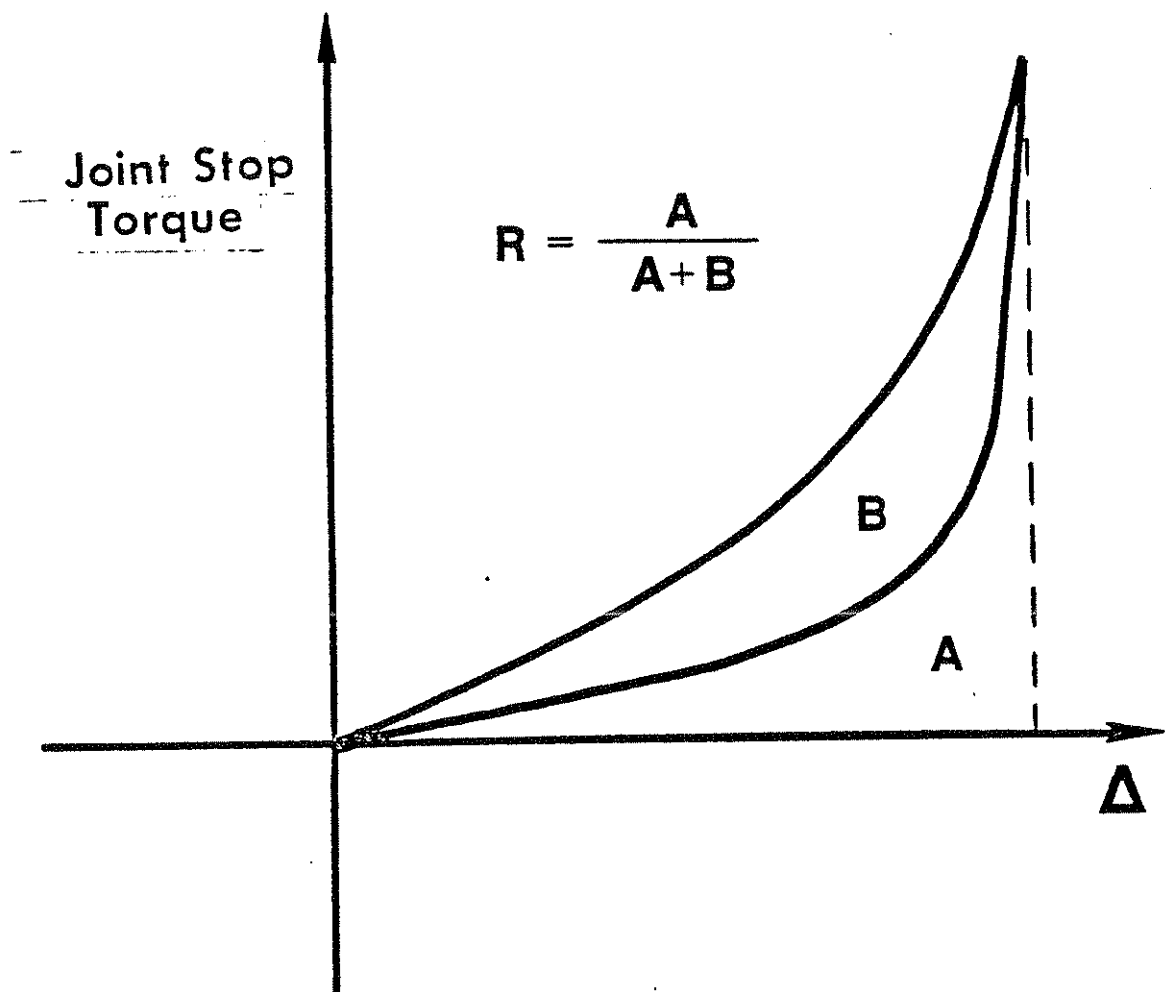


FIGURE 2-10 R-ratio for energy conserved at joint stop

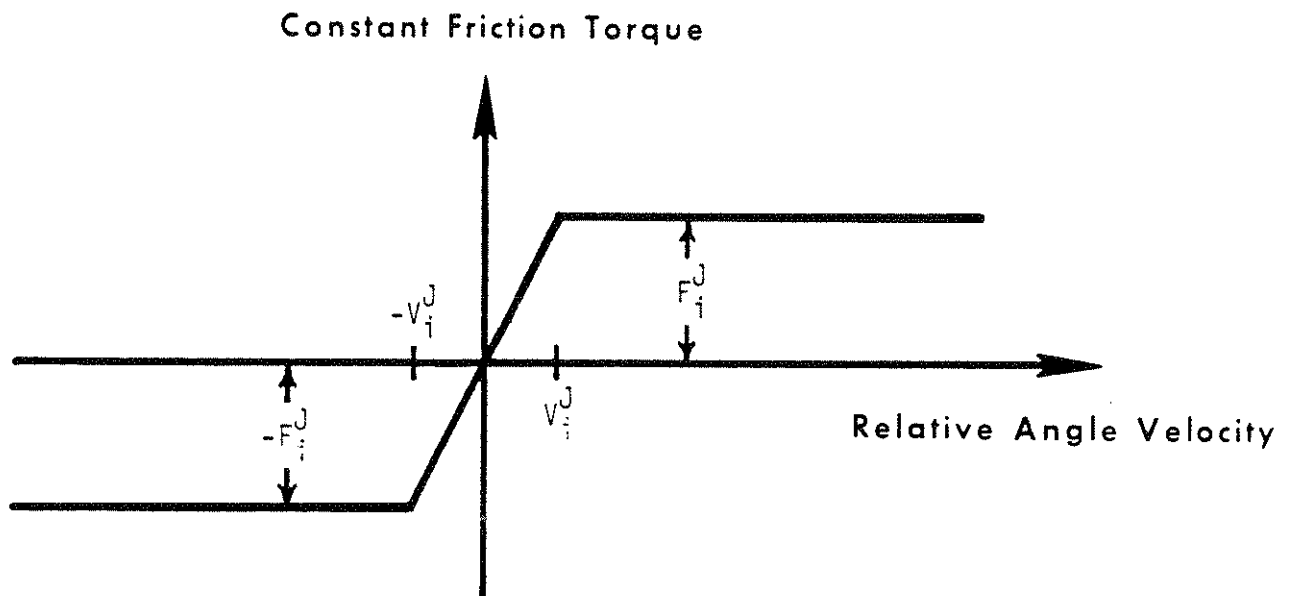


FIGURE 2-11 Joint friction at joint "i"

NOTE: It is estimated for 50th-percentile-male values for mass, moment of inertia, and link lengths and an integration time step of one millisecond that a threshold velocity V_i^J of 300-400 deg/sec or greater should be used for a joint with a constant friction torque of 1000 in-lb or 113 N-m. For greater values of constant friction and time step, proportionately greater values of threshold velocity should be used. Minimum threshold velocities are in inverse proportion to masses and moments of inertia.

constant friction joint torque. Both quantities are illustrated by Figure 2-11. The value in field 5 is the constant torque level, F_i^J , for joint "i." The quantity V_i^J in field 6 is the velocity threshold for constant friction; it is the minimum relative angle velocity for which the full friction torque results. Torques for relative angle velocities less than the velocity threshold in absolute value are calculated with a linear ramp, as illustrated in the figure. Constant friction is not a component of torque appropriately used for modeling the human being since human joints are virtually frictionless. It is very useful, however, in simulating anthropomorphic dummies. (See footnote with Figure 2-11.)

This completes discussion of the primary joint parameters for a typical joint, the knee. Input data requirements are identical in form for the upper spine, lower spine, hip, upper arm-upper torso joint, and elbow except that parameter values are entered on the 207, 208, 209, 211, and 212 cards, respectively.

2.3.6 The Neck Joints

The upper and lower neck joints in the MVMA 2-D model are atypical joints in an important sense. They are allowed to have visco-elastic properties in flexion different from those in extension. While the "typical" joints discussed above can have asymmetric joint-stop positions, still the torque-producing elements are the same for positive and negative relative angle motions. There are two joint parameter cards for each of the two neck joints. Flexion data for the upper and lower neck joints, i.e., for forward bending, are entered on Cards 205 and 206. Field 7 may be left blank since the positive-most stop must be for extension, not flexion. Data for backward bending of the neck, i.e., extension, are entered on Cards 215 and 216. Here, field 8 may be left blank, and extension stop

angle values are entered in field 7.

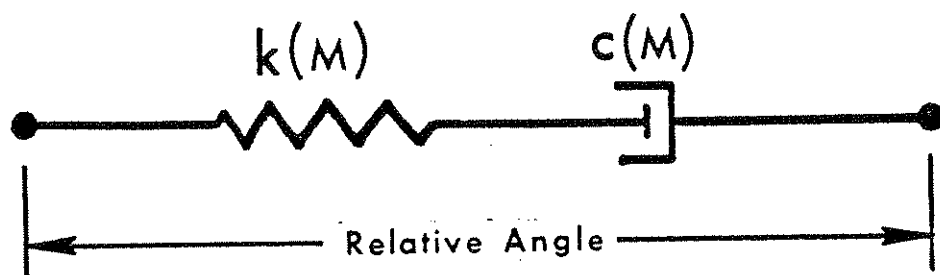
2.4 Muscle Tension

None of the previously described viscoelastic joint torque elements can be used to adequately model muscle tension. Moderate levels of muscle contraction generally have a significant effect on the crash dynamics, especially for low-g impacts, so analytical representation of the effect is of obvious value. The MVMA-2D model determines generalized forces for muscle tension torques at the eight joints. A similar torque is calculated to resist angular motion of the shoulder link. Muscle tension resistance to elongation of the neck and shoulder links is also modeled.

Experimental investigation of the knee joint indicates that this property is properly represented by a Maxwell element, i.e., a spring and damper in series, with spring and damping coefficients that are simple functions of the degree of muscle activation, M .^{*} Such an element is shown in Figure 2-12. The equations which accompany the figure give these coefficients as linear functions of the absolute value of M . This Maxwell element can be considered to be an "active" element since its coefficients are functions of the degree of muscle activation, M . It is clear that when the muscles are completely relaxed, i.e., $M = 0$, the Maxwell element has no effect on motion at the joint since C is then zero. The quantities a_1 , a_2 , a_3 , and M will now be discussed in some detail.

Dynamic torques resulting from muscle elements are determined by the program by solving first-order differential equations in muscle torque simultaneously with the system of second-order equations of motion. The torques M , however, are inputted by the user

* Moffatt, C.A., Harris, E. H., and Haslam, E. T., "An Experimental and Analytic Study of the Human Leg," Journal of Biomechanics, Vol. 2, No. 4, October 1969, pp. 373-387.



$$k = a_1 + a_2 |M|$$

$$c = a_3 |M|$$

$M = M(t)$, muscle activity level

FIGURE 2-12 Muscle element

as time-dependent levels of muscle activation. $M(t)$ for any particular joint is generally bounded by the maximum static moment that the vehicle occupant would be able to generate voluntarily.* Typically, the dependence on time is as shown in Figure 2-13. t_R is the reflex time, a non-zero value whenever the vehicle occupant is not pre-tensed because of awareness of impending impact. t_C is the contraction time, the time required for muscle activity to peak from a state of rest. Values of t_R and t_C for muscles at all joints are typically 50 msec and 120 msec, respectively.**

a_1 , a_2 , and a_3 are constants for the subject and the joint. Arguments relating these quantities to muscle tissue properties -- material properties -- allow the development of scaling laws for going from joint to joint in an individual or from individual to individual for the same joint.*** A necessary assumption is that the material properties, i.e., constitutive properties, of all striated (or skeletal) muscle in humans are constant from body part to body part and from individual to individual. The scaling laws and a schematic illustrating some of the parameters are shown in Figure 2-14. The MVMA-2D muscle model, based directly on angular motion, is somewhat artificial in that muscle moments are really a result of lineal action of a muscle with a moment arm. This results in no analytical difficulties, however, since all lineal muscle coefficients can be related to effective angular coefficients by the effective moment arm, L , illustrated in Figure 2-14. Strictly,

* Peak $M(t)$ is normally less than about one-third the static moment that can be generated against a reaction surface.

** $t_R + t_C$ is called the muscle response time.

*** Bowman, B. M., "An Analytical Model of a Vehicle Occupant for Use in Crash Simulations," Doctoral Thesis, Univ. of Mich., 1971.

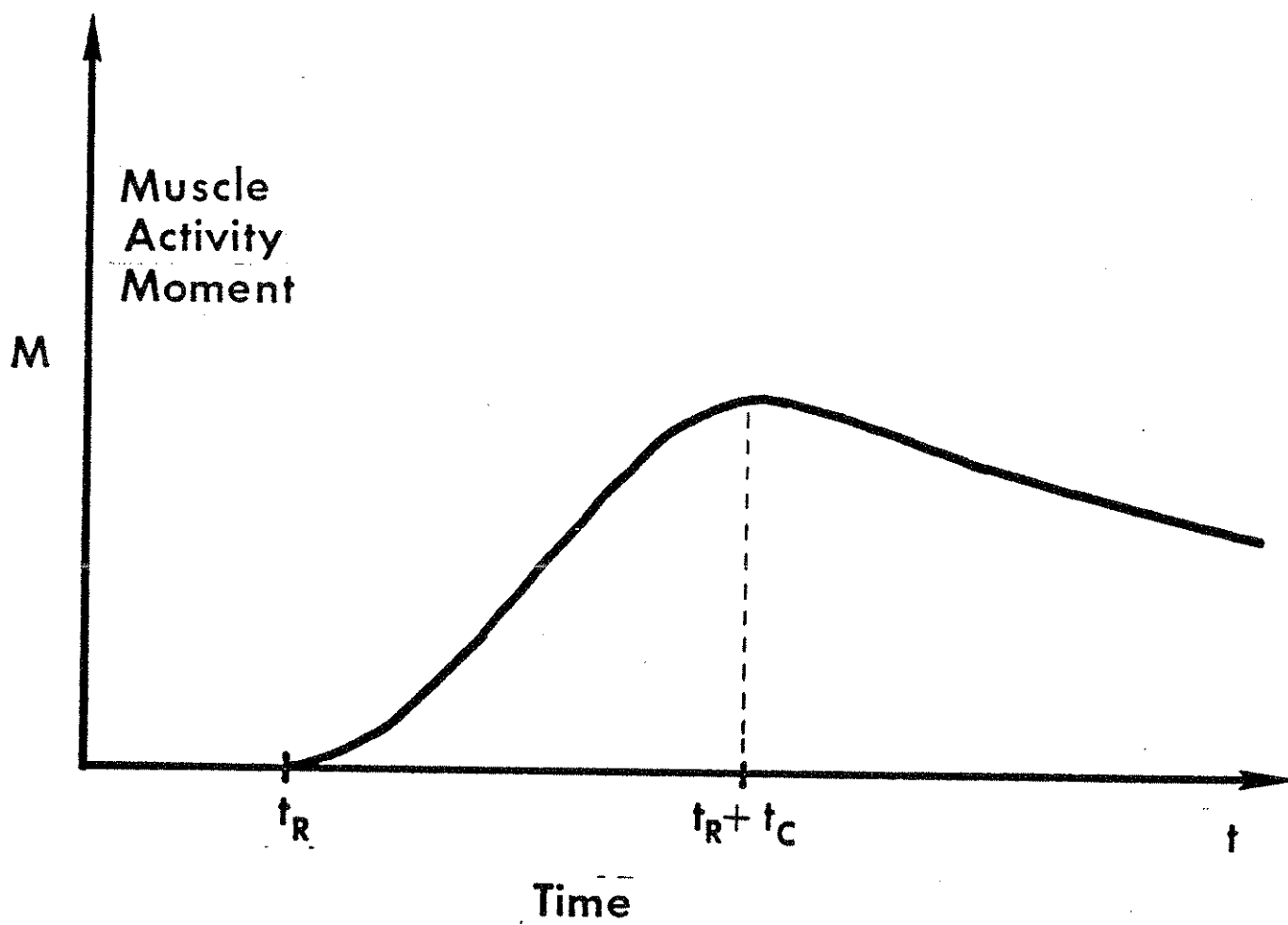


FIGURE 2-13. Muscle activity moment as a function of time

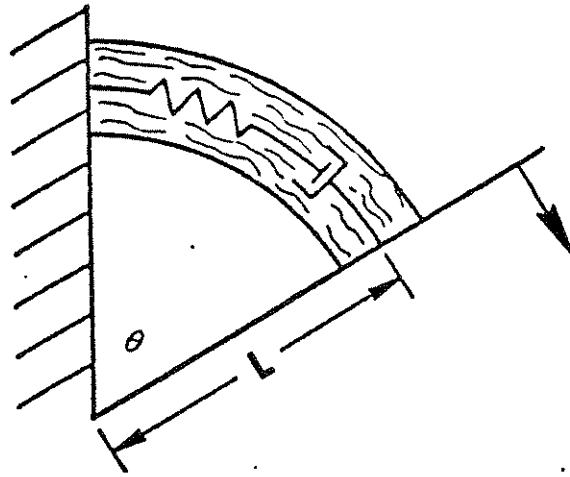


FIGURE 2-14 Muscle at a joint

SCALING LAWS RELATING MUSCLE PARAMETERS
FOR JOINTS I AND II:

$$a_{1,II} = \left(\frac{L_{II}}{L_I} \right)^2 a_{1,I} \frac{|F_{\max,II}|}{|F_{\max,I}|}$$

$$a_{2,II} = \left(\frac{L_{II}}{L_I} \right) a_{2,I}$$

$$a_{3,II} = \left(\frac{L_{II}}{L_I} \right) a_{3,I}$$

$$\text{where } |F_{\max,j}| = |M_{\max,j}| / L_j$$

NOTE: I and II indicate either two joints for the same individual or the same joint for two individuals. $M_{\max,j}$ is the maximum static torque that can be voluntarily generated at joint j . $F_{\max,j}$ is the maximum static tension that can be generated in the muscle element under the same conditions. For scaling from individual to individual for the same joint, $|F_{II}|/|F_I|$ can reasonably be taken as $(m_{II}/m_I)^{2/3}$, where m is total body mass.

the effective moment arm is a function of the articulation angle, θ , but it is assumed constant in this model.

The literature at present contains little experimental information relating to the values of a_1 , a_2 , a_3 , and $M(t)$. HSRI has successfully used values determined from certain published data for the knee and by scaling on the basis of available anthropometric data for 50th percentile males.* The available values which are pertinent to MVMA 2-D simulations are shown in Figure 2-15.**

Cards 227-237 contain the muscle element coefficients a_1 , a_2 , a_3 , which, together with tabular time-dependent muscle tensions $|M|$ from 238-Cards, define the Maxwell coefficients of the composite musculature at a joint. Example data cards are shown in

Figure 2-16.

Values for the coefficients a_1 , a_2 , and a_3 are entered in the first three fields of Cards 227 to 234 for the joints numbered 1 through 8, as illustrated earlier in Figure 2-7. Field 4 should contain a zero or be left blank. A name of up to eight alphanumeric characters must be entered in field 5. This name serves as an identifier of a table for $M(t)$ which must be defined for the composite musculature at each joint. The user can approximate any function $M(t)$ as closely as desired by prescribing a sufficient number of coordinate pairs. The time for each pair is entered in field 2 of a 238-Card and a positive value for $M(t)$ is entered in field 3. The name of the table for which the coordinate pair in fields 2 and 3 is a point is entered in field 1. This name will be identical to one of the table names defined in field 5 of a card 227 to 237. If it is desired to use the same muscle contraction function $M(t)$ for more than one joint, it is

* Ibid.

** The shoulder muscle tension parameter values are little better than guesses.

Upper neck joint and lower neck:

$$a_1 = 1.476 \text{ lb in/deg}$$

$$a_2 = 0.153 \text{ deg}^{-1}$$

$$a_3 = 0.0129 \text{ sec/deg}$$

$$|M|_{\max} = 210 \text{ lb in}$$

Neck element elongation:

$$a_1 = 42.3 \text{ lb/in}$$

$$a_2 = 4.4 \text{ in}^{-1}$$

$$a_3 = 0.37 \text{ sec/in}$$

$$|F|_{\max} = 210 \text{ lb.}$$

**Shoulder-upper torso joint:

$$a_1 = 0.15 \text{ lb in/deg}$$

$$a_2 = 0.153 \text{ deg}^{-1}$$

$$a_3 = 0.0129 \text{ sec/deg}$$

$$|M|_{\max} = 5 \text{ lb in}$$

**Shoulder element elongation:

$$a_1 = 4.23 \text{ lb/in}$$

$$a_2 = 4.4 \text{ in}^{-1}$$

$$a_3 = 0.37 \text{ sec/in}$$

$$|F|_{\max} = 200 \text{ lb}$$

Knee:

$$a_1 = 10.44 \text{ lb in/deg}$$

$$a_2 = 0.105 \text{ deg}^{-1}$$

$$a_3 = 0.0088 \text{ sec/deg}$$

$$|M|_{\max} = 4320 \text{ lb in (two knees together)}$$

FIGURE 2-15 Muscle element parameters

not necessary to define separate tables with 238-Cards.

In addition to the antagonistic muscles effective at the eight joints in Figure 2-7, three other muscle elements may be similarly defined. Cards 236 and 237 are used for elements which restrict elongation of the neck and shoulder links. Card 235 is for muscle restricting shoulder link angulation. These three elements of the occupant linkage are discussed in detail in Module 3.

The numbers in Figure 2-16 are from Figure 2-15, and for each muscle element, a pre-tensed and constant state of contraction at the 50% level is assumed.

Figure 2-17 provides an exercise for the user. Suppose that a vehicle occupant becomes aware of impending impact 20 msec before impact and that involuntary muscle contraction begins after a reflex time of 54 msec. Suppose the time-dependent shape of the elbow contraction moment curve $M(t)$ is as in Figure 2-13. Assume that $M_{\text{max, elbow}}$ is 720 lb in and that the contraction moment peaks at 40% of the voluntary maximum level after a contraction time of 120 msec. Show that the cards in Figure 2-17 reasonably define the composite muscle element effective at the elbow. (Arbitrary values were selected for a_1 , a_2 , and a_3 on Card 234.)

1.476	.153	.0129	0.	NECKMUS	227
1.476	.153	.0129	0.	NECKMUS	228
42.3	4.4	.37	0.	NLMUS	236
.15	.153	.0129	0.	SHTMUS	235
4.23	4.4	.37	0.	SHLMUS	237
10.44	.105	.0088	0.	KNEEMUS	232
NECKMUS	0.	105.			238
NECKMUS	0.	105.			238
NLMUS	0.	105.			238
NLMUS	0.	105.			238
SHTMUS	0.	2.5			238
SHTMUS	0.	2.5			238
SHLMUS	0.	100.			238
SHLMUS	0.	100.			238
KNEEMUS	0.	2160.			238
KNEEMUS	0.	2160.			238

FIGURE 2-16 Muscle tension parameter cards

1.6	.11	.0115	0.	ELBOWMUS	234
ELBOWMUS0.		0.			238
ELBOWMUS34.		0.			238
ELBOWMUS64.		45.			238
ELBOWMUS90.		126.			238
ELBOWMUS133.		267.			238
ELBOWMUS154.		288.			238
ELBOWMUS175.		270.			238
ELBOWMUS280.		180.			238

FIGURE 2-17 Cards for time-dependent muscle activity

2.5 Scaling Relations

Good biomechanical and anthropometric data are important for successful use of any crash victim simulator. It will often be the case that the user has established a good data set for one segment of the population, e.g., 35 to 44 year old males of 50th percentile stature and weight, but that he has little data for other population segments. It is generally possible by applying scaling relations to good data for one population segment to develop reasonable data for other segments.

It must always be kept in mind, however, that scaling is only a substitute for more direct development of biomechanical and anthropometric data. Its use should always be influenced by whatever data is available for the population segment of interest. Good engineering judgment is of obvious value in blending the use of available data and the use of scaling.

An understanding of the assumptions that lie behind scaling relations is important for their intelligent use. This is also important in allowing the modeler to make a subjective estimate of how good his scaled values are likely to be. The scaling relations given in Figure 2-18 are valid with the following conditions:

- 1) All internal and external length measures of the "scaled" biomechanical system (subscript 2) are proportionate to the corresponding measures of the "scaled to" system (subscript 1) by the same proportionality constant. That is, linear scaling in size is assumed.

- 2) Corresponding body parts of the two systems have equal mass densities.

- 3) Corresponding anatomical elements of the two systems have the same material constitutive properties. This means that material parameters such as Young's modulus (E) are the same for corresponding elements while the strengths of the elements will not be the same if they are of different size.

It is clear from these conditions that biomechanical scaling will be better between some population segments than between others. Condition 1, linear scaling in size, is probably the primary weakness in

SCALING RELATIONS

	$M = \text{mass}$
LENGTH:	$L_1 = L_2 (M_1/M_2)^{1/3}$
AREA:	$A_1 = A_2 (M_1/M_2)^{2/3}$
VOLUME:	$V_1 = V_2 (M_1/M_2)$
MASS:	$m_1 = m_2 (M_1/M_2)$
MOMENT OF INERTIA:	$I_1 = I_2 (M_1/M_2)^{5/3}$
DAMPING COEFFICIENT:	$C_1 = C_2 (M_1/M_2)^{2/3}$
LINEAL SPRING CONSTANTS:	$K_1^{(n)} = K_2^{(n)} (M_1/M_2)^{(2-n)/3}$ where $F = K^{(1)} \delta + K^{(2)} \delta^2 + \dots$
TORSIONAL SPRING CONSTANTS:	$K_{1\theta}^{(n)} = K_{2\theta}^{(n)} (M_1/M_2)$ where $T = K_{\theta}^{(1)} \Delta\theta + K_{\theta}^{(2)} (\Delta\theta)^2 + \dots$

FIGURE 2-18 Parameter Scaling Relations

human scaling.* The reason is that body proportions are functions of age and sex. For example, better results can be expected for scaling from 35-44 year-old males to 18-24 year-old males than from 35-44 year-old males to 6-9 year-old females. But it is also clear from the conditions of validity that scaling between segments of the human population has a considerably firmer basis than scaling from lower primates to humans, which is a common technique used in the development of human injury tolerance data.

The relations in Figure 2-18 will not be derived here. It might be instructive for the student to try to demonstrate that the first-order spring coefficient $K^{(1)}$, i.e., the linear stiffness, for lengthwise deformation of a cylindrically-shaped anatomical element is properly scaled by $K_1^{(1)} = K_2^{(1)} (M_1/M_2)^{1/3}$. This relation is the special case of the seventh relation in the figure for order n equal to 1.**

Figure 2-19 is a list of selected references which have been useful in defining vehicle-occupant anthropometry for MVMA-2D model data sets.

The user is again advised always to take due consideration of the conditions of validity for the scaling relations. Scaling can be very useful, but the limitations of its application must be understood.

* It is better not to scale for lengths if values can be obtained independently. Other quantities may still be scaled reasonably on the basis of mass.

** Hint: The linear stiffness is equal to AE/l , where A is the cross-sectional area, E is Young's modulus, and l is the length of the element.

SELECTED REFERENCES FOR ANTHROPOMETRIC DATA

1. Chandler, R. F., C. E. Clauser, J. T. McConville, H. M. Reynolds and J. W. Young, "Investigation of Inertial Properties of the Human Body," Final Report, DOT-HS-801-430, NHTSA, Washington, D.C. 1974.
2. Clauser, C. E., J. T. McConville and J. W. Young, "Weight, Volume and Center of Mass of Segments of the Human Body," AMRL-TR-69-70, Wright-Patterson AFB, Ohio, 1969.
3. Clauser, C. E., P. Tucker, J. T. McConville, E. Churchill, L. L. Laubach, and J. Reardon, "Anthropometry of Air Force Women," AMRL-TR-10-5, Wright-Patterson AFB, Ohio (AD 743 113), 1972.
4. Damon, A., H. W. Stoudt, and R. A. McFarland, "The Human Body in Equipment Design," Harvard University Press, Cambridge (revised 1974) 1966.
5. Dempster, W. T., "Space Requirements of the Seated Operator," WADC-TR-55-159, Wright-Patterson AFB, Ohio (AD 87 892), 1955.
6. Garrett, J. W. and K. W. Kennedy, "A Collation of Anthropometry," AMRL-TR-68-1 (2 Vols.) Wright-Patterson AFB, Ohio, (AD 723 629) March 1971.
7. Grunhofer, H. J. and G. Kroh (eds.), "A Review of Anthropometric Data of German Air Force and United States Air Force Flying Personnel 1967-1968," AGARDograph No. 205, Advisory Group for Aerospace Research and Development, NATO, Neuilly-sur-Seine, France (AD N75 22635) 1975.
8. Reynolds, H. M., C. E. Clauser, J. T. McConville, R. Chandler, and J. W. Young, "Mass Distribution Properties of the Male Cadaver," SAE Transactions No. 750424, Warrendale, Pa., 1975.
9. Reynolds, H. M., J. W. Young, J. T. McConville, and R. G. Snyder, "Development and Evaluation of Masterbody Forms for Three-Year Old and Six-Year Old Child Dummies," DOT-HS-801 811, NHTSA, Washington, D.C., 1976.
10. Snyder, R. G., C. Owings, M. Spencer, and L. W. Schneider, "Anthropometry of U.S. Infants and Children," SAE Report No. 750423, 1975.
11. United States Department of Health, Education and Welfare. Public Health Service, National Center for Health Statistics, Series 11, Nos. 8, 14, 35, 104, 120, 123, 124, 126, 132, and 143. Rockville, Md., 1965-1974. (Anthropometry on U.S. Civilian population from age 6 through 79).

FIGURE 2-19 Selected References for Anthropometric Data

MODULE 3--NECK AND SHOULDER MODELS

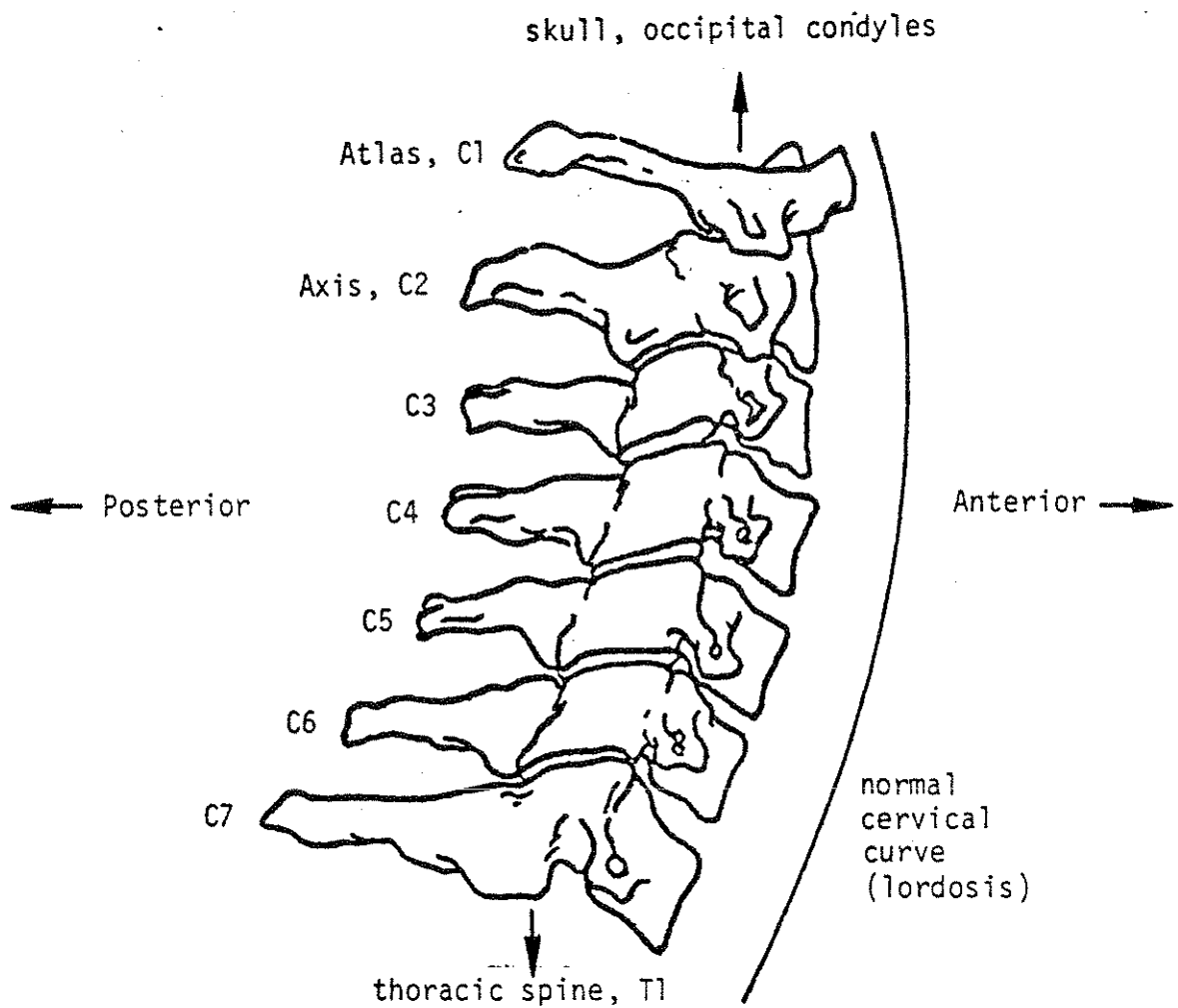
3.1 The Neck

The cervical spine is that portion of the spinal column from the skull to the thoracic spine. It supports the head and provides mobility and flexibility in the neck.

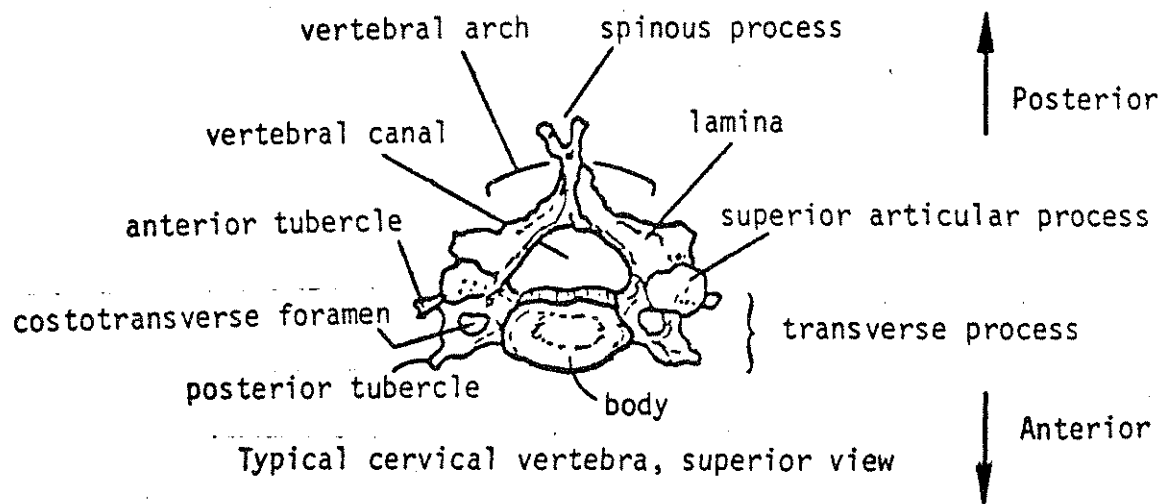
Viewed as a mechanical system, the human neck is complex. The MVMA 2-D occupant model is a lumped-parameter system. While the neck representation in the model is more complex than that in other full-body motion simulators in current use, it still adds only three degrees of freedom to the occupant model. The user is therefore neither required nor allowed to define values for more than a relatively few biomechanical neck parameters. The following discussion is an introduction to the anatomy of the neck. The purpose of this introduction is not to define quantities for which values must be provided, since no anatomical detail is included in the analytical neck model, but rather to help the user to develop good judgment and insight in the use of the model and interpretation of results.

3.1.1 The Anatomy of the Neck

There are three primary types of structural components in the cervical spine -- vertebrae, intervertebral discs, and ligaments. Of the thirty-three vertebrae in the human spinal column, seven are in the neck. Figure 3-1 shows a lateral view of the cervical spine. The seven vertebrae are conventionally designated C1 through C7, where C1 is the uppermost vertebra, commonly called the atlas. Also shown in this figure is a superior view of a typical cervical vertebra, any below the axis, C2. The anterior portion of each vertebra is a solid vertebral body, which imparts strength to the spinal column and bears the weight of the head. A bony vertebral arch is attached to the posterior portion of the body. It encloses and protects the spinal cord. This arch also furnishes bony projections and processes, to which ligaments and muscles attach. The inferior portion of the skull, or occiput, is closely attached to the cervical spine by some of these ligaments and muscles.



The cervical spine, lateral view



Typical cervical vertebra, superior view

FIGURE 3-1 The cervical vertebrae

The skull is supported on the spinal column by two rounded, bony protuberances of the occiput. These protuberances are called the occipital condyles, and they are accommodated by two hollow recesses on the superior surface of the first cervical vertebra, the atlas.

The x-rays in Figure 3-2 show the cervical spine in neutral, hyperflexed, and hyperextended positions. Note that in the neutral position, the normal cervical spine is already in slight extension, a rearward bending with convexity forward. This normal cervical curvature is called lordosis, and it results from the greater depth of the intervertebral discs anteriorly rather than posteriorly. Greater articulation in the sagittal plane can occur at the occipital condyles than at any interspace below the atlas in the cervical spine.* Values of from 20 to 35 degrees of total motion are reported by various investigators. Below the atlas, there is considerable variation in the average ranges of motion at the different vertebral levels. The range of motion values given in Figure 3-3 are averages for twenty normal adults and are typical of values reported in the literature. C7 is adjacent to the first thoracic vertebra, conventionally designated T1. The thoracic part of the spinal column itself is relatively immobile, and the transition interspace C7-T1 has less range in sagittal plane motion than the cervical interspaces above it. After the atlanto-occipital joint at the condyles, most motion occurs at the mid-levels of the cervical spine.

Except between the occipital bone of the skull and the atlas, and between the atlas and axis, the vertebrae are separated by elastic-discs of cartilage called intervertebral discs. These are firmly joined to the vertebral bodies, anterior to the spinal canal, and allow movement of the spinal column because of their elasticity. The walls of a disc, called the annulus fibrosus, are a heavy layer of fibrous cartilage. The fibers are directed obliquely and thus prevent excessive movement in any direction. The annulus fibrosus encloses a semigelatinous substance and a kernel of elastic, compressed tissue called the nucleus pulposus. The semifluid character of the interior of the disc serves to

*The midsagittal plane is the plane of symmetry. Any parallel plane is called a sagittal plane.



Neck Flexion



Neck in Neutral Position



Neck Extension

FIGURE 3-2 X-rays of a normal human neck in the neutral position and in full voluntary flexion and extension

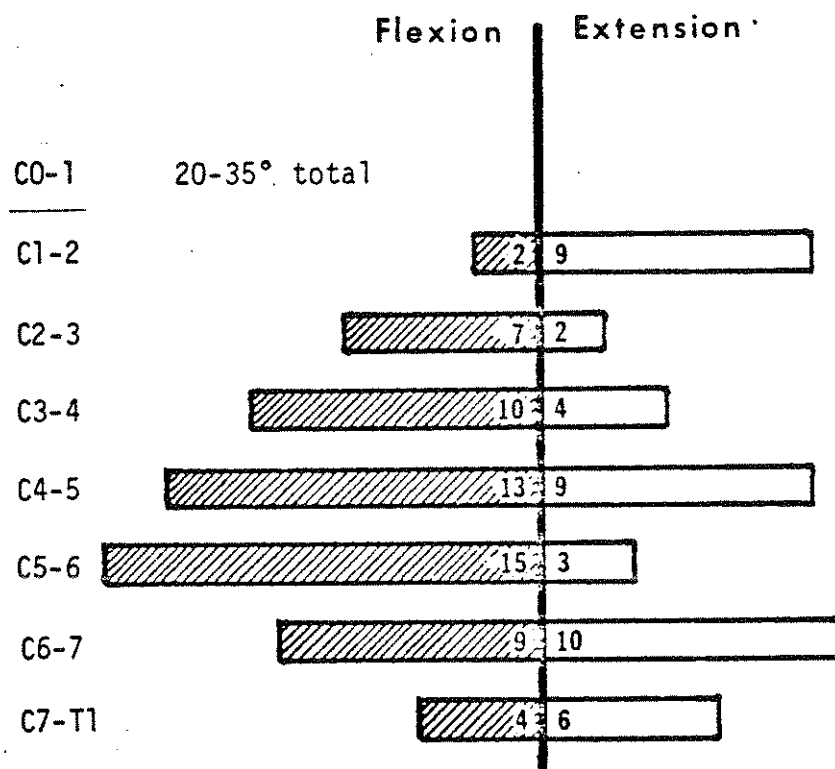


FIGURE 3-3 Average range of flexion and extension (in degrees) at each vertebral level in 20 normal adults

distribute compression forces equally over the surfaces of opposing vertebrae. The intervertebral discs in the neck are resilient and rugged, less likely to rupture during dynamic loading than the vertebrae are to fracture.

In addition to vertebrae and discs, ligaments are an important structural component of the cervical spine. Ligaments in the neck are bands of connective tissue -- tough, flexible, and in some cases elastic -- which extend between the vertebrae. Some connect vertebrae to the occipital region of the skull and intervertebral discs to one another. The most important function of the cervical ligaments is in maintaining stability. They serve to maintain the apposition of component parts of joints and allow and limit the appropriate range of motion for each joint.

Muscles are not components of the cervical spine, but they do significantly affect head and neck dynamics. They assist the vertebrae, discs, and ligaments in resisting tension and torsional loads. Six major muscles control movements of the head and seven control neck movement. The approximate origin and insertion points and the line of action of the most important of these muscles are indicated in Figure 3-4.

3.1.2 The MVMA-2D Neck Model

It is clear that even in motion confined to the midsagittal plane the cervical spine has many degrees of freedom. Even if the intervertebral discs were assumed to be non-deforming in shear, tension, and compression, eight degrees of freedom might reasonably be defined for angular motions of the seven cervical vertebrae and the skull in the midsagittal plane. In the MVMA-2D simulation, angular motions of the head and neck are lumped at two articulations. In Figure 3-5 these joints are illustrated at the positions of the occipital condyles and the C7-T1 intervertebral disc. The user is free, however, to define their positions as he chooses by selecting input data appropriately. The two joints of the analytical model are not joined by a rigid link but rather by deformable viscoelastic elements, so a third degree of freedom is a mode for compression and elongation of the neck. Motion in this mode tends to be small even in high-G environments since the intervertebral discs are stiff.

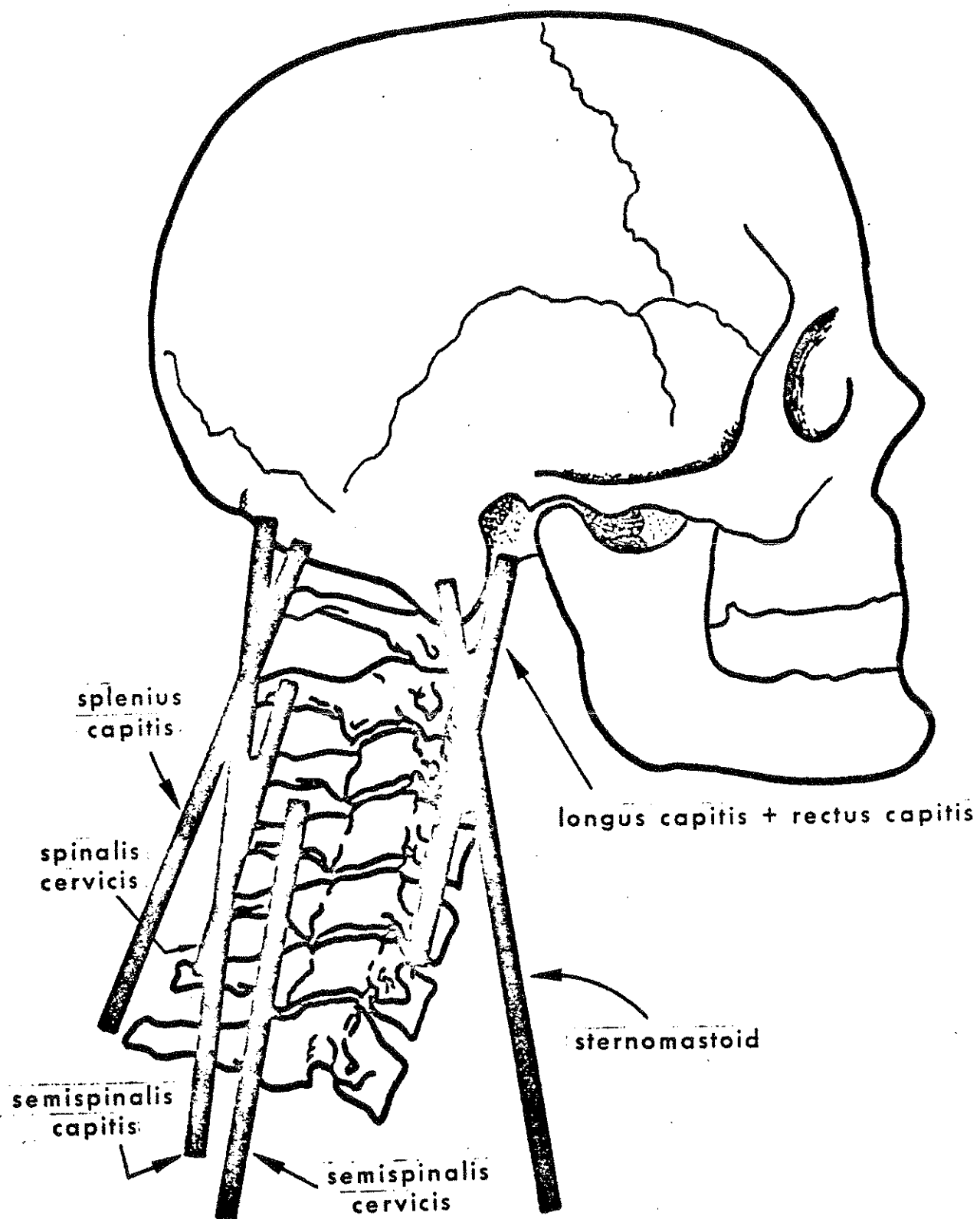


FIGURE 3-4 The major muscle groups controlling head and neck movements

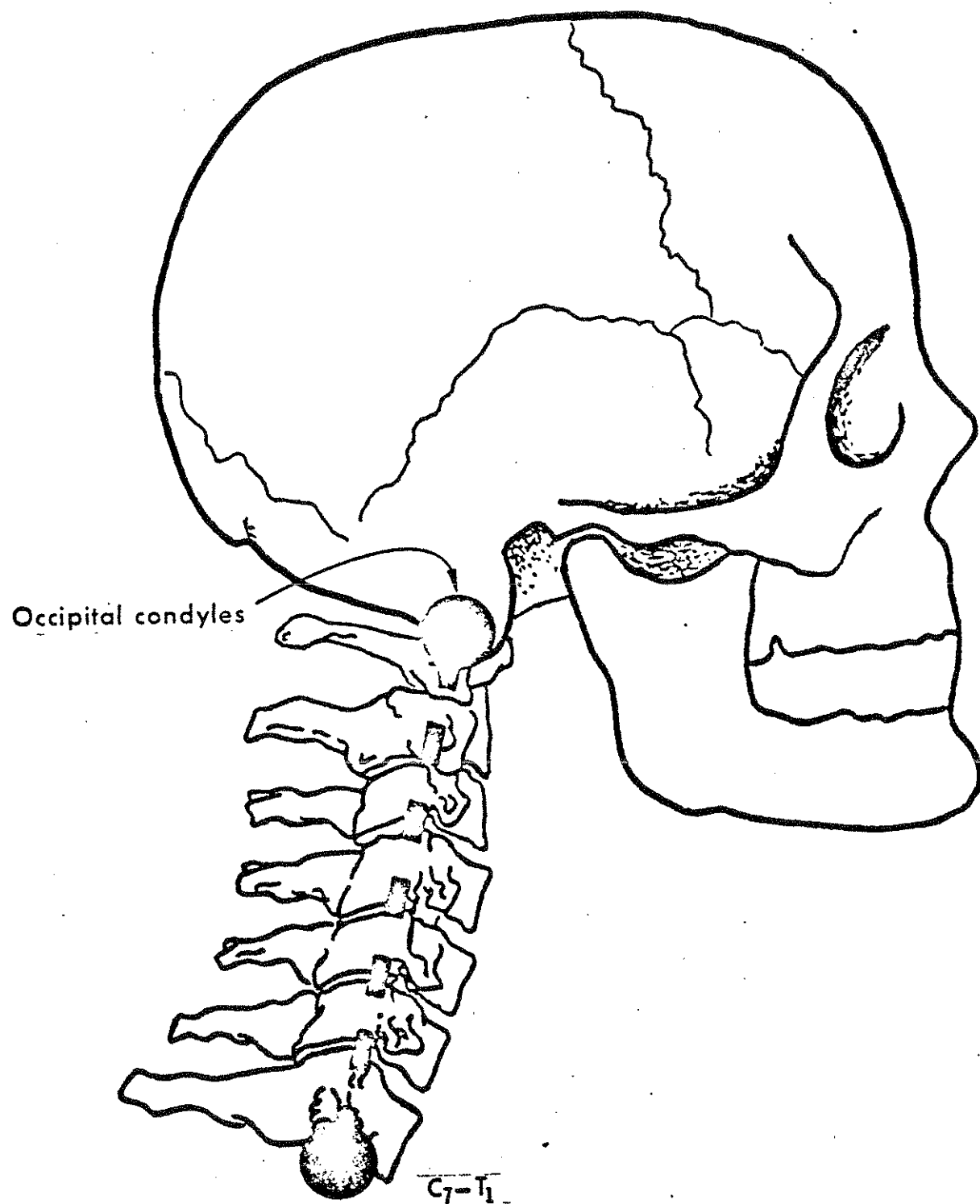


FIGURE 3-5 The MVMA-2D two-joint, extensible neck

Figure 3-6 illustrates various geometrical quantities for which the user must assign values. Example data cards are shown in Figure 3-8. The position of the upper neck articulation is defined with respect to the head center of mass in the head coordinate system. The quantity C is the rearward offset of the joint from the superior-inferior head axis, and its value is entered in field 1 of Card 201. A value of ℓ_1 , entered in field 1 of Card 202, positions the joint downward from the head center of mass. The lower neck articulation is constrained to lie on the longitudinal principal axis of the upper torso link, so a single length, ℓ_2 , is required to define its location. This is the distance of the C7-T1 joint from the center of mass of the upper torso, and its value is put in field 2 of Card 202. Additionally, the neck length is required, i.e., the straight-line distance between the neck articulations. As previously mentioned, the neck can undergo compression and elongation, so its length is not constant. The inputted neck length is the value at time zero and this is assumed to be its unstrained length. The initial value for L_n is entered in field 5 of Card 303. The initial rate of neck elongation (\dot{L}_n), normally 0., is also required on Card 303, in field 6.

The mass of the extensible neck is lumped at the extremities of the element, at the head-neck and neck-torso joints. The total neck mass is entered in field 9 of Card 203, and the decimal fraction which is to be placed at the upper joint is in field 9 of Card 202. The neck mass is not required to be non-zero.

The complex of motion-restricting elements in the cervical spine previously described must be lumped by assigning values for composite torsional viscoelastic elements at the two joints and lineal viscoelastic elements between the joints. While this limits the degree to which model predictions can agree with reality, performance of the lumped-parameter, three-degree-of-freedom, head-neck system has been shown to be good. And from a practical point of view, this simplification of the real biomechanical system makes the model usable because empirical values for composite neck characteristics are much easier to determine than values required to describe an anatomically detailed analytical model.

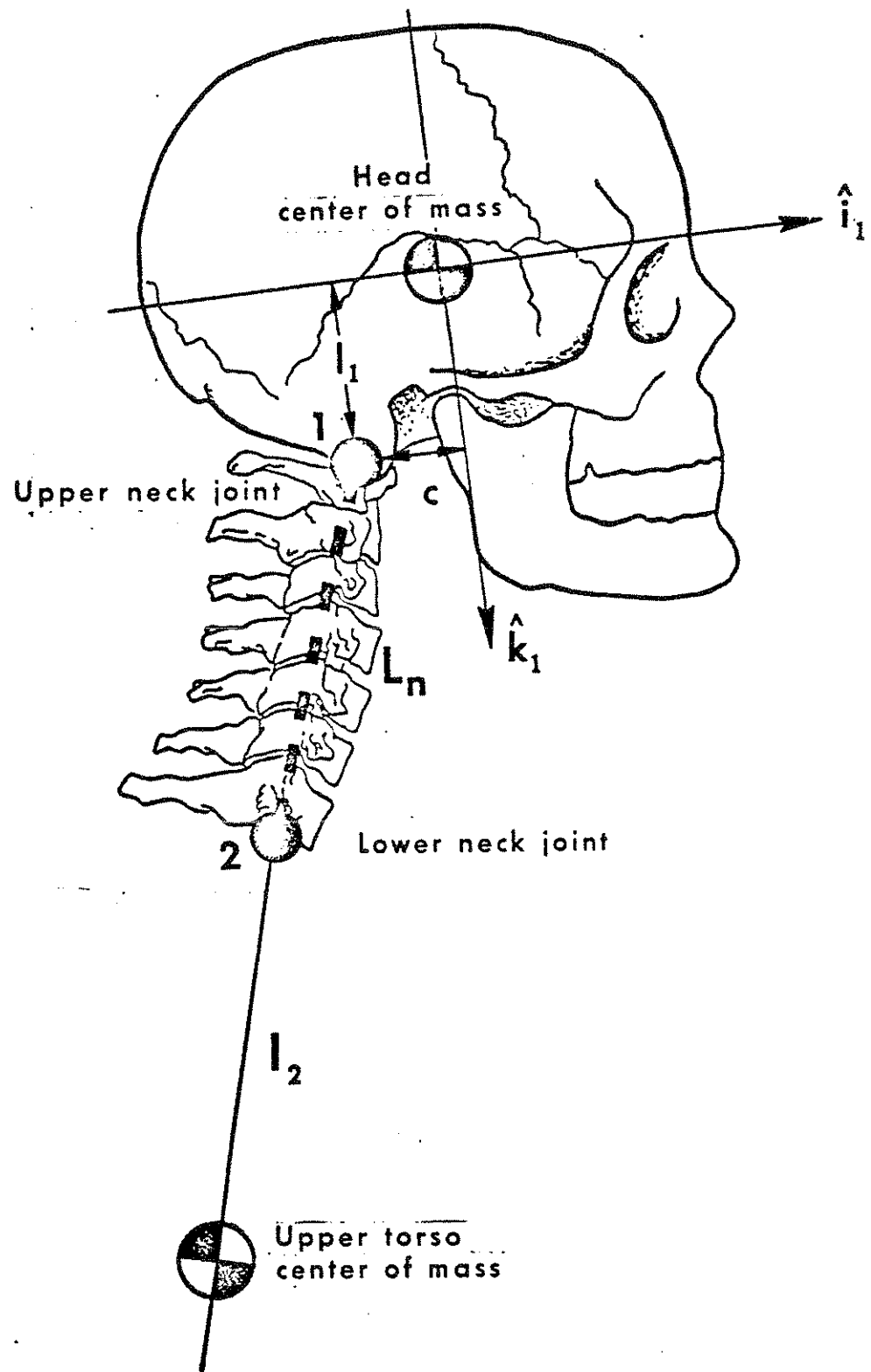


FIGURE 3-6 MVMA-2D extensible neck geometry

Viscoelastic joint parameters are fully discussed in Module 2. Several types of elements are defined for each joint in the occupant linkage, including the neck joints. These include a linear spring for angulation away from an equilibrium joint angle, a nonlinear spring for angular deformation of motion-limiting "joint stops," a viscous damper, a constant-friction torque producer, and a Maxwell element with coefficients that are functions of a user-defined, time-dependent level of muscle activation. Hysteretic energy loss for deformation of a joint stop can be simulated by specification of a restitution coefficient. For the neck joints, these viscoelastic elements, except for muscle tension, may have different coefficient values for flexion and extension. Flexion data for the upper and lower neck joints are entered on Cards 205 and 206; extension data are entered on Cards 215 and 216. Neck muscle-element data are specified on Cards 227, 228, and 238.

A viscous damper with a nonlinear spring in parallel resist neck compression and elongation. They are illustrated in Figure 3-7. These elements represent resistance of discs and ligaments to lineal deformation. The spring and damping coefficients need not have the same values for compression and elongation. Elongation coefficients are on the 213-Card. Spring rates for tension forces proportional to the magnitudes of the first, second, and third powers of neck elongation are entered in fields 1, 2, and 3. Field 4 contains the value for the linear viscous friction coefficient. Card 242, for neck compression coefficients, is identical in form. The input value for initial neck length on Card 303 is used as the unstrained length of the nonlinear springs for neck elongation and compression. Therefore, it is not possible to enter data which result in a non-zero initial compressive neck load, as would be the normal condition for a seated occupant. This small initial imbalance is inconsequential.

Since muscles cannot push, but can only pull, neck muscles cannot help to limit compression of the cervical spine. Muscle contraction can, however, act against elongation of the neck. Muscle parameters for the effective axial component are entered on Card 236, and the time-dependent level of muscle activation is entered in tabular form with 238-Cards. The modeling of muscle

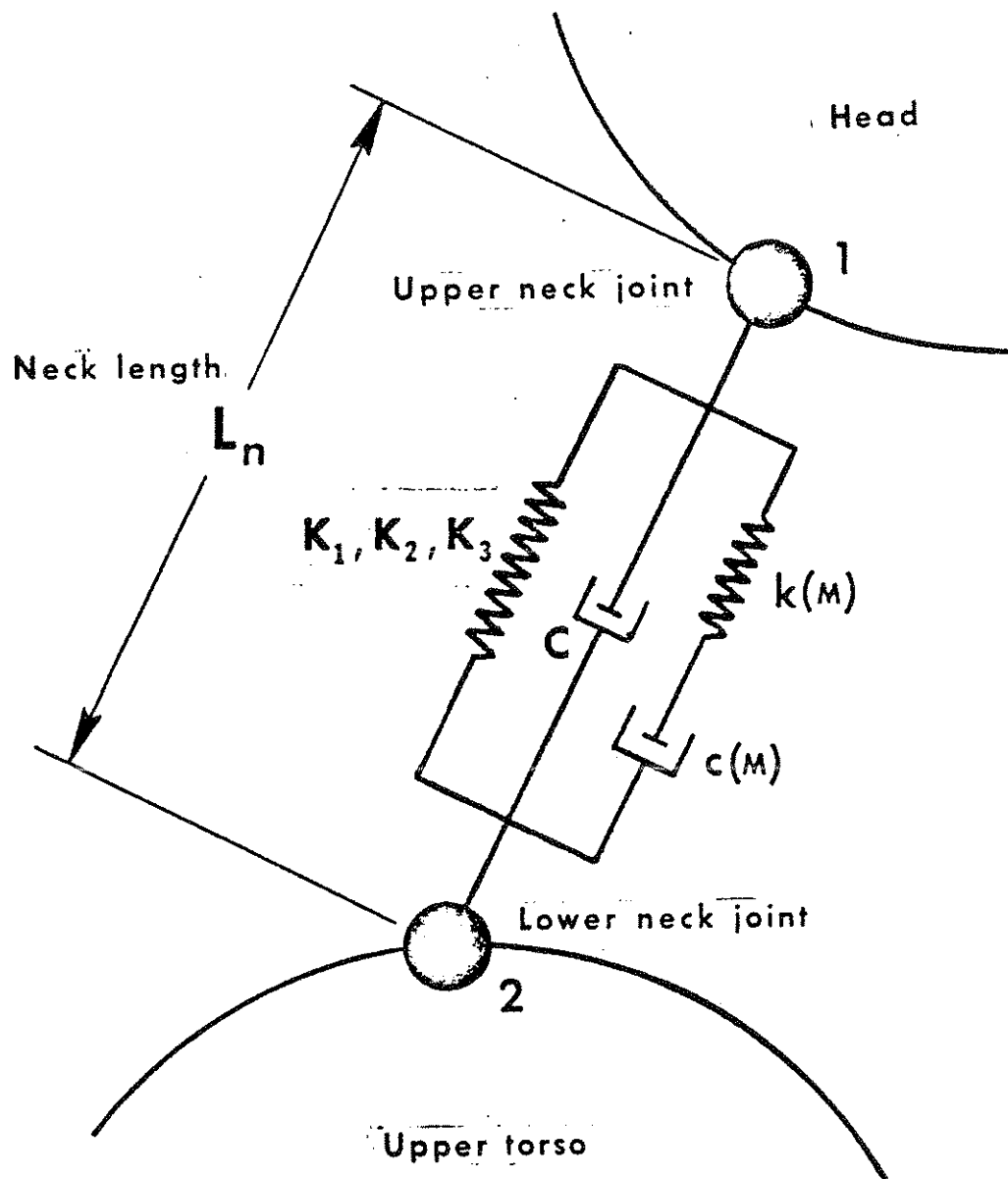


FIGURE 3-7 Lineal viscoelastic components in MVMA-2D extensible neck

action in the MVMA 2-D simulator is presented in detail in Module 2.

Example data cards with values for the neck parameters discussed in this module are shown in Figure 3-8. All values on these cards are for a 161 lb. male of average stature.

3.1.3 Special Uses of the Neck Model

Discussion of the neck model will be concluded with notes regarding some common special uses of the model. Users occasionally find reason to simulate a one-joint neck with the MVMA-2D model. This may be in connection with parallel simulations made with occupant dynamics simulators that have one-degree-of-freedom, pin-joint necks. It may be that the types of experimental data the user has available suggest the use of a one-joint neck. Or it may be that the MVMA-2D model is being used to simulate some mechanical linkage other than a human or human analog. The MVMA-2D model does not allow the removal of degrees of freedom through specification of constraints, so the user must accomplish this by proper selection of parameter values. Conceptually, the three-degree-of-freedom neck could be reduced to one degree of freedom, a single articulation, by setting the neck length equal to zero and setting the neck-length stiffness and torsional stiffnesses for one neck joint equal to infinity. In practice this cannot be done. The length of the neck link should not be allowed to approach zero because the coefficient matrix of the system of Lagrange differential equations then approaches singularity. Near this singular condition, loss of precision in the numerical integration is excessive and the computer simulation will soon abort. If neck length is small but remains greater than a certain magnitude, say one-tenth inch, precision might be saved by using a reduced value for the integration time step. The problem with setting spring rates equal to arbitrarily large values is of a similar nature, i.e., a "blow up" of the run will result from loss of precision unless an unreasonably small value of the integration time step is used. Even this may be insufficient because of round-off errors.

Figure 3-9 illustrates a solution to this modeling problem. The neck length is effectively reduced to zero by placing the upper neck joint at a position well within the head and by using

.97	11.93	5.47	4.25	16.0		12.6	1.74	0.	201
1.64	4.00	3.46	1.65	7.28	11.3	5.28	12.3	.33	202
.0234	.1087	.0183	.0480	.1006	.0541	.0290	.0257	.0088	203
.146	2.603	.473	1.766	2.394	3.020	.547	1.644		204
0.	.231	0.	.09	0.	1.		5.	.5	205
0.	.077	0.	.27	0.	1.		-71.	.5	206
0.	.231	0.	.09	0.	1.	25.		.5	215
0.	.077	0.	.27	0.	1.	53.		.5	216
934.	0.	1494.	9.92						213
934.	0.	1494.	9.92						242
3.6	-20.	0.	0.	-90.	40.	0.	-50.		217
0.	0.	3.996	0.	4.41	0.				303
.475	.153	.0129	0.	MNH					227
1.476	.153	.0129	0.	MNT					228
75.2	5.84	.490	0.	MN					236
MNH	0.	34.3							238
MNH	300.	34.3							238
MNT	0.	105.							238
MNT	300.	105.							238
MN	0.	131.							238
MN	300.	131.							238

FIGURE 3-8 Example data cards for MVMA-2D neck

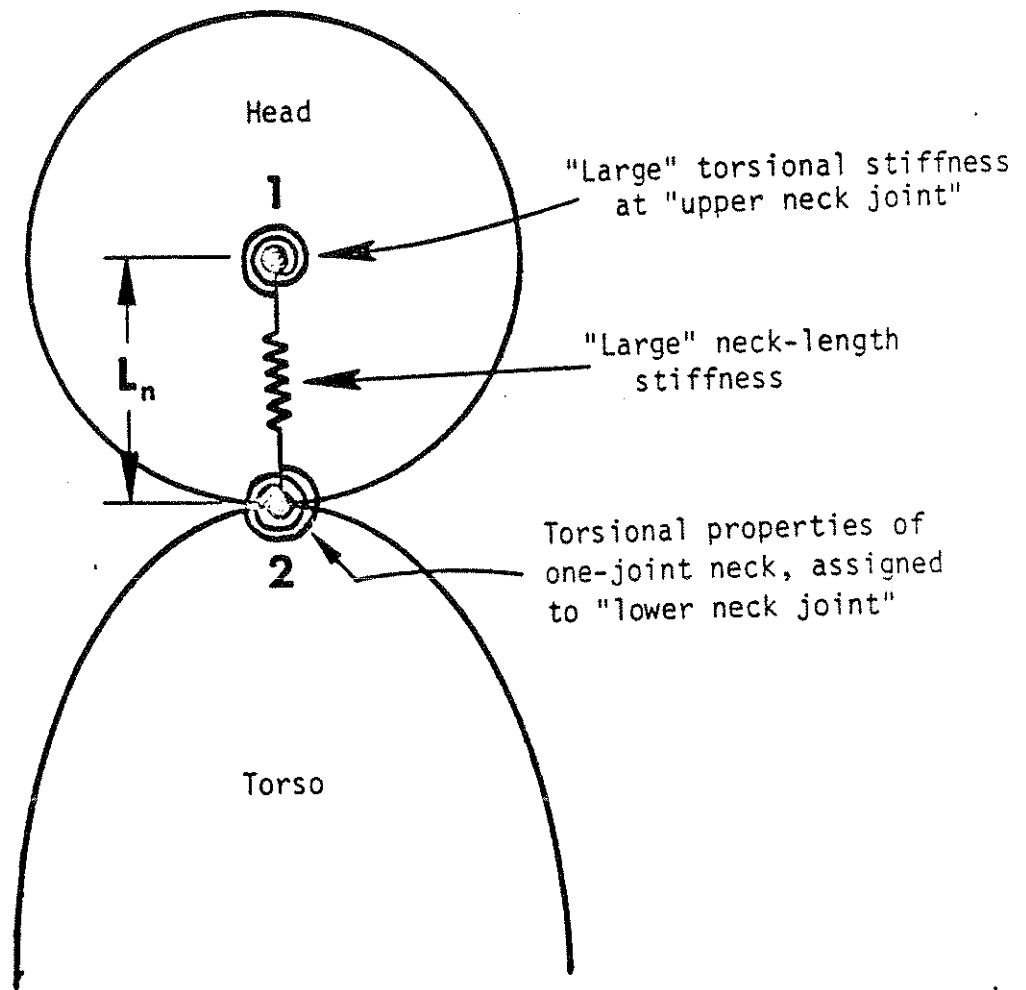


FIGURE 3-9 Effective reduction of MVMA 2-D two-joint extensible neck to a pin-joint neck

a large, but not too large, value for neck-length stiffness. The neck line will then be simply a line of material points in the head if the neck and head can be made to articulate together at the torso juncture. This can be accomplished by fixing the neck line to the head with a large, but not too large, torsional spring at the upper neck joint and assigning the torsional properties of the desired one-joint neck to the lower neck joint.

The general rule to be followed in selecting artificially large stiffnesses for spring elements in the linkage is that the period of the largest natural frequency in the system should be at least ten times, and probably twenty times, as large as the integration time step. A similar rule relates maximum allowable damping rates to integration time step. These two rules are outlined by Figure 3-10. The inequality for the damping rule in the lower figure is easily solved by using Newton's method or by iteration. The solution curve is shown in Figure 3-11 for the range .001 to .1 of the parameter ϵ .*

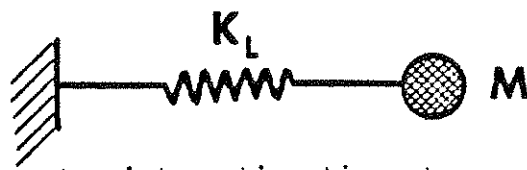
Reasonable estimates for the largest allowable values of the stiff linear and torsional springs for the artificially constrained neck just discussed are easily found. Conservative estimates may be found by assuming the mass and moment of inertia of the torso to be infinite, or large with respect to the values for the head, because true natural frequencies must be less than those estimated in this way. Suppose the head weight is 10 pounds and the principal moment of inertia is 0.2 lb sec²/in. Suppose it is desired, if possible, to run the simulation with a 1 ms integration time step. Then, applying the formulas from Figure 3-10, one obtains

$$\begin{aligned} \text{Maximum linear stiffness} &\leq 4 \left(\frac{10}{386.1} \right) \left(\frac{.05\pi}{.001} \right)^2 \\ &= 2600 \text{ lb/in} \end{aligned}$$

and

$$\begin{aligned} \text{Maximum torsional stiffness} &\leq 4(.2) \left(\frac{.05\pi}{.001} \right)^2 \\ &= 20,000 \text{ in lb/rad} \\ &= 340 \text{ in lb/deg} \end{aligned}$$

* Reasonable values for ϵ are probably .001 to .01.



K_L, K_T = linear and torsional spring rates

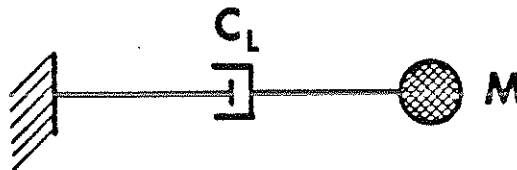
M, I = mass and moment of inertia

Δt = integration time step
 T = period of natural frequency

K-rule

$$.05 \text{ (or } .1) \geq \frac{\Delta t}{T} = \frac{\Delta t}{2\pi} \sqrt{\frac{K_L}{M}}$$

$$\rightarrow \Delta t \leq \frac{\pi}{10 \sqrt{\frac{K_L}{M}}} \quad \text{or} \quad \Delta t \leq \frac{\pi}{10 \sqrt{\frac{K_T}{I}}}$$



C_L, C_T = linear and torsional damping coefficients

C-rule

For a relative error of less than ϵ introduced into \dot{x} at each time step,

$$\left| 1 - e^{\frac{-C_L}{M} \Delta t} / \left(1 - \frac{C_L}{M} \Delta t \right) \right| < \epsilon. \quad \text{Therefore,}$$

$$e^{\frac{-C_L}{M} \Delta t} + \frac{C_L}{M} \Delta t (1+\epsilon) < 1 + \epsilon \quad \text{or} \quad e^{\frac{-C_T}{I} \Delta t} + \frac{C_T}{I} \Delta t (1+\epsilon) < 1 + \epsilon$$

FIGURE 3-10 Maximum stiffness and damping values for numerical stability with integration time step Δt

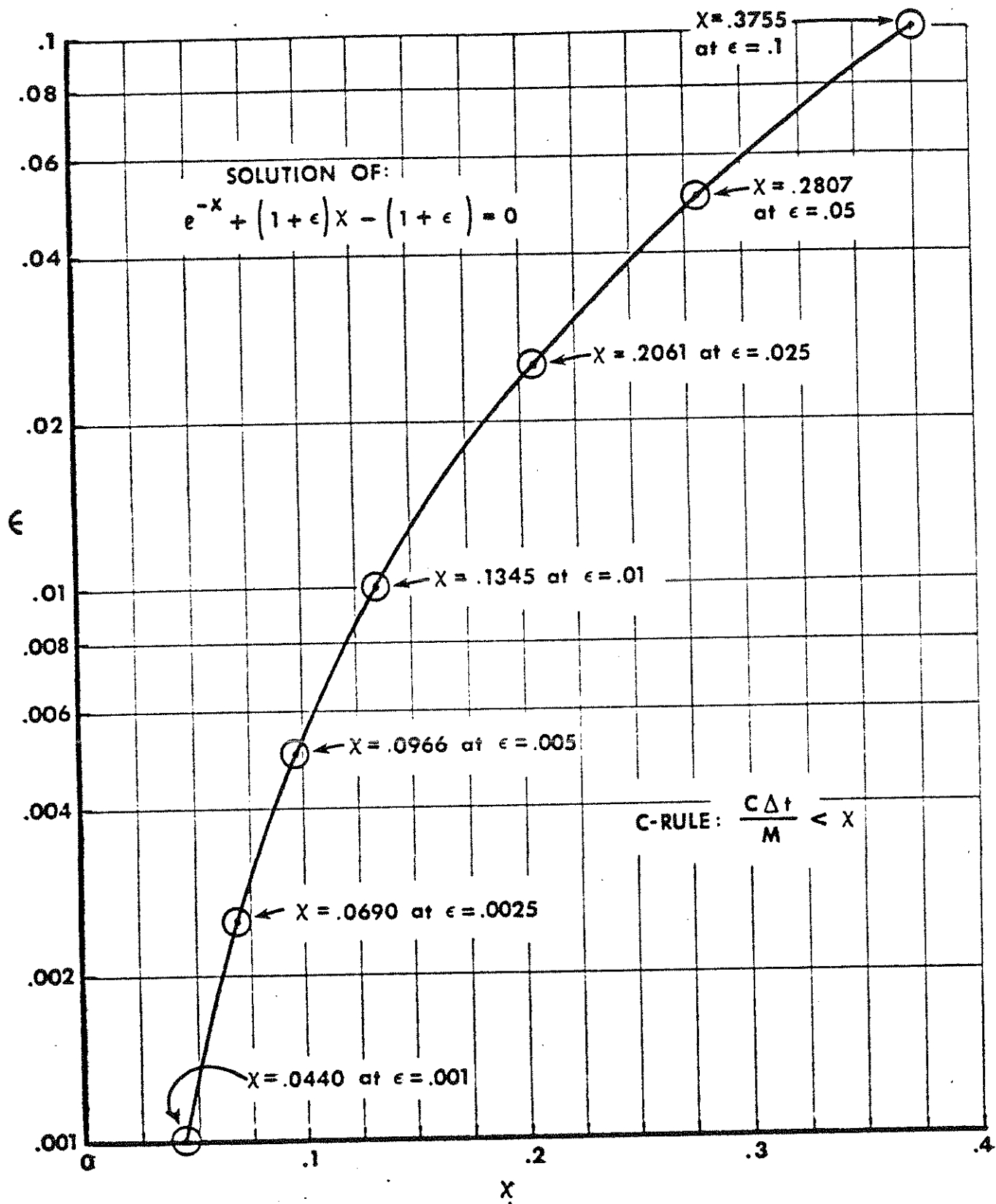


FIGURE 3-11 Solution of $e^{-x} + (1+\epsilon)x - (1+\epsilon) = 0$ for x With ϵ As a Parameter

3.2 The Shoulder

3.2.1 The Anatomy of the Shoulder

The shoulder is a composite system that consists of four skeletal elements and three joints. The shoulder complex and its separate skeletal parts are illustrated in Figure 3-12. In order of their positions in the linkage, the skeletal elements are: 1) the sternum, or breastbone; 2) the clavicle, or collar bone; 3) the scapula, or shoulder blade; and 4) the humerus, or upper arm bone. The three joints are the articulations between these four skeletal parts, and their names are derived from the skeletal parts that they join. Thus, the first two joints are the sternoclavicular joint and the claviscapular joint. The third is called the glenohumeral joint. Its name is derived from the glenoid fossa, the depressed surface on the scapula in which the head of the humeral bone rotates.

Twelve separate ligaments affix to the four skeletal elements. They transmit torques from one element to another as muscles are contracted, and they limit the motions that the shoulder complex can undergo freely. The continuous boundary of the range of relatively free motion that can occur at a single joint or a composite of several joints is called a "joint sinus." It is sometimes called an "excursion cone" since in three-dimensional space the extreme range of the motion pattern is typically a conical surface swept out by a skeletal link.

The clavicle, when moved to its extreme positions in all directions permitted by the sternoclavicular joint, describes a conical joint sinus with an elliptical opening. This joint sinus is illustrated in Figure 3-13. The elliptical base of the cone is shown in the lower figure. The anterior-posterior dimension of the base is typically 3.5 inches and the vertical dimension is usually about 2.5 inches. Further motion of the clavicle tending to enlarge the sinus is resisted by the binding of ligaments and by the pressing together of articular surfaces.

Figure 3-14 shows actions that result in direct translatory, or "shrugging," motions of the shoulder mass. These are shoulder pro-

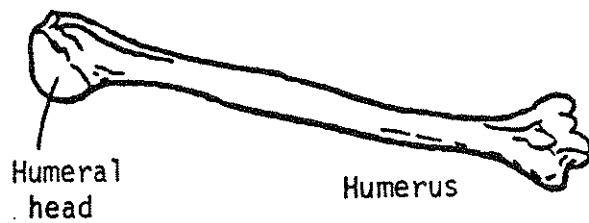
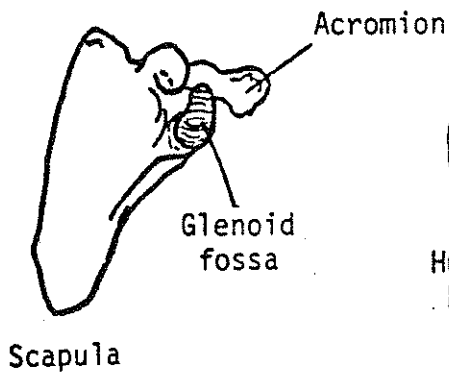
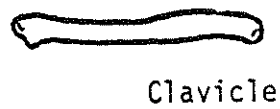
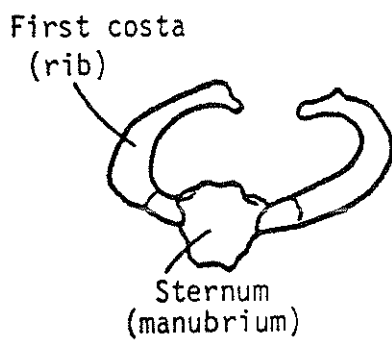
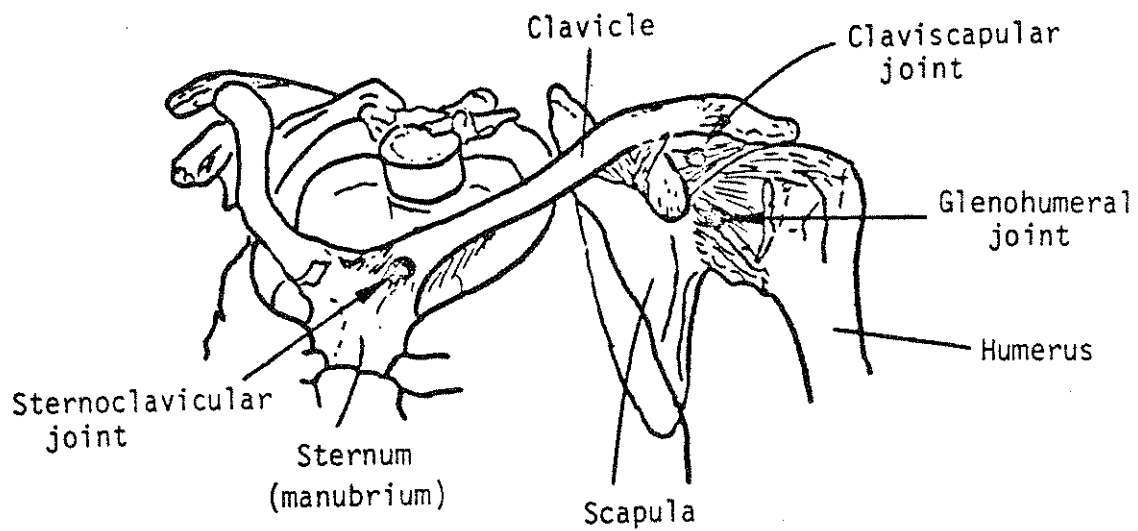


FIGURE 3-12 The shoulder complex and its skeletal parts

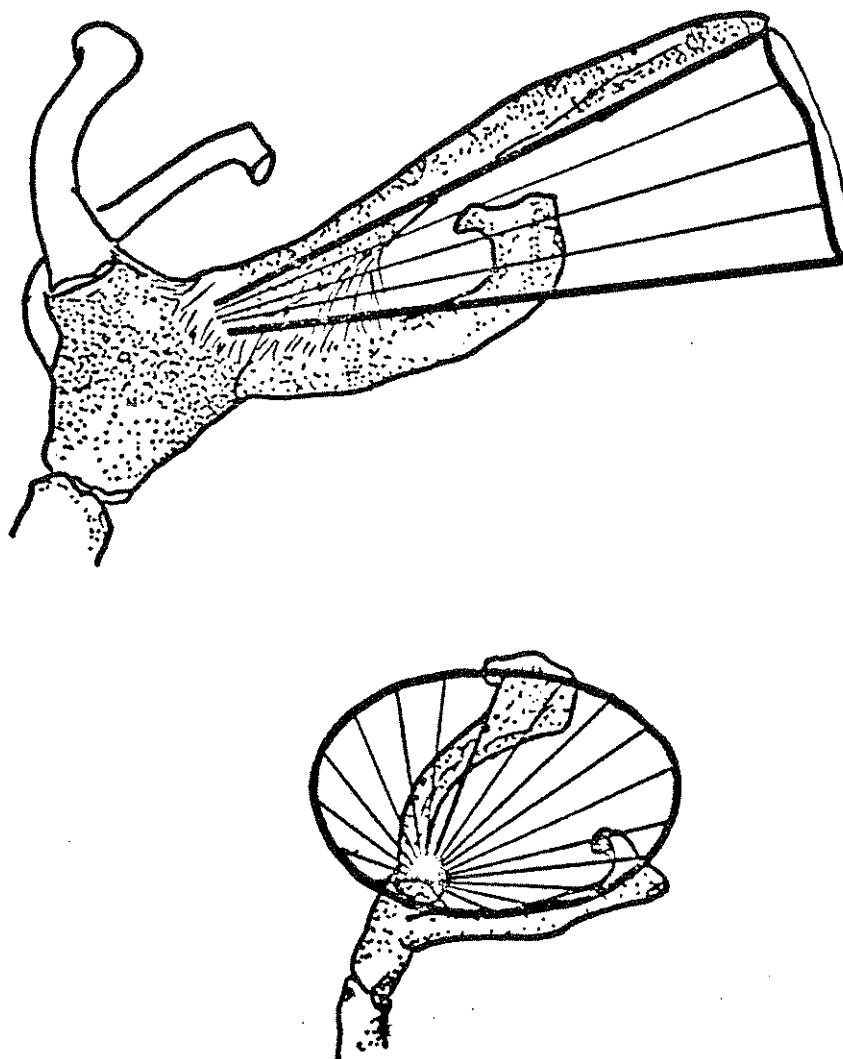


FIGURE 3-13 Joint sinus of sternoclavicular joint

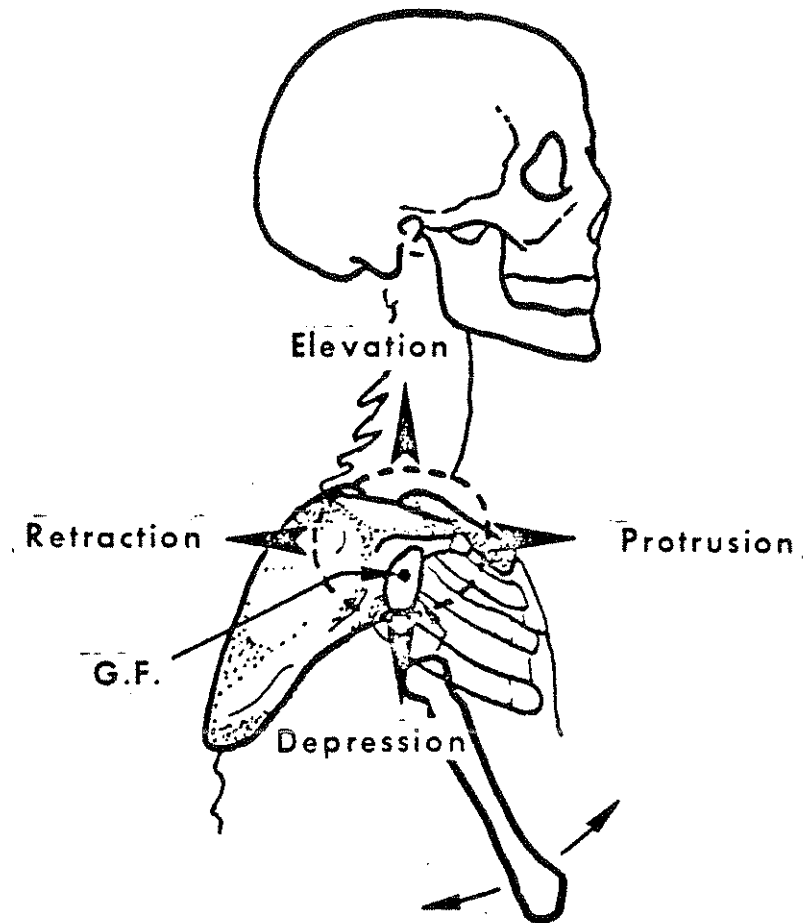


FIGURE 3-14 Maximum range of motion of the glenoid fossa (shoulder socket) in shrugging movements

trusion, shoulder retraction, shoulder elevation, and shoulder depression. They are combined motions of the clavicle and scapula. The point marked "G.F." is the rest position of the mean center of the glenoid fossa on the scapula, the socket in which the humeral head articulates. The dashed ellipse is the maximum range of motion of this point when the arm (humerus) is hanging straight down.

More or less independently from these claviscapular motions, articulations of the humerus occur at the glenohumeral joint. The joint sinus is large since ligaments between the scapula and the humerus allow the arm considerable freedom of movement. The maximum range of the humeral link from adduction to abduction (toward and away from the body) is about 100 degrees. As long as the humerus is not rotated axially, the glenohumeral sinus from anterior to posterior is about 160 degrees. With axial rotation of the humerus, the range of motion of the upper arm can exceed 180 degrees, being limited to an approximately overhead position in the one extreme and to a position somewhat back of vertical when downward.

3.2.2 The MVMA-2D Shoulder Model

The shoulder model used in the MVMA Two-Dimensional Crash Victim Simulator has three degrees of freedom which represent the composite claviscapular shrugging motions and sagittal-plane articulation of the upper arm at the shoulder socket, the glenoid fossa. These are the motions just discussed and illustrated in Figure 3-14. The model is simplified analytically by the assumption that the joint sinus for clavicle and scapula translatory movements is circular in cross section rather than elliptical as shown in the figure. Further, the rest point of the glenoid fossa is assumed to be at the center of the circle rather than below it. In Figure 3-15, joint 9 is the rest position of the glenoid fossa. Its fixed location on the upper torso link is defined by the constants θ_c and L_{27} , both determined from user-specified input data. This point is at the center of a circle with radius specified by the user which represents the translatory range of motion of the glenoid fossa. Joint 7 is the time-varying position of the glenoid fossa, together with the humeral head. Excursion of this point away from point 9 is resisted by linear spring and damping elements until

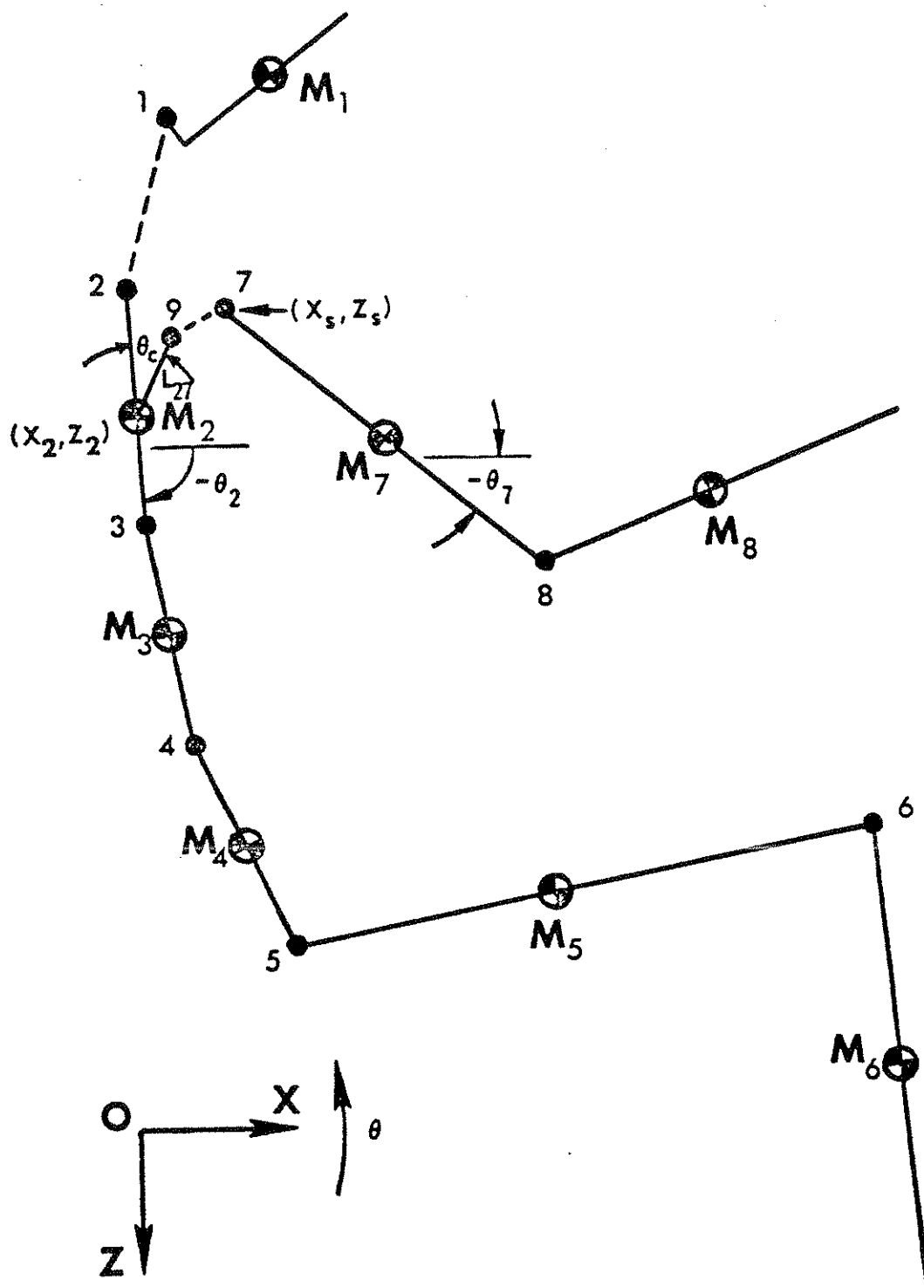


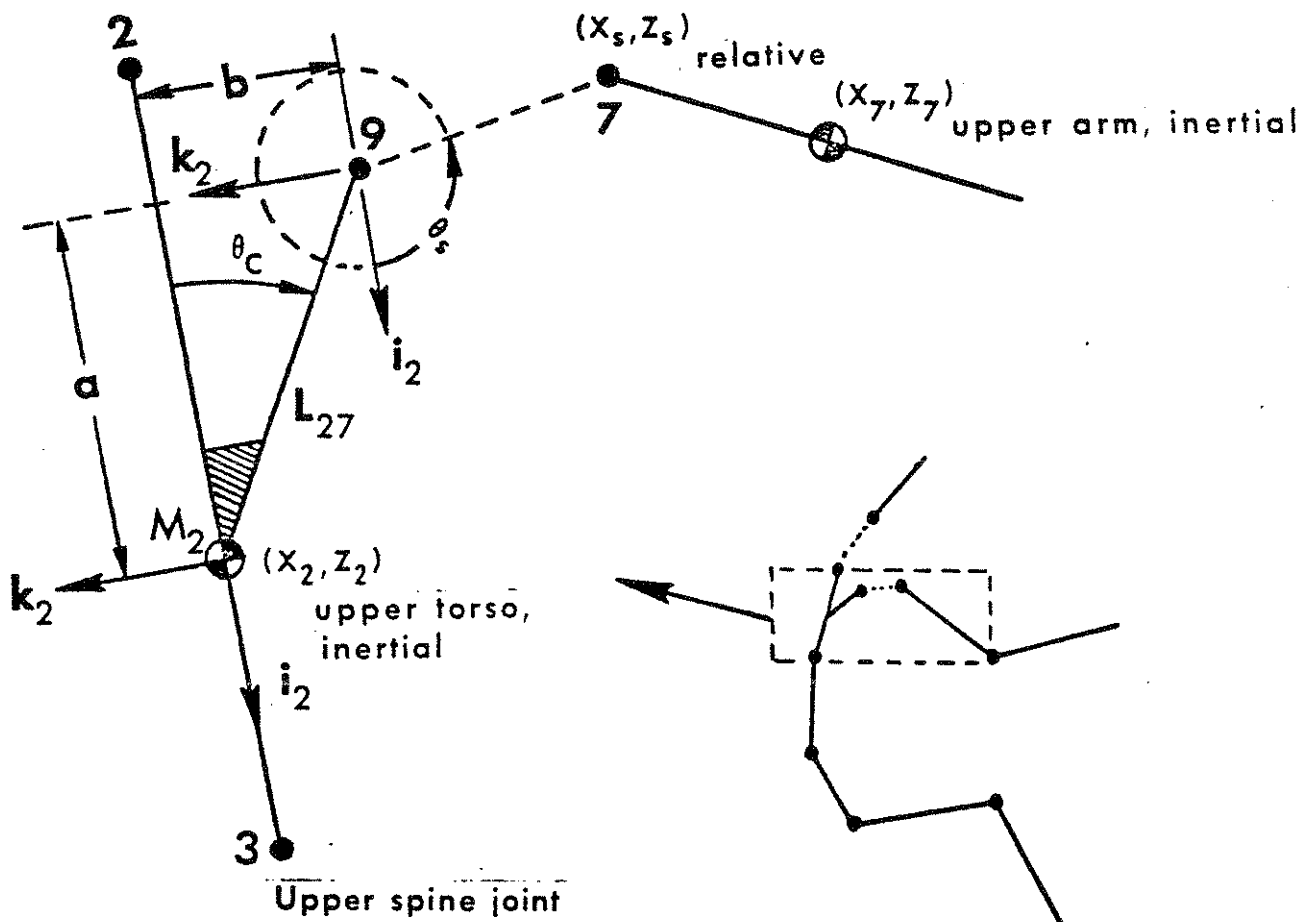
FIGURE 3-15 Articulated body schematic showing three-degree-of-freedom shoulder

the joint sinus circle is reached. Excursions exceeding the radius of this circle are resisted further by quadratic and cubic spring elements since such motions can occur only with stretching of clavicular and scapular ligaments. The dashed line between joints 7 and 9 is most accurately pictured as the projection onto the X-Z plane of the straight line joining the sternoclavicular joint with the glenohumeral joint. The angle between this dashed line and the upper arm has no physical significance. Thus, sagittal-plane articulation of the upper arm at the shoulder socket, i.e., θ_7 -motion about point 7, is restricted by viscoelastic elements fixed to the upper torso. Joint stop positions of the upper arm with respect to the upper torso as well as all of the types of viscoelastic elements discussed in this module with regard to the neck, and in Module 2, are user-prescribed input data.

The analytical shoulder model is shown in somewhat more detail in Figure 3-16, and example shoulder data cards are shown in Figure 3-17. The radius of the joint sinus circle about the rest position of the shoulder socket is entered in field 7 of Card 214. The rest position itself is located with respect to the center of mass of the upper torso element by the coordinates a and b, which are defined in fields 8 and 9 of Card 201. The linear, quadratic, and cubic spring coefficients for elements which resist excursion of joint 7, previously discussed, are entered in the first three fields of this card. A restitution coefficient, the ratio of conserved to total loading energy, is entered in field 9 for hysteretic unloading from excursions beyond the joint sinus circle. A viscous friction coefficient is entered in field 4. The initial x- and z-coordinates of the shoulder socket in the upper torso system but relative to the rest position, point 9, are entered in fields 1 and 3 of Card 304. Normally, these values will be 0. since the shoulder socket is normally in its rest position at onset of a simulated crash.

Other input cards which relate to excursion of the shoulder socket from its rest position are Cards 239, 240, and 241 -- all optional. As it may not be true that resistance to such motion away from point 9 is the same in all directions, the constant linear, quadratic, and cubic spring coefficients entered on Card 214 may

Lower neck joint



$$\vec{r}_{9 \rightarrow 7} = x_s \mathbf{i}_2 + z_s \mathbf{k}_2$$

$$\theta_c = \text{constant}$$

$$L_{27} = \text{constant}$$

FIGURE 3-16 Shoulder Joint

be replaced if desired by periodic functions of the angle θ_s . If the linear coefficient is to be a tabular, periodic function of θ_s , then a 239-Card must be present for each point. The first and last of these cards contain 0. and 360. in field 1 and, in field 2, identical values for the linear spring coefficient at θ_s equal to zero. Intervening 239-Cards specify the coordinate pairs for θ_s and the spring coefficient between 0 degrees and 360 degrees. 240- and 241-Cards are used similarly for the quadratic and cubic coefficients.

Joint parameters affecting sagittal-plane articulation of the upper arm at the shoulder socket are defined on Card 211. These are completely analogous to parameters defined for other body joints on Cards 207 to 212, which are discussed in Module 2. The linear torque rest angle is entered in field 7 of Card 217.

Three muscle elements can be defined for the shoulder complex. One is a force producer which limits excursion of joint 7. Two are torque producers, limiting θ_s -motion and motion of the upper arm relative to the torso. The parameters for these elements are entered on Cards 237, 235, and 233, respectively. Muscle activity levels are defined as functions of time with 238-Cards, as described fully in Module 2.

Example input data for the shoulder complex are shown in Figure 3-17. Note in particular the resistance to translatory "shrugging" motions illustrated by the values in fields 1, 2, 3, and 7 of Card 214 and by the 240-Cards. The student should be able to demonstrate that, in the situation represented, there is no resistance to translatory motions of the shoulder socket within a distance of 2. inches from the rest position and that restoring forces for excursions, D , greater than 2. inches are proportional to the quantity $(D - 2. \text{ inches})$ squared. Further, resistance to depression of the shoulder socket is twice as large as resistance to elevation for equal deformations of the circular joint sinus, and values for forces resisting protrusion and retraction are intermediate.

0.	0.	0.	0.		2.		.6	214	
1.11	7.99	9.41	4.25	16.0	0.	1.00	0.	201	
0.	0.	0.	0.					304	
0.	550.							240	
25.	515.							240	
90.	400.							240	
115.	375.							240	
180.	275.							240	
250.	420.							240	
270.	450.							240	
330.	525.							240	
360.	550.							240	
0.	.156	0.	0.	0.	1.	45.	-165.	.5	211
3.6	-20.	0.	0.	-90.	40.	0.	-50.		217

FIGURE 3-17 Example data cards for MVMA-2D shoulder

MODULE 4 - CONTACT SURFACES ATTACHED TO THE OCCUPANT

4.1 Occupant Profiles: General

Modules 2 and 3 describe the occupant linkage adequately only for the simulation of free motion problems. In those modules, link lengths, joint characteristics, and mass and moment of inertia properties are defined. No part of the occupant description in those modules is directly relevant to the application of external forces to the linkage. While one can imagine problems of free motion of the human linkage that would be of interest in certain types of studies, they are of no interest in crash simulations. Means must be provided for generating forces for occupant interactions with restraint systems and surfaces of the vehicle interior. In general, this necessitates description of the geometry of the interacting systems.

This module deals with the description of occupant geometry, i.e., with the definition of the planar occupant profile. The MVMA-2D model provides for generation of forces from belts, airbag, occupant contact with vehicle surfaces, and interaction between body parts. The MVMA-2D belt models, discussed in Module 9, do not require the definition of an occupant profile. The other force producers mentioned here do depend on an occupant profile, and their descriptions are discussed in this module. Since it was convenient to use different analytical techniques for each of the force producers, the occupant contact-sensing profile is defined for each, independently, by a different set of input parameters.

4.2 Occupant Profile for Interaction with Vehicle Surfaces

The most important of the three occupant profiles to be discussed in this module is for sensing occupant interaction with vehicle-interior surfaces. It is the most important in that it will be defined for virtually all crash simulations while the occupant profiles discussed in the last two sections of this module are associated with special options of the model and are far less commonly used.

This contact-sensing occupant profile is a set of ellipses of

arbitrary number and dimensions, fixed to body links at arbitrary positions. The only restriction is that either the major or minor axis of each ellipse must be parallel to the body link to which it is attached. Figure 4-1 illustrates an example set of occupant contact-sensing ellipses.* Material properties may be assigned for each ellipse, or an ellipse can be specified as rigid.

Forces between the occupant and the vehicle interior are generated by the model as a result of interaction of a profile of occupant ellipses such as those in Figure 4-1 with a user-defined vehicle-interior profile. Module 5 details the description of this profile so it will be only summarized here. This profile is a set of connected or disconnected straight line segments. An example profile of five segments is illustrated in Figure 4-1, but any number may be prescribed and their lengths and locations are arbitrary. As with contact ellipses, they may be assigned material properties or be specified as rigid.

An untutored user of the MVMA-2D model would soon develop, on his own, a proficiency in defining occupant ellipse profiles appropriate for his various simulations. Nonetheless, a discussion is presented here of several considerations that are normally made. Several points can be made by examining Figure 4-1. The following seven subsections pertain to these points.

4.2.1 Specification of Unnecessary Ellipses. First, it may very well be that, in this example, the head ellipse is unnecessary for a front-end collision. For the vehicle-interior profile shown, it seems unlikely that any head contacts could occur within the time frame of a crash history. While the specification of this head ellipse can do no harm, the only need for its presence is to sense possible contacts; hence, its presence may represent a (small) modeling inefficiency since wasted computations and storage result. Similarly, the knee and hand ellipses are probably unnecessary for a frontal impact. While no significant increase in computational expense would result from specifying three unnecessary contact ellipses, the careful user will seldom go wrong in trying to model a crash event as efficiently as possible.**

*Most model users find scale drawings and ellipse and circle templates to be of value for data preparation.

**A point for defining a complete occupant profile is that it would be good for all crashes and interiors.

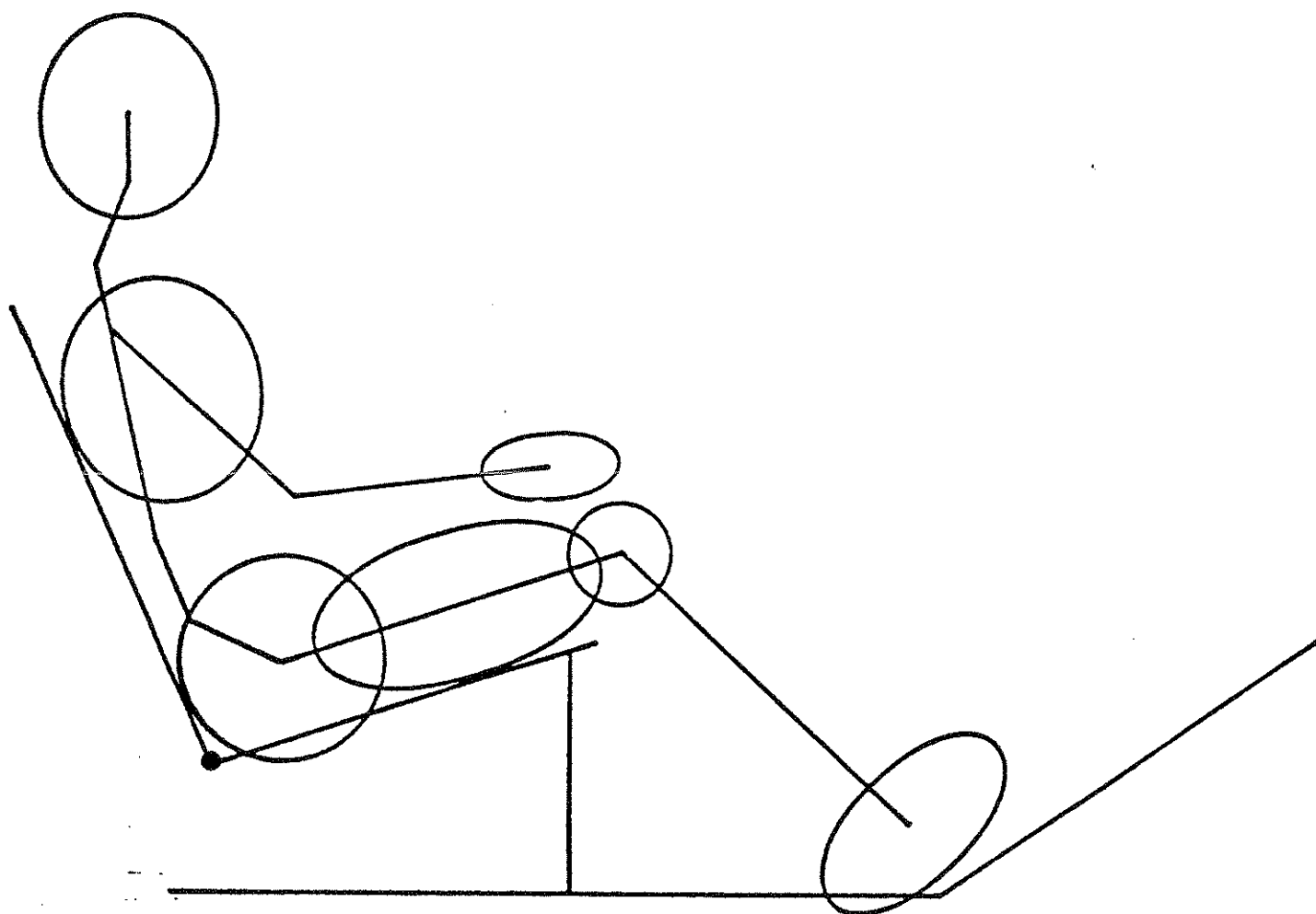


FIGURE 4-1 Example Occupant Profile of Contact Sensing Ellipses for Interaction with Vehicle Interior Surfaces

4.2.2 Incomplete Specification of Ellipses. Second, for a rear impact, the addition of an elbow ellipse might be appropriate as the elbow joint might otherwise pass unimpeded through the seatback line. However, the effect of arm contacts on overall body dynamics is often considered not to be of importance, so this may not be necessary.

4.2.3 Inhibition Switches. Third, the so-called "inhibition switches" for contact interactions should be used for most simulations. These are defined by entries on 102- and 106-Cards and are discussed in detail later in this module. Suffice it to say here that these cards can be used to specify either allowed interactions or interactions that are not to be considered by the model, i.e., "inhibited" interactions. The purpose of specifying allowed or disallowed interactions is usually to make it unnecessary for the computer model to check all combinations of occupant ellipses and vehicle-interior regions for potential interaction. In many simulations, the user can be sure that certain interactions will not occur, so use of 106-Cards will effect a reduction in computation expense. For example, for a frontal impact involving the occupant of Figure 4-1, restrained by a lap belt, it would be reasonable to specify the following allowed interactions: THORAX against SEATBACK, HIP against SEATBACK, HIP against SEATCUSHION, THIGH against SEATCUSHION, KNEE against SEATCUSHION, FOOT against FLOORPAN, and FOOT against TOEBOARD. These are seven interactions for which forces could result. Since there are potentially seven ellipses interacting with five vehicle-interior regions, or 35 total potential interactions, use of the 106-Cards reduces in this instance by 80% the number of potential interactions that the computer model must consider.

4.2.4 Spaces in Occupant Profile. Fourth, "holes" in the occupant profile are sometimes of consequence and sometimes not. For example, Figure 4-1 shows several spaces between ellipses along the occupant linkage, but the ellipses present are adequate for reasonable interaction with the defined vehicle-interior profile. No ellipse should be required at a mid-torso location because the hip and thorax ellipses at either end of the torso adequately account for interaction against the single line of the seat back. Holes in the occupant profile at the neck, arms, and lower legs are of no consequence for this case because

there are no vehicle surfaces which are likely to pass through the interspaces. If, on the otherhand, the vehicle-interior profile included a panel region in front of the occupant, it would probably be important to add a contact-sensing profile for the lower leg, which might otherwise pass upward through the panel area with the knee and foot straddling the panels. An ellipse might be needed at a mid torso location for a rear collision.

4.2.5 Use of a Circle Instead of Ellipse. Fifth, a contact-sensing circle is often just as suitable as an ellipse. The thorax ellipse in Figure 4-1 is a true ellipse, not a circle. But there is clearly no advantage in using an ellipse here.

The only possible interaction of the thorax is with the seat back, and a circle could be attached to the upper torso link which would produce virtually identical deflections of the seat back for all likely positions and orientations of the body linkage. Use of a circle instead will result in a negligible reduction in computation expense, but the circle may be considerably easier to position properly on the upper torso link.

4.2.6 Use of Several Circles Instead of Ellipse. Sixth, a single narrow ellipse sometimes defines a segment of the occupant profile inadequately and should be replaced by two or more circles. Figure 4-2 illustrates such a case. The point on each ellipse and circle perimeter of maximum distance into the material side of the line segment is called a "contact point," and, for each, the maximum penetration distance defines the deflection. The algorithm for determining contact forces, discussed in Module 6, will normally find a non-zero force for a deflection δ greater than zero whenever the contact point is between the end-points of the line segment. The force is normally zero whenever the contact point is outside the line segment. The ellipse in Figure 4-2 clearly should have an interaction force with the line segment AB. But it will not, even though the "deflection" δ_E is greater than zero, since the contact point lies outside the line segment. Use of the three circles in place of the narrow ellipse is superior since, while the contact point of one circle is outside the segment AB, two circles lie within the segment. The deflection δ_C will produce a reasonable force. A general rule to follow is that a contact-sensing ellipse should not be longer than any line segment that it must contact for there to be proper resistance to occupant motion.

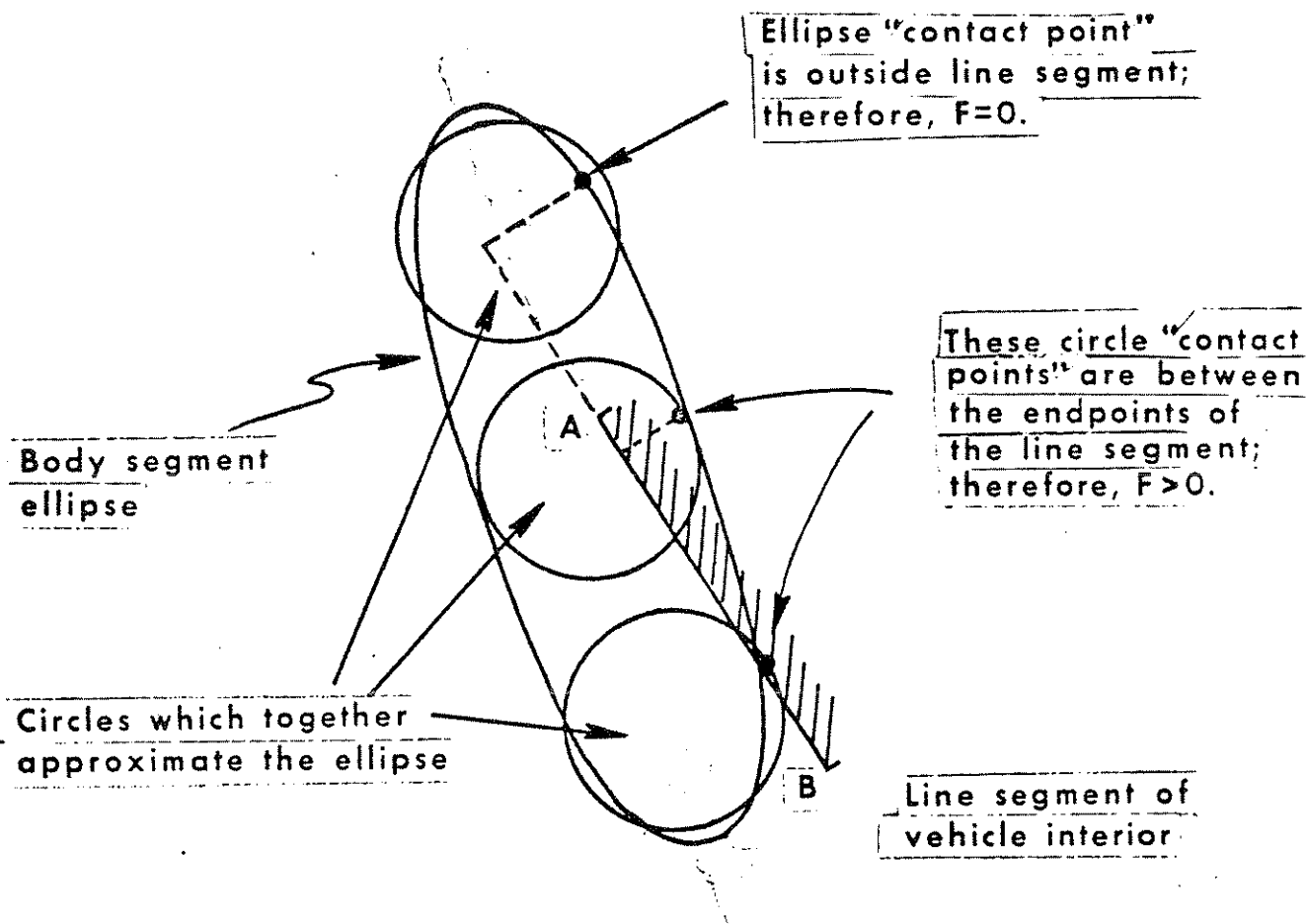


FIGURE 4-2 A Contact Sensing Ellipse and a Better Representation of the Body Segment Profile With Circles

4.2.7 Compliance of the Occupant-Vehicle Interface. Seventh, it is important when assigning material properties to keep in mind that forces for contacts of the occupant with the vehicle interior can be influenced significantly by the force-deflection characteristics of the portion of the body involved. Very often users of crash simulation models concern themselves only with the force-deflection characteristics of elements of the vehicle interior and use rigid contact ellipses or circles on the occupant. This invariably results in effective stiffnesses for occupant-interior interactions that are too large. Consequently, resulting model predictions of peak forces and G-levels are generally too high. The MVMA-2D model allows separate definition of material properties for contact ellipses and vehicle-interior surfaces. The user should define a material for both elements of an interaction whenever data is available unless one element is considerably softer than the other. In this case, the stiffer element may reasonably be specified as rigid.

Figure 4-3 illustrates example force-deflection curves for the chest and a padded panel which it is assumed to strike.* Whenever the chest and panel are in contact, their total relative displacement δ will be the sum of separate chest and panel deflections, δ_c and δ_p . That is,

$$\delta = \delta_c + \delta_p \quad (4.1)$$

For forces less than 450 lbs, each material has constant stiffness, i.e., it is linear. This force corresponds to 1.5 inches of deflection for the chest and 0.9 inches for the panel. Hence, the composite force-deflection relationship for the materials is linear for deflections up to 1.5 + 0.9, or 2.4 inches. The maximum total deflection for which the force is proportional to deflection may be determined in another way. For forces up to 450 lb, the interaction can be thought of as two springs in series with a combined deflection of δ . It is easily shown that for two such springs, with stiffnesses K_c and K_p , the composite stiffness is

$$K = \frac{K_c K_p}{K_c + K_p} \quad (4.2)$$

* A more reasonable chest loading curve would rise more steeply and level off at 800-1200 pounds.

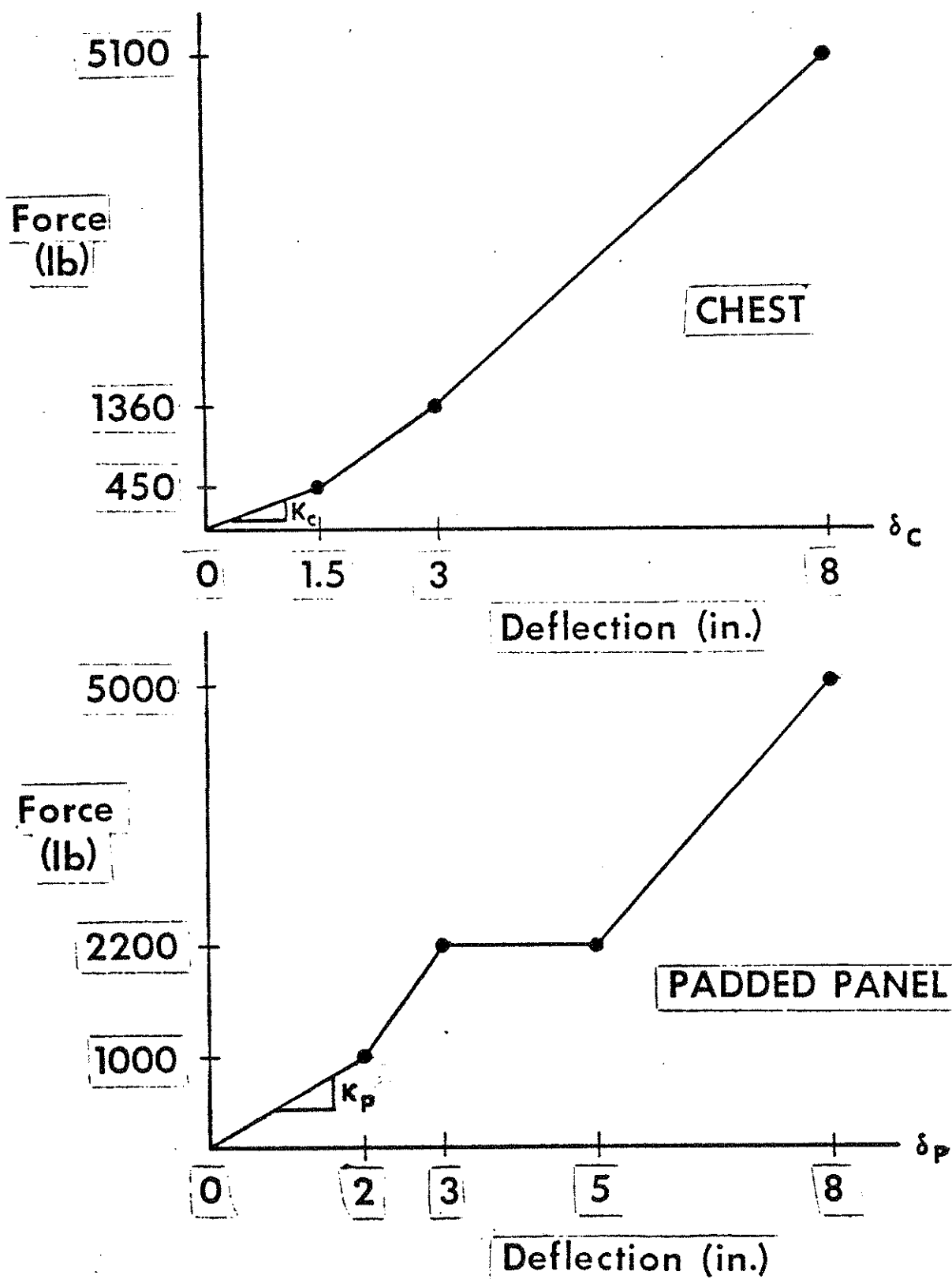


FIGURE 4-3 Example Force-Deflection Curves for the Chest and a Padded Panel

For this example, it is seen from the figure that $K_c = 450/1.5 = 300$ lb/in and $K_p = 1000/2 = 500$ lb/in so that the composite stiffness is $K = 187.5$ lb/in. The composite deflection corresponding to the maximum force for linearity is therefore $\delta = F/K = 450/187.5 = 2.4$ inches. Note that the composite stiffness is less than either of the separate components. This is true in general as can be seen by rewriting equation (4.2) as:

$$K = \left(\frac{K_p}{1 + \frac{K_p}{K_c}} \right) \quad (4.3)$$

It is clear from this form of the equation that K is less than K_p . K is also less than K_c since K_c and K_p are interchangeable.

If at some instant of time, in a simulation with both materials defined, the peak total chest-panel deflection is 2.4 inches, the resulting force will, of course, be 450 lb. Suppose, however, that a peak deflection of 2.4 inches occurs in a simulation which uses the panel material in Figure 4-3 but assumes a rigid chest. The force on the chest is seen to be far greater, namely, 1480 lb. If the panel is assumed rigid in a simulation with a deformable chest, then a 2.4 inch peak deflection would represent 996 lb. These forces are considerably greater than 450 lb, but the significance of using a rigid material has been somewhat overstated. If two simulations differed in no way from the one with mutual chest-panel deformation of 2.4 inches except for having either a rigid chest or rigid panel, respectively, then their peak chest loads would in fact be expected to be less than 1480 and 996 pounds -- but still considerably more than 450. The reason for this is that, in a simulation with one rigid material, occupant momentum would be maximally transferred to the vehicle with a peak deflection of less than 2.4 inches because the force for any given value of deflection is greater.

Figure 4-4 gives peak forces which would result for several different values of total deflection. It would be an instructive exercise for the student to develop these values from the information in Figure 4-3.

Simulation	$\delta = \delta_c + \delta_p$	δ_c (in)	δ_p (in)	F (lb)
Chest deformable	1.0	.625	.375	187.5
	2.4	1.5	0.9	450.
Panel deformable	4.0	2.2229	1.7771	888.55
	7.0	4.1230	2.8770	2200.
Chest rigid	1.0	0	1.0	500.
	2.4	0	2.4	1480.
Panel deformable	4.0	0	4.0	2200.
	7.0	0	7.0	4066.7
Chest deformable	1.0	1.0	0	300.
	2.4	2.4	0	996.
Panel rigid	4.0	4.0	0	2108.
	7.0	7.0	0	4352.

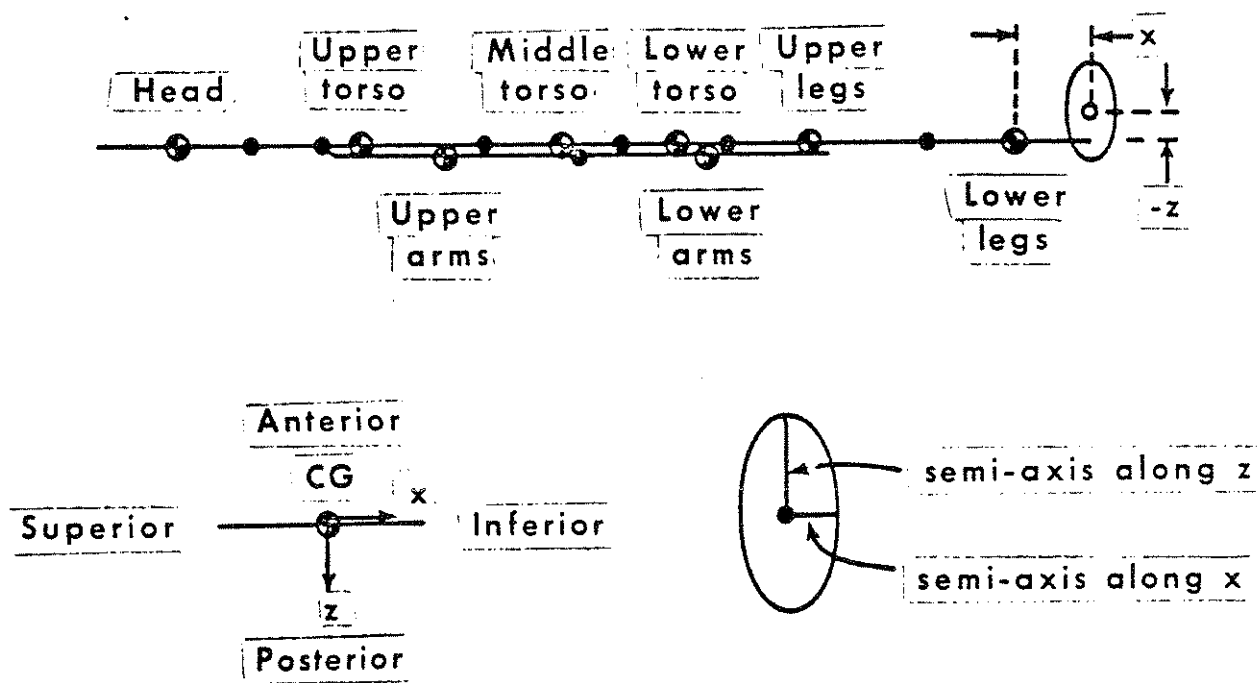
FIGURE 4-4 Chest Loads for Example Force-Deflection Curves

4.2.8 Specification of Data. Data cards relevant to ellipses which interact with vehicle surfaces are Cards 102, 106, 219 through 226, and 412. The data deck must include one 219-Card for each ellipse the user wishes to define. Each ellipse is identified by a user-defined name of up to sixteen alphanumeric characters entered in the first two fields. The 16-character name of a material assigned to the ellipse is entered in fields 3 and 4. If the ellipse is to be considered as rigid, then these two fields are left blank. Each ellipse is attached to one of eight body links, and the link number is entered in field 5 of the 219-Card. The head is link 1; the upper, middle, and lower torso elements are 2, 3, and 4; the upper and lower legs are 5 and 6; and the upper and lower arms are 7 and 8. There is no restriction on the number of ellipses on any link. The example 219-Card in Figure 4-5 is for a chest ellipse attached to the upper torso link. The value in field 6 pertains to the frictional characteristics of the ellipse and will be explained later with 412-Cards.

The data deck must also include one 220-Card for each ellipse. Values on this card locate the ellipse on the body link and prescribe its dimensions. The ellipse name already defined on a 219-Card is in fields 1 and 2. The x- and z- coordinates of the ellipse center in body segment coordinates are entered in fields 3 and 4. Figure 4-6 illustrates the definition of these coordinates with an example for a foot ellipse. Note that the occupant linkage is flat on its back with arms at the side and the legs along the positive x-axis. Z is positive downward, and ellipse coordinate values are measured from the center of gravity of the body link to which the ellipse is attached. The example data in Figure 4-5 are for a chest ellipse centered .5 inches anteriorly from the upper torso link line and .68 inches from the upper torso center of gravity toward the neck. The semi-axis ellipse dimension along the x-coordinate axis, i.e., along the link line, is entered in field 5. The semi-axis z-dimension is in field 6. Thus, the example values in Figure 4-5 are for a chest ellipse with a superior-inferior length of 11.04 inches and an anterior-posterior length of 8.88 inches. Note that there is no provision for orienting ellipse axes at an arbitrary angle from body segment axes.

THORAX	CHESTMATERIAL		2.	1.				219
THORAX	-.5	-.68	5.52	4.44				220
CHESTMATERIAL	0.	0.	0.	100.	101.	0.	0.	221
CHESTMATERIAL	10.				CSTAT	I	CGR	222
CGR	-1.	.1						223
CGR	-1.	.4						224
CSTAT	0.	0.						225
CSTAT	1.5	450.						225
CSTAT	3.	1360.						225
CSTAT	8.	5100.						225
I	-1.	0.						226
3.	0.	0.	0.	0.	0.	10.	.000001 2.	102
1.	3.	.4						412
1.	8.	.35						412
THORAX	PADDED PANEL							106
THORAX	SEATBACK							106
PADDED PANEL	3.	3.	1.	0.	0.			402
SEATBACK	1.	8.	1.	0.	0.			402

FIGURE 4-5 Example Data Cards for a Contact-Sensing Ellipse.



Example for a 'foot' ellipse

FIGURE 4-6 Definition of Location and Dimensions of Contact-Sensing Ellipses

Material property specifications for ellipses are made with Cards 221 through 226. Since material properties are discussed in detail in Module 6, which deals specifically with the generation of forces between interacting occupant and vehicle systems, only the general content of these cards will be discussed here.

The Cards 221 through 226 in Figure 4-5 completely specify example loading and unloading characteristics of the thorax. These cards define a material arbitrarily called CHESTMATERIAL, already identified on Card 219 as the material of the ellipse called THORAX. Values on Card 221 identify deflections at the peak and cutoff of the inertial spike curve, at the yield point, and at the beginning and end of material breakdown. A force saturation level can also be defined with the 221-Card, but the zeroes in fields 8 and 9 of the example data specify a material which does not saturate. Names are entered on the 222-Card for tabular or polynomial representation of: 1) the static force-deflection loading curve; 2) the ratio of permanent deformation to maximum deformation upon complete unloading, as a function of maximum deflection (G-ratio); 3) the fraction of total loading energy not lost to hysteretic absorption upon complete unloading, as a function of maximum deflection (R-ratio); and 4) the so-called "inertial spike" curve, a force-deflection loading curve which may be superimposed upon the static loading curve to represent the effects on impact forces of mass and loading rate. In the example data, the 223- and 224-Cards define constant values for the permanent-deformation and conserved-energy ratios, from which unloading hysteresis is determined. The four 225-Cards define table points for the chest static force-deflection loading curve shown previously in Figure 4-3. Coefficients for a sixth-order polynomial for the inertial spike curve are given on Card 226, all coefficients zero.

The material properties specified on Cards 221 through 226 allow the determination of contact forces normal to the vehicle-interior surface. Friction force components can be determined as well, however. 412-Cards are used for the specification of coefficients of friction. Friction coefficients are defined not for materials but rather for pairings of "classes" of potentially interacting ellipses and regions. For example, knee and chest ellipses might be of the same ellipse friction class if both are covered with cloth. The head would probably be of a different

friction class. Similarly, a seat back and a padded panel would likely belong to different region friction classes because of different surface roughnesses. Each ellipse must be assigned to one of five ellipse friction classes by entering 1., 2., 3., 4., or 5. in field 6 of its 219-Card. Each region of the vehicle interior, discussed in Module 5, is assigned to one of ten friction classes by an entry in field 4 of its 402-Card. Thus, up to 50 combinations of ellipse and region classes can be assigned friction coefficients. In the example data of Figure 4-5, the thorax ellipse is of ellipse friction class 1, as indicated by the 1. in field 6 of Card 219. The values in field 4 of the 402-Cards indicate that the PADDED PANEL and SEATBACK regions have region friction classes of 3 and 8. Each 412-Card has an ellipse class in field 1 and a region class in field 2. A coefficient of friction for this pairing is in field 3. Thus, the constant coefficient of friction between the thorax and the seatback, for example, is .35.

The use of so-called "inhibition switches" for the purpose of allowing or disallowing specific potential interactions was discussed earlier. The user sets these switches for the computer model by making entries on the 102-Card and on 106-Cards. The field of the 102-Card that is pertinent to ellipse-region interactions is the fifth. A 0. is entered if all pairs of ellipse and region names entered on 106-Cards are to be considered allowable interactions, and a 1. is entered if all pairs are to be disallowed, or "inhibited." On the 106-Cards, 16-character ellipse names are in field 1 and 2, and 16-character region names are in fields 3 and 4. Examination of the example data will show that the only regions with which the THORAX ellipse can interact are PADDED PANEL and SEATBACK. An equivalent specification of switches would be to enter a 1. in field 5 of Card 102 and to include in the data set one 106-Card for the THORAX ellipse for each other region name in the vehicle interior. Whether a 0. or a 1. is better used in field 5 of Card 102 depends on whether the set of allowed ellipse-region interactions or the complementary set of disallowed interactions is smaller.

4.3 Occupant Profile for Interaction Between Body Segments

A second type of interaction which involves body ellipses is contact

between body parts. Examples of such an interaction are the head striking the knee, the chest striking the upper leg, and the chin striking the sternum. Specifications for ellipse location, dimensions, and material properties are made as described in the preceding discussion of the occupant profile for interaction with vehicle surfaces. The pertinent data cards are 219 through 226.

In any simulation, the same ellipses defined for interaction with vehicle surfaces may be used for determining contact forces between body parts. This is not required, however. Separate ellipses can be defined for this purpose only, if desired. Any ellipse can be made invisible to any other ellipse and to any region of the vehicle interior by inhibition specifications on 106-Cards.

The previous discussion of inhibition cards was limited to their application to ellipse-region interactions. Allowed or disallowed ellipse-ellipse interactions can also be specified on 106-Cards by entering a second ellipse name in fields 3 and 4 instead of a region name. Two entries on the 102-Card are pertinent. The value in field 6 is a global control over the calculation of forces for this type of interaction. It must be 0. if any interactions between body parts are to be allowed. If it is set to 1., then no such interactions will be considered regardless of 106-Cards which may be present for ellipse-ellipse interactions. If a 0. is entered and no 106-Cards are present in the data deck, then all pairings of ellipses except for those on the same body link will be considered. Since ellipses on the same body link can never interact, such ellipses can be overlapped or superimposed without the necessity of disallowing their interaction with inhibition switch settings. The second pertinent value on the 102-Card is in field 4. A 0. indicates that 106-Cards identify allowable ellipse-ellipse interactions, and a 1. means the specified interactions are disallowed.

Regardless of whether the user provides circles or true ellipses, the algorithm which determines deflections models each interaction as one circle against another. This algorithm replaces a user-supplied ellipse either by a circle fixed to the body element or by a circle which is positioned along the major axis of the ellipse so that its distance from a similar circle on another body element is minimum. This is illustrated

by Figure 4-7. Approximating an ellipse by a circle positioned along the major axis essentially reduces the ellipse to parallel lines with a semi-circular cap at each end.

Whether the algorithm uses a circle of fixed position or of varying position along the major axis depends on whether the ellipse approximates a circle. A parameter value required for the criterion for degree of approximation is one of two additional data inputs that must be made by the user. The criterion is as follows: Let "a" and "c" be the major and minor semi-axes of the ellipse and β be the non-dimensional value entered in field 8 of Card 103; the ellipse is replaced for the purpose of ellipse-ellipse interactions by a circle fixed at the center of the ellipse if $c/a \geq \beta$. The radius R of the approximating circle is taken as C, the semi-minor ellipse axis. This case is illustrated in Figure 4-8.

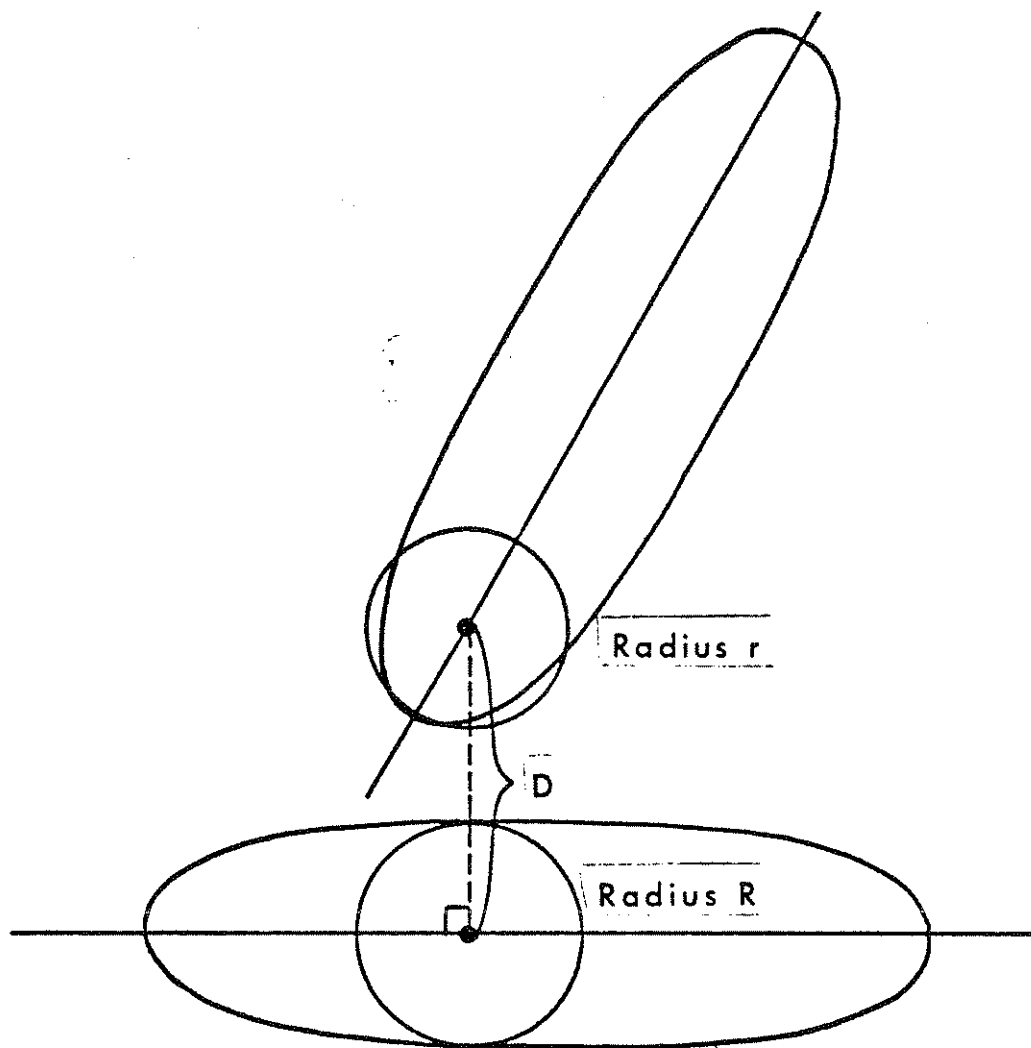
If an ellipse fails the circle-replacement test just outlined, then the ellipse is represented by a circle of varying position. Again, the circle radius is taken as C. The algorithm requires for this case a second parameter value entered on the 103-Card, in field 9. This non-dimensional parameter, called γ , defines the range on either side of the ellipse center that is allowed for the replacement circle. In Figure 4-9, "l" is the maximum allowed distance between the centers of the ellipse and its replacement circle, and it is determined as

$$l = \gamma (a - R) .$$

Note that $\gamma = 1$ puts the circle flush to the end of the ellipse.

Reasonable values of β and γ for most simulations are .75 and .9.* These are the values shown in the example data of Figure 4-10. The user should be able to establish that these data are for a long, narrow ellipse attached to the upper legs parallel to the femur line on the front side of the thigh. For the data values given, the ellipse will be represented by a 0.01 inch radius circle of varying position and with a total range of 14.382 inches. In effect, it is a straight-line segment. The effective ellipse length is 14.402 inches.

* Values of 1. and 1. are often used.



$$\delta = R + r - D$$

$$\text{Deflection} = \begin{cases} \delta & \text{if } \delta > 0 \\ 0 & \text{if } \delta \leq 0 \end{cases} \begin{cases} \text{(circles overlapping)} \\ \text{(circles separated)} \end{cases}$$

FIGURE 4-7 Ellipse Replacement Circles at Positions of Nearest Approach

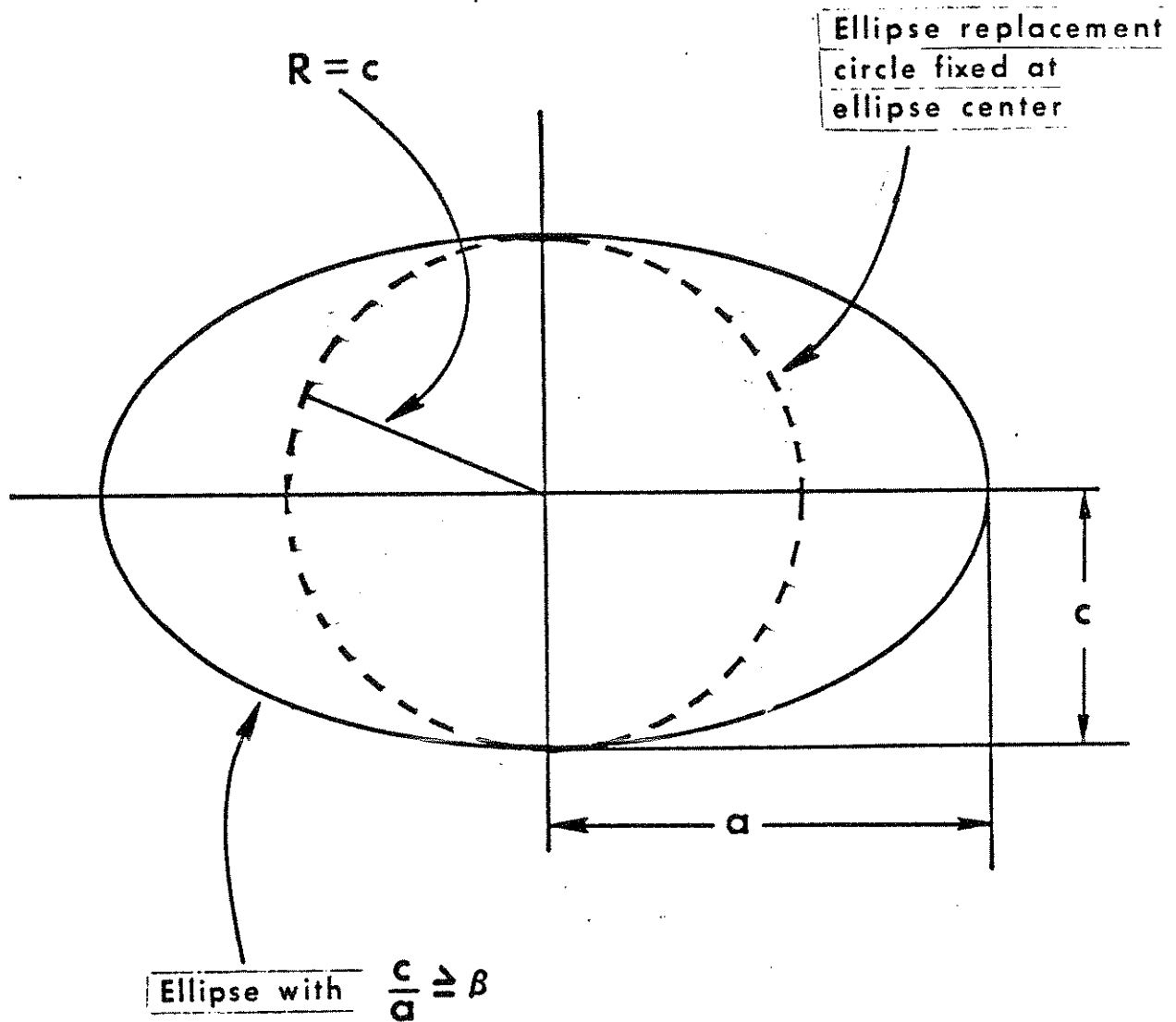


FIGURE 4-8 Approximation of an Ellipse by a Replacement Circle of Fixed Position

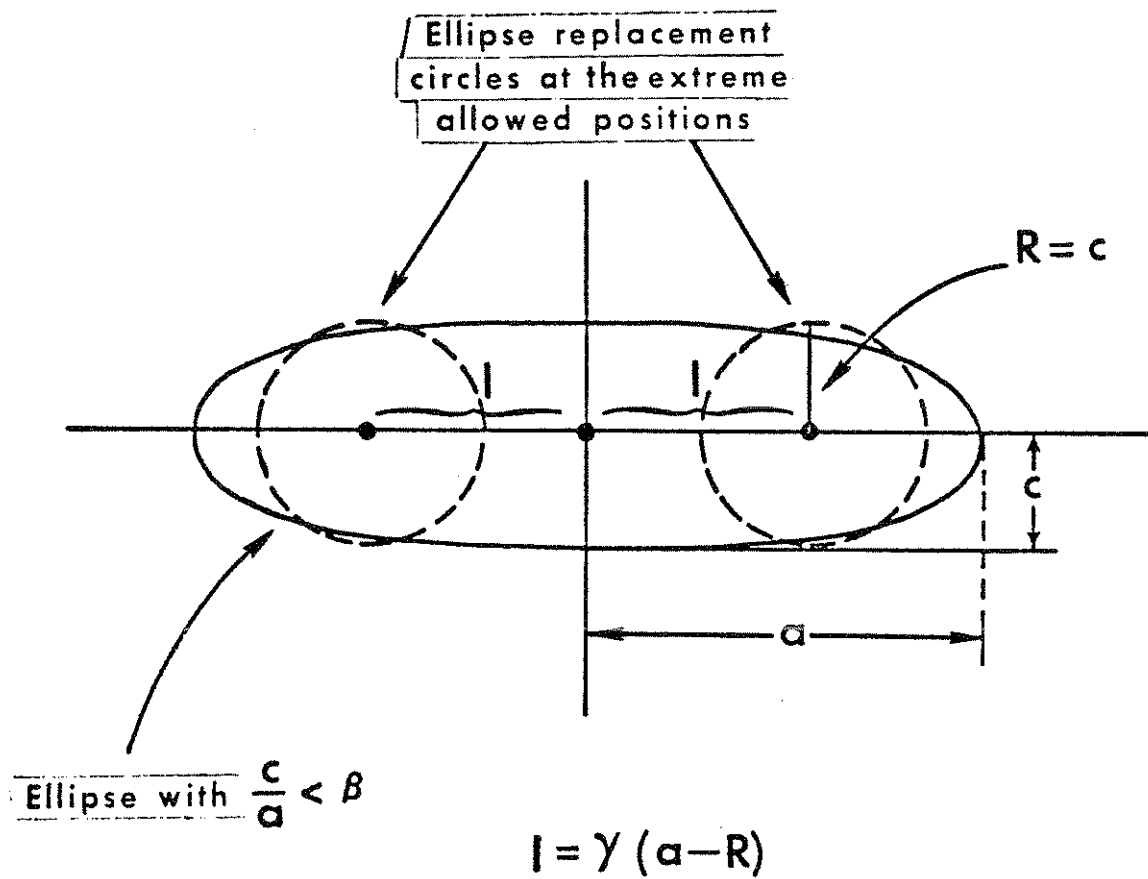


FIGURE 4-9 Approximation of an Ellipse by a Replacement Circle of Varying Position

3.	0.	0.	0.	0.	0.	10.	.000001	2.	102
.2	.02	100000.	15000.	10.	.05	10.	.75	.9	103
FEMURLINEELLIPSETHORAX									106
FEMURLINEELLIPSE				5.	1.				219
FEMURLINEELLIPSE2.			1.4	8.	.01				220

FIGURE 4-10 Example Data Cards for a Special Ellipse on the Upper Legs Link

4.4 Occupant Profile for Interaction with Airbag

The third type of occupant profile senses contact with the airbag. Cards 903, 907, 908, and 909 define this profile as a series of straight line segments. Figure 4-11 illustrates the profile, which consists of the line segments from b-c at the head to 9-10 at the lower legs.

Airbag forces and moments are applied to the occupant only at segments C-1, 1-2, 3-4, 5-6, and 7-8, but the airbag submodel makes use of the entire profile. The user is required to define the locations of eight points on the occupant frontal profile, each fixed with respect to some body link as indicated in Figure 4-12. The points in the figure which are defined on cards 907, 908, and 909 are (ξ_i, ζ_i) with "i" equal to 1, 2, 4, 6, 7, 8, 9, and 10. It is clear that as articulation occurs at body joints, any successive points of this group that are not defined with respect to the same body link will undergo relative motion. Solid line segments in the contact line profile are fixed in length and orientation by the input data. Dashed lines will vary in both length and orientation with respect to all body links; these are determined by the computer model from the input data so as to make the contact profile continuous. The first eight fields of Card 907 are used for coordinate pairs (ξ_i, ζ_i) with successive values of i equal to 1, 2, 3, and 4. No values are required for point 3, so fields 5 and 6 are left blank. Similarly, four points are accommodated by Card 908. No input is required for point 5, however, so the coordinates of points 6 through 8 are in fields 3 through 8. Points 9 and 10 are defined in the first four fields of Card 909.

The last required entry is on the 903-Card. In field 7 is entered a value for average head radius. It is used to help define the two line segments on the head, b-c and C-1 in Figure 4-11. Example data cards for this occupant profile are shown in Figure 4-13.

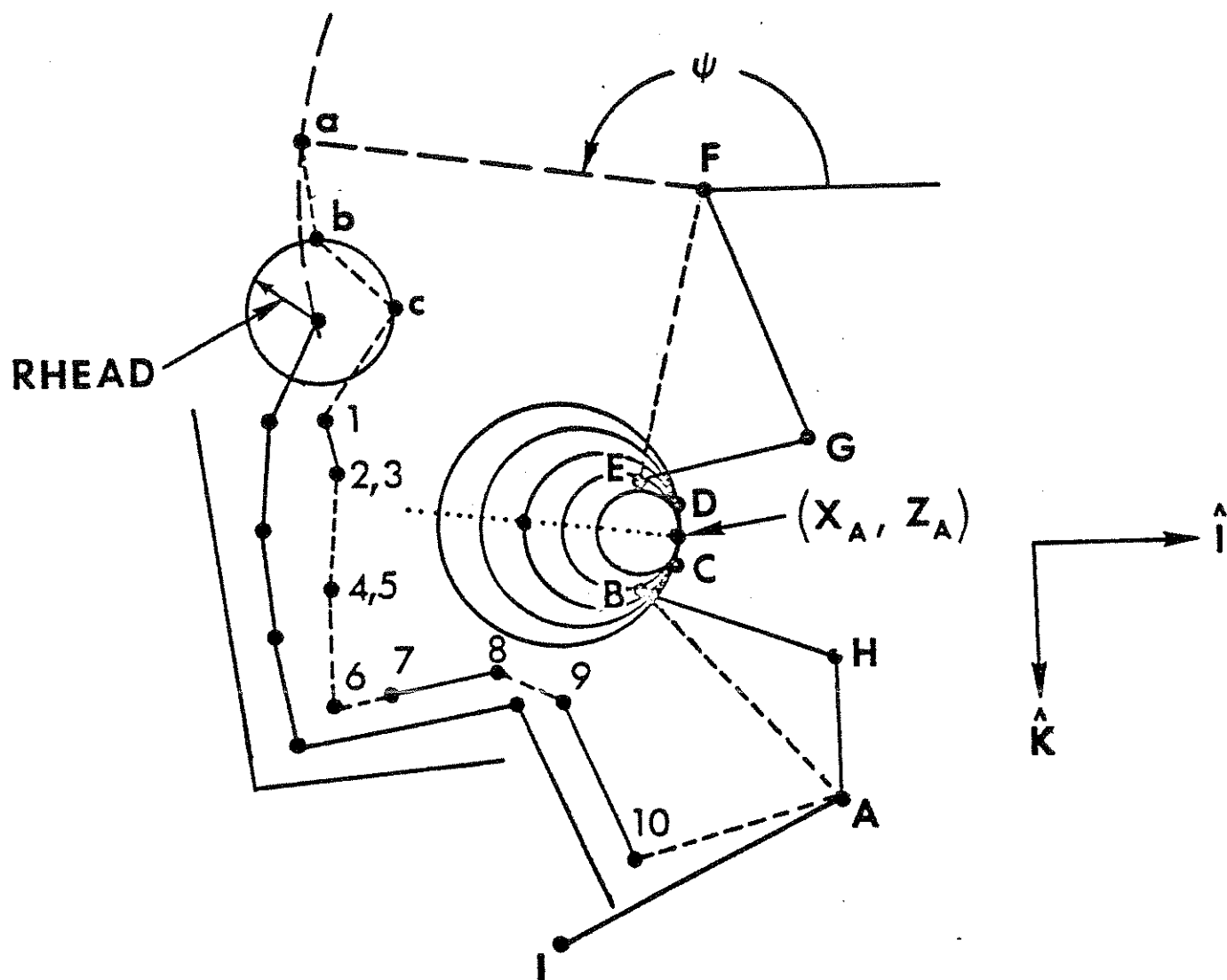


FIGURE 4-11 MVMA 2-D Airbag Model

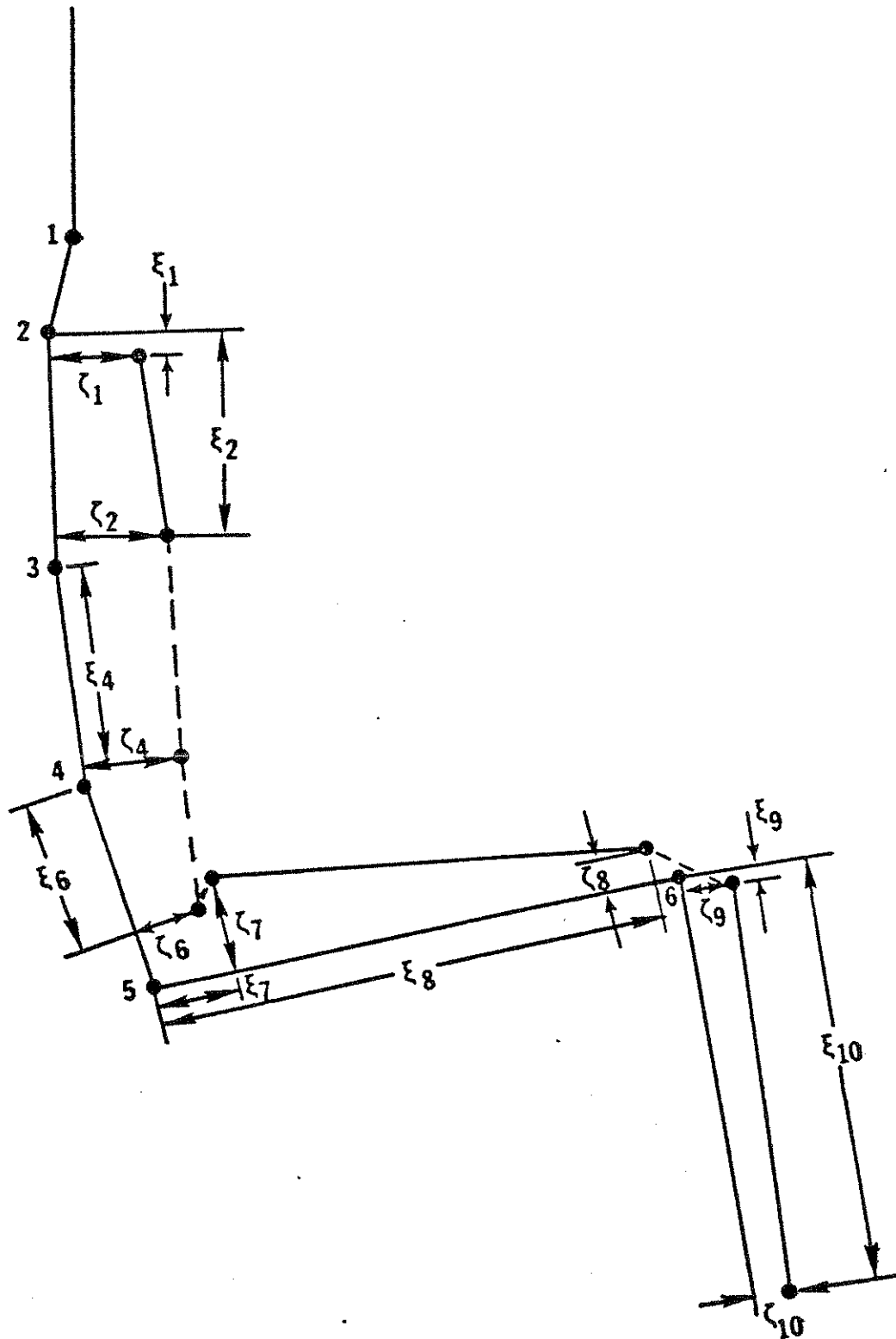


FIGURE 4-12 Airbag Contact Lines on Occupant

55.15	2116.8	1.4		.25	150.	6.		903
0.	4.	8.	4.			8.	4.	907
		2.	4.	4.	2.	20.	1.	908
0.	1.	20.	1.					909

FIGURE 4-13 Example Cards for Airbag-Sensing Profile on Occupant

MODULE 5 - CONTACT SURFACES ATTACHED TO THE VEHICLE

5.1 The Occupant Compartment

The MVMA-2D model is a predictive tool for estimating the dynamic response of a human or an anthropomorphic dummy in a crash environment. The mathematical simulation of a specific event requires the definition of: 1) an occupant model; and 2) a crash environment. The occupant model is described primarily in Modules 2, 3, and 4 while the elements of the expansive term "crash environment" are described in the remaining modules. The crash environment is comprised of all elements of the total system which cause external forces to be developed on the occupant. These include: 1) surfaces of the vehicle-interior profile; 2) restraint systems; and 3) vehicle motion. This module deals with the first of these, occupant-compartment surfaces.

Forces between the occupant and the vehicle interior are generated by the model as a result of interaction of a profile of occupant ellipses with the user-defined vehicle-interior profile. This profile is a set of connected or disconnected straight-line segments. An example profile of eleven segments is illustrated in Figure 5-1, but any number may be prescribed and their lengths and locations are arbitrary. The line segments may be assigned material properties or they may be specified as rigid.

In most instances, the model user will specify line segments of fixed position within a coordinate frame which has three degrees of freedom for user-prescribed occupant-compartment motion. This is appropriate for simulation of any crash with a human or human analog inside an occupant compartment that does not suffer intrusion or collapse as a result of the impact. However, model options allow the user two variations. 1) First, motion of segments of the vehicle-interior profile within the original space of the occupant compartment can be prescribed. Time-dependent positioning of the segments might model either direct intrusion in the case of a side-impact simulation or secondary frontal interior displacements resulting from gross deformation of the engine compartment. For the occupant compartment illustrated in Figure 5-1, this would most likely involve the elements PANEL,

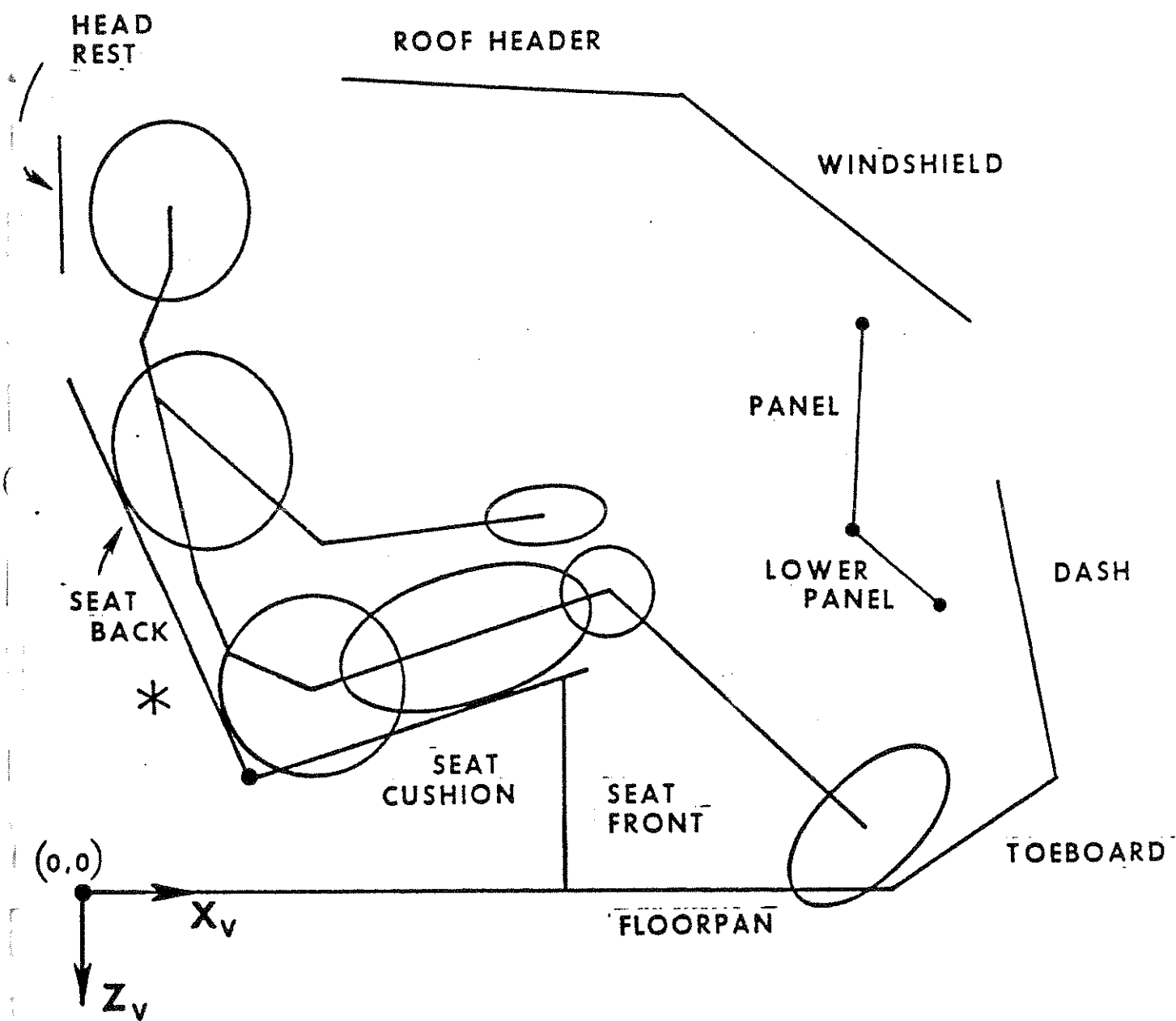


FIGURE 5-1 Example Profile of Vehicle-Interior Surfaces

LOWER PANEL, DASH, and TOEBOARD. 2) Second, the position of any line segment can be defined with respect to the inertial frame, if desired, instead of with respect to a vehicle-fixed coordinate frame. This option is only a convenience for users with occasional diverse applications for the model. With vehicle motion taken into account, it is always possible to make any such simulation without the use of this option.

5.2 Vehicle Interior Regions and Line Segments

5.2.1 Regions. The user defines a contact-sensing vehicle-interior profile as a set of "regions." A region is a set of straight-line segments characterized by the following features.

1) The line segments comprising a region are connected end to end. There may be an arbitrary number of segments in a region, with as few as one.

2) All line segments in a region are considered to have the same load-deflection characteristics since materials are prescribed for regions, not for segments.

Several points are illustrated by Figure 5-1. a) First, the roof and windshield lines, although connected, would surely be separate regions in any reasonable simulation. The reason is that these surfaces should have different load-deflection properties. b) Second, the two panel segments, the seat back plus seat cushion, and the floorpan plus toeboard might reasonably be made two-segment regions since the line segments are connected and may very well have the same load-deflection properties. c) Third, regions in the profile may be disconnected even though segments within a region may not be. The user is invited to demonstrate that two segments in the profile shown must be regions in themselves and that an absolute minimum of six regions must be defined for this configuration.

Only two data cards are required to define each region in the profile. These are cards 401 and 402. Example cards for a region consisting of the two panel segments in Figure 5-1 are shown in Figure 5-2. Fields 1 and 2 of the 401-Card contain a user-defined region name of up to sixteen alphanumeric characters. Fields 3 and 4 contain the

PADDED PANEL	PANELMAT	0.	1.	1.	1.	401			
PADDED PANEL	2.	1.	1.	0.	0.	402			
PANEL	PADDED PANEL	1.	.1	1.	1.	409			
PANEL	4.	0.	0.	0.	0.	410			
PANEL	0.	43.0	-36.8	41.7	-25.3	411			
PANEL	30.	43.0	-36.8	41.7	-25.3	411			
PANEL	70.	43.7	-38.7	38.7	-28.3	411			
PANEL	300.	43.7	-38.7	38.7	-28.3	411			
LOWER PANEL	PADDED PANEL	1.	.1	1.	2.	409			
LOWER PANEL	4.	0.	0.	0.	0.	410			
LOWER PANEL	0.	41.7	-25.3	44.8	-22.2	411			
LOWER PANEL	30.	41.7	-25.3	44.8	-22.2	411			
LOWER PANEL	70.	38.7	-28.3	40.6	-24.4	411			
LOWER PANEL	300.	38.7	-28.3	40.6	-24.4	411			
.2	.02	1000.	15000.	6.	.05	10.	1.	1.	103

FIGURE 5-2 Example Data Cards for a Region

region material name. In the example data, these are PADDED PANEL and PANELMAT. Any material referenced on a 401-Card must be defined in the data deck by a set of Cards 403 through 408. Input data cards for a material called PANELMAT are described later in this module. (See Fig. 5-9). The values in fields 5 through 8 of the 401-Card and field 5 of Card 402 indicate options to be used in the determination of region contact forces. All such options are discussed in Module 6. For each 401-Card in the data deck, there must be a 402-Card which contains in its first two fields the region-identifying name from the 401-Card. In field 3 is entered the number of line segments in the region. In the present example, this value is 2. Field 4 identifies a "friction class" for the region, which is defined later in this module. The user indicates in fields 6 and 7 the reference frames for input and output of region line-segment endpoint coordinates. If input data (on 411-Cards) positioning region line segments are to be interpreted as inertial coordinates, then a 1. is entered in field 6. A 0. means that input coordinate values for segments of this region are in a vehicle-fixed reference frame. If the user requests time-dependent output of region or segment coordinates,* then motion in the inertial frame will be printed if a 1. is entered in field 7 of the 402-Card; motion (if any) in the vehicle-fixed frame will be printed if a 0. is entered.

5.2.2 Line Segments. Various specifications are required for each line segment in a region. A 409-Card, a 410-Card, and at least one 411-Card must be provided. If the segment is stationary with respect to the reference frame indicated in field 6 of the region 402-Card, then a single 411-Card is needed. If the segment is moving, perhaps for the representation of intrusion as discussed earlier, then a tabular, time-dependent, motion history is prescribed for the segment with 411-Cards. In this case, one 411-Card is required for each time point in the table.

The 409-Card for the segment contains in fields 1 and 2 a segment name of up to sixteen alphanumeric characters. In Figure 5-2, there is

* See description of Cards 107, 1001, and 1002 and output categories 2 and 3 in Module 12.

one 409-Card for each segment in the region PADDED PANEL. These are PANEL and LOWER PANEL. The name of the region to which the 409-Card segment belongs is entered in fields 3 and 4. The value in field 8 indicates the segment position within its region. The user can choose the segment at either end of the region arbitrarily as the "first" segment, but the remaining segments in the region must then be numbered consecutively to the other end. For the example data, if the "first" segment of region PADDED PANEL is line AB, then field 8 of the 409-Card for segment PANEL must contain a 1. and field 8 of the card for segment LOWER PANEL consequently must contain a 2.*

Cards 410 and 411 also contain in their first two fields the alphanumeric segment name. In field 3 of Card 410 is entered the number of time points for which the location of the segment is to be specified. A 1., of course, indicates a non-moving segment. This value will always equal the number of 411-Cards present for the segment. If the segment is stationary, then field 3 of the one 411-Card must contain any negative value. Otherwise, this field contains the time in milliseconds for which the line segment location is specified by the coordinates in fields 4 through 7. The x- and z-coordinates of the first endpoint of the segment are in fields 4 and 5. Fields 6 and 7 contain the coordinates of the second endpoint. Several notes should be made regarding the use of 411-Cards.

- 1) The reference frame for coordinate values is indicated in field 6 of the region 402-Card.

- 2) The "first endpoint" of a segment is the end toward lower-numbered segments within the region.

- 3) The coordinates of the first endpoint of the second segment in a region should be identical to the coordinates of the second endpoint of the first segment, etc.

- 4) Segment endpoint coordinate values for time zero are not allowed to be such that an extension of the segment would pass exactly through the origin of the inertial reference frame.

- 5) 411-Cards for each line segment must be ordered with respect to time.

- 6) Segment endpoint coordinates are determined by linear interpolation between times for inputted table points.

*Fields 5 and 7 of Card 409 are discussed later in this module.
Field 6 is discussed in Module 6-2.

7) Since both endpoints of a segment are prescribed by the user, it is possible for the segment length to change with time.

The user may wish to demonstrate that the example 411- Cards in Figure 5-2 are for PADDED PANEL region segments which rotate upward and back from their initial positions in the vehicle. Figure 5-3 illustrates the panel displacement. All motion occurs between 30 and 70 msec. Note that since the 409-Card field-8 values indicate that PANEL and LOWER PANEL are the first and second segments, respectively, in the region, the point B in Figure 5-3 is both the second endpoint of the segment "PANEL" and the first endpoint of the segment "LOWER PANEL."

Two fields on the 103-Card that are pertinent to line segment specification and several fields on the 409- and 410-Cards have not yet been discussed. Fields 4 through 7 of Card 410 are not pertinent to this module; they are dealt with in Module 6. Likewise, field 6 of Card 409 is left for Module 6.

Fields 6 and 7 of Card 103 are used when contact region line segments are specified to move as a function of time. The lower portion of Figure 5-4 shows example x-motion for one endpoint of a line segment. The points 0, 1, 2, and 3 might be defined, for example, by field-6 entries on four successive 411-Cards. The 103-Card entries are used to avoid abrupt changes in velocity at line-segment endpoints, such as illustrated by the dashed lines in the upper portion of the figure. Let the quantities in fields 6 and 7 be called N and α . The ramp length ϵ used to make the velocity continuous is determined from these quantities by evaluation of the following expression:

$$\epsilon = \min \{ \alpha(t_2 - t_1), N \Delta t \} ,$$

where Δt is the integration time step. If $N \Delta t$ is less than $\alpha(t_2 - t_1)$, then $\epsilon = N \Delta t$ is used, where N is the number of integration time steps which will span the ramp connecting the two velocity levels. If $\alpha(t_2 - t_1)$ is less than $N \Delta t$, then $\epsilon = \alpha(t_2 - t_1)$ is used; this is a decimal fraction of the duration of the velocity level following a discontinuity at t_1 . Suggested values for these non-dimensional quantities are $N = 10$. and $\alpha = .05$.

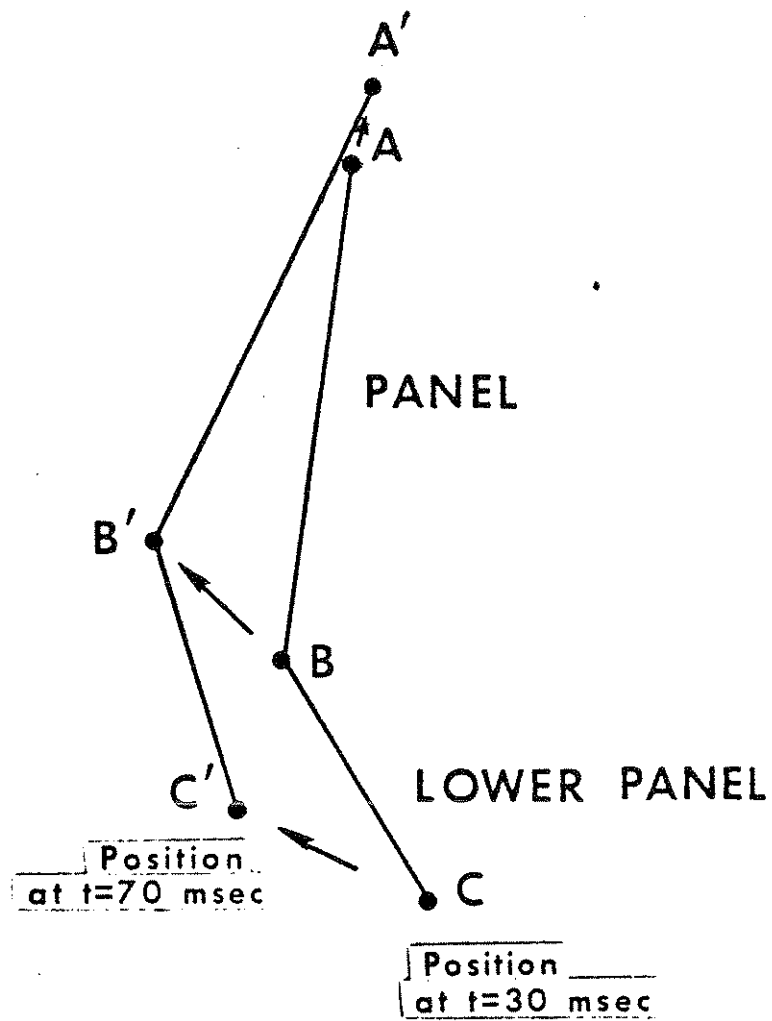


FIGURE 5-3 Padded Panel Region Displacement for Example Data

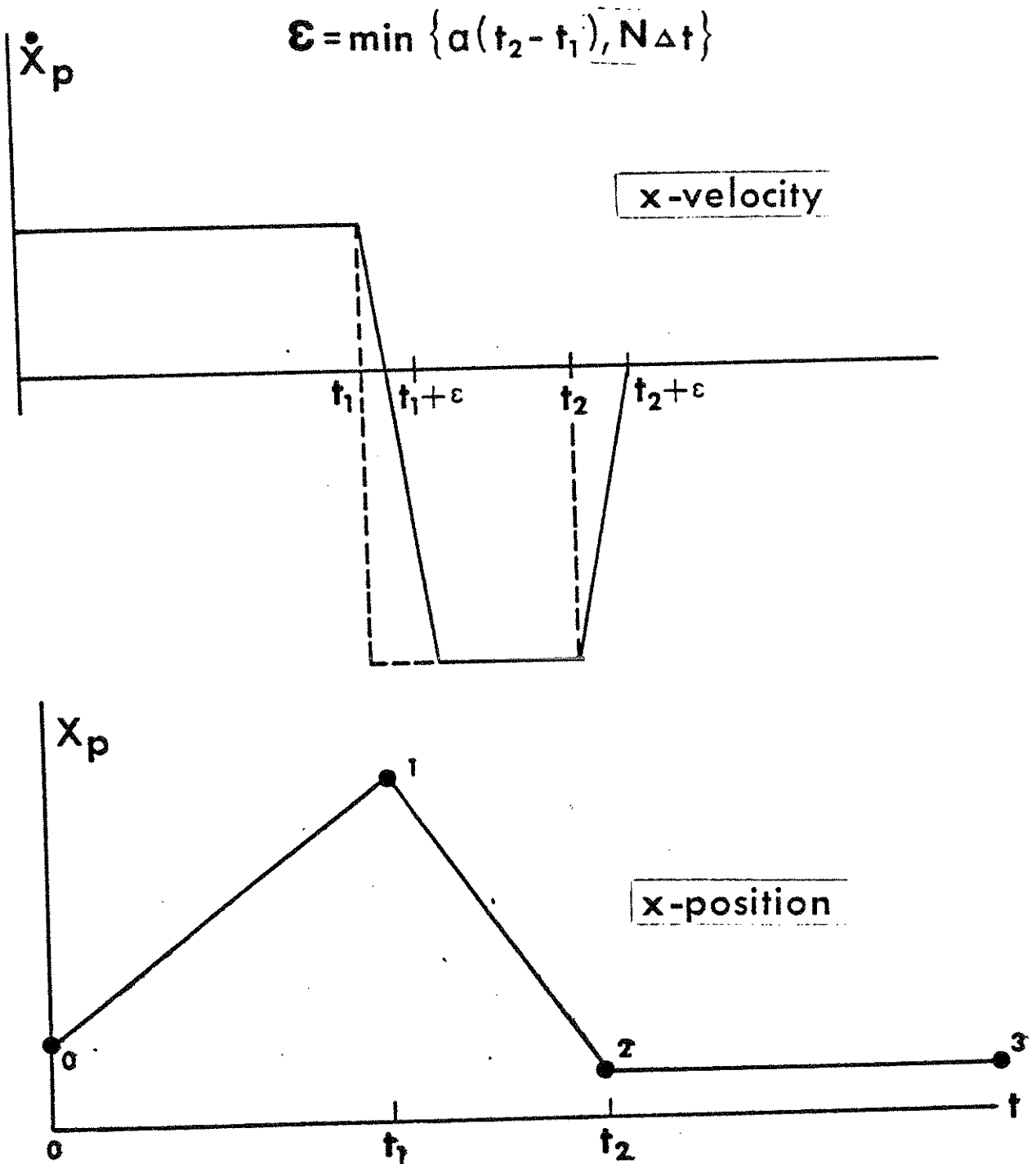


FIGURE 5-4 A Line-Segment Endpoint Coordinate and its Velocity as a Function of Time

Two fields, 5 and 7, remain to be discussed on Card 409. The value in field 7 for each line segment is its "direction factor." The direction factor indicates the side of the line segment which produces contact forces. This is illustrated in Figure 5-5 for the panel segments previously discussed. The value of a direction factor is always either 1. or -1. It is dependent on whether the inertial origin lies behind or in front of the contact surface at time zero. If the inertial origin is on the side of the surface which should be contacted, then the direction factor is D. F. = 1. Figure 5-5 illustrates three different cases for the two-segment PADDED PANEL region. In the upper figure, the direction factor for both segments is 1. In the middle figure both are -1. The line segments in the lower figure have direction factors of different sign. A useful exercise for the student would be to determine the direction factors for all vehicle-interior line segments in Figure 5-1. Assume that the origin of the inertial reference frame at time zero is at the star (asterisk) behind the seat back. The correct values for direction factors for the eleven line segments, beginning with the ROOFHEADER and following the vehicle-interior profile clockwise, are:

1., 1., 1., 1., 1., 1., 1., -1., 1., -1., and 1.

One additional entry is required on the 409-Card for each segment. This is the so-called "penetration limit," in field 5. The penetration limit is used by the computer model to help identify a case in which an ellipse is behind a line segment but no force is to be calculated. Such a case is illustrated by Figure 5-6, which shows a three-segment panel. The knee has an apparent deflection of ℓ_0 into the UPPER PANEL in the position shown,* but a legitimate non-zero force should be predicted only if the knee passes around the panel area and strikes the UPPER PANEL from above. Since the knee location in the normal seated position might very well be as shown in the figure, the penetration limit has pertinence to the specification of conditions at time zero. In particular, its value must be less than the initial distance, ℓ_0 .

* Also, the contact point C.P. is within the projected points A' and D' of the UPPER PANEL segment, AD.

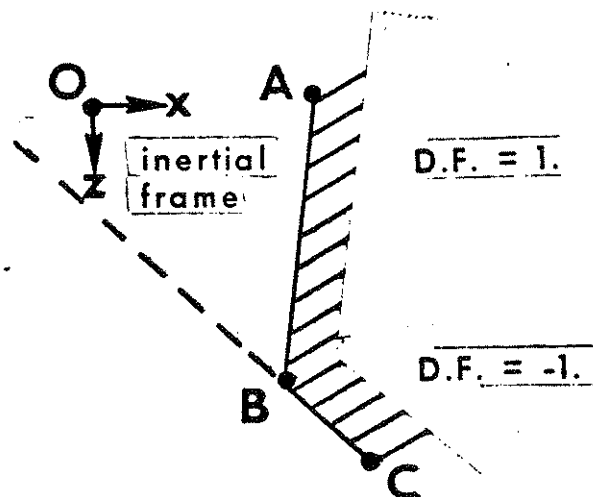
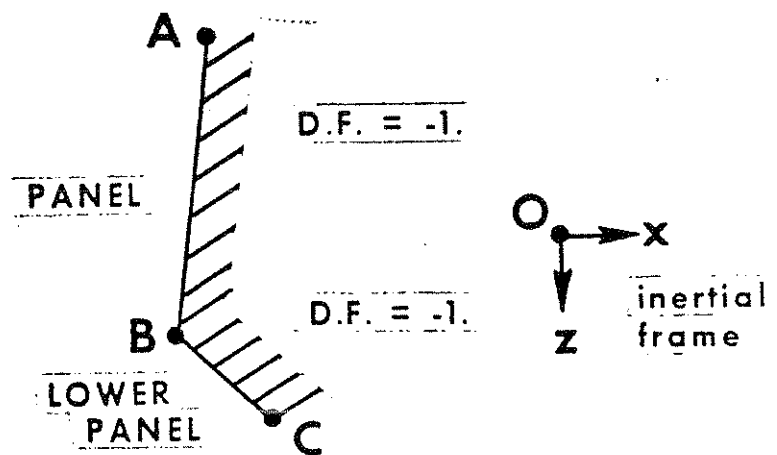
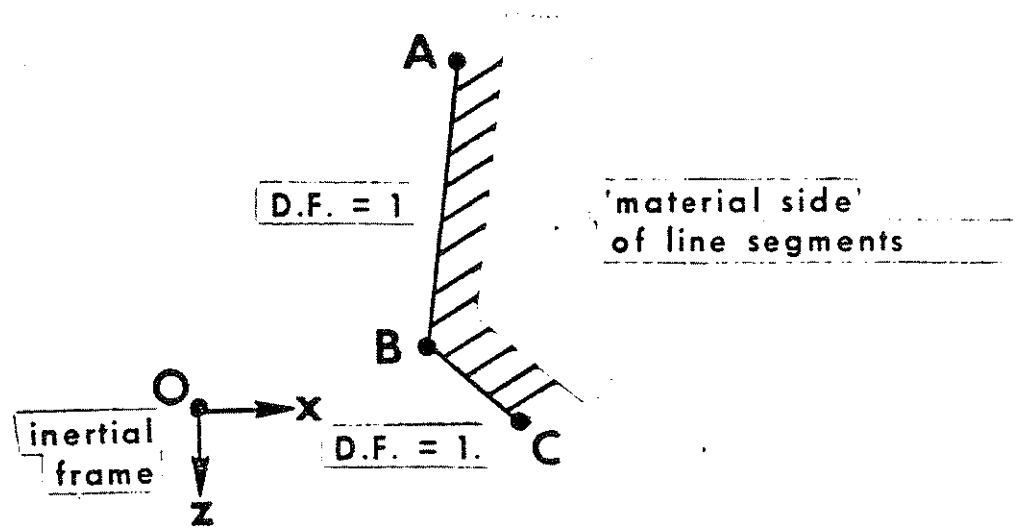


FIGURE 5-5 Line-Segment Direction Factors, Defined at $t = 0$

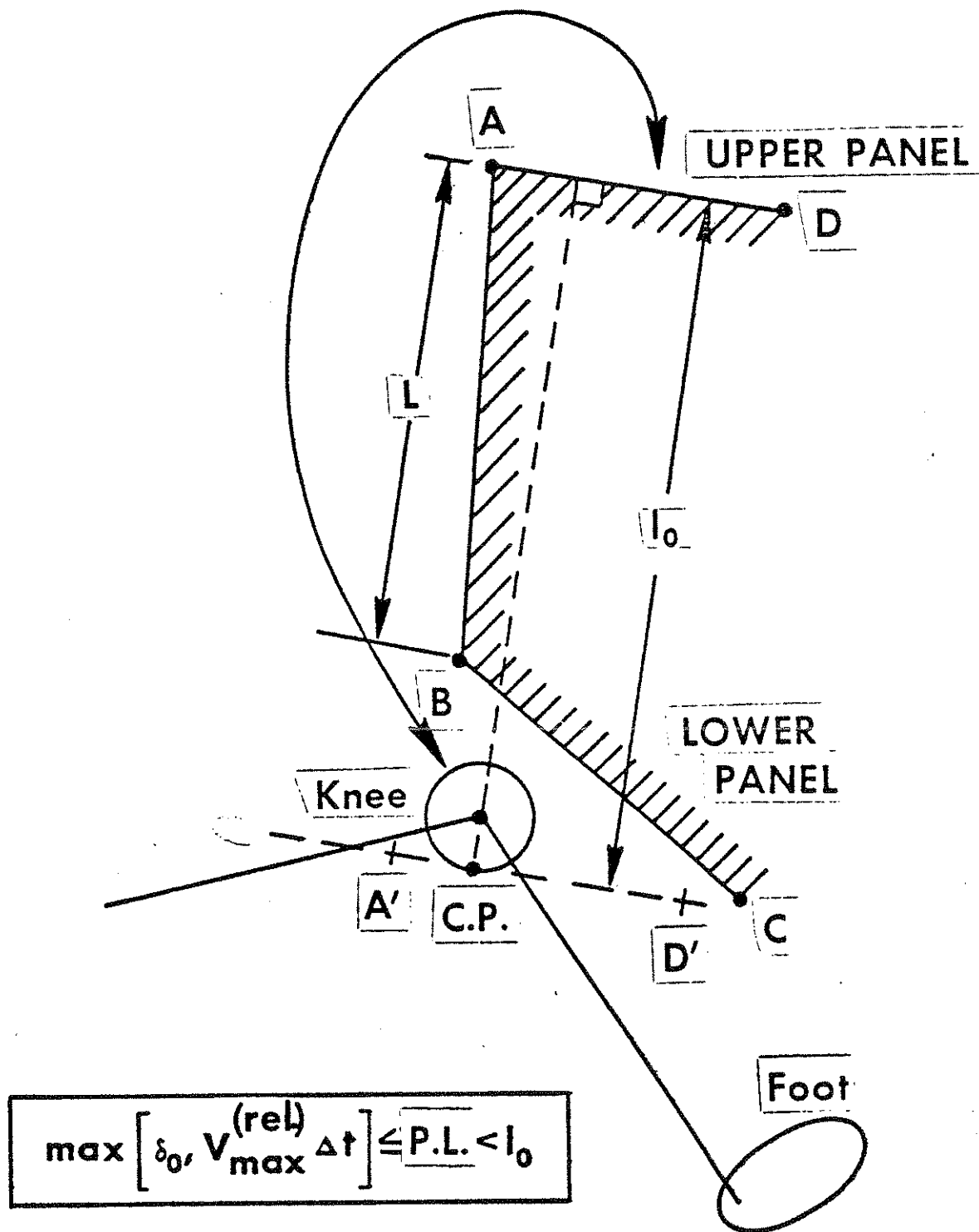


FIGURE 5-6 Selection of Value for Line-Segment Penetration Limit

In effect, the penetration limit defines the depth of a component of the vehicle interior which might be contacted from either side.* Thus, in the figure, the length L would be a reasonable value for the penetration limit of the UPPER PANEL. But the student should not be given the impression that extreme attention must be given to the selection of a value for this quantity. The computer logic only requires a value which satisfies the following inequality:

$$\max(\delta_0, v_{\max}^{(\text{rel.})} \Delta t) \leq \text{P.L.} < x_{t=0} = x_0.$$

Here, P.L. is the penetration limit. Δt is the integration time step, x_0 is the maximum initial apparent (non-force producing) deflection of all ellipses against the line segment, and δ_0 is the maximum real (force producing) initial deflection of all ellipses against the line segment. $v_{\max}^{(\text{rel.})} \Delta t$ is the maximum change of deflection which is expected in one time integration step, which is to say that $v_{\max}^{(\text{rel.})}$ is the maximum speed at which an ellipse is expected to approach the contact surface. Since $v_{\max}^{(\text{rel.})}$ is limited roughly to the crash impact velocity, a reasonable lower bound for P.L. is easily established for a surface that has no real initial deflections ($\delta_0 = 0$). If, for example, the impact velocity is 30 mph, or 528 in/sec, and the integration time step is 1. msec, then $\text{P.L.} \geq .528$ inches. The user could set the penetration limit to 5. inches and be assured that it is almost certainly well within both bounds. But in practice, P.L. is best set equal to its lower bound: $\text{P.L.} = \max(\delta_0, v_{\max}^{(\text{rel.})} \Delta t)$. The small value will eliminate the possibility of a sudden, large, anomalous force when an ellipse is near the edge of a contact surface. This is explained in Module 6, Part 2, which deals with the generation of contact forces.

5.3 Inhibition of Contact Interaction

The so-called "inhibition switches" for contact interactions between occupant ellipses and vehicle regions should be used for most simulations. These are defined by entries on 102- and 106-Cards. These cards can be used to specify either allowed interactions or interactions that are not to be considered by the model, i.e., "inhibited" interactions. The purpose of specifying allowed or disallowed interactions is usually to make it unnecessary for the computer model to check all combinations of occupant ellipses and vehicle-interior regions for potential interaction. In many simulations, the user can be sure that certain interactions will not occur so use of 106-Cards will effect a reduction in computation expense. Assume

* Here, two sides are the upper and lower panels.

that each vehicle-interior line segment in Figure 5-7 is a separate region. For a frontal impact involving the occupant illustrated, restrained by a lap belt, it would be reasonable to specify the following allowed interactions: HEAD against PANEL, THORAX against SEAT BACK, HIP against SEAT BACK, HIP against SEAT CUSHION, THIGH against SEAT CUSHION, KNEE against SEAT CUSHION, HAND against PANEL, FOOT against TOEBOARD, and FOOT against DASH. These are ten interactions for which forces could result. Since there are potentially seven ellipses interacting with eleven vehicle interior regions, or 77 total potential interactions, use of the 106-Cards reduces in this instance by 87% the number of potential interactions that the computer model must consider.

Example contact inhibition cards are shown in Figure 5-8. Field 5 of the 102-Card is pertinent to ellipse-region interactions. A 0. is entered if all pairs of region* and ellipse names entered on 106-Cards are to be considered allowable interactions, and a 1. is entered if all pairs are to be disallowed, or "inhibited." On the 106-Cards, 16 character ellipse names are in fields 1 and 2, and 16-character region names are in fields 3 and 4. The example cards allow the ten interactions previously mentioned. An equivalent specification of switches would be to enter a 1. in field 5 of Card 102 and to include in the data set one 106-Card for each of the 67 disallowed interactions. Whether a 0. or a 1. is better used in field 5 of Card 102 depends on whether the set of allowed ellipse-region interactions or the complementary set of disallowed interactions is smaller.

5.4 Material Property Specifications

Material property specifications for regions are made with Cards 403 through 408. Only the general content of these cards will be discussed here since material properties are discussed in detail in Module 6, which deals specifically with the generation of forces between interacting occupant and vehicle systems.

The Cards 403 through 408 in Figure 5-9 completely specify example loading and unloading characteristics of a panel region.

* All line segments in the region are thus simultaneously allowed or disallowed to interact with the ellipse.

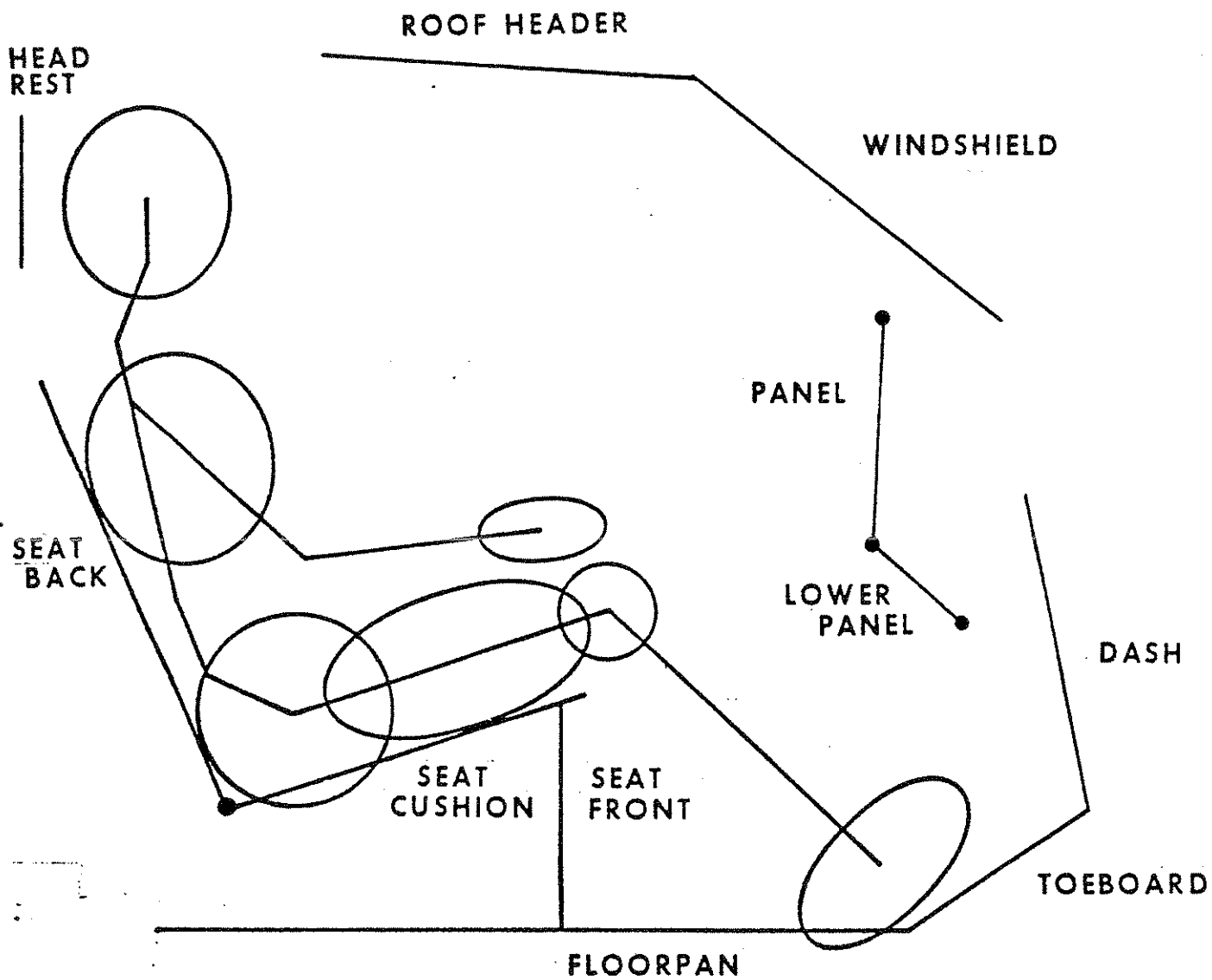


FIGURE 5-7 Seven Occupant Ellipses and Eleven Line Segments for Potential Contact

3.	0.	0.	0.	0.	1.	10.	.000001	2.	102
HEAD	PANEL								106
THORAX	SEAT BACK								106
HIP	SEAT BACK								106
HIP	SEAT CUSHION								106
THIGH	SEAT CUSHION								106
KNEE	SEAT CUSHION								106
HAND	PANEL								106
FOOT	FLOORPAN								106
FOOT	TOEBOARD								106
OOT	DASH								106

FIGURE 5-8 Example Data Cards Specifying Allowed Contact Interactions.

ADDED PANEL	PANELMAT	0.	1.	1.	1.			401
PANELMAT	0.	0.	.1	100.	101.	0.	0.	403
PANELMAT	10.				PSTAT	I	PGR	404
PGR	-1.	.7						405
PGR	-1.	.15						406
PSTAT	0.	0.						407
PSTAT	2.	1000.						407
PSTAT	3.	2200						407
PSTAT	5.	2200.						407
PSTAT	8.	5000.						407
I	-1.	0.						408

FIGURE 5-9 Data Cards for Example Vehicle-Interior Region Material.

These cards define a material arbitrarily called PANELMAT, already identified on Card 401 in Figure 5-2 as the material of the region called PADDED PANEL. Values on Card 403 identify deflections at the peak and cutoff of the inertial spike curve, at the yield point, and at the beginning and end of material breakdown. A force saturation level can also be defined with the 403-Card, but the zeroes in fields 8 and 9 of the example data specify a material which does not saturate. Names are entered on the 404-Card for tabular or polynomial representation of: 1) the static force-deflection loading curve; 2) the ratio of permanent deformation to maximum deformation upon complete unloading, as a function of maximum deflection (G-ratio); 3) the fraction of total loading energy not lost to hysteretic absorption upon complete unloading, as a function of maximum deflection (R-ratio); and 4) the so-called "inertial spike" curve, a force-deflection loading curve which may be superimposed upon the static loading curve to represent the effects on impact forces of mass and loading rate. In the example data, the 405- and 406-Cards define constant values for the permanent-deformation and conserved-energy ratios, from which unloading hysteresis is determined. The four 407-Cards define table points for the panel static force-deflection loading curve shown in Figure 5-10. Coefficients for a sixth-order polynomial for the inertial spike curve are given on Card 408, all coefficients zero.

5.5 Contact Surface Friction

The material properties specified on Cards 403 through 408 allow the determination of contact forces normal, or perpendicular to the vehicle interior surface. Friction force components can be determined as well, however. 412-Cards are used for the specification of coefficients of friction. Friction coefficients are defined not for materials but rather for pairings of "classes" of potentially interacting ellipses and regions. For example, a seat back and a seat cushion might be of the same region friction class if they are covered with the same fabric. Similarly, a floorpan and a panel would likely belong to different region friction classes because of different surface roughnesses. Each region of the vehicle interior must be assigned to

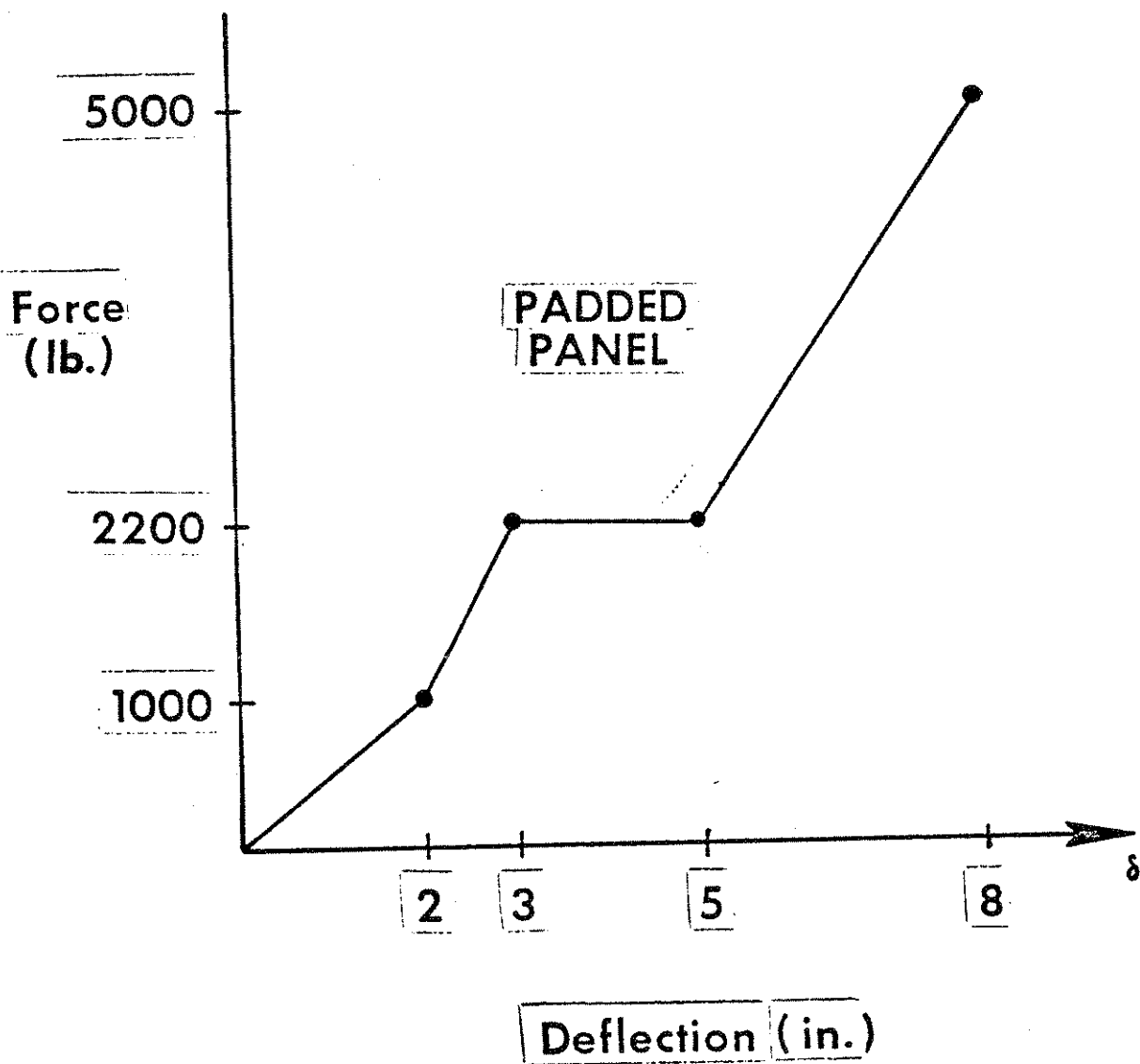


FIGURE 5-10 Example Static Load-Deflection Curve for a Panel Region

one of ten friction classes by entering an integer 1. through 10. in field 4 of its 402-Card. Ellipses, discussed in Module 4, are assigned to one of five ellipse friction classes by entering 1., 2., 3., 4., or 5. in field 6 of its 219-Card. Thus, up to 50 combinations of ellipse and region classes can be assigned friction coefficients. In the example data of Figure 5-11, the values in field 4 of the 402-Cards indicate that the PANEL and SEAT BACK regions have region friction classes of 3 and 8. The thorax ellipse is of ellipse friction class 1, as indicated by the 1. in field 6 of Card 219.

Each 412-Card has an ellipse class in field 1 and a region class in field 2. Fields 3, 4, and 5 contain polynomial coefficients for a deflection-dependent coefficient of friction. These are μ_0 , μ_1 , and μ_2 in the following relation:

$$\mu = \mu_0 + \mu_1\delta + \mu_2\delta^2,$$

where $F_{\text{friction}} = \mu F_{\text{normal}}$.

The first coefficient, μ_0 , is the constant coefficient of friction normally defined. Non-zero values for μ_1 and μ_2 provide a dependence on deflection that represents tangential resistance to "plowing" at the ellipse-region interface. The last card in the example data of Figure 5-11 is for a friction coefficient of .25 for zero deflection, .35 for two inches of deflection, and .65 for five inches of deflection. The user should be able to demonstrate that the tangential force for this friction coefficient equals the constant force normal to the surface when the deflection is 7.29 inches.

THORAX	CHESTMAT	2.	1.		219
PANEL	4.	3.	1.	0.	402
SEAT BACK	1.	8.	1.	0.	402
1.	3.	.4			412
1.	8.	.25	.03	.01	412

$$\mu = \mu_0 + \mu_1 \delta + \mu_2 \delta^2$$

$$F_{\text{friction}} = \mu F_{\text{normal}}$$

FIGURE 5-11 Example Data Cards for Coefficients of Friction

MODULE 6 -- GENERATION OF CONTACT FORCES ON THE OCCUPANT: Part 1

6.1 Generation of Contact Forces

Occupant motion within the vehicle both determines and is determined by forces acting on the occupant linkage. Figure 6-1 illustrates the relationship between the motion and the forces. At some instant of time, usually called $t = 0$, the position and velocity conditions of the occupant relative to a vehicle-fixed reference frame must be known. From these, the instantaneous state of displacements between body and vehicle elements, and hence the interaction forces, may be determined. Further, the instantaneous interaction forces thus found, together with the motion equations of classical mechanics, namely Newton's Laws, determine the instantaneous accelerations as $a = F/m$, or $\{a\} = [M]^{-1} \{F\}$ in a vector formulation. Integration of the accelerations then yields the occupant velocities and positions at a new time, different from the time at which forces were determined by an arbitrarily small amount, dt or Δt . New position and velocity conditions having been determined, new deflections can be determined and so forth so that the entire time histories for motion and forces are established.

The vector $\{F\}$ in block 4 of Figure 6-1 is a function of position and velocity coordinates and the interaction forces from block 3. The interaction forces include restraint system loads, which are discussed in Modules 9 and 10, and "contact forces," with which this module deals. Contact forces are those forces resulting from direct interaction between body parts or between a body part and a surface of the occupant compartment. Figure 6-1 indicates in block 1 that occupant and vehicle positions and velocities must be known before interaction forces may be determined. Modules 2, 4, and 7 are relevant to occupant conditions for block 1, and pertinent vehicle specifications are described in Modules 5 and 8.

The subject of this module is determination of contact-interaction deflections and resulting forces in blocks 2 and 3. A logically

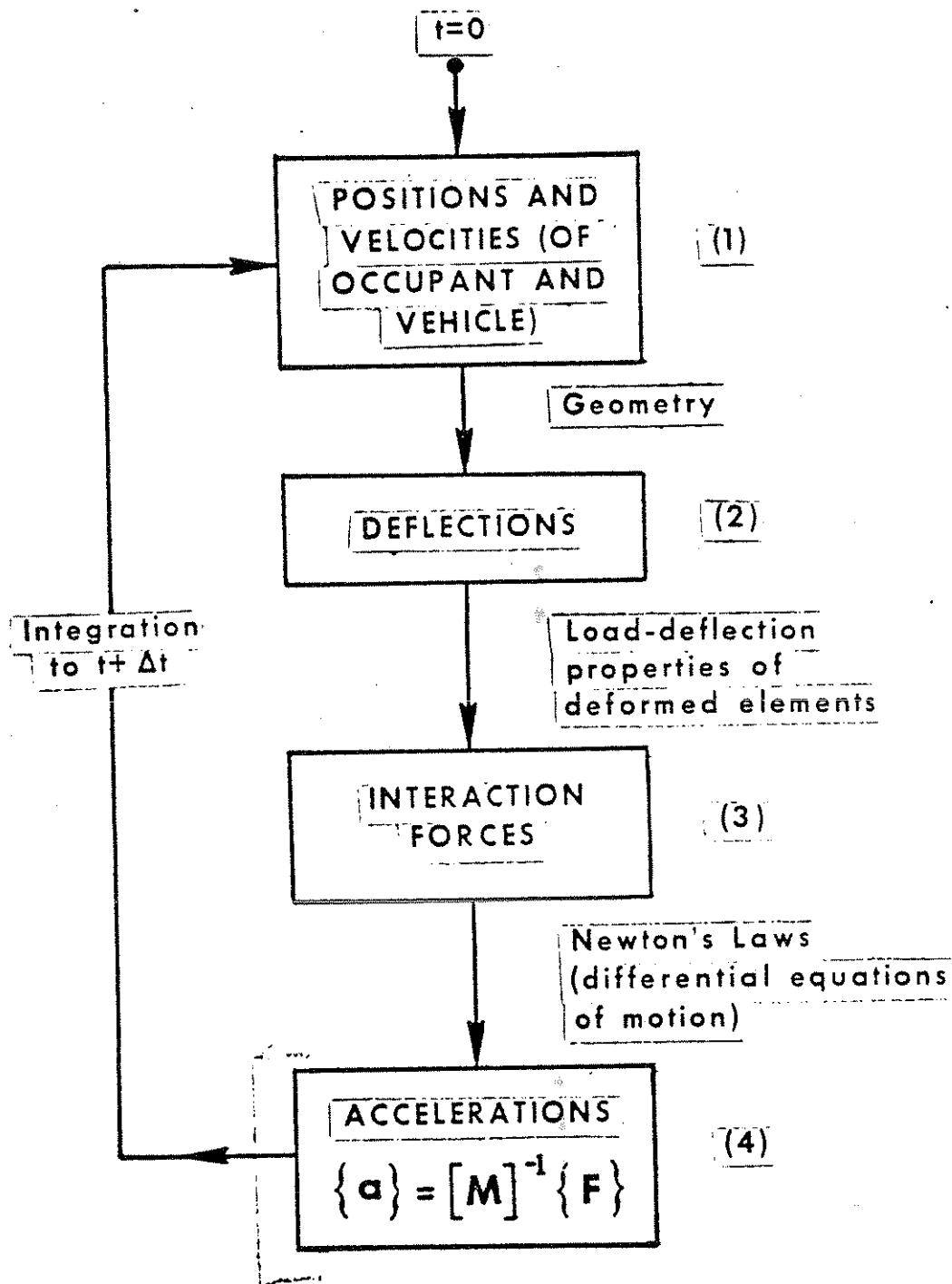


FIGURE 6-1 Relationship of Position Conditions and Interaction Forces Within the Framework of an Initial Value Problem

ordered development of contact forces by the computer model is a necessity. A description of these same ordered steps is a suitable framework for the explanation of related input requirements for the MVMA-2D model. Thus, the development shown in Figure 6-2 is both a flow for the computational algorithm and an outline of this module.

6.2 Determination of Deflections

6.2.1 Ellipse Against Line Segment. Module 4 describes the user-supplied profile of contact-sensing ellipses which may be attached to the occupant linkage. The prescription of line segments which constitute the vehicle-interior profile is described in Module 5. A contact force vector is generated whenever a body ellipse intersects a line segment. Figure 6-3 illustrates such a case. The deflection δ is defined as the distance of maximum penetration of the ellipse beyond the line. Note from the lower figure that this definition still applies if the body ellipse has passed completely beyond the resisting surface.

The user may find it useful occasionally to be able to evaluate a deflection for given ellipse and line segment positions. This might be done if accuracy is desired for defining the initial occupant configuration* or in connection with debugging a computer simulation. The pertinent equations are presented in Figure 6-4 and 6-5 for reference and may also be found in Volume 1 of the MVMA-2D manuals and in Module 7. The body link angles in these equations are the internal angles, generalized coordinates, defined in Module 7 and illustrated in Figure 6-6. Whether the deforming element in a contact interaction is the ellipse or the line segment is not implicit in the definition of deflection. This is dependent upon material specifications. Figure 6-4 illustrates a rigid ellipse against a deforming line segment, but with different material specifications the deflection could be shared or could be solely in the ellipse.

*See Module 7.

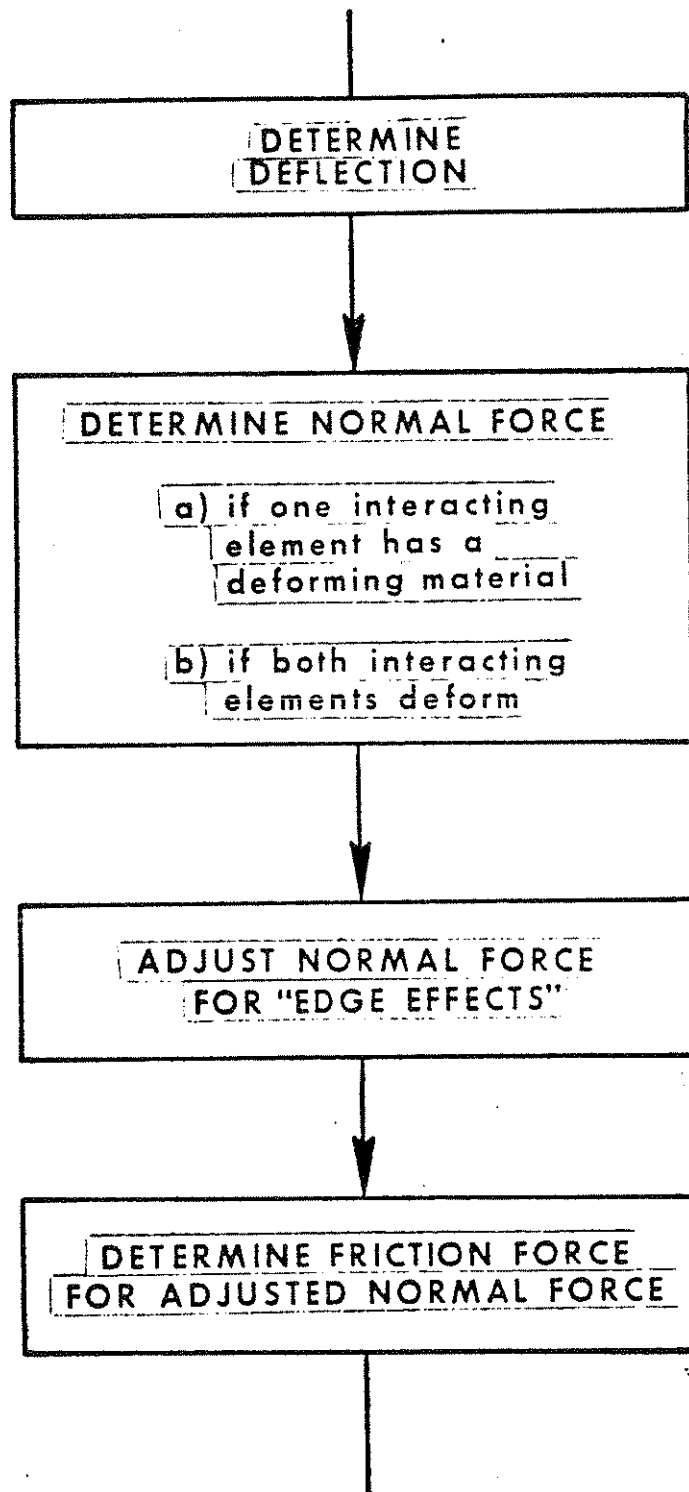


FIGURE 6-2 Development of Interaction Forces

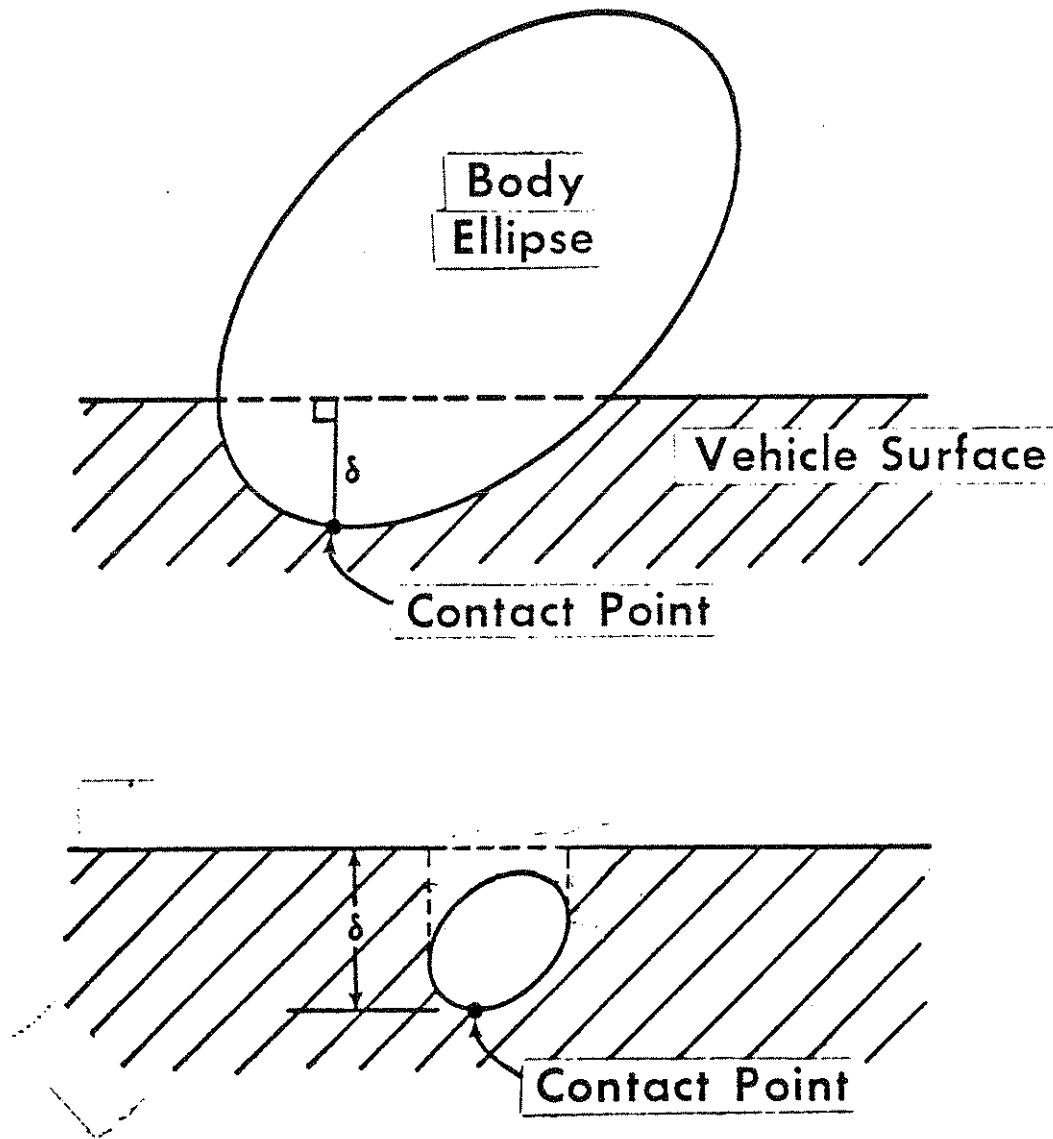
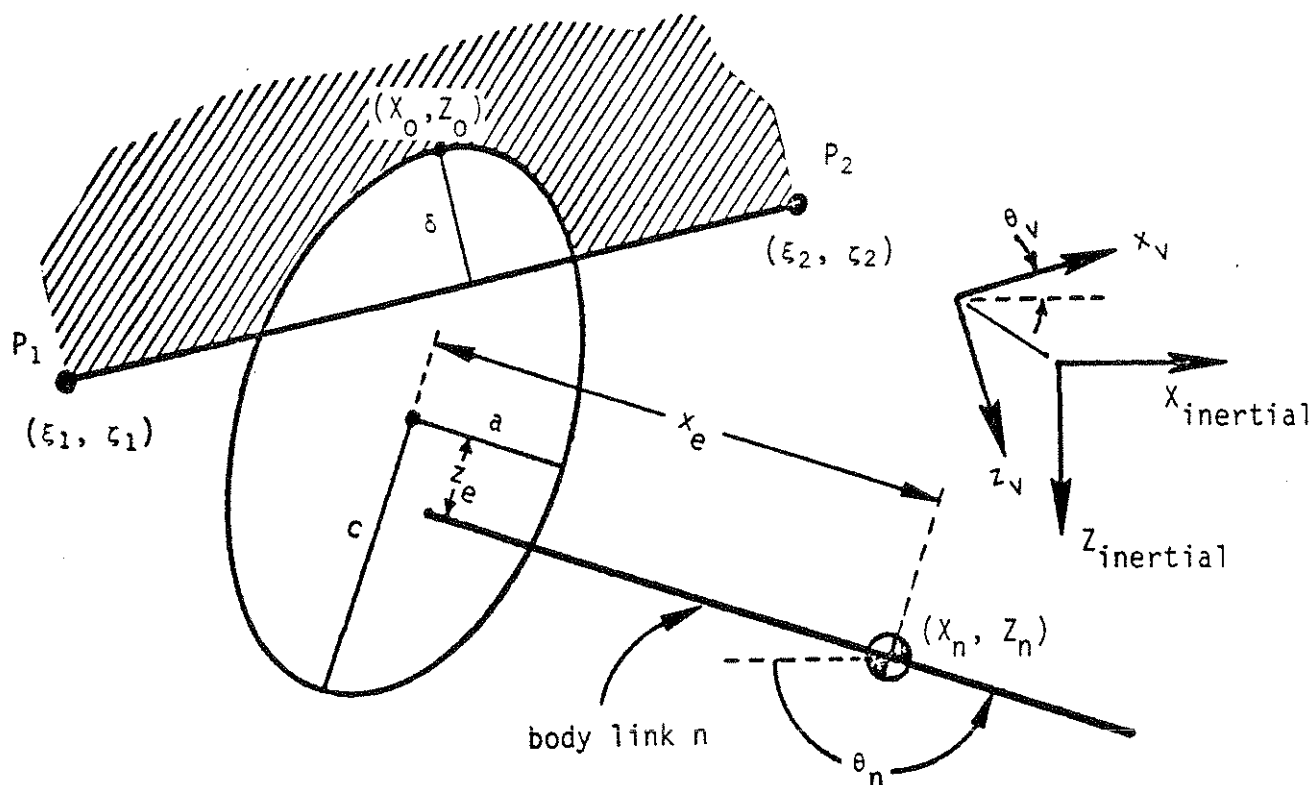


FIGURE 6-3 Deflection Between a Straight-Line Segment and an Ellipse



Definitions

- n = body segment number for the ellipse (1, ..., 8) (Card 219, field 5).
- a = x-semi-axis length (Card 220, field 5).
- c = z-semi-axis length (Card 220, field 6).
- θ_n = angle of body link n (see Card 301 for $t = 0$ and Figure 6-5).
- θ_v = vehicle pitch angle (see Card 601 for $t = 0$ and Card 604).
- (x_e, z_e) = coordinates of ellipse center in body segment system (Card 220, fields 3 and 4).
- (ξ_i, ζ_i) = coordinates of line-segment endpoint P_i ($i = 1, 2$) in vehicle system (Card 411, fields 4-7).
- (x_n, z_n) = inertial coordinates of CG of body segment n [function of x_2 and z_2 (from Card 303 for $t = 0$), body link angles (see Card 301 for $t = 0$ and Figure 6-5), and link lengths (Cards 201 and 202); see Section 2.1 of Volume 1].
- (u_4, u_5) = inertial coordinates of ellipse center.
- (x_0, z_0) = inertial coordinates of contact point.
- δ = deflection.

FIGURE 6-4 Constants and Variables Relevant to Evaluation of Ellipse-Line Deflection

EQUATIONS

$$p = \xi_2 - \xi_1$$

$$r = \zeta_1 - \zeta_2$$

$$s = \xi_1 \zeta_2 - \zeta_1 \xi_2$$

$$A = r \cos \theta_v + p \sin \theta_v$$

$$C = -r \sin \theta_v + p \cos \theta_v$$

$$D = s$$

$$\mu_1 = \frac{1}{2}(a^2 \cos^2 \theta_n + c^2 \sin^2 \theta_n)$$

$$\mu_2 = \frac{1}{2}(c^2 - a^2) \sin \theta_n \cos \theta_n$$

$$\mu_3 = \frac{1}{2}(a^2 \sin^2 \theta_n + c^2 \cos^2 \theta_n)$$

$$\mu_4 = X_n + X_e \cos \theta_n + Z_e \sin \theta_n$$

$$\mu_5 = Z_n - X_e \sin \theta_n + Z_e \cos \theta_n$$

$$k = \sqrt{\frac{2}{\mu_1 A^2 + 2\mu_2 AC + \mu_3 C^2}}$$

$$X_o = \mu_4 \pm k (\mu_1 A + \mu_2 C)$$

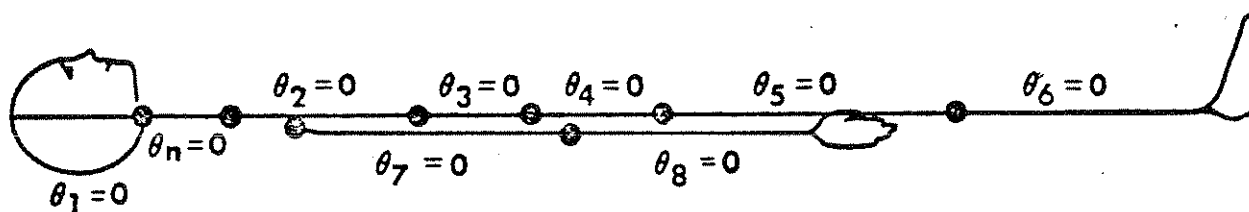
$$Z_o = \mu_5 \pm k (\mu_2 A + \mu_3 C)$$

One sign for k gives the point of maximum penetration, the "contact point." The other sign gives the point directly opposite the ellipse center, i.e., the point of "minimum penetration."

$$\delta = \left| \frac{Ax_o + Cz_o + D}{\sqrt{A^2 + C^2}} \right|$$

FIGURE 6-5 Evaluation of Deflection Between a Straight-Line Segment and an Ellipse.

$\theta_1, \theta_2, \theta_3, \theta_4, \theta_5, \theta_6, \theta_7, \theta_8, \theta_n = 0$ (analysis and computer code)



Analysis
or Code

Input or Output

$$\theta_i = \theta_i + \theta_v - 180^\circ \quad (i = 1, 2, 3, 4, n)$$

$$\theta_i = \theta_i + \theta_v \quad (i = 5, 6, 7, 8)$$

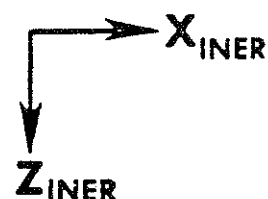


FIGURE 6-6 Occupant Model Configuration with all Internal Link Angles Equal to Zero (NOT for input or output)

6.2.2 Ellipse Against Ellipse. Module 4 explains how ellipses attached to different body segments are approximated, for the purpose of considering potential interactions between ellipses, by circles of varying position. An ellipse-ellipse contact force will be produced if the ellipse replacement circles overlap.

Figure 6-7 illustrates contact interactions between replacement circles for progressively greater deflections. In each instance, R and r are the radii of the circles, and D is the distance between their centers. A resulting force is applied to the body link of each ellipse as a vector along the line between the centers of the circles.

6.3 Material Properties

Contact forces in the MVMA-2D model are directly dependent on deformations of the interacting elements but not on deformation rates. The user prescribes for each body-segment ellipse and each vehicle-interior region a material with resistive properties that depend only on deflection. This is not to say that the loading history of a material is not considered; deformations beyond a user-defined yield point, or "elastic limit," can result in hysteretic energy loss and permanent deformation of the element upon unloading. Also, reloading from a partially unloaded state is complex.

The various material properties that can be specified by the user are described in the following sections. Data cards referenced here are 403 through 408, which are implied in Volume 2 of the MVMA-2D manuals to be for region materials since they appear with region cards 401 and 402. However, material property specifications for ellipses and belts have the same form.* Ellipse material cards, 221 through 226, and belt cards, 704 through 709, can be identified with the region material cards, 403 through 408. Strictly, it is unnecessary ever to use any cards but 403 through 408 to specify the properties of a material since these cards contain no reference to regions.

* Belt material specifications can be made optionally in terms of strain, instead of deflection.

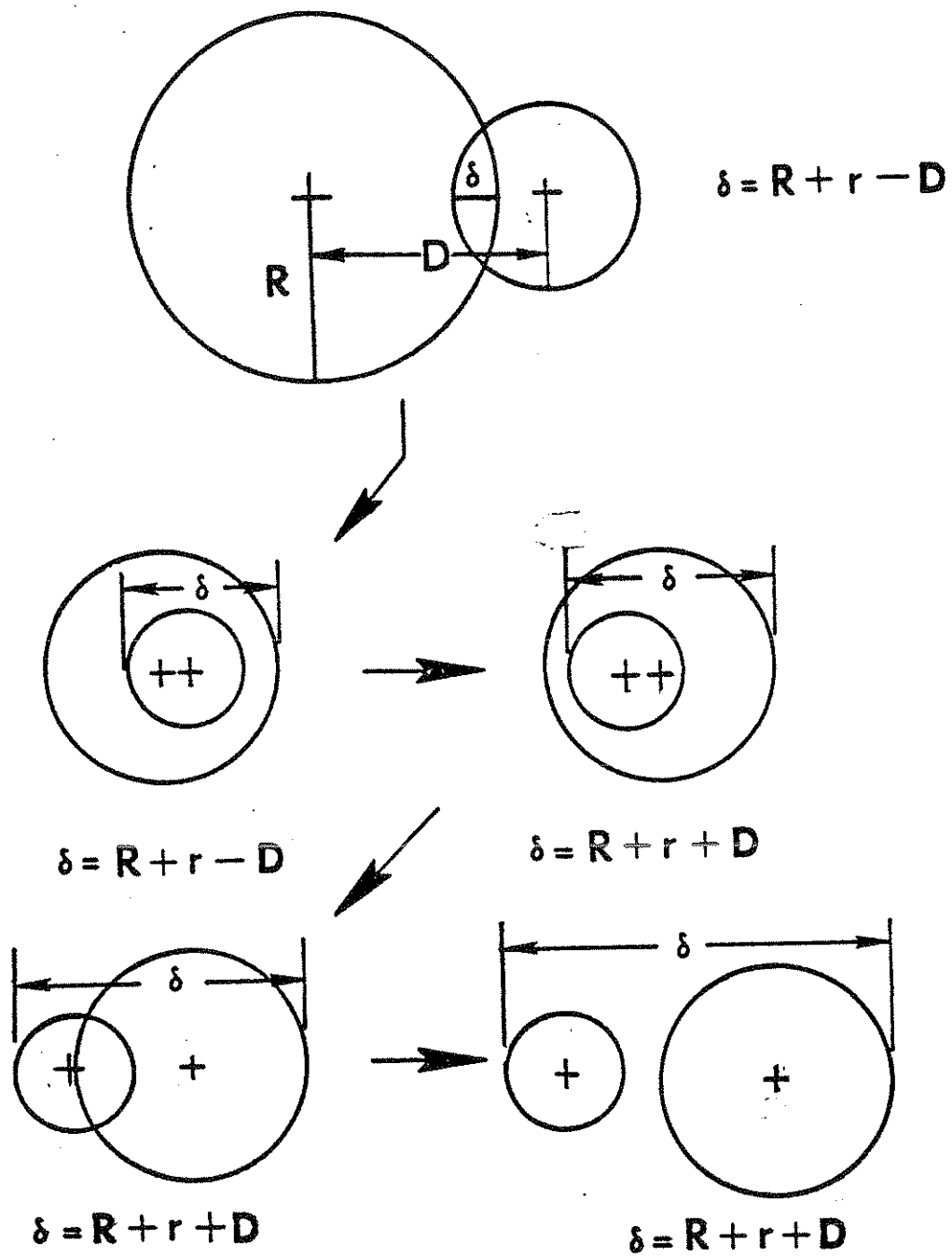


FIGURE 6-7 Deflection Between Ellipse Replacement Circles

Conversely, Cards 221 through 226, for example, could be used for a region material.

6.3.1 Loading: Static Curve. An element is undergoing "loading" whenever its material deformation is increasing with time. Note that this does not mean that the load, or force, is necessarily increasing with time or with deflection. The user is required to prescribe a static loading curve for each material name defined within the data set.*

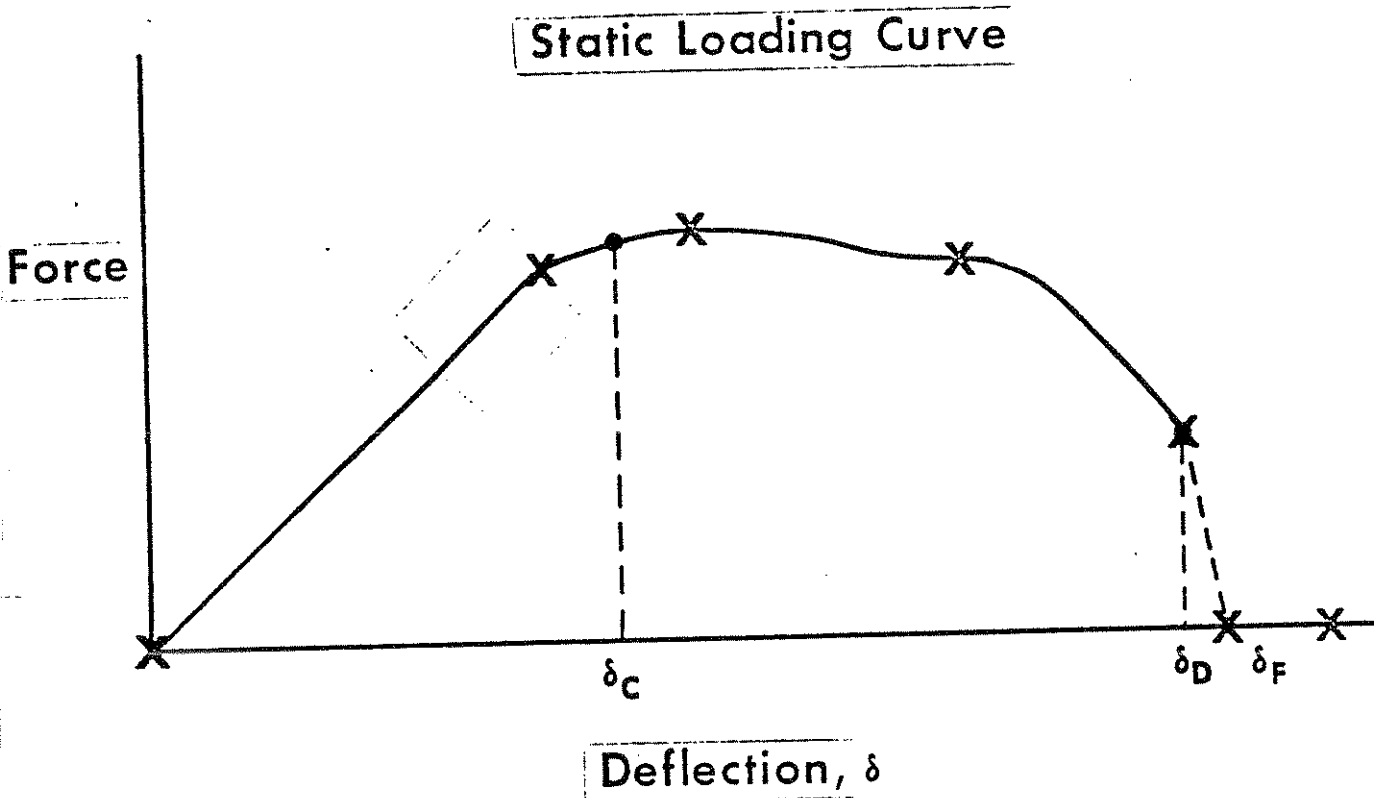
Suppose that an element is tested in quasi-static loading by pressing against it a rigid form, either flat, elliptical, or circular in shape in accordance with the definitions of deflections earlier in this module. A load-deflection curve such as illustrated in Figure 6-8 could be established. It can be represented as accurately as necessary by a piecewise-linear approximation. For example, the curve shown is adequately defined for simulation purposes in tabular form by coordinate pairs of force and deflection values of the points marked with an "X." The user may prescribe a tabular static loading curve or, optionally, a polynomial curve of order six, viz.,

$$F = C_1\delta + C_2\delta^2 + C_3\delta^3 + C_4\delta^4 + C_5\delta^5 + C_6\delta^6.$$

The tabular form of the curve is generally used, but sometimes it is convenient to fit a polynomial to the load-deflection data. Seldom are more than the first three coefficients used. The most common use of the polynomial is for specifying a constant load-deflection slope C_1 with all other coefficients zero. C_1 is a proportionality factor between force and deflection, i.e., a linear spring stiffness. An equivalent way of defining a linear load-deflection curve is to enter a two-point table; the first point would be (0., 0.) and the second would be ($C_1 \Delta$, Δ), where Δ is an arbitrary value of deflection greater than the greatest deflection expected for the material in a simulation:

Three points pertinent to continued static loading are labeled

* Material names are defined on Card 219 for ellipses, Card 401 for regions, and Cards 702, 703, and 710-716 for belts.



δ_c = yield point (elastic limit)

δ_D = breaking point

δ_F = end of breakdown curve

FIGURE 6-8 Static Loading Curve

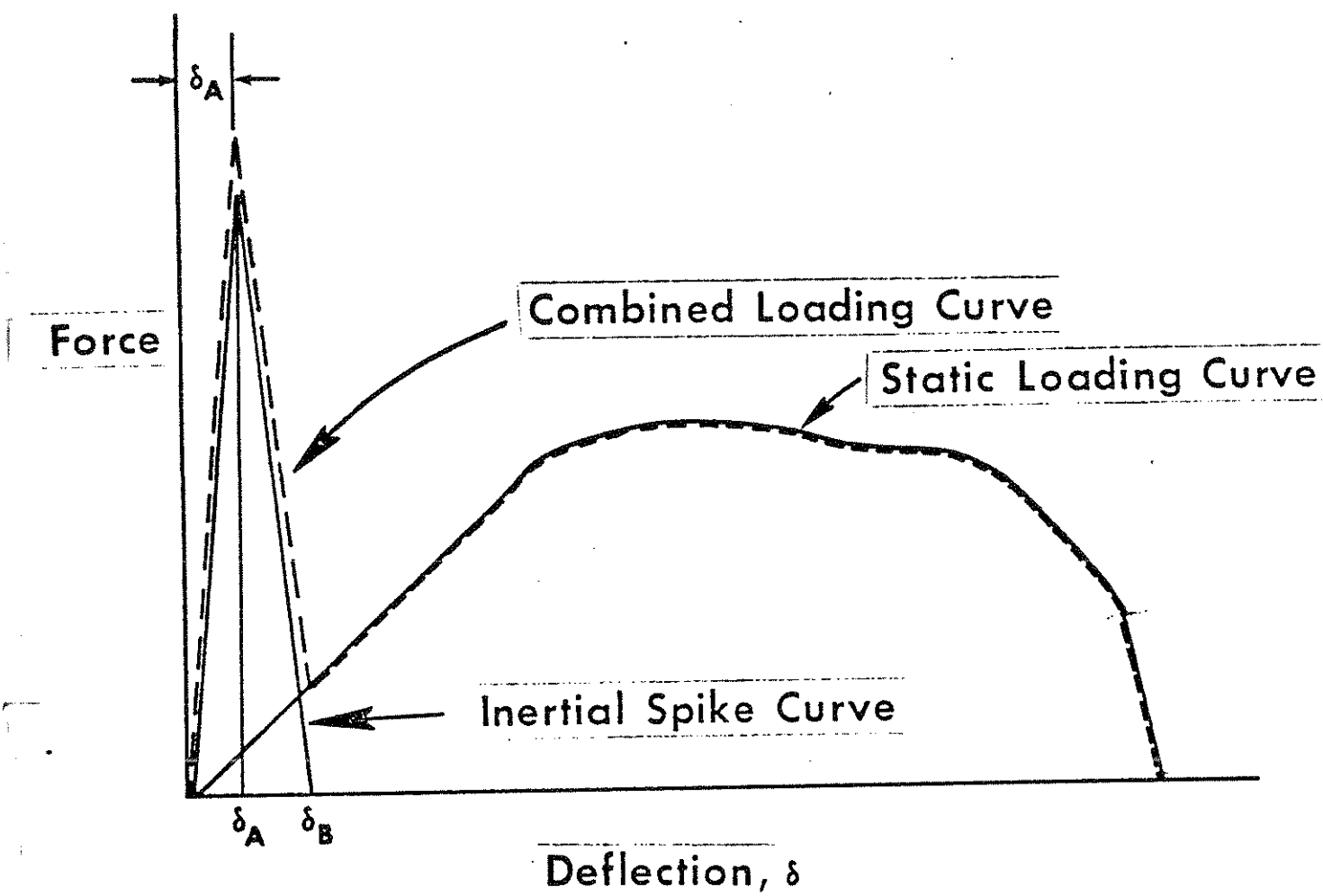
in Figure 6-8. These are deflections δ_C , δ_D , and δ_F , all user-defined input parameters. δ_C is deflection at the material yield point, or "elastic limit." Note that it is not identified with the limit of material linearity. Its proper definition relates to characteristics of the material in unloading. Unloading from peak deflections less than δ_C are backward along the loading curve, i.e., they occur without permanent deformation of the material and without energy loss. There are no restrictions on δ_C except that it be greater than or equal to zero.* The deflections δ_D and δ_F relate to material, or structural, breakdown. All points on the user-defined static loading curve beyond δ_D are ignored by the computer model. This value is the deflection at which the material begins to fail. Continued loading to δ_F or beyond will complete breakdown of the material, as illustrated in the figure.**

6.3.2 Loading: Inertial Spike Curve. The so-called "inertial spike curve" is a model feature which can be used to account for dynamic effects on the force-producing capability of a material. This is the only model feature through which mass- and rate-dependence of material properties can be represented, even indirectly. It is observed that initial impact against a deforming surface is often accompanied by a high force spike which diminishes rapidly with increasing deflection and which does not reappear with repeated loadings. Such an inertial spike force can be specified by the user as a tabular or polynomial function of deflection. This curve is added to the static load-deflection curve previously discussed.

Figure 6-9 illustrates an inertial spike curve and the combined loading curve. Values for δ_A and δ_B in the figure are supplied by the user. δ_A is the deflection at which inertial effects of the surface break down irreparably. This means that once deflection exceeds δ_A , subsequent re-loadings from deflections less than δ_A will be along the static curve, not the combined curve. δ_A is often

* All reasonable values of δ_C are less than δ_D .

** δ_F must be greater than δ_D .



$\delta_A =$ deflection at peak of inertial spike curve

$\delta_B =$ deflection at cutoff of inertial spike curve

FIGURE 6-9 Inertial Spike Curve

set either to zero or to the deflection at the peak of the inertial spike curve. There are no restrictions on its value, but certainly it is most reasonably set to some value less than or equal to deflection at the peak. δ_B is the deflection at which all inertial effects cease. The inertial spike curve, whether tabular or polynomial in form, must be zero at δ_B . δ_B must be in the closed interval from δ_A to δ_D : $\delta_A \leq \delta_B \leq \delta_D$.

6.3.3 Loading: Force Saturation. Figure 6-10 illustrates the loading curve for an element which deforms plastically once the load has reached a specific value. The force saturation level is at load F_{\max} , an input parameter. Force saturation affects only static loading. Whenever the saturation force limit is exceeded by the static curve, the regular loading sequence is superceded. The inertial spike curve is unaffected; if loading is on the combined static and inertial spike curve when F_{\max} is reached, only the static component will be limited to F_{\max} .

6.3.4 Unloading. An element is undergoing "unloading" whenever its material deformation is decreasing with time. While it is not necessarily true that force increases with deflection in a loading material, the decreasing deflection for unloading of a reasonably specified material will be accompanied by decreasing force. Figure 6-11 illustrates the loading curve for a material which surely requires specifications relating to unloading because unloading back along the loading curve from any deformation which exceeds δ_p would involve force increase for decreasing deflection. Unloading curves are calculated by the computer model from user-prescribed specifications. These are discussed in later sections of this module.

δ_C , the deflection at the material "elastic limit," was discussed earlier in this module. If material deflection once exceeds δ_C , then any subsequent unloading will not be back along the loading curve but instead will be along a curve which lies below the loading curve. It might be noted in connection with Figure 6-11 that, while there are no restrictions on the user-supplied value for δ_C , it cannot reasonably be greater than δ_p for a material with a loading peak as illustrated.

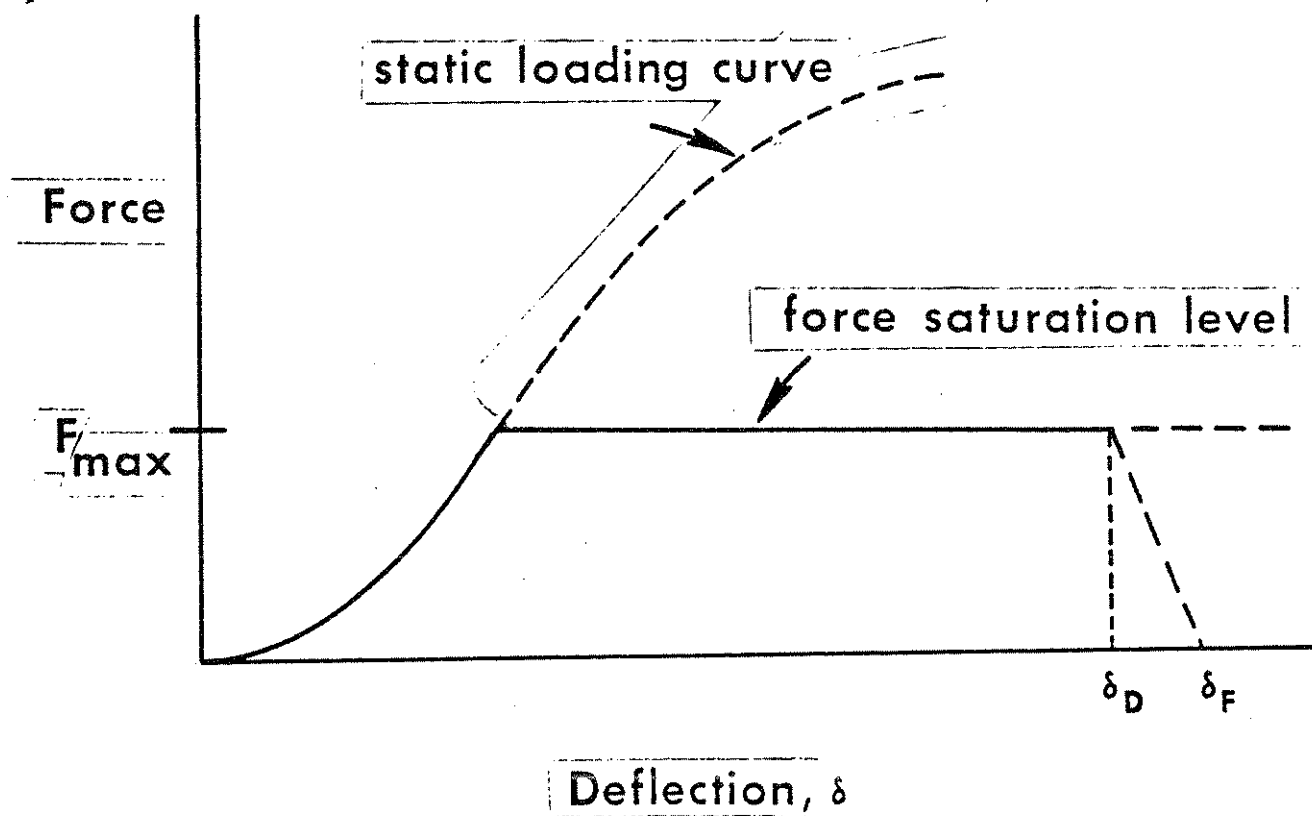


FIGURE 6-10 Static Loading Curve with Force Saturation

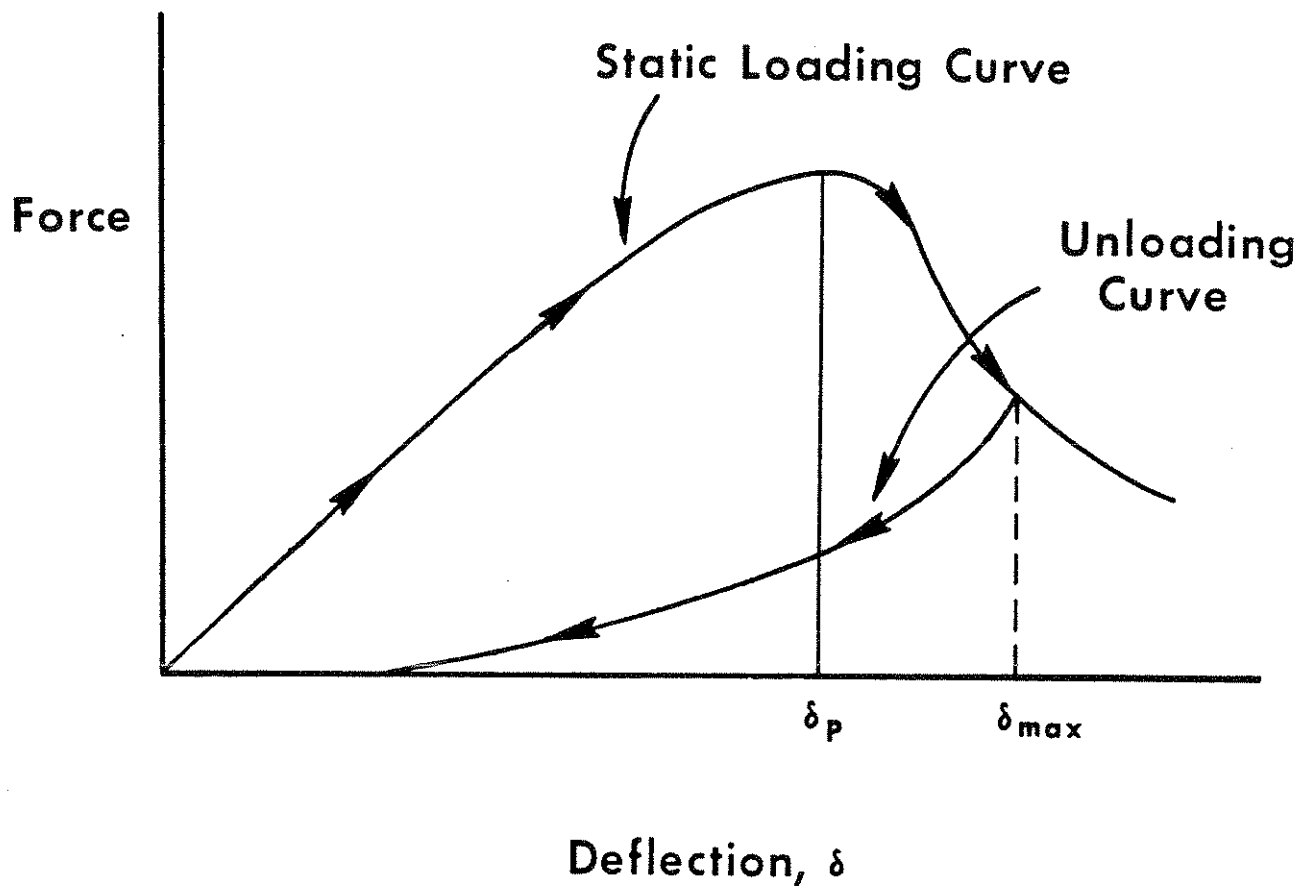


FIGURE 6-11 Unloading From Deflections Greater Than δ_p

6.3.5 Unloading: Permanent Deformation. Figure 6-12 illustrates unloading from a turnaround deflection δ_{\max} greater than δ_c . On complete unloading from beyond the elastic limit, the force usually returns to zero before the deflection. In other words, there is usually a permanent deformation of the surface, represented in the figure by the deflection ω .

In general, the permanent deformation increases with increasing turnaround deflections. The upper portion of Figure 6-13 illustrates the typical dependence of permanent deformation on deflection. For deflections up to the elastic limit, the permanent deformation is zero. As deflection increases without bound, the permanent deformation approaches the value of the turnaround deflection. This characteristic of the material is illustrated in a completely equivalent way in the lower figure. The lower curve is simply the upper curve divided by deflection, point for point.

$$G(\delta_{\max}) = \frac{\omega(\delta_{\max})}{\delta_{\max}} .$$

That is, the lower curve defines, as a function of δ_{\max} , a non-dimensional ratio of the permanent deflection to the turnaround deflection. This function is zero for deflections up to the elastic limit and approaches 1. as δ_{\max} increases without bound. The function has been called the "G-ratio," and in the MVMA-2D model it is a user-supplied input for each material. It may be entered in tabular form or it may be assigned a constant value. It should be noted, however, that a constant can be used with safety only if there are a priori reasons to expect a particular approximate maximum deflection of the material for the specific crash simulation. The reason for this is that for most materials the G-ratio changes rapidly with increasing deflection past the yield point.

6.3.6 Unloading: Hysteretic Energy Absorption. Figure 6-14 illustrates again an example loading-unloading cycle. Since the integral to δ_{\max} of the force times an incremental deflection, namely, the area under the static loading curve, is the work done in reaching the turnaround deflection, δ_{\max} , unloading along a

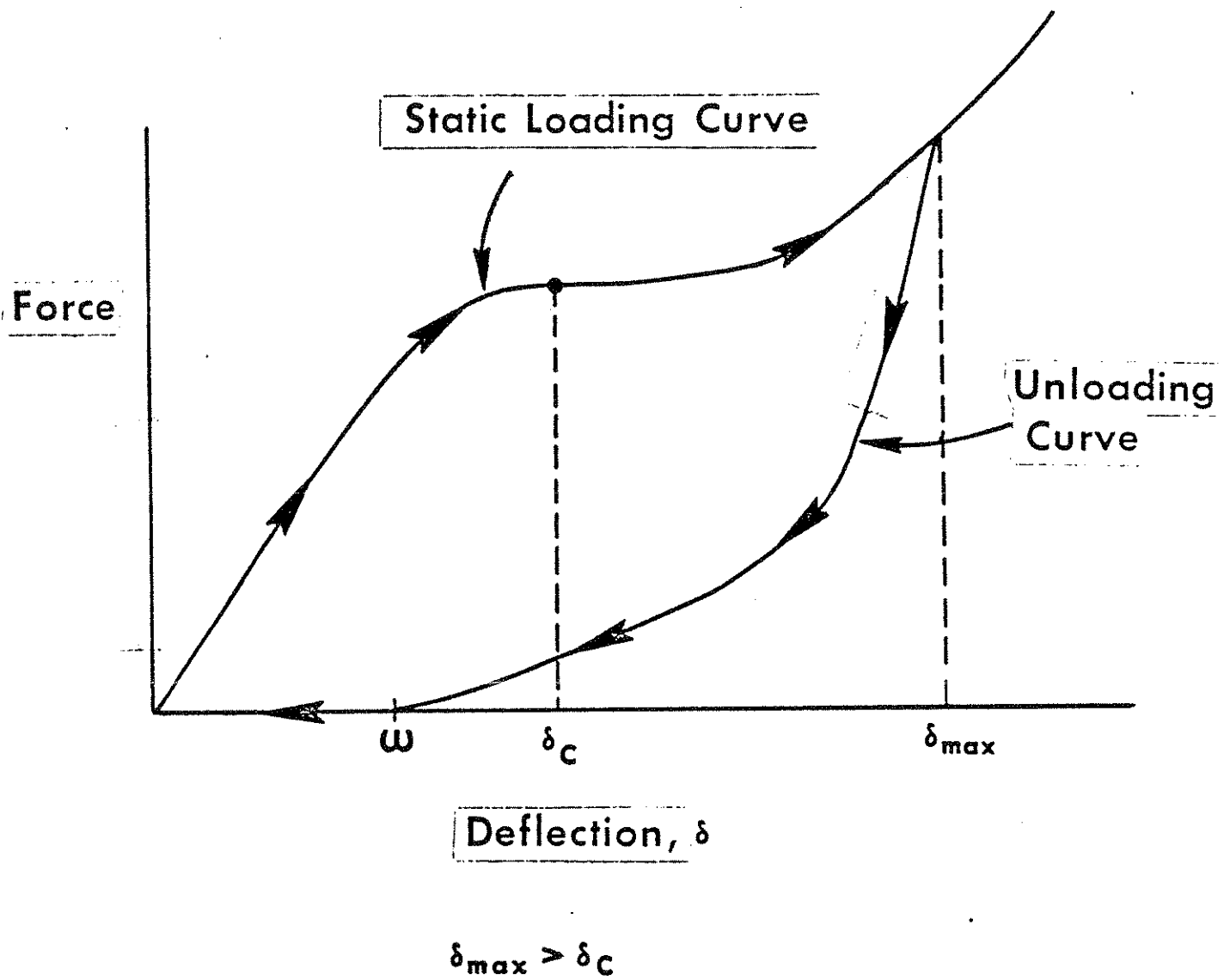


FIGURE 6-12 Unloading With Permanent Deformation from Deflections Greater Than δ_c

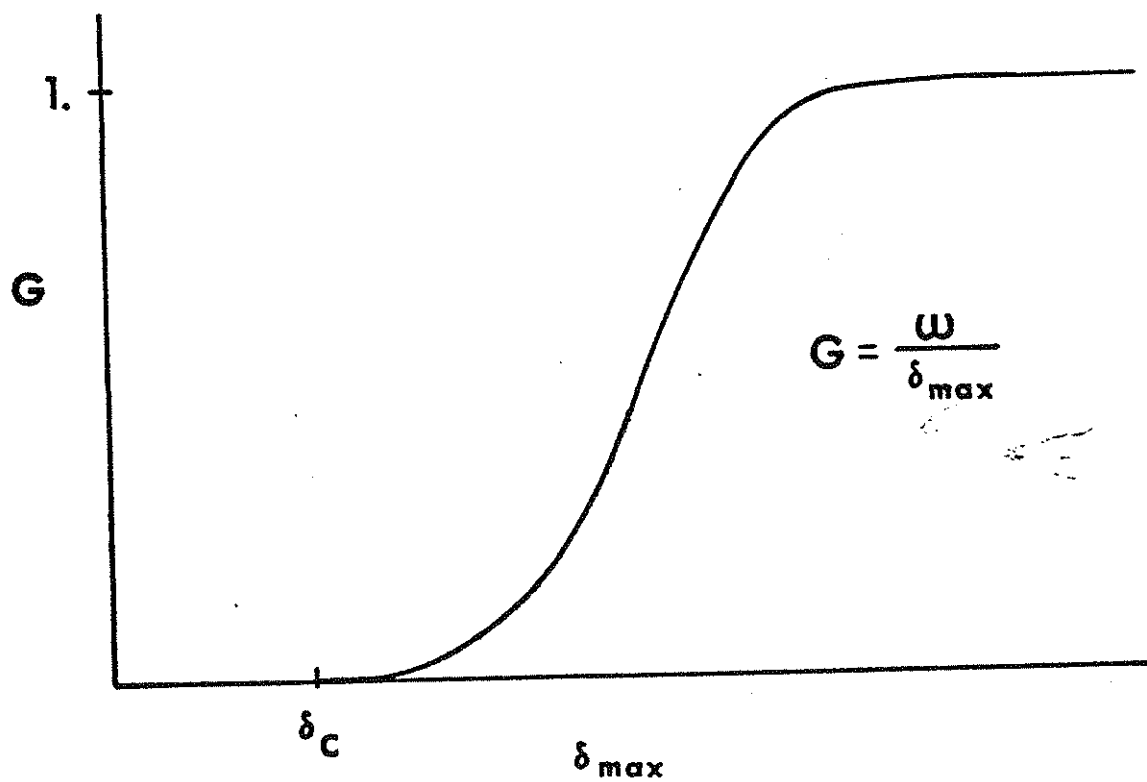
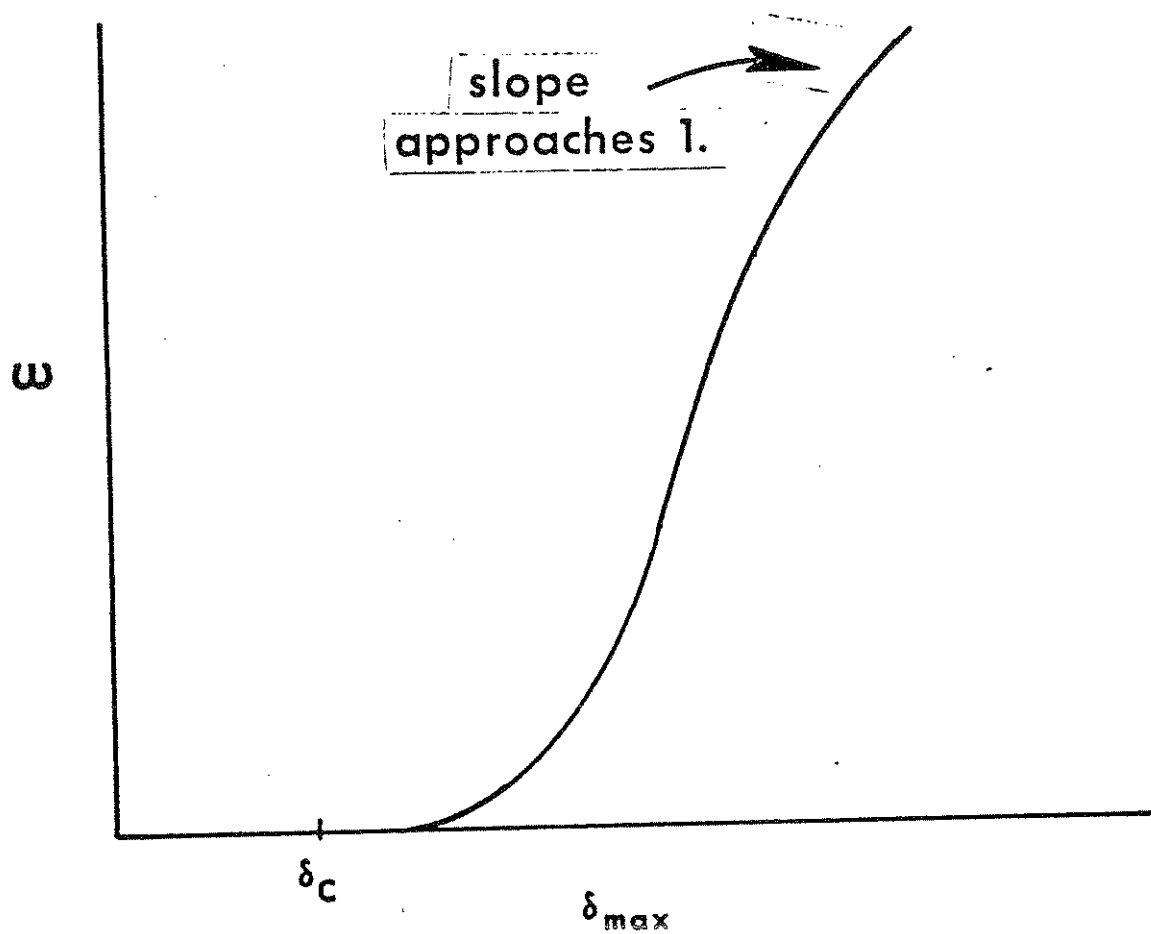


FIGURE 6-13 Permanent Deformation ω and G-ratio As Functions of Maximum Deflection

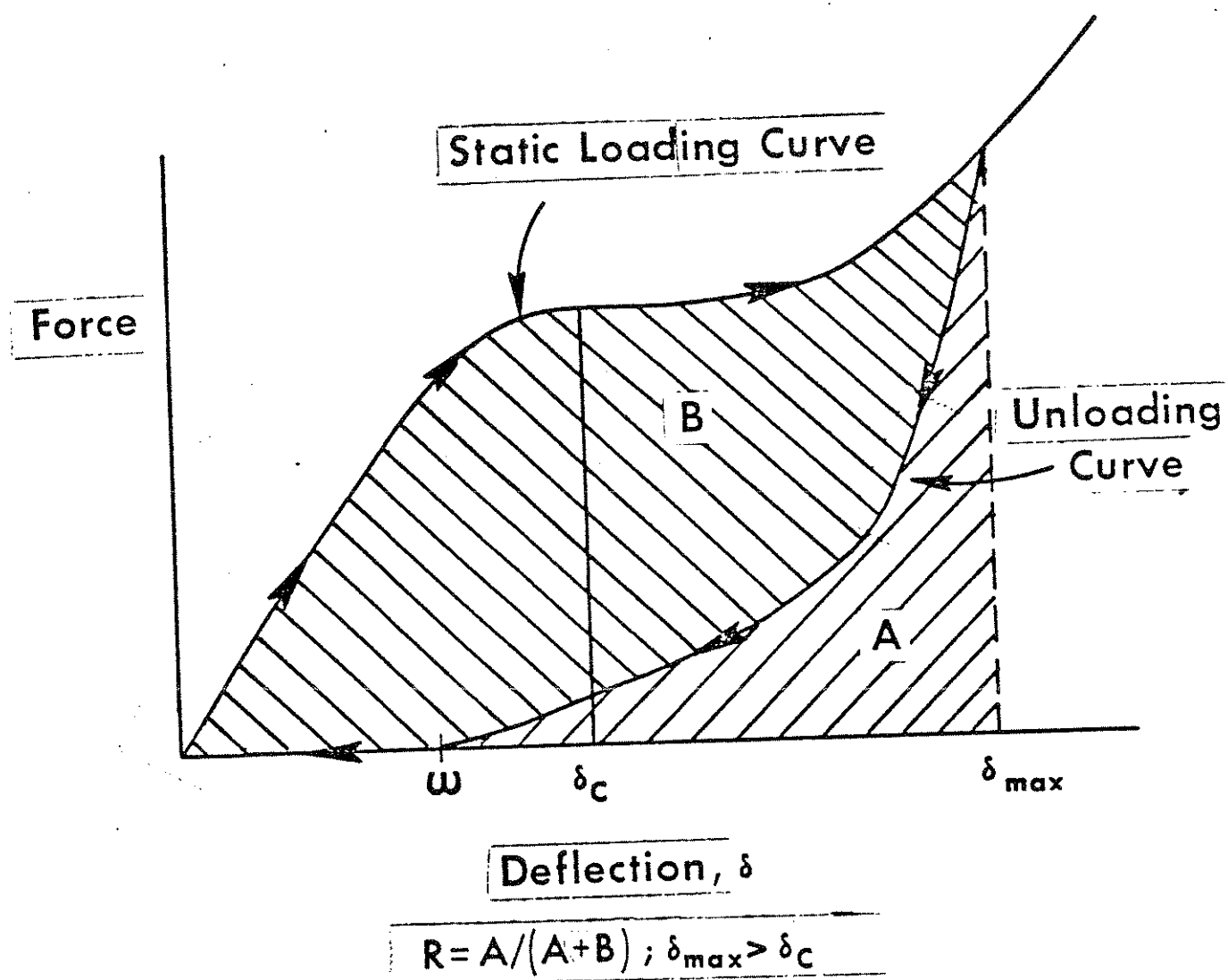


FIGURE 6-14 Unloading with Energy Loss from Deflections Greater Than δ_c

curve which lies under the loading curve means that there is a hysteretic energy loss. Energy is absorbed by heating or by mechanical breakdown of the material. In the figure, area B equals the absorbed energy. Area A is the restored, or conserved, energy. Just as permanent deformation is in general a function of turnaround deflection, so is the amount of energy restored upon complete unloading. For each material, a non-dimensional ratio of restored energy to total loading energy can be defined in parallel to the G-ratio for permanent deformation. This quantity is called the "R-ratio" and it is clearly a function of turnaround deflection, namely

$$R(\delta_{\max}) = \frac{A(\delta_{\max})}{A(\delta_{\max}) + B(\delta_{\max})}.$$

The model user supplies the R-ratio either as a tabular function of δ_{\max} or as a constant. Figure 6-15 illustrates the typical dependence of the R-ratio on δ_{\max} .

The R-ratio is used together with the G-ratio by the computer model for calculating an unloading curve whenever unloading from a deflection greater than δ_c begins. The unloading curve is normally quadratic in form, and its coefficients are determined so that unloading occurs with the appropriate permanent deformation and restored energy. Strictly, the G- and R-ratios are not independent quantities as there exists a constraint between their values. This is discussed in the last section of Module 6, Part 2.

6.3.7 Unloading: Force Saturation. Either of two types of unloading from a force-saturation level can be specified by the model user. Both are illustrated in Figure 6-16. The standard method is to unload with a specified slope, β , an input parameter. Alternatively, the G-ratio is used to determine a permanent deformation, to which unloading occurs along a straight-line segment.

6.3.8 Rigid-Rigid Interactions. Contact ellipses, vehicle-interior regions, and even belts can be specified as rigid by leaving blank fields of 219-Cards (fields 3 and 4), 401-Cards (3 and 4), the 702-Card (1 and 2), the 703-Card (1, 2, 5, and 6), and Cards 710

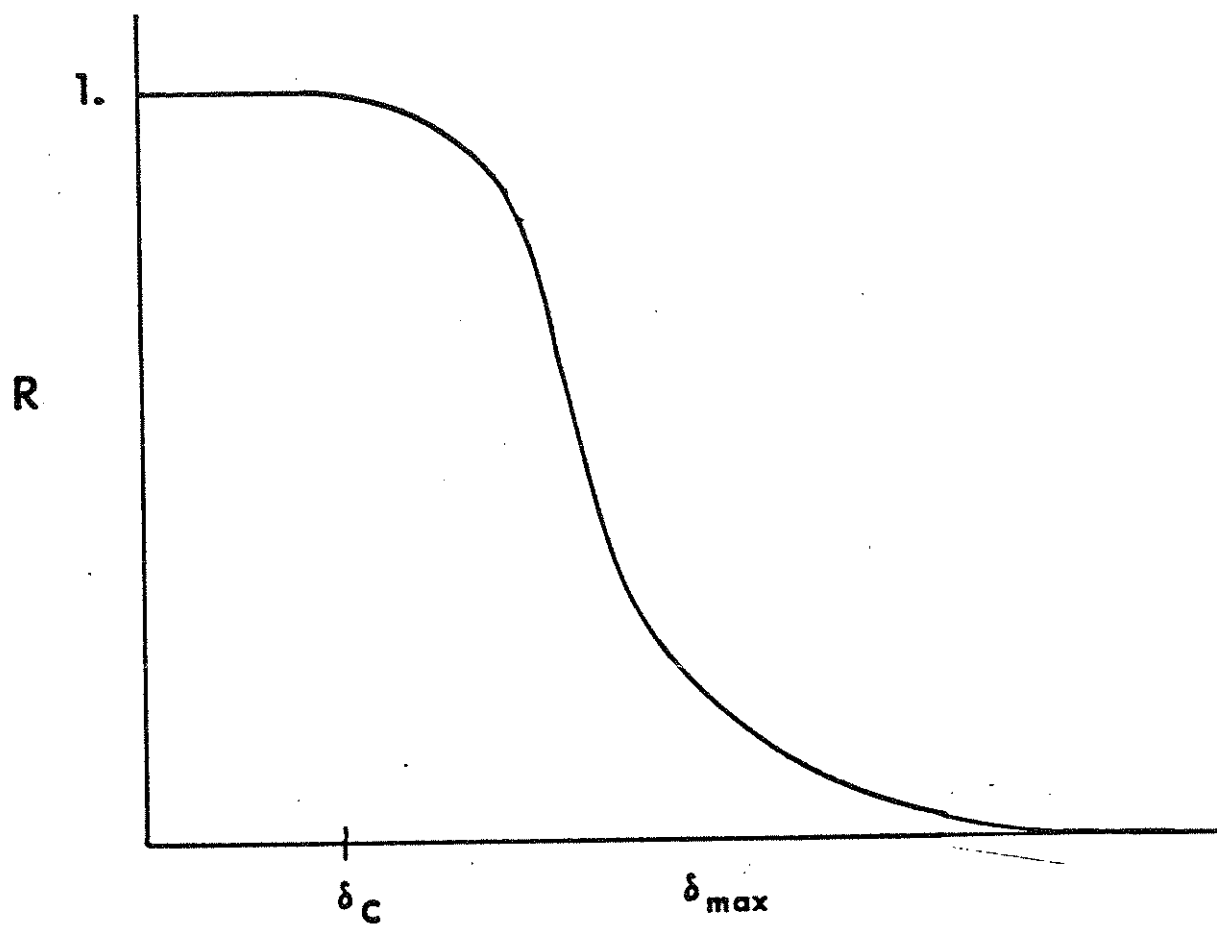


FIGURE 6-15 R-ratio as a Function of Maximum Deflection

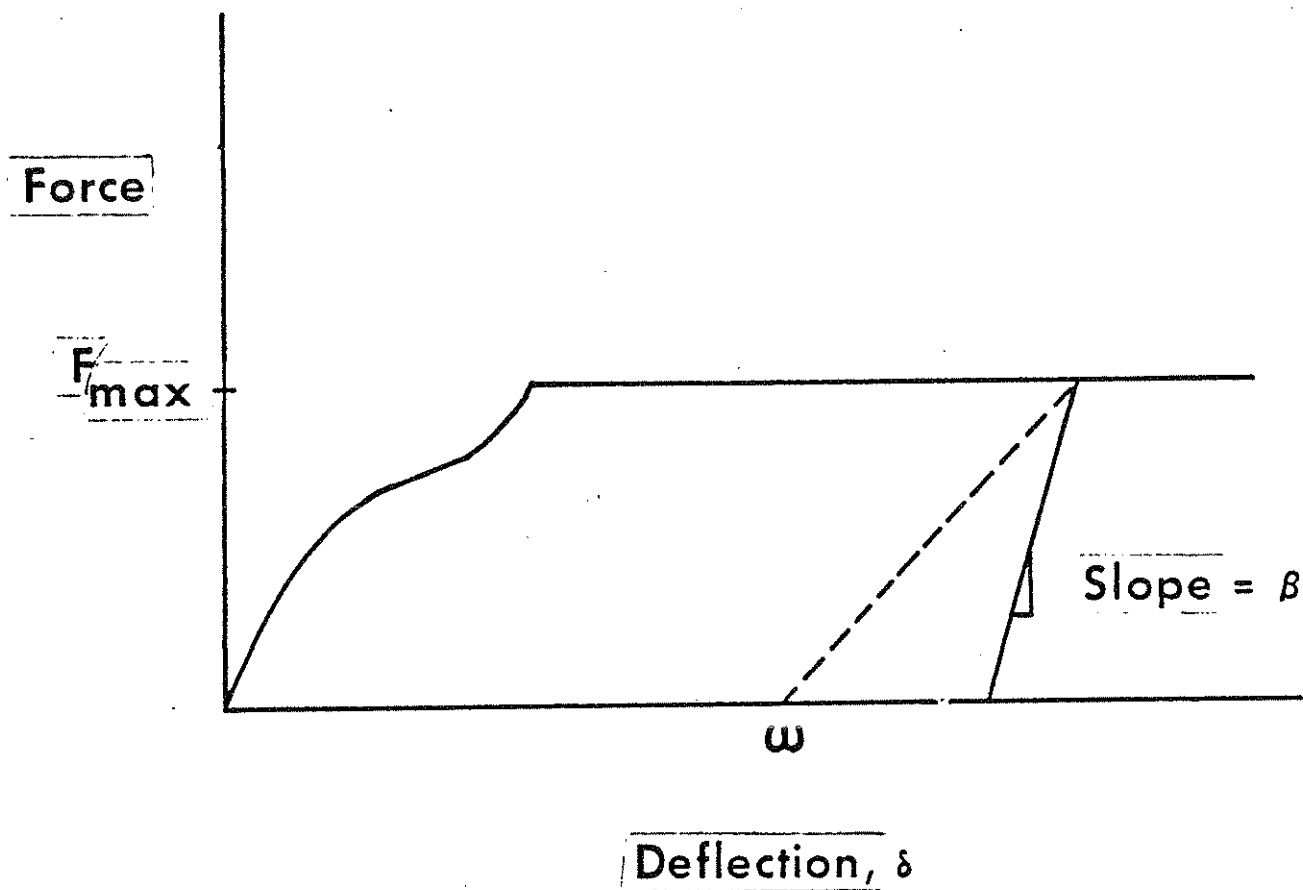


FIGURE 6-16 Unloading from Force Saturation

through 716 (6 and 7). If a rigid element interacts with a deformable element, then all deformation is attributed to the deformable element and its material properties are used. If, however, two rigid elements interact, then a special linear stiffness value is used. This value is user-defined and is usually taken as 15,000 lb/in. This stiffness is entered in field 4 of Card 103. A value is specified in field 3 of that card for a maximum allowed force for rigid-rigid interactions. Normally, a large value is used, such as 100,000 lbs.

6.3.9 Material Property Data Cards. All data which relate to the material properties discussed in the foregoing sections may be entered on Cards 403 through 408. The content of the pertinent fields of those cards will now be identified. Example data cards for windshield glass are shown in Figure 6-17.

There must be one 403-Card and one 404-Card for each material. The first two fields of these cards contain a sixteen-character alphanumeric material name. The deflection parameters δ_A , δ_B , δ_C , δ_D , and δ_F illustrated in Figures 6-8 and 6-9 are in fields 3 through 7 of Card 403. Required and suggested conditions to be imposed on the quantities have been previously discussed. The required conditions are, in summary:

$$0 \leq \delta_A \leq \delta_B \leq \delta_D < \delta_F; \text{ and } \delta_C \geq 0$$

Fields 8 and 9 of this card control force saturation, which is illustrated in Figure 6-16. The force saturation level is entered in field 8, and the slope of the desired straight-line unloading curve is in field 9. Any negative value entered in field 9 will cause the slope of the unloading curve to be determined from the G-ratio. If the force-saturation option is not to be used, then fields 8 and 9 must be zero or blank.

On Card 404, the user defines eight-character alphanumeric names in fields 7 and 8 for the static and inertial spike loading curves. The single name entered in field 9 is used for both G- and R-ratios. All three of these eight-character names must be defined for each material. Field 3 is the only other pertinent field on the 404-Card. It contains the allowed convergence error for force balance between

WINDSHIELD GLASS.5	1.	0.	100.	101.	0.	0.	403
WINDSHIELD GLASS5.				WS	WI	WGR	404
WGR	0.	0.					405
WGR	.5	0.					405
WGR	.51	.85					405
WGR	1.	.95					405
WGR	6.	.99					405
WGR	0.	1.					406
WGR	.5	1.					406
WGR	.51	.1					406
WGR	1.	.05					406
WGR	6.	.01					406
WS	-1.	108.8	50.0	-10.9	1.		407
WI	-1.	3000.	1000.	-8000.	4000.		408
SEATCUSHION MATL5.				SSTAT	I	CUSHGR	404
SEATBACK MATL	5.			SSTAT	I	BACKGR	404
MATERIAL NAME	5.			STATIC	I	GRNAME	404
I	-1.	0.					408

FIGURE 6-17 Example Material Property Data Cards

mutually deforming surfaces. This is discussed in Module 6, Part 2. A value of 5. lbs. is usually suitable.

At least one 405- and one 406-Card must be present in the data deck for each G- and R- name on any 404-Card, in field 9. G- and R-ratio values are entered on 405- and 406-Cards, respectively. Table points for piecewise-linear representation of G and R curves such as illustrated in Figures 6-13 and 6-15 are entered in fields 2 and 3, the deflection value in field 2 and the G or R value in field 3. There will be one card for each table point. Should it be desired to specify a constant value, independent of deflection, then any negative value is entered in field 2 and the constant value for G or R is in field 3. The G-ratio should never be set to 1. nor should the R-ratio be 0.

The static loading curve may be specified as described earlier as a tabular or polynomial function of deflection. A curve must be prescribed for each static curve name on any 404-Card, in field 7. Curve specifications are made on 407-Cards, which contain the eight-character static curve name in field 1. If the force is to be a polynomial function of deflection, then a negative value is entered in field 2 and the polynomial coefficients for the first six powers of δ are entered in fields 3 through 8. Since a field may be left blank in place of entering a zero, and since a linear stiffness is often assumed, i.e., $F = C_1\delta$, it is common to leave all coefficient fields blank except for field 3. A tabular static curve is prescribed point-by-point, one 407-Card per table point. The deflection value is entered in field 2 and the force value is in field 3. As for all tables which the model user may define, the first point must be for a zero abscissa value -- in this case, zero deflection.

The inertial spike curve is prescribed in just the same manner as the static loading curve. Field 1 in this case contains the inertial spike name from field 8 of a 404-Card. The inertial spike curve should go to zero at a deflection of δ_B , which is entered on the 403-Card. The user should be able to demonstrate that the polynomial curve specified on the 408-Card of the example data peaks at 1000 lb. at a deflection of .5 inches. The onset slope, 3000 lb/in, is

50% greater than the slope of straight-line rise to peak force. The curve diminishes to 0. at a deflection of 1. inch.

It should be made clear to the user that static and inertial spike loading curves and G- and R-ratio functions defined with Cards 405 through 408 need not be unique to a material. In other words, these curves can be shared by materials. The example data in Figure 6-17 illustrate 404-Cards for seat cushion and seatback materials that have the same loading characteristics but different G- and R-ratios for unloading. Since the inertial spike feature is not used for most materials, it is often convenient to define it once as zero, as shown in the last card (408) in the example data. The name on the 408-Card may then be used wherever needed for 404-Cards, in field 8. It is also worth mentioning that the material itself need not be unique to an ellipse or region. Any number of ellipses and regions may be assigned the same material properties by referencing the same sixteen-character material name.

MODULE 6 -- GENERATION OF CONTACT FORCES ON THE OCCUPANT: Part 2

6.4 Shared Deflection

Whenever two deformable elements contact each other, both will deform. In the MVMA-2D model, this is called "shared deflection" or "mutual deformation." Figure 6-18 illustrates such an interaction for an ellipse and a line segment. Interacting ellipses could be considered just as well. Given only the position of the ellipse and the position of the line, the total deflection δ is determined. The component deflections δ_1 and δ_2 , however, depend on the material properties of the interacting elements. The compressive forces in the elements will be equal. Therefore, in order to determine the interaction force F , the computer model solves the following equations for δ_1 and δ_2 :

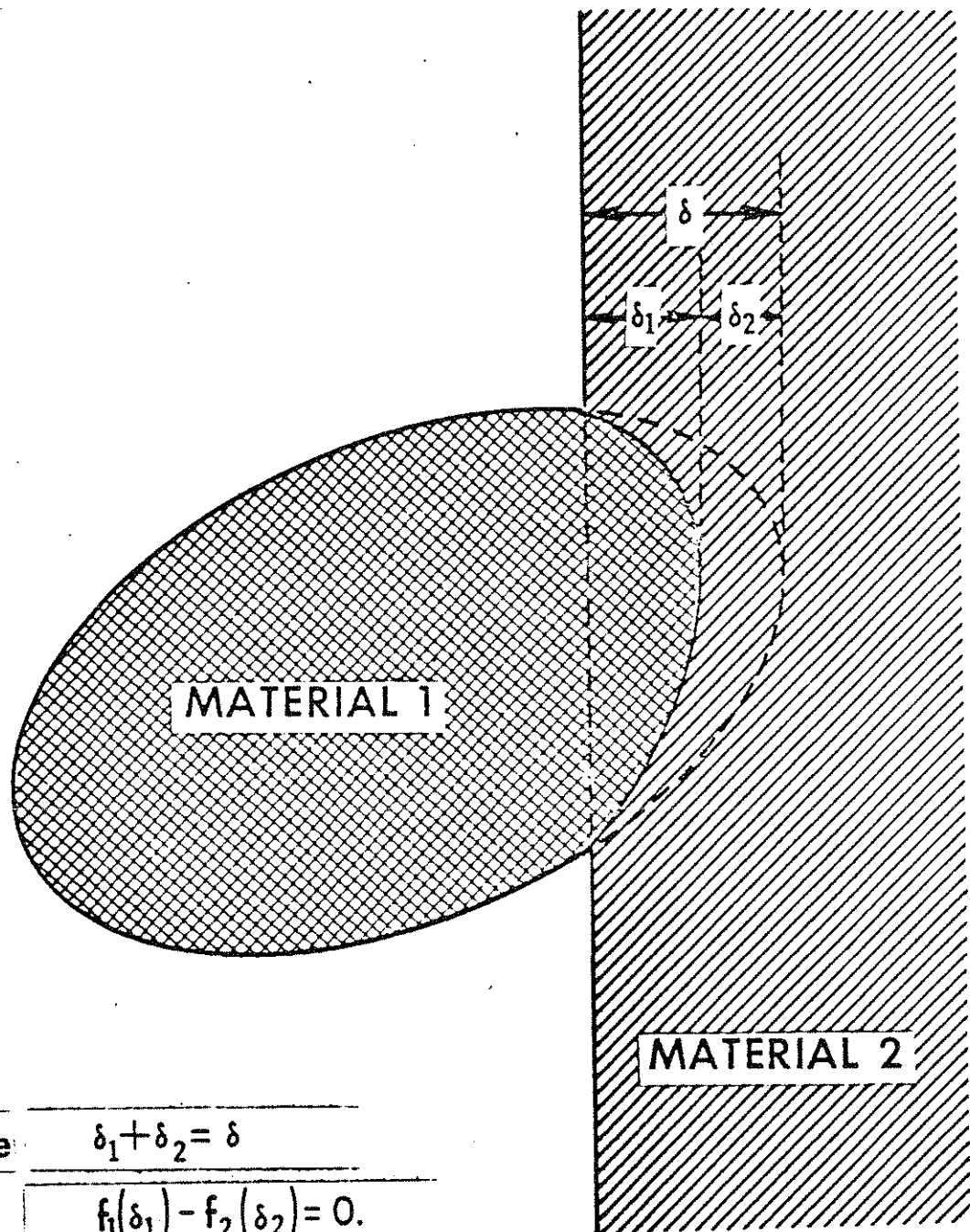
$$\delta_1 + \delta_2 = \delta$$

$$f_1(\delta_1) - f_2(\delta_2) = 0.$$

Here, the total deflection δ is a known value at each instant of time. f_1 and f_2 are the functional relationships between force and deflection for the two materials, defined by the user on Cards 403 through 408. The solution of these equations yields F as

$$F = f_1(\delta_1) = f_2(\delta_2).$$

The solution algorithm involves an iterative procedure, and it requires five control values specified by the user. Two are convergence epsilons, ϵ_1 and ϵ_2 , one for each material. The force balance is considered to be good enough when $f_1(\delta_1)$ is within ϵ of $f_2(\delta_2)$, where $\epsilon = \min \{\epsilon_1, \epsilon_2\}$. ϵ_1 and ϵ_2 are defined for the two materials in field 3 of Card 222, 404, or 705. The value commonly used for this parameter is 5. lbs. Three of the control values are specified once and are used for all shared-deflection interactions. They are in fields 1, 2, and 5 of Card 103. Fields 1 and 2 contain the maximum and minimum allowed trial adjustments of the component deflection



Solve	$\delta_1 + \delta_2 = \delta$
	$f_1(\delta_1) - f_2(\delta_2) = 0.$
Then,	$F = f_1(\delta_1) = f_2(\delta_2).$

FIGURE 6-18 Mutual Deformation of an Ellipse and a Line

values at any iteration step. Values of .2 and .02 inches are suitable.* The value in field 5 is the maximum number of deflection adjustments allowed for finding force balance at any time step. Ten adjustments will be adequate for almost all combinations of materials if the other suggested shared-deflection control values are used.

Module 4 contains an example which illustrates the importance of defining material properties for both ellipses and vehicle-interior surfaces whenever possible. Very often users of crash simulation models concern themselves only with the force-deflection characteristics of elements of the vehicle interior and use rigid contact ellipses or circles on the occupant. This invariably results in effective stiffnesses for occupant-interior interactions that are too large. Consequently, resulting model predictions of peak forces and G-levels are generally too high. Both materials for an interaction should be defined whenever data is available unless one is considerably softer than the other. In this case, the stiffer element, whether ellipse or line, may reasonably be specified as rigid.

6.5 Edge Effects

The foregoing sections define deflection and explain the determination of a deflection-dependent normal force from prescribed material properties. Nothing has yet been said about the precise circumstances under which a normal force will be calculated. That is, when is a contact interaction considered to have taken place.

Only the interaction between an ellipse and a line needs to be discussed. One obvious requirement for production of a contact force by the simulation model is that there be a positive relative displacement between the ellipse and the line. A non-zero force should clearly be determined for the deflection δ shown in Figure 6-18. But Figure 6-19 illustrates a case where the deflection δ , as previously defined, is positive yet there should be no interaction force because the ellipse passes to one side of the line segment. It is

*These values may reasonably be selected as 500 lb/K and 1. lb/K, where K is the maximum slope of any loading curve which may participate in shared deflection.

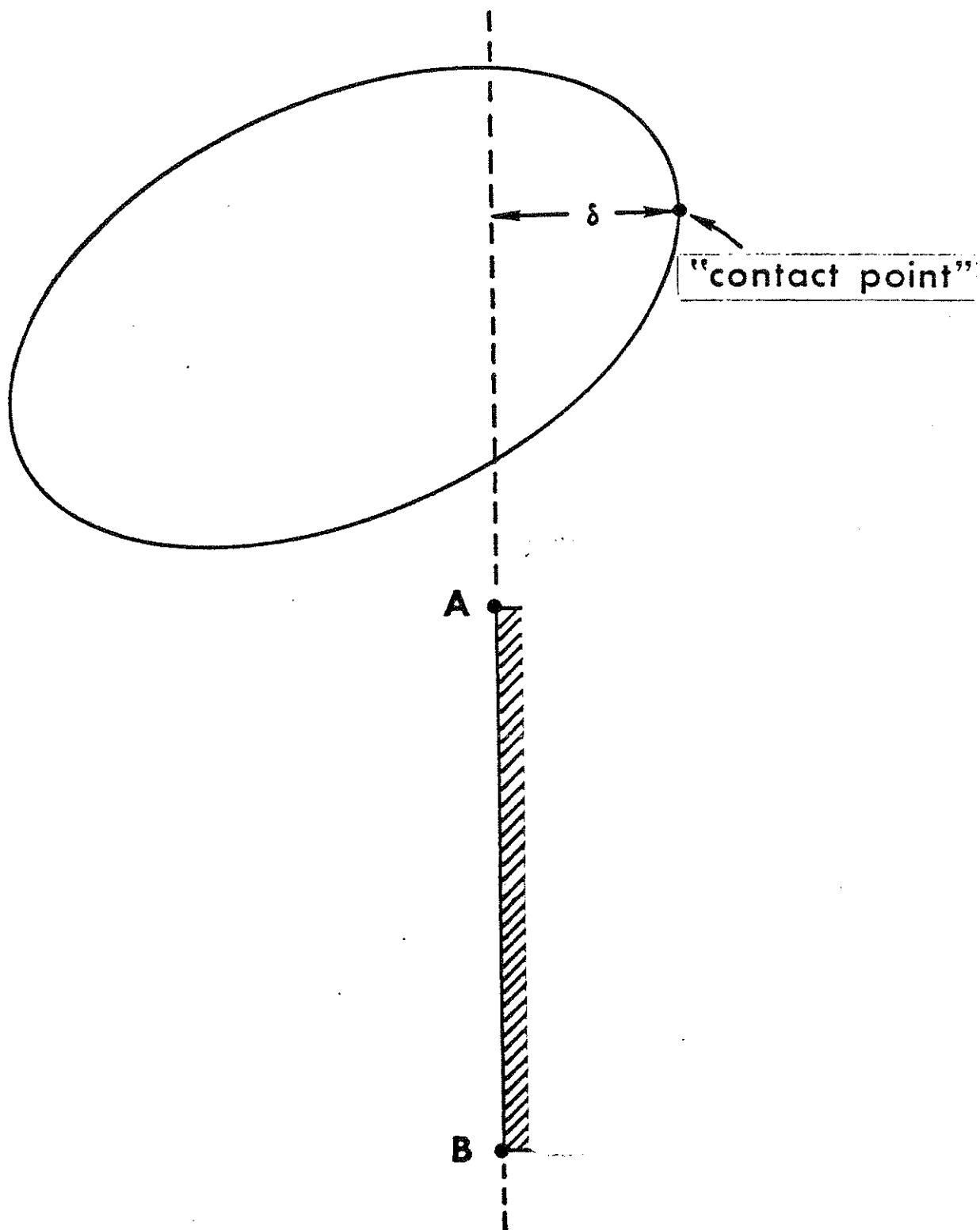


FIGURE 6-19 An Ellipse Which Misses a Line Segment to the Side

obviously necessary to consider not only deflection against the extended line defined by the segment endpoints A and B but also the position of the ellipse relative to the endpoints themselves.

Figure 6-20 illustrates an intermediate condition. While the so-called "contact point" is beyond the endpoint A, still there is an apparent interaction between the ellipse and the segment and a means should be provided for estimating an appropriate force. If the ellipse in the figure were moved upward so that the contact point lay far beyond the edge of the line segment, a zero interaction force should clearly be predicted. Such a condition has already been illustrated in Figure 6-19. If, on the other hand, the ellipse were moved downward so that the contact point lay halfway between the line-segment endpoints, then an interaction force appropriate for firm contact should be predicted. The model provides a means by which diminishing normal forces can be calculated as an ellipse moves from firm contact through intermediate positions such as illustrated in Figure 6-20 to positions off the edge of the segment where forces become zero.

The user supplies for each line segment a value for a parameter called an "edge constant." Whenever there is a positive relative displacement between an ellipse and the line, a so-called "effectiveness factor" is calculated for the interaction as a function of the edge constant and of the position of the contact point relative to the extent of the segment. The effective force is found by multiplying the deflection-dependent normal force determined from material properties by the effectiveness factor, E . That is,

$$F_{\text{eff.}} = E F(\delta) .$$

The definition of the effectiveness factor is illustrated by Figure 6-21. This figure shows E as a function of a non-dimensional coordinate called " s ," which ranges from 0 to 1 as the position of the contact point varies from endpoint A of the line segment to endpoint B. The quantity s takes on negative values for contact point positions beyond endpoint A and values greater than 1 for positions beyond endpoint B. The effectiveness factor is symmetric about the midpoint of the line segment, and it has the value 1 for contact point

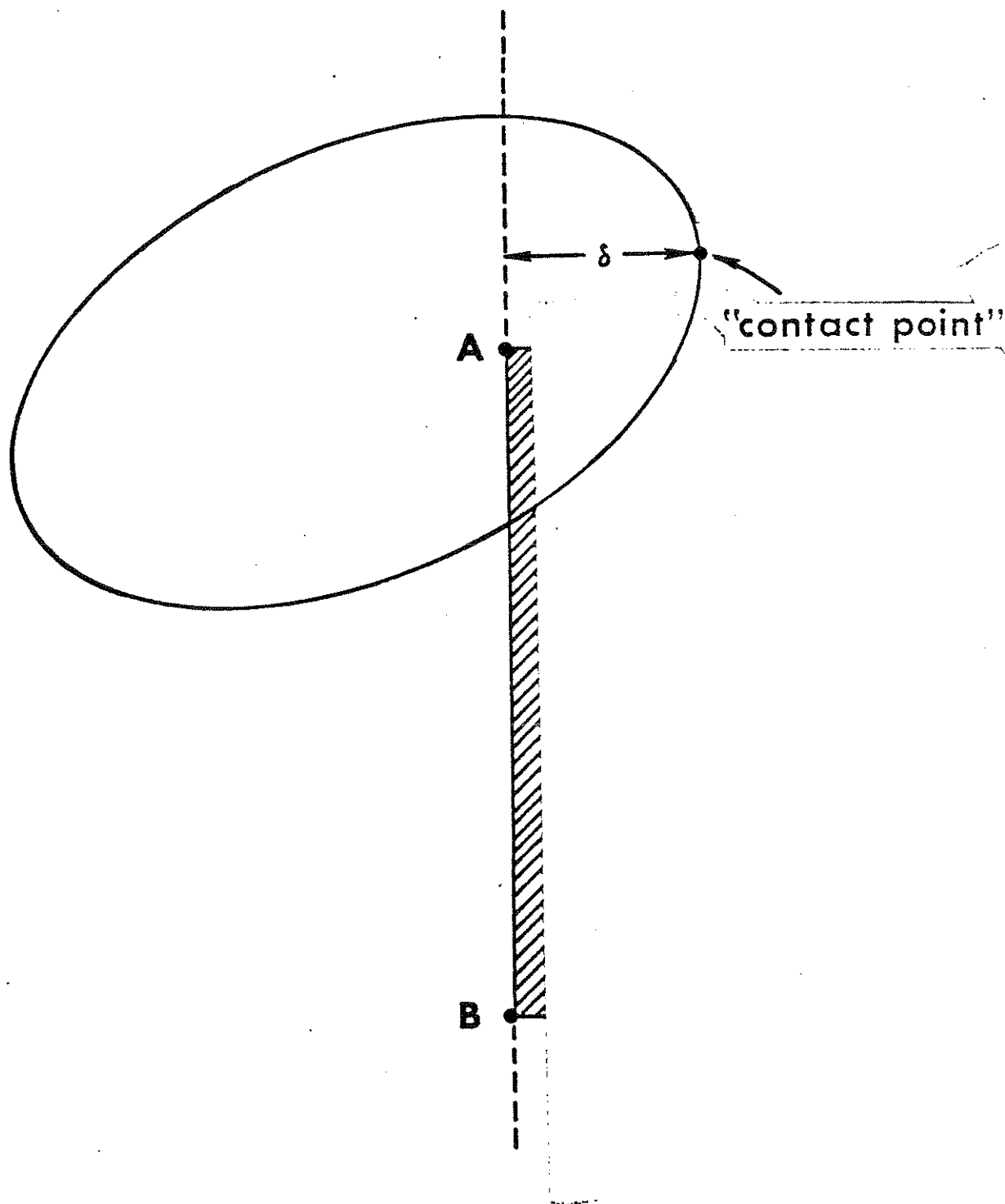


FIGURE 6-20 An Ellipse Contacting a Line Segment Near Its Edge

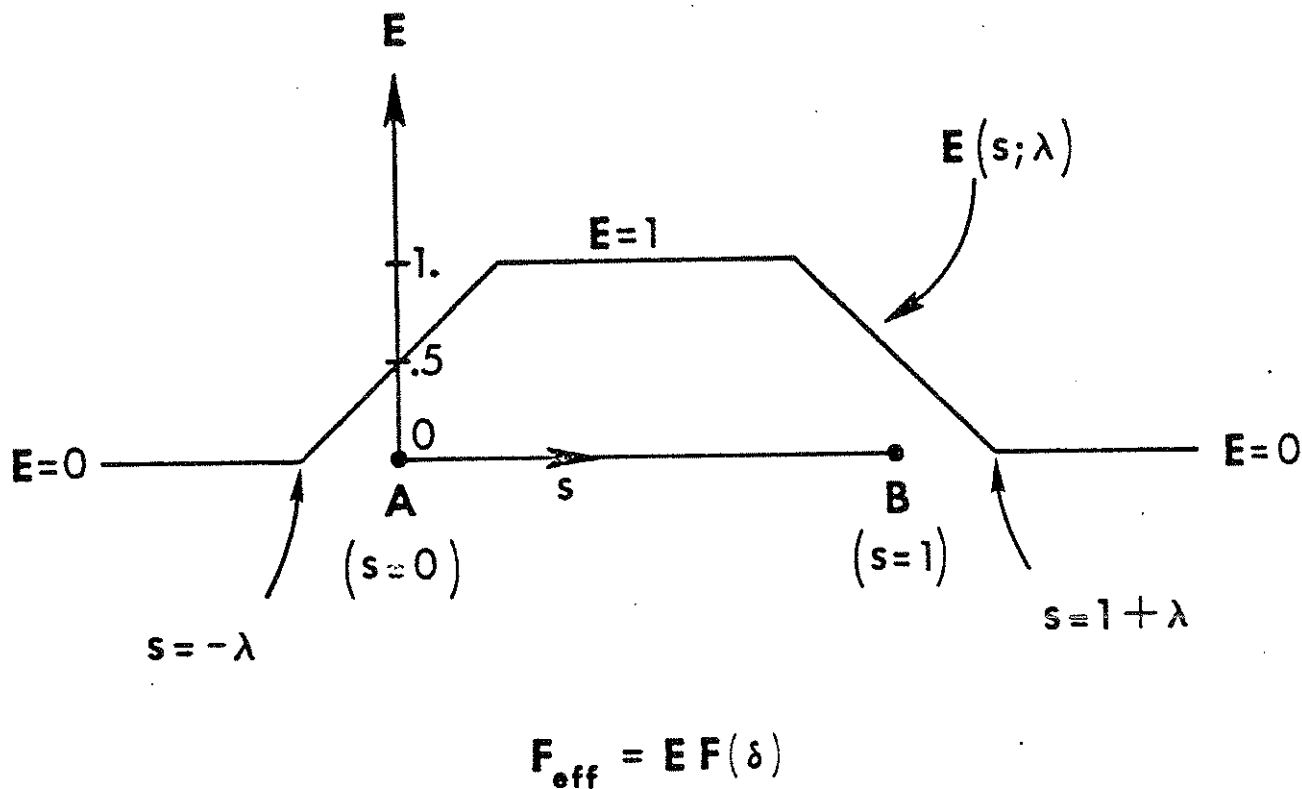


FIGURE 6-21 Effectiveness Factor E as a Function of s , the Position of Contact Point with Respect to Line Segment, With Edge Constant λ as a Parameter

positions near the middle of the segment, i.e., where ellipse contact with the segment is firm. Unit value for the effectiveness factor results in undiminished forces for contacts here. The extent of the firm area of the segment is defined by the user-prescribed edge constant, λ , which is a parameter of the graph for E. The effectiveness factor increases linearly from 0 to 1 from a contact point position of non-dimensional distance λ beyond an endpoint to a position of distance λ within the endpoint. Thus, the effectiveness factor is always .5 for contact precisely at an endpoint, and the effective force is zero for any contact beyond an endpoint by a non-dimensional distance greater than λ . The user should be able to show that if the length of the contact surface is L, then the length of the firm middle area is $(1-2\lambda)L$.

The two extreme forms of the effectiveness factor are illustrated in Figure 6-22. In the upper figure, for an edge constant of 0, an undiminished force results for all contacts within the segment endpoints, but the effective force is zero for any contact beyond an endpoint. In the lower figure, the surface softens away from the center.

The user prescribes an edge constant value for each line segment of the vehicle interior. Each edge constant must be from 0. to .5:

$$0 \leq \lambda \leq .5$$

These values are entered in field 6 of the 409-Cards.

The edge constant for a particular contact surface is sometimes selected on the basis of a comparison between its length, L, and the semi-major axis, S, of the most important or most likely ellipse to interact with the surface. Thus, $\lambda = S/L$. Here, $S = \max\{a, c\}$, where a and c are shown in Figure 6-4.

6.6 Contact Surface Friction

In addition to a force component normal to the contact surface, the interaction force vector includes a friction component parallel to the surface.* This component is determined as the

*Friction forces are calculated only for interactions between an ellipse and a line, not between ellipses.

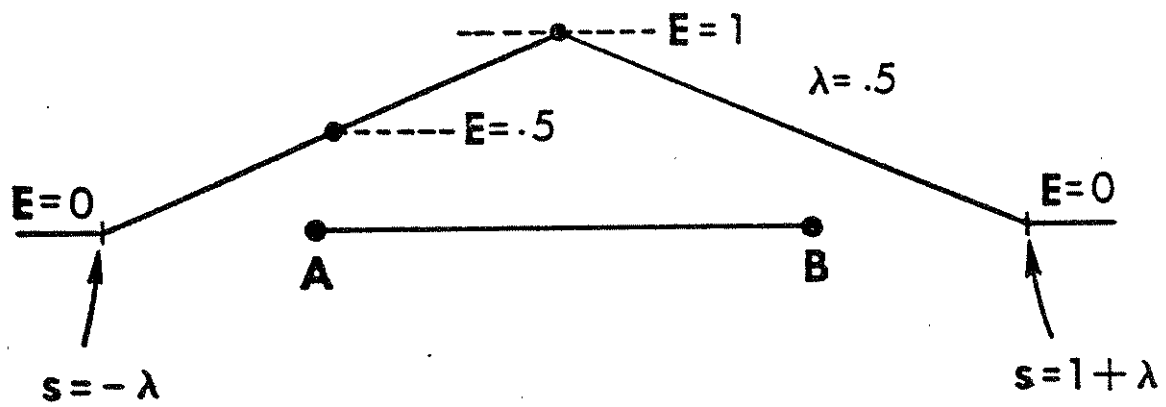
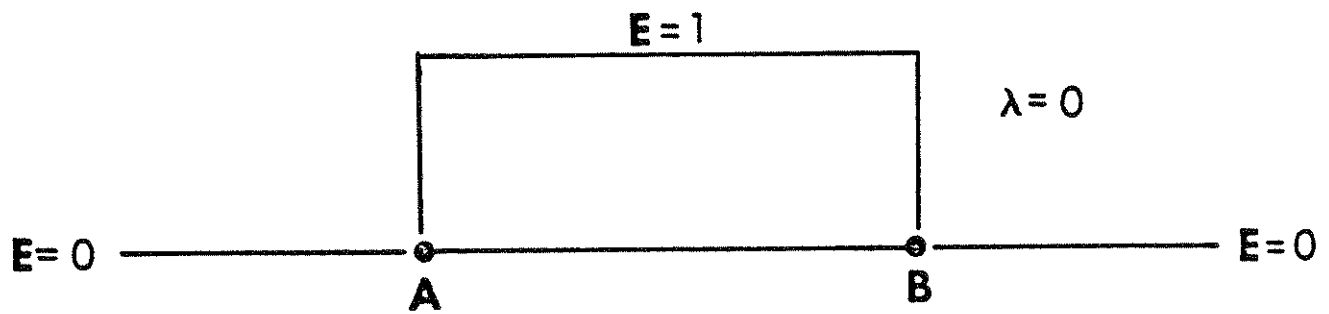


FIGURE 6-22 Effectiveness Factors for Edge Constant Values of 0. and .5

product of a user-defined coefficient of friction and the effective normal force resulting from edge-factor adjustment. Figure 6-23 illustrates the friction-force component.

Modeling of friction should not be neglected by the user since it can sometimes significantly affect results. Typical friction coefficients for interactions within the occupant compartment are in the range .25 to .75. Figure 6-23 is proportioned for a coefficient value of $\bar{\mu} = .4$ and shows that while the magnitude of the resultant force vector may be very little different from the normal component alone, the direction of the resultant may be significantly different.

In the MVMA-2D model, friction coefficients are defined not for materials but rather for pairings of "classes" of potentially interacting ellipses and regions. For example, a seat back and a seat cushion might be of the same region friction class if they are covered with the same fabric. On the otherhand, the head and foot (shoe) ellipses would likely belong to different ellipse friction classes because of different surface characteristics. Each region of the vehicle interior, discussed in Module 5, is assigned to one of ten friction classes by entering an integer 1. through 10. in field 4 of its 402-Card. Ellipses, discussed in Module 4, are similarly assigned to one of five ellipse friction classes by entering 1., 2., 3., 4., or 5., in field 5 of its 219-Card. Thus, up to 50 combinations of ellipse and region classes can be assigned friction coefficients. In example data of Figure 6-24, the values in field 4 of the 402-Cards indicate that regions PANEL and SEAT BACK have region friction classes of 3 and 8. The thorax ellipse is of ellipse friction class 1, as indicated by the 1. in field 6 of Card 219.

412-Cards are used for the specification of coefficients of friction. Each 412-Card has an ellipse class in field 1 and a region class in field 2. Fields 3, 4, and 5 contain polynomial coefficients for a deflection-dependent coefficient of friction. These are μ_0 , μ_1 , and μ_2 in the following relation:

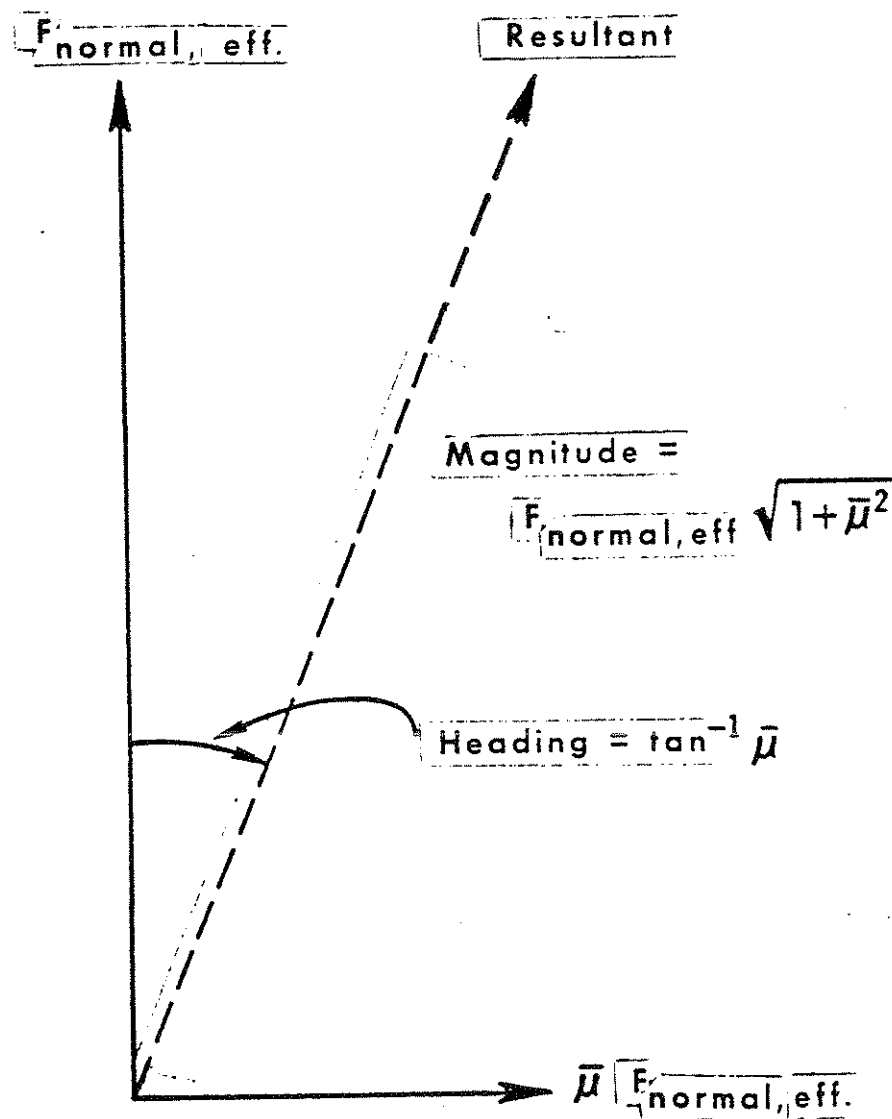


FIGURE 6-23 Resultant Interaction Force Vector For Friction
Coefficient $\bar{\mu} = .4$: Resultant = $1.08 F_{\text{normal}}$,
Heading = 21.8°

3.	0.	0.	0.	0.	1.	10.	.000001	2.	102
THORAX		CHESTMAT		2.	1.				219
PANEL		4.	3.	1.	0.				402
SEAT BACK		1.	8.	1.	0.				402
1.	3.	.4							412
1.	8.	.25	.03	.01					412

$$\mu = \mu_0 + \mu_1\delta + \mu_2\delta^2$$

FIGURE 6-24 Example Data Cards for Coefficients of Friction

$$\mu = \mu_0 + \mu_1 \delta + \mu_2 \delta^2$$

The first coefficient, μ_0 , is the constant coefficient of friction normally defined. Non-zero values for μ_1 and μ_2 provide a dependence on deflection that represents tangential resistance to "plowing" at the ellipse-region interface. The polynomial coefficients on the last card in the example data of Figure 6-24 give a friction coefficient of .25 for zero deflection, .35 for two inches of deflection, and .65 for five inches of deflection.

Figure 6-25 pertains to an additional parameter needed for determination of frictional forces. Strictly, the coefficient of friction used by the computer model is not μ , as determined from the polynomial coefficients, but

$$\bar{\mu} = C\mu$$

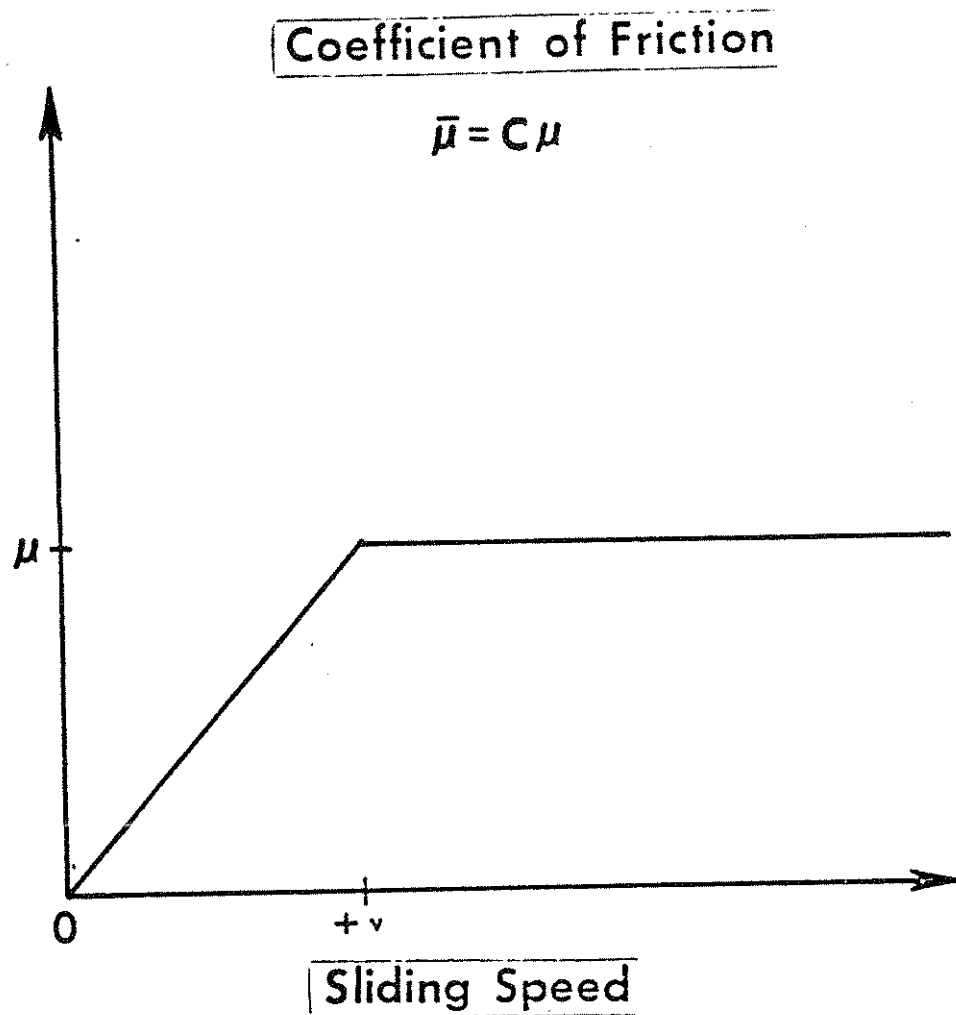
where the coefficient C depends on the sliding speed. Since the friction force is opposite in direction to the sliding velocity, this coefficient is needed to insure friction force continuity as the sliding velocity changes sign. C is a linear ramp, from 0. at a sliding speed of zero to 1. at speed equal to a user-supplied ramp length, v , and for all speeds greater than v .^{*} The value for this parameter is entered in field 7 of Card 102, and 10 in./sec. is suggested. This is normally much smaller than speeds of the occupant relative to the vehicle interior and yet sufficiently large to insure against frictional forces that change too rapidly.

6.7 Special Contact Force Adjustment Features

The MVMA-2D model has five contact force options that are presently inoperative because of incomplete computer code. User-prescribed switch settings which would invoke any of these options are ignored by the computer model, but such settings cause a warning to be printed. The pertinent switches are defined in fields 5 through 8 of the 401-Card for each region and field 5 of the region 402-Card. All switches should be set to "off" by the user by entering values of 0., 1., 1., 1., and 1. in these fields, as shown in Figure 6-26.

These options are described in detail in Volumes 1 and 2 of

^{*} Thus, the coefficient of friction used is an adjusted sliding-friction coefficient. The effective static coefficient is zero.



$$\mu = C\mu = C(\mu_0 + \mu_1\delta + \mu_2\delta^2)$$

FIGURE 6-25 Adjustment of Coefficient of Friction for Small Sliding Speeds

REGIONNAME	MATERIALNAME	0.	1.	1.	1.		401
REGIONNAME	3.	3.	1.	0.	0.		402
MATERIALNAME	5.	blank	blank	blank	STATIC	INERTIALGRNAME	404
LINESEGMENTNAME	1.	blank	blank	blank	blank		410

FIGURE 6-26 Example Cards With Data Relating To Contact Force
Adjustment Options

the MVMA-2D manuals. They are described briefly here:

1) Multiple ellipse forces acting on one line segment may be scaled so that they sum to the maximum of the separate forces. (switch = field 6 of Card 401)

2) A special force apportionment may be used when an ellipse contacts more than one line segment simultaneously. (switch = field 7 of Card 401)

3) A line segment being deflected by an ellipse need not present a straight line profile to a second approaching ellipse. (switch = field 8 of Card 401)

4) Region structural deformation resulting from occupant impact is allowed. (switch = field 5 of Card 402)

5) Permanent material deformation may be coupled with structural response (4). (switch = field 5 of Card 401)

Fields 4 through 6 of 404-Cards and 4 through 7 of 410-Cards are for values relating to options 3, 4, and 5. They may be left blank since any values entered will be ignored.

6.8 Modeling Notes

As the user gains experience, improvement in modeling technique will result in more effective and more efficient simulation of the crash event. Points relevant to effective modeling procedure are made throughout the modules of the MVMA-2D Tutorial System. The notes which follow all relate to contact forces and are largely miscellaneous.

1) The R-ratio, or energy restitution coefficient, for soft biological tissues in general decreases rapidly as a function of deflection. While the appropriate value for zero deflection is 1., values of .1 or less are appropriate for peak deflections which might occur in a crash. This can be understood intuitively by considering a fall victim who lands on a concrete surface in a prone, face-down orientation from a fall height of ten feet. His bounce height divided by ten feet provides a rough estimate for an average, overall R-ratio.

2) While the user of the MVMA-2D model is required to provide R-ratios and G-ratios separately for the calculation of unloading curves, they cannot in reality be independent. For example, a G-ratio near 1. can be consistent only with R-ratios near zero as illustrated by Figure 6-27. An unloading curve for any combination of G and R values could be determined which would satisfy both the permanent-deflection and restored-energy requirements, but only concave-upward unloading curves are reasonable for deflections beyond the yield point. The straight-line unloading to ω shown in the figure is thus the limit of reasonable curves. Since the area under the curve is maximized by straight-line unloading, the R-ratio for any value of maximum deflection should always be less than or equal to the energy ratio $C/(C+D)$.

The user may occasionally specify incompatible G- and R-ratios for unloading from a particular loading curve. Should G and R be incompatible for some δ_{\max} , then the computer model will by default accept the G-ratio and unload to ω on a straight-line curve, ignoring the R value. A warning is printed, but results will normally be reasonable. The condition can be corrected if desired by reducing either G or R, but experience has shown that reducing G is generally better.

If the user wants to be entirely certain that G and R functions are compatible, it is necessary to verify that condition (8) in Figure 6-28 is satisfied for all values of δ_{\max} . A commonly used loading curve is one of constant slope, or stiffness. The curve for a stiffness K is illustrated in Figure 6-29. The user may wish to demonstrate as an exercise that, for such a loading curve, the following inequality relating G and R should be satisfied for all turnaround deflections δ_{\max} :

$$R(\delta_{\max}) \leq 1 - G(\delta_{\max}).$$

3) It should be kept in mind that G- and R-ratios determined quasi-statically may be different from values appropriate for a dynamic interaction. If statically determined values are used, an implicit assumption is that the material is capable of responding in-

$$\omega = G(\delta_{\max}) \delta_{\max}$$

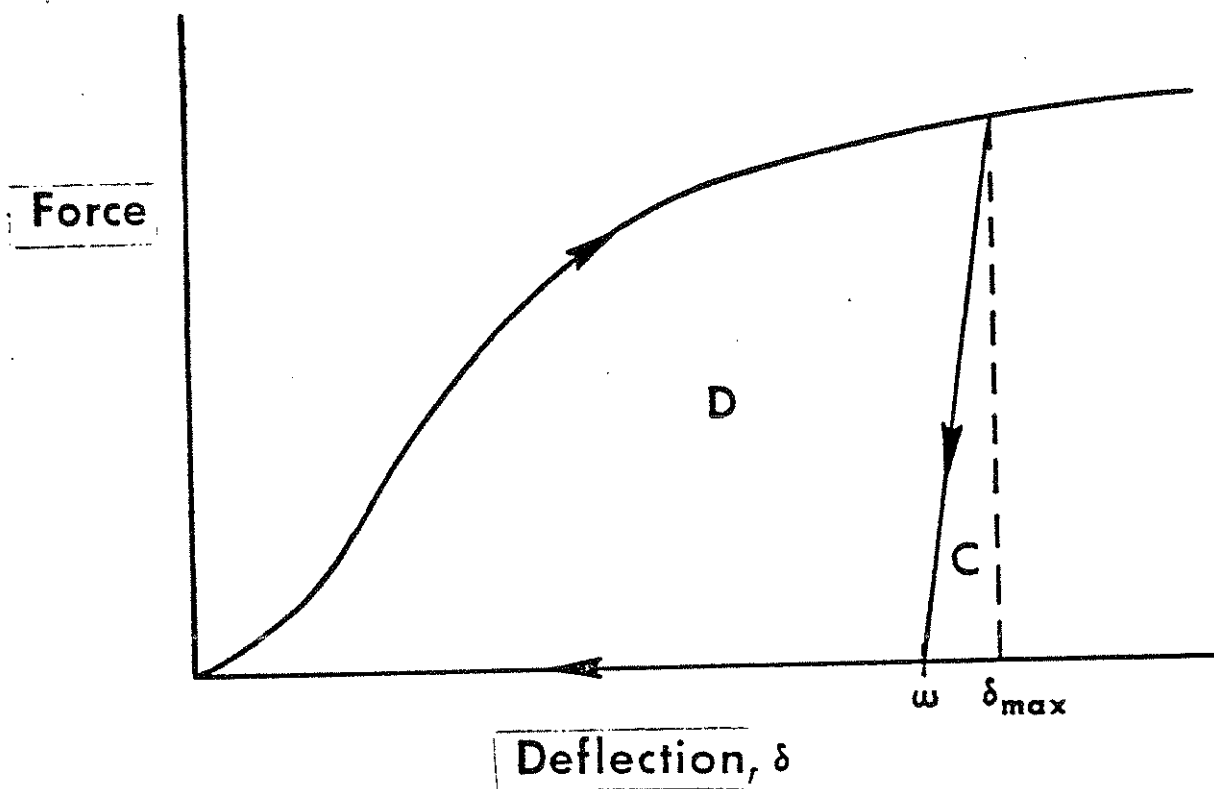


FIGURE 6-27 Maximum-Energy Unloading for a G-Ratio Near to 1.

- (1) δ_{\max} = maximum deflection
- (2) $G = g(\delta_{\max})$ [G-ratio; input]
- (3) $R = r(\delta_{\max})$ [R-ratio; input]
- (4) $F_{\max} = f(\delta_{\max})$ [loading curve; input]
- (5) $\omega = G\delta_{\max}$ [permanent deformation]
- (6) $C = (\delta_{\max} - \omega) F_{\max}/2$ [area under straight line unloading]
- (7) $A_L = C + D = a(\delta_{\max}) = \int_0^{\delta_{\max}} f(x) dx$
[area under loading curve]
- (8) $R \leq C/A_L$ for all δ_{\max}

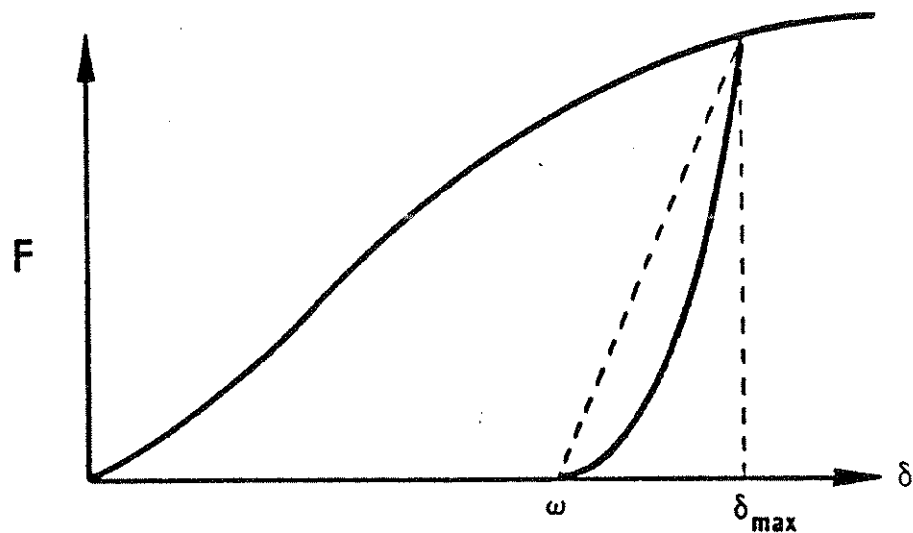
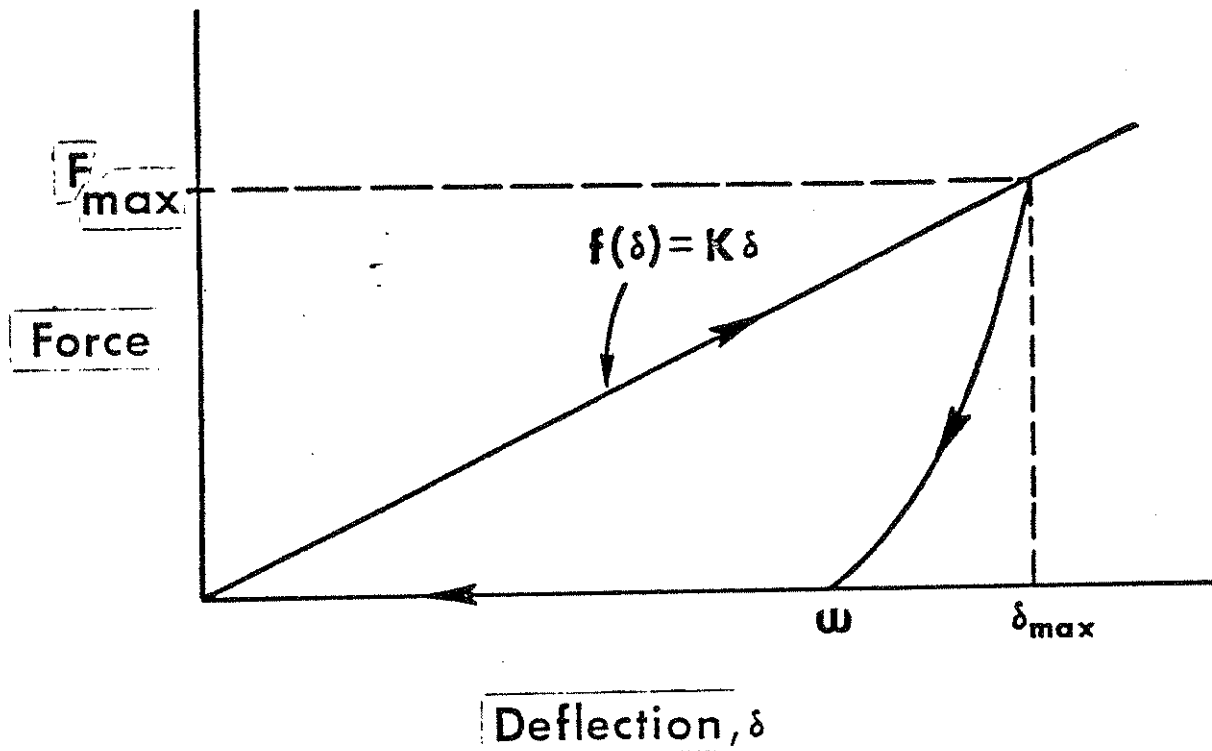


FIGURE 6-28 Determination of Compatibility of R-Ratio with a Specified G-Ratio



$$R(\delta_{\max}) \leq 1 - G(\delta_{\max})$$

FIGURE 6-29 G-R Compatibility Constraint for Constant Stiffness Loading Curve

stantaneously to changes in deflection, that is, that there is no dependence on rate of unloading. The degree to which static and dynamic values differ depends, of course, on the material, but in general, the G-ratio will be larger and R smaller for fast unloading, such as would occur in a crash, than for quasi-static unloading.

4) When using a polynomial to approximate a monotonic function of deflection,* the user should check to be certain that coefficient values determined by satisfying various magnitude and slope conditions define a polynomial that is indeed monotonic in the deflection range of interest. There is no guarantee, for example, that a general cubic polynomial determined by fitting four point-wise monotonic points will not have a "dip" between the first and second points or a "hump" between the third and fourth points.

5) It may sometimes be useful to superimpose either ellipses or vehicle-interior regions and to assign different material properties to the duplicate elements. With proper use of inhibition switches, it is then possible in effect for the same physical element to offer different resistances to different elements which may contact it. This might be done, for example, for an occupant-compartment surface for which the resistance to deformation cannot be well-approximated solely as a function of deflection but is significantly dependent as well on the displaced area or volume. If a single ellipse interacts with the surface, then an appropriate force-deflection loading curve can be defined; but this curve would be inappropriate for a second interacting ellipse that is significantly smaller or larger.

6) An example in Module 4 illustrates that a good general rule to follow is that a contact-sensing ellipse should not be made longer than any line segment that it must contact for there to be proper resistance to occupant motion. A related rule is that there is generally no benefit in breaking a straight-line region surface into a set of shorter straight-line segments of the same force-deflection properties. No deterioration of simulation results should occur, but unless the special force adjustment options discussed earlier in

* For example, a static loading curve

this module are operative, there will be no improvement in results while model execution cost will increase.

7) If possible, the user should avoid modeling the vehicle interior with line segments which meet at acute angles,* as illustrated in Figure 6-30. This may result in sudden, unreasonably large forces on the occupant after an ellipse passes near the vertex. Such forces can result if the ellipse passes around the corner so that the first effective deflection between the line segment and the ellipse contact point is large.

The most effective way of lessening the likelihood of occurrence of this problem in the case that acute angles must be used in the vehicle interior is to set the "penetration limits" for the line segments to properly small values.** The penetration limit is an input parameter discussed in Module 5, and a value is specified for each line segment in field 5 of Card 409. One way of recognizing as false a sudden, large deflection such as shown in the figure is to compare it with the maximum change of deflection which is possible in one time integration step. If the first effective deflection is larger than the maximum possible change in one time step, then the deflection is false and no forces should be calculated while the ellipse remains behind the line segment. Clearly, the smallest false deflections which can be recognized in this manner are just larger than the product of the time step Δt and the speed at which an ellipse approaches the contact surface, say $v^{(rel)}$. Therefore, the computer model will recognize most false deflections by comparing the deflection with a penetration limit set to $v_{max}^{(rel)} \Delta t$, where $v_{max}^{(rel)}$, the maximum speed at which an ellipse is ever expected to approach the surface, can be taken as the crash impact velocity, a reasonable limiting value. Thus, for an impact velocity of 30 mph, or 528 in/sec, and an integration time step of 1. msec, penetration limits may be set to .528 inches and no false deflections greater than .528 inches will be accepted as real by the computer model.

*Angles between 0° and 90° .

** The problem may also occur if one side (AB) of the angle is missing and even for an obtuse angle ($>90^\circ$) if one side is too "soft."

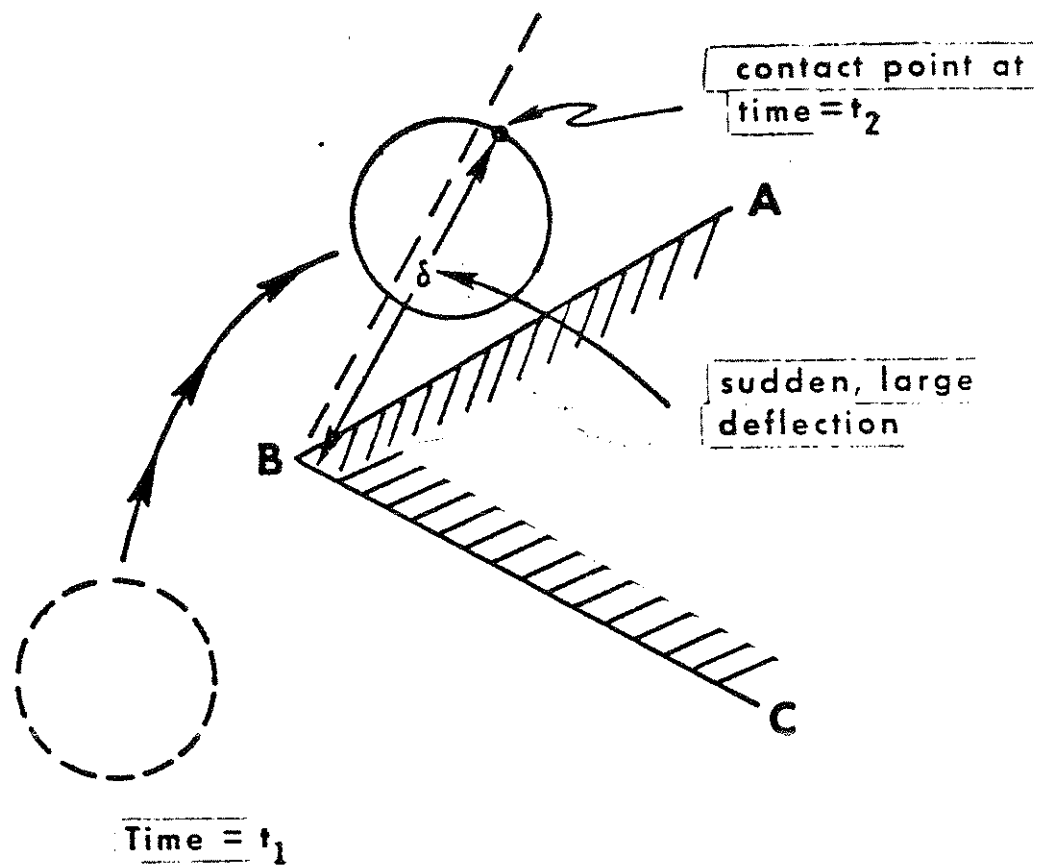


FIGURE 6-30 A Sudden, Large Deflection Near an Acute Angle

Penetration limit values should not be taken as significantly less than $v_{\max}^{(rel)} \Delta t$ since real interactions between ellipses and line segments might then be identified as false.

8) A model option that is only indirectly related to contact forces is the application of prescribed, time-dependent forces to the head. This feature has been useful in simulation of non-crash events where head forces were known but the kinetics were unknown. Applied head forces are prescribed with Cards 605 and 606, which are discussed in Module 8.

MODULE 7 - OCCUPANT POSITIONING WITH RESPECT TO THE VEHICLE

7.1 Generalized Coordinates

The problem of determining occupant dynamics in a crash environment can be simply stated. A description of a biomechanical system, the occupant, is given. A description of a potentially interacting mechanical system, the occupant compartment, is given. The motion in space of the occupant compartment as a function of time is specified. And finally, the occupant's position and orientation and their rates of change are specified for some single instant of time. It is required to determine the motion of the occupant and the forces which describe his interaction with the vehicle interior (See Figure 7-1).

This module deals with the description of occupant position and orientation. Since the user of the simulation model is required to specify occupant position and orientation and their rates of change for some instant of time, arbitrarily assigned the value $t = 0$, this module is pertinent to preparation of input data sets. It is also pertinent to interpretation of model output since "occupant motion" is nothing more than time-histories of occupant position and orientation. Rates of change with respect to time of these histories, viz., velocities and accelerations, are equivalent descriptions of the motion and are normally printed together with the position history.

Consider a system of " n " particles confined to a plane, and let the positions of all points in the plane be defined in an arbitrarily positioned, non-accelerating orthogonal axis system with coordinates X and Z , as indicated in Figure 7-2. This is a so-called "inertial coordinate frame." In general, " $2n$ " coordinate values must be

**COMPUTER SIMULATION
OF OCCUPANT DYNAMICS
IN A CRASH ENVIRONMENT**

GIVEN (Input):

- 1) Description of a biomechanical system representing the occupant
- 2) Description of a mechanical system representing the occupant compartment
- 3) Time-history of occupant compartment motion
- 4) Occupant position at onset of crash

DETERMINED (Output):

- 1) Occupant motion
- 2) Forces on Occupant
- 3) Derived descriptions and measures of the crash dynamics

FIGURE 7-1 Computer Simulation of Occupant Dynamics

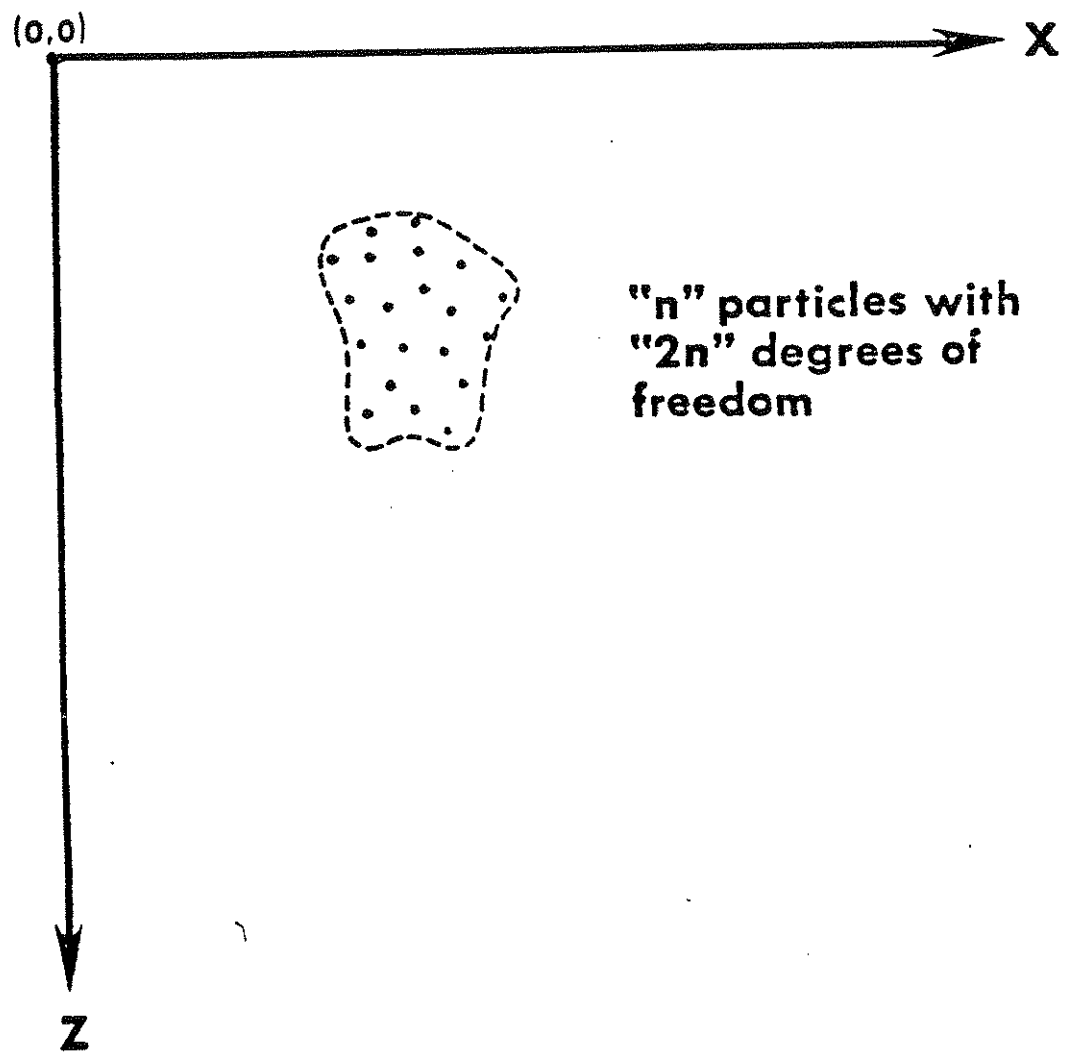


FIGURE 7-2 " n " Free Particles in an Inertial Coordinate Frame

specified to completely define the state of the system at any instant of time, i.e., there are " $2n$ " degrees of freedom. However, if constraints exist on the positions of particles relative to each other, then fewer than " $2n$ " coordinate values are sufficient. If there exist " $2n - 3$ " independent positional constraints, then the system of particles is called a "rigid body." (See Figure 7-3.) There remain three independent modes of motion of this system, and as " n " approaches infinity there are infinitely many equivalent ways that three independent degrees of freedom may be defined. It is most convenient and conventional to locate an arbitrary point in the rigid body, normally the center-of-mass point, by the two cartesian coordinates x and z . The third coordinate is the angle of intercept between the x - or z -axis of the inertial frame and an extended line drawn between two specified but arbitrary points in the rigid body. In Figure 7-3, the three quantities x_A , z_A , and θ_{BC} are so-called "generalized coordinates" for the rigid body. It might be noted here that any material line in the body parallel to the one specified for defining the angular coordinate is just as suitable and will have the same intercept angles with the inertial axes. A common misconception is that a rotation is defined with respect to some "center of rotation" or "pivot point." This is clearly not the case.

If a system of particles is not rigid, then one additional generalized coordinate must be defined for each positional constraint fewer than $2n - 3$ which exists for the system. Figure 7-4 illustrates the MVMA 2-D man model linkage, which consists of eight rigid-body elements. If this were not a kinematically constrained linkage,

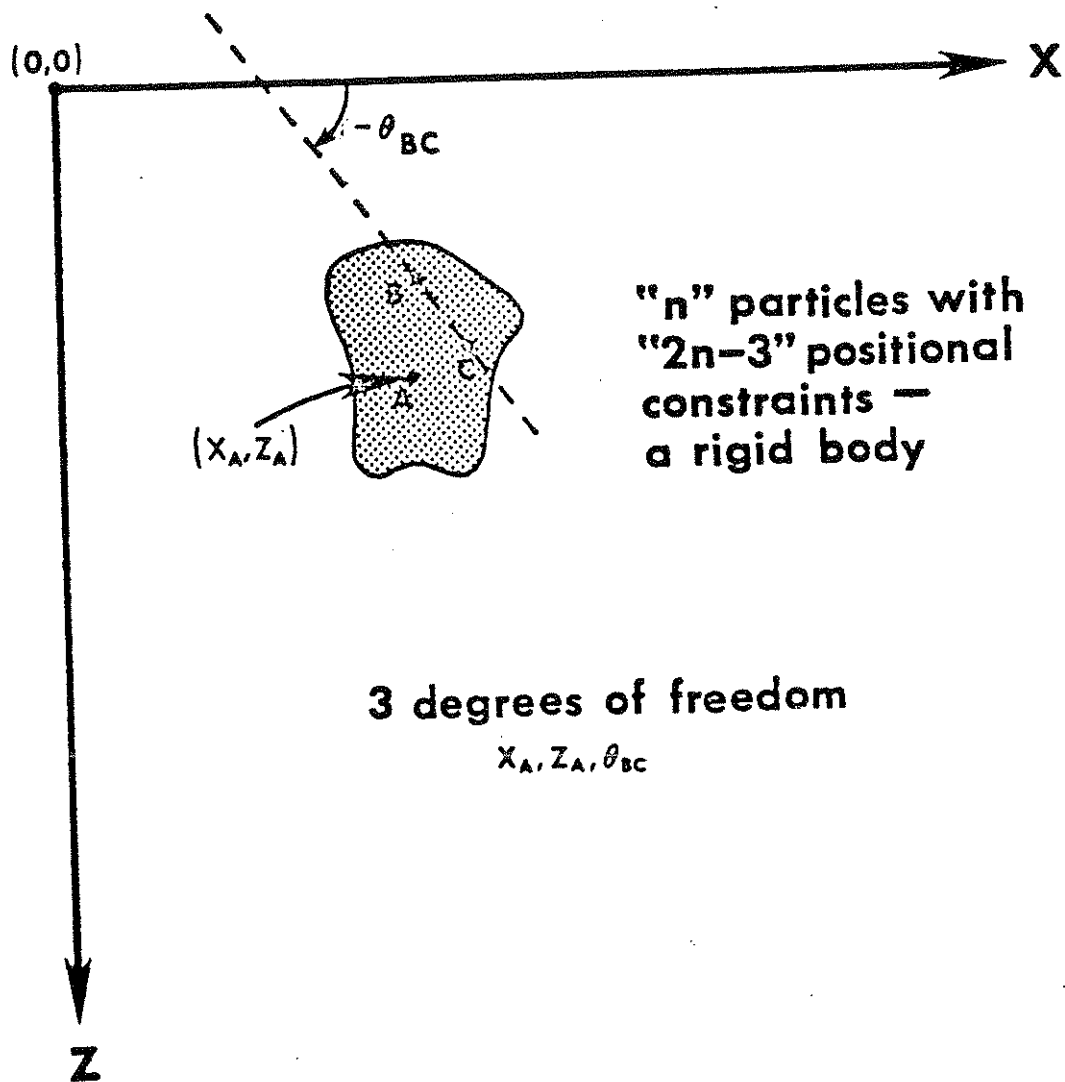
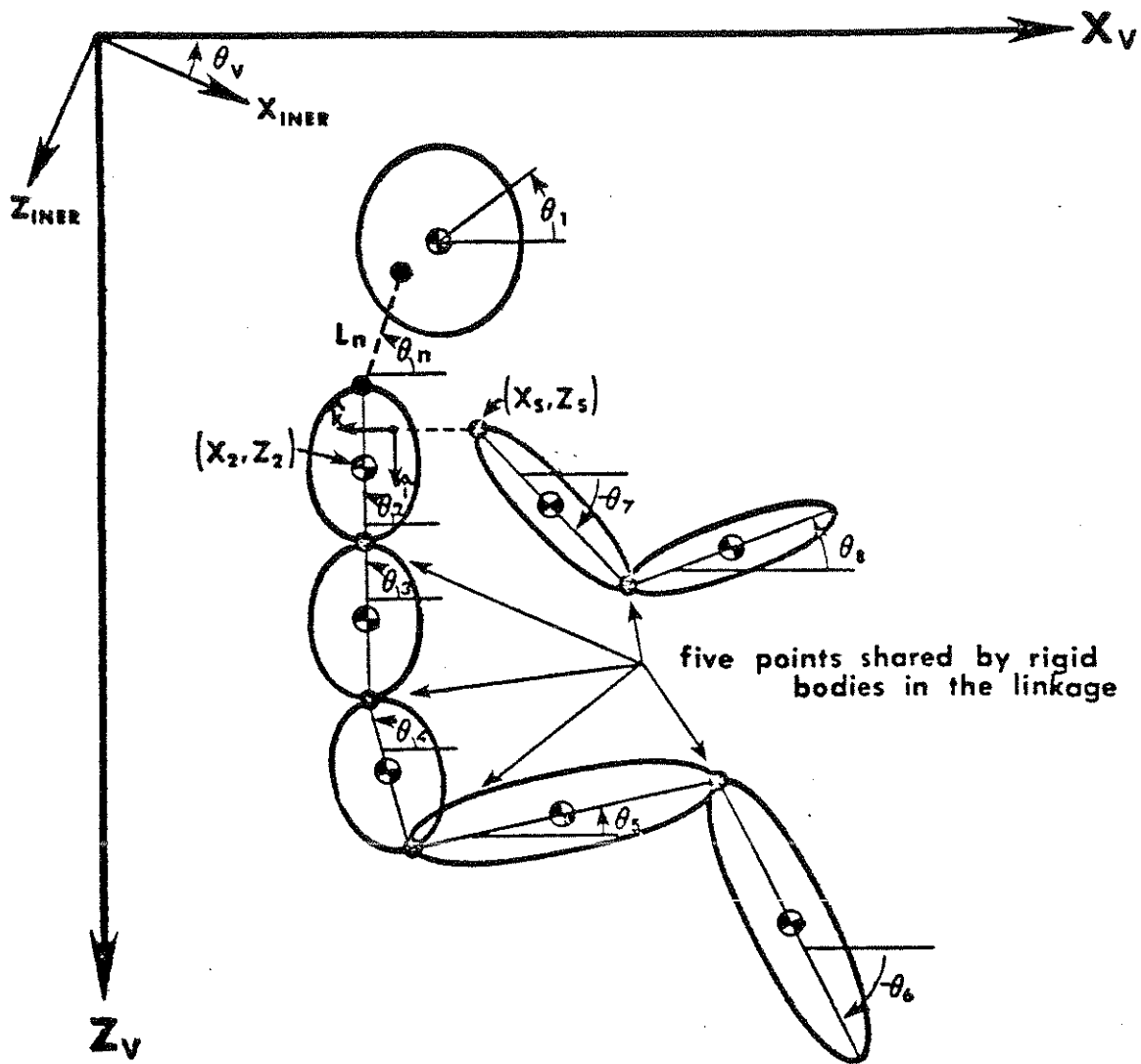


FIGURE 7-3 A Rigid Body in 2-Space, with Three Degrees of Freedom



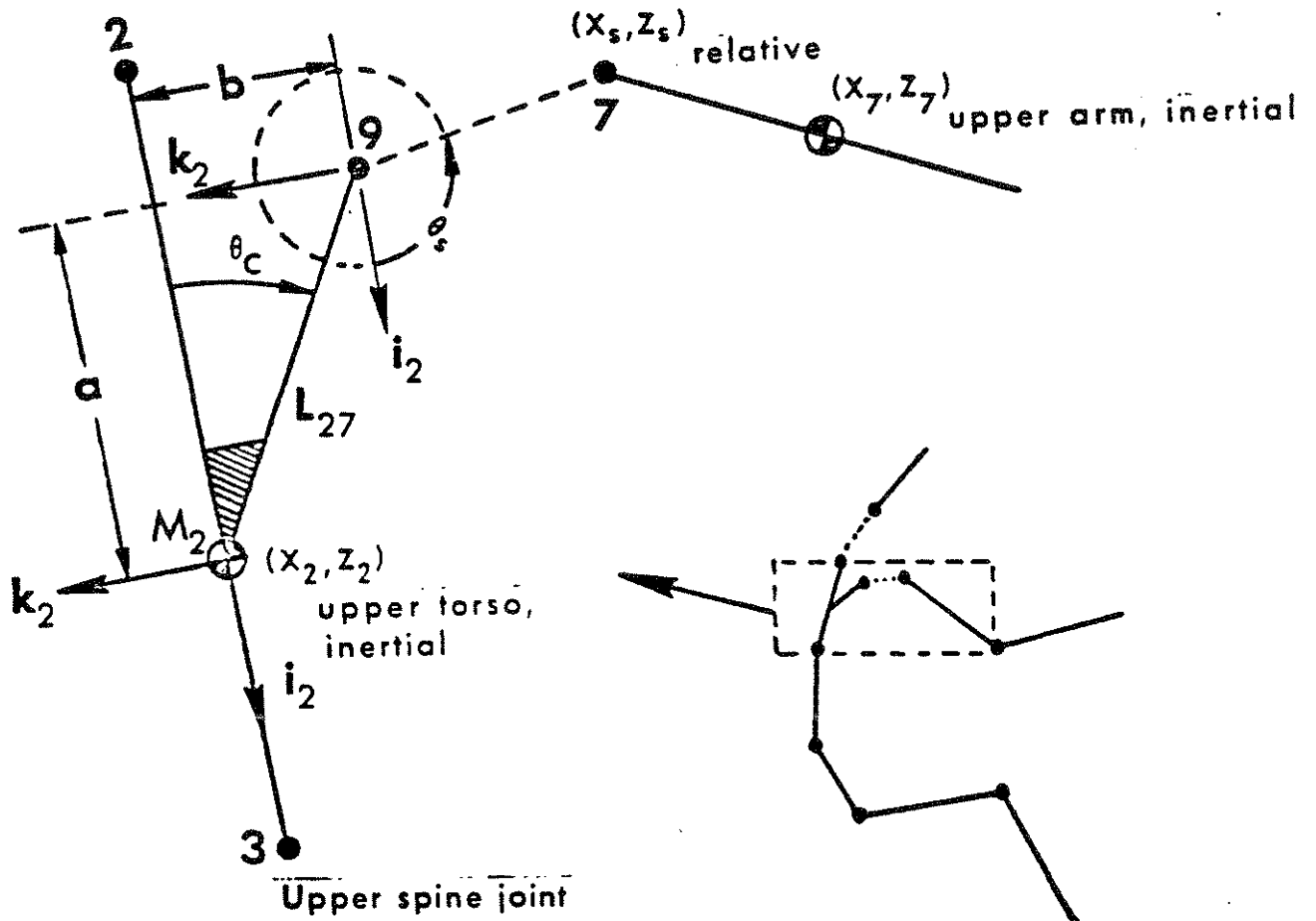
14 generalized coordinates: $X_2, Z_2, \theta_1, \theta_2, \theta_3, \theta_4, \theta_5, \theta_6,$
 $\theta_7, \theta_8, \theta_n, L_n, X_s, Z_s$

FIGURE 7-4 Occupant Model Generalized Coordinates for Input and Output (absolute coordinates defined with respect to vehicle axes)

twenty-four generalized coordinates would be required to define the position and orientation of the system, three for each rigid-body element. There are, however, five points shared by the rigid-body elements, at body joints, and for each, the X and Z coordinate values of one particle point are made redundant. Thus there are ten positional constraints. Consequently, the linkage shown in Figure 7-4 has only fourteen degrees of freedom, and fourteen suitable generalized coordinates are indicated. Eleven have been chosen to be relative to the axis system (X_V, Z_V) . They are nine link angles, θ_1 to θ_8 plus θ_n , and two cartesian coordinates of the upper torso element center of mass, X_2 and Z_2 . Three coordinates were more conveniently defined as relative to points in the linkage. They are L_n , the length of the extensible neck link, and (X_S, Z_S) , the coordinates in a coordinate frame fixed to the upper torso element of the end of the upper arm element. The coordinates X_S and Z_S represent shoulder flexibility in the linkage and they are more clearly illustrated in Figure 7-5. Joint properties and dimensional parameters of the linkage, such as the locations of body link centers of mass with respect to articulation points, are discussed fully in Modules 2 and 3.

The differential equations of motion for the occupant which are numerically integrated by the computer model are derived in terms of generalized coordinates defined relative to an inertial frame. This definition of coordinates is pertinent to the analytical equations of motion in Volume 1 of the MVMA-2D manuals and to the computer model code. The average user of the MVMA-2D simulation, however, will be concerned only with model input and output, and for both,

Lower neck joint



$$\vec{r}_{9 \rightarrow 7} = x_s i_2 + z_s k_2$$

$$\theta_c = \text{constant}$$

$$L_{27} = \text{constant}$$

FIGURE 7-5 Shoulder Joint

coordinate values are relative to an arbitrarily positioned coordinate frame in the vehicle. (This is discussed fully in Module 8.) These coordinates differ additionally from computer-model internal coordinates in the definition of five of the body link angles, each different by 180° . This is apart from the potential difference due to a non-zero inertial vehicle angle, θ_V . Figure 7-4, already discussed, illustrates an occupant orientation with non-zero values for all vehicle-relative input coordinates. Figure 7-6 illustrates an orientation in which all angle coordinates are zero. The body linkage of a person touching his toes while doing sit-ups approximates this orientation. The legs are straight out to the right, parallel to the vehicle x-axis, and the torso is completely forward and down, with articulation at the hip only. The arms are extended straight ahead toward the feet. Figure 7-7 illustrates the null orientation for internal coordinates and is presented here only for the benefit of the occasional user who may have reason to study the analytical formulation of the motion equations or the associated computer code. It should be instructive to the student to demonstrate that the equations given with Figure 7-7 accurately relate the external (input and output) and internal angular link coordinates.

$\theta_1, \theta_2, \theta_3, \theta_4, \theta_5, \theta_6, \theta_7, \theta_8, \theta_n = 0$ (input or output)

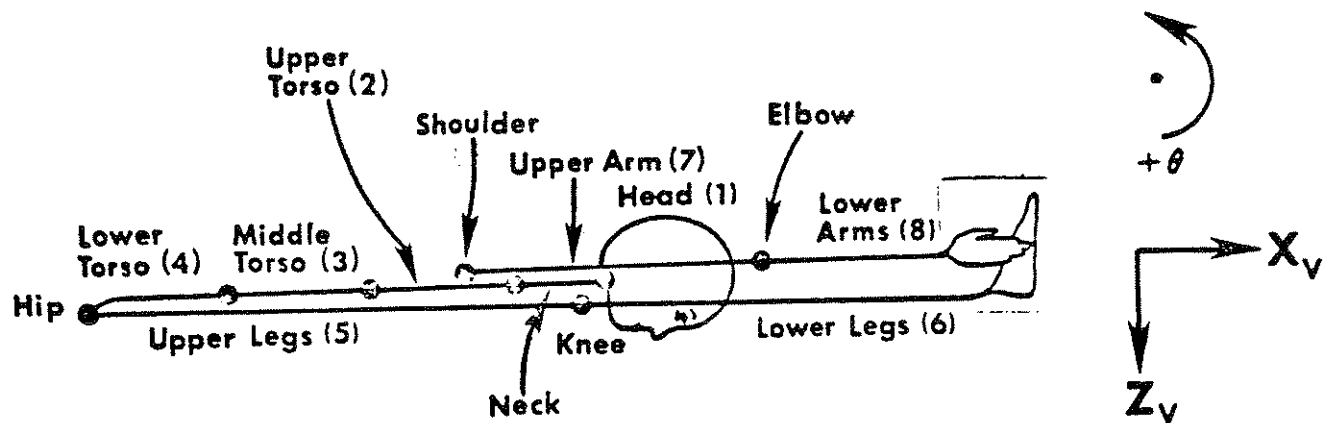
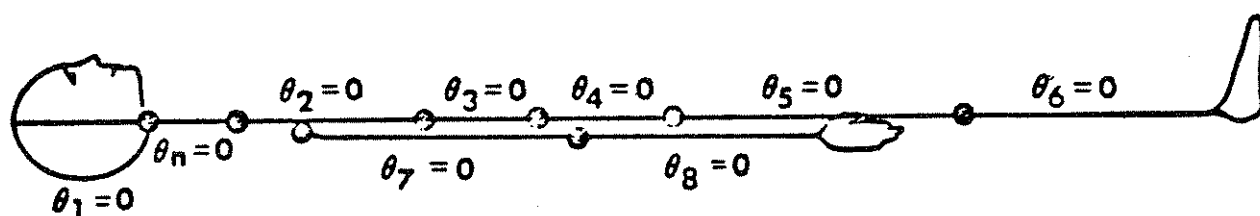


FIGURE 7-6 Occupant Model Configuration with all Body Link Angles Equal to Zero, for INPUT or OUTPUT

$\theta_1, \theta_2, \theta_3, \theta_4, \theta_5, \theta_6, \theta_7, \theta_8, \theta_n = 0$ (analysis and computer code)



Analysis
or Code

Input or Output

$$\theta_i = \theta_i + \theta_v - 180^\circ \quad (i = 1, 2, 3, 4, n)$$

$$\theta_i = \theta_i + \theta_v \quad (i = 5, 6, 7, 8)$$

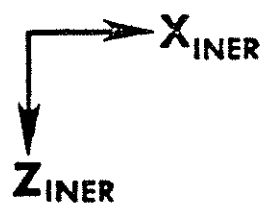


FIGURE 7-7 Occupant Model Configuration with all Internal Link Angles Equal to Zero (NOT for input or output)

7.2 Initial Positioning of Occupant - Data Cards

The input data which relate to the position and orientation of the occupant within the vehicle at crash onset are contained entirely in four data cards -- Cards 301, 302, 303, and 304. Figure 7-8 illustrates cards with values for a seated driver. Initial body link angles, θ_1 to θ_8 plus θ_n , are entered in the first nine fields of Card 301. The units are degrees and angles are defined, as previously discussed, by Figures 7-4 and 7-6. The initial link angular velocities are in the first nine fields of Card 302. Their values will normally all be zero since the occupant is not generally in motion with respect to the vehicle at crash onset. Initial conditions for the linear generalized coordinates are entered on Cards 303 and 304. The x- and z-coordinates of the upper torso center of mass, X_2 and Z_2 , relative to the vehicle origin, are in fields 1 and 3 of Card 303. Their units are inches or centimeters. The initial neck length, i.e., the separation between joints 1 and 2, is entered in field 5 with the same units. The initial velocities for these three linear coordinates are entered in fields 2, 4, and 6, and they will normally be zero. In the event that they are non-zero, however, entries are made with units of ft/sec or m/sec for the torso velocities and in/sec or cm/sec for the initial rate of neck elongation. The shoulder joint coordinates, illustrated in Figure 7-5, are on Card 304. X_s and Z_s are in fields 1 and 3, and their initial velocities are in fields 2 and 4. All four of these values are normally zero because there is generally no relative motion within the occupant linkage before crash onset. The coordinates X_s and Z_s are normally zero initially because those values define

a rest position for the shoulder linkage, which is discussed in detail in Module 3. Rate units are in/sec or cm/sec.

90.	87.	106.	154.	21.	-50.	-82.	40.	75.	301
0.	0.	0.	0.	0.	0.	0.	0.	0.	302
20.5	0.	-29.7	0.	4.41	0.				303
0.	0.	0.	0.						304

FIGURE 7-8 Example Initial Position Data for Seated Driver

7.3 Initial Positioning of Occupant - Equilibrium Considerations

The MVMA Two-Dimensional Crash Victim Simulator has been applied in various ways for the modeling of dynamical systems. A broad range of front and rear impacts for driver and passenger have been simulated. The applications include simulating anthropomorphic dummy drops onto a hard surface and human fall victims striking yielding and unyielding surfaces. They include simulating pedestrians struck by a vehicle. Simulations have been done of laboratory tests in which lateral neck response of human subjects was measured when the head was jerked to the side by a falling weight. Use of the MVMA-2D model need not be restricted to simulating human or human-analog systems. While it could be used to simulate a hanging to help determine force levels for vertebral fracture, it could also be used to model a particle subject to a two-dimensional force field or a three-ball billiards shot on a four-cushioned table. Diverse applications are possible if the user is clever in utilizing the many features of the model.

It is unfortunate that the most common application of the model, simulation of vehicle occupant dynamics, presents a difficulty presented by few of the special model applications -- namely, proper specification of the initial position and orientation of the mechanical linkage. (See Figure 7-9.) The special model applications, while often requiring a certain amount of ingenuity and imagination in the construction of input data sets, normally involve simpler mechanical systems than the occupant/vehicle-interior system; and in particular there is normally no special difficulty in initializing the simpler systems for the desired state of force balance or imbalance. On the other hand, initial positioning of the occupant within the

occupant compartment requires special care by the user because several variously-directed force vectors are required on the seated-occupant linkage to balance gravity. In practice it is not possible to specify the initial position so that the sums of all moments and all forces on all body parts are equal to zero. The user should attempt to approximate this condition of equilibrium, however, if it is intended that the occupant be seated at rest at crash onset. The best measure of his success is probably the nearness to zero of the values calculated by the model at time zero for body link angular accelerations and upper-torso and hip resultant linear accelerations. If these values are small in comparison with the maximum values attained in the simulation, then the initial imbalance is probably not significant.

Forces between the occupant and the vehicle interior are generated by the model as a result of interactions between a user-defined occupant profile and a user-defined vehicle-interior profile. Example profiles are illustrated in Figure 7-9. The contact-sensing occupant profile is a set of ellipses of arbitrary number and dimensions, fixed to body links at arbitrary positions. The only restriction is that either the major or minor axis of each ellipse must be parallel to the body link to which it is attached. Material properties may be assigned for each ellipse, or an ellipse can be specified as rigid, as desired. The contact-sensing vehicle-interior profile is a set of connected or disconnected straight-line segments. Any number may be prescribed, and their lengths and locations are arbitrary. As with contact ellipses, they may be assigned material properties or be specified as rigid. Modules 4, 5, and 6 detail the generation of forces between interacting vehicle-interior and occupant profiles.

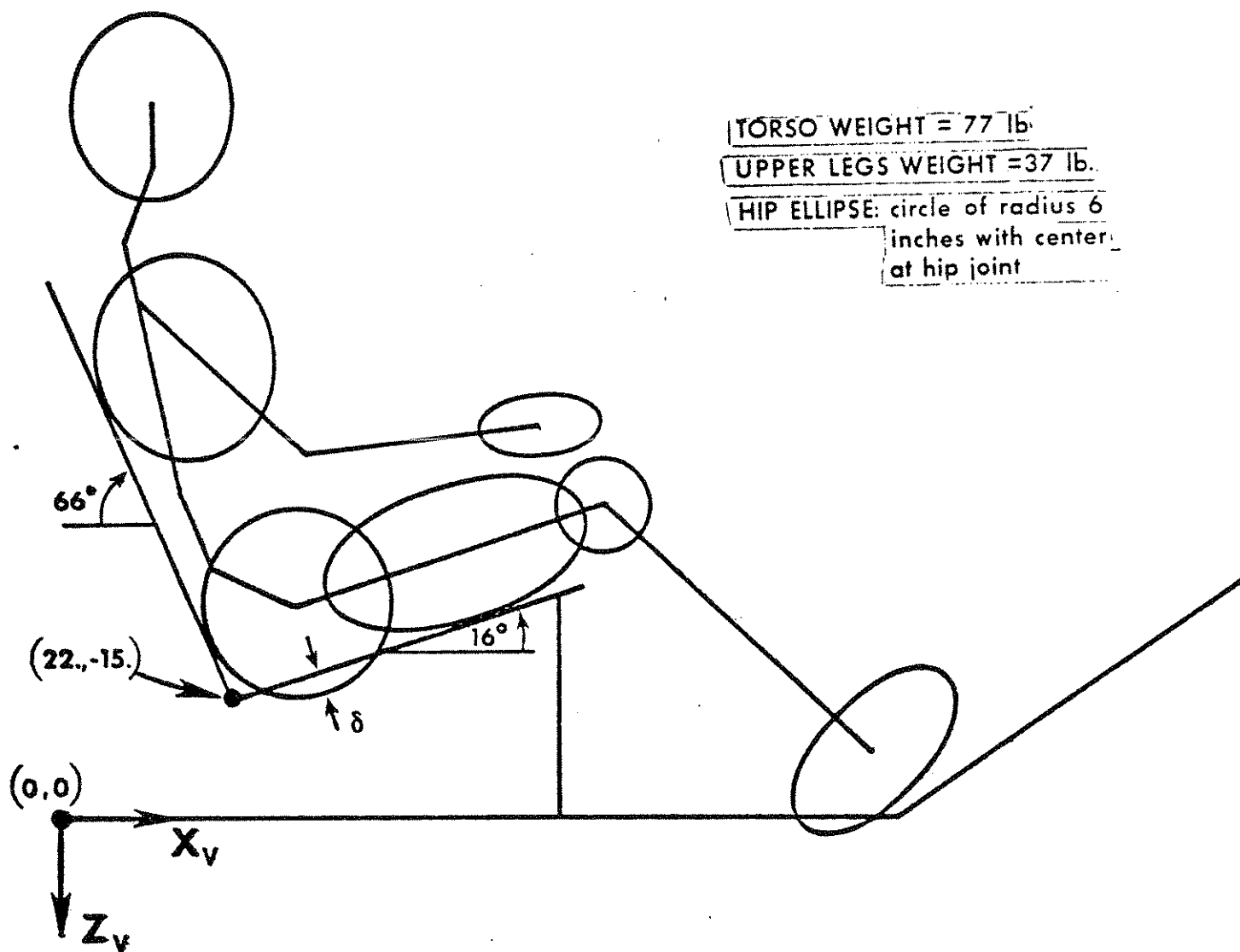


FIGURE 7-9 Seated Occupant in Position of Approximate Equilibrium

The foregoing summary is sufficient explanation for the purposes of this module.

In lieu of a pre-processor computer model or special subroutines, the user himself must establish an initial positioning for approximate equilibrium. One reasonable way to proceed is as follows. First decide on all body-segment masses and body dimensions, including link lengths and sizes and attachment positions of ellipses which define the contact-sensing profile. Decide on the positions in the vehicle of all segments of the vehicle-interior profile. Next, determine what material stiffnesses will be assigned for all ellipses and vehicle-interior line segments. On the basis of the material stiffnesses of the hip ellipse and the seat cushion line, determine the total hip plus seat cushion deformation required to produce a vertical component of seat force which will balance the weight of the torso segments plus one half of the upper legs segment. Similarly determine the total deformation required for the materials of the floorpan and of a contact ellipse at the foot in order to produce a force which will balance the weight of the lower legs plus half the upper-leg weight. It is reasonable to position the hip ellipse so that it is tangent to the seat back, producing no normal force. Thus, it is now possible, using scale drawings or analytic geometry, to establish the coordinates of the hip joint and upper and lower leg angles which will result in the desired initial deformations at the seat cushion and floorpan.

With the hip-joint position already established, values for the torso link angles can next be determined which will make the torso contact

ellipses tangent to the seat back. If desired, they can instead be determined so that torso-ellipse deformations of the seat back produce forces with moments about the hip which balance torso gravitational moments about the hip. However, the force and moment imbalances that result from assuming a zero initial deflection, or simply from making a reasonable estimate of a non-zero initial deflection, will not be significant to the crash dynamics. It is important, however, that the occupant be positioned properly with respect to vehicle-interior surfaces that he might strike, such as the windshield. Therefore, if torso contact ellipses are made tangent to a seatback line, this line should be at the deflected position of the seat back, not at the undeflected surface. Finally, the coordinates of the hip joint position together with the established torso link angles and dimensions completely determine the coordinates X_2 and Z_2 of the upper torso center of gravity. It is necessary in assigning initial head, neck and arm angles to be certain that contact ellipses attached to the head and arm segments are not in position to interact with a head rest, the seat back, the seat cushion, or any other vehicle interior segment. The procedure described here can be modified if thigh or knee ellipses are present and in potential contact with the seat.

Figure 7-9 is a schematic of the seated occupant. In the example which follows, the proper location in vehicle coordinates is determined for the center of a contact-sensing circle at the hip. Many users of the MVMA-2D model will prefer to use scale drawings to solve problems such as this, and in that connection it is mentioned here that it is often worthwhile to make templates for the body contact-sensing ellipses. The solution given here is analytical.

In order that a hip circle of radius 6 inches be tangent to the seat back, its center must lie on a line parallel to and 6 inches from the seat-back line. The slope intercept-equation of a straight line has the form

$$z = (\text{slope}) x + (z\text{-intercept})$$

and therefore the equation for the seat-back line is

$$z = (\tan 66^\circ) x + (-15 - 22 \tan 66^\circ)$$

or

$$z = 2.246 x - 64.41.$$

The distance of a point (x_c, z_c) from a line

$$Ax + Cz + D = 0$$

is

$$0 \leq \delta = \frac{Ax_c + Cz_c + D}{\pm \sqrt{A^2 + C^2}}$$

Therefore, the center of the hip circle must lie on the line

$$6 = \frac{2.246 x_c - z_c - 64.41}{+\sqrt{(2.246)^2 + (-1)^2}}$$

The "plus" sign is required for the radical in order that the distance to points (x_c, z_c) on the hip-circle line, which is on the opposite side of the seat-back line from the origin, be positive. Thus, the condition of tangency of the hip circle to the seat back is

$$.9135 x_c - .4067 z_c - 32.20 = 0 \quad (7.1)$$

A second condition to be satisfied is that the hip circle must deflect the seat cushion by an amount δ which will produce a z-component of force sufficient to balance the weight of the torso plus half the upper legs weight. This means that the center of the hip circle must

lie on a line of distance $6'' - \delta$ from the seat-cushion line. Proceeding as before, we find the equation of the seat-cushion line to be

$$.2867 x + z + 8.692 = 0.$$

The center of the hip circle therefore satisfies the condition

$$6 - \delta = \frac{.2867 x_c + z_c + 8.692}{-\sqrt{(.2867)^2 + (1)^2}} \quad (7.2)$$

It is now necessary to determine the deflection δ . Suppose that both the hip circle and the seat cushion can undergo deflection and that their force-deflection curves are as shown in Figure 7-10. If the torso weight is 77 lb and the upper legs weight is 37 lb, the force to be balanced in the z-direction is $F = 77 + 37/2 = 95.5$ lb. The force normal to the seat cushion line must therefore be $95.5 \cos 16^\circ = 91.8$ lb. From the force-deflection equation for the seat cushion, given with Figure 7-10, the seat cushion deflection which will produce this force is found as the solution of the equation:

$$91.8 = 88.45\delta - 33\delta^2 + 9.36\delta^3.$$

The solution may be found iteratively, graphically, or by other means to be

$$\delta_{sc} = 1.533''.$$

The hip-circle deflection necessary for 91.8 lb is found similarly as the solution of

$$91.8 = 10 + (\delta - .5) \frac{990}{.5},$$

or

$$\delta_H = .541''.$$

Consequently, the total deflection of hip and seat cushion is

$$\delta = \delta_H + \delta_{sc} = 2.074''.$$

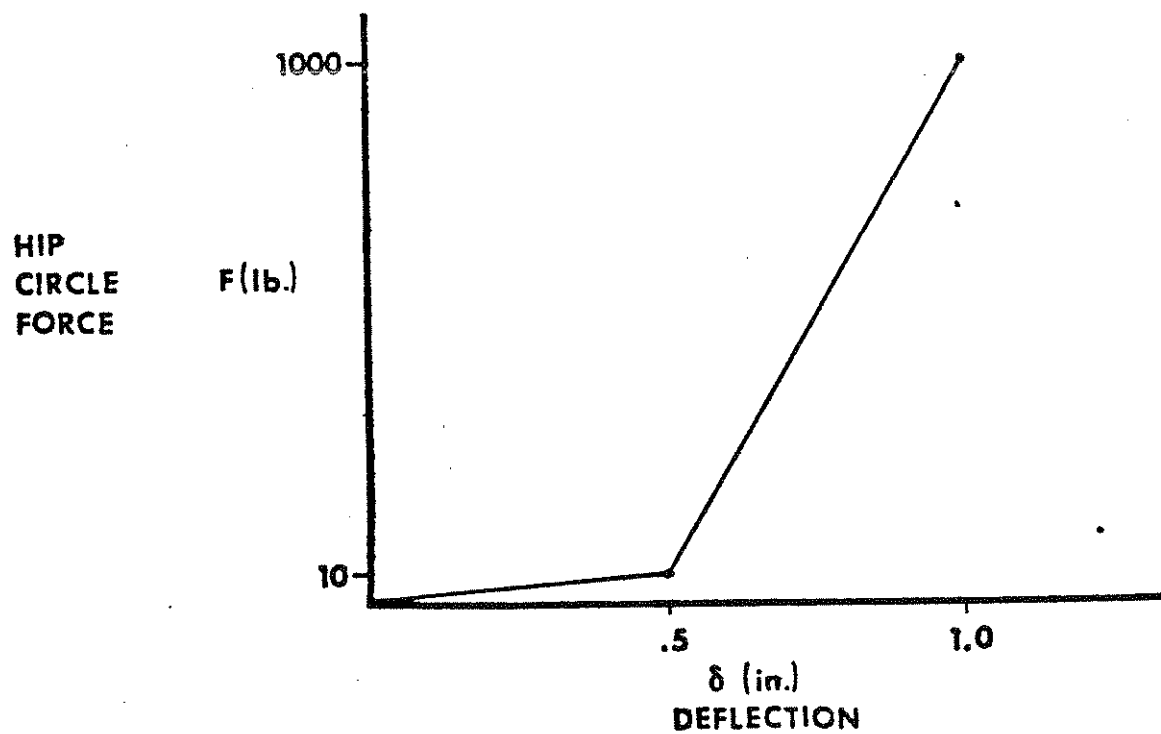
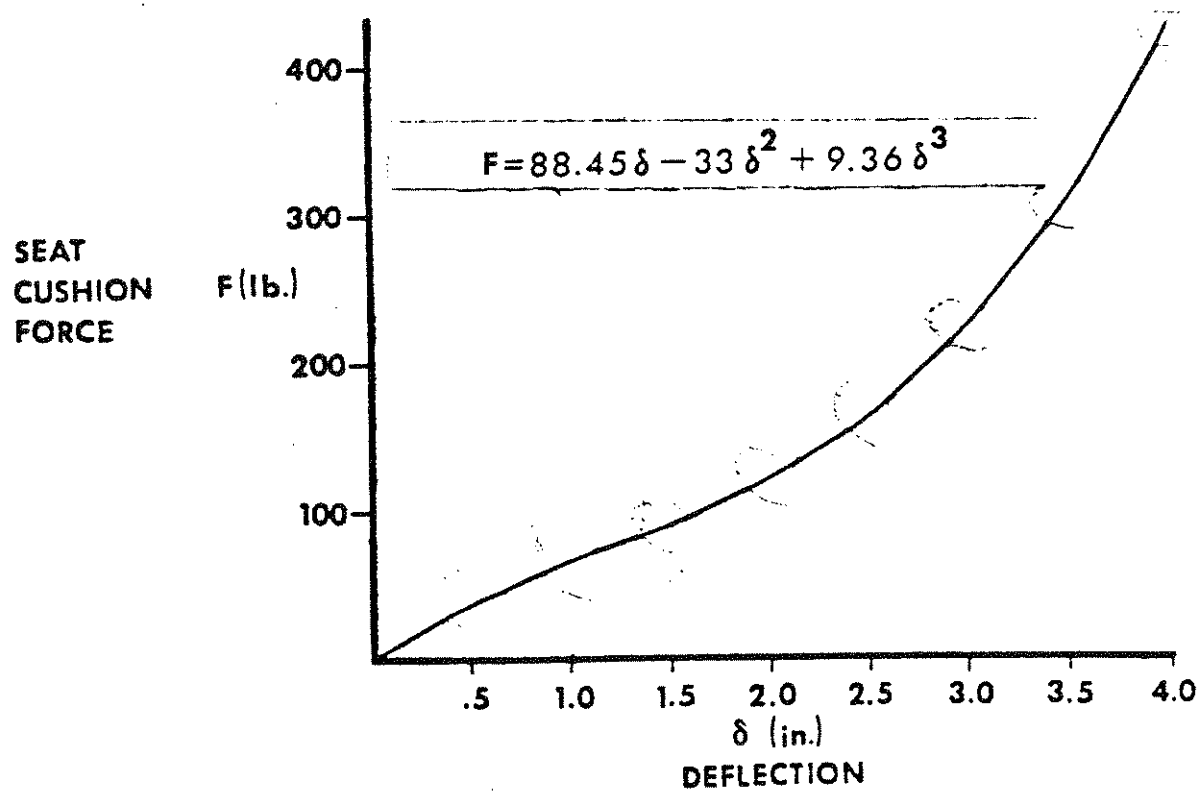


FIGURE 7-10 Force-Deflection Curves for Seat Cushion and Hip Circle

Substituting this value for δ into equation (7.2) gives

$$.2756 x_c + .9613 z_c + 12.28 = 0 \quad (7.3)$$

as the condition for proper seat cushion deflection.

The intersection of the two lines given by equations (7.1) and (7.3) is the required location of the center of the hip circle.

Solution of these simultaneous equations yields

$$x_c = 26.22"$$

$$z_c = -20.29" .$$

Since for this example the hip circle is centered at the hip joint, we do not need to lay off from this point to determine the hip joint coordinates. They are

$$x_H = 26.22"$$

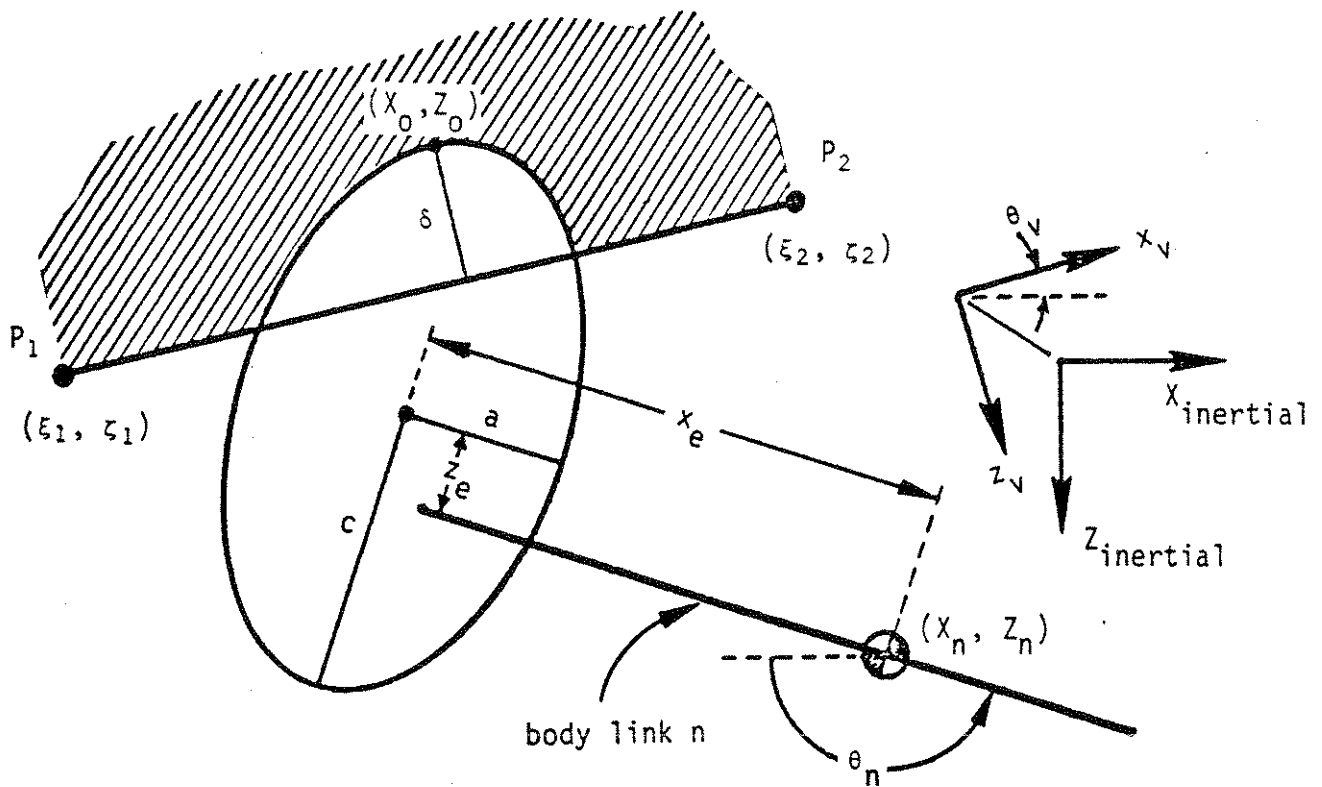
$$z_H = -20.29" .$$

No further details will be presented here for the determination of the initial position data. The user should be able to follow the general procedure outlined earlier in this section. The step following the establishment of H-point coordinates (x_H , z_H) should be to strike off arcs from the H-point of radii equal to the lengths of the upper leg and lower torso links. These arcs will be the loci of prospective locations of the knee joint and lower spine joint.

If the initial occupant configuration involves deflection between a non-circular ellipse and a line segment, then the analysis is somewhat more complex than in the foregoing example. For an ellipse, the analysis must involve the relationship of deflection to ellipse orientation, ellipse size, ellipse position, and line position. The less mathematically-oriented user will perhaps prefer to use scale

drawings to solve such a problem. However, for the analyst, pertinent equations are presented in Figures 7-11 and 7-12 for reference and may also be found in Volume 1 and Module 6.

After completing the determination of initial position and orientation data, and before making a computer run for the crash simulation, the user may wish to see a computer-generated schematic of the vehicle and occupant represented by the established data set. The MVMA-2D model will produce such a schematic in print-plot form without execution of the "GO" processor, i.e., without performing an integration for occupant dynamics. The print-plot schematic can be produced by running only the input and output processors, "IN" plus "OUT." Cards 1500 and 1501 are used for this purpose as explained in Module 12. If printout of initial force and acceleration values is desired in addition to the schematic, then the execution processor, "GO," can be run as well, say, to $t = 1$ msec.



Definitions

- n = body segment number for the ellipse (1, ..., 8) (Card 219, field 5).
- a = x-semi-axis length (Card 220, field 5).
- c = z-semi-axis length (Card 220, field 6).
- θ_n = angle of body link n (see Card 301 for $t = 0$ and Figure 6-5).
- θ_v = vehicle pitch angle (see Card 601 for $t = 0$ and Card 604).
- (x_e, z_e) = coordinates of ellipse center in body segment system (Card 220, fields 3 and 4).
- (ξ_i, ζ_i) = coordinates of line-segment endpoint P_i ($i = 1, 2$) in vehicle system (Card 411, fields 4-7).
- (x_n, z_n) = inertial coordinates of CG of body segment n [function of x_2 and z_2 (from Card 303 for $t = 0$), body link angles (see Card 301 for $t = 0$ and Figure 6-5), and link lengths (Cards 201 and 202); see Section 2.1 of Volume 1].
- (μ_4, μ_5) = inertial coordinates of ellipse center.
- (x_0, z_0) = inertial coordinates of contact point.
- δ = deflection.

FIGURE 7-11 Constants and Variables Relevant to Evaluation of Ellipse-Line Deflection

EQUATIONS

$$p = \xi_2 - \xi_1$$

$$r = \zeta_1 - \zeta_2$$

$$s = \xi_1 \zeta_2 - \zeta_1 \xi_2$$

$$A = r \cos \theta_v + p \sin \theta_v$$

$$C = -r \sin \theta_v + p \cos \theta_v$$

$$D = s$$

$$\mu_1 = \frac{1}{2}(a^2 \cos^2 \theta_n + c^2 \sin^2 \theta_n)$$

$$\mu_2 = \frac{1}{2}(c^2 - a^2) \sin \theta_n \cos \theta_n$$

$$\mu_3 = \frac{1}{2}(a^2 \sin^2 \theta_n + c^2 \cos^2 \theta_n)$$

$$\mu_4 = X_n + X_e \cos \theta_n + Z_e \sin \theta_n$$

$$\mu_5 = Z_n - X_e \sin \theta_n + Z_e \cos \theta_n$$

$$k = \sqrt{\frac{2}{\mu_1 A^2 + 2\mu_2 AC + \mu_3 C^2}}$$

$$X_0 = \mu_4 \pm k (\mu_1 A + \mu_2 C)$$

$$Z_0 = \mu_5 \pm k (\mu_2 A + \mu_3 C)$$

One sign for k gives the point of maximum penetration, the "contact point." The other sign gives the point directly opposite the ellipse center, i.e., the point of "minimum penetration."

$$\delta = \left| \frac{Ax_0 + Cz_0 + D}{\sqrt{A^2 + C^2}} \right|$$

FIGURE 7-12 Evaluation of Deflection Between a Straight-Line Segment and an Ellipse.

7.4 Initial Equilibrium -- Other Considerations

Strictly, the initial values for body link angles are independent and arbitrary since they are generalized coordinates. But their values are restricted not only by the considerations just discussed for initial equilibrium in the vehicle but also by anatomical considerations. Initial deformation of a joint stop cannot be justified if the stop is intended to be a "hard" limitation to voluntary relative motion at the joint; deformation in this case can be allowed only after impact. Thus, for example, the initial head, neck, and upper torso angles should not result in relative angles at the neck joints which exceed the joint-stop limits for the neck indicated on Cards 205, 206, 215, and 216.

It is appropriate to note here a small initial imbalance over which the user has no control. The value on Card 303 for initial neck length is used also as the unstrained length for nonlinear springs which resist neck elongation and compression. Therefore, it is not possible to enter data which result in a non-zero initial compressive neck load, as would be the normal condition for a seated occupant. This initial imbalance is inconsequential.

One model input parameter which is indirectly pertinent to the specification of initial conditions is not discussed in this module. This is the so-called "penetration limit," which is used by the computer model to help identify a case in which an ellipse is initially behind a line segment but no force is to be calculated. In effect, it defines the depth of a component of the vehicle interior. This is a line-segment parameter on 409-Cards and it is discussed in detail in Module 5.

MODULE 8 -- CRASH DECELERATION PROFILES AND HEAD APPLIED FORCES

8.1 Vehicle Motions

The crash victim's environment is made to be dynamic by specifying a vehicular motion. If the crash victim is a pedestrian, the vehicle might be moving with constant speed or it might be accelerating or decelerating. If the crash victim is an occupant of either a struck vehicle or a striking vehicle, he is normally initially at rest with respect to the vehicle. He interacts dynamically with the vehicle interior and restraint systems only as a result of occupant compartment acceleration or deceleration. Therefore, unless the model is being used to solve a free motion problem, it is always necessary to prescribe a vehicular motion.

Figure 8-1 is a schematic of the planar vehicle. Point "0" is the origin of a coordinate system fixed to the occupant compartment. Its location in the vehicle is arbitrary; it might, for example, be a point on the toeboard. While occupant position and the location of points defining the vehicle interior are prescribed with respect to this point, it is necessary to describe the motion of this point with respect to an inertial reference frame. In addition to horizontal and vertical motions for point "0" (X_V and Z_V), it is necessary to know the angular vehicle motion as a function of time. The sense of each of the three vehicle degrees of freedom (X_V , Z_V , and θ_V) is shown in the figure. Vehicle motion is prescribed with Cards 601, 602, 603, 604, and accompanying unnumbered cards.

8.1.1 Data Requirements. Initial values for the x- and z-coordinates of point "0" in the inertial frame are required in fields 1 and 3 of Card 601, and the x- and z- components of the initial velocity vector of this point are required in fields 2 and 4. Similarly, the initial pitch angle and pitch angular velocity are entered in fields 5 and 6. If velocities of the vehicle degrees of freedom are to vary with time, time-dependent accelerations must be prescribed. In order that vehicle accelerations can be specified with greatest possible ease, it is not required that the linear accelerations be defined

Inertial reference frame

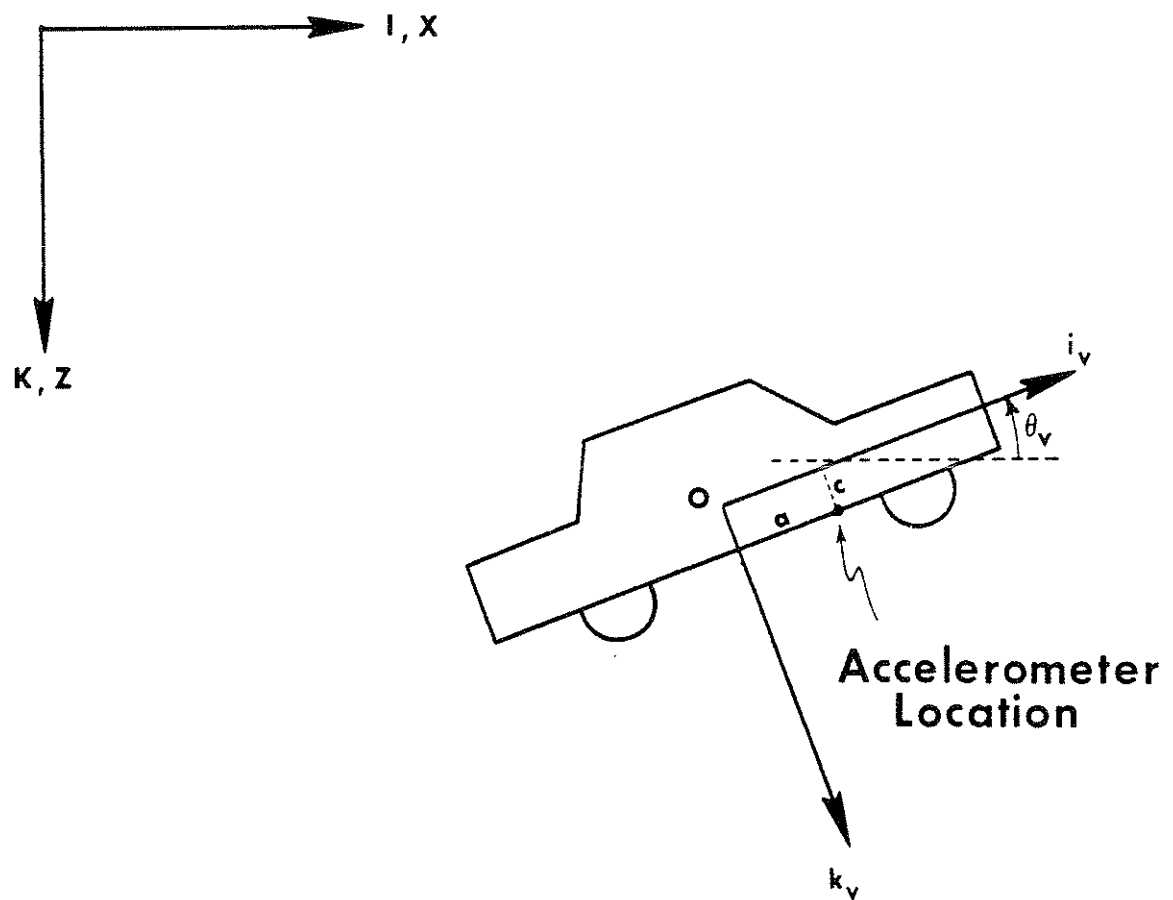


FIGURE 8-1 Vehicle Coordinates

at the point "0," but rather at an arbitrary point in the occupant compartment, where, for example, a biaxial accelerometer might be mounted. The location of that point in vehicle coordinates, that is, relative to point "0," must be specified in fields 7 and 8 of Card 601.

Acceleration histories are inputted as tabular functions of time. The number of points in the x-acceleration table is entered in field 1 of Card 602. This number must be between 2. and 200. Field 2 should contain a 1. if the accelerations are in g units and a 0. if in in/sec^2 or m/sec^2 . If vehicle accelerations are defined with respect to the vehicle coordinate frame, i.e., as accelerometer readings, then field 3 should contain a 0. If vehicle accelerations are defined instead with respect to the inertial reference frame, field 3 of Card 602 should contain a non-zero value;* in this case, the acceleration components must be for the vehicle origin, "0," not for a specified accelerometer location. The coordinates of the points in the x-acceleration table are entered on unnumbered cards following the 602-Card. Each card contains coordinates of four points. The time in milliseconds is placed in fields 1, 3, 5, and 7 and the corresponding x-acceleration values in fields 2, 4, 6, and 8. The first eight fields on each card are filled before proceeding to the next card. Card 603 and following unnumbered cards are similarly used for specifying z-accelerations.

The pitch angular acceleration table is defined by Card 604. Pitch acceleration data are entered on succeeding unnumbered cards in the previously described manner. The 604-Card requires only two entries -- the number of points in the table in field 1 and a units indicator in field 2, 0. if deg/sec^2 and 1. if rad/sec^2 .

8.1.2 Example Data. As an example of the preparation of vehicle-motion input data cards, consider a hypothetical 30 mph frontal barrier collision. Suppose that linear acceleration data is obtained from a biaxial accelerometer fastened to the frame of the vehicle and located

* Other names commonly used for the inertial reference frame are "spaced-fixed frame," "lab frame," and "absolute frame."

at a point 18 inches behind and 3. inches below an arbitrarily defined vehicle origin, say, a point on the toeboard. In accordance with the sign convention illustrated in Figure 8-1, fields 7 and 8 of Card 601 are -18. and 3., respectively. The example data cards are shown in Figure 8-2. Definition of the beginning of the crash, that is, $t = 0$, is arbitrary, but is reasonably taken as the time at which accelerations begin to deviate from zero. Suppose that at this instant the vehicle origin, "0," at the toeboard in this example, is 120. inches forward of the inertial-frame reference point and 14. inches above.* Then fields 1 and 3 of Card 601 should be 120. and -14. Field 2 is 44. ft/sec, i.e., 30 mph, and field 4 is 0. since there is no initial vertical velocity. The initial vehicle pitch angle and angular velocity are both zero, so 0's are entered in fields 5 and 6 of the 601-Card.

The user can always approximate a continuous accelerometer trace to any desired degree of accuracy by connected straight-line segments. Figure 8-3 shows piecewise-linear approximations of hypothetical accelerometer traces for a 30 mph frontal barrier collision. If values are used directly from accelerometer traces in order to specify vehicle motion, field 3 of Cards 602 and 603 must be 0. since the linear acceleration components are with respect to the vehicle axes and not the inertial reference frame. Since values may be entered in g-units from Figure 8-3, field 2 of Cards 602 and 603 is 1. It is seen that seven input points are sufficient to define the piecewise-linearized trace for the horizontal component of vehicle acceleration and ten points are sufficient for the vertical component. The 602- and 603-Cards therefore have a 7. and a 10. in their respective first fields. Pairs of coordinate values for these eighteen table points follow the 602- and 603-Cards on unnumbered

* It is often convenient to define the inertial frame reference point as coincident with the vehicle origin at time zero. The initial vehicle x- and z-coordinate values would obviously both be 0. in this case.

30MPH FRONT BARRIER								600
120.	44.	-14.	0.	0.	0.	-18.	3.	601
7.	1.	0.						602
0.	0.	25.	-17.3	65.	-15.2	75.	-20.	
85.	-20.	120.	0.	2000.	0.			
11.	1.	0.						603
0.	0.	20.	-5.	40.	-5.	55.	10.1	
80.	11.1	90.	-4.	105.	-9.	120.	-8.	
130.	0.	2000.	0.					
11.	1.							604
0.	0.	2.	-32.	45.	-32.	46.	90.	
76.	60.	90.	75.	96.	-68.	126.	-68.	
130.	0.	2000.	0.					

FIGURE 8-2 Deceleration Pulse Data Cards

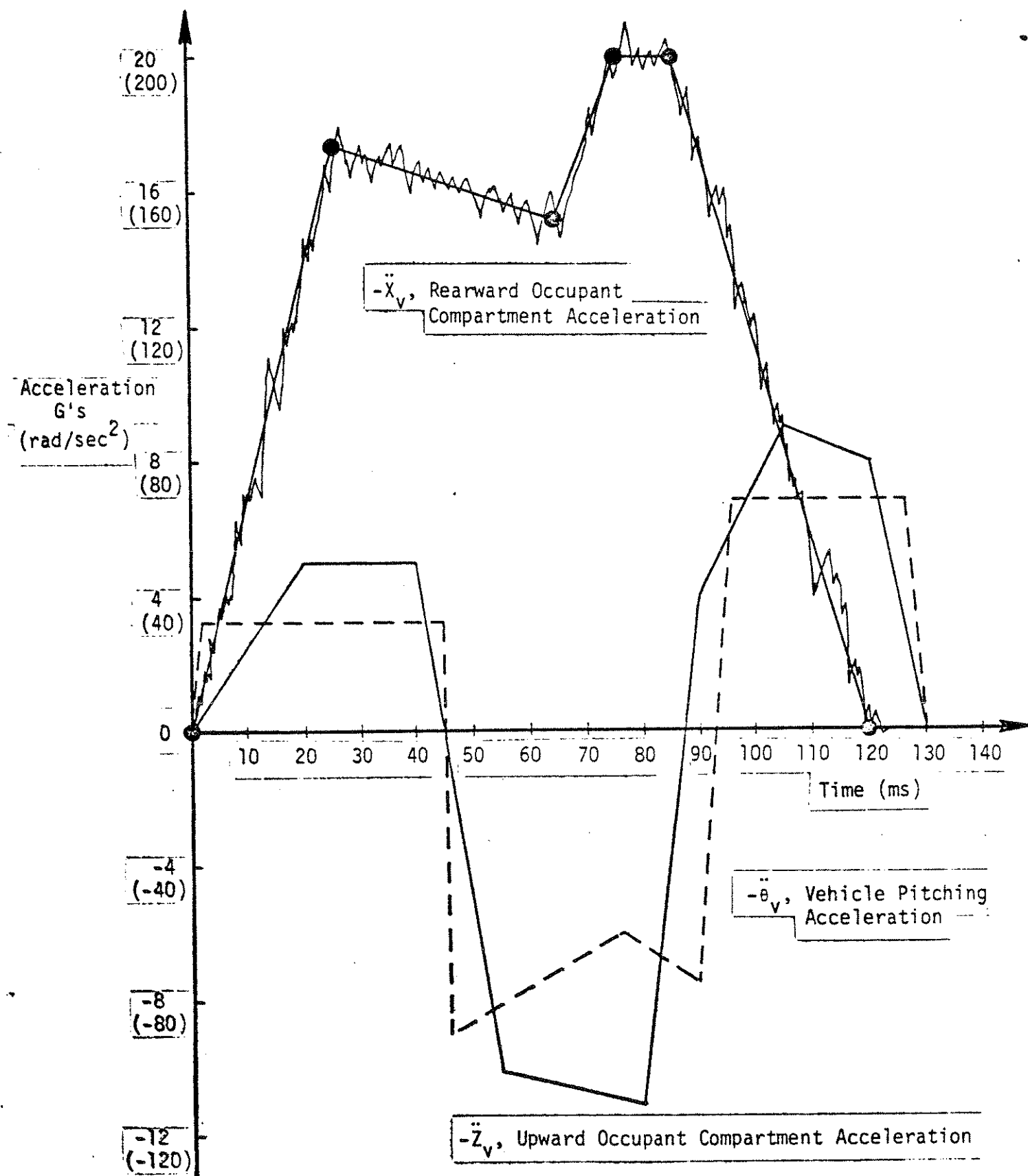


FIGURE 8-3 Vehicle Acceleration Profiles

cards, time values in milliseconds and accelerations in g's. For example, the second point on the x-acceleration trace is -17.3 g at 25 msec. Fields 3 and 4 of the first card after the 602-Card accordingly contain 25. and -17.3.

The angular acceleration trace in Figure 8-3 might have been obtained from an angular accelerometer, from analysis of non-coincident linear accelerometer data, or from film analysis. Like the x- and z-accelerations in the figure, this trace is a piecewise-linear approximation of a more complex profile. Values used from the trace are in rad/sec^2 so field 2 of Card 604 contains a 1. The ten points which define this acceleration profile are entered on the unnumbered cards following the 604-Card.

8.1.3 Acceleration Components in Different Frames of Reference.

If linear vehicle acceleration components for the foregoing example had been determined in the inertial frame (for "0") instead of as accelerometer measurements in the vehicle frame, the necessary data could be input just as easily. In this case, field 3 of Cards 602 and 603 would be set to 0. in order to indicate inertial accelerations. This option was previously explained.

Whether the model user inputs vehicle acceleration components relative to the inertial frame or in the vehicle frame of reference generally depends on the source of his data. The linear acceleration profiles may be entered in whichever form is more convenient. It is unnecessary for the purpose of defining input data for the user to understand the analytical relationship between acceleration components in these two reference frames. It is not a consideration in the specification of data. But it is clear that an analytical relationship between them does exist since there is no model provision allowing the accelerometer location to change with time in the vehicle-fixed coordinate frame.*

The following simple transformation relates the inertial components to components measured in the rotating vehicle coordinate system.

* That is, the quantities a and c in Figure 8-1 are constants, not functions of time.

Where θ_v is the vehicle pitch angle,

$$\ddot{x}_{v,"0"}^{(\text{inertial})} = \ddot{x}_{v,"0"}^{(\text{vehicle frame})} \cos \theta_v + \ddot{z}_{v,"0"}^{(\text{vehicle frame})} \sin \theta_v$$

$$\ddot{z}_{v,"0"}^{(\text{inertial})} = -\ddot{x}_{v,"0"}^{(\text{vehicle frame})} \sin \theta_v + \ddot{z}_{v,"0"}^{(\text{vehicle frame})} \cos \theta_v$$

where

$$\ddot{x}_{v,"0"}^{(\text{vehicle frame})} = \ddot{x}_{\text{accelerometer}} - c \ddot{\theta}_v + a \dot{\theta}_v^2$$

$$\ddot{z}_{v,"0"}^{(\text{vehicle frame})} = \ddot{z}_{\text{accelerometer}} + a \ddot{\theta}_v + c \dot{\theta}_v^2$$

These relations are pertinent to understanding the printed output of vehicle motion. Although the user is allowed to prescribe acceleration components in the vehicle-fixed frame, inertial components are calculated by the computer model for output and for use in the equations of motion.

The inertial components are, of course, identical to the vehicle-relative components whenever the vehicle is not pitched. These results can be seen to follow from the transformation relations by setting the pitch angle, θ_v , equal to zero. As an exercise, the student might try to demonstrate for the example crash defined by the profiles in Figure 8-3 that, while the accelerometer peaks are -20 g's and +11.1 g's for x- and z- motions, the peak inertial accelerations are -20.2 g's and + 9.8 g's. Acceleration data for the profiles in Figure 8-3 are in Figure 8-2, and the vehicle pitch angle as a function of time is shown in Figure 8-4.* Assume the accelerometer to be at the vehicle origin.

8.2 Head Applied Forces

Crash deceleration profiles provide an indirect forcing excitation to the occupant linkage. It is indirect in that crash forces on the occupant result only when prescribed vehicle motion causes interaction with occupant-compartment surfaces and restraint systems. The MVMA Two-Dimensional Crash Victim Simulator provides as well for a special, direct forcing excitation that has found occasional use. This is the direct application of a time-dependent force vector to any desired point on the head. Both the magnitude and direction of the vector can be time dependent since the X- and Z-components are separately

* The pitch angle in Figure 8-4 is the second integral of the pitch angular acceleration in Figure 8-3.

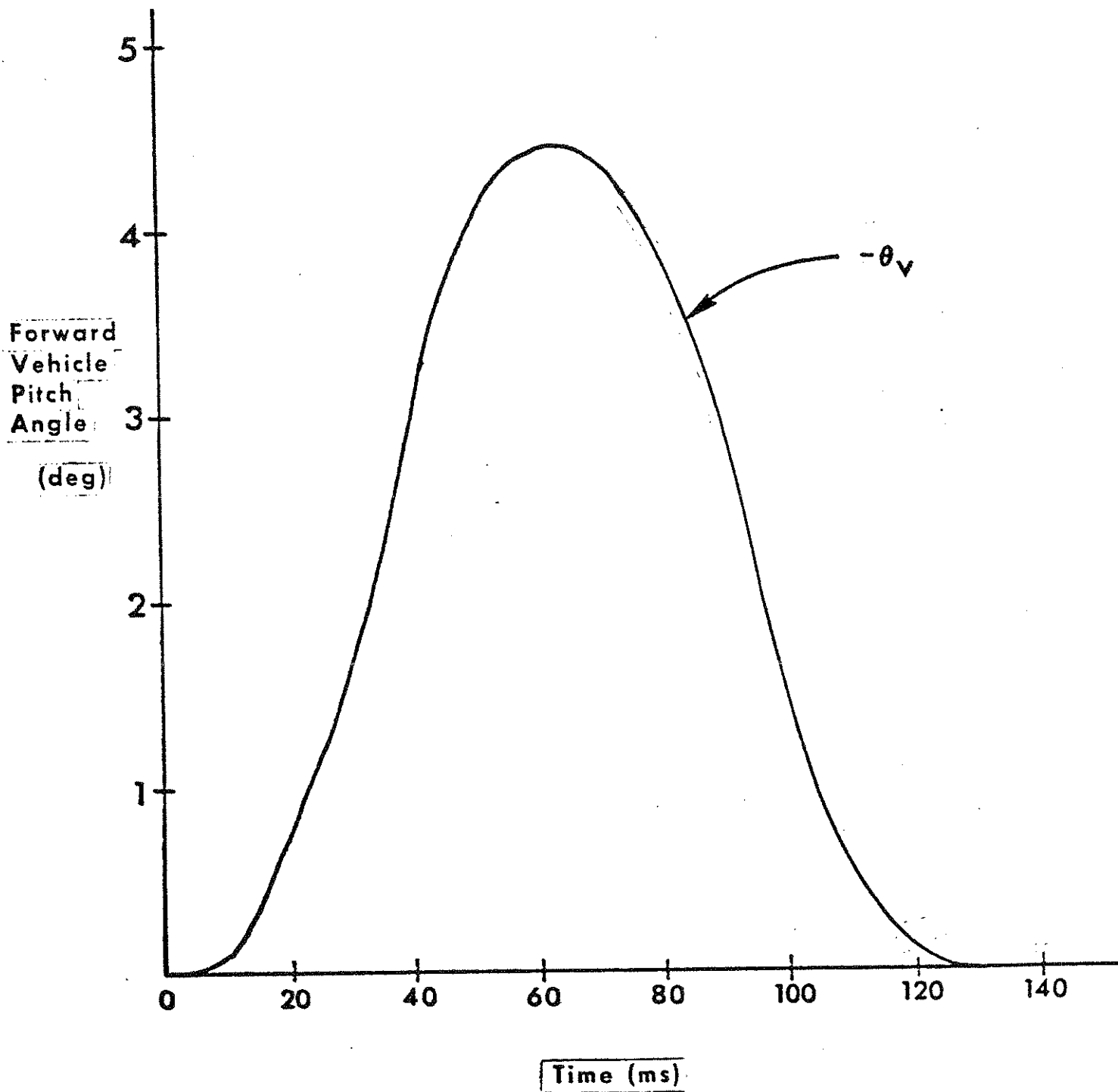


FIGURE 8-4 Vehicle Pitch Angle

specified. Figure 8-5 shows the head and the components of an applied force vector.

The force components are specified as time-dependent tables. A single 605-Card is required. Field 1 should contain a name assigned to the table for F_x ; it may be any combination of up to eight alphanumeric characters. Field 2 similarly contains a name for the z-component. The value entered for field 3 indicates whether force components are to be interpreted as relative to the inertial coordinate axes or the rotating head system. A zero is entered if they are in the inertial frame and a non-zero value otherwise. Fields 4 and 5 contain the X and Z coordinates in the head system of the point of application of the force vector, "a" and "c" in Figure 8-5. One 606-Card is required for each point in the two applied force tables. Field 1 of each 606-Card must contain the name assigned to the force table in field 1 or field 2 of the 605-Card. The time for the table point is in field 2 of the 606-Card and the force component value is in field 3.

Figure 8-6 illustrates a 500 lb., 10 msec half-sine force applied at the base of the skull in a superior and anterior direction, 30° above the inertial horizontal axis. The force is applied at a point 4 inches posterior and 1.2 inches inferior of the head center of gravity. In accordance with the sign convention indicated in Figure 8-5, values of "a" equal to 1.2 and "c" equal to -4. are entered in fields 4 and 5 of Card 605. The data cards for this example are shown in Figure 8-7. The sinusoidal force pulses are approximated by piecewise-linear forms, and the resulting time and force values are entered on 606-Cards. Field 3 of Card 605 contains a 0. since force components are defined in the inertial frame for this example.

Diverse applications might be made of this model feature. One use to which it has been put was to aid in the empirical determination of a composite lateral bending stiffness of the neck for small deformations. An experiment was devised in which a short-duration, low-level force could be applied laterally to a subject's head. The subject was seated, and a sideboard prevented any torso motion. The force pulse was recorded as a function of time, and angular head acceleration was determined from accelerometers mounted on a

6/28/79

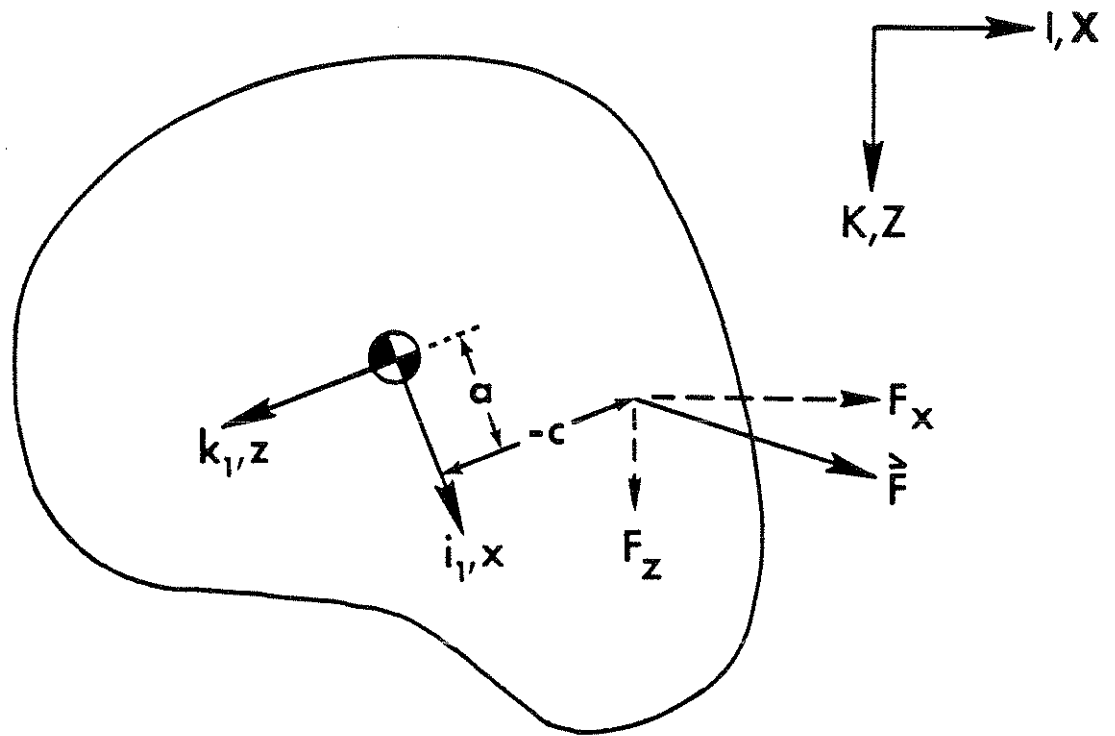
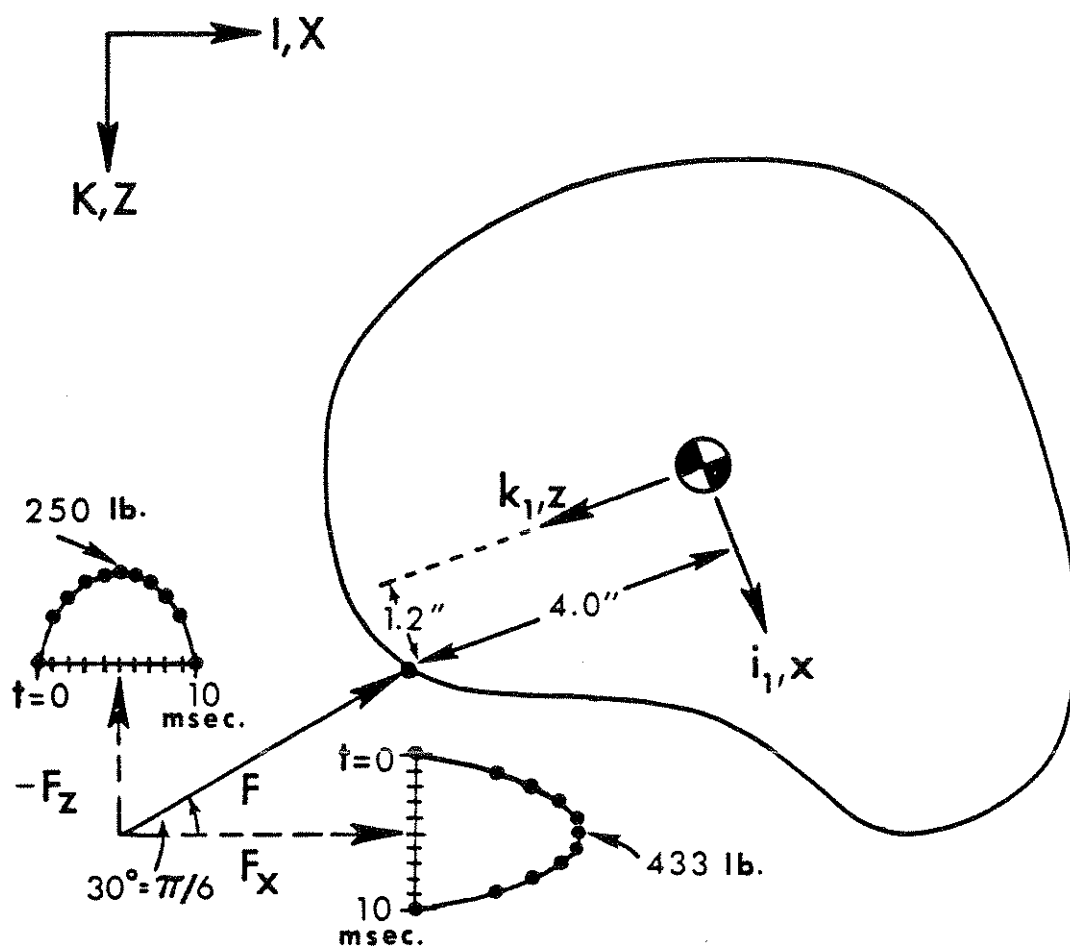


FIGURE 8-5 Schematic of Force Applied to Head



$$F_x = 500 \cos \pi/6 \sin \left(\frac{2\pi}{.02} t \right)$$

$$F_z = -500 \sin \pi/6 \sin \left(\frac{2\pi}{.02} t \right)$$

FIGURE 8-6 Example of Data for Force Applied to Head

FX	FZ	0.	1.2	-4.	605
FX	0.	0.			606
FX	1.	133.8			606
FX	2.	254.5			606
FX	3.	350.3			606
FX	4.	411.8			606
FX	5.	433.0			606
FX	6.	411.8			606
FX	7.	350.3			606
FX	8.	254.5			606
FX	9.	133.8			606
FX	10.	0.			606
FX	2000.	0.			606
FZ	0.	0.			606
FZ	1.	-77.3			606
FZ	2.	-146.9			606
FZ	3.	-202.3			606
FZ	4.	-237.8			606
FZ	5.	-250.			606
FZ	6.	-237.8			606
FZ	7.	-202.3			606
FZ	8.	-146.9			606
FZ	9.	-77.3			606
FZ	10.	0.			606
FZ	2000.	0.			606

FIGURE 8-7 Head Applied Force Data Cards

6/28/79

bite-bar structure. The experiment was then simulated with the MVMA-2D model. Primary inputs to the model were head mass and moment of inertia and neck mass, all estimated from cadaver data, and neck length, determined from X-rays of the subjects. The elastic torsional stiffness coefficients K_θ at the upper and lower neck joints were considered to be adjustable parameters for a series of computer simulations which used measured head force as a driving excitation. Neck stiffnesses appropriate for small lateral bending deflections of the head and neck were thus determined as the values K_θ which gave the best fit of simulated angular acceleration response to experimentally measured response.

MODULE 9 -- BELT RESTRAINT SYSTEMS

9.1 Introduction

The MVMA Two-Dimensional Crash Victim Simulator includes two independent belt system models for optional usage. The first is illustrated by Figure 9-1 and consists of: a) a one-piece lap belt attached to the lower torso element and anchored at each end to the vehicle; b) an upper torso harness strap attached to the upper torso element and anchored to the vehicle; c) a lower torso harness strap attached arbitrarily to any torso element and anchored to the vehicle. The second, a more complex system, is illustrated by Figure 9-2 and includes the following features: a) seven belt segments which may be independent or, at option, may be paired in certain combinations to act as a lesser number of separate lengths of webbing by use of various free slipping and friction elections at the torso and lap and at slip points; b) a slip point in the three-belt upper harness system; c) a slip point between the lower torso and lap sections; d) optionally, inertia reels (either vehicle-sensitive or webbing-sensitive) at three of the four anchor locations.

9.2 A Three-Belt Submodel

9.2.1 Anchors and Attachment Points. The simpler of these two belt-restraint submodels is effectively a three-belt system. The two-segment lap belt shown in Figure 9-1 is treated by the computer model as a single piece of webbing that slides freely over the pelvis through a user-specified point, called an "attachment point," on the lower-torso element. Thus, a lap-belt tension is determined from the elongation or strain of the total belt length, with no adjustment for possible friction effects, and the established tension is applied at the attachment point on the body through both the inboard and outboard segments. For example, if the projections in the X-Z plane of the inboard and outboard lap belt anchors are made coincident by the user, then the magnitude of the lap-belt force vector acting at the attachment point will be $2F$, where F is the tension in the lap-belt webbing. In general, the lap-belt segments are not coincident, nor are they of equal length, since the anchor positions

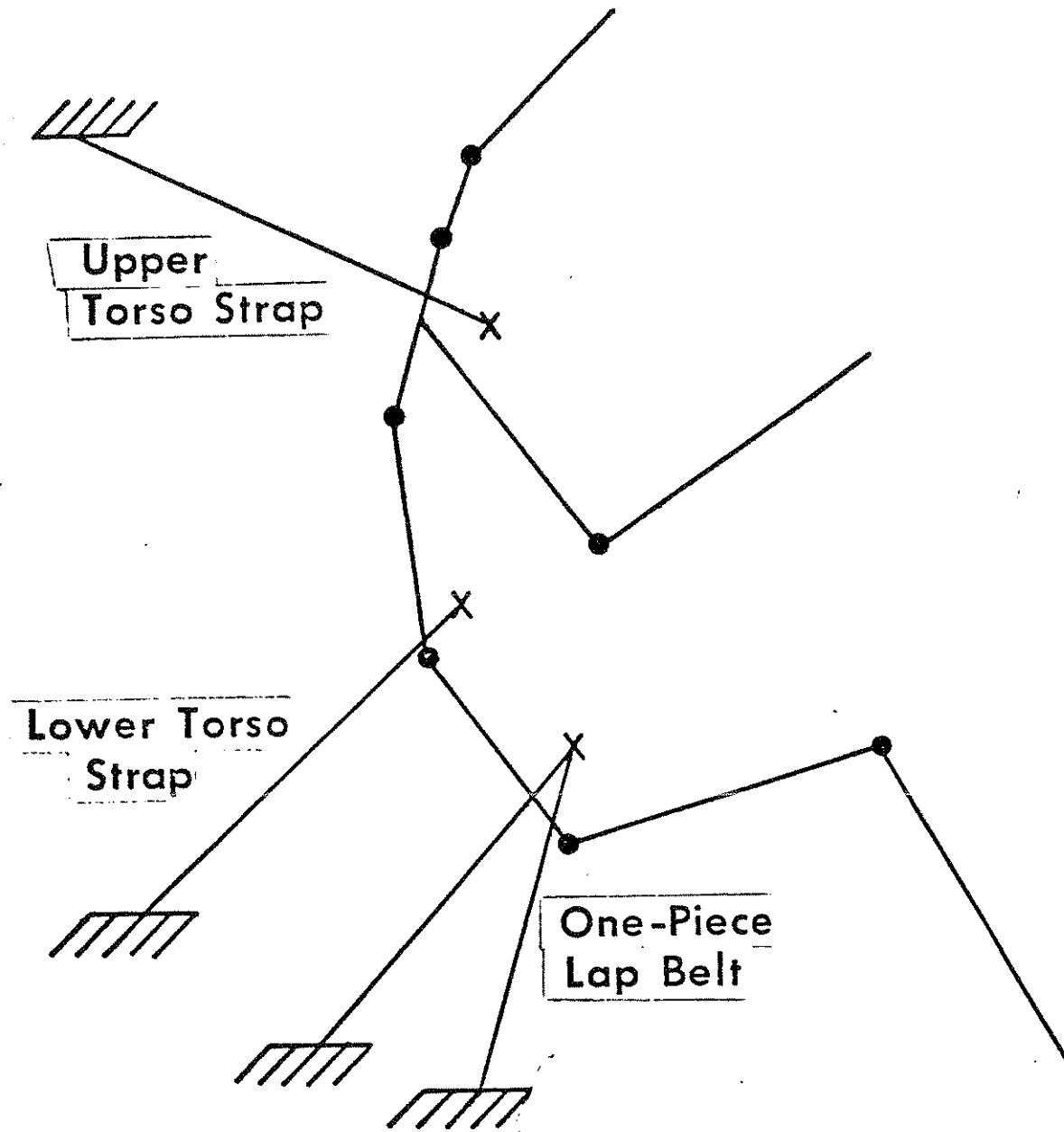


FIGURE 9-1 Simple Belt System

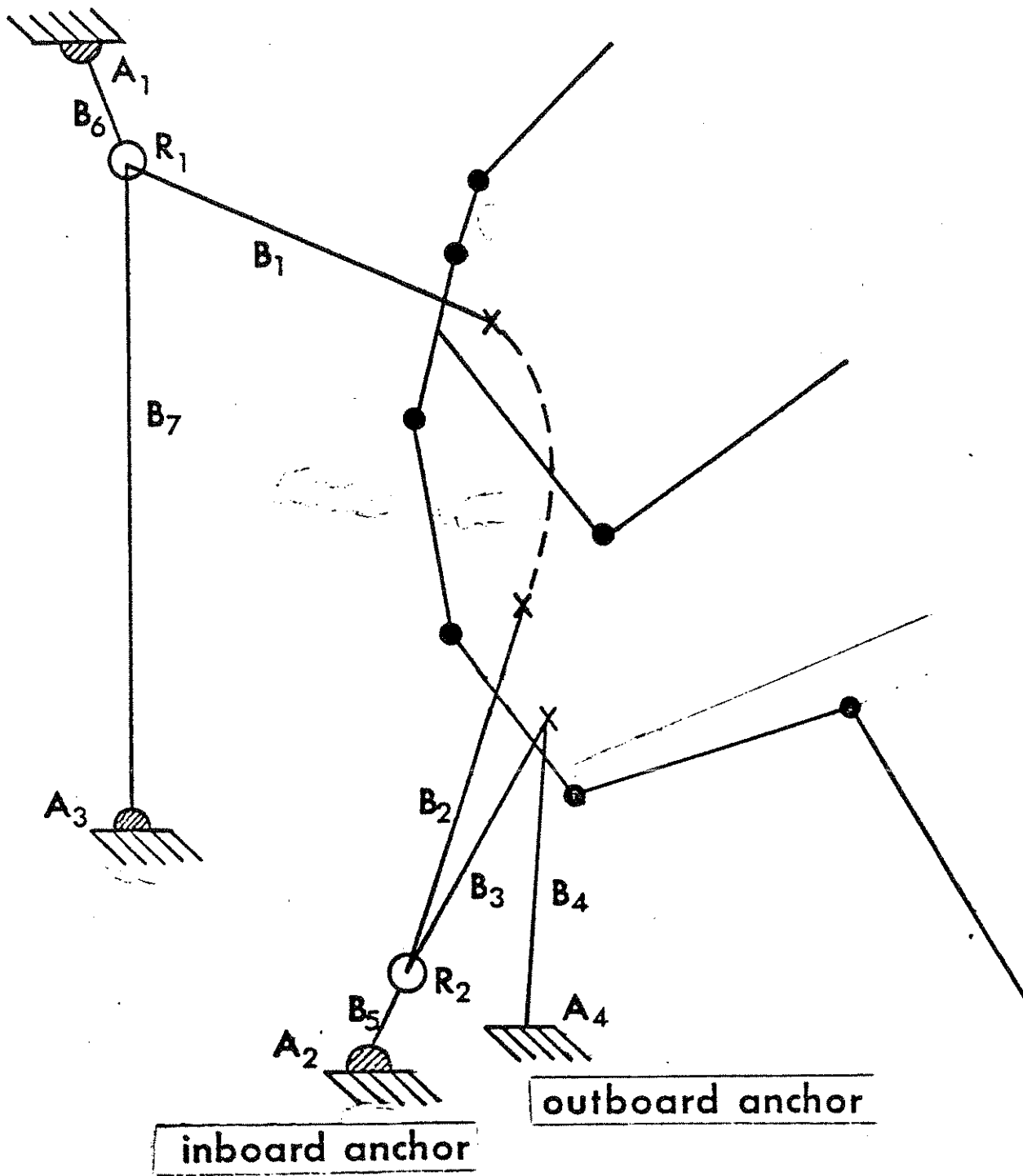


FIGURE 9-2 Advanced Belt System

in the vehicle, as well as the attachment point on the lower-torso segment, can be specified arbitrarily by the user.

The torso harness restraint consists of two individual straps: an upper strap attached to a fixed point on the upper torso segment and a lower strap attached to a fixed point on the upper-, mid-, or lower-torso segment. Unlike for the lap belt, the two segments of the torso harness are independent pieces of webbing. Each extends from an anchor point positioned arbitrarily in the vehicle* to an attachment point fixed on a torso element. Thus, a "no-slip" condition is assumed at the torso for each belt segment, and entirely independent belt tensions are calculated for the two segments. There is no necessity to define equivalent webbing properties for the two segments. Indeed, specification of different force-producing characteristics for these two segments is a means sometimes used for simulating slipping and friction for the torso restraint of the three-belt submodel.

9.2.2 Deflection and Strain. Loading curves for the three pieces of webbing may be prescribed either as force-deflection relations or force-strain relations. The type of specification must be the same for all belts in the system. Whether force-deflection or force-strain relations are used generally depends on the form of available data. Force-strain specifications are probably more common.

For determination of belt forces in the three-belt system, belt deflection is defined as the difference between stretched belt length and the length of the taut, but unstretched, webbing. This is illustrated in Figure 9-3. For each belt in the three-belt system, the input parameters pertinent to determination of belt deflection are the unstretched webbing length l_0 , the initial slack Δ , and the vehicle coordinates and body segment coordinates, respectively, of the belt anchor and the attachment point on the body.** These

*See Module 8 for user specification of the vehicle coordinate frame.

** The seven-belt system requires different specifications.

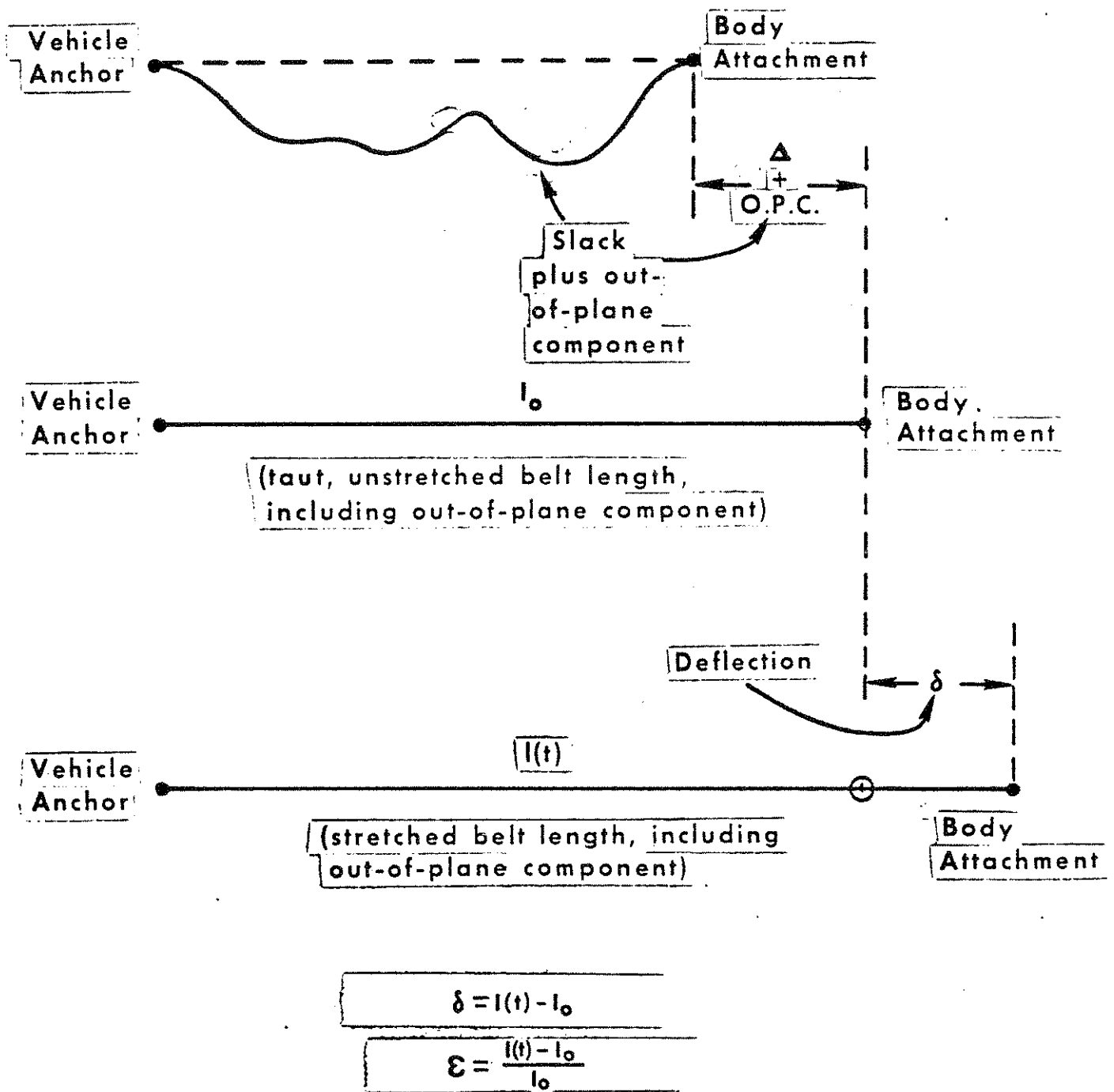


FIGURE 9-3 Definition of Belt Deflection

values do not over-specify the belt geometry, as might be thought, because the defined belt length ℓ_0 should not in general be a projection onto the x-z plane but rather is the total belt length in three dimensions. The specification of both unstretched belt length and initial slack along with initial endpoint coordinates allows calculation by the computer model of the proper initial "out-of-plane" component of webbing length, O.P.C in the figure.* The stretched belt length $\ell(t)$ is calculated as the straight-line distance in the x-z plane between the instantaneous positions of the belt anchor and attachment point plus the constant value determined for the initial out-of-plane length. Since the input constant ℓ_0 , the unstretched belt length, includes the out-of-plane component by definition, the belt deflection at time t is

$$\delta = \ell(t) - \ell_0.$$

The strain is defined as the ratio of belt elongation to total initial belt length, i.e.,

$$\epsilon = \frac{\ell(t) - \ell_0}{\ell_0}$$

9.2.3 Material Properties. Loading curves for belts, whether in terms of deflections or strains, may be defined either in polynomial or tabular form. Specification of loading curves is described in detail in Module 6, Part 1, and will not be discussed here. Both static and "inertial spike" loading curves may be assigned for belt materials, and unloading characteristics may be prescribed in terms of deflection-dependent "G- and R-ratios," which determine permanent deformation and restored energy upon complete unloading.

9.2.4 Mutual Deformation of Body and Belt. One force-generation feature of the MVMA-2D model that is discussed in detail in Modules 4 and 6, Part 2, has a special application in the calculation of belt forces, so it is discussed further here. This feature is

* If the specified unstretched belt length and the initial belt geometry are incompatible with a specified initial slack, then a negative out-of-plane component is calculated to accommodate the requested slack.

the "shared-deflection," or "mutual-deformation," algorithm. The normal use of this algorithm is for determination of the contributions of a non-rigid body ellipse and a non-rigid contact surface to the total relative displacement, or deflection, between the two.* The compressive force for such an interaction is always less than the force for an interaction with the same total deflection but with one of the interacting elements rigid instead of yielding. Therefore, allowing for realistic mutual deformation of interacting elements softens peak forces and G-levels.

It can sometimes be useful to employ this feature to account for the effect of body compliance (or even belt slipping) at the belt-occupant interface. This is the "attachment point," previously discussed, which is defined by the user as a fixed point on a body segment. By using the mutual deformation feature, this point can be made to relax, in a sense, in the direction of the applied belt tension. The effective belt deformation, and thus its tension, is therefore reduced.** This feature is not used for determining a belt force unless a body "material" is defined and explicitly specified for this use on the appropriate data card.

9.2.5 Data Cards for the Three-Belt Submodel. Whether or not belt restraint-system data are present in a data set for an MVMA-2D simulation, a belt-system control switch on Card 102 must be properly set. If the value in field 1 of this card is 0., then no belt forces will be determined even though the data set may include cards with belt-system specifications. A value of 1. or 2. indicates that the three-belt submodel is to be used. If a 1. is entered, then only lap-belt forces will be determined. Lap-belt and shoulder-harness forces will all be determined if a 2. is entered. This switch should be set to 3. whenever advanced belt-system forces are to be determined.

Figure 9-4 illustrates belt geometry for the three-belt submodel. All belt anchor points, shown as A_1 , A_2 , A_3 and A_4 , are prescribed

* Shared deflection is resolved also for interactions between two non-rigid body ellipses.

** In a strict sense, however, the attachment point is still fixed with respect to the body-segment coordinate frame, so the line of action of the belt force is unchanged.

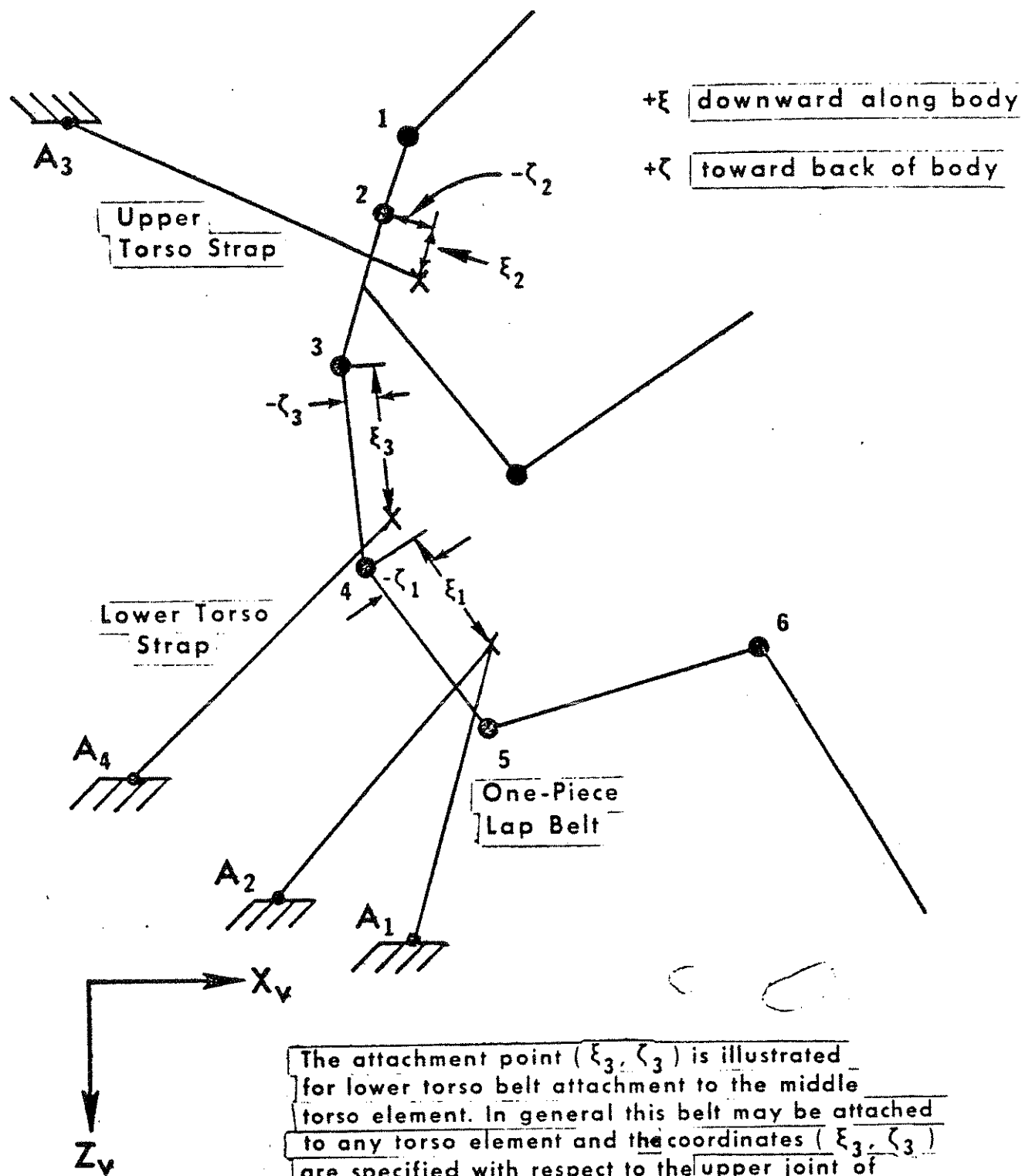


FIGURE 9-4 Three-Belt System Geometry

by the user in the vehicle coordinate frame (defined in Module 8). The X- and Z- coordinates of these points are entered in pairs in the first eight fields of Card 501. Anchors 1 and 2 are interchangeable; either may be considered the inboard or outboard lap belt anchor. The three belt attachment points are defined relative to body joints by ξ - ζ coordinates, as illustrated in Figure 9-4. The upper torso-harness strap must be attached to the upper torso element and the lap belt attachment must be on the lower torso element. The lower torso-harness strap, however, may be attached to any desired torso element by entering a 2., 3., or 4. in field 7 of Card 702 for attachment to the upper-, middle-, or lower-torso element, respectively. The point (ξ_3 , ζ_3) is illustrated in the figure for attachment to the middle torso element. In general, these coordinates should be specified with respect to the upper joint of the torso element to which the belt is attached. ξ - ζ coordinates for the three belts are entered in pairs in fields 4 through 9 of Card 218.

All remaining data required by the three-belt submodel are entered on Cards 701 through 709. Example data cards are shown in Figures 9-5a and 9-5b. The total lap-belt webbing length is entered in field 1 of Card 701. The unstretched lengths for the upper- and lower-segments of the shoulder harness are entered in fields 3 and 5 of Cards 701 and 702, respectively. Initial slacks for the three belts are specified in fields 2 and 4 of Card 701 and field 6 of Card 702.

Loading and unloading properties of a belt, whether for the three-belt submodel or the advanced belt-system submodel, are prescribed on Cards 704 through 709. If the properties of all belt segments are different, then for each segment there will be one complete set of Cards 704-709 in the data set. The contents of these cards are entirely parallel to Card 403-408 specifications, which are discussed in detail in Module 6, Part 1. (Indeed, as explained in that module, these cards may be used interchangeably.) Fields 1 and 2 of both Cards 704 and 705 contain a user-defined, sixteen-character alphanumeric name for a material. This name serves to identify the loading and unloading characteristics specified in the remaining fields of Cards 704 through 709 with any belt for which this same string of alphanumeric characters is specified as a material

2.	0.	0.	0.	1.	1.	10.	.000001	3.	102
1.49	5.28	0.	4.3	-3.	5.5	-3.7	4.3	-3.	218
-127.8	-7.4	-127.8	-7.4	-134.8	-43.8	-125.2	-10.5		501
34.0	0.	70.2	.5	7000.	7000.	1.			701
LAPBELTMAT				21.1	.5	4.	0.		702
UTBELTMAT				LTBELTMAT					703
LAPBELTMAT	0.	0.	0.	1.	2.	0.	0.		704
LAPBELTMAT	5.				LAPS	I	LAPGR		705
LAPGR	0.	0.							706
LAPGR	.02	.05							706
LAPGR	.06	.4							706
LAPGR	.1	.6							706
LAPGR	.2	.84							706
LAPGR	.3	.94							706
LAPGR	.0	1.							707
LAPGR	.02	.95							707
LAPGR	.06	.6							707
LAPGR	.1	.4							707
LAPGR	.2	.15							707
LAPGR	.3	.1							707
LAPS	0.	0.							708
LAPS	.03286	250.							708
LAPS	.28618	4250.							708
I	-1.	0.							709

FIGURE 9-5a Example Data Cards for the Three Belt System

UTBELTMAT	0.	0.	0.	1.	2.	0.	0.	704
UTBELTMAT	5.				UTS	I	LTGR	705
UTGR	0.	0.						706
UTGR	.025	.05						706
UTGR	.075	.4						706
UTGR	.125	.6						706
UTGR	.25	.84						706
UTGR	.375	.94						706
UTGR	0.	1.						707
UTGR	.025	.95						707
UTGR	.075	.6						707
UTGR	.125	.4						707
UTGR	.25	.15						707
UTGR	.375	.1						707
UTS	0.	0.						708
UTS	.041075	500.						708
UTS	.1994	4500.						708
LTBELTMAT	0.	0.	0.	1.	2.	0.	0.	704
LTBELTMAT	5.				LTS	I	LTGR	705
LTGR	0.	0.						706
LTGR	.0154	.05						706
LTGR	.0462	.4						706
LTGR	.0769	.6						706
LTGR	.1538	.84						706
LTGR	.2308	.94						706
LTGR	0.	1.						707
LTGR	.0154	.95						707
LTGR	.0462	.6						707
LTGR	.0769	.4						707
LTGR	.1538	.15						707
LTGR	.2308	.1						707
LTS	0.	0.						708
LTS	.02528	500.						708
LTS	.12270	4500.						708

FIGURE 9-5b Example Data Cards for the Three-Belt System

name. Such a specification is required for each belt, and the three sixteen-character material names for the three-belt system are entered in fields 1 and 2 of Card 702, fields 1 and 2 of Card 703, and fields 5 and 6 of Card 703. As explained previously, belt material specifications are optionally in terms of force-deflection relations or force-strain relations. If force-deflection characteristics are prescribed on the material property cards, then a 1. should be entered in field 8 of Card 702. A 0. indicates specification of force-strain properties.*

Three optional assignments on Cards 702 and 703 are the sixteen-character names for "body" materials which are to deform mutually with the belts. This feature was discussed in Section 9.2.4. The pertinent fields are 3 and 4 of Card 702 for the lap belt, fields 3 and 4 of Card 703 for the upper strap of the shoulder harness, and fields 7 and 8 of Card 703 for the lower strap. No body deformation will be considered in determination of a belt force if the fields for the body material name are left blank. If a name is entered, however, the data set must include material-property specifications for this material on Cards 221-226, 403-408, or 704-709. There is no requirement that these material properties bear any relation to body-ellipse properties that may have been prescribed for the determination of vehicle-interior contact forces.

Finally, fields 5, 6, and 7 of Card 701 relate to failure of the three-belt system. The lap-belt and torso-belt breaking forces are entered in fields 5 and 6. The time duration for belt failure in field 7 ensures that after a belt force exceeds its breaking level the force will be reduced gradually to zero. A value of 1. ms is often used. The belt-failure mechanism can be defined alternatively by specifying the webbing loading curves so that loads reduce to zero after breaking deflections, or strains, are reached.**

* If the advanced belt system is used, then the switch setting is defined oppositely (1. for force-strain) and the value is entered in field 2 of Card 717.

** Parameters on Cards 704 and 708 must be appropriately prescribed.

9.3 An Advanced Belt-System Submodel

9.3.1 General Description. Figure 9-6 is a schematic of a second optional belt restraint-system submodel. This seven-segment system is called the "advanced belt system."

The system has four anchor points, designated as A_1 , A_2 , A_3 , A_4 . Any of the anchors A_1 , A_2 , A_3 may be inertia reels of either the vehicle-sensitive type or webbing-sensitive type. The anchor A_4 cannot have an inertia reel; the outboard lap belt segment, if present, fastens securely to this anchor. In Figure 9-6 and in all other figures in this module, a solid semi-circle at an anchor position indicates an optional inertia reel.

The system includes two slip points where three belt segments come together. One is in the upper harness system and one is between the lower-torso and lap sections. The slip points are shown as open circles, R_1 and R_2 in Figure 9-6, and hereafter will be called the "upper ring" and the "lower ring." The rings may be fastened to ring straps, which lead to anchors A_1 and A_2 , or they may be fixed to the vehicle frame at anchor locations A_1 and A_2 , in which case the corresponding ring straps (B_6 and B_5 , or either) are absent. Belt segments B_5 and B_6 are always "independent" of other belt segments since they fasten to the slip rings. Through each ring, however, passes a strap of webbing shown in the figure as a pair of belt segments, either B_1 and B_7 or B_2 and B_3 . At option, the members of these pairs can be made independent by prohibiting slipping of the combined strap through the ring. In this case the ring location is a juncture of three independent straps of webbing. The pairs B_1 - B_7 and B_2 - B_3 , however, may be considered common straps that may slip freely through their respective rings or with an amount of frictional resistance which depends on the resultant normal force at the ring.

The upper and lower torso belts, B_1 and B_2 , may be independent or the separate belt forces may be made interdependent by use of inter-belt influence options. These are of three types: a) a force adjustment determined on the basis of normal-force friction at the torso surface; b) an adjustment for maintaining a force-difference saturation level;

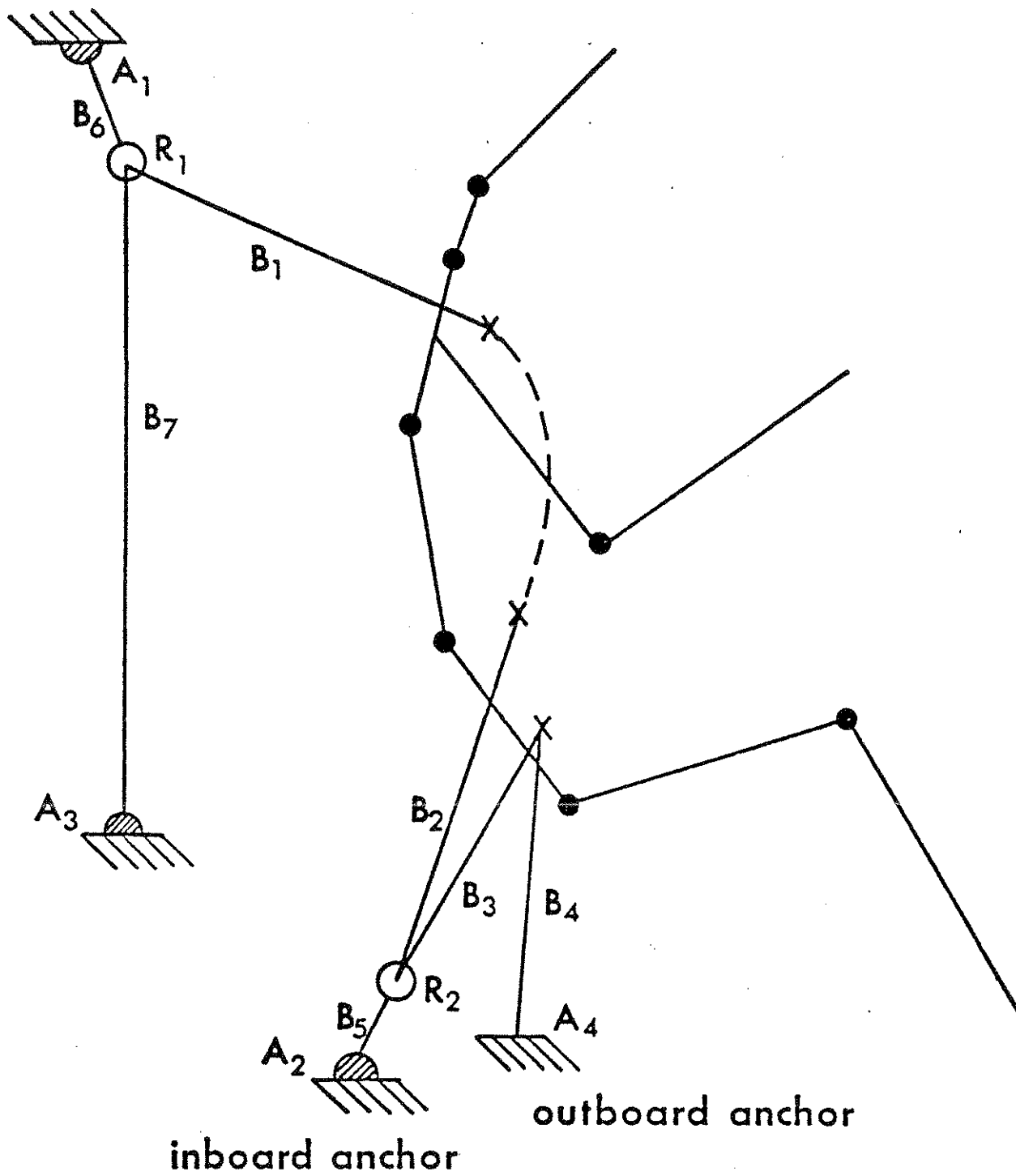


FIGURE 9-6 Advanced Belt System

c) a positive or negative percentage influence on one belt force on the other. In addition, a free-slipping option is available for the torso-belt and lap-belt combinations.* Torso and lap belt segments attach to the occupant at points on the torso elements. The upper torso belt attachment is on the upper torso element and the attachment for lap belt segments is on the lower torso. The user may specify an attachment on any of the three torso elements for the lower torso belt.

Force-deformation relations for belt segments may be specified in either tabular or polynomial form. They may be either force-strain relations or force-deflection relations, but a mixture for the various belt segments is not allowed.

9.3.2 Deflection and Strain. Belt deflection for the simpler three-belt submodel was defined in Section 9.2.2 and illustrated by Figure 9-3. Belt deflection is defined in the same manner for the advanced belt system, i.e.,

$$\delta(t) = l(t) - l_0$$

where: 1) $l(t)$ is the straight-line distance in the x-z plane between the instantaneous positions of the belt-segment endpoints plus the initial out-of-plane component of belt length, and 2) l_0 is the unstretched belt length, including the out-of-plane component. For both belt systems, in order to evaluate $\delta(t)$, it is necessary to know the unstretched belt length l_0 , the out-of-plane length O.P.L., and the initial slack Δ associated with the belt segment (See Figure 9-3). However, while the three-belt submodel accepts unstretched length and slack as input and calculates the out-of-plane length, O.P.L., as previously explained, the advanced belt-system submodel accepts slack and out-of-plane length as input and calculates the total, unstretched belt length, l_0 . Since these specifications and others differ for the optional belt submodels, different input data cards are used for the two. The three-belt submodel cards have been described in Section 9.2.5, and cards required for the advanced belt system are described

* All of these features are adapted from the belt model used in the HSRI Six-Mass, Three-Dimensional Crash Victim Simulator.

in Section 9.3.8.

Determination of strain is necessary if force-strain properties are prescribed for the belt system. Strain is found as

$$\epsilon = \frac{l(t) - l_0}{l_0}.$$

9.3.3 Material Properties. Loading and unloading characteristics for belts may be specified as described in detail in Module 6, Part 1, and in brief in Section 9.2.3.

It was previously mentioned that, for certain belt-system specifications, the segment pairs B_1 - B_7 and B_2 - B_3 may be considered to be single pieces of webbing that pass through slip points rather than attaching independently to anchors (or rings). Explanation of such specifications is given later in Section 9.3.8.1, but it should be made clear that the tension in any one-piece segment pair (possibly adjusted for friction effects) is determined from the total deflection, or total strain, of the combined lengths of webbing. In addition to the pairs B_1 - B_7 and B_2 - B_3 , this can be true also for the pairs B_1 - B_2 and B_3 - B_4 if "force equalization" (free slipping) options are selected. (See Section 9.3.4). If a belt-system design modeled by the user includes a belt pair that will be considered as a single piece of webbing by the MVMA-2D model, then the user should designate the same material name for the two segments. Whenever a belt pair must be treated as a common strap, the computer model will arbitrarily use the material for the first member of the pair if the designated materials for the separate segments are different.

Mutual deformation of the occupant and belts may be modeled for the advanced belt system as well as for the three-belt system. This feature has been discussed in Section 9.2.4.

9.3.4 Force Equalization. Both the torso belt pair, B_1 and B_2 , and the lap belt pair, B_3 and B_4 (or both) can be "force equalized" by setting belt-system switches appropriately in the input data. The force-equalization option is a means for determining equal tensions

in both segments of a pair of belts that might be considered as a single piece of webbing instead of fastening independently to a user-defined attachment point on the occupant. Thus, this option for the advanced belt system is identical to the standard treatment of the combined two-segment lap belt discussed in Section 9.2.1 for the three belt submodel. A single tension is determined for a deflection equal to the summed segment deflections over a webbing length equal to the summed segment lengths, including a specified out-of-plane component. This tension is assigned separately to both segments of the pair. The belt forces thus produced correspond to a condition of free slipping around the occupant at the attachment point.

9.3.5 Torso-Belt Interbelt Influence. In general, friction and belt-system geometry factors lead to unequal belt tensions. Three optional methods are available to allow the tension in one torso belt to influence the tension in the other. They are described in the following three sections. The computer program logic allows any of these three influences to be applied to the torso belt pair (B_1 and B_2) even if it has previously been force-equalized by the method of the preceding section. However, examination of the pertinent equations in Volume 1 of the MVMA-2D manuals would show that equalized force values are further modified only by the "percentage influence" method. The user is directed to Volume 1 for a more detailed description of these features than is given in the following sections.

9.3.5.1 Normal-Force Friction. The first interbelt influence option is intended to simulate the effect of static and sliding friction between belts and the occupant. This is done by allowing the torso-belt pair to "relax," in effect, toward the belt segment of greater tension. Normal-force friction effects are approximated from an estimate of the normal force where the webbing is in contact with the occupant. Three system parameters are prescribed by the user for this option. The first two are static and sliding coefficients of friction for the belt-occupant interface, μ_s and μ_k , respectively. The static friction coefficient is in general at least as large as the sliding friction coefficient ($\mu_s \geq \mu_k$) although this is not a requirement.

Free slipping results if μ_s and μ_k are specified as zero.* A non-slip condition is guaranteed by specifying a very large value for the static coefficient.

The third input parameter, ζ , is a nondimensional quantity which must have a value from 0 to 1: $0 \leq \zeta \leq 1$. If ζ is 1, then the negative friction-force effect that is applied to the torso belt segment with greater tension will be applied also as a positive effect to the segment with smaller tension.** If ζ is 0, then the belt with greater tension will still be affected (negatively) by the established friction-force "adjustment," but the belt with smaller tension will be unaffected. For values of ζ between 0 and 1, the belt with smaller tension will be affected by an intermediate (positive) adjustment. ζ is the fraction of the negative friction-force adjustment that is to be applied positively to the belt with smaller tension. Limited experience with this feature of the advanced belt system submodel indicates that a value for ζ of about .5 may be most reasonable for most shoulder harness arrangements.

9.3.5.2 Force Difference Saturation. An interbelt influence option can be selected which will simulate the effect of belt friction in an entirely different manner. Here, a "saturation force difference" is prescribed by the user for the torso belt pair. Whenever the difference in tension between the two belts exceeds this force saturation value, the greater of the forces is reduced by an amount such that the difference in tensions is equal to the saturation value. The tension in the other belt is unchanged. This adjustment of the force difference is intended to represent partial slipping against static friction. The only quantity that the user must define if this option is used is the value for the saturation force difference.

9.3.5.3 Percentage Influence. The third interbelt influence option allows the user to specify a positive or negative fraction of the tension of one torso belt which will be applied as an additive adjust-

* ζ , the third parameter, must be 1 for free slipping to result.

** The computer code does not allow force adjustments to do more than equalize the belt tensions, i.e., the belt segment with originally greater tension cannot have the smaller tension after adjustment for friction effects.

ment to the tension of the other. Thus, one belt is designated by the user as an "influencing belt." Its tension is not adjusted, but it determines the adjustment to the other belt of the pair. In conjunction with this option, the user supplies a "maximum influence-force bound." If the force adjustment, in absolute value, is greater than this bound, then the bound itself is applied as the adjustment (with proper sign). The "percentage influence" option is more artificial than the other torso interbelt influence options, but it has nevertheless found useful application.

9.3.6 Inertia Reels. A maximum of three anchors, A_1 , A_2 , and A_3 (see Figure 9-6), may have inertia reels of either the vehicle-sensitive or webbing-sensitive type. The associated belts are B_6 , B_5 , and B_7 , respectively. A vehicle-sensitive reel can be made to lock at some specified time, or alternatively, when either of two conditions occurs: a) the resultant inertial acceleration at the anchor location exceeds, in absolute value, a specified limit; or b) vehicle pitch exceeds, in absolute value, a specified limit. A webbing-sensitive reel will lock either when the rate of belt feed-out or the acceleration of belt feed-out exceeds a specified limit. Since belt feed-out rate and acceleration are obtained from rough numerical differentiations, the modeled webbing-sensitive reels may not be as well behaved as vehicle-sensitive reels. Once a reel of either type locks it will remain locked for the duration of the crash history.

9.3.7 Slip Points. The upper and lower slip points, or rings, if present, are either fixed to the vehicle frame or fastened to the end of ring straps, B_5 and B_6 . If a ring is not anchored to the vehicle, then its location at any value of time is determined by the condition that x- and z-forces at the ring location sum to zero. This involves solving simultaneous nonlinear equations for the ring coordinates, and some of the required input data are specifications for the numerical solution algorithm.

The primary characteristic of the rings is that the webbing straps passing through them are allowed to slip either freely, or with a desired amount of frictional resistance, or not at all. Free slip-

ping is handled by determining a deflection for the combined belt segment (either B_1-B_7 or B_2-B_3) and then setting both belt segment tensions equal to the resulting belt force. The "no slip" case is handled by treating the individual segments as independent straps. The case of non-zero frictional resistance to slipping is treated by including a torso-belt tension adjustment determined by multiplying a user-prescribed coefficient of friction by a calculated estimate of the normal force at the ring.

9.3.8 Data Cards for the Advanced Belt-System Submodel.

9.3.8.1 Anchor Types and Ring Types. All user-specified data relating to

1. anchor types, and
2. slip point characteristics

are entered on Card 720. The anchors A_1 , A_2 , A_3 , and A_4 are assigned anchor type designation numbers in the first four fields. Figure 9-7 illustrates the four anchor types that can be specified. If an anchor location has no associated belt in some user-defined restraint-system configuration, then a 0. is entered on the 720-Card for that anchor. The anchor is a "type 0" anchor. The other three anchor types are designated by 1., 2., and 3. A "type 1" anchor fixes a belt firmly to the vehicle frame. A "type 2" anchor is any inertia reel, whether vehicle-sensitive or webbing-sensitive. A "type 3" anchor is a slip ring that is fastened firmly to the vehicle frame.

Type designation numbers are also required on Card 720 for the two slip points, or rings. Figure 9-8 illustrates the three ring types that can be specified. A ring is "type 1" if belt segments leading to it fasten firmly to the ring. Note that wherever belt segments 1, 2, or 3 fasten securely to the vehicle frame, a "type 1" ring is specified even though no ring exists, and a "type 3" anchor is prescribed. If a belt strap passes through a ring, then that ring is either "type 2" or "type 3." It is "type 3" if free-slipping occurs at the ring and "type 2" if slipping occurs with frictional resistance. The ring type designation numbers for rings 1 and 2 are entered in fields 5 and 6. A coefficient of friction for belt slipping must be specified for each ring of "type 2." The friction coefficient


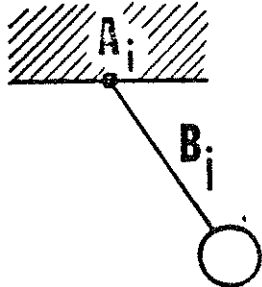
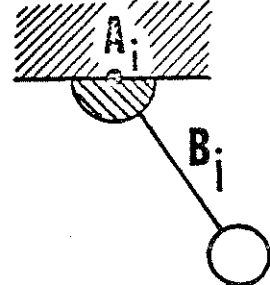
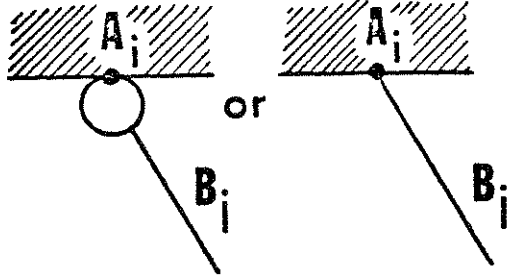
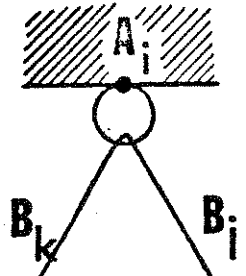
SCHEMATIC	ANCHOR TYPE DESIGNATION	ALLOWED INDEX VALUES
 <p>no belt</p>	$ANCHOR_i = 0$	$i = 1, 2, 3, 4$
	$ANCHOR_i = 1$	$i = 1, j = 6$ $i = 2, j = 5$ $i = 3, j = 7$ $i = 4, j = 4$ (no ring)
	$ANCHOR_i = 2$	$i = 1, j = 6$ $i = 2, j = 5$ $i = 3, j = 7$
	$ANCHOR_i = 3$	$i = 1 \text{ or } 3, j = 1, RING_1 = 1$ $i = 2, j = 2 \text{ and/or } 3, RING_2 = 1$
	$ANCHOR_i = 3$	$i = 1, j = 1, k = 7, RING_1 = 2 \text{ or } 3$ $i = 2, j = 2, k = 3, RING_2 = 2 \text{ or } 3$

FIGURE 9-7 Belt Anchor Type Designation for Anchor "i"

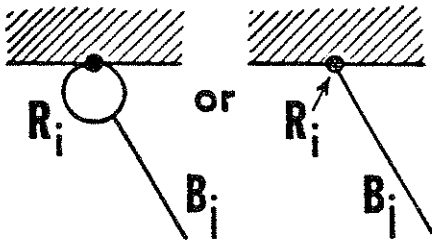
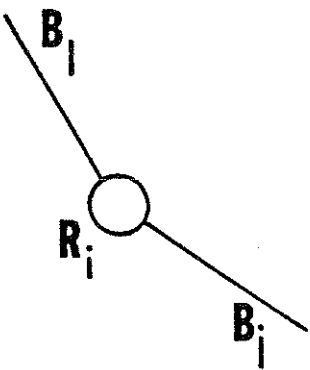
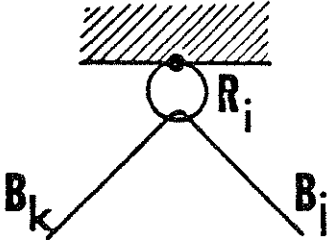
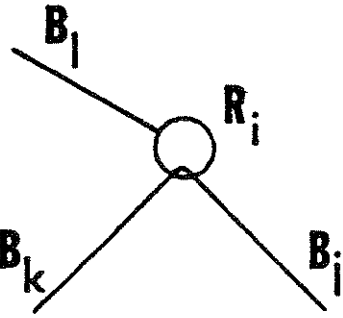
SCHEMATIC	RING TYPE DESIGNATION	ALLOWED INDEX VALUES
	$RING_i = 1$	$i = 1, j = 1, ANCHOR_1 = 3$ $i = 2, j = 2 \text{ or } 3, ANCHOR_2 = 3$ $i = 2, j = 2 \text{ and } 3, ANCHOR_2 = 3$
	$RING_i = 1$	$i = 1, j = 1, \ell = 6, ANCHOR_1 = 1 \text{ or } 2$ $i = 1, j = 1, \ell = 7, ANCHOR_3 = 1 \text{ or } 2$ $i = 1, j = 1, \ell = 6 \text{ and } 7, ANCHOR_1 \text{ and } ANCHOR_3 = 1 \text{ or } 2$ $i = 2, j = 2, \ell = 5, ANCHOR_2 = 1 \text{ or } 2$ $i = 2, j = 2, \ell = 3 \text{ and } 5, ANCHOR_2 = 1 \text{ or } 2$
	$RING_i = 2 \text{ or } 3$	$i = 1, j = 1, k = 7, ANCHOR_1 = 3 \text{ (or } 0)$ $i = 2, j = 2, k = 3, ANCHOR_2 = 3$
	$RING_i = 2 \text{ or } 3$	$i = 1, j = 1, k = 7, \ell = 6, ANCHOR_1 = 1 \text{ or } 2$ $i = 2, j = 2, k = 3, \ell = 5, ANCHOR_2 = 1 \text{ or } 2$

FIGURE 9-8 Designation of Ring-Belt Relationship for Slip Point "i"

is entered in field 7 for ring 1 and in field 8 for ring 2.

As an example use of the advanced belt-system submodel, Figure 9-9 illustrates simulation of the three-belt system discussed in Section 9.2 and illustrated by example data in Figure 9-5. Equivalent data for a representation of that system by the seven-belt submodel are shown in Figure 9-10. The user should be able to demonstrate the correctness of the anchor type and ring type designations in fields 1 through 6 of Card 720. Belt segment B_3 (shown dashed in Figure 9-9) is effectively absent since a very large slack is specified on Card 712. Belt segment B_4 represents the two lap belt segments together, for which coincident x-z plane projections are prescribed in the example data of Figure 9-5.

9.3.8.2 Belt Segment Specifications. For each belt segment present in the restraint system design, the data set must include one of the cards 710 through 716. These seven cards are for belt 1 through belt 7, respectively, as indicated in Figure 9-11.

The first two fields of each card contain x- and z-coordinates of the belt attachment point. Figure 9-12 illustrates the definition of these coordinates. They are specified in a system fixed to the torso segment to which the belt is attached, with the x-coordinate measured along the centerline from the upper joint of the segment and the z-coordinate measured perpendicularly toward the front of the body.* Attachment points for the lap belt segments (B_3 and B_4) should be coincident. Attachment point coordinates for the ring straps (B_5 and B_6) and the upper torso belt extension (B_7) need not be specified since these belt segments do not extend to the torso.

Figure 9-13 shows a belt system with one inertia reel, two slip points, and one ring strap. Example data cards for this system are shown in Figure 9-14. Card 715 is not included since the upper ring strap is not present in this belt-system configuration.

Anchor point coordinates are entered in fields 3 and 4 of Cards

* While belt attachment points are measured from joints for input, the internal values in the computer program are with respect to torso segment centers of gravity.

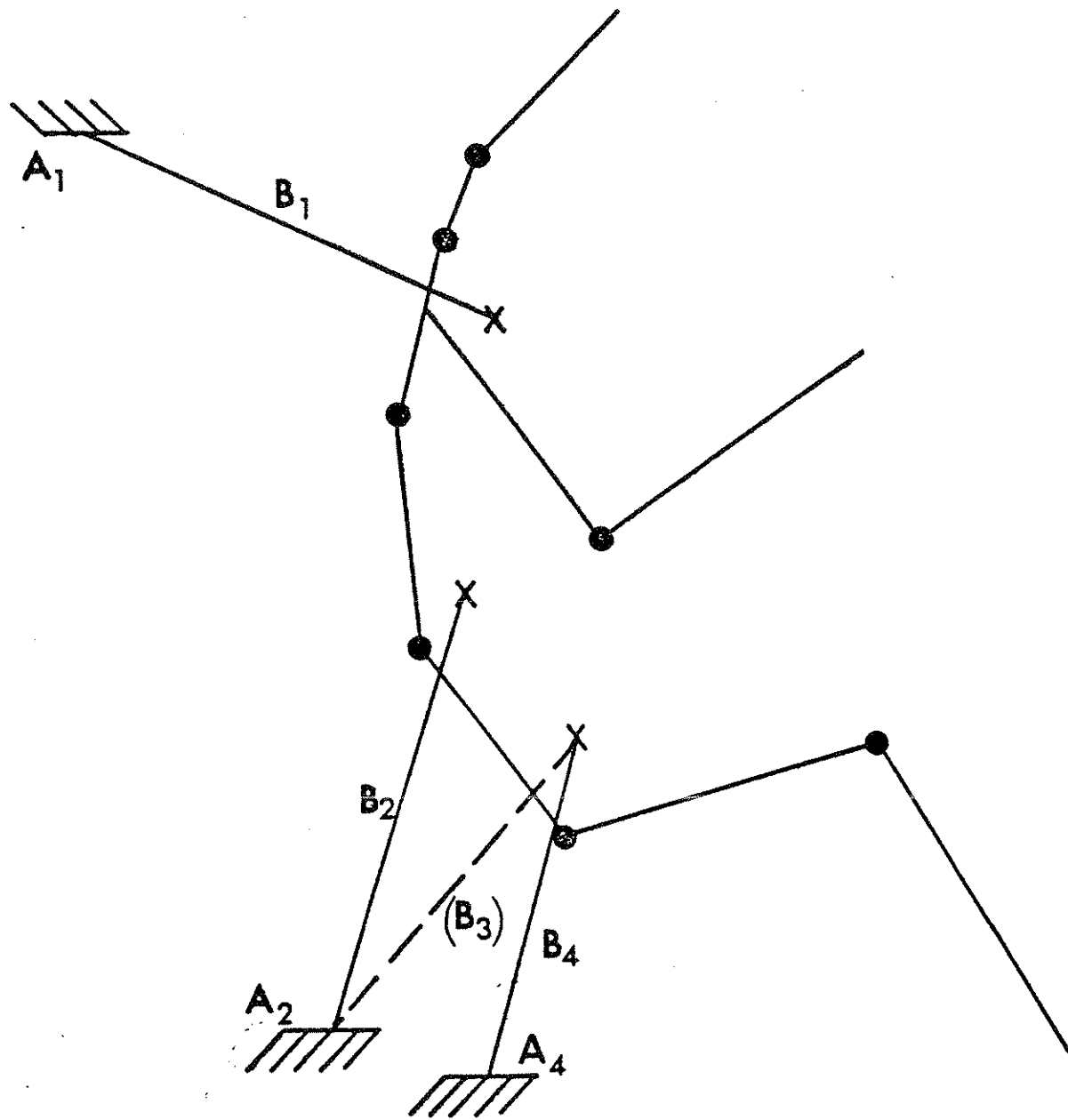


FIGURE 9-9 Simulation of a Three-Belt System Using the Advanced Belt-System Submodel

3.	0.	0.	0.	1.	1.	10.	.000001	3.	102
5.5	3.7	-134.8	-43.8	.5	UTBELTMAT				710
4.3	3.	-125.2	-10.5	.5	LTBELTMAT				711
4.3	3.	-125.2	-10.5	1000.	LAPBELTMAT2				712
4.3	3.	-127.8	-7.4	0.	LAPBELTMAT2				713
0.	1.	4.	0.	0.	0.	0.			717
3.	3.	0.	1.	1.	1.				720
LAPBELTMAT2	0.	0.	0.	1.	2.	0.	0.		704
LAPBELTMAT2	5.				LAPS2	I	LAPGR		705
LAPGR	0.	0.							706
LAPGR	.02	.05							706
LAPGR	.06	.4							706
LAPGR	.1	.6							706
LAPGR	.2	.84							706
LAPGR	.3	.94							706
LAPGR	0.	1.							707
LAPGR	.02	.95							707
LAPGR	.06	.6							707
LAPGR	.1	.4							707
LAPGR	.2	.15							707
LAPGR	.3	.1							707
LAPS2	0.	0.							708
LAPS2	.03286	500.							708
LAPS2	.28618	8500.							708
I	-1.	0.							709
Material properties for UTBELTMAT and LTBELTMAT									
are as specified in Figure 9-5b.									

FIGURE 9-10 Data cards for advanced belt system representation of the three-belt system data set in Figure 9-5.

BELT INDEX SPECIFICATIONS (Advanced Belt-Restraint Submodel)		
CARD NO.	BELT INDEX	BELT SEGMENT IDENTIFICATION
710	1	Upper torso belt
711	2	Lower torso belt
712	3	Inboard lap belt
713	4	Outboard lap belt
714	5	Lower ring strap
715	6	Upper ring strap
716	7	Upper torso belt extension

FIGURE 9-11 Belt Index Specifications

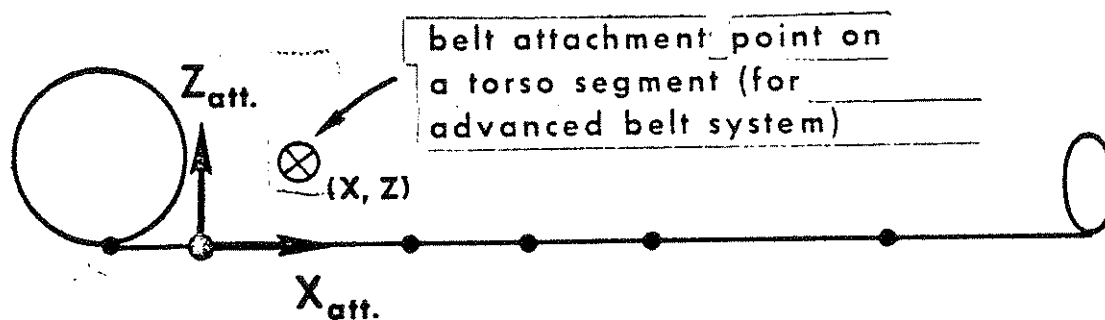
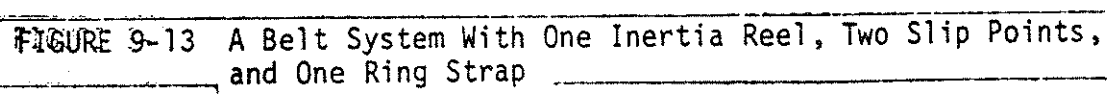


FIGURE 9-12 Belt Attachment Point Coordinates for Advanced Belt-Restraint Submodel



3.	0.	0.	0.	1.	1.	10.	.000001 3.	102
5.5	3.7	-134.8	-43.8	.5	BELTMAT			710
3.5	3.			.5	BELTMAT			711
4.3	3.			0.	BELTMAT			712
4.3	3.	-127.8	-7.4	0.	BELTMAT			713
		-127.0	-8.1	8.	STRAPMAT			714
		-134.8	-7.4	36.4	BELTMAT			716
2.	1.	4.	0.	0.	0.	0.		717
	10.	2.						718
				250.				719
3.	1.	2.	1.	2.	2.	.3	.3	720
1.	-1.	.4	14.					723

Force-strain material property data
must be provided for materials BELTMAT
and STRAPMAT.

FIGURE 9-14 Data for a belt system with one inertia reel, two slip points,
and one ring strap.

710 through 716 for each belt segment which extends to a fixed point on the vehicle frame, to a ring that is fastened to the vehicle frame, or to an inertia reel. These points are specified in the vehicle coordinate system, which is defined in Module 8. Anchor point coordinates are specified for the upper ring strap (B_6) if it is present rather than for the upper torso belt (B_1). Similarly, anchor coordinates are specified for the lower ring strap (B_5) if it is present rather than for the lower torso belt (B_2) and the inboard lap belt (B_3). The anchor points for belts 2 and 3, when required, should be coincident.

An entry must be made in field 5 of each of the cards 710 through 716 present in the data set. For belt segments 1 through 4, this value is for the initial slack associated with the belt. Negative values may be entered if initial belt tension is desired. For belts 5 through 7 the value entered is for the initial segment webbing length, including desired slack.

Fields 6 and 7 contain a sixteen-character alphanumeric name for the belt material. For each different belt material name referenced on Cards 710 through 716, the data set must include a set of material property cards 704 through 709, as described previously for the three-belt submodel in Section 9.2.5.

Fields 8 and 9 are used only if mutual deformation is desired between a belt segment and the body element to which it is attached. For belts 1 through 4, a sixteen-character alphanumeric name entered in these fields designates a body material, and a complete set of material property specifications must be supplied for each such material.

9.3.8.3 System Specifications. Entries on all remaining belt cards pertain not to specific belt segments but rather to the belt system as a whole. They are "system parameters."

Card 718 is needed whenever the belt system includes a ring strap. The values on this card are control parameters for the algorithm which determines the ring location for a force balance at

each instant of time. Only fields 2 and 3 of this card are used.* In field 2 is entered the maximum number of trial adjustments of the ring coordinates x and z that is allowed for each determination of the force balance. The iterative process is terminated either when this limit has been reached** or when the force imbalance has been made less than a convergence epsilon, which is entered in field 3. The recommended values for these controls are 10. iterations and 2. lb, respectively. The user should avoid unnecessary specification of greatly different stiffnesses for belts which lead to a ring since many iteration steps may then be required for finding a force balance.

Card 717 defines miscellaneous system parameters. The value in field 2 indicates whether prescribed deformation-dependent belt material properties are to be treated as functions of belt deflection or belt strain. A 0. is entered for deflection-dependent properties and any non-zero value for strain-dependent properties. The field-3 value indicates the torso element to which the "lower torso belt" (B_2) is attached, 2. for the upper element, 3. for the middle, and 4. for the lower. Fields 4 and 5 are the out-of-plane components of separation between the torso-belt attachment points and lap-belt attachment points, respectively. Values need not be entered in these fields unless fields 6 and 7 have non-zero values, which indicate that the force-equalization (free-slipping) option discussed in Section 9.3.4 is to be used for torso belts and lap belts, respectively.

The remaining field of Card 717 for which a value is required is field 1. The value entered indicates the desired type of interbelt influence for the torso belts. A 0. may be entered if it is desired to use none of the interbelt influence options. Values of 1., 2., and 3. indicate, respectively, the options for normal-force friction, force-difference saturation, and percentage influence. The characteristics for the selected option are specified on Card 719. Fields 1, 2, and 3 are pertinent if normal-force friction is selected. They contain

* The algorithm presently used replaces the one documented in the MVMA-2D manuals, June 1974.

** In this case a warning message is printed, the best trial solution discovered is retained, and program execution continues.

values for the sliding and static coefficients of friction between torso harness and the torso and the parameter ζ , which was discussed in Section 9.3.5.1. If force-difference saturation is selected, then only a value for the saturation level is required; it is entered in field 5. For the percentage influence option, values are required in three fields. The influencing belt is designated by the value in field 4, 1. for the upper torso belt and -1. for the lower torso belt. The positive or negative fraction of the tension of the influencing belt which is to be applied as an additive adjustment to the other belt is specified in field 7. The third parameter is in field 6; it is the upper bound for percentage-influence force adjustment.

9.3.8.4 Inertia Reel Specifications. If an inertia reel is indicated for anchor A_1 , A_2 , or A_3 by the anchor type designation on Card 720 (see Section 9.3.8.1), then the properties of the inertia reel must be specified on one of the cards 721, 722, or 723, respectively. Any inertia reel may be either vehicle-sensitive or webbing-sensitive, as indicated by values of 1. or 0., respectively, in field 1. For a vehicle-sensitive reel, the "lock" condition can be specified either as a lock time or as a pair of values for maximum vehicle pitch and maximum resultant acceleration at the anchor location. The fields for these three quantities are 2, 3, and 4. If a lock time is specified in field 2, then fields 3 and 4 must be left blank. If the pair of values is specified in field 3 and 4, then -1. must be entered in field 2. A webbing-sensitive reel can be made to lock either on the basis of a limiting velocity or a limiting acceleration for belt feed-out. The fields for these two quantities are 5 and 6. Only one value may be specified, and -1. must be entered in the field not used.* Each inertia reel present requires the presence of belt B_5 , B_6 , or B_7 and, thus, one of the Cards 714, 715, or 716.

9.4 Modeling Considerations

9.4.1 Static Tests. Figure 9-15 illustrates a device that might be used for laboratory determination of the breaking strength of belt webbing. Data from such a test might also be used for defining the

* Values standardly used for some of these lock-condition parameters are 14° pitch and 0.4 g resultant acceleration for the vehicle-sensitive reel and 0.6 to 0.9 g's belt feed-out acceleration for the webbing-sensitive reel.

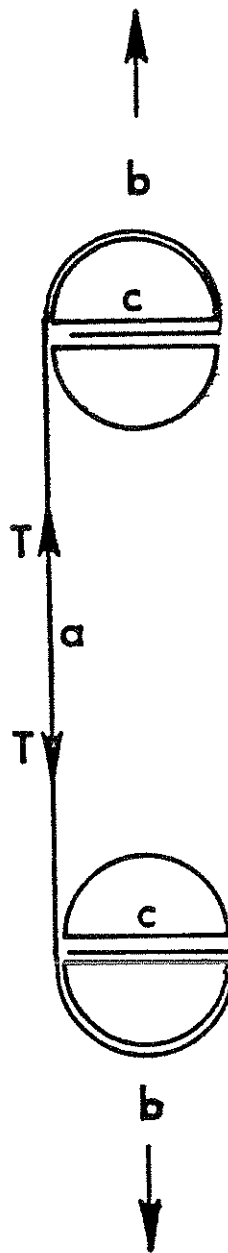


FIGURE 9-15 Belt Strength Test Device

force-strain properties of the webbing for input to a mathematical model. It is merely noted here that if a test device such as shown is used, strain must be determined as a function of slippage at "b" and possibly "c" since for non-zero slippage the length of segment "a" is not the effective webbing length.

9.4.2 , Adjustment of Loading Properties. An MVMA-2D data set may sometimes define a belt-system configuration that differs from the true restraint system. For example, a restraint system might include double upper-torso restraints, symmetric straps, one over each shoulder. The MVMA Two-Dimensional model can be used to simulate such a system with the single shoulder strap that can be defined by the user. It is necessary only to double the force components of the force-deflection or force-strain loading curve for that belt segment.

Another example of necessary adjustment of input data is illustrated by Figure 9-16. Suppose the true belt system includes the elements shown in the upper part of the figure and that the coefficient of friction for webbing sliding through the slip point is zero. Such a system might be simplified for simulation with the three-belt submodel as illustrated in the lower part of the figure. Suppose that force-strain data are available for the webbing of the true system and that it is used directly for the simplified system. Then, while the anchor and attachment point specifications are unchanged in simplifying the true system, account must be taken of the fact that the apparent belt length, ℓ , in the simplified system is less than the total belt length of the true system, L . Belt length should be specified not as ℓ , the straight-line distance between the anchor and the initial position of the attachment point, but instead as L . This will result in calculation of strains appropriate for the prescribed material properties. Whatever initial slack condition might have been prescribed for the true system may still be prescribed for the simplified system. Alternatively, if the force-strain curve is linear, ℓ may be taken as the torso belt length, and the force components of the true loading curve must then be increased by the factor L/ℓ .

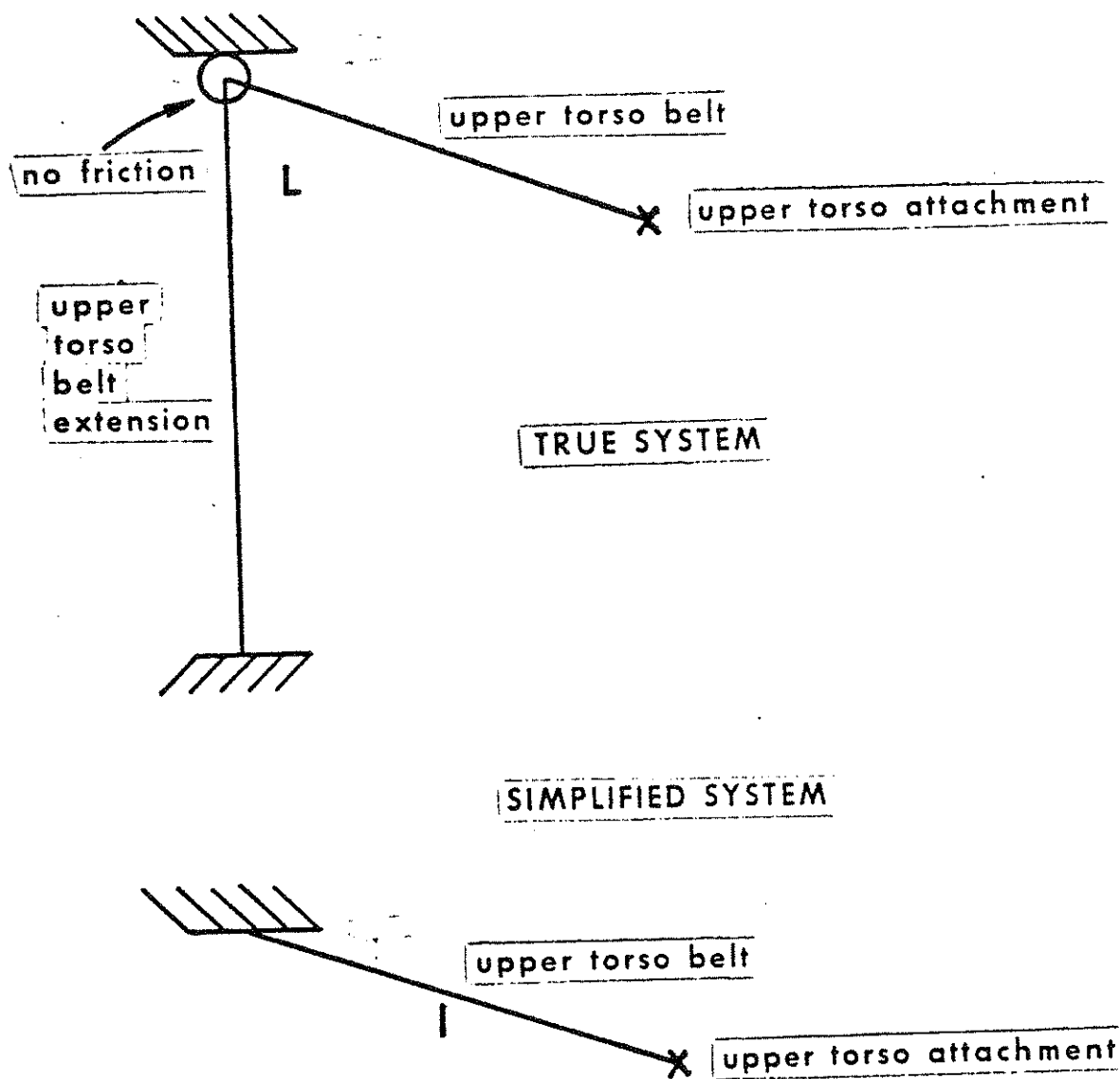


FIGURE 9-16 An Example Simplification of a Restraint System

These are only two examples of ways in which artificial loading properties might be prescribed for representing one belt-system configuration by a different one, whether of necessity or for economizing the determination of belt forces. The user may wish to demonstrate as an exercise that the belt stiffness data of the 708-Cards shown in Figure 9-10 are appropriate for making the system shown in Figure 9-9 equivalent to the system defined by the data in Figure 9-5 (specifically, the 708-Cards for material LABELMAT).

9.4.3 Special Uses of Loading Curves. The user should keep in mind the possibility of modifying loading curves for the purpose of modeling phenomena that cannot be represented directly by use of model features. Figure 9-17 illustrates an example. The first part of the curve represents resistance to a large amount of belt slip, after which a real belt load results from belt elongation.

9.4.4 Special Uses of Contact Surfaces. If it is found that a restraint-system design cannot be adequately represented by the belt segments of the seven-belt submodel, contact surfaces can often be used to define suitable artificial, supplementary belt segments. An example is shown in Figure 9-18. A contact surface is assigned the material properties of the belt represented, and a rigid occupant contact circle is prescribed for interaction with this surface. Inhibition cards* are included in the data deck which guarantee that the "belt surface" and "belt circle" will interact with no other elements of the system. The surface and circle are positioned so that initial belt slack is properly represented. This technique is best used for belts that are independent of other belts in the system and do not change angle significantly with occupant motion.

* Cards 106. See Modules 4 and 5.

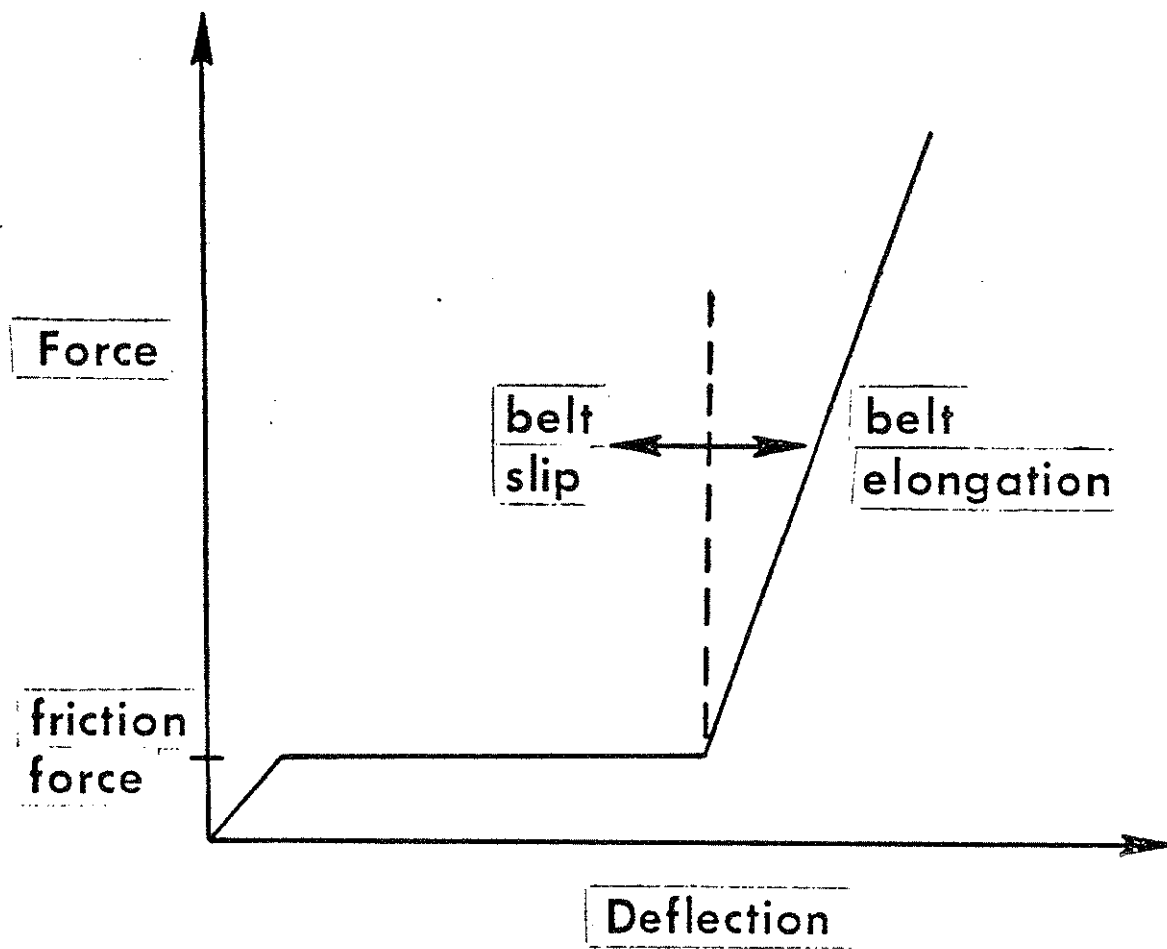


FIGURE 9-17 Modified Loading Curve for Modeling Belt Slip

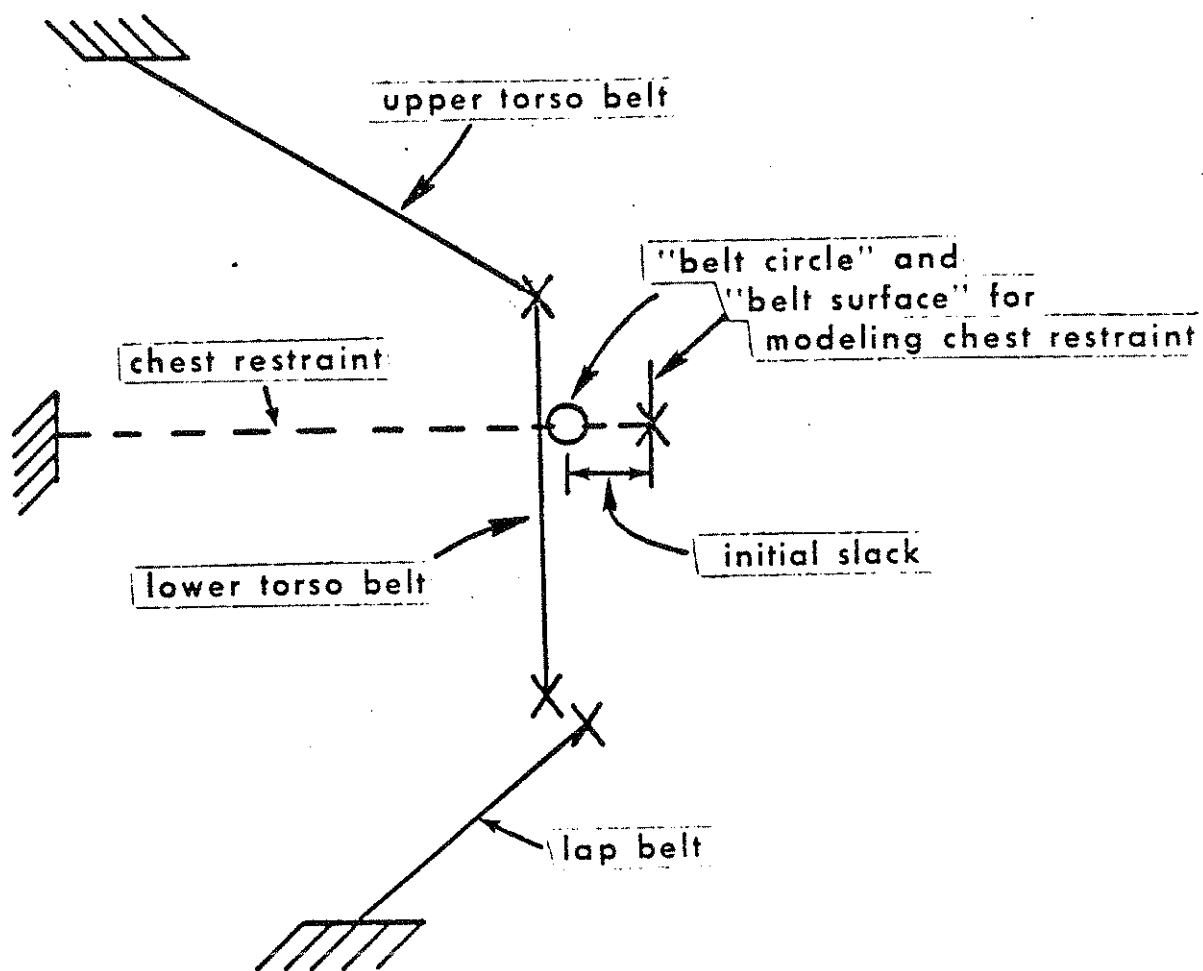


FIGURE 9-18 Modeling of an Artificial Belt Segment

MODULE 10 -- AIRBAG RESTRAINT SYSTEM

10.1 Airbag Submodel: General Description

An airbag submodel may be used optionally with the MVMA-2D Crash Victim Simulator. The estimation of bag forces is based on solution of the differential equations of gas thermodynamics. The airbag can contact both the occupant and vehicle interior. Restraining forces due to the internal pressure and skin tension are generated when the bag is fully inflated. The shape of the bag is allowed to conform to that of the occupant and the vehicle interior with free sections of the perimeter defined as circular segments. When the pressure in the bag reaches a specified level, gas is allowed to flow out of the bag through defined orifices.

10.2 Airbag Enclosure

The airbag expands within a closed area illustrated in Figure 10-1. The area is defined by: a) five inputted straight line segments attached, respectively, to the upper torso, middle torso, lower torso, upper legs, and lower legs (segments 1-2, 2-4, 4-6, 7-8, and 9-10) (907-909 cards); b) calculated straight-line segments joining the endpoints of the five primary line segments; c) two calculated straight-line segments approximating the front of the head; d) from one to five inputted frontal interior line segments (special entries on standard 411 cards); 3) a roof line extending to above and behind the head; f) and two calculated line segments which close the area (a-b and 10-A in Figure 10-1).

The bag source, or "attachment point," is shown in Figure 10-1 as point (X_A, Z_A) . This point is inputted in vehicle coordinates

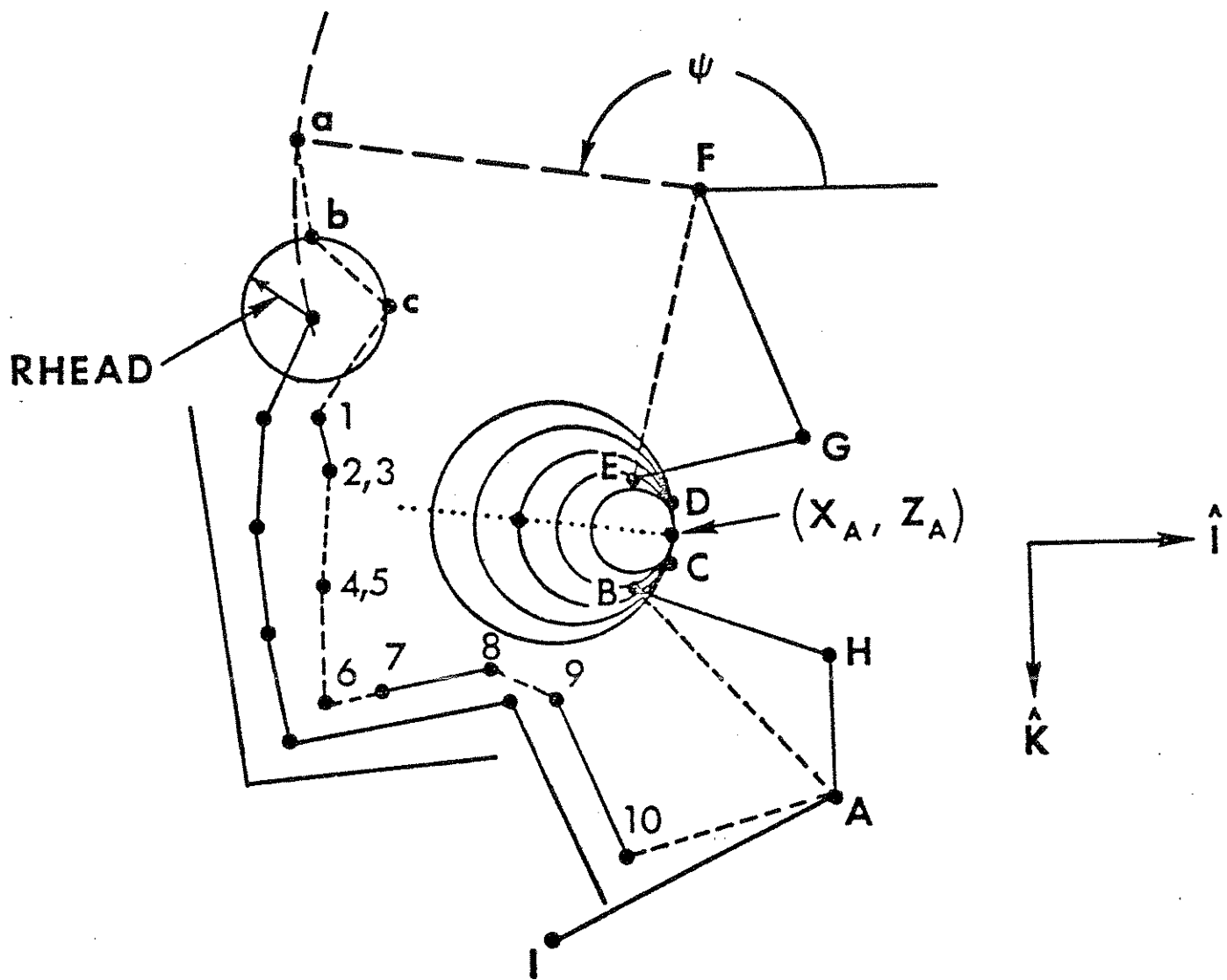


FIGURE 10-1 MVMA 2-D Airbag Model

on the 901 and 902 Cards as will be explained later. The bag source is fixed in the vehicle; it cannot move with either the steering assembly system or any part of the vehicle interior. The airbag itself, however, will react against line segments which define a frontal interior profile. This profile is comprised of from one to five connected line segments generated by the user's defining two to six points. The profile for airbag contact is normally identical to the profile of instrument panel lines, etc., defined for interaction with the vehicle occupant. Figure 10-1, however, illustrates a bag-sensing profile which is less detailed than the occupant-sensing profile. Six entries on 411-Cards define the points A, B, C, D, E, F and thus the line segments AB, BC, CD, DE, and EF. These five segments, the maximum number allowed, can only approximate the occupant-sensing profile, shown by solid lines. Since this profile is a reaction surface for the airbag, the user should make the approximation to the true interior line most accurate near the bag source. All vehicle-interior line-segment endpoints can be prescribed as functions of time, and the airbag will sense any collapse of the lines AB, BC, CD, DE, and EF about it. These lines are sensitive only to airbag contact while the example vehicle-interior configuration defined by FGEDCBHAI is sensitive only to interaction with contact ellipses. Airbag forces and moments are applied to the occupant at segments C-1, 1-2, 3-4, 5-6, 7-8.

10.3 Assumptions

The approach chosen for developing an analytical submodel for inflatable occupant restraints was to produce the simplest model

that would provide acceptable agreement with experimental data. Assumptions made in the formulation of the analytical model were based upon both analysis of the physical processes involved and observation of high-speed movies of tests of prototype inflatable safety restraints. User experience with the model may suggest alteration of some of the assumptions or generalization of some of the algorithms used to cover a wider variety of physical situations. Observation of high-speed movies of tests led to three assumptions (See Figure 10-2).

1. No restraint force is exerted upon the occupant until the occurrence of full bag inflation, which is defined as the condition in which the calculated perimeter of the deformed or undeformed bag equals the inputted filled-bag perimeter. This is equivalent to stating that the mass of the bag and its contents can be neglected.

2. The skin of the bag does not stretch.

3. The perimeter of the bag cross section in the plane of motion conforms to the shape of the automobile interior or to the occupant wherever they touch. Elsewhere the perimeter is described by circular arcs.

Five other assumptions were made to simplify the model.

1. Tangential forces between the occupant and the bag are negligible in comparison with normal forces.

2. Thermodynamic properties of the gas in the bag are calculated using adiabatic expansion of ideal nitrogen, neglecting potential energy of the gas. Flow of gas through the deflation membranes is calculated assuming unchoked flow through a converging nozzle.

3. Bag pressure does not affect the rate of inflation by the gas generator, which delivers gas at a predetermined rate. This implies that the area of the cross section of the bag increases

SUMMARY OF ASSUMPTIONS IN AIRBAG SUBMODEL ANALYSIS

- 1. The occupant feels constraint forces only after bag is fully expanded.**
- 2. The skin of the bag does not stretch.**
- 3. The bag cross-section perimeter is circular except where it conforms to the shape of the vehicle interior or to the occupant.**
- 4. Tangential bag forces are negligible.**
- 5. Adiabatic expansion of ideal nitrogen is assumed.**
- 6. Bag pressure does not affect the rate of inflation, which is specified by the user.**
- 7. The attachment point is fixed in the occupant compartment.**
- 8. The effect of skin tension can be approximated from bag pressure, occupant width, and depth of penetration into the bag.**

FIGURE 10-2 Summary of Assumptions in Airbag Submodel Analysis

6/28/79

at a predetermined rate until the bag is filled.

4. The point at which the bag attaches to the automobile interior is fixed with respect to the interior. This means that the bag may not be attached to a collapsible steering column.

5. Restraint force due to tension in the skin of the bag, caused primarily by the bag wrapping around the sides of the occupant, is approximated by a simple algorithm which takes into account the most important variables: pressure in the bag, width of the occupant and depth of penetration into the bag.

10.4 Simulation Description

The differential equations for occupant motion require values for forces and moments, from all sources, acting on the occupant. At each step of the numerical integration, a central routine calls the airbag submodel, presents it with an updated occupant and vehicle position, and receives in return updated forces and moments on the occupant due to the airbag. Basic organization of the airbag simulation is shown in Figure 10-3.

The airbag is inflated at a time-dependent rate specified by the user; inlet mass flow rate is a tabular input to the simulation. Energy absorption by the bag results by either or both of two means, controllable by the user. First, exhaust gas may be vented through user-defined orifices, as illustrated in Figure 10-4. Second, the venting of gas over the surface of the bag may be simulated by defining the porosity of the bag fabric. These features of the airbag submodel will be discussed in detail with the description of input data requirements.

6/28/79

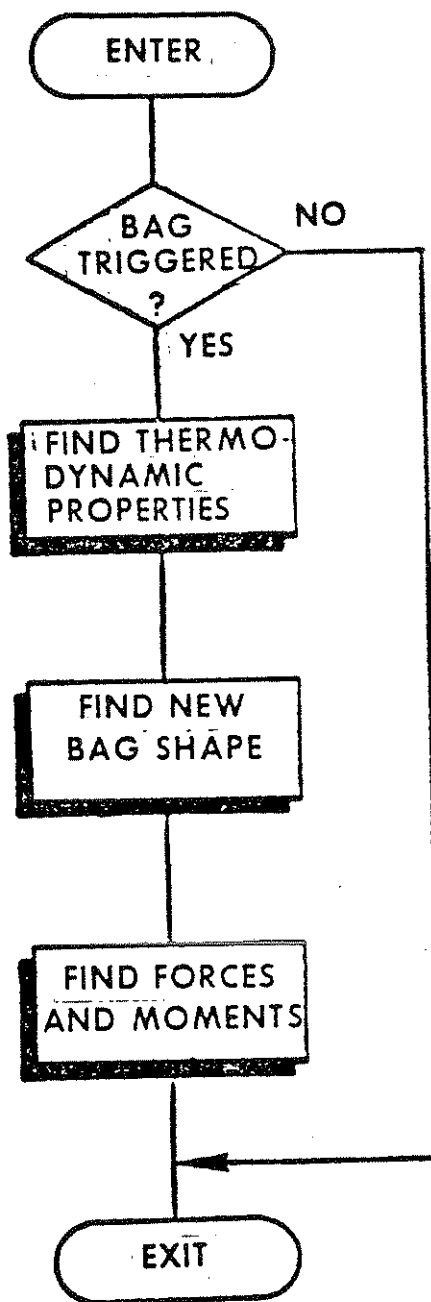


FIGURE 10-3 General Organization of the Airbag Simulation

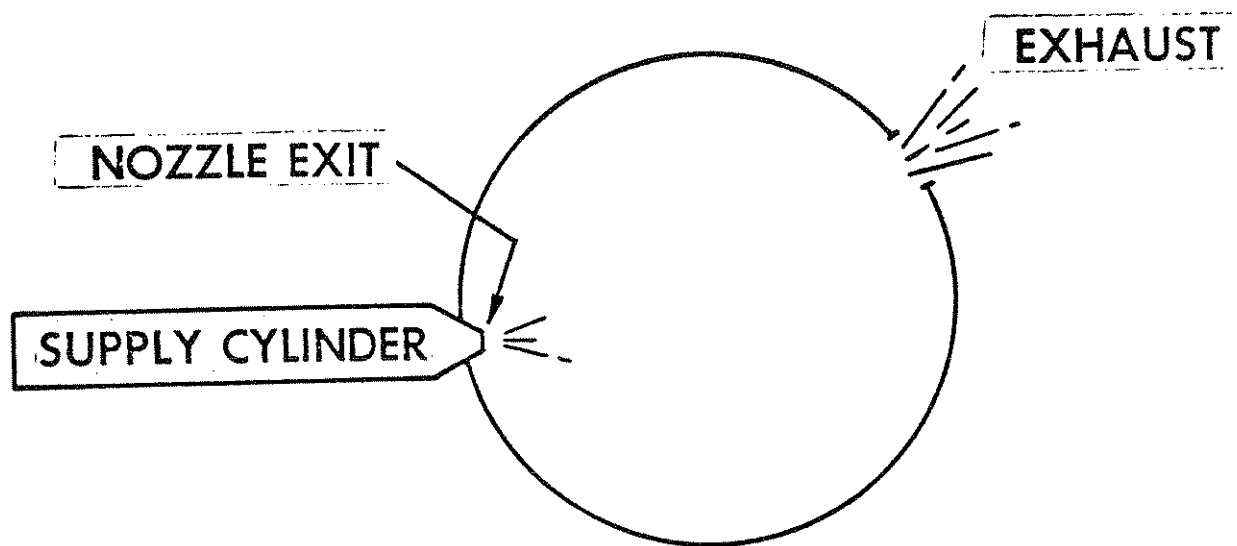
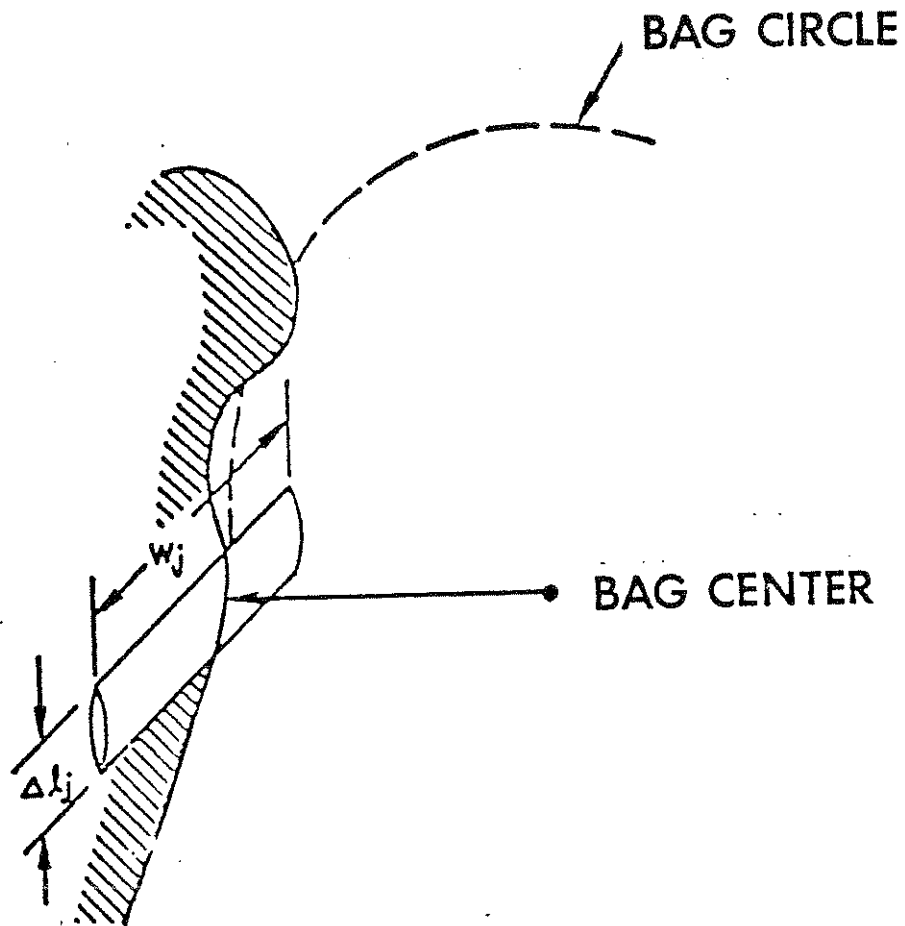


FIGURE 10-4 Supply Cylinder and Bag

The bag may be arbitrarily positioned within the passenger compartment; for example, on the instrument panel. A vector heading must be specified to define an axis along which the bag center progresses as the bag becomes an ever-expanding circle. This axis is illustrated in Figure 10-1. The heading angle remains constant until contact occurs with bounding segments of the closed area in which the airbag expands, previously illustrated in Figure 10-1. After such contact, the heading of the bag center motion is adjusted in order to balance z-direction forces on the bag. It is assumed that forces on the bag in the vehicle x-direction caused by contact with the occupant are balanced by forces caused by contact with the interior.

Forces on the occupant are calculated as a sum of elemental forces from elemental areas of contact between bag and occupant as shown in Figure 10-5. Forces are accumulated for each of the body segments representing head, torso and upper legs. Moments on each segment are calculated in the same process. Each elemental force is made up of two parts: one caused by pressure inside the bag and the other by tension in the bag skin. The first of these is calculated from the elemental length of bag contact, the width of the occupant at that point, and the pressure in the bag. The skin tension force results from the tendency of the bag to wrap around the sides of the occupant. Since this simulation calculates the shape of the bag only in the plane of motion, skin tension force can only be roughly approximated. The variables of strongest influence on skin tension force are pressure inside the bag, width of the occupant at each contact position, and the distance the occupant has penetrated into the bag at all points on the airbag perimeter.



Δl_j = Incremental length of contact in plane of motion.
 w_j = Width of occupant at this increment

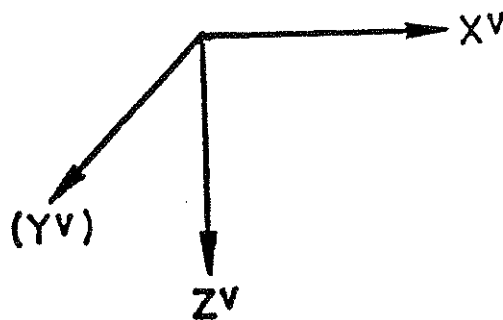


FIGURE 10-5 Incremental Force Generation

The approximation used is an attempt to take all three of these factors into account without unduly increasing the complexity of the analysis.

10.5 Input Data Cards

Data pertinent to the airbag submodel are entered primarily on Cards 901 through 909. Other relevant cards are 102 and 411. The presence of airbag data within a completely assembled set of data for an MVMA-2D crash simulation will not in itself result in inclusion of airbag effects in the crash dynamics. It is necessary for the user to indicate that airbag interaction with the occupant is to be considered by setting a control switch on Card 102. Field 2 of this card must contain a non-zero value if the airbag is to be deployed. Card 102 is shown in Figure 10-6 along with other cards for an example airbag data set.

Special entries are required on at least two, but not more than six, 411-Cards in any simulation in which the airbag is to be deployed. These cards are used normally for specifying the location of endpoints of straight line segments which define the vehicle interior profile seen by occupant contact-sensing ellipses. These cards are also used, however, to specify points of a frontal interior profile against which the airbag can react when it interacts with the occupant. These two vehicle interior profiles have been discussed previously and are illustrated in Figure 10-1. If points of the occupant-sensing profile are felt to adequately define the bag-sensing profile, then such line segment endpoints as are ap-

1.	1.	0.	0.	1.	1.	10.	.000001	5.	102
WINDSHIELD		-1.	25.	-46.	25.	-16.	4.		411
PANEL		-1.	25.	-16.	25.	-5.			411
LOWER	PANEL	-1.	25.	-5.	40.	0.	3.		411
TB		-1.	40.	0.	34.	11.	2.		411
FL		-1.	34.	11.	0.	12.	1.		411
0.	161.	36.	1.	30.	75.4	2.	12.	25.	901
-14.	40.	8.	20.	20.	20.	20.		0.	902
55.15	14.7	1.4		.25	150.	6.			903
12.									904
0.	84.9	10.	50.	20.	30.7	30.	19.6		
40.	12.9	50.	8.7	60.	6.	70.	4.		
80.	3.1	90.	2.3	100.	1.7	200.	1.		
2.									905
0.	-52.6	200.	-52.6						
0.	4.	8.	4.			8.	4.		907
		2.	4.	4.	2.	20.	1.		908
0.	1.	20.	1.						909

FIGURE 10-6 Airbag Input Data

appropriate, from two to six, may be made to serve double duty. An independently defined bag-sensing profile may be used instead, if desired, by adding 411-Cards for line segments of a vehicle interior region which is not allowed to interact with body segment ellipses. (Allowed or disallowed contact interactions are specified on 106-Cards, which are discussed in Module 6.) In either case, the values in fields 4 and 5 of any 411-Card for time equal to zero are used as coordinates of a point of the bag-sensing profile if field 8 of the card contains a 1., 2., 3., 4., 5., or 6. If there are to be "n" line segments in the profile, then there must be "n + 1" 411-Cards with values from 1. to "n + 1" in field 8. The "n + 1" points so designated are connected in order of the numbers in field 8 to define the "n" segments. Point 1 should be near the bottom of the toeboard and point "n + 1" should be for a point near the top of the windshield. The example 411-Cards in Figure 10-6 define a three-segment bag-sensing profile.

Values are required for various constant airbag system parameters on Cards 901, 902, and 903. The first field of Card 901 must contain a zero or be left blank. In field 2 is entered the angle, in degrees, of the line from the attachment point along which the bag center progresses as the bag expands. This angle is measured counterclockwise from the vehicle's x-axis. The value of 161° in the example data of Figure 10-6 is typical. Bag width, i.e., the out-of-plane dimension, is entered in field 3, and the perimeter of the bag when fully inflated is in field 6. Fields 4 and 5 contain two quantities that can be fully understood only

with an examination of some of the computer code. They are a perimeter iteration tolerance and a maximum allowed count for that iteration. Suffice it to say that values of 1. inch and 30. are appropriate.

One of the two deflation mechanisms mentioned earlier is the venting of gas through orifices after the rupture of deflation membranes. The pressure differential necessary to burst a membrane is entered in field 7 of Card 901. The area of one deflation membrane is entered in field 8. Explicit assumptions made in the calculation of the exhaust mass flow rate are: 1) that unchoked flow through an orifice occurs with no losses, i.e., with a value of 1 for the orifice discharge coefficient; and, 2) that the bag has two deflation orifices. Since the exhaust mass flow rate is directly proportional to the discharge coefficient and to the area of a deflation membrane, the user may effectively adjust the pre-assumed values for discharge coefficient and number of orifices by adjusting the value for deflation membrane area appropriately. The student should be able to satisfy himself that the value of 12. square inches in field 8 of Card 901 might be for a bag with two 12 square-inch orifices with discharge coefficients of 1, or that it could equally well be for a bag with three orifices, one with area 10 in^2 and a discharge coefficient of 1. and two others, each with an area of 8 in^2 and a discharge coefficient of .875.

The X- and Z-coordinates in the vehicle system of the bag attachment point are entered in field 9 of Card 901 and field 1 of Card 902. Temperature of the supply gas ($^{\circ}\text{F}$ or $^{\circ}\text{C}$), if constant, is in field 2

of Card 902. Occupant out-of-plane widths for head, shoulders, torso, hip, and thighs (two legs) are required in fields 3 through 7. Field 8 is unused and may be left blank. The bag fire time is entered in field 9. This value is generally in near coincidence with the first deviation from zero of the vehicle deceleration profiles but will normally depend on a Δv -threshold at the sensor.

Seven values are required on Card 903. The gas constant is in field 1. The value of 55.15 ft/°F in the example data is for nitrogen.

53.3 ft/°F is appropriate for air. The exhaust pressure is in field

2. Since this must be one atmosphere, the value entered should be 14.7 lb/in² if the simulation is done in English units or 10.135 N/cm² if done in Metric units. In field 3 should be entered the ratio of specific heat at constant pressure to the specific heat at constant volume. For real gases, the specific heats and also their ratio are dependent on temperature, but for the temperature range likely for air-bag simulations, a mean ratio of 1.4 is accurate for either nitrogen or air. Field 4 is unused and may be left blank. A mean value of the specific heat at constant pressure is required in field 5; .25 BTU/lb°F is an approximate value for both nitrogen and air. The angle for the roof line with respect to the x-axis of the vehicle is needed in field 6 to help define the closed area in which the airbag expands. This is the angle ψ in Figure 10-1. Model results are insensitive to the value inputted with any reasonable bag location as long as the projected roof line passes above the head. A value of 150° is reasonable. The last required entry on the 903-Card is a value in field 7 for average head radius. It is used to help define the line segments bc and cl in Figure 10-1.

Three types of tabular input are specified with Cards 904, 905

and 906 and unnumbered cards which follow them. Card 904 contains one value, in field 1 -- the number of time points at which mass influx rate will be specified. The computer model determines the influx rate for all non-specified times by linear interpolation. Coordinate pairs which define the mass influx rate profile are entered on unnumbered cards immediately following the 904-Card, four time-rate pairs per card, in order. Field 1 of each such card contains a time value in msec, time and influx rate values alternating in the first eight fields. Supply gas temperature versus time is similarly defined by Card 905 and following unnumbered cards.

One of two deflation mechanisms has previously been discussed, viz., the venting of gas through orifices after the rupture of deflation membranes. The second optional method is the venting of gas through porous bag fabric over the surface of the bag. The user is required to specify bag porosity as a function of pressure differential. Field 1 of Card 906 indicates the number of points in the table and following cards contain pressure-porosity pairs, four pairs to a card. The units of porosity are volume of gas (at the temperature and pressure of the occupant environment) per unit area per minute. The user may, if desired, combine the two available deflation mechanisms in any crash simulation. If it is desired to use only bag-porosity deflation, it is necessary to ensure against gas loss through the deflation orifices, which are an integral feature of the airbag model. This may be done by specifying an unrealistically large value in field 7 of Card 901 for the pressure differential necessary to burst a deflation membrane or by setting the deflation membrane area equal to zero in field 8 of Card 901. If energy absorption is to result only from

venting of gas through orifices, then Card 906 and accompanying un-numbered cards should be omitted from the data deck.

Three remaining cards complete the data requirements for the air-bag submodel. Bag forces on the occupant result from interaction of the airbag with the occupant profile. Cards 907, 908, and 909 define this occupant profile as a series of straight line segments. These are illustrated in Figure 10-7. The user is required to define the locations of eight points on the occupant frontal profile, each fixed with respect to some body link as indicated. The points in Figure 10-7 which are defined on cards 907, 908, and 909 are (ξ_i, ζ_i) with "i" equal to 1, 2, 4, 6, 7, 8, 9, and 10. It is clear that as articulation occurs at body joints, any successive points of this group that are not defined with respect to the same body link will undergo relative motion. Solid line segments in the contact line profile are fixed in length and orientation by the input data. Dashed lines will vary in both length and orientation with respect to all body links; these are determined by the computer model from the input data so as to make the contact profile continuous.

The first eight fields of Card 907 are used for coordinate pairs (ξ_i, ζ_i) with successive values of i equal to 1, 2, 3, and 4. No values are required for point 3, so fields 5 and 6 are left blank. Similarly, four points are accommodated by Card 908. No input is required for point 5, however, so the coordinates of points 6 through 8 are in fields 3 through 8. Points 9 and 10 are defined in the first four fields of Card 909.

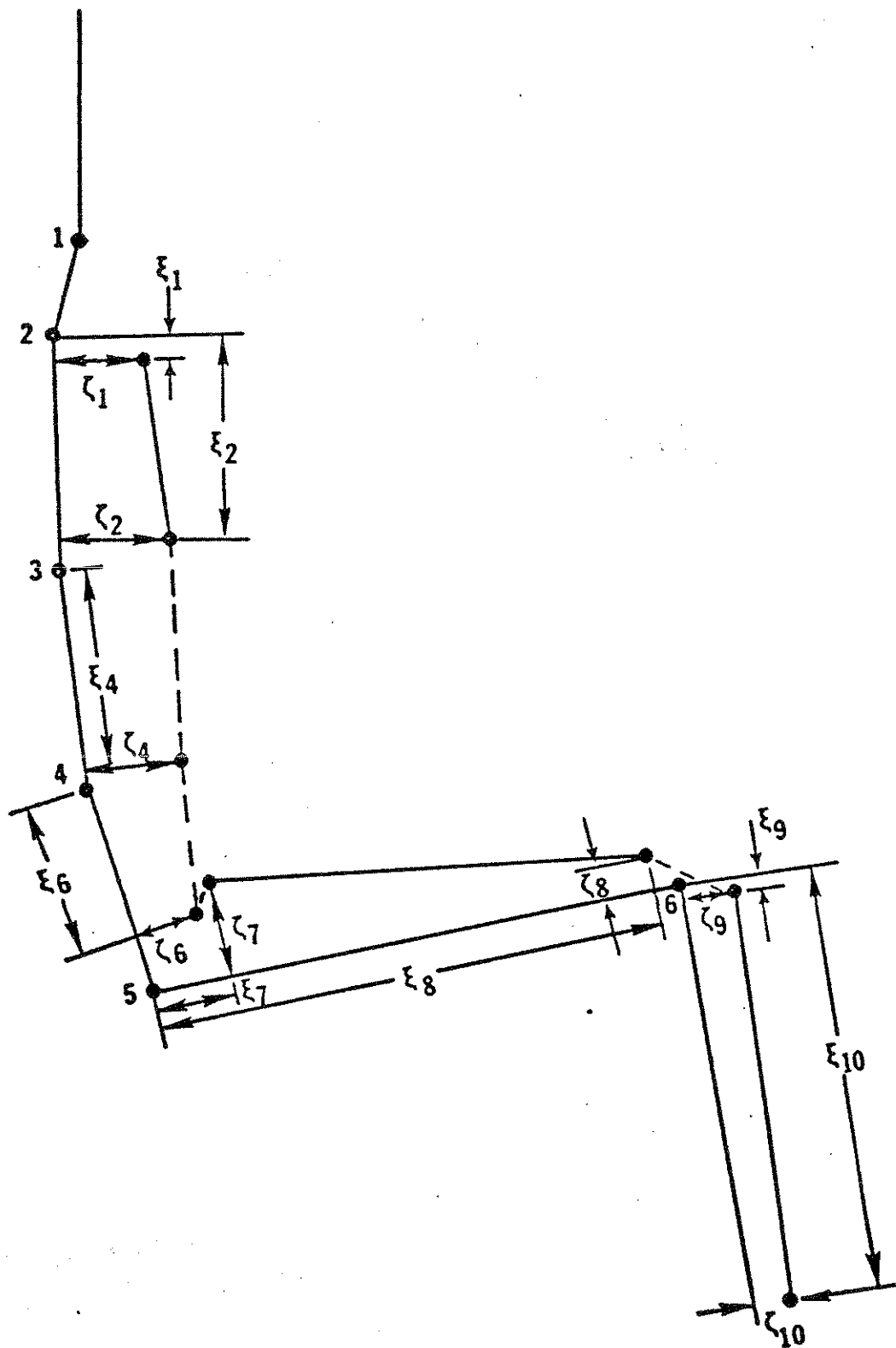


FIGURE 10-7 Airbag Contact Lines on Occupant

MODULE 12 - MODEL OPERATION

12.1 Model Architecture

The MVMA Two-Dimensional Crash Victim Simulation is a large and complex computer program. Some of the input quantities to the MVMA 2-D Model deal with the alternatives in operation of the computer program as opposed to the description of the situation being simulated. Understanding of some of the program controls entails some knowledge of the architecture of the model program.

The MVMA 2-D computer model is organized as a multiprocessor in that it is divided into five parts which operate in turn. The first processor is called the Input Pre-Processor, or INP. It reads data cards and writes the main program for the second processor. The second processor is called the Input Processor, or IN. It packs input data into binary tables and records those tables for use by subsequent processors. It also writes two programs needed by the third processor, including the main program. The third processor is called the Dynamics Solution Processor, or GO. It reads the binary tables, solves the equations of motion, and incorporates the computed results into the binary tables. The fourth processor is the Output Pre-Processor, or OUTP. It reads data cards and writes three programs needed by the fifth processor, including the main program. The fifth processor is called the Output Processor, or OUT. It reads the binary tables produced by the other processors and prints a comprehensive summary of all recorded information as the user specifies.

The binary tables which are used for communication between processors are stored in four external files. These files can be used as a complete summary of this computer run for input into post-processors such as the Validation Command Language or a graphics package. The four files are called NU, MU, MV, and NP, respectively for the four variables used to reference the logical device numbers to which they are attached. NU is a direct access data set which contains all input quantities and all fixed-length computed results. MU is a sequential data set which contains head, chest, and hip acceleration information for every integration time step. MV is a direct access data set which contains the variable-length computed results, which include contact interactions, region movement, and region summary

quantities. NP is a sequential data set which contains the special information needed for production of the stick-figure printer-plot output. Figure 12-1 summarizes the intercommunication between the five processors by means of the four external files.

12.2 Output Categories

The computed results are broken into subjects or categories which correspond to output pages for the fixed-length output and to "typical output pages" for the variable-length output. There are forty-five such subjects or categories and these are numbered 1 through 40 and 46 through 50. In addition to these, there are six special types of output which it was convenient to put in the same numbering scheme even though they are not recorded in the same manner. These categories are numbered 0 and 41 through 45. Figure 12-2 lists all fifty-one categories.

Categories 1-40 and 46-50 may be optionally recorded on the binary files NU and MV under control of the recording switches specified by the user on Cards 107 through 110, fields 1 through 9 and Card 111, fields 1 through 4 respectively. These switches are set non-zero to inhibit the recording of the information for the respective categories. Example images of Cards 107 through 111 and all other data cards discussed in this module are shown in Figure 12-13 at the end of the module.

The input to OUTP allows a specification of which categories are to be printed during the execution of OUT and the order in which the categories are to appear. OUTP and OUT may be re-run with the specification of different choices of categories as many times as desired as long as the binary tables remain undisturbed. A particular category will appear in the output of OUT if the category was recorded by GO and was specified as desired in the input to OUTP. Input cards 1001 and 1002 are used to specify which categories are desired to be printed. All input cards numbered 1001 and higher are to be inputted to OUTP. Cards 1001 and 1002 are the only two input cards which are not fixed-format fields. These cards contain a listing of the category numbers in the order in which they are to appear in the printout. The category number zero is used for the output of the input values and must occur first if it occurs at all. The category numbers are separated by commas. In order to simplify the presentation of a consecutive sequence of integers (either ascending or descending),

6/28/79

Category Number	Description
0	Formatted Printout of Input Quantities
1	Vehicle Response
2	Real Line Region Parameters
3	Real Line Region Individual Line Segment Movement
4	Contact Forces Including Occupant-Vehicle, Occupant- Belt, Occupant-Occupant
5	Neck Reaction Forces
6	Unfiltered Body Accelerations (Head, Chest, Pelvis)
7	Filtered Body Accelerations (Head, Chest, Pelvis)
8	Unfiltered Severity Indices
9	Filtered Severity Indices
10	Body Link Angles
11	Body Link Angular Velocities
12	Body Link Angular Accelerations
13	Body Joint Coordinates
14	Body Joint Velocities
15	Body Joint Torques
16	Body Joint Absorbed Energies
17	Body Kinetic Energies
18	Airbag Variables
19	Airbag Contact Forces
20	Airbag Center of Mass Forces and Moments
21	Neck Joint Coordinates
22	Shoulder Joint Coordinates
23	Joint Torque Elastic Components
24	Joint Torque Joint-Stop Components
25	Joint Torque Friction Components
26	Joint Torque Viscosity Components
27	Joint Absorbed Energy Joint Stop Components
28	Joint Absorbed Energy Friction Components
29	Joint Absorbed Energy Viscosity Components
30	Center of Mass X-Component Forces
31	Center of Mass Z-Component Forces

FIGURE 12-2a List of Output Categories

Category Number	Description
32	Center of Mass Resultant Moments
33	Steering Column Coordinates
34	Steering Column Generalized Coordinates
35	Steering Column Forces and Moments
36	Forces and Moments on Body Due to Steering Column
37	Neck and Shoulder Forces
38	Muscle Tension Forces
39	Muscle Tension Energy Absorption
40	Femur and Tibia Accelerations and Loads
41	Joint Relative Angle Comparisons Against Upper and Lower Test Values
42	Standard List of Quantities to be Compared Against Test Values
43	Individual Type A Comparisons
44	Individual Type B Comparisons
45	Printer-Plots of Stick Figures
46	Head Center-of-Gravity Motion
47	Chest Center-of-Gravity Motion
48	Hip Motion
49	Joint Relative Angles
50	Joint Relative Angle Velocities

FIGURE 12-2b List of Output Categories

a special abbreviation of a sequence is recognized by OUTP. The abbreviation lists the category number of the end of the sequence which is to appear first followed by a hyphen (minus sign) followed by the category number of the end of the sequence which is to appear last. The whole sequence abbreviation is separated from other category numbers or other sequence abbreviations by commas.

Category numbers are also used in specifying input to the Type A and Type B comparisons which will be discussed later in this module.

12.3 General Model Controls

The general model controls are specified on Cards 101 and 102 and will be described here in the order they are found on those two cards.

The MVMA 2-D CVS Model is capable of accepting input and producing output in either metric units or in American standard (English) units. Field 1 of Card 101 is used to specify a switch which is set to 0 for metric units and set non-zero for English units. Figure 12-3 contains the metric/English conversion constant used in the model.

Field 2 must be set to 1 since the fixed-step Runge-Kutta is the only integration method currently implemented. Field 3 specifies the acceleration due to gravity to be operative during the simulation.

It is sometimes useful to edit acceleration values which are close to zero back to zero. This procedure can improve the appearance of the tabulated results and rarely can affect the accuracy of a computation. Field 4 is used to control the editing facility built into the MVMA 2-D model. If field 4 is 0, editing is not done. If field 4 is positive, the value will be the cut-off point between the acceleration magnitude values reset to zero and those which are unaltered.

Fields 5 through 9 contain the simulation beginning time, ending time, integration time step, tabular output time step, and the time step for plot recording, respectively. The beginning time is normally set to zero. The final time will be set to 200 milliseconds beyond the beginning time if it does not exceed the beginning time. If the integration time step is not positive, it is set to 1 msec. If the tabular output time step is not positive, it is set to the maximum

METRIC/ENGLISH SYSTEM CONVERSION CONSTANTS

PHYSICAL QUANTITY	CONVERSION RELATION
Length	1 in. = 2.54 cm*
Length	1 ft. = .3048 m*
Length	39.370075 in. = 1 m
Force	1 lb. = 4.4482216 N
Mass	1 lbm = .45359237 kg*
Mass	1 lb-sec ² /in. = 175.12684 kg
Mass	1 slug = 14.593903 kg.
Moment of Inertia	1 lb-sec ² -in = 0.11298483 kg-m ²
Torque	1 lb-in = 0.11298483 N-m
Energy	1 in-lb = 0.11298483 N-m
Linear Spring Coefficient	1 lb/in. = 1.7512684 N/cm
Second Order Coefficient	1 lb/in ² = 0.68947573 N/cm ²
Third Order Coefficient	1 lb/in ³ = 0.27144714 N/cm ³
Fourth Order Coefficient	1 lb/in ⁴ = 0.10686895 N/cm ⁴
Fifth Order Coefficient	1 lb/in ⁵ = 0.042074390 N/cm ⁵
Sixth Order Coefficient	1 lb/in ⁶ = 0.016564721 N/cm ⁶
Pressure	1 lb/in ² = 0.68947573 N/cm ²
Pressure	1 atm. = 14.696 lb/in ² = 1.0132535 x 10 ⁵ N/m ²
Gas Constant	1 ft-lb/(lbm °F) = 5.38032 Joules/(kg °C)
Specific Heat	1 BTU/lb-°F = 1 kg-cal/kg-°C = 4.1868 Joules/gm-°C*
Earth Standard Gravity	1 E.S.G. = 9.80665 m/sec ² * = 32.174049 ft/sec ² = 386.08858 in/sec ²

* Exact conversion

FIGURE 12-3 Metric/English System Conversion Constants

of 5 msec. and the integration time step. If the tabular output time step is not an integral multiple of the integration time step, it is set to the closest integral multiple of the integration time step. Likewise, if the plot recording time step is not an integral multiple of the tabular output time step, it is set to the closest integral multiple of the tabular output time step. If the plot recording time step is zero, no plot recording is done.

Four optional subsystems are available within the MVMA 2-D Man Model for two belt models, an airbag model and an energy-absorbing steering column model. These four options are controlled by three switches which are specified using the first three fields of Card 102. The first of these switches has the four possible values (0 to 3) which signify respectively no belts, standard lap belt only, standard lap belt and shoulder harness, and the advanced belt system. The other two switches deal with airbag and steering column respectively and are set non-zero to indicate use of the respective subsystem.

Field 8 is used to specify a relative error bound which will be used to recognize a singular matrix during the inversion step. 0.000001 is the recommended value.

Field 9 contains an execution time limit. During the run, if the execution time exceeds the limit, the run will be terminated. If field nine is set zero, the testing of execution time is inhibited.

12.4 Auxiliary Printed Output

The G0 processor has a large number of optional printout capabilities called auxiliary or Debug Printout. These optional printouts are organized under sixteen time-dependent four-level switches. The four levels are off, primary, secondary, and tertiary and are represented by zero, one, two and three respectively. A complete description of the debug switches and the printout they control is found in Section 4.3.5 of Volume 3. Switch 16, level 3 causes the termination of the run and a dump if subroutine ABDUMP has been implemented.

The desired debug printout is specified using fields 1 through 8 on Cards 104 and 105. Each successive pair of fields on these

two cards define one of the eight possible time points for hexadecimal debug switch settings. Each such pair of fields has the effective time in milliseconds in the odd-numbered field and the hexadecimal debug switch setting in the even-numbered field. The pairs of fields are filled in ascending order of time starting with the first pair of fields and continuing with each consecutive pair for fields as needed. The first effective time must either equal or exceed the beginning time specified in field 8 of Card 101. If the first effective time exceeds the beginning time, an all-zero hexadecimal debug switch setting is presumed until the first effective time.

Each hexadecimal debug switch setting contains a representation of the values of all sixteen debug switches at the effective time. The recommended procedure for generating hexadecimal debug switch settings is illustrated by Figure 12-4.

Field 9 of the 104-Card contains a switch which when set zero specifies that the debug switch settings apply to all four evaluations necessary at each integration step. If this switch is set non-zero, the debug switch settings apply only to the fourth evaluation at each integration step. A non-zero setting for this switch nearly always provides adequate debugging information and considerably reduces the volume of printout.

Field 9 of the 105-Card contains a switch which controls the auxiliary output of the Input Processor. If the switch is set zero, a packing dictionary and binary file index summary are printed. If the switch is set non-zero, the auxiliary output is not printed. It is advisable to obtain this output as a standard operating procedure.

12.5 Accelerometer Location

For determination of several output quantities, two occupant accelerometers, one in the head and one in the chest, are represented in the model. The chest accelerometer can be placed anywhere along the upper torso centerline, and its position is measured from the lower neck joint. This coordinate is entered in field 2 of Card 218. The head accelerometer is not confined to the head centerline and its position is specified in fields 1 and 3 of the same card. Field 1 is

Procedure Step	Example																																								
A. Determine desired values for each debug switch at each effective time. See Tables 70, 71, 72, 73, and 75 in Volume 3. Steps B through D are carried out for each time in turn.	<p>(1) At t = 0, switches 1, 4, 9, 13 are 0, switches 2, 3, 15, 16 are 1, switches 5, 6, 10, 11 are 2 and switches 7, 8, 12, 14 are 3.</p> <p>(2) At t = 5 msec, switches 11 and 12 are 3, switch 16 is 1, and the rest are 0.</p> <p>(3) At t = 59 msec all switches are 0.</p> <p>(4) At t = 103 msec all switches are 1.</p> <p>(5) At t = 157 msec all switches except 16 are 3, and switch 16 is 2 (full debug).</p> <p>(6) At t = 159 msec all switches are 0 (no debug).</p> <p>(7) At t = 162 msec switches 1, 2, 3, 6 are 1, the rest are 0.</p> <p>(8) At t = 164 msec all switches are 3 (full debug, termination of run and dump).</p>																																								
B. Write out the values of each switch in binary in ascending switch number.	<p>For t = 0</p> <table><tr><td>1</td><td>2</td><td>3</td><td>4</td><td>5</td><td>6</td><td>7</td><td>8</td><td>9</td><td>10</td></tr><tr><td>00</td><td>01</td><td>01</td><td>00</td><td>10</td><td>10</td><td>11</td><td>11</td><td>00</td><td>10</td></tr><tr><td>11</td><td>12</td><td>13</td><td>14</td><td>15</td><td>16</td><td></td><td></td><td></td><td></td></tr><tr><td>10</td><td>11</td><td>00</td><td>11</td><td>01</td><td>01</td><td></td><td></td><td></td><td></td></tr></table>	1	2	3	4	5	6	7	8	9	10	00	01	01	00	10	10	11	11	00	10	11	12	13	14	15	16					10	11	00	11	01	01				
1	2	3	4	5	6	7	8	9	10																																
00	01	01	00	10	10	11	11	00	10																																
11	12	13	14	15	16																																				
10	11	00	11	01	01																																				
C. Replace each four binary bits by the corresponding hexadecimal digit in turn*	1 4 A F 2 B 3 5																																								
D. Enter the effective time in milliseconds in the next unused odd-numbered (not field 9) field and the eight digit hexadecimal number in the next unused even-numbered field.	<p>0. 14AF2B35</p> <p>Figure 12-13 contains the complete 104 and 105 cards for the total example specified in step A of this procedure.</p>																																								

FIGURE 12-4 Hexadecimal Debug Switch Setting Generation

* The hexadecimal representations of the binary numbers 0 through 1111 are 0 through 9 followed by A through F.

the component of the head accelerometer position measured along the head centerline from the upper neck joint. Field 3 is the posterior component of the position of the head accelerometer measured from the head centerline.

12.6 Generation of Page Titles

The regular output of the MVMA Two-Dimensional CVS Model is provided with automatic titling based on the contents of cards 100, 200, 300, 400, 500, 600, 700, 800, and 900. Card 100 will be treated as seventy-two columns of general run title. The contents of the other cards appear in part in the title. The title consists of two lines formatted from this information together with the date, the time, job identification and page number. Figure 12-5 shows the layout of this information in the title and states which columns of each of the forenamed input cards are incorporated.

12.7 End of Input Processor Data Deck

The end of the data deck for the Input Pre-Processor is marked by the presence of a 1000-Card. All fields on this card are ignored.

12.8 Output Processor Control Cards

The rest of this module deals with the input control cards inputted to the Output Pre-Processor. These cards all have identification numbers exceeding 1000. Cards 1001 and 1002 have already been discussed in Section 12.2.

The first two fields of the 1003-Card contain controls for the auxiliary output from the Output Pre-Processor. The first of these fields contains a switch which when set non-zero causes intermediate printout from the HIC computation to be printed. The second of these fields acts both as a switch and a designation of a logical device number upon which a separate printout of peak head acceleration and three millisecond average acceleration are to be put out. If this field is zero, the peak head acceleration and three millisecond average acceleration are not desired.

Title Line	Title Columns	Input Card Number	Input Card Columns	Description
1	1	-	-	Eject Page
	2 - 4	-	-	Blank
	5 - 16	-	-	Date: Month, Day Year, if FDATER implemented
	17 - 24	-	-	Time: Hour, Minute, Second if FDATER implemented
	25 - 29	-	-	Blank
	30 -101	100	1 - 72	General Run Title
	102 -106	-	-	Blank
	107 -114	-	-	Job Name if USERZZ implemented
	115 -118	-	-	Blank
	119 -132	-	-	Page Number
2	1	-	-	Blank
	2 - 20	200	1 - 19	Occupant Identification
	21 - 39	300	1 - 19	Occupant Orientation
	40 - 58	400	1 - 19	Interior Description
	59 - 77	500	1 - 19	Interior Configuration
	78 - 96	600	1 - 19	Acceleration Profile
	97 -115	700	1 - 19	Belt Description
	116 -132	800	1 - 17	Steering Column Description
		900 or whichever occurs last in data deck	1 - 17	Airbag Description Defaulted to "MVMA 2-D,VER3"

FIGURE 12-5 Layout of Automatic Title

The third field of Card 1003 also acts as a switch which if non-zero causes the output processor to repeat the filtering and computation of special indices whether it has been previously done or not. If this switch is set zero and if the output processor has been previously run on a set of binary catch files, the filtering and the computation of special indices are not repeated.

Field 4 of Card 1003 contains the distance along the upper leg centerline from the hip joint to a simulated femur-load sensor mounted on the upper leg centerline. Field 5 is the amount of upper leg mass between the sensor and the knee.

Card 1004 contains four filtering controls and four HIC controls. Section 4.4.2.3 of Volume 3 describes the low-pass filtering technique. Field 1 is the number (NPP) of filter weights on one side of the symmetric sum exclusive of the center weight. Field 2 is the cut-off frequency (FC) that is, the frequency marking the upper bound of the passband. Figure 12-6 illustrates the gain characteristics.

Field 3 is the terminal frequency (FT), that is, the frequency which marks the start of the stopband and the end of the roll-off band. The quantity NPP cannot exceed 500 without redimensioning of storage arrays. FC cannot exceed half the sampling frequency. Further, the product of the ratio of the roll-off bandwidth to the sampling frequency and NPP must be as large as 1. for reasonable filtering accuracy. In order to compute the symmetric sums within NPP points of two endpoints, it is necessary to extend the data for NPP points around each endpoint. Field 4 is a switch which when zero implies that a polar image will be used at the two endpoints and which when non-zero implies that a mirror image will be used at the two endpoints. Figure 12-7 illustrates the difference between polar and mirror images. It is thought that polar images usually yield better results.

The four HIC controls begin with field 5 of Card 1004. Field 5 is the fraction of the maximum HIC below which scanning is stopped. Field 6 contains the number of time points over which HIC is to be computed. Fields 7 and 8 contain the number of points by which the outside and inside loops are incremented for comparison of all

Characteristics of a Martin-Graham Digital Filter

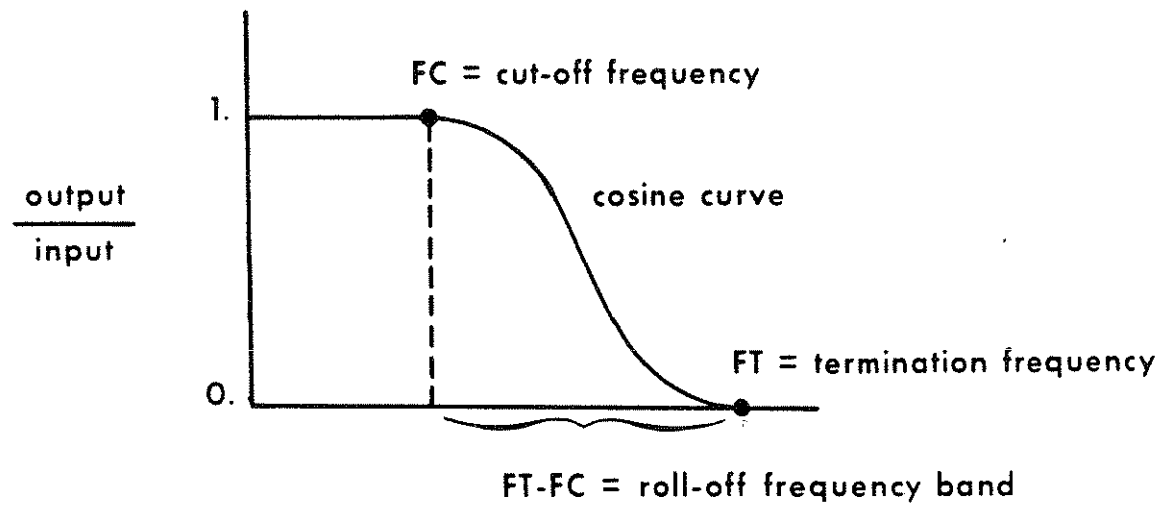


FIGURE 12-6 Characteristics of a Martin-Graham Digital Filter

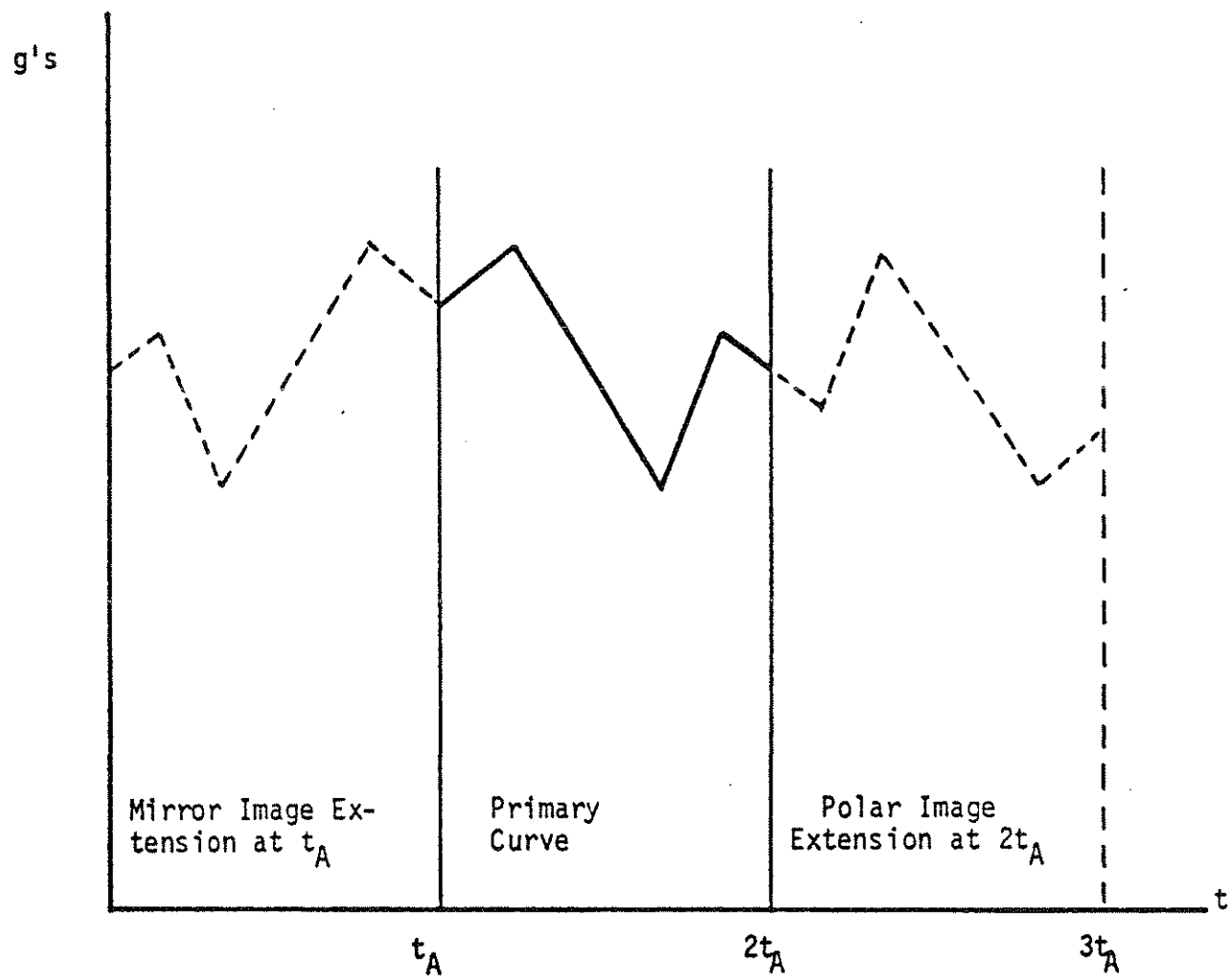


FIGURE 12-7 Mirror and Polar Images

of points. These two increments are used to decrease the expense of the HIC computation and each must be set at least to 1 or may be greater if sufficient time points are being used.

12.9 Output Comparisons

Cards 1100 through 1107 are used to supply high and low test values for relative angles at all of the eight joints. Fields 1 and 2 of each of these cards contain the high and low test values respectively. Figure 12-8 relates the individual card identification numbers with the connected body parts and joint angle name. If the joint relative angle exceeds the high test value or fails to exceed the low test value, an entry stating the quantity name, peak value, time of peak, violation duration, beginning time of violation, and ending time of violation appears on the joint test summary page. If both high and low test values are zero, the test is not carried out.

Cards 1200 and 1201 are used to specify test values for eighteen injury-related quantities. Figure 12-9 lists the eighteen quantities in the order of testing. Each test is made only if the corresponding specified test value is greater than zero. The absolute value of each quantity is tested for exceeding the test value. The output produced prints the quantity name, the peak value, the time at which the peak occurs, the time duration during which the quantity exceeds an inputted test value together with the points in time at which the quantity exceeds and then returns below the test value. This output is repeated for each new violation time range. The first nine test values are specified in Card 1200, fields 1 through 9 respectively. The second nine test values are specified in Card 1201, fields 1 through 9. Card 1202 is used to specify a name for a face ellipse in columns 1 through 15 and a name for a chest ellipse in columns 17 through 32. The interaction force quantities associated with these ellipses are used in the appropriate tests.

CARD ID	BODY PARTS CONNECTED	JOINT ANGLE NAME
1100	Head to Neck	Upper Neck
1101	Neck to Upper Torso	Lower Neck
1102	Upper Torso to Middle Torso	Upper Spine
1103	Middle Torso to Lower Torso	Lower Spine
1104	Upper Leg to Lower Torso	Hip
1105	Lower Leg to Upper Leg	Knee
1106	Upper Arm to Upper Torso	Shoulder
1107	Lower Arm to Upper Arm	Elbow

FIGURE 12-8 Relationship of Test Value Card ID Numbers to Joints

Number	Quantity Description
1	Head frontal acceleration at the center of gravity (Anterior-posterior, A-P)
2	Head vertical acceleration at the center of gravity (Superior-inferior, S-I)
3	Head resultant acceleration at the center of gravity
4	Head angular acceleration
5	Head injury criterion (HIC)
6	Face loads as measured on a deformable head contact ellipse
7	Chest deflection as measured on a deforming chest contact ellipse
8	Chest load as measured on a deforming chest contact ellipse
9	Chest frontal acceleration at the center of gravity (A-P)
10	Chest vertical acceleration at the center of gravity (S-I)
11	Chest resultant acceleration at the center of gravity (3 msec average)
12	Chest frontal severity index (A-P)
13	Chest vertical severity index (S-I)
14	Chest resultant severity index
15	Pelvic horizontal acceleration at the hip joint
16	Pelvic vertical acceleration at the hip joint
17	Pelvic resultant acceleration at the hip joint
18	Femur load at a specified point along the length representing the location of a sensor

FIGURE 12-9 List of Injury Related Test Quantities

Two types of general comparison are available for any variable against fixed limits or against any other variable. The class of variables which can be compared consists of all quantities which have been recorded for printing. The total specification for one of these quantities involves at least two numbers and in some cases one or two sixteen-character names. The two numbers are the category number and the column number (ignoring time except in category one) on the printed page. If the category number is two or three, the name of the region in question is also required to make the specification unique. If the category number is four, three different possibilities exist. These possibilities deal with the type of interaction (ellipse-line, ellipse-ellipse, and belt) and are summarized in Fig. 12-10. An alphabetical listing of all printed quantities together with category number and column number will be found in Volume 3 in Table 114. Belt names are not user-supplied. The belt names which have been assigned are shown in Fig. 12-11.

Card 1300 is used to specify a comparison of Type A in which a single general variable is compared against high and low test values. The printout is similar to that produced for the Joint Relative Angle Tests and for the Standard List Tests. The first two fields contain the category number and the column number respectively. Fields 3 and 4 contain the first name, and fields 5 and 6 contain the second name. These fields should be left blank if the corresponding name is unneeded. Field 7 contains the high test value and field 8 contains the low test value.

Cards 1400 and 1401 are used to specify a comparison of Type B in which two general variables are compared in time against each other. The produced output lists each of the variables, their difference, and an indication of which is larger. The first six fields of Card 1400 contain a general variable specification as discussed in the preceding paragraph. Field 7 is an optional ordering number among Type B Comparisons. The Ordering Number, if specified, serves a dual function of specifying an ordering of printout which may be different from the ordering of input cards and of providing a means of matching the first half of the comparison specification (Card 1400) with the second half of the comparison specification (Card 1401) independent of the order of cards in the input deck. If the Ordering

of crash events. Field 2 of Card 1500 controls whether the input based plot is desired. If this field is zero, the plot is desired. The plot is identified by a time value of -1000. The plot can be produced even if the output processors are run after the input processors without the intermediate execution of the Dynamics Solution Processor.

Fields 1, 7, 8, and 9 of Card 1501 control the production of the time series of plots. Field 1 is the number of plots to be produced from computed information. This value may not exceed 27. Field 7 is a switch which when set zero causes the time points at which plots are to be produced to be read from up to three 1502 cards. These time points are specified using all nine fields of the 1502 cards in the order in which they occur in the input deck. These time points must appear as an ascending sequence.

If field 7 of Card 1501 is non-zero, plots at equal increments are desired and are controlled by fields 8 and 9. Field 8 is the first time at which a plot is desired, and field nine is the time increment between plots. If field 9 is zero, all recorded plots are desired.

Whichever way desired plot times are specified, it may come about that plotting is desired for a time at which no plotting information was recorded. If this condition arises, a plot is produced at the closest recorded time unless a plot has already been produced at that time, in which case the plot is inhibited.

12.11 End of Output Processor Data Deck

The 1600-Card marks the end of the data deck for the Output Pre-Processor in the same way that the 1000-Card marks the end of the data for the Input Pre-Processor.

12.12 Example Input Cards

Figure 12-14 contains examples of the cards discussed in this module. Cards 104 and 105 show the completed debug cards for the example given in Figure 12-4. Belt angles, joint absorbed energy, body kinetic energy, and femur and tibia quantity output are all inhibited. The default order of output pages is explicitly written out on the 1001 and 1002-Cards. The joint test is used to analyze when the upper

6/28/79

joint stop comes on. Head frontal acceleration is tested for magnitude exceeding fortyg's. Filtered head resultant acceleration is compared against filtered chest resultant acceleration. The printer plot cards are those used to produce Figure 12-12.

MAIN TITLE FOR RUN									100	
1.	1.	32.174	0.	0.	180.	1.	5.	10.	101	
2.	0.	0.	0.	1.	1.	10.	.000001	5.	102	
0.	14AF2B355.		00000F0159.		00000000103.		555555551.		104	
157.	FFFFFFFFE159.		00000000162.		54100000164.		FFFFFFFFF0.		105	
0.	0.	0.	0.	1.	0.	0.	0.	0.	107	
0.	0.	0.	0.	0.	0.	1.	1.	0.	108	
										109
										110
0.	0.	0.	1.	0.	0.	0.	0.	0.	111	
2.75	7.	0.	0.	0.	1.8	-1.96	14.12	-5.07	218	
										1000
0,1,46-48,10-14,21,22,37,5,38,49,50,15,23-26,2-4,18-20,33-36,30-32,16,									1001	
27-29,39,17,40,6,9,45									1002	
0.	0.	0.	11.55	.025						1003
40.	500.	560.	0.	.85	181.	5.	5.	1004		
-8.	-25.2									1102
40.									1200	
7.	3.									1400
7.	6.									1401
0.	0.	0.	64.	1.	-40.	10.	0.	1500		
19.	0.	0.	1.	1.	0.	1.	0.	10.	1501	
										1600

FIGURE 12-14 Example Data Cards

MODULE 13 -- EXAMPLE CRASH SIMULATIONS

The purpose of this module is to give the user of the Tutorial System a "hands-on" feeling for input data sets required for exercising the MVMA 2-D Crash Victim Simulator and for the output which is generated. Data decks are described and assembled in this module for the following two simulations:

1. a 30-mph frontal barrier crash with vehicle interior deformation and a dummy passenger restrained only by a knee bar; and,
2. a crash with similar occupant and vehicle configurations except that the occupant is restrained additionally by a torso harness.

13.1 Introduction

It is normally convenient to construct a data set card by card, beginning with Card 100 and proceeding through Card 1600. However, a complete data set can also be viewed as a collection of subsets which may be dealt with individually. In this module, discussion of the construction of data sets is in terms of eighteen largely independent subsets. These are identified in Figure 13-1. Data subsets developed for one simulation can be assembled with subsets developed for other simulations to yield a complete data deck for a new simulation. As long as the user keeps in mind and takes account of the various dependencies between some of the subsets, a completely satisfactory composite data deck will result.

13.2 Input Data for Example 1

The first example to be considered is simulation of a 30-mph frontal barrier crash with a dummy passenger restrained only by a knee bar. The frontal portion of the vehicle interior displaces toward the occupant. Figure 13-2 is a schematic of the occupant and vehicle interior configuration at crash onset. The following sections (13.2.1 through 13.2.11) discuss the construction of the data set for Example 1, which is shown in its entirety in Figure 13-14.

Arbitrary Decomposition of MVMA 2-D Data Set Into Subsets

DATA SUBSET	CARD NUMBERS
Title Cards	100, 200, ..., 900
General Controls for IN and GO	101, 102, 103
Debugging Printout Controls	104, 105
Categories of Output Variables to be Stored	107 - 111
Vehicle Motion	601 - 604
Occupant Description	201 - 242
Occupant Position	217, 301-304
Vehicle Interior	401 - 411
Friction Characteristics	412
Allowed or Disallowed Contact Interactions	106
Belt Restraint System	218, 501, 701-723
Airbag Restraint System	901 - 909
End of Data Deck for INP	1000
Categories of Output Variables to be Printed	1001, 1002
HIC, Femur Loads, and Filtering	1003, 1004
Potential Injury Indicators	1100 - 1401
Printer-Plot Stick Figure Time Sequence	1500 - 1502
End of Data Deck for OUTP	1600

FIGURE 13-1 Arbitrary Decomposition of MVMA 2-D Data Set Into Subsets

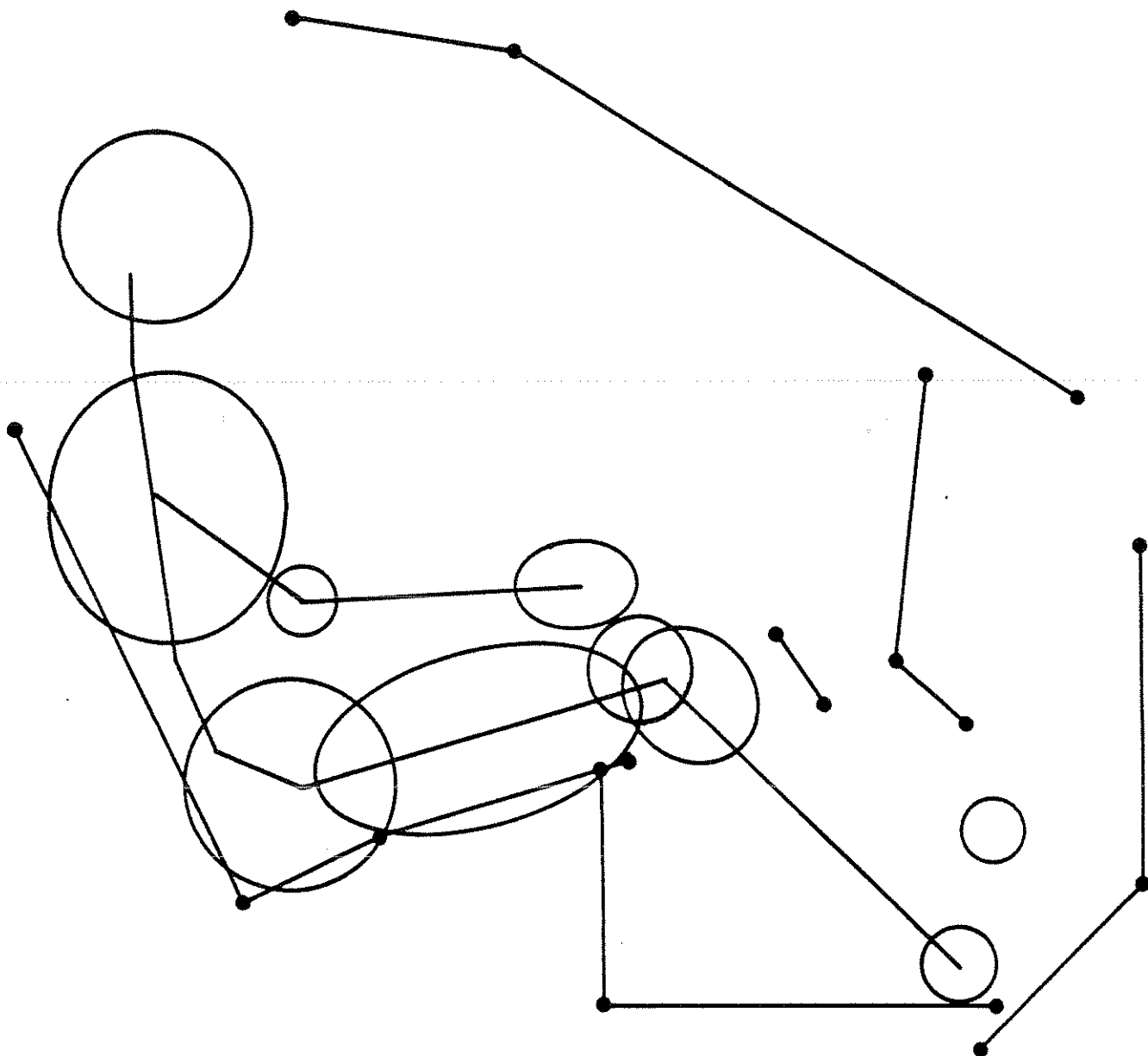


FIGURE 13-2 Occupant and Vehicle Interior Configuration for Example 1

13.2.1 Title Cards. Each page of output for a simulation is headed by titles which may be supplied on Cards 100, 200, 300, ..., 900. These cards are discussed in Module 12. The 100-Card is for a "run title," which should be centered in the first 72 columns and which will appear on the first line of each page of printout. (See Figure 13-3). The second line of page heading consists of the concatenated content of Cards 200, 300, ..., 900. Each of these cards is normally used for description of a specific simulation characteristic. For example, as indicated in Volume 2 of the MVMA 2-D report, the 700-Card normally describes the type of belt restraint system used. However, there are no restrictions on the content of these cards. The 19-column sub-title fields of Cards 200, 300, ..., 700 plus the 17-column field of either Card 800 or Card 900 (only one may be used) can be used together for any 131-character description of the simulation.

The title cards for Example 1 have been grouped together at the beginning of the data set except for the 200- and 300-cards, which have both been used for occupant description and are placed with the occupant data cards (see Figure 13-7). It might be again noted, as explained in Module 1, that data cards can be positioned within the data deck in any order, without attention to card identification number. Exceptions to this are the 1000- and 1600-cards, which serve as "end-of-data-deck" markers and must be the last cards of the data decks for the Input and Output Pre-processors, respectively.

13.2.2 General Controls for IN and GO. A number of general controls are required for the operation of the Input (IN) and Execution (GO) Processors. These are on Cards 101, 102, and 103, which are discussed in Modules 4, 5, 6, 9, 10, and 12.* Some of the most important of these controls specify: 1) the system of units (metric or English) for the simulation; 2) crash duration, integration time step, and time increment for printing of output; 3) use or non-use of the various restraint system options; 4) interpretation of "inhibition cards" for allowed or disallowed contact interactions; and 5) limits for the algorithm which

*The user is referred to Figure 1-26 of Module 1 for aid in finding discussion in Modules 2 through 12 of the parameter in any data card field.

	MVMA 2-D TUTORIAL EXAMPLE #1	100
KNEE BAR		400
JCC. COMP. DISPL.		500
30MPH FRONT BARRIER		600
NO BELTS		700

FIGURE 13-3 Title Cards for Example 1

1.	1.	32.174	0.	0.	200.	1.	5.	10.	101
0.	0.	0.	0.	0.	0.	10.	.000001	5.	102
.2	.05	100000.	15000.	10.	.05	10.	1.	1.	103

FIGURE 13-4 General Controls for IN and GO for Example 1

determines shared-deflection force balance. Simulation Examples 1 and 2 of this module are both for 200 msec duration, one msec integration time step, and five msec printout interval. The simulations are made with English system data. Figure 13-4 shows Cards 101 through 103.

13.2.3 Vehicle Motion. The vehicle motion, or more precisely, occupant compartment motion, is described with Cards 601 through 604. This prescription of the "crash history" is the subject of Module 8. Cards for the 30-mph frontal barrier crash of Example 1 are shown in Figure 13-5. Initial position and velocity values for vehicle horizontal, vertical, and pitch coordinates are on Card 601, together with two coordinates for an accelerometer location. The remaining cards specify acceleration histories for the three vehicle degrees of freedom.

The horizontal motion for this example, illustrated by the acceleration profile in Figure 13-6, is defined by twenty-three time-acceleration points on cards following the 602-card. The crash represented is for an impact velocity of 30 mph, a ΔV of 32.83 mph, 33.9 g's peak acceleration, and a stopping distance (or "crush") of 21.8 inches.

13.2.4 Occupant Description. Most of the Cards 201 through 242 are used for prescribing occupant parameters. Cards 201 through 216 plus 227 through 242 describe mass and moment of inertia properties for the body links, link lengths, and joint properties.* Cards 219 and 220 define ellipses which represent the contact-sensing profile of the body. Loading and unloading characteristics of body materials are prescribed on Cards 221 through 226.** The data in Figure 13-7 are preliminary data compiled by HSRI from several sources for a GM Hybrid II dummy. Toe and heel ellipses have been positioned for a foot in a flexed configuration since the MVMA 2-D model does not include an articulation at the ankle joint.

Values pertinent to initial joint torques are on Card 217 (see Section 13.2.5). Head and chest accelerometers are located by values on the 218-Card (see Figure 13-27).

* Much larger threshold velocities (field 6, Cards 205-216) should have been used. See Figure 2-11.

** See Modules 2, 3, 4, and 6 for discussion of occupant parameters.

0.	44.	0.	0.	0.	0.	0.	0.	501
23.	1.	1.						602
0.	-1.7	1.	-1.4	7.	-33.9	12.	2.8	
13.5	3.9	18.	-21.2	21.5	-12.4	28.	-9.2	
32.	-24.0	33.	-24.0	36.	-9.9	37.	-9.9	
42.	-26.9	47.	-31.8	50.	-25.9	54.	-27.2	
58.	-32.2	61.	-29.0	76.	-6.9	90.	-1.4	
100.	-1.4	120.	0.	300.	0.			
2.	1.	1.						603
0.	0.	300.	0.					
2.	1.							504
0.	0.	300.	0.					

FIGURE 13-5 Vehicle Motion Cards for Example 1

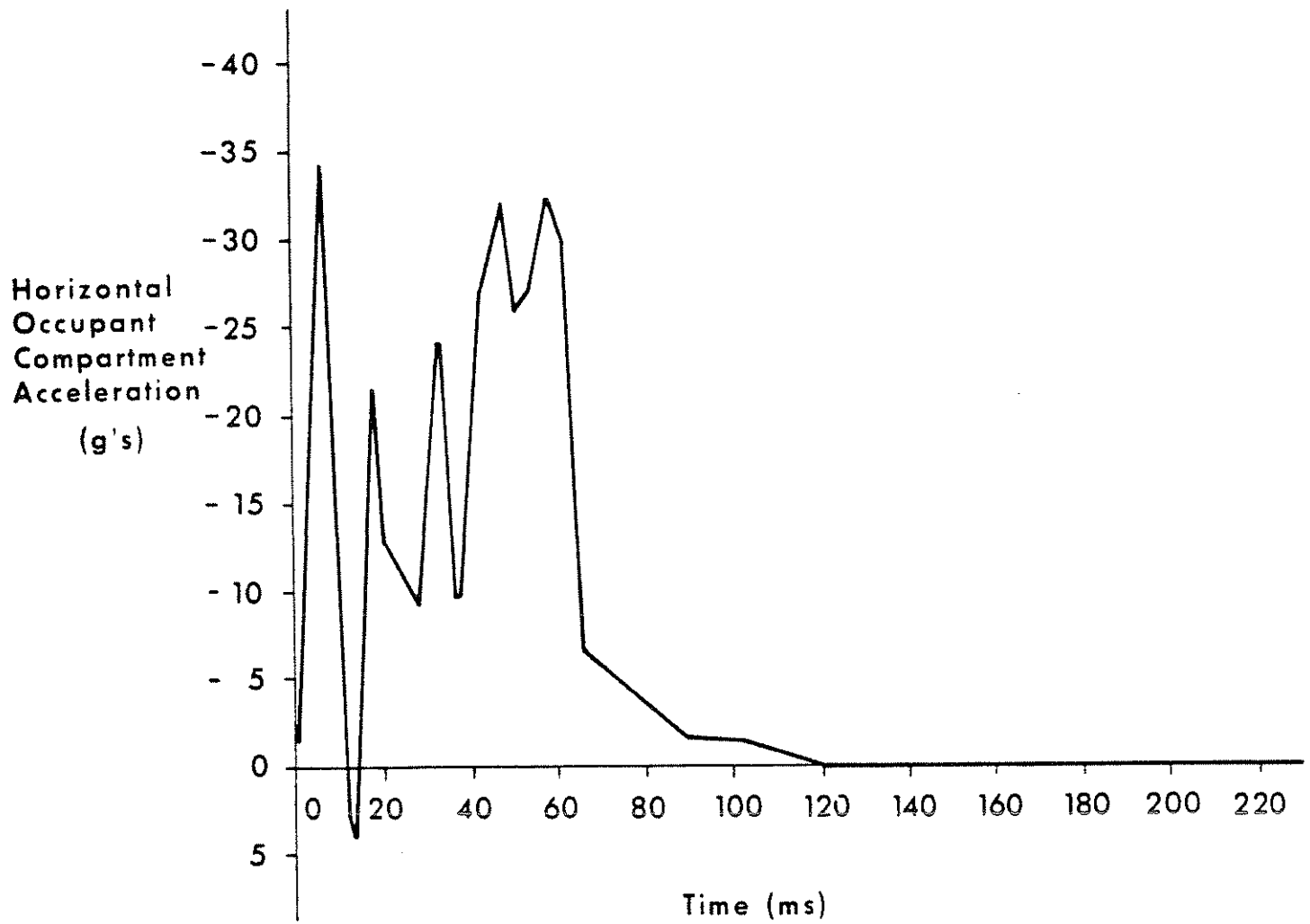


FIGURE 13-6 Horizontal Component of Vehicle Acceleration for Example i

GM HYBRID II DUMMY									200
(PRELIMINARY DATA)									300
1.1	13.44	3.4	5.	15.8		10.3	3.25	-.88	201
2.75	7.	1.7	4.2	8.2	9.3	5.	5.8	.5	202
.0259	.0951	.0052	.0992	.0932	.0518	.022	.0256	.007	203
.108	1.97	.04	1.53	1.38	2.82	.18	.62		204
12.8	.58	0.	.52	17.4	1.		-25.	.35	205
12.9	.58	0.	.52	17.4	1.		-22.	.35	206
72.	15.	0.	.66	1000.	1.	-8.	-25.5	.35	207
102.5	-7.624	.1944	.66	1000.	1.	-33.999	-34.001	.35	208
84.44	-4.810	.1053	0.	850.	1.	-49.999	-50.001	.5	209
0.	29.8	0.	0.	204.	1.	135.	0.	.5	210
0.	10.	0.	0.	222.	1.	28.	-197.	.5	211
0.	10.	0.	0.	64.	1.	0.	-165.	.5	212
751.	0.	757.	1.98						213
20.	230.	0.	0.			2.		.5	214
38.	.58	0.	.52	0.	1.	-1.		.16	215
38.	.58	0.	.52	0.	1.	2.		.16	216
751.	0.	757.	1.98						242
HEAD				1.	3.				219
THORAX		CHESTMATL		2.	1.				219
HIP		HIPMATL		4.	1.				219
THIGH				5.	1.				219
KNEE				5.	1.				219
SHANK				6.	1.				219
HEEL				6.	2.				219
TOE				6.	2.				219
ELBOW				7.	1.				219
HAND				8.	3.				219
HEAD	0.	.5	.5	4.	4.				220
THORAX	-.5	-.68	5.52	4.44					220
HIP	-.12	0.	4.5	4.5					220
THIGH	-.5	-.1	7.	3.					220
KNEE	7.	-.4	2.25	2.25					220
SHANK	-7.54	0.	3.	2.4					220
HEEL	8.57	0.	1.2	1.2					220
TOE	5.61	-5.16	1.2	1.2					220
ELBOW	5.3	0.	1.5	1.5					220
HAND	5.6	-.4	2.72	1.52					220
CHESTMATL	0.	0.	0.	100.	101.	0.	0.		221
CHESTMATL	5.				CSTAT	IZERO	CGR		222
CGR	-1.	.1							223
CGR	0.	1.							224
CGR	.01	.64							224
CGR	.3	.5							224
CGR	1.35	.45							224
CSTAT	0.	0.							225
CSTAT	.01	1125.							225
CSTAT	.05	1460.							225
CSTAT	.3	1350.							225
CSTAT	.4	1260.							225
CSTAT	1.1	1260.							225
CSTAT	4.25	12600.							225
IZERO	-1.	0.							226
HIPMATL	0.	0.	0.	100.	101.	0.	0.		221
HIPMATL	5.				CSTAT	IZERO	CGR		222

FIGURE 13-7 Occupant Parameter Cards for Example 1

13.2.5 Occupant Position. The seated occupant at "time zero" for Example 1 is shown in Figure 13-2. Data are required for initial positioning of the occupant. In addition, a value is needed for the initial velocity for each occupant degree of freedom (see Module 7). As the occupant for Example 1 is initially at rest within the occupant compartment, which is normally the case for crash simulations, these initial velocities -- fourteen fields of Cards 302, 303, and 304 -- are all 0. in the data of Figure 13-8.

The initial position data are on Cards 217, 301, 303, and 304. First, initial position values are required for the fourteen occupant degrees of freedom. These are the initial link angles (301), neck length (303), shoulder position (304), and horizontal and vertical locations within the occupant compartment of the upper torso center of gravity (303). For the two example simulations, initial link angles and upper torso CG location were estimated from scale drawings of the "time zero" occupant and vehicle-interior configurations, so the values in Figure 13-8 produce only approximate initial occupant equilibrium. The resulting total initial upward force on the occupant, for example, is 207.1 lb, which does not equal the occupant weight, 163.7 lb. The initial imbalance is not great enough to significantly affect the simulation results.

Values on Card 217 are for the so-called "joint equilibrium angles." The values in the example data have been selected to equal initial relative joint angles, which may be determined by subtracting link angles on Card 301. As explained in Module 2, this results in zero initial values for the linear components of joint torques.

13.2.6 Vehicle Interior. A vehicle interior with which the occupant is to interact must be prescribed by the user. Two types of data are required. The first of these describes the geometrical profile of the interior in the plane of occupant motion. (See Module 5.) The primary elements of this description are the endpoint coordinates of line segments which comprise so-called vehicle-interior "regions," a "region" being a set of connected straight-line segments having the same material properties. Figure 13-9 shows the vehicle interior profile defined for Example 1. Region and segment names are indicated,

-11.	-8.	-18.	-34.	-50.	0.	0.	0.		217
78.5	97.5	115.5	149.5	19.5	-45.	-41.	3.	89.5	301
0.	0.	0.	0.	0.	0.	0.	0.	0.	302
12.2	0.	-21.4	0.	3.28	0.				303
0.	0.	0.	0.						304

FIGURE 13-8 Occupant Position Cards for Example 1

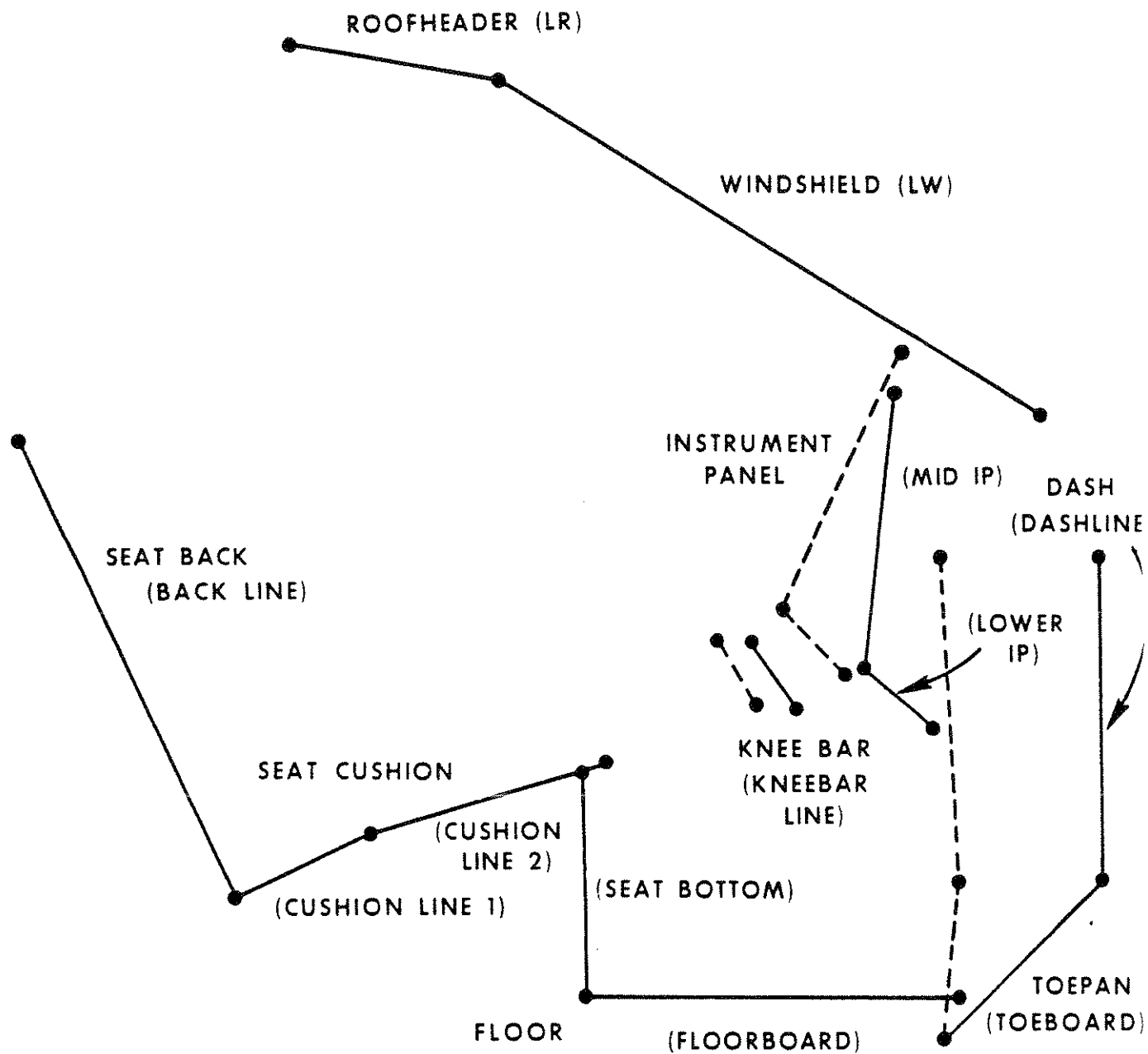


FIGURE 13-9 Vehicle Interior Profile for Example 1

segment names in parentheses. Solid lines indicate positions of line segments before frontal interior penetration into the occupant compartment, which begins at 40 ms. All penetration occurs between 40 and 80 ms, and the dashed lines represent the deformed vehicle interior. Note that the toeboard segment decreases considerably in length. There is no restriction that segment lengths be held constant while undergoing motion. Data for one of the penetrating regions of the vehicle interior, the INSTRUMENT PANEL region, are illustrated in Figure 13-10. The INSTRUMENT PANEL profile is defined entirely by Cards 401, 402, 409, 410, and 411.

The second type of data required for the vehicle interior describes material characteristics, i.e., loading and unloading properties of regions of the defined profile. Data are on Cards 403 through 408. With regard to material specifications in Figure 13-10 for the INSTRUMENT PANEL, there are two points worthy of note. First, the use of the name IZERO on Card 404 for the inertial spike curve illustrates that curve names may be shared by materials; no inertial spike data (Card 408) appear here for material IPMAT since the inertial spike curve IZERO is defined elsewhere in the data set for a different material (see Card 226 in Figure 13-7). It is also allowable to specify the same material name for different regions or ellipses while defining the material properties only once within the data set. Second, the dependence of the R-ratio (for energy restitution) on maximum deformation is indicated on the 406-Cards and has been established to be compatible with the G-ratio (for permanent deformation) on Cards 405 and the loading curve from Cards 407. This is important to guarantee proper unloading behavior for the material. Determination of G- and R-ratio compatibility is described in Module 6, Part 2 (see Figure 6-28).

13.2.7 Friction Characteristics. Frictional forces between the occupant and elements of the vehicle interior can be large enough to have a considerable effect on the magnitude and direction of the resultant force vector at the interaction interface. It is therefore important in simulations to account for frictional forces accurately. The user of the MVMA 2-D model assigns each body ellipse and each vehicle interior region to a "friction class;" this is done with entries on Cards 219 and 402. Coefficients of friction are specified

INSTRUMENT PANEL	IPMAT	0.	1.	1.	1.	401
INSTRUMENT PANEL	2.	4.	1.	0.	0.	402
MID IP	INSTRUMENT PANEL	5.	0.	1.	1.	409
MID IP	4.					410
MID IP	0.	44.9	-27.3	43.7	-15.9	411
MID IP	40.	44.9	-27.3	43.7	-15.9	411
MID IP	80.	45.6	-29.3	40.6	-18.9	411
MID IP	300.	45.6	-29.3	40.6	-18.9	411
LOWER IP	INSTRUMENT PANEL	5.	.5	1.	2.	409
LOWER IP	4.					410
LOWER IP	0.	43.7	-15.9	46.8	-12.8	411
LOWER IP	40.	43.7	-15.9	46.8	-12.8	411
LOWER IP	80.	40.6	-18.9	42.6	-14.9	411
LOWER IP	300.	40.6	-18.9	42.6	-14.9	411

IPMAT	0.	0.	0.	100.	101.	0.	0.	403
IPMAT	5.	0.	0.	0.	IPSTAT	IZERO	IPGR	404
IPGR	0.	0.						405
IPGR	2.	.75						405
IPGR	40.	.75						405
IPGR	0.	1.						406
IPGR	1.	.25						406
IPGR	2.	.1						406
IPGR	8.	.1						406
IPGR	8.4	.15						406
IPSTAT	0.	0.						407
IPSTAT	.165	80.						407
IPSTAT	.375	480.						407
IPSTAT	.665	750.						407
IPSTAT	.780	760.						407
IPSTAT	1.25	500.						407
IPSTAT	1.75	580.						407
IPSTAT	2.54	225.						407
IPSTAT	2.87	255.						407
IPSTAT	3.44	300.						407
IPSTAT	4.54	380.						407
IPSTAT	4.63	250.						407
IPSTAT	8.	250.						407
IPSTAT	12.	3850.						407

FIGURE 13-10 Data Cards for Definition of Geometrical Profile and Material Properties for a Typical Region

on 412-Cards for combinations of ellipse and region friction classes. Figure 13-11 shows the 412-Cards in the data set for Example 1. There is one card for each pairing of friction classes represented in the set of contact interactions which can occur in this simulation. For any simulation, coefficients of friction will default to 0. for any pairing not represented by a 412-card. Note that the first data card in Figure 13-11 includes coefficients for tangential forces proportional to the first and second powers of deflection, as explained in Module 6-2. For this example, the values represent plowing resistance to relative motion between the SEAT CUSHION and SEAT BACK regions and contacting body ellipses.

13.2.8 Interaction "Inhibition" Cards. Modules 4 and 5 discuss the use of 106-Cards for specification of allowed or disallowed combinations of potentially-interacting body ellipses and vehicle interior regions. "Allowed" combinations are normally specified when the number of probable interactions is less than the number of improbable interactions. This is judged to be the case for the first simulation example, so twenty-one allowed interactions have been specified between the ten body ellipses and nine vehicle-interior regions. These are shown in Figure 13-12. One card has been included for an allowed interaction between body ellipses THIGH and THORAX.

13.2.9 Belt Restraint System. Example 1 is a simulation for an unrestrained occupant. As an illustration that it is unnecessary to remove restraint system data from the data deck for such a simulation, belt system data cards are included in the complete data deck for Example 1 shown in Figure 13-14. (These are Cards 218, 501 and 701 through 709). It is necessary only to set the belt system usage switch in field 1 of Card 102 to its "off" value, zero.

13.2.10 End of Data Deck for INP. The last card in the data deck for the Input Processor, IN, must be the 1000-Card. It is blank except for the card identification number in columns 77 through 80. (See Figure 13-14.)

1.	1.	.25	.125	.125	412
1.	2.	.5			412
1.	3.	.5			412
1.	4.	.4			412
2.	2.	.8			412
3.	1.	.4			412
3.	2.	.5			412
3.	4.	.4			412
3.	5.	.67			412
3.	6.	.9			412

FIGURE 13-11 Data Cards for Coefficients of Friction for Example 1

HEAD	ROOFHEADER	106
HEAD	WINDSHIELD	106
HEAD	INSTRUMENT PANEL	106
THORAX	SEAT BACK	106
THORAX	SEAT CUSHION	106
THORAX	INSTRUMENT PANEL	106
HIP	SEAT BACK	106
HIP	SEAT CUSHION	106
HIP	FLOOR	106
THIGH	SEAT CUSHION	106
KNEE	INSTRUMENT PANEL	106
KNEE	KNEE BAR	106
SHANK	INSTRUMENT PANEL	106
SHANK	KNEE BAR	106
HEEL	FLOOR	106
HEEL	DASH	106
TOE	DASH	106
HEEL	TOEPAN	106
TOE	TOEPAN	106
HAND	SEAT CUSHION	106
HAND	INSTRUMENT PANEL	106
THIGH	THORAX	106

FIGURE 13-12 Interaction "Inhibition" Cards for Example 1

13.2.11 Output Processor Controls. Cards 1001 through 1600 constitute a separate data deck from Cards 100 through 1000, described in the preceding sections and read by the Input Pre-Processor. Cards 1001 through 1600 are read by the Output Pre-Processor. These cards control post-processing and printout of data calculated and stored by the Dynamic Solution Processor (or "Execution Processor," G0). These data and data generated by the Input Processor are stored in four external files (see Module 12); as long as the files are maintained intact, they can be processed by the Output Processor any number of times, using different control Cards 1001 through 1600.

13.2.11.1 Output Categories for Printout. The entire Output Pre-Processor data deck for Example 1 consists of seven cards. These are shown in Figure 13-13. The first two cards, 1001 and 1002, are used for specification of categories of calculated data for which printout is desired and the order of printout for these categories. The forty-five categories of results which may be printed are identified by Category Number in Figures 1-21 and 12-2 of Modules 1 and 12. The ordering for printout shown for Example 1 in Figure 13-13 is identical to the default ordering which would result if the 1001- and 1002-Cards were omitted from the data deck.* All categories are requested for Example 1. Requests for printout for categories for which no data are stored will be ignored by the Output Processor.

13.2.11.2 HIC, Femur Loads, and Filtering. Various data explained in Module 12 are required on Cards 1003 and 1004 for the post-processor functions of filtering of occupant accelerations and determination of HIC and femur loads.

13.2.11.3 Potential Injury Indicators. In addition to HIC and femur loads, other potential injury indicators can be determined and printed by the Output Processor. These are also discussed in Module 12. They are requested by using Cards 1100 through 1401, none of which are included in the data deck for Example 1.

* The default ordering minus printout of the input data summary, Category 0, can be obtained by using a 1001-Card which contains only "-1" in columns one and two.

0, 1, 46-48, 10-14, 21, 22, 37, 38, 49, 50, 15, 23-26, 2-5, 18-20, 33-36, 30-32, 16,									1001
27-29, 39, 17, 40, 6-9, 45									1002
0.	0.	0.	11.55	.025					1003
40.	500.	560.	0.	.85	201.	5.	5.		1004
0.	0.	-3.	62.	5.	-44.	10.	0.		1500
21.	0.	0.	1.	1.	0.	1.	0.	10.	1501
									1600

FIGURE 13-13 Output Processor Data Deck for Example 1

6/28/79

13.2.11.4 Printer-Plot Stick Figures. As explained in Module 12, a time sequence of printer-plot pages can be produced which depict the occupant and all lines of the vehicle interior. A control for storing data required for production of this printout is on Card 101, read by the Input Pre-Processor and shown in Figure 13-4. Controls for producing the printout are read from Cards 1500 through 1502 by the Output Pre-Processor. The most important data on these cards are margin coordinates which frame the printer-plot image within the vehicle coordinate system and the simulation times to be included in the time sequence of printouts.

13.2.11.5 End of Data Deck for OUTP. As for the Input Pre-Processor data deck, a single card is required to mark the end of the Output Pre-Processor data deck. It is Card 1600, which is blank except for the card identification number.

13.3 Selected Output from Simulation Example 1

Selected pages of printout from the MVMA 2-D Crash Victim Simulator are shown as Figures 13-15 through 13-26. Figure 13-14 contains the data cards for Example 1 which generated the simulation results shown.

The MVMA 2-D model has undergone continuous development and improvement since its inception, and it is expected that it will continue to undergo change. Consequently, numerical results in Figures 13-15 through 13-26 should not be compared with results that MVMA 2-D users might obtain by using the data set for Example 1 for simulation with their own installations of the model. Rather, these figures are to be viewed as illustrative of the format of MVMA 2-D printout.*

13.3.1 Data Set Echo. Both the Input and Output Pre-Processors always produce "echoes" of their data decks. An example page from the Input Pre-Processor "echo" for Example 1 is shown as Figure 13-15. The eight-column data fields are separated by asterisks.

13.3.2 Summary of Input Data. Figure 13-16 is an example page of printout of a summary of the input data. The entire input data summary for Example 1 is 63 pages. This printout is produced whenever category 0 is requested on the 1001-Card.

*Results in Figures 13-18.1, 13-18.2, 13-18.3, 13-22, and 13-23 are not consistent with other results since they were taken from a different simulation.

13.3.3 Printer-Plot Stick Figure Sequence. The data decks for Example 1 cause printer-plot stick figure output to be generated for each 10 ms of simulation time. Selected "frames" of the time sequence are shown as Figure 13-17.

13.3.4 Printout of Numerical Results. Nine example pages of printout of numerical results are shown in Figures 13-18 through 13-26. The definition of most output variables is clear. However, aid is provided for the user in interpreting output in a section of Volume 2 of the MVMA 2-D report entitled, "Description of Normal Output."

Only two special notes will be made here regarding output variables. First, femur and tibia loads (Figure 13-24) must be interpreted as for two legs combined. That is, values for one leg are obtained by dividing by two. Second, GMR Severity Indices are calculated for head and chest in addition to values for the standard Gadd Severity Index. The GMR index is defined in a section of Volume 3 of the MVMA 2-D report entitled, "Special Indices." It differs from Gadd index in that its calculation involves raising acceleration values to powers which vary with acceleration level rather than the constant power 2.5.

MVMA 2-D TUTORIAL EXAMPLE #1									100
KNEE BAR									400
JCC. COMP. DISPL.									500
30MPH FRONT BARRIER									600
NO BELTS									700
1.	1.	32.174	0.	0.	200.	1.	5.	13.	101
0.	0.	0.	0.	0.	0.	10.	.000001	5.	102
.2	.05	100000.	15000.	10.	.05	10.	1.	1.	103
0.	44.	0.	0.	0.	0.	0.	0.		501
23.	1.	1.							602
0.	-1.7	1.	-1.4	7.	-33.9	12.	2.8		
13.5	3.9	18.	-21.2	21.5	-12.4	28.	-9.2		
32.	-24.0	33.	-24.0	36.	-9.9	37.	-9.9		
42.	-26.9	47.	-31.8	50.	-25.9	54.	-27.2		
58.	-32.2	61.	-29.0	76.	-5.9	90.	-1.4		
100.	-1.4	120.	0.	300.	0.				
2.	1.	1.							603
0.	0.	300.	0.						
2.	1.								504
0.	0.	300.	0.						
GM HYBRID II DUMMY									200
(PRELIMINARY DATA)									300
1.1	13.44	3.4	5.	15.8		10.3	3.25	-.88	201
2.75	7.	1.7	4.2	8.2	9.3	5.	5.8	.5	202
.0759	.0951	.0052	.0992	.0932	.0518	.022	.0256	.007	203
.108	1.07	.04	1.53	1.38	2.82	.18	.62		204
12.8	.58	0.	.52	17.4	1.		-25.	.35	205
12.9	.58	0.	.52	17.4	1.		-22.	.35	206
72.	15.	0.	.66	1000.	1.	-8.	-25.5	.35	207
102.5	-7.624	.1044	.66	1000.	1.	-33.999	-34.001	.35	208
84.44	-4.810	.1053	0.	850.	1.	-49.999	-50.001	.5	209
0.	29.8	0.	0.	204.	1.	135.	0.	.5	210
0.	10.	0.	0.	222.	1.	28.	-197.	.5	211
0.	10.	0.	0.	64.	1.	0.	-165.	.5	212
751.	0.	757.	1.98						213
20.	230.	0.	0.			2.		.5	214
38.	.58	0.	.52	0.	1.	-1.		.16	215
38.	.58	0.	.52	0.	1.	2.		.16	216
751.	0.	757.	1.98						242
HEAD									219
THORAX									219
CHESTMATL									219
HIP									219
HIPMATL									219
THIGH									219
KNEE									219
SHANK									219
HEEL									219
TOE									219
ELBOW									219
HAND									219
HEAD									220
THORAX									220
HIP									220
THIGH									220
KNEE									220
SHANK									220
HEEL									220
TOE									220
ELBOW									220
HAND									220
CHESTMATL									221

FIGURE 13-14 Complete Data Set for Simulation Example 1 (page 1 of 6)

CHESTMATL	5.					CSTAT	IZERO	CGR	222
CGR	-1.	.1							223
CGR	0.	1.							224
CGR	.01	.64							224
CGR	.3	.5							224
CGR	1.35	.45							224
CSTAT	0.	0.							225
CSTAT	.01	1125.							225
CSTAT	.05	1460.							225
CSTAT	.3	1350.							225
CSTAT	.4	1260.							225
CSTAT	1.1	1260.							225
CSTAT	4.25	12600.							225
IZERO	-1.	0.							226
HIPMATL	0.	0.	0.	100.	101.	0.	0.		221
HIPMATL	5.				CSTAT	IZERO	CGR		222
-11.	-8.	-18.	-34.	-50.	0.	0.	0.		217
78.5	97.5	115.5	149.5	19.5	-45.	-41.	3.	89.5	301
0.	0.	0.	0.	0.	0.	0.	0.	0.	302
12.2	0.	-21.4	0.	3.23	0.				303
0.	0.	0.	0.						304
SEAT BACK	SEAT MATERIAL	0.	1.	1.	1.	1.			401
SEAT BACK	1.	1.	1.	0.	0.				402
SEAT MATERIAL	0.	0.	1.6	3.5	4.	0.	0.		403
SEAT MATERIAL	5.				SSEAT	IZERO	GRSEAT		404
GRSEAT	-1.	.1							405
GRSEAT	-1.	.5							406
SSEAT	0.	0.							407
SSEAT	.8	150.							407
SSFAT	1.6	400.							407
SSEAT	3.	2000.							407
SSFAT	3.5	4000.							407
SSEAT	4.	0.							407
BACK LINE	SEAT BACK	5.	0.	-1.	1.				409
BACK LINE	1.								410
BACK LINE	-1.	6.2	-25.8	15.44	-4.96				411
SEAT CUSHION	SEAT MATERIAL	0.	1.	1.	1.				401
SEAT CUSHION	2.	1.	1.	0.	0.				402
CUSHION LINE 1	SEAT CUSHION	5.	.164	1.	1.				409
CUSHION LINE 1	1.								410
CUSHION LINE 1	-1.	15.44	-4.96	28.	-9.92				411
CUSHION LINE 2	SEAT CUSHION	5.	.5	-1.	2.				409
CUSHION LINE 2	1.								410
CUSHION LINE 2	-1.	28.	-9.92	32.24	-10.64				411
FLOOR	FMATL	0.	1.	1.	1.				401
FLOOR	2.	2.	1.	0.	0.				402
SEAT BOTTOM	FLOOR	5.	0.	-1.	1.				409
SEAT BOTTOM	1.								410
SEAT BOTTOM	-1.	31.2	-8.	31.2	-.84				411
FLOORBOARD	FLOOR	5.	0.	-1.	2.				409
FLOORBOARD	1.								410
FLOORBOARD	-1.	31.2	-.84	49.	-.84				411
TOEPAN	FMATL	0.	1.	1.	1.				401
TOEPAN	1.	2.	1.	0.	0.				402
TOERBOARD	TOEPAN	5.	0.	1.	1.				409
TOERBOARD	4.								410
TOERBOARD	0.	47.3	1.1	54.7	-5.6				411
TOERBOARD	40.	47.3	1.1	54.7	-5.6				411
TOERBOARD	80.	47.3	1.1	47.9	-5.6				411
TOERBOARD	300.	47.3	1.1	47.9	-5.6				411

FIGURE 13-14 Complete Data Set for Simulation Example 1 (page 2 of 6)

KNEE BAR	SHEET METAL	0.	1.	1.	1.		401
KNEE BAR	1.	3.	1.	0.	0.		402
SHEET METAL	0.	0.	.5	8.	9.	10000.	403
SHEET METAL	5.				SSHEET	1ZERO	404
GRSHEET 0.	0.					GRSHEET	405
GRSHEET 0.5	0.						405
GRSHEET 5.5	0.9						405
GRSHEET 0.	1.						406
GRSHEET .5	1.						406
GRSHEET 2.	.7						406
GRSHEET 4.	.2						406
GRSHEET 5.5	.15						406
GRSHEET 8.	.1						406
GRSHEET 9.	.01						406
SSHEET 0.	0.						407
SSHEET 2.	1500.						407
SSHEET 4.	1500.						407
SSHEET 5.5	10000.						407
SSHEET 8.	10000.						407
SSHEET 9.	0.						407
KNEEBAR LINE	KNEE BAR	5.	0.5	1.	1.		409
KNEEBAR LINE	4.						410
KNEEBAR LINE	0.	40.4	-13.2	38.9	-16.4		411
KNEEBAR LINE	60.	40.4	-13.2	38.9	-16.4		411
KNEEBAR LINE	80.	38.9	-13.2	37.4	-16.4		411
KNEEBAR LINE	300.	38.9	-13.2	37.4	-16.4		411
ROOFHEADER	RMATL	0.	1.	1.	1.		401
ROOFHEADER	1.	6.	1.	0.	0.		402
LR	ROOFHEADER	5.	0.	1.	1.		409
LR	1.						410
LR	-1.	18.2	-43.4	28.0	-41.7		411
WINDSHIELD	WINDSHIELD GLASS	0.	1.	1.	1.		401
WINDSHIELD	1.	5.	1.	0.	0.		402
LW	WINDSHIELD	5.	0.	1.	1.		409
LW	1.						410
LW	-1.	27.8	-41.3	51.6	-26.3		411
INSTRUMENT PANEL	INSTRUMENT PANEL	0.	1.	1.	1.		401
INSTRUMENT PANEL	2.	4.	1.	0.	0.		402
MID IP	INSTRUMENT PANEL	5.	0.	1.	1.		409
MID IP	4.						410
MID IP	0.	44.9	-27.3	43.7	-15.9		411
MID IP	40.	44.9	-27.3	43.7	-15.9		411
MID IP	80.	45.6	-29.3	40.6	-18.9		411
MID IP	300.	45.6	-29.3	40.6	-18.9		411
LOWER IP	INSTRUMENT PANEL	5.	.5	1.	2.		409
LOWER IP	4.						410
LOWER IP	0.	43.7	-15.9	46.8	-12.8		411
LOWER IP	40.	43.7	-15.9	46.8	-12.8		411
LOWER IP	80.	40.6	-18.9	42.6	-14.9		411
LOWER IP	300.	40.6	-18.9	42.6	-14.9		411
DASH	DASHMATL	0.	1.	1.	1.		401
DASH	1.	2.	1.	0.	0.		402
DASHLINE	DASH	5.	0.	1.	1.		409
DASHLINE	4.						410
DASHLINE	0.	54.7	-5.6	54.2	-20.1		411
DASHLINE	40.	54.7	-5.6	54.2	-20.1		411
DASHLINE	80.	47.9	-5.6	47.4	-20.1		411
DASHLINE	300.	47.9	-5.6	47.4	-20.1		411
DASHMATL	0.	0.	0.	100.	101.	0.	403
DASHMATL	5.				DSTAT	1ZERO	404
						OGR	

FIGURE 13-14 Complete Data Set for Simulation Example 1 (page 3 of 6)

DGR	0.	0.							405
DGR	.001	.01							405
DGP	10.	.01							405
DGR	0.	1.							406
DGR	.001	.91							406
DGR	.75	.8							406
DGR	1.5	.5							406
DGR	10.	.3							406
DSTAT	0.	0.							407
DSTAT	0.75	2100.							407
DSTAT	1.5	9000.							407
DSTAT	40.	9000.							407
RMATL		0.	0.	0.	100.	101.	0.	0.	403
RMATL		5.	0.	0.	0.	RSTAT	IZERO	DGR	404
RSTAT	-1.	1200.	-65.36	67.38	-29.36	4.78			407
WINDSHIELD GLASS	.5	1.	0.	0.	100.	101.	0.	0.	403
WINDSHIELD GLASS	.5	0.	0.	0.	0.	WSTAT	WI	WGR	404
WGR	0.	0.							405
WGR	.5	0.							405
WGR	.51	.65							405
WGR	1.	.75							405
WGR	6.	.8							405
WGR	0.	1.							406
WGR	.5	1.							406
WGR	.51	.1							406
WGR	1.	.05							406
WGR	6.	.01							406
WSTAT	-1.	108.8	50.0	-10.9	1.				407
WI	-1.	3000.	1000.	-8000.	4000.				408
IPMAT		0.	0.	0.	100.	101.	0.	0.	403
IPMAT		5.	0.	0.	0.	IPSTAT	IZERO	IPGR	404
IPGR	0.	0.							405
IPGR	2.	.75							405
IPGR	40.	.75							405
IPGR	0.	1.							406
IPGR	1.	.25							406
IPGR	2.	.1							406
IPGR	8.	.1							406
IPGR	8.4	.15							406
IPSTAT	0.	0.							407
IPSTAT	.165	80.							407
IPSTAT	.375	480.							407
IPSTAT	.665	750.							407
IPSTAT	.780	760.							407
IPSTAT	1.25	500.							407
IPSTAT	1.75	580.							407
IPSTAT	2.54	225.							407
IPSTAT	2.87	255.							407
IPSTAT	3.44	300.							407
IPSTAT	4.54	380.							407
IPSTAT	4.63	250.							407
IPSTAT	8.	250.							407
IPSTAT	12.	3850.							407
FMATL		0.	0.	0.	100.	101.	0.	0.	403
FMATL		5.	0.	0.	0.	FSTAT	IZERO	FGR	404
FGR	0.	0.							405
FGR	2.	.7							405
FGR	0.	1.							406
FGR	2.	.2							406
FSTAT	0.	0.							407

FIGURE 13-14 Complete Data Set for Simulation Example 1 (page 4 of 6)

FSTAT	.25	100.								407
FSTAT	.5	400.								407
FSTAT	.75	1200.								407
FSTAT	1.	2400.								407
FSTAT	1.5	4000.								407
FSTAT	2.	4600.								407
FSTAT	3.	5000.								407
FSTAT	4.	5200.								407
FSTAT	6.	5400.								407
FSTAT	10.	5600.								407
FSTAT	16.	10000.								407
1.	1.	.25	.125	.125						412
1.	2.	.5								412
1.	3.	.5								412
1.	4.	.4								412
2.	2.	.8								412
3.	1.	.4								412
3.	2.	.5								412
3.	4.	.4								412
3.	5.	.67								412
3.	6.	.9								412
HEAD		POOFHEADER								106
HEAD		WINDSHIELD								106
HEAD		INSTRUMENT PANEL								106
THORAX		SEAT BACK								106
THORAX		SEAT CUSHION								106
THORAX		INSTRUMENT PANEL								106
HIP		SEAT BACK								106
HIP		SEAT CUSHION								106
HIP		FLOOR								106
THIGH		SEAT CUSHION								106
KNEE		INSTRUMENT PANEL								106
KNEE		KNEE BAR								106
SHANK		INSTRUMENT PANEL								106
SHANK		KNEE BAR								106
HEEL		FLOOR								106
HEEL		DASH								106
TOE		DASH								106
HEEL		TOEPAN								106
TOE		TOEPAN								106
HAND		SEAT CUSHION								106
HAND		INSTRUMENT PANEL								106
THIGH		THORAX								106
2.75	7.	0.	0.	0.	1.9	-1.96	14.12	-5.07		218
0.	0.	0.	0.	0.	-33.52	17.	-1.2			501
100.	0.	15.13	-.00178	6600.	6600.	10.				701
NO STRENGTH				14.04	-.00172	2.	1.			702
6% WEARING #1				6% WEARING #2						703
6% WEARING #1	0.	0.	0.16	14.36	15.04	0.	0.			704
6% WEARING #1	5.				SBELT1	IZERO	GBELT1			705
GBELT1	0.	0.								706
GBELT1	.16	0.								706
GBELT1	1.37	.56								706
GBELT1	6.15	.95								706
GBELT1	40.	.95								706
GBELT1	0.	1.								707
GBELT1	1.37	.33								707
GBELT1	2.06	.19								707
GBELT1	6.15	.05								707
GBELT1	40.	.05								707

FIGURE 13-14 Complete Data Set for Simulation Example 1 (page 5 of 6)

SBELT1	0.	0.							709
SREL1	.533	1500.							708
SREL1	9.91	2000.							708
SREL1	11.28	5300.							708
SREL1	14.36	6600.							708
SBELT1	15.04	0.							708
6% WEARING #2	0.	0.	.155	13.85	14.51	0.	0.		704
6% WEARING #2	5.				SBELT2	IZERO	GBELT1		705
SREL2	0.	0.							708
SREL2	.396	1150.							708
SREL2	9.56	1650.							708
SREL2	10.9	5300.							708
SBELT2	13.85	6600.							708
SREL2	14.51	0.							708
NO STRENGTH	0.	0.	0.	10.	11.	0.	0.		704
NO STRENGTH	5.				SNOSTR	IZERO	GNOSTR		705
GNOSTR	-1.	0.							706
GNOSTR	-1.	1.							707
SNOSTR	-1.	0.							708
									1000
0, 1, 46-48, 10-14, 21, 22, 37, 38, 49, 50, 15, 23-26, 2-5, 18-20, 33-36, 30-32, 16,									1001
27-29, 39, 17, 40, 6-9, 45									1002
0.	0.	0.	11.55	.025					1003
40.	500.	560.	0.	.85	201.	5.	5.		1004
0.	0.	-3.	62.	5.	-44.	10.	0.		1500
21.	0.	0.	1.	1.	0.	1.	0.	10.	1501
									1600

FIGURE 13-14 Complete Data Set for Simulation Example 1 (page 6 of 6)

```

1 100 *      *      *      MVH*A 2-D TU*TORIAL E*XAMPLE #*1      *      *      *
2 400 *      KNEE *BAR      *      *      *      *      *      *      *
3 500 *OCC. COM*P. DISPL*      *      *      *      *      *      *      *
4 600 *30MPH PR*ONT BARR*IER      *      *      *      *      *      *      *
5 700 *      NO B*ELTS      *      *      *      *      *      *      *
6 101 *1.      *1.      *32.174 *0.      *0.      *200.      *1.      *5.      *10.      *
7 102 *0.      *0.      *0.      *0.      *0.      *0.      *10.      *.000001 *5.      *
8 103 *.2      *.05      *100000. *15000. *10.      *.05      *10.      *.1.      *.1.      *
9 601 *0.      *.44.      *0.      *0.      *0.      *0.      *0.      *0.      *
10 602 *23.      *1.      *1.      *      *      *      *      *      *
11      *      0.0 *      -1.70*      1.00*      -1.40*      7.00*      -33.90*      12.00*      2.80*      0.0 *
12      *      13.50*      3.90*      18.00*      -21.20*      21.50*      -12.40*      28.00*      -9.20*      0.0 *
13      *      32.00*      -24.00*      33.00*      -24.00*      36.00*      -9.90*      37.00*      -9.90*      0.0 *
14      *      42.00*      -26.90*      47.00*      -31.80*      50.00*      -25.90*      54.00*      -27.20*      0.0 *
15      *      58.00*      -32.20*      61.00*      -29.00*      76.00*      -6.90*      90.00*      -1.40*      0.0 *
16      *      100.00*      -1.40*      120.00*      0.0 *      300.00*      0.0 *      0.0 *      0.0 *      0.0 *
17 603 *2.      *1.      *1.      *      *      *      *      *      *      *
18      *      0.0 *      0.0 *      300.00*      0.0 *      0.0 *      0.0 *      0.0 *      0.0 *      0.0 *
19 604 *2.      *1.      *      *      *      *      *      *      *      *
20      *      0.0 *      0.0 *      300.00*      0.0 *      0.0 *      0.0 *      0.0 *      0.0 *      0.0 *
21 200 *GM HYBRI*D II DUM*MY      *      *      *      *      *      *      *
22 300 *(PRELIMI*NARY DAT*A)      *      *      *      *      *      *      *
23 201 *1.1      *13.44      *3.4      *5.      *15.8      *      *10.3      *3.25      *-1.88      *
24 202 *2.75      *7.      *1.7      *4.2      *8.2      *9.3      *5.      *5.8      *.5      *
25 203 *.0259      *.0951      *.0052      *.0982      *.0932      *.0518      *.022      *.0256      *.007      *
26 204 *.198      *1.97      *.04      *1.53      *1.38      *2.82      *.18      *.62      *      *
27 205 *12.8      *.58      *0.      *.52      *17.4      *1.      *      *-25.      *.35      *
28 206 *12.8      *.58      *0.      *.52      *17.4      *1.      *      *-22.      *.35      *
29 207 *72.      *15.      *0.      *.66      *1000.      *1.      *-8.      *-25.5      *.35      *
30 208 *102.5      *-7.624      *.1944      *.66      *1000.      *1.      *-33.999      *-34.001      *.35      *
31 209 *94.44      *-4.810      *.1053      *0.      *850.      *1.      *-49.999      *-50.001      *.5      *
32 210 *0.      *29.8      *0.      *0.      *204.      *1.      *135.      *0.      *.5      *
33 211 *0.      *10.      *0.      *0.      *222.      *1.      *28.      *-197.      *.5      *
34 212 *0.      *10.      *0.      *0.      *64.      *1.      *0.      *-165.      *.5      *
35 213 *751.      *0.      *757.      *1.98      *      *      *      *      *      *
36 214 *20.      *230.      *0.      *0.      *      *      *2.      *      *.5      *
37 215 *38.      *.58      *0.      *.52      *0.      *1.      *-1.      *      *.16      *
38 216 *38.      *.58      *0.      *.52      *0.      *1.      *2.      *      *.16      *
39 242 *751.      *0.      *757.      *1.98      *      *      *      *      *      *
40 219 *HEAD      *      *      *1.      *3.      *      *      *      *      *
41 219 *THORAX      *      *CHESTMAT*L      *2.      *1.      *      *      *      *
42 219 *HIP      *      *HIPMATL      *4.      *1.      *      *      *      *
43 219 *THIGH      *      *      *5.      *1.      *      *      *      *
44 219 *KNEE      *      *      *5.      *1.      *      *      *      *
45 219 *SHANK      *      *      *6.      *1.      *      *      *      *
46 219 *HEEL      *      *      *6.      *2.      *      *      *      *
47 219 *TOE      *      *      *6.      *2.      *      *      *      *
48 219 *ELBOW      *      *      *7.      *1.      *      *      *      *
49 219 *HAND      *      *      *8.      *3.      *      *      *      *
50 220 *HEAD      *      *0.      *.5      *4.      *4.      *      *      *      *
51 220 *THORAX      *      *-1.5      *-1.68      *5.52      *4.44      *      *      *      *
52 220 *HIP      *      *-1.12      *0.      *4.5      *4.5      *      *      *      *
53 220 *THIGH      *      *-1.5      *-1.1      *7.      *3.      *      *      *      *
54 220 *KNEE      *      *7.      *-1.4      *2.25      *2.25      *      *      *      *
55 220 *SHANK      *      *-7.54      *0.      *3.      *2.4      *      *      *      *
56 220 *HEEL      *      *8.57      *0.      *1.2      *1.2      *      *      *      *
57 220 *TOE      *      *5.61      *-5.16      *1.2      *1.2      *      *      *      *
58 220 *ELBOW      *      *5.3      *0.      *1.5      *1.5      *      *      *      *
59 220 *HAND      *      *5.6      *-1.4      *2.72      *1.52      *      *      *      *

```

FIGURE 13-15 Input Processor Data Deck Echo for Example 1 (example page)

BODY PARAMETERS			
BODY SEGMENT LENGTHS (IN)		END OF LINK TO CENTER-OF-MASS LENGTHS (IN)	
HEAD LENGTH=	1.10	HEAD/NECK JOINT-HEAD CM LENGTH=	2.75
UPPER TORSO LENGTH=	13.44	NECK-CHEST CM LENGTH=	7.00
MIDDLE TORSO LENGTH=	3.40	UPPER TORSO JOINT-MIDDLE TORSO CM LENGTH=	1.70
LOWER TORSO LENGTH=	5.00	LOWER TORSO JOINT-LOWER TORSO CM LENGTH=	4.20
HIP-KNEE LENGTH=	15.80	UPPER TORSO JOINT-UPPER TORSO CM LENGTH=	8.20
UPPER TORSO-SHOULDER=	0.0	HIP-UPPER LEG CM LENGTH=	9.30
SHOULDER-ELBOW LENGTH=	10.30	KNEE-LOWER LEG CM LENGTH=	5.00
1 REST POINT OF SHOULDER=	3.25	SHOULDER-UPPER ARM CM LENGTH=	5.80
2 REST POINT OF SHOULDER=	-0.88	ELBOW-LOWER ARM CM LENGTH=	
MASS OF BODY SEGMENTS (LBS SEC**2 IN)			
HEAD MASS=	0.03	CHEST MASS=	0.10
MIDDLE TORSO MASS=	0.01	LOWER TORSO MASS=	0.10
UPPER LEG (BOTH LEGS)=	0.09	UPPER ARM (BOTH ARMS)=	0.02
LOWER LEG (BOTH LEGS)=	0.05	LOWER ARM (BOTH ARMS)=	0.03
UPPER TORSO-NECK MASS=	0.00	UPPER TORSO-NECK MASS=	0.00

MOMENTS OF INERTIA (ABOUT CM)		INITIAL BODY LINK ANGLES (RELATIVE TO VEHICLE)	
(LBS SEC**2 IN)	(DEG)	(RELATIVE TO VEHICLE)	(DEG/SEC)
HEAD	0.20	78.50	0.0
UPPER TORSO	1.97	97.50	0.0
MIDDLE TORSO	0.04	115.50	0.0
LOWER TORSO	1.53	149.50	0.0
UPPER LEG	1.38	19.50	0.0
LOWER LEG	2.82	-45.00	0.0
UPPER ARM	0.18	-41.00	0.0
LOWER ARM	0.62	3.00	0.0
NECK	0.0	89.50	0.0
INITIAL ANGULAR VELOCITIES (RELATIVE TO VEHICLE)			
			(DEG/SEC)

OCCUPANT JOINT PARAMETERS			
LINEAR ANGULAR DEFLECTION CORP. (IN-LBS/DEG)		QUADRATIC ANGULAR DEFLECTION CORP. (IN-LBS/DEG**2)	
HEAD-NECK FORWARD	12.80	0.58	0.0
NECK-UPPER TORSO FORWARD	12.80	0.58	0.0
UPPER SPINE	72.00	15.00	0.0
LOWER SPINE	102.50	-7.62	0.19
HIP	84.44	-4.81	0.11
KNEE	0.0	29.80	0.0
UPPER ARM-UPPER TORSO	0.0	10.00	0.0
ELBOW	0.0	10.00	0.0
HEAD-NECK REAR	38.00	0.58	0.0
NECK-UPPER TORSO REAR	38.00	0.58	0.0
NECK (EXTENSIBLE) **	751.00	0.0	757.00
SHOULDER (EXTENSIBLE) **	20.00	230.00	0.0
NECK (COMPRESSIBLE) **	751.00	0.0	757.00
CUBIC ANGULAR DEFLECTION CORP. (IN-LBS/DEG**3)			
CONSERVED-ABSORBED ENERGY RATIO			

** UNITS FOR THE NECK (EXTENSIBLE), (COMPRESSIBLE) AND SHOULDER (EXTENSIBLE) PARAMETERS ARE GIVEN IN THE ROW BELOW (LB/IN**2) (LB/IN**3)

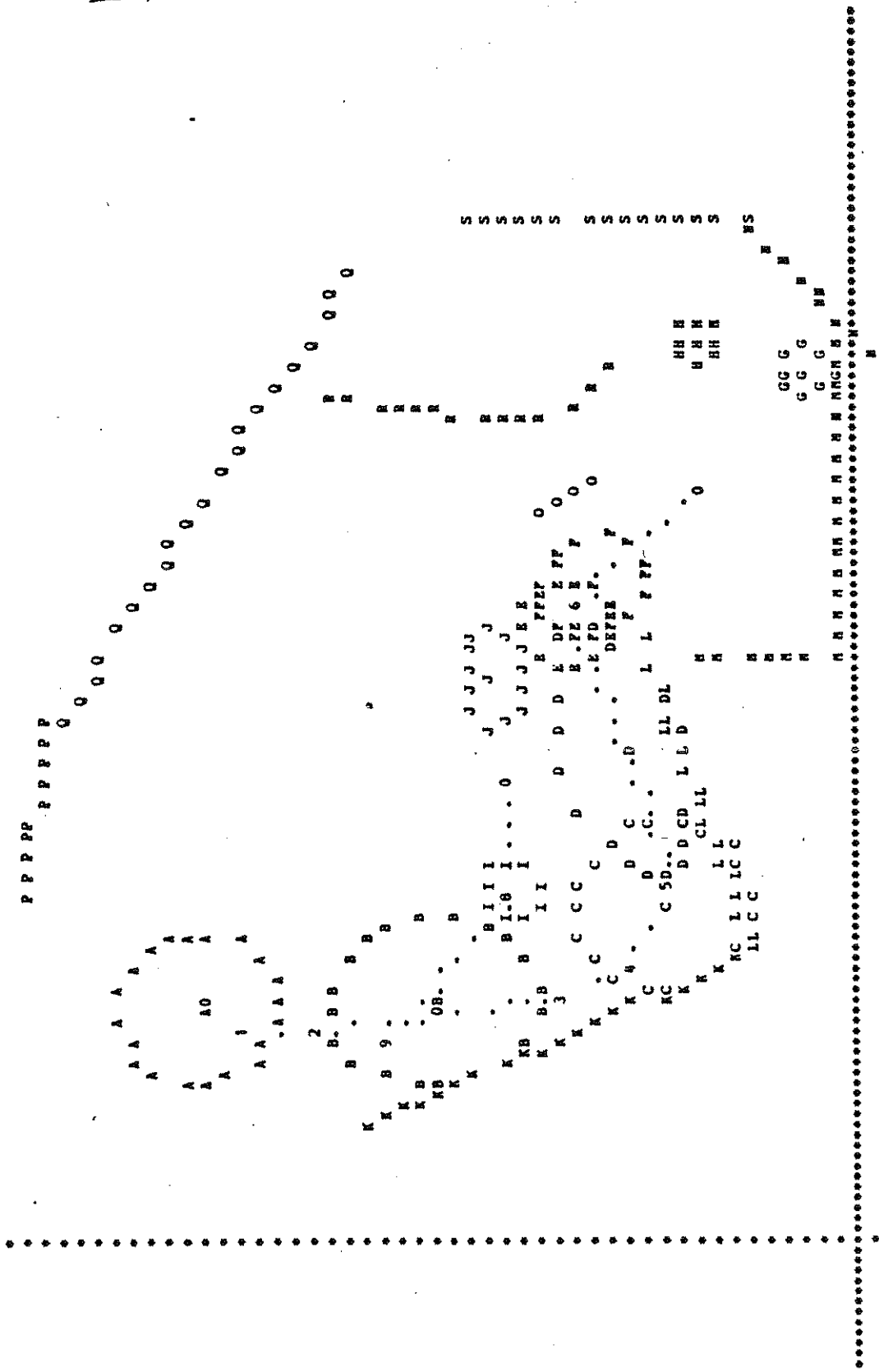
FIGURE 13-16 Summary of Input Data (example page)

JUN 24, 197702:00:20
GM HYBRID II DUMMY (PRELIMINARY DATA)

PAGE 130-45
HYNA 2-D, VER. 3

KNEE BAR OCC. COMP. DISPL. 30MPH FRONT BARRIER
NO BELTS

STICK FIGURE PRINTER PLOT FRAME FOR TIME= 0.0 MSEC.



COORDINATE RANGES FOR PLOT ARE X= -6.56 (AT LEFT) TO 65.56 (AT RIGHT) AND Z= 5.00 (AT BOTTOM) TO -44.00 (AT TOP)
SCALE FACTOR IS (IN) = 5.547 (IN) , X AND Z POINT RESOLUTION ERRORS EQUAL RESPECTIVELY 0.277 AND 0.462 (IN) IN SCALE.

FIGURE 13-17a Printer-Plot Time Sequence for Example 1 (0 ms)

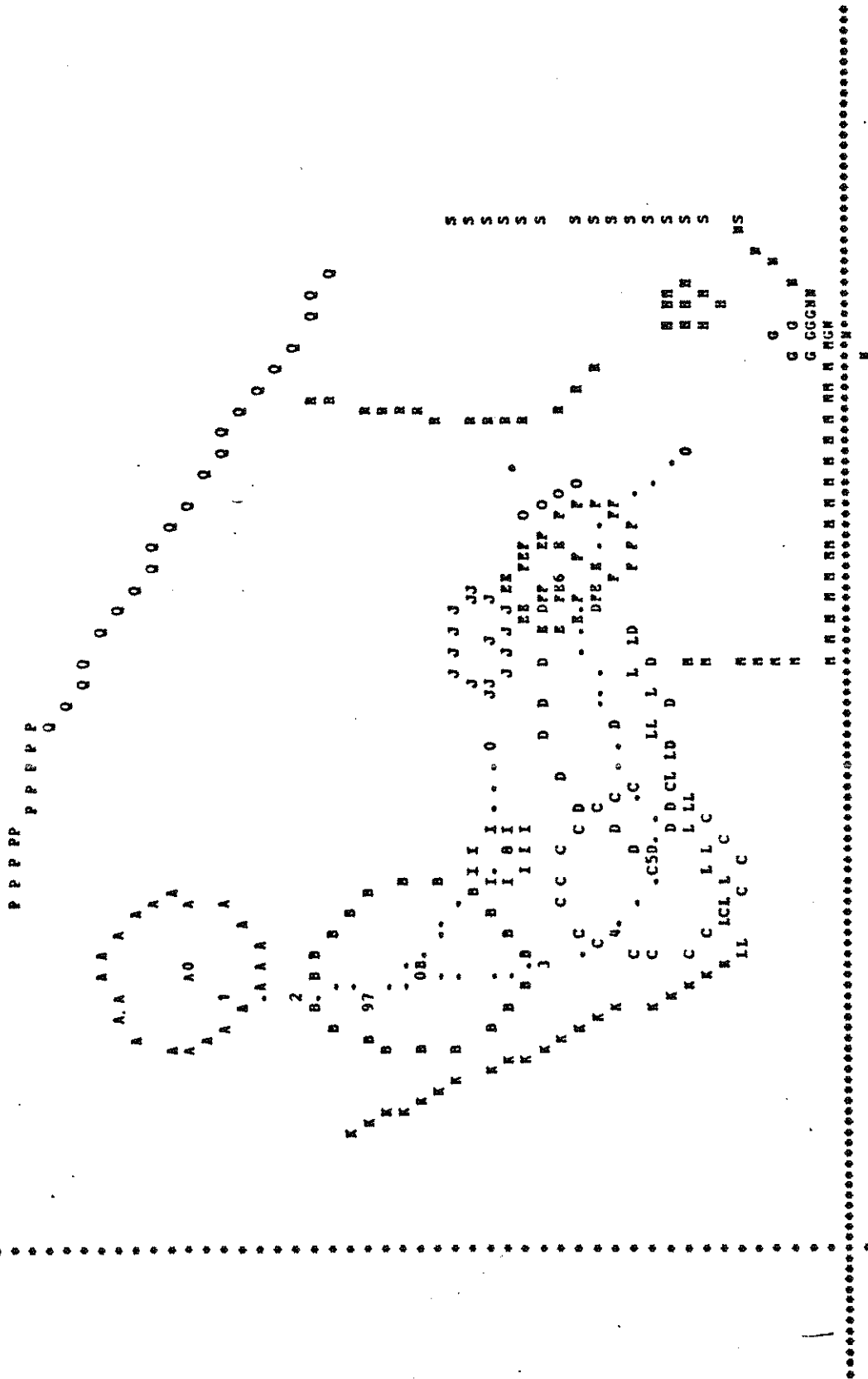
JUN 24, 197702:00:20
 GN HYBRID II DUMMY (PRELIMINARY DATA)

KNEE BAR
 OCC. COMP. DISPL. 30MPH FRONT BARRIER

NO BELTS

PAGE 133-45
 NVNA 2-D, VER. 3

STICK FIGURE PRINTER PLOT FRAME FOR TIME= 30.00 MSEC.



COORDINATE RANGES FOR PLOT ARE X= -6.56 (AT LEFT) TO 65.56 (AT RIGHT) AND Z= 5.00 (AT BOTTOM) TO -44.00 (AT TOP)
 SCALE FACTOR IS (IN) = 5.547 (IN) , X AND Z POINT RESOLUTION ERRORS EQUAL RESPECTIVELY 0.277 AND 0.462 (IN) IN SCALE.

FIGURE 13-17b Printer-Plot Time Sequence for Example 1 (30 ms)

NO BELTS
60.00 MSEC.

STICK FIGURE PRINTER PLOT FRAME FOR TIME*

JUN 24, 197702:00:20
GM HYBRID II DUMMY (PRELIMINARY DATA)

COOR. RANGES FOR PLOT ARE X= -6.56 (AT LEFT) TO 65.56 (AT RIGHT) AND Z= 5.00 (AT BOTTOM) TO -44.00 (AT TOP)
SCALE FACTOR IS (IN) = 5.547 (IN) , X AND Z POINT RESOLUTION ERRORS EQUAL RESPECTIVELY 0.277 AND 0.462 (IN) IF SCALE.

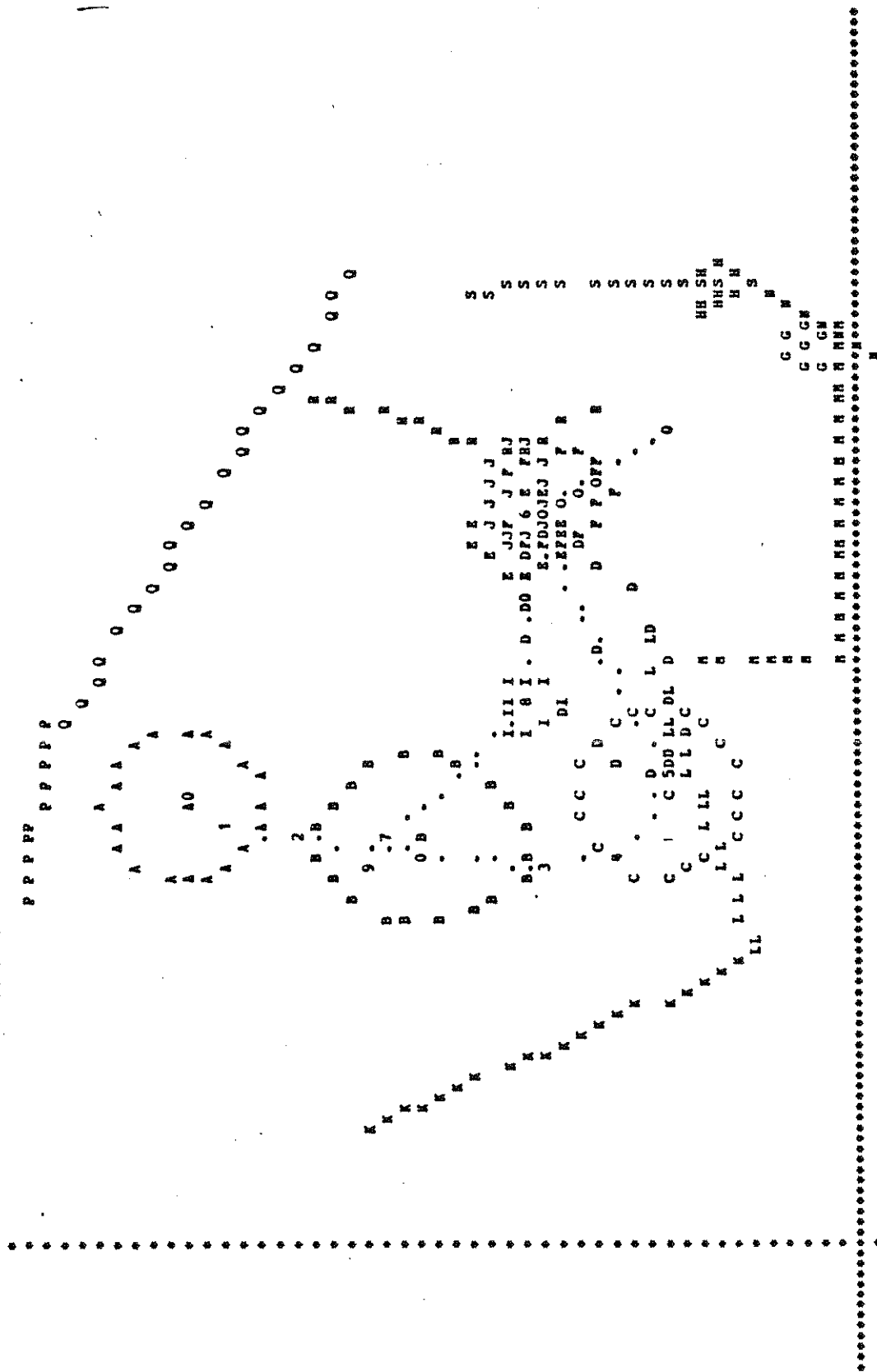
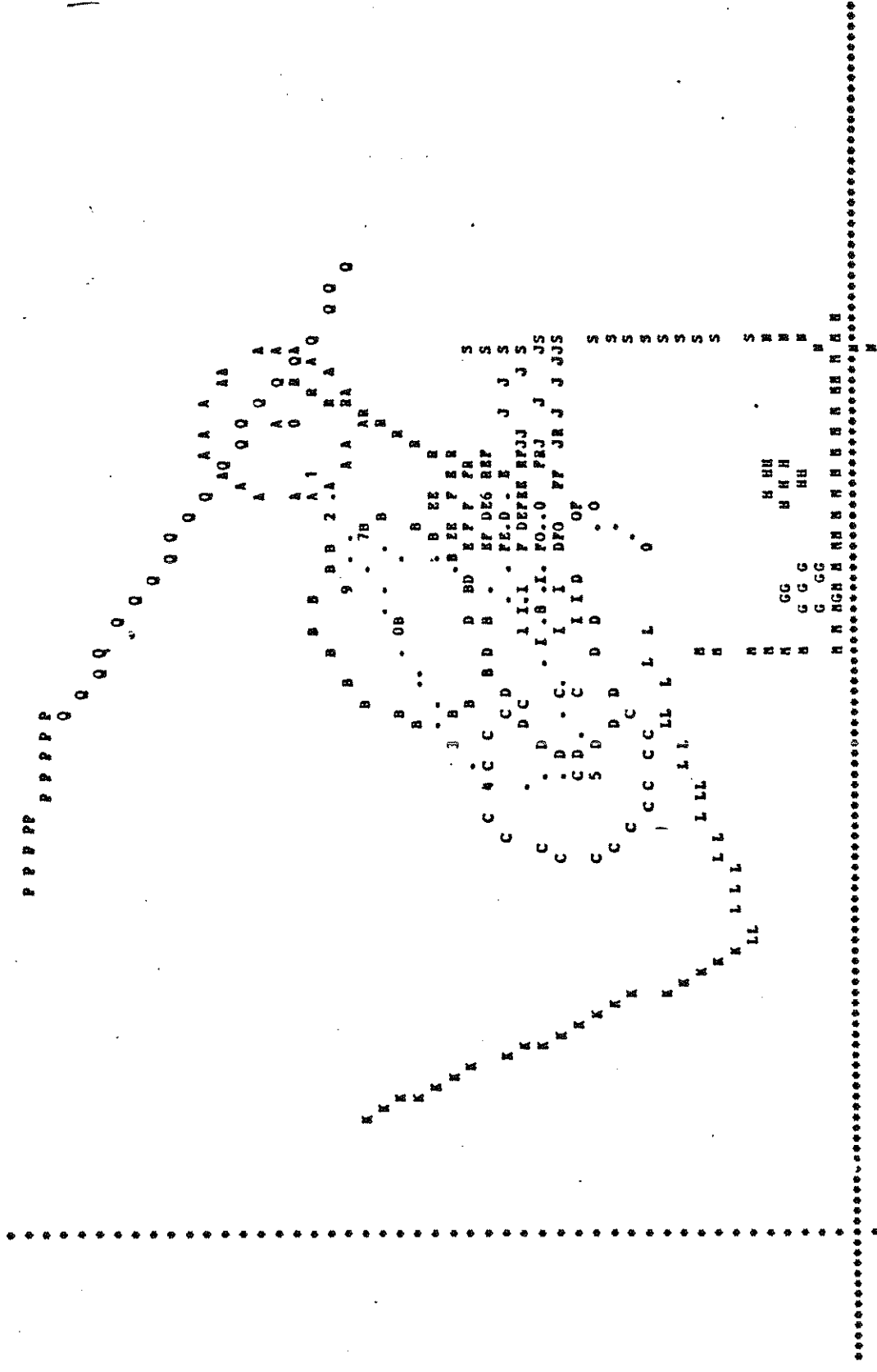


FIGURE 13-17c Printer-Plot Time Sequence for Example 1 (60 ms)

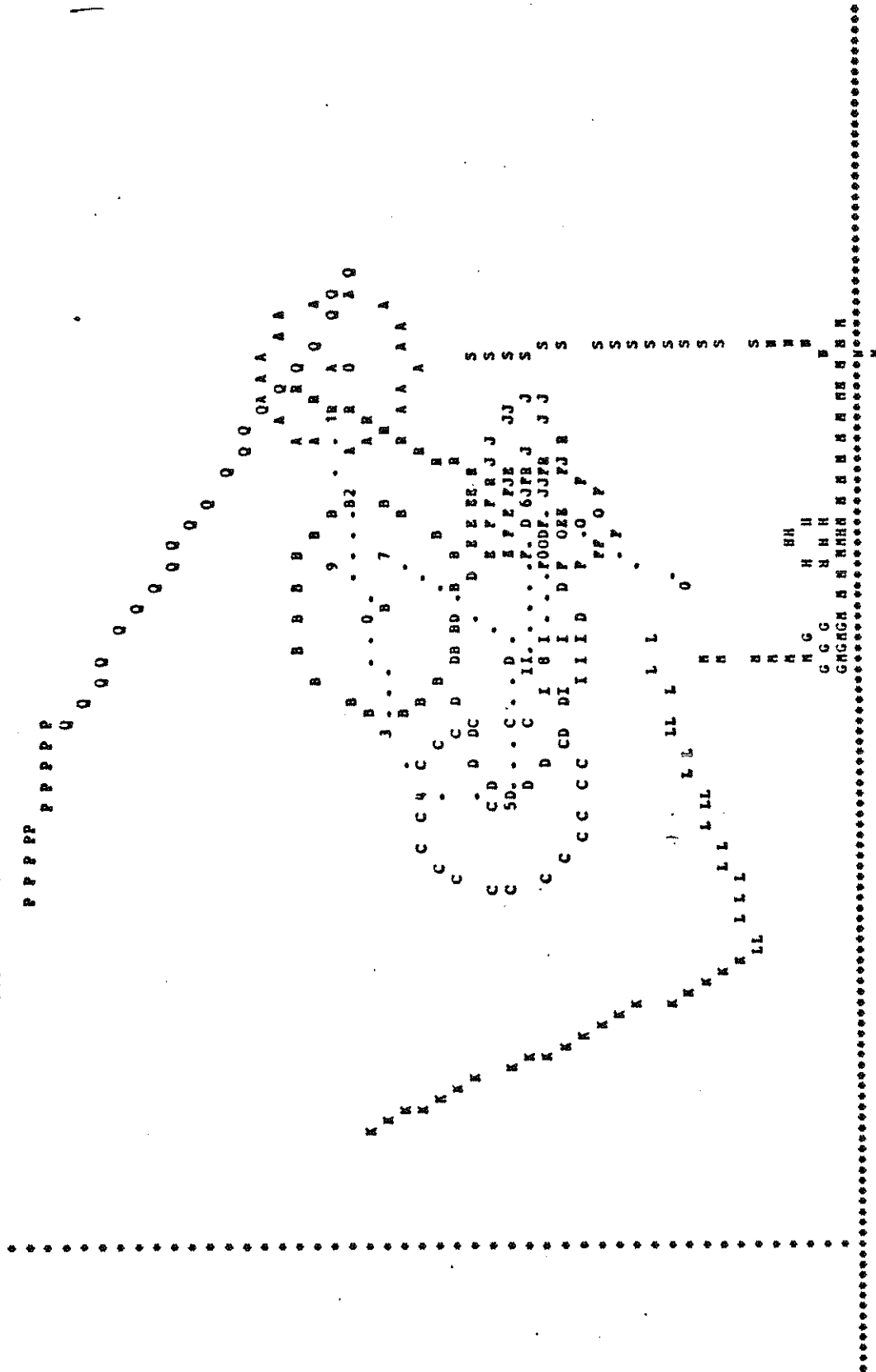


COORDINATE RANGES FOR PLOT ARE X= -6.56 (AT LEFT) TO 65.56 (AT RIGHT) AND Z= 5.00 (AT BOTTOM) TO -44.00 (AT TOP)
 SCALE FACTOR IS (IN) = 5.547 (IN) , X AND Z POINT RESOLUTION ERRORS EQUAL RESPECTIVELY 0.277 AND 0.462 (IN) IN SCALE.
 FIGURE 13-17e Printer-Plot Time Sequence for Example 1 (100 ms)

JUN 24, 197702:00:20
GN HYBRID II DUMMY (PRELIMINARY DATA)

PAGE 142-45
MVNA 2-D, VER. 3

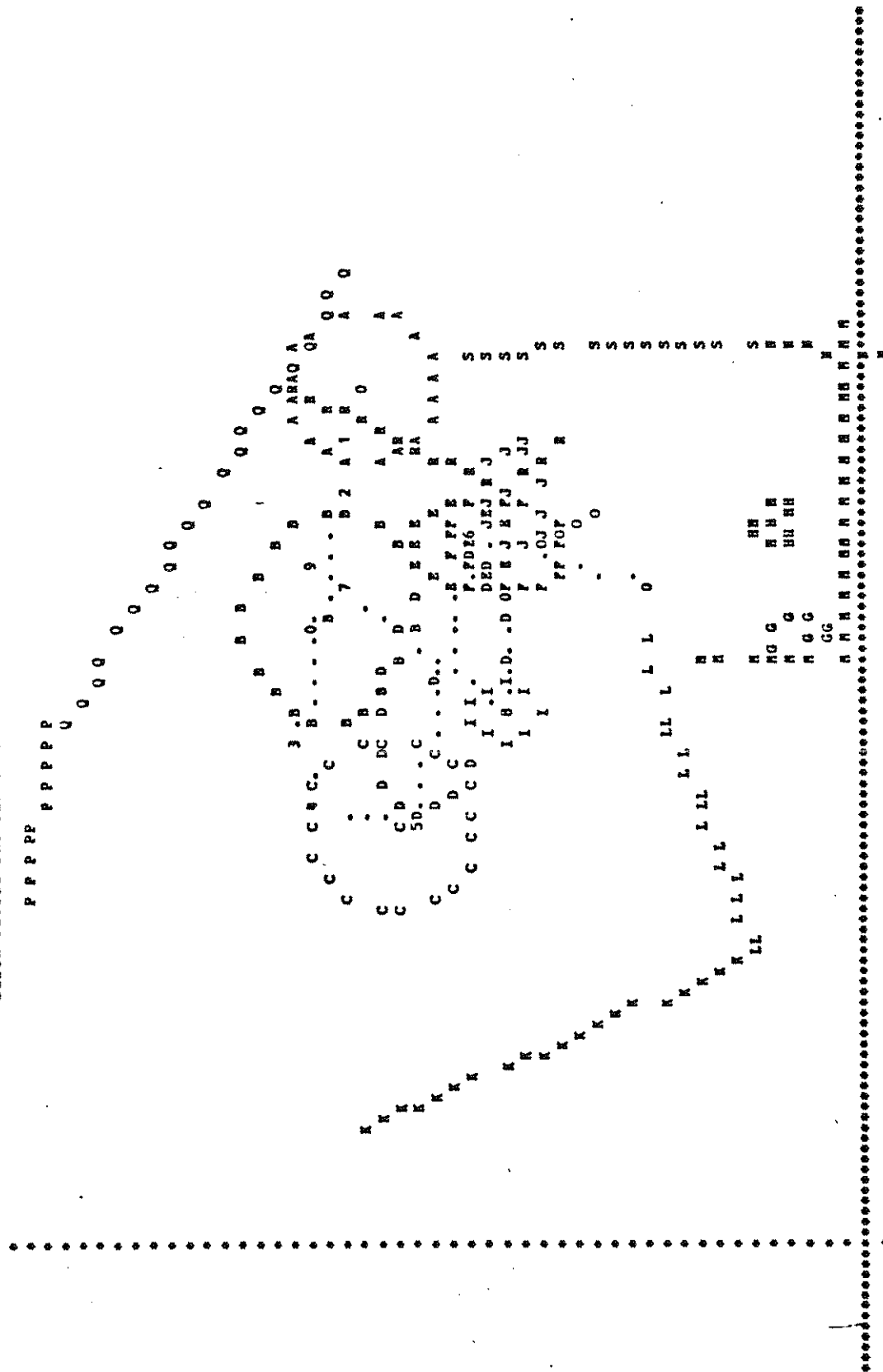
MVNA 2-D TUTORIAL EXAMPLE #1
KNEE BAR OCC. COMP. DISPL. JORPH FRONT BARRIER NO BELTS
STICK FIGURE PRINTER PLOT FRAME FOR TIME= 120.00 MSEC.



COORDINATE RANGES FOR PLOT ARE X= -6.56 (AT LEFT) TO 65.56 (AT RIGHT) AND Z= 5.00 (AT BOTTOM) TO -48.00 (AT TOP)
SCALE FACTOR IS (IN) = 5.547 (IN) , X AND Z POINT RESOLUTION ERRORS EQUAL RESPECTIVELY 0.277 AND 0.462 (IN) IN SCALE.

FIGURE 13-17f Printer-Plot Time Sequence for Example 1 (120 ms)

JUN 24, 197702:00:20 NVHA 2-D TUTORIAL EXAMPLE #1
GM HYBRID II DUMMY (PRELIMINARY DATA) KNEE DAE OCC. COMP. DISPL. 30MPS FRONT BARRIER NO BELTS
STICK FIGURE PRINTER PLOT FRAME FOR TIME= 150.00 MSEC.

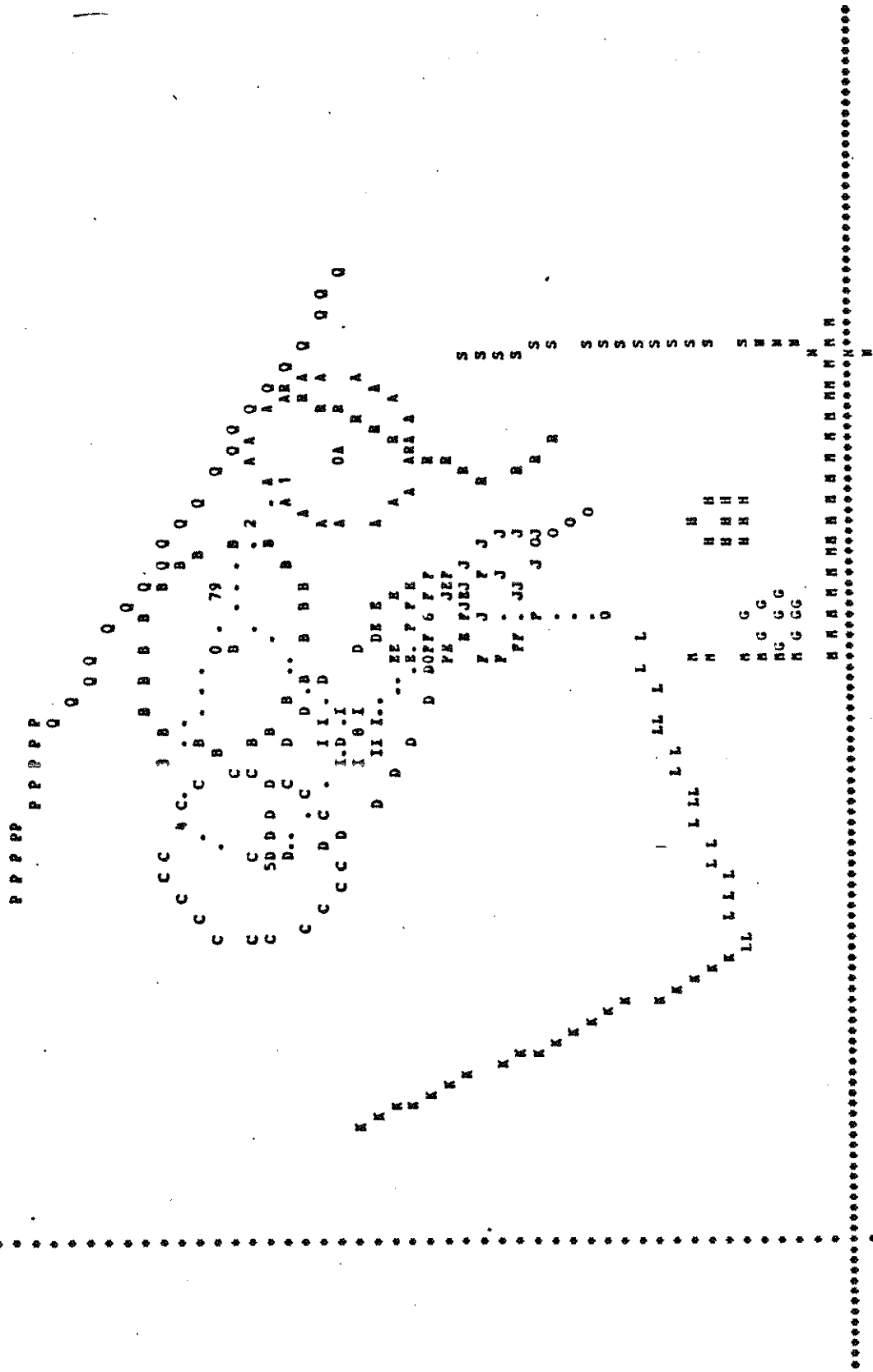


COORDINATE RANGES FOR PLOT ARE X= -6.56 (AT LEFT) TO 65.56 (AT RIGHT) AND Z= 5.00 (AT BOTTOM) TO -44.00 (AT TOP)
SCALE FACTOR IS (IN) = 5.547 (IN) , X AND Z POINT RESOLUTION ERRORS EQUAL RESPECTIVELY 0.277 AND 0.462 (IN) IN SCALE.

FIGURE 13-17g Printer-Plot Time Sequence for Example 1 (150 ms)

KNEE BAR OCC. COMP. DISPL. 30MPH FRONT BARRIER NO BELTS

STICK FIGURE PRINTER PLOT FRAME FOR TIME= 200.00 MSEC.



COORDINATE RANGES FOR PLOT ARE X= -6.56 (AT LEFT) TO 65.56 (AT RIGHT) AND Z= 5.00 (AT BOTTOM) TO -99.00 (AT TOP)
 SCALE FACTOR IS (IN) = 5.507 (IN) , X AND Z POINT RESOLUTION ERRORS EQUAL RESPECTIVELY 0.277 AND 0.462 (IN) IN SCALE.

FIGURE 13-17h Printer-Plot Time Sequence for Example 1 (200 ms)

HEAD CENTER OF MASS MOTION

(POSITIONS AND VELOCITIES RELATIVE TO VEHICLE FRAME)
 (ACCELERATIONS RELATIVE TO INERTIAL FRAME)

TIME (MSEC)	X (IN)	X-VEL. (IN/SEC)	X-ACCEL. (G'S)	Z (IN)	Z-VEL. (IN/SEC)	Z-ACCEL. (G'S)	HEAD ANGLE (DEG)	ANG. VEL. (DEG/SEC)	ANG. ACC. (RAD/SEC**2)
0.0	12.94	0.0	-0.000	-34.10	0.0	1.000	78.50	0.0	-0.00
5.00	12.97	20.29	-1.965	-34.09	0.94	0.476	78.49	6.59	-551.04
10.00	13.20	69.32	-1.904	-34.09	0.52	-0.140	78.42	-9.45	-556.95
15.00	13.56	71.71	-1.755	-34.09	-0.92	-0.523	78.27	-27.66	-566.14
20.00	13.98	101.85	-1.811	-34.10	-2.82	-0.652	78.02	-44.44	-582.18
25.00	14.55	126.56	-1.830	-34.12	-4.85	-0.705	77.70	-59.41	-588.09
30.00	15.24	149.00	-1.733	-34.14	-7.08	-0.940	77.30	-75.22	-596.04
35.00	16.08	190.11	-1.468	-34.19	-9.96	-1.469	76.81	-94.22	-607.21
40.00	17.13	218.32	-0.517	-34.25	-14.53	-2.648	76.22	-116.07	-584.23
45.00	18.32	275.10	1.937	-34.33	-20.74	-3.291	75.61	-129.48	-450.39
50.00	19.86	346.27	4.840	-34.45	-27.26	-3.151	74.98	-122.48	-243.80
55.00	21.73	406.64	9.350	-34.60	-33.10	-2.312	74.36	-139.87	131.93
60.00	23.95	462.77	9.613	-34.77	-33.12	3.540	73.60	-181.86	13.58
65.00	26.54	548.85	7.928	-34.91	-16.51	14.496	72.55	-249.73	-7.06
70.00	29.49	594.65	2.859	-34.90	22.52	26.240	71.18	-314.76	-88.51
75.00	32.36	541.53	-81.864	-34.61	111.70	61.654	69.79	-37.40	2854.46
80.00	34.96	520.33	-5.835	-33.90	159.95	13.709	69.99	-93.22	-1547.61
85.00	37.54	576.22	-19.247	-33.33	189.55	18.504	68.41	-518.69	-1653.52
90.00	39.94	465.36	-28.412	-31.98	235.22	27.831	64.95	-837.46	-966.97
95.00	43.12	360.94	-62.636	-33.70	259.38	-16.455	58.44	-2474.69	-11601.15
100.00	43.73	260.57	-51.994	-29.54	204.00	-26.712	43.26	-2840.28	3087.70
105.00	44.89	217.67	-10.903	-28.60	173.61	-15.327	30.43	-2415.08	1035.27
110.00	45.90	177.36	-34.519	-27.81	143.79	-12.955	19.37	-1927.01	2419.62
115.00	46.62	197.90	-41.020	-27.12	132.74	-5.796	11.33	-1292.02	2166.99
120.00	46.97	33.86	-33.042	-26.49	117.15	-11.867	6.18	-809.57	817.05
125.00	47.31	14.36	-16.823	-25.96	94.38	-11.908	2.65	-642.20	242.87
130.00	46.88	31.99	-2.747	-25.54	73.75	-8.932	-0.45	-600.85	157.31
135.00	46.72	20.69	3.321	-25.21	59.57	-6.156	-3.34	-558.16	127.29
140.00	46.58	25.37	0.386	-24.94	48.29	-6.077	-6.04	-525.40	87.96
145.00	46.45	31.47	-6.638	-24.73	34.14	-8.869	-8.65	-529.89	-163.62
150.00	46.25	-46.01	-8.099	-24.61	15.35	-10.014	-11.44	-590.87	-204.86
155.00	45.99	-59.52	-5.561	-24.58	-2.77	-9.321	-14.53	-642.69	-351.92
160.00	45.67	-66.41	-1.768	-24.63	-17.13	-6.700	-17.95	-708.89	-395.16
165.00	45.34	-60.85	0.717	-24.74	-24.29	-3.194	-21.67	-767.50	-519.80
170.00	45.91	-65.20	0.127	-24.87	-26.84	1.409	-25.72	-846.31	312.56
175.00	44.63	-63.65	0.577	-25.01	-28.43	-1.145	-29.99	-860.65	64.55
180.00	44.36	-63.86	-1.376	-25.16	-32.09	-2.173	-34.16	-803.16	607.71
185.00	44.94	-67.47	-2.610	-25.33	-39.98	-2.702	-37.85	-692.96	792.72
190.00	43.69	-69.37	-3.423	-25.55	-47.34	-1.931	-41.02	-622.64	533.47
195.00	43.35	-66.82	2.711	-25.83	-51.61	-1.326	-43.86	-532.31	47.39
200.00	43.03	-61.20	3.020	-26.05	-49.86	1.500	-46.37	-465.61	327.76

FIGURE 13-18.1 Head Center of Mass Motion for Example 1

(see footnote, page 348.)

CHEST CENTER OF MASS MOTION

(POSITIONS AND VELOCITIES RELATIVE TO VEHICLE FRAME)
(ACCELERATIONS RELATIVE TO INERTIAL FRAME)

TIME (MSEC)	X (IN)	X-VEL. (IN/SEC)	X-ACCEL. (G'S)	Z (IN)	Z-VEL. (IN/SEC)	Z-ACCEL. (G'S)
0.0	12.20	0.0	-3.586	-21.40	0.0	-0.603
5.00	12.22	15.09	-13.974	-21.40	-1.30	4.549
10.00	12.44	66.20	-14.432	-21.41	-1.95	4.632
15.00	12.78	65.93	-14.642	-21.42	-3.06	4.429
20.00	13.16	92.93	-14.832	-21.44	-4.57	4.164
25.00	13.63	114.00	-15.116	-21.46	-6.64	3.799
30.00	14.28	132.00	-15.342	-21.50	-9.72	3.212
35.00	15.03	167.34	-16.552	-21.56	-13.89	1.979
40.00	15.90	185.66	-18.230	-21.64	-20.25	3.089
45.00	16.00	210.25	-18.659	-21.75	-24.12	2.277
50.00	18.08	252.02	-22.085	-21.88	-30.31	-0.821
55.00	19.39	271.06	-10.819	-22.06	-40.69	-7.453
60.00	20.81	297.95	-8.731	-22.28	-44.67	-1.530
65.00	22.36	321.30	-6.256	-22.50	-43.57	-1.668
70.00	24.01	336.52	-2.067	-22.72	-44.10	-1.040
75.00	25.72	344.00	-16.667	-22.93	-40.96	4.263
80.00	27.42	333.17	-23.955	-23.10	-23.55	8.191
85.00	23.02	303.03	-29.137	-23.17	-3.94	8.065
90.00	30.42	255.43	-29.800	-23.14	13.40	4.402
95.00	31.51	159.57	-44.250	-23.25	-102.59	-68.862
100.00	32.24	153.70	-16.108	-23.78	-101.82	3.352
105.00	32.83	106.93	-17.277	-24.27	-92.02	6.972
110.00	33.26	68.27	-17.384	-24.68	-74.66	8.514
115.00	33.54	46.58	-8.863	-25.03	-65.55	2.736
120.00	33.74	34.70	-13.138	-25.35	-62.85	-12.330
125.00	33.89	22.06	-3.773	-25.68	-67.94	-3.043
130.00	33.96	12.12	-6.464	-26.03	-71.31	-1.000
135.00	33.99	-1.77	-7.545	-26.39	-74.03	-1.896
140.00	33.95	-15.19	-5.782	-26.77	-78.89	-3.327
145.00	33.85	-22.32	-1.559	-27.19	-87.39	-5.247
150.00	33.73	-23.67	-0.202	-27.65	-95.56	-4.495
155.00	33.61	-24.37	0.378	-28.14	-100.26	-4.891
160.00	33.49	-24.79	0.378	-28.65	-104.73	-5.143
165.00	33.36	-24.94	1.073	-29.19	-103.54	-4.595
170.00	33.23	-26.67	2.600	-29.74	-112.91	12.160
175.00	33.09	-27.36	3.627	-30.29	-109.44	12.303
180.00	32.95	-25.74	1.926	-30.83	-106.75	14.043
185.00	32.83	-22.95	5.411	-31.35	-101.98	15.071
190.00	32.73	-20.27	4.638	-31.84	-95.37	14.219
195.00	32.63	-18.17	-2.294	-32.30	-90.63	0.492
200.00	32.54	-20.56	-1.773	-32.75	-87.66	-0.180

FIGURE 13-18.2 Chest Center of Mass Motion for Example 1

(see footnote, page 348.)

HIP MOTION

(POSITIONS AND VELOCITIES RELATIVE TO VEHICLE FRAME)
 (ACCELERATIONS RELATIVE TO INERTIAL FRAME)

TIME (MSEC)	X (IN)	X-VEL. (IN/SEC)	X-ACCEL. (G'S)	Z (IN)	Z-VEL. (IN/SEC)	Z-ACCEL. (G'S)
0.0	18.81	0.0	-0.533	-9.41	0.0	-1.626
5.00	18.24	17.57	4.479	-9.41	-1.88	1.380
10.00	19.06	63.13	4.151	-9.42	-2.67	1.484
15.00	19.38	61.15	3.734	-9.44	-2.96	1.319
20.00	19.74	85.98	3.225	-9.45	-3.57	1.136
25.00	20.22	104.15	2.592	-9.47	-4.66	0.893
30.00	20.77	118.29	1.376	-9.49	-5.74	0.460
35.00	21.44	147.88	-1.449	-9.53	-8.98	-0.815
40.00	22.20	151.32	-11.577	-9.58	-11.33	-2.461
45.00	22.97	157.44	-21.461	-9.63	-6.90	1.121
50.00	23.75	145.58	-36.379	-9.65	-1.55	-1.885
55.00	24.29	107.11	-54.473	-9.67	-6.93	0.208
60.00	24.82	67.82	-53.964	-9.69	-4.86	4.745
65.00	25.07	34.35	-44.454	-9.72	-9.86	-8.828
70.00	25.14	-2.29	-36.416	-9.93	-26.74	-18.825
75.00	25.66	-26.57	-10.904	-10.10	-70.61	-14.022
80.00	24.92	-26.54	0.927	-10.52	-99.06	-12.099
85.00	24.80	-19.98	4.790	-11.09	-130.53	-14.423
90.00	24.73	-7.30	9.259	-11.83	-163.72	-14.741
95.00	24.75	13.55	8.292	-12.73	-199.64	-31.099
100.00	24.86	26.66	-7.208	-13.89	-219.61	2.225
105.00	24.91	-16.83	-36.866	-14.86	-199.57	13.978
110.00	24.67	-73.60	-18.051	-15.91	-182.16	2.961
115.00	24.29	-72.55	11.041	-16.73	-186.66	-1.414
120.00	23.97	-49.62	11.224	-17.66	-186.52	11.255
125.00	23.76	-36.83	2.687	-18.59	-187.14	1.924
130.00	23.59	-33.19	1.333	-19.52	-183.81	1.868
135.00	23.43	-31.37	0.751	-20.42	-178.54	3.419
140.00	23.27	-30.51	-0.082	-21.30	-171.31	3.953
145.00	23.12	-31.06	-0.478	-22.13	-162.76	3.774
150.00	22.66	-32.39	-1.025	-22.94	-157.29	3.757
155.00	22.79	-32.75	-1.575	-23.71	-152.67	4.653
160.00	22.62	-35.57	-2.149	-24.46	-147.46	5.091
165.00	22.44	-36.65	-2.459	-25.18	-142.65	4.979
170.00	22.25	-38.29	0.932	-25.88	-136.50	-7.019
175.00	22.06	-38.62	1.033	-26.56	-134.51	-5.740
180.00	21.86	-39.12	1.242	-27.22	-131.59	-6.322
185.00	21.67	-39.33	1.411	-27.87	-127.06	-6.665
190.00	21.47	-39.16	1.387	-28.50	-124.67	-5.968
195.00	21.28	-39.55	1.453	-29.12	-121.55	2.393
200.00	21.09	-36.93	1.256	-29.72	-118.93	2.426

FIGURE 13-18.3 Hip Motion for Example 1

(see footnote, page 348.)

TIME	HEAD	NECK	UPPER TORSO	MID TORSO	LOW TORSO	BODY LINK ANGLES		(DEGREES)		(RELATIVE TO VEHICLE)			
						UPPER TORSO	MID TORSO	LOW TORSO	UPPER LEG	LOWER LEG	SHOULDER	UPPER ARM	LOWER ARM
0.0	78.50	89.50	97.50	115.50	149.50	149.50	149.50	19.50	-45.00	---	---	-41.00	3.00
5.0	79.48	89.46	97.51	115.43	149.54	149.54	149.54	19.47	-45.00	---	---	-41.00	3.00
10.0	78.39	89.43	97.46	115.42	149.58	149.58	149.58	19.38	-45.02	---	---	-41.02	3.01
15.0	78.24	89.32	97.36	115.43	149.61	149.61	149.61	19.26	-45.06	---	---	-41.05	3.02
20.0	78.02	89.15	97.20	115.39	149.61	149.61	149.61	19.13	-45.11	---	---	-41.08	3.02
25.0	77.72	88.92	96.97	115.27	149.60	149.60	149.60	18.99	-45.16	---	---	-41.12	3.02
30.0	77.36	88.61	96.65	115.04	149.56	149.56	149.56	18.83	-45.17	---	---	-41.23	2.99
35.0	76.90	88.18	96.19	114.65	149.50	149.50	149.50	18.63	-45.14	---	---	-41.48	2.90
40.0	76.29	87.68	95.47	114.09	149.39	149.39	149.39	18.45	-45.33	---	---	-41.93	2.75
45.0	75.61	87.05	94.18	112.98	149.15	149.15	149.15	19.29	-47.69	---	---	-42.62	2.53
50.0	74.94	86.10	91.87	110.89	148.49	148.49	148.49	22.12	-51.13	---	---	-43.77	2.28
55.0	74.24	84.58	88.20	107.34	147.28	147.28	147.28	25.64	-54.87	---	---	-45.34	1.97
60.0	73.52	82.27	82.97	102.13	145.06	145.06	145.06	28.83	-58.65	---	---	-47.39	1.54
65.0	72.91	79.00	76.43	95.90	141.16	141.16	141.16	32.33	-63.13	---	---	-53.15	1.32
70.0	71.19	74.91	68.79	87.91	135.61	135.61	135.61	35.73	-68.08	---	---	-61.29	0.86
75.0	69.89	70.71	60.40	79.37	128.60	128.60	128.60	37.60	-72.74	---	---	-69.37	-0.27
80.0	70.18	67.90	52.00	70.76	120.62	120.62	120.62	38.00	-77.54	---	---	-75.39	-2.03
85.0	68.66	63.23	43.87	62.19	113.17	113.17	113.17	37.29	-82.98	---	---	-82.65	-3.20
90.0	65.21	57.51	35.75	54.07	107.44	107.44	107.44	34.98	-84.08	---	---	-94.60	-2.37
95.0	56.91	44.75	29.68	44.51	103.15	103.15	103.15	29.18	-97.34	---	---	-105.80	-0.88
100.0	40.47	34.64	25.42	44.61	100.95	100.95	100.95	19.68	-107.17	---	---	-112.47	0.60
105.0	27.24	27.16	21.32	40.80	98.68	98.68	98.68	10.56	-115.53	---	---	-117.05	1.98
110.0	16.17	20.32	17.67	36.45	93.01	93.01	93.01	3.65	-120.15	---	---	-120.35	3.13
115.0	8.62	15.00	14.27	32.64	87.24	87.24	87.24	0.49	-117.93	---	---	-122.74	4.06
120.0	4.10	10.96	10.74	28.73	83.56	83.56	83.56	-1.08	-115.81	---	---	-123.92	4.73
125.0	1.24	7.92	7.10	25.45	81.21	81.21	81.21	-2.40	-114.72	---	---	-123.89	5.04
130.0	-1.05	5.47	3.50	22.02	79.85	79.85	79.85	-4.12	-113.19	---	---	-123.29	4.88
135.0	-3.25	3.25	0.04	19.18	79.01	79.01	79.01	-6.05	-111.70	---	---	-122.83	3.97
140.0	-5.39	0.96	-3.27	17.17	78.61	78.61	78.61	-8.09	-110.28	---	---	-123.38	2.04
145.0	-7.50	-1.56	-6.31	15.95	78.41	78.41	78.41	-10.17	-108.88	---	---	-125.40	-0.95
150.0	-9.81	-4.31	-8.94	15.37	78.12	78.12	78.12	-12.27	-107.46	---	---	-128.05	-4.50
155.0	-12.67	-7.25	-10.96	14.57	77.76	77.76	77.76	-14.39	-105.99	---	---	-130.21	-8.16
160.0	-16.21	-10.21	-12.55	14.00	77.19	77.19	77.19	-16.50	-104.47	---	---	-131.81	-11.86
165.0	-20.29	-13.37	-13.80	13.54	76.60	76.60	76.60	-18.62	-102.90	---	---	-133.06	-15.61
170.0	-24.84	-16.81	-14.76	13.08	75.89	75.89	75.89	-20.72	-101.27	---	---	-133.99	-19.40
175.0	-29.55	-20.37	-15.52	12.54	74.98	74.98	74.98	-22.83	-99.60	---	---	-134.74	-23.22
180.0	-33.98	-23.68	-16.23	11.93	73.84	73.84	73.84	-24.94	-97.89	---	---	-135.35	-27.08
185.0	-37.96	-26.64	-16.91	11.10	72.48	72.48	72.48	-27.08	-96.14	---	---	-135.90	-30.96
190.0	-41.56	-29.22	-17.57	10.12	70.97	70.97	70.97	-29.22	-94.35	---	---	-136.44	-34.86
195.0	-44.72	-31.34	-18.35	9.21	69.59	69.59	69.59	-31.40	-92.55	---	---	-137.16	-38.77
200.0	-47.47	-33.24	-19.19	8.28	68.38	68.38	68.38	-33.60	-90.74	---	---	-137.96	-42.65

FIGURE 13-19 Body Link Angles for Example 1

JUN 24, 197702:00:20

GM HYBRID II DUMMY (PRELIMINARY DATA)

KNEE BAR

NMMA

2-D TUTORIAL EXAMPLE #1

OCC. COMP. DISPL. 30MPH FRONT BARRIER

NO BELTS

PAGE 67-12
NMMA 2-D, VER.:

(RELATIVE TO INERTIAL FRAME)

(DEG/SEC**2)

ACCELERATION OF BODY LINK ANGLES

TIME	HEAD	NECK	UPPER TORSO	MID TORSO	LOW TORSO	UPPER LEG	LOWER LEG	SHOULDER	UPPER ARM	LOWER ARM
0.0	-0.08	2938.40	-3248.21	2979.45	4793.00	-3645.51	-492.10	---	-0.02	-0.00
5.0	25857.73	-223587.69	127969.00	-527872.88	144861.88	-13590.84	7348.74	---	-38930.38	13606.55
10.0	29682.09	-233848.44	127889.50	-473227.00	90787.13	782.02	5714.10	---	-39166.94	13556.36
15.0	28032.93	-233876.63	127401.56	-475440.25	91681.69	933.72	6171.09	---	-39402.73	13480.65
20.0	30796.70	-237296.81	126878.81	-477046.81	92156.88	1007.69	6765.30	---	-34780.67	10397.41
25.0	31065.69	-237736.81	125699.25	-478322.31	92567.80	613.75	7717.36	---	-40171.68	13262.19
30.0	29287.89	-233934.06	123251.13	-484735.19	99429.88	-1695.69	9112.70	---	-19912.01	566.06
35.0	27216.75	-229205.13	116945.88	-481020.38	96750.88	-4410.46	4634.26	---	-20102.70	261.85
40.0	-33603.26	205130.31	-141076.81	460340.63	-134661.63	48445.60	-112498.75	---	-19932.46	-227.75
45.0	-24473.03	158491.75	-130632.50	315852.69	-80942.63	91546.75	-375308.94	---	-19197.52	-1011.97
50.0	-14550.74	124068.88	-136785.69	249910.44	-70707.81	29565.52	-183277.44	---	-16947.72	-2294.53
55.0	9319.91	-161231.31	7418.38	-317691.06	-7141.34	-1596.45	59359.55	---	-13162.18	-4054.77
60.0	1737.15	-170728.31	22284.50	-306341.13	-40286.15	57256.60	4843.56	---	-245395.88	34988.09
65.0	1549.49	-153355.75	28247.05	-271429.44	-33563.59	19158.34	26113.83	---	-58629.13	-17853.61
70.0	-3405.37	-136127.00	36042.57	-275813.69	-16945.75	-80090.50	23158.45	---	18040.09	-31443.95
75.0	16372.25	205956.06	-50444.42	194833.13	-76379.06	-49146.36	-7571.30	---	106407.75	-26885.63
80.0	-96307.94	7449.24	-49430.32	234451.81	-19378.71	-42686.88	-22981.67	---	-66920.06	14910.29
85.0	-89125.44	57954.29	-57992.70	198039.13	41107.65	-54579.84	-34902.36	---	-223432.44	25324.41
90.0	-54990.81	33871.97	-59382.40	172857.94	66169.88	-60121.92	-41638.49	---	35846.14	-22035.46
95.0	-481964.38	80945.63	32022.68	-564191.50	246550.50	-86629.88	-8456.13	---	223792.94	4476.54
100.0	191133.19	32120.41	20808.85	-13572.79	12974.57	12510.36	51409.51	---	71766.19	-4169.37
105.0	56210.35	73014.13	11303.79	-49897.39	-153452.50	84620.00	141207.38	---	34124.68	-14371.46
110.0	157107.05	73777.63	13517.83	30420.26	6924.27	184807.06	324180.50	---	34541.01	-8421.68
115.0	123203.38	60756.18	-8628.77	-3753.18	98450.81	56039.26	-186156.88	---	50151.01	-10198.30
120.0	72155.31	-16942.42	26096.33	-85527.69	61935.59	-4262.55	-116811.44	---	50917.07	-14588.93
125.0	30849.06	-21004.46	23278.25	-83631.31	62039.53	-27827.26	40552.36	---	20514.27	-17491.39
130.0	2141.99	9876.37	5073.38	25533.01	21175.43	-8123.35	-5669.99	---	-4410.66	-29606.40
135.0	2242.21	-3047.31	5569.14	34190.18	18337.61	-4428.91	-2817.41	---	-41723.62	-42299.68
140.0	2273.97	-9536.70	10364.16	32448.52	8191.64	-1620.30	-567.86	---	-62486.91	-43318.28
145.0	-9534.13	-13067.22	18933.00	23103.40	-4346.64	27.79	886.93	---	-45861.91	-27245.51
150.0	-21488.26	-3365.79	18227.15	21133.92	-11828.38	373.08	1876.43	---	22844.40	-2654.75
155.0	-27100.18	13181.14	3114.47	72380.44	-26001.77	3929.86	2620.24	---	27059.45	-665.82
160.0	-34574.75	16094.84	75.71	76495.44	-30481.41	4961.23	3133.62	---	29287.47	731.46
165.0	-34013.80	16916.27	-1945.95	73574.13	-35436.34	5397.42	3340.20	---	30517.90	1711.29
170.0	-23751.43	-70955.06	78437.54	-282697.88	5336.14	-12588.36	4993.33	---	31289.14	1908.91
175.0	32805.65	-171129.69	110062.56	-376787.00	68659.88	-14978.75	6152.11	---	-19876.87	-4740.37
180.0	39366.07	-174374.88	110553.00	-387197.56	70503.81	-15331.14	6615.40	---	-19874.18	-3640.73
185.0	40980.61	-184915.63	111065.75	-385713.50	72637.19	-15013.99	6929.22	---	-20506.83	-2494.84
190.0	22463.36	34291.04	-19406.22	52206.05	-664.37	300.91	-719.20	---	-21528.57	-1297.61
195.0	8957.54	52111.74	-23009.35	68026.94	-3645.16	1325.42	-886.49	---	-22236.98	2.06
200.0	7900.23	151368.13	-109302.94	439788.88	-106996.69	20469.91	-5362.71	---	-21304.69	1470.21

FIGURE 13-20 Body Link Angle Accelerations for Example 1

6/28/79

REGION LINE SEGMENT MOVEMENT FOR INSTRUMENT PANEL (IN)
 (X,Z) W.R.T. VEHICLE FRAME
 REGION CONTAINS 2 LINE SEGMENTS

TIME	A			1 (MID IP)			2 (LOWER IP)			3 (X,Z)			4 (X,Z)			5 (X,Z)		
	X	Z		X	Z		X	Z		X	Z		X	Z		X	Z	
0.0	44.90	-27.30		43.70	-15.90		46.80	-12.80		0.0	0.0		0.0	0.0		0.0	0.0	
5.00	44.90	-27.30		43.70	-15.90		46.80	-12.80		0.0	0.0		0.0	0.0		0.0	0.0	
10.00	44.90	-27.30		43.70	-15.90		46.80	-12.80		0.0	0.0		0.0	0.0		0.0	0.0	
15.00	44.90	-27.30		43.70	-15.90		46.80	-12.80		0.0	0.0		0.0	0.0		0.0	0.0	
20.00	44.90	-27.30		43.70	-15.90		46.80	-12.80		0.0	0.0		0.0	0.0		0.0	0.0	
25.00	44.90	-27.30		43.70	-15.90		46.80	-12.80		0.0	0.0		0.0	0.0		0.0	0.0	
30.00	44.90	-27.30		43.70	-15.90		46.80	-12.80		0.0	0.0		0.0	0.0		0.0	0.0	
35.00	44.90	-27.30		43.70	-15.90		46.80	-12.80		0.0	0.0		0.0	0.0		0.0	0.0	
40.00	44.90	-27.30		43.70	-15.90		46.80	-12.80		0.0	0.0		0.0	0.0		0.0	0.0	
45.00	44.99	-27.55		43.31	-16.27		46.28	-13.06		0.0	0.0		0.0	0.0		0.0	0.0	
50.00	45.07	-27.80		42.93	-16.65		45.75	-13.32		0.0	0.0		0.0	0.0		0.0	0.0	
55.00	45.16	-28.05		42.54	-17.02		45.23	-13.59		0.0	0.0		0.0	0.0		0.0	0.0	
60.00	45.25	-28.30		42.15	-17.40		44.70	-13.85		0.0	0.0		0.0	0.0		0.0	0.0	
65.00	45.34	-28.55		41.76	-17.77		44.18	-14.11		0.0	0.0		0.0	0.0		0.0	0.0	
70.00	45.42	-28.80		41.38	-18.15		43.65	-14.37		0.0	0.0		0.0	0.0		0.0	0.0	
75.00	45.51	-29.05		40.99	-18.52		43.13	-14.64		0.0	0.0		0.0	0.0		0.0	0.0	
80.00	45.60	-29.30		40.60	-18.90		42.60	-14.90		0.0	0.0		0.0	0.0		0.0	0.0	
85.00	45.60	-29.30		40.60	-18.90		42.60	-14.90		0.0	0.0		0.0	0.0		0.0	0.0	
90.00	45.60	-29.30		40.60	-18.90		42.60	-14.90		0.0	0.0		0.0	0.0		0.0	0.0	
95.00	45.60	-29.30		40.60	-18.90		42.60	-14.90		0.0	0.0		0.0	0.0		0.0	0.0	
100.00	45.60	-29.30		40.60	-18.90		42.60	-14.90		0.0	0.0		0.0	0.0		0.0	0.0	
105.00	45.60	-29.30		40.60	-18.90		42.60	-14.90		0.0	0.0		0.0	0.0		0.0	0.0	
110.00	45.60	-29.30		40.60	-18.90		42.60	-14.90		0.0	0.0		0.0	0.0		0.0	0.0	
115.00	45.60	-29.30		40.60	-18.90		42.60	-14.90		0.0	0.0		0.0	0.0		0.0	0.0	
120.00	45.60	-29.30		40.60	-18.90		42.60	-14.90		0.0	0.0		0.0	0.0		0.0	0.0	
125.00	45.60	-29.30		40.60	-18.90		42.60	-14.90		0.0	0.0		0.0	0.0		0.0	0.0	
130.00	45.60	-29.30		40.60	-18.90		42.60	-14.90		0.0	0.0		0.0	0.0		0.0	0.0	
135.00	45.60	-29.30		40.60	-18.90		42.60	-14.90		0.0	0.0		0.0	0.0		0.0	0.0	
140.00	45.60	-29.30		40.60	-18.90		42.60	-14.90		0.0	0.0		0.0	0.0		0.0	0.0	
145.00	45.60	-29.30		40.60	-18.90		42.60	-14.90		0.0	0.0		0.0	0.0		0.0	0.0	
150.00	45.60	-29.30		40.60	-18.90		42.60	-14.90		0.0	0.0		0.0	0.0		0.0	0.0	
155.00	45.60	-29.30		40.60	-18.90		42.60	-14.90		0.0	0.0		0.0	0.0		0.0	0.0	
160.00	45.60	-29.30		40.60	-18.90		42.60	-14.90		0.0	0.0		0.0	0.0		0.0	0.0	
165.00	45.60	-29.30		40.60	-18.90		42.60	-14.90		0.0	0.0		0.0	0.0		0.0	0.0	
170.00	45.60	-29.30		40.60	-18.90		42.60	-14.90		0.0	0.0		0.0	0.0		0.0	0.0	
175.00	45.60	-29.30		40.60	-18.90		42.60	-14.90		0.0	0.0		0.0	0.0		0.0	0.0	
180.00	45.60	-29.30		40.60	-18.90		42.60	-14.90		0.0	0.0		0.0	0.0		0.0	0.0	
185.00	45.60	-29.30		40.60	-18.90		42.60	-14.90		0.0	0.0		0.0	0.0		0.0	0.0	
190.00	45.60	-29.30		40.60	-18.90		42.60	-14.90		0.0	0.0		0.0	0.0		0.0	0.0	
195.00	45.60	-29.30		40.60	-18.90		42.60	-14.90		0.0	0.0		0.0	0.0		0.0	0.0	
200.00	45.60	-29.30		40.60	-18.90		42.60	-14.90		0.0	0.0		0.0	0.0		0.0	0.0	

FIGURE 13-21 Example Region Line Segment Movement from Example 1

OCT 18, 1978 02:51:55

GM HYBRID II DUMMY (PRELIMINARY DATA)

KNEE BAR

NVMA 2-D TUTORIAL EXAMPLE #1

OCC. COMP. DISPL. 30MPH FRONT BARRIER

NO DELTS

(7-77)

PAGE 104-04

CONTACT INTERACTION BETWEEN

ELLIPSE HIP MADE OF HIPKATL

AND

LINE CUSHION LINE 1 WHICH IS AN ELEMENT OF REGION SEAT CUSHION MADE OF SEAT MATERIAL

INITIAL LINE LENGTH = 13.50 (IN) EDGE CONSTANT = 3.164

TIME (MSEC)	DEFLECTION		DEFL. RATE LINE (IN/SEC)	ELLIPSE (IN/SEC)	LINE (IN)	FORCE		TANGHTL. (LB)	CONTACT LOCATION ON LINE		CONTACT LOCATION IN SPACE		CONTACT LOCATION ON BODY SEG.	
	LINE (IN)	ELLIPSE (IN)				NORMAL (LB)	POSITION (NORDIN.)		RATE (IN/SEC)	X (IN)	Z (IN)	X (IN)	7 (IN)	
3.0	0.87	0.00	0.	0.	0.	174.4	0.0	0.0	0.311	0.	19.67	-5.69	2.43	2.77
5.0	0.88	0.00	5.	0.	0.	176.2	80.6	80.6	0.313	17.	22.31	-5.69	2.43	2.77
10.0	0.95	0.00	21.	0.	0.	198.0	95.5	95.5	0.328	59.	24.94	-5.70	3.43	2.77
15.0	1.06	0.00	20.	0.	0.	231.4	123.9	123.9	0.351	57.	27.54	-5.72	3.42	2.77
20.0	1.18	0.00	29.	0.	0.	268.6	153.2	153.2	0.376	81.	30.13	-5.73	3.42	2.78
25.0	1.33	0.00	34.	0.	0.	318.4	204.1	204.1	0.410	98.	32.70	-5.75	3.42	2.77
30.0	1.51	0.00	38.	0.	0.	374.6	272.7	272.7	0.449	112.	35.23	-5.77	3.43	2.77
35.0	1.73	0.00	46.	0.	0.	514.8	458.3	458.3	0.496	141.	37.72	-5.81	3.43	2.77
40.0	1.95	0.01	45.	0.	1.	802.4	782.1	782.1	0.549	145.	40.13	-5.86	3.43	2.76
45.0	2.19	0.01	50.	6.	36.	1071.1	1208.0	1208.0	0.604	150.	42.38	-5.91	3.45	2.74
50.0	2.42	0.03	44.	36.	18.	1333.8	1747.8	1747.8	0.659	138.	44.35	-5.94	3.48	2.70
55.0	2.51	0.15	-5.	-3.	-3.	1415.1	2075.7	2075.7	0.705	106.	45.92	-5.98	3.54	2.62
60.0	2.49	0.29	-3.	-18.	-21.	1356.4	2114.3	2114.3	0.737	73.	47.02	-6.04	3.64	2.48
65.0	2.48	0.33	-22.	-21.	-32.	1146.5	1712.6	1712.6	0.773	29.	47.66	-6.11	3.79	2.22
70.0	2.42	0.27	-50.	-32.	-2.	579.2	724.2	724.2	0.782	25.	47.93	-6.29	3.90	1.95
75.0	2.24	0.14	-104.	-2.	-3.	209.5	196.5	196.5	0.793	37.	47.91	-6.63	4.18	1.34
80.0	1.83	0.07	-127.	-3.	-3.	133.5	84.2	84.2	0.809	51.	47.78	-7.13	4.32	0.74
85.0	1.26	0.06	-151.	-3.	0.	41.3	15.4	15.4	0.832	69.	47.61	-7.75	4.38	0.15
90.0	0.57	0.04	0.	0.	0.	0.0	0.0	0.0	0.0	0.	47.45	-8.52	4.37	-0.32
95.0	0.0	0.0	0.	0.	0.	0.0	0.0	0.0	0.0	0.	0.0	0.0	0.0	0.0
100.0	0.0	0.0	0.	0.	0.	0.0	0.0	0.0	0.0	0.	0.0	0.0	0.0	0.0
105.0	0.0	0.0	0.	0.	0.	0.0	0.0	0.0	0.0	0.	0.0	0.0	0.0	0.0
110.0	0.0	0.0	0.	0.	0.	0.0	0.0	0.0	0.0	0.	0.0	0.0	0.0	0.0
115.0	0.0	0.0	0.	0.	0.	0.0	0.0	0.0	0.0	0.	0.0	0.0	0.0	0.0
120.0	0.0	0.0	0.	0.	0.	0.0	0.0	0.0	0.0	0.	0.0	0.0	0.0	0.0
125.0	0.0	0.0	0.	0.	0.	0.0	0.0	0.0	0.0	0.	0.0	0.0	0.0	0.0
130.0	0.0	0.0	0.	0.	0.	0.0	0.0	0.0	0.0	0.	0.0	0.0	0.0	0.0
135.0	0.0	0.0	0.	0.	0.	0.0	0.0	0.0	0.0	0.	0.0	0.0	0.0	0.0
140.0	0.0	0.0	0.	0.	0.	0.0	0.0	0.0	0.0	0.	0.0	0.0	0.0	0.0
145.0	0.0	0.0	0.	0.	0.	0.0	0.0	0.0	0.0	0.	0.0	0.0	0.0	0.0
150.0	0.0	0.0	0.	0.	0.	0.0	0.0	0.0	0.0	0.	0.0	0.0	0.0	0.0
155.0	0.0	0.0	0.	0.	0.	0.0	0.0	0.0	0.0	0.	0.0	0.0	0.0	0.0
160.0	0.0	0.0	0.	0.	0.	0.0	0.0	0.0	0.0	0.	0.0	0.0	0.0	0.0
165.0	0.0	0.0	0.	0.	0.	0.0	0.0	0.0	0.0	0.	0.0	0.0	0.0	0.0
170.0	0.0	0.0	0.	0.	0.	0.0	0.0	0.0	0.0	0.	0.0	0.0	0.0	0.0
175.0	0.0	0.0	0.	0.	0.	0.0	0.0	0.0	0.0	0.	0.0	0.0	0.0	0.0
180.0	0.0	0.0	0.	0.	0.	0.0	0.0	0.0	0.0	0.	0.0	0.0	0.0	0.0

FIGURE 13-22 Example (A) Ellipse-line Contact Interaction from Example 1

FIGURE 13-22 Example (A) Ellipse-Line Contact Interaction from Example 1

(see footnote, page 348)

6/28/79

CONTACT INTERACTION BETWEEN

ELLIPSE HEAD ASSUMED TO BE RIGID

AND

LINE LM WHICH IS AN ELEMENT OF REGION WINDSHIELD MADE OF WINDSHIELD GLASS

INITIAL LINE LENGTH = 20.13(IN) EDGE CONSTANT = 0.0

TIME (MSEC)	DEFLECTION		DEFL. RATE (IN/SEC)	ELLIPSE (IN)	FORCE		TANGTL. (LB)	CONTACT LOCATION ON LINE		CONTACT LOCATION IN SPACE		CONTACT LOCATION ON BODY SPG.	
	LINE (IN)	ELLIPSE (IN)			NORMAL (LB)	HORNL (LB)		POSITION (NONDIM.)	RATE (IN/SEC)	X (IN)	Z (IN)	X (IN)	Z (IN)
0.0	0.0	0.0	0.0	0.0	0.0	0.0	0.0	0.0	0.0	0.0	0.0	0.0	0.0
5.00	0.0	0.0	0.0	0.0	0.0	0.0	0.0	0.0	0.0	0.0	0.0	0.0	0.0
10.00	0.0	0.0	0.0	0.0	0.0	0.0	0.0	0.0	0.0	0.0	0.0	0.0	0.0
15.00	0.0	0.0	0.0	0.0	0.0	0.0	0.0	0.0	0.0	0.0	0.0	0.0	0.0
20.00	0.0	0.0	0.0	0.0	0.0	0.0	0.0	0.0	0.0	0.0	0.0	0.0	0.0
25.00	0.0	0.0	0.0	0.0	0.0	0.0	0.0	0.0	0.0	0.0	0.0	0.0	0.0
30.00	0.0	0.0	0.0	0.0	0.0	0.0	0.0	0.0	0.0	0.0	0.0	0.0	0.0
35.00	0.0	0.0	0.0	0.0	0.0	0.0	0.0	0.0	0.0	0.0	0.0	0.0	0.0
40.00	0.0	0.0	0.0	0.0	0.0	0.0	0.0	0.0	0.0	0.0	0.0	0.0	0.0
45.00	0.0	0.0	0.0	0.0	0.0	0.0	0.0	0.0	0.0	0.0	0.0	0.0	0.0
50.00	0.0	0.0	0.0	0.0	0.0	0.0	0.0	0.0	0.0	0.0	0.0	0.0	0.0
55.00	0.0	0.0	0.0	0.0	0.0	0.0	0.0	0.0	0.0	0.0	0.0	0.0	0.0
60.00	0.0	0.0	0.0	0.0	0.0	0.0	0.0	0.0	0.0	0.0	0.0	0.0	0.0
65.00	0.0	0.0	0.0	0.0	0.0	0.0	0.0	0.0	0.0	0.0	0.0	0.0	0.0
70.00	0.0	0.0	0.0	0.0	0.0	0.0	0.0	0.0	0.0	0.0	0.0	0.0	0.0
75.00	0.67	0.0	195.0	0.0	950.5	636.8	0.0	0.247	518.0	55.80	-38.17	-3.91	-0.33
80.00	1.45	0.0	144.0	0.0	234.9	157.4	0.0	0.338	525.0	58.30	-37.46	-3.91	-0.35
85.00	2.11	0.0	114.0	0.0	369.2	247.4	0.0	0.432	528.0	60.73	-36.60	-3.93	-0.24
90.00	2.55	0.0	56.0	0.0	463.2	310.3	0.0	0.525	518.0	63.00	-35.57	-3.97	0.00
95.00	2.67	0.0	5.0	0.0	489.6	320.1	0.0	0.614	467.0	64.98	-34.34	-4.00	0.45
100.00	2.67	0.0	-10.0	0.0	449.8	301.4	0.0	0.635	335.0	66.44	-33.29	-3.87	1.50
105.00	2.60	0.0	-12.0	0.0	130.2	87.2	0.0	0.739	286.0	67.46	-32.42	-3.55	2.34
110.00	2.53	0.0	-14.0	0.0	65.8	44.1	0.0	0.786	237.0	68.32	-31.67	-3.13	2.98
115.00	2.40	0.0	-47.0	0.0	46.4	31.1	0.0	0.822	170.0	68.07	-30.99	-2.76	3.40
120.00	2.08	0.0	-77.0	0.0	4.4	3.0	0.0	0.846	97.0	69.01	-30.37	-2.48	3.63
125.00	1.67	0.0	-84.0	0.0	0.0	0.0	0.0	0.858	0.0	68.83	-29.85	-2.29	3.78
130.00	1.27	0.0	-77.0	0.0	0.0	0.0	0.0	0.863	0.0	68.48	-29.43	-2.11	3.90
135.00	0.92	0.0	-64.0	0.0	0.0	0.0	0.0	0.865	0.0	68.10	-29.10	-1.93	4.00
140.00	0.63	0.0	-52.0	0.0	0.0	0.0	0.0	0.867	0.0	67.74	-28.82	-1.76	4.09
145.00	0.39	0.0	-44.0	0.0	0.0	0.0	0.0	0.868	0.0	67.37	-28.61	-1.60	4.17
150.00	0.19	0.0	-36.0	0.0	0.0	0.0	0.0	0.865	0.0	66.96	-28.48	-1.42	4.24
155.00	0.03	0.0	-28.0	0.0	0.0	0.0	0.0	0.858	0.0	66.47	-28.45	-1.22	4.31
160.00	0.0	0.0	0.0	0.0	0.0	0.0	0.0	0.0	0.0	0.0	0.0	0.0	0.0
165.00	0.0	0.0	0.0	0.0	0.0	0.0	0.0	0.0	0.0	0.0	0.0	0.0	0.0
170.00	0.0	0.0	0.0	0.0	0.0	0.0	0.0	0.0	0.0	0.0	0.0	0.0	0.0
175.00	0.0	0.0	0.0	0.0	0.0	0.0	0.0	0.0	0.0	0.0	0.0	0.0	0.0
180.00	0.0	0.0	0.0	0.0	0.0	0.0	0.0	0.0	0.0	0.0	0.0	0.0	0.0

FIGURE 13-23 Example (B) Ellipse-Line Contact Interaction from Example 1

JUN 24, 197702:00:20
GM HYBRID II DUMMY (PRELIMINARY DATA)
HVMA 2-D TUTORIAL EXAMPLE #1
KNEE BAR OCC. COMP. DISPL. 303PH PRONT BARRIER NO BELTS
FEMUR AND TIBIA LOADS (LB)
WITH FEMUR SENSOR LOCATED 11.55(IN) FROM HIP

TIME	FEMUR		TIBIA	
	AXIAL AT	SHEAR AT	AXIAL AT	AXIAL AT
0.0	8.1	KNEE	KNEE	FOOT
5.00	-92.2	-4.6	-34.6	2.5
10.00	-131.2	-40.3	-66.6	7.3
15.00	-131.0	-68.8	14.8	-85.1
20.00	-131.9	-64.8	5.5	-82.3
25.00	-137.2	-61.1	-2.2	-77.6
30.00	-138.2	-60.0	-6.6	-72.2
35.00	-168.6	-52.9	-39.8	-64.0
40.00	321.6	-59.5	-56.9	-69.5
45.00	655.0	420.3	-498.8	470.8
50.00	1027.6	864.9	-1091.0	1145.5
55.00	1623.2	1383.9	-724.0	996.4
60.00	1517.9	2162.4	-572.7	903.9
65.00	670.8	2035.3	-1065.1	1130.8
70.00	26.2	1048.9	-871.8	718.6
75.00	106.1	221.0	-190.2	104.9
80.00	159.5	99.0	-151.4	107.4
85.00	212.7	71.6	-182.7	133.8
90.00	233.2	90.4	-255.7	175.7
95.00	-73.9	102.3	-281.3	175.8
100.00	1237.8	2.4	-236.7	103.8
105.00	5027.1	1627.2	-361.1	-624.0
110.00	1262.3	5848.4	-770.9	-1599.5
115.00	-577.4	1406.7	-1605.8	1367.9
120.00	-178.9	-750.1	-763.1	1028.1
125.00	97.7	-259.7	-332.6	410.7
130.00	-15.7	62.6	-168.7	132.3
135.00	-32.4	-26.7	-101.9	105.1
140.00	-43.9	-31.7	-87.0	92.4
145.00	-50.0	-34.1	-68.0	73.6
150.00	-54.7	-34.5	-49.7	54.3
155.00	-58.7	-35.3	-36.1	39.1
160.00	-63.6	-36.3	-15.5	16.5
165.00	-66.9	-38.4	-3.5	2.1
170.00	-77.9	-40.4	6.0	-10.0
175.00	-89.1	-43.8	-31.4	23.8
180.00	-94.0	-48.8	-30.6	18.7
185.00	-98.7	-51.6	-26.1	9.8
190.00	-23.0	-54.8	-20.7	-0.3
195.00	-25.4	-23.9	8.5	-17.8
200.00	-9.3	-26.5	12.4	-23.7
		-26.4	52.7	-58.6

FIGURE 13-24 Femur and Tibia Loads for Example 1

TIME	HEAD				CHEST				HIP			
	A-F	S-I	RESULTANT	A-P	S-I	RESULTANT	X	Z	RESULTANT	X	Z	RESULTANT
0.0	-0.199	0.980	1.000	0.485	-0.667	0.825	-0.543	-1.605	0.825	-0.543	-1.605	0.825
5.00	-2.445	0.877	2.598	-13.023	-3.607	13.513	-7.311	-3.560	13.513	-7.311	-3.560	13.513
10.00	-2.663	0.351	2.686	-12.607	-5.371	13.703	-6.601	1.691	13.703	-6.601	1.691	13.703
15.00	-2.617	0.011	2.617	-12.485	-5.667	13.711	-7.084	1.495	13.711	-7.084	1.495	13.711
20.00	-2.750	-0.003	2.750	-12.269	-6.024	13.668	-7.651	1.286	13.668	-7.651	1.286	13.668
25.00	-2.813	-0.073	2.814	-12.003	-6.445	13.623	-8.456	0.991	13.623	-8.456	0.991	13.623
30.00	-2.748	-0.390	2.776	-11.642	-6.751	13.458	-9.708	-0.115	13.458	-9.708	-0.115	13.458
35.00	-2.781	-1.103	2.991	-10.557	-8.369	13.471	-12.670	-1.231	13.471	-12.670	-1.231	13.471
40.00	1.134	-4.373	4.518	10.622	-0.935	18.646	-10.521	1.756	18.646	-10.521	1.756	18.646
45.00	-1.060	-5.353	5.457	19.145	-0.700	19.158	-21.853	0.728	19.158	-21.853	0.728	19.158
50.00	-3.815	-5.419	6.627	22.133	-1.332	22.173	-35.665	-1.752	22.173	-35.665	-1.752	22.173
55.00	-8.429	-4.341	9.481	10.842	-6.295	12.537	-56.717	3.199	12.537	-56.717	3.199	12.537
60.00	-10.226	1.000	10.275	8.828	-0.296	8.833	-54.579	5.142	8.833	-54.579	5.142	8.833
65.00	-11.206	12.104	16.495	6.004	0.950	6.079	-45.198	-6.229	6.079	-45.198	-6.229	6.079
70.00	-11.306	24.231	26.739	2.150	-0.393	2.196	-36.477	-19.870	2.196	-36.477	-19.870	2.196
75.00	56.073	94.908	110.235	12.636	12.000	17.426	-10.807	-14.942	17.426	-10.807	-14.942	17.426
80.00	0.875	9.974	10.012	13.738	21.866	25.824	0.685	-12.808	25.824	0.685	-12.808	25.824
85.00	9.894	20.242	22.530	14.280	27.616	30.910	4.391	-15.541	30.910	4.391	-15.541	30.910
90.00	13.299	35.806	38.196	14.253	27.616	31.077	9.313	-15.512	31.077	9.313	-15.512	31.077
95.00	44.284	-4.257	44.488	4.549	9.229	35.108	5.461	-32.311	35.108	5.461	-32.311	35.108
100.00	45.479	33.763	56.642	-4.470	13.903	14.628	-5.946	2.218	14.628	-5.946	2.218	14.628
105.00	14.325	5.420	15.316	-4.470	28.843	29.187	-59.711	12.448	29.187	-59.711	12.448	29.187
110.00	21.388	41.426	46.621	-4.260	16.458	17.001	-5.284	7.818	17.001	-5.284	7.818	17.001
115.00	12.403	44.020	45.733	-3.344	6.851	7.623	19.113	-1.738	7.623	19.113	-1.738	7.623
120.00	11.993	29.908	32.223	-0.590	3.982	4.026	9.071	-3.636	4.026	9.071	-3.636	4.026
125.00	9.871	13.695	16.882	1.392	8.286	8.402	4.707	-4.425	8.402	4.707	-4.425	8.402
130.00	8.464	2.364	8.787	3.746	7.309	8.213	2.324	1.906	8.213	2.324	1.906	8.213
135.00	6.523	-0.424	6.537	3.885	7.597	8.532	1.156	3.230	7.597	1.156	3.230	7.597
140.00	6.028	3.664	7.054	3.959	5.553	6.820	0.143	3.904	5.553	0.143	3.904	5.553
145.00	6.681	7.831	10.294	4.691	2.200	5.181	-0.540	3.972	5.181	-0.540	3.972	5.181
150.00	6.463	7.646	10.012	4.534	0.244	4.540	-0.951	3.459	4.540	-0.951	3.459	4.540
155.00	5.137	3.769	6.372	5.612	0.349	5.622	-1.703	4.906	5.622	-1.703	4.906	5.622
160.00	3.390	-0.649	3.451	5.076	-0.164	5.078	-2.191	5.009	5.078	-2.191	5.009	5.078
165.00	1.762	-2.546	3.097	4.155	-1.329	4.362	-2.460	4.858	4.362	-2.460	4.858	4.362
170.00	0.819	-1.543	1.747	-10.363	-7.022	12.518	0.444	-5.550	12.518	0.444	-5.550	12.518
175.00	-0.777	6.008	6.058	-12.334	-10.251	16.039	0.620	-7.161	16.039	0.620	-7.161	16.039
180.00	0.111	7.204	7.205	-13.245	-10.712	17.035	0.844	-7.429	17.035	0.844	-7.429	17.035
185.00	0.339	4.197	4.210	-13.012	-10.063	16.450	0.952	-7.271	16.450	0.952	-7.271	16.450
190.00	1.342	-0.110	1.346	-0.765	1.817	1.972	1.318	2.332	1.972	1.318	2.332	1.972
195.00	1.970	-2.370	3.082	-0.101	2.335	2.338	1.097	2.826	2.338	1.097	2.826	2.338
200.00	2.001	-2.148	2.936	13.684	6.315	15.071	-3.436	12.620	6.315	-3.436	12.620	6.315

FIGURE 13-25 Unfiltered Head, Chest, and Hip Accelerations for Example 1

SEVERITY INDICES FOR UNFILTERED ACCELERATIONS

HEAD										CHEST									
HIC= 491.21, BEG. TIME= 65.00, END TIME= 125.00					3 MSEC AVER= 133.633 AT TIME= 92.00					3 MSEC AVER= 145.528 AT TIME= 91.00									
3 MSEC AVER= 107.979 AT TIME= 74.00					3 MSEC AVER= 74.00					3 MSEC AVER= 74.00					3 MSEC AVER= 74.00				
PEAK= 128.533 AT TIME= 74.00					PEAK= 74.00					PEAK= 74.00					PEAK= 74.00				
SEVERITY INDEX					GMR MODIFIED S.I.					SEVERITY INDEX					GMR MODIFIED S.I.				
TIME	A-P	S-I	RESULTANT	A-P	S-I	RESULTANT	A-P	S-I	RESULTANT	A-P	S-I	RESULTANT	A-P	S-I	RESULTANT	A-P	S-I	RESULTANT	
0.0	0.0	0.0	0.0	0.0	0.0	0.0	0.0	0.0	0.0	0.0	0.0	0.0	0.0	0.0	0.0	0.0	0.0	0.0	
5.00	0.02	0.00	0.02	0.01	0.01	0.01	0.01	0.01	0.01	1.54	0.10	1.76	0.03	0.00	0.00	0.04	0.00	0.04	
10.00	0.09	0.00	0.08	0.01	0.01	0.01	0.01	0.01	0.01	4.44	0.34	5.15	0.08	0.00	0.00	0.12	0.00	0.12	
15.00	0.13	0.00	0.14	0.01	0.05	0.01	0.01	0.01	0.01	7.31	0.61	8.59	0.13	0.01	0.01	0.19	0.01	0.19	
20.00	0.19	0.00	0.20	0.01	0.18	0.01	0.01	0.01	0.01	10.08	0.96	12.03	0.18	0.01	0.01	0.27	0.01	0.27	
25.00	0.26	0.00	0.26	0.02	0.25	0.01	0.01	0.01	0.01	12.70	1.39	15.45	0.22	0.01	0.01	0.34	0.01	0.34	
30.00	0.32	0.00	0.33	0.02	0.27	0.02	0.02	0.02	0.02	15.11	1.95	18.84	0.25	0.01	0.01	0.41	0.01	0.41	
35.00	0.38	0.01	0.39	0.02	0.28	0.02	0.02	0.02	0.02	17.22	2.72	22.17	0.27	0.01	0.01	0.48	0.01	0.48	
40.00	0.40	0.09	0.51	0.02	0.28	0.02	0.02	0.02	0.02	19.28	3.18	26.72	0.47	0.02	0.02	0.70	0.02	0.70	
45.00	0.41	0.35	0.78	0.03	0.20	0.02	0.02	0.02	0.02	28.53	3.19	34.30	0.92	0.02	0.02	1.16	0.02	1.16	
50.00	0.45	0.71	1.22	0.04	0.28	0.03	0.02	0.02	0.02	30.26	3.19	44.04	1.74	0.03	0.03	1.98	0.03	1.98	
55.00	0.96	0.99	2.15	0.04	0.28	0.03	0.03	0.03	0.03	42.63	3.89	49.68	1.94	0.04	0.04	2.24	0.04	2.24	
60.00	2.35	1.06	3.69	0.05	0.29	0.04	0.04	0.04	0.04	44.30	4.03	51.57	1.95	0.04	0.04	2.25	0.04	2.25	
65.00	4.22	1.79	6.65	0.07	0.30	0.12	0.12	0.12	0.12	45.08	4.04	52.36	1.95	0.05	0.05	2.25	0.05	2.25	
70.00	6.35	9.41	17.83	0.09	0.98	1.46	1.46	1.46	1.46	45.29	4.04	52.58	1.95	0.06	0.06	2.26	0.06	2.26	
75.00	60.00	232.11	332.96	42.98	202.04	250.77	250.77	250.77	250.77	45.46	4.23	53.03	1.96	0.07	0.07	2.29	0.07	2.29	
80.00	73.35	292.79	417.04	44.38	238.40	312.54	312.54	312.54	312.54	48.37	11.00	64.32	2.02	0.55	0.55	3.56	0.55	3.56	
85.00	73.90	296.62	422.13	44.39	238.61	312.91	312.91	312.91	312.91	52.13	26.57	86.37	2.11	2.80	2.80	7.94	2.80	7.94	
90.00	76.66	318.40	449.03	44.44	243.69	320.41	320.41	320.41	320.41	56.17	47.67	114.70	2.22	6.59	6.59	14.69	6.59	14.69	
95.00	147.65	328.43	535.66	92.19	245.32	377.27	377.27	377.27	377.27	689.44	50.99	764.71	467.56	6.70	6.70	490.30	6.70	490.30	
100.00	244.74	347.77	666.76	161.54	250.31	493.44	493.44	493.44	493.44	692.16	53.28	770.33	467.57	6.74	6.74	490.38	6.74	490.38	
105.00	263.00	356.92	698.96	165.44	251.32	504.84	504.84	504.84	504.84	692.24	62.91	780.20	467.57	7.95	7.95	491.63	7.95	491.63	
110.00	269.47	375.89	728.22	165.86	257.68	516.82	516.82	516.82	516.82	692.41	76.10	793.91	467.57	9.37	9.37	493.17	9.37	493.17	
115.00	274.68	439.38	802.39	166.13	268.04	556.32	556.32	556.32	556.32	692.54	77.61	795.68	467.57	9.38	9.38	493.17	9.38	493.17	
120.00	271.09	486.09	854.60	166.16	304.71	576.74	576.74	576.74	576.74	693.18	71.83	796.71	467.59	9.38	9.38	493.20	9.38	493.20	
125.00	279.20	497.65	869.95	166.18	305.82	578.68	578.68	578.68	578.68	693.18	78.37	797.25	467.60	9.38	9.38	493.20	9.38	493.20	
130.00	280.60	498.66	872.77	166.19	305.83	578.72	578.72	578.72	578.72	693.27	78.95	798.02	467.60	9.38	9.38	493.20	9.38	493.20	
135.00	281.35	498.66	873.54	166.19	305.83	578.72	578.72	578.72	578.72	693.42	79.76	799.09	467.60	9.38	9.38	493.21	9.38	493.21	
140.00	281.83	498.69	874.06	166.19	305.84	578.72	578.72	578.72	578.72	693.57	80.36	799.94	467.61	9.38	9.38	493.21	9.38	493.21	
145.00	282.32	499.17	875.22	166.20	305.84	578.73	578.73	578.73	578.73	693.76	80.53	800.36	467.61	9.39	9.39	493.21	9.39	493.21	
150.00	282.68	500.12	877.00	166.20	305.85	578.74	578.74	578.74	578.74	693.99	80.54	800.62	467.61	9.39	9.39	493.21	9.39	493.21	
155.00	283.40	500.53	878.10	166.20	305.85	578.75	578.75	578.75	578.75	694.34	80.54	800.97	467.61	9.40	9.40	493.21	9.40	493.21	
160.00	283.61	500.56	878.36	166.20	305.86	578.75	578.75	578.75	578.75	694.67	80.54	801.30	467.61	9.42	9.42	493.21	9.42	493.21	
165.00	283.67	500.58	878.45	166.20	305.86	578.75	578.75	578.75	578.75	694.90	80.54	801.55	467.61	9.43	9.43	493.21	9.43	493.21	
170.00	283.67	500.63	878.51	166.21	305.86	578.75	578.75	578.75	578.75	695.14	80.62	801.92	467.61	9.43	9.43	493.22	9.43	493.22	
175.00	283.68	500.77	878.67	166.21	305.86	578.76	578.76	578.76	578.76	697.37	81.93	806.10	467.64	9.44	9.44	493.35	9.44	493.35	
180.00	283.68	501.40	879.31	166.23	305.87	578.76	578.76	578.76	578.76	700.18	83.65	811.44	467.69	9.46	9.46	493.57	9.46	493.57	
185.00	283.68	501.82	879.74	166.23	305.87	578.76	578.76	578.76	578.76	703.14	85.26	816.83	467.74	9.47	9.47	493.78	9.47	493.78	
190.00	283.70	501.86	879.80	166.24	305.87	578.76	578.76	578.76	578.76	704.44	85.91	819.13	467.76	9.47	9.47	493.84	9.47	493.84	
195.00	283.72	501.88	879.86	166.24	305.88	578.76	578.76	578.76	578.76	704.44	85.96	819.18	467.77	9.47	9.47	493.84	9.47	493.84	
200.00	283.76	501.93	879.95	166.24	305.88	578.76	578.76	578.76	578.76	704.64	86.05	819.53	467.79	9.48	9.48	493.86	9.48	493.86	

FIGURE 13-26 Severity Indices for Unfiltered Accelerations for Example 1

13.4 Input Data for Example 2

The second example data set includes the same 30-mph frontal barrier crash acceleration profile as used for Example 1. Simulation Example 2 is similar to Example 1 in other ways also. It uses the same occupant description data subset and the occupant is positioned within the vehicle in an identical manner. The vehicle interior used is basically the same. The primary difference between Examples 1 and 2 is that while both occupants are restrained by a knee bar, the occupant in Example 2 is additionally restrained by a torso harness. There are a number of other differences in the data sets. None of these should affect the crash dynamics; they have been included to illustrate various program options.

13.4.1 Belt Restraint System. The three-belt submodel described in Module 9 is used for this simulation. Since simulation Example 1 was for an occupant unrestrained by belts, the belt system usage switch in field 1 of Card 102 was set to 0. For Example 2, however, Card 102 in Figure 13-30 is seen to have a 2. in field 1. This indicates usage of the three-belt submodel with both lap and torso restraints. Since it is desired for this simulation to have only the torso harness and the knee bar as restraints, and not a lap belt, the belt system data subset shown in Figure 13-27 includes some specifications worthy of note.

While any of the seven belt segments of the Advanced Belt-Restraint Submodel may be included or omitted from a belt system design, the Three-Belt Submodel is not as flexible. It must include either both lap belt and torso harness or the lap belt alone. Therefore, in the data subset shown, in order to effectively eliminate the lap belt, a belt material named NO STRENGTH is defined by 704- and 705-Cards and is prescribed a zero stiffness with a 708-Card. This belt material is assigned to the lap belt on Card 702.

The torso belts are each pre-tensioned to 5 lb. This is done by assigning negative values for initial slack on Cards 701 and 702. Belt anchor locations and attachment points on the occupant are prescribed on Cards 501 and 218.

2.75	7.	0.	0.	0.	1.8	-1.96	14.12	-5.07	218
0.	0.	0.	0.	0.	-33.52	17.	-1.2		501
100.	0.	15.13	-.00178	6600.	6600.	10.			701
NO STRENGTH				14.04	-.00172	2.	1.		702
6% WEAVING #1				6% WEBBING #2					703
6% WEAVING #1	0.	0.	0.16	14.36	15.04	0.	0.		704
6% WEAVING #1	5.				SBELT1	IZERO	GBELT1		705
GBELT1	0.	0.							706
GBELT1	.16	0.							706
GBELT1	1.37	.56							706
GBELT1	6.15	.95							706
GBELT1	40.	.95							706
GBELT1	0.	1.							707
GBELT1	1.37	.33							707
GBELT1	2.06	.19							707
GBELT1	6.15	.05							707
GBELT1	40.	.05							707
SBELT1	0.	0.							708
SBELT1	.533	1500.							708
SBELT1	9.91	2000.							708
SBELT1	11.28	5300.							708
SBELT1	14.36	6600.							708
SBELT1	15.04	0.							708
5% WEAVING #2	0.	0.	.155	13.85	14.51	0.	0.		704
6% WEAVING #2	5.				SBELT2	IZERO	GBELT1		705
SBELT2	0.	0.							708
SBELT2	.396	1150.							708
SBELT2	9.56	1650.							708
SBELT2	10.9	5300.							708
SBELT2	13.85	6600.							708
SBELT2	14.51	0.							708
NO STRENGTH	0.	0.	0.	10.	11.	0.	0.		704
NO STRENGTH	5.				SNOSTR	IZERO	GNOSTR		705
GNOSTR	-1.	0.							706
GNOSTR	-1.	1.							707
SNOSTR	-1.	0.							708

FIGURE 13-27 Belt Restraint System Cards for Example 2

13.4.2 Auxiliary Debugging Printout. Module 12 explains the use of 104- and 105-Cards for obtaining "debugging" printout of intermediate results from the Execution Processor. Time-dependent, multi-level switches may be set for sixteen divisions of program variables. Figure 13-28 illustrates specifications for debugging printout for Example 2 from 0 to 3 ms and from 198 to 200 ms inclusive. Printout beginning at times zero will be for switches 1, 7, 9, 10, 11, and 16 at levels 3, 1, 3, 3, 2, and 2, respectively. At 1.1 ms, switches 7 and 16 are set to 0, and at 3.1 ms all debugging printout is suppressed. At 198 ms, all sixteen switches are set at level 1; debugging printout continues through the end of the simulation (200 ms for Example 2) since the switches are not reset to 0. Field 9 of Card 104 is set to 1. in order to limit debugging printout to each final evaluation for the four-step Runge-Kutta integration. A "packing dictionary," which is often useful in interpreting debugging printout, is requested by defaulting the ninth field of Card 105 to 0. by omission of the card from the data deck.

13.4.3 Output Variable Storage. Section 13.2.11.1 has explained the use of Cards 1001 and 1002 for specifying categories of calculated data for which printout is desired. It should be kept in mind that in order for the Output Processor to print out variables in response to specifications on Cards 1001 and 1002, those variables must first be stored in an external file. Specification of categories which are to be stored during execution of the "GO" processor for possible later printout is made separately through use of Cards 107 through 111. For Example 1, these cards were omitted from the data deck and thus, by default, all categories were stored for printout. However, the data deck for Example 2 includes the cards shown in Figure 13-29. Only variables for categories for which a "0." is specified will be written to the external file for possible printout. Use of Cards 107 through 111 is explained in Module 12.

13.4.4 Other "Example 2" Modifications. Additional differences between the data decks for Example 1 and Example 2 include the following. (These can be seen in comparing the appropriate sections of their complete data decks, which are shown in Figures 13-14 and 13-30.) First, the vehicle interior for Example 2 does not include the ROOFHEADER,

0.	C004F8021.1	C000F8003.1	00000000198.	555555551.	104
----	-------------	-------------	--------------	------------	-----

FIGURE 13-28 Debugging Printout Specifications for Example 2

0.	1.	1.	0.	0.	0.	1.	0.	1.	107
0.	0.	0.	0.	0.	0.	1.	1.	1.	108
1.	1.	0.	0.	0.	0.	0.	0.	1.	109
1.	1.	0.	0.	0.	1.	1.	1.	1.	110
0.	1.	1.	0.	0.	0.	0.	0.	0.	111

FIGURE 13-29 Specifications for Storage of Output Categories for Example 2

WINDSHIELD, and INSTRUMENT PANEL regions. Second, the 106-Cards are absent from the data deck, and interaction "inhibition" controls on Card 102 are redefined so that all potential ellipse-line interactions are investigated. Third, the THORAX and HIP ellipses have been made rigid since materials were defined for them for Example 1 only because of the possibility of THORAX-INSTRUMENT PANEL and HIP-FLOOR interactions. Finally, printout of the summary of the input data is often not desired; it is suppressed for Example 2 by removing Category 0 from the string on Card 1001. Alternatively, a 1001-Card containing only "-1" in columns one and two could have been used. This requests the default ordering for Categories 1 through 40 and 46 through 50 with omission of printout of the input data summary, Category 0.

13.5 Selected Output from Simulation Example 2

Selected pages of printout produced by the complete Example 2 data deck in Figure 13-30 are shown as Figures 13-31 through 13-36. These are: a printer-plot stick figure sequence; example debugging printout; belt system data; body link angle accelerations; head, chest, and hip accelerations; and HIC and Severity Indices.

MVMA 2-D TUTORIAL EXAMPLE #2										100
KNEE BAR										400
300. COMP. DISPL.										500
30MPH FRONT BARRIER										600
FORCE-LIM. HARNESS										700
NO LAP BELT										800
1.	1.	32.174	0.	0.	200.	1.	5.	10.		101
2.	0.	0.	0.	1.	1.	10.	.000001	5.		102
.2	.05	100000.	15000.	10.	.05	10.	1.	1.		103
0.	C004F8021.1		C000F8003.1		00000000198.		555555551.			104
0.	1.	1.	0.	0.	0.	1.	0.	1.		107
0.	0.	0.	0.	0.	0.	1.	1.	1.		108
1.	1.	0.	0.	0.	0.	0.	0.	1.		109
1.	1.	0.	0.	0.	1.	1.	1.	1.		110
0.	1.	1.	0.	0.	0.	0.	0.	0.		111
0.	44.	0.	0.	0.	0.	0.	0.			601
23.	1.	1.								602
0.	-1.7	1.	-1.4	7.	-33.9	12.	2.8			
13.5	3.9	18.	-21.2	21.5	-12.4	28.	-9.2			
32.	-24.0	33.	-24.0	36.	-9.9	37.	-9.9			
42.	-26.9	47.	-31.9	50.	-25.9	54.	-27.2			
58.	-32.2	61.	-29.0	76.	-6.9	90.	-1.4			
100.	-1.4	120.	0.	300.	0.					
2.	1.	1.								603
0.	0.	300.	0.							
2.	1.									604
0.	0.	300.	0.							
GM HYBRID II DUMMY										200
(PRELIMINARY DATA)										300
1.1	13.44	3.4	5.	15.8		10.3	3.25	-.88		201
2.75	7.	1.7	4.2	8.2	9.3	5.	5.8	.5		202
.0250	.0951	.0052	.0992	.0932	.0518	.022	.0256	.007		203
.198	1.07	.04	1.53	1.39	2.82	.18	.62			204
12.8	.59	0.	.52	17.4	1.		-25.	.35		205
12.8	.59	0.	.52	17.4	1.		-22.	.35		206
72.	15.	0.	.66	1000.	1.	-8.	-25.5	.35		207
102.5	-7.624	.1944	.66	1000.	1.	-33.999	-34.001	.35		208
84.44	-4.810	.1053	0.	850.	1.	-49.999	-50.001	.5		209
0.	29.8	0.	0.	204.	1.	135.	0.	.5		210
0.	10.	0.	0.	222.	1.	28.	-197.	.5		211
0.	10.	0.	0.	64.	1.	0.	-165.	.5		212
751.	0.	757.	1.98							213
20.	230.	0.	0.			2.		.5		214
38.	.58	0.	.52	0.	1.	-1.		.16		215
38.	.58	0.	.52	0.	1.	2.		.16		216
751.	0.	757.	1.98							242
HEAD				1.	3.					219
THORAX				2.	1.					219
HIP				4.	1.					219
THIGH				5.	1.					219
KNEE				5.	1.					219
SHANK				6.	1.					219
HEEL				6.	2.					219
TOE				6.	2.					219
ELBOW				7.	1.					219
HAND				8.	3.					219
HEAD		0.	.5	4.	4.					220
THORAX		-.5	-.68	5.52	4.44					220
HIP		-.12	0.	4.5	4.5					220
THIGH		-.5	-.1	7.	3.					220

FIGURE 13-30 Complete Data Set for Simulation Example 2 (page 1 of 5)

KNEE	7.	-4	2.25	2.25					220
SHANK	-7.54	0.	3.	2.4					220
HEEL	8.57	0.	1.2	1.2					220
TOE	5.61	-5.16	1.2	1.2					220
ELBOW	5.3	0.	1.5	1.5					220
HAND	5.6	-4	2.72	1.52					220
CHESTMATL	0.	0.	0.	100.	101.	0.	0.		221
CHESTMATL	5.				CSTAT	IZERO	CGR		222
CGR	-1.	-1							223
CGR	0.	1.							224
CGR	.01	.64							224
CGR	.3	.5							224
CGR	1.35	.45							224
CSTAT	0.	0.							225
CSTAT	.01	1125.							225
CSTAT	.05	1460.							225
CSTAT	.3	1350.							225
CSTAT	.4	1260.							225
CSTAT	1.1	1260.							225
CSTAT	4.25	12600.							225
IZERO	-1.	0.							226
HIPMATL	0.	0.	0.	100.	101.	0.	0.		221
HIPMATL	5.				CSTAT	IZERO	CGR		222
-11.	-9.	-19.	-34.	-50.	0.	0.	0.		217
78.5	97.5	115.5	140.5	19.5	-45.	-41.	3.	89.5	301
0.	0.	0.	0.	0.	0.	0.	0.	0.	302
12.2	0.	-21.4	0.	3.29	0.				303
0.	0.	0.	0.						304
SEAT BACK	SEAT MATERIAL		0.	1.	1.	1.			401
SEAT BACK	1.	1.	1.	0.	0.				402
SEAT MATERIAL	0.	0.	1.6	3.5	4.	0.	0.		403
SEAT MATERIAL	5.				SSEAT	IZERO	GRSEAT		404
GRSEAT	-1.	.1							405
GRSEAT	-1.	.5							406
SSEAT	0.	0.							407
SSEAT	.8	150.							407
SSEAT	1.6	400.							407
SSEAT	3.	2000.							407
SSEAT	3.5	4000.							407
SSEAT	4.	0.							407
BACK LINE	SEAT RACK		5.	0.	-1.	1.			409
BACK LINE	1.								410
BACK LINE	-1.	6.2	-25.8	15.44	-4.96				411
SEAT CUSHION	SEAT MATERIAL		0.	1.	1.	1.			401
SEAT CUSHION	2.	1.	1.	0.	0.				402
CUSHION LINE 1	SEAT CUSHION		5.	.164	1.	1.			409
CUSHION LINE 1	1.								410
CUSHION LINE 1	-1.	15.44	-4.96	28.	-9.92				411
CUSHION LINE 2	SEAT CUSHION		5.	.5	-1.	2.			409
CUSHION LINE 2	1.								410
CUSHION LINE 2	-1.	28.	-9.92	32.24	-10.64				411
FLOOR	FMATL		0.	1.	1.	1.			401
FLOOR	2.	2.	1.	0.	0.				402
SEAT BOTTOM	FLOOR		5.	0.	-1.	1.			409
SEAT BOTTOM	1.								410
SEAT BOTTOM	-1.	31.2	-8.	31.2	-.84				411
FLOORBOARD	FLOOR		5.	0.	-1.	2.			409
FLOORBOARD	1.								410
FLOORBOARD	-1.	31.2	-.84	49.	-.84				411
TOEPAN	FMATL		0.	1.	1.	1.			401

FIGURE 13-30 Complete Data Set for Simulation Example 2 (page 2 of 5)

TOEPAN	1.	2.	1.	0.	0.			402
TOBOARD	TOEPAN		5.	0.	1.	1.		409
TOBOARD	4.							410
TOBOARD	0.	47.3	1.1	54.7	-5.5			411
TOBOARD	40.	47.3	1.1	54.7	-5.6			411
TOBOARD	80.	47.3	1.1	47.9	-5.6			411
TOBOARD	300.	47.3	1.1	47.9	-5.6			411
KNEE BAR	SHEET METAL		0.	1.	1.	1.		401
KNEE BAR	1.	3.	1.	0.	0.			402
SHEET METAL	0.	0.	.5	8.	9.	10000.	10000.	403
SHEET METAL	5.				SSHEET	IZERO	GRSHEET	404
GRSHEET 0.	0.							405
GRSHEET 0.5	0.							405
GRSHEET 5.5	0.9							405
GRSHEET 0.	1.							406
GRSHEET .5	1.							406
GRSHEET 2.	.7							406
GRSHEET 4.	.2							406
GRSHEET 5.5	.15							406
GRSHEET 9.	.1							406
GRSHEET 9.	.01							406
SSHEET 0.	0.							407
SSHEET 2.	1500.							407
SSHEET 4.	1500.							407
SSHEET 5.5	10000.							407
SSHEET 9.	10000.							407
SSHEET 9.	0.							407
KNEEBAR LINE	KNEE BAR		5.	0.5	1.	1.		409
KNEEBAR LINE	4.							410
KNEEBAR LINE	0.	40.4	-13.2	38.9	-16.4			411
KNEEBAR LINE	40.	40.4	-13.2	38.9	-16.4			411
KNEEBAR LINE	80.	38.9	-13.2	37.4	-16.4			411
KNEEBAR LINE	300.	38.9	-13.2	37.4	-16.4			411
DASH	DASHMATL		0.	1.	1.	1.		401
DASH	1.	2.	1.	0.	0.			402
DASHLINE	DASH		5.	0.	1.	1.		409
DASHLINE	4.							410
DASHLINE	0.	54.7	-5.6	54.2	-20.1			411
DASHLINE	40.	54.7	-5.6	54.2	-20.1			411
DASHLINE	80.	47.9	-5.6	47.4	-20.1			411
DASHLINE	300.	47.9	-5.6	47.4	-20.1			411
DASHMATL	0.	0.	0.	100.	101.	0.	0.	403
DASHMATL	5.				DSTAT	IZERO	DGR	404
DGR	0.	0.						405
DGR	.001	.01						405
DGR	10.	.01						405
DGR	0.	1.						406
DGR	.001	.91						406
DGR	.75	.8						406
DGR	1.5	.5						406
DGR	10.	.3						406
DSTAT	0.	0.						407
DSTAT	0.75	2100.						407
DSTAT	1.5	9000.						407
DSTAT	40.	9000.						407
FMATL	0.	0.	0.	100.	101.	0.	0.	403
FMATL	5.	0.	0.	0.	FSTAT	IZERO	FGR	404
FGR	0.	0.						405
FGR	2.	.7						405
FGR	0.	1.						406

FIGURE 13-30 Complete Data Set for Simulation Example 2 (page 3 of 5)

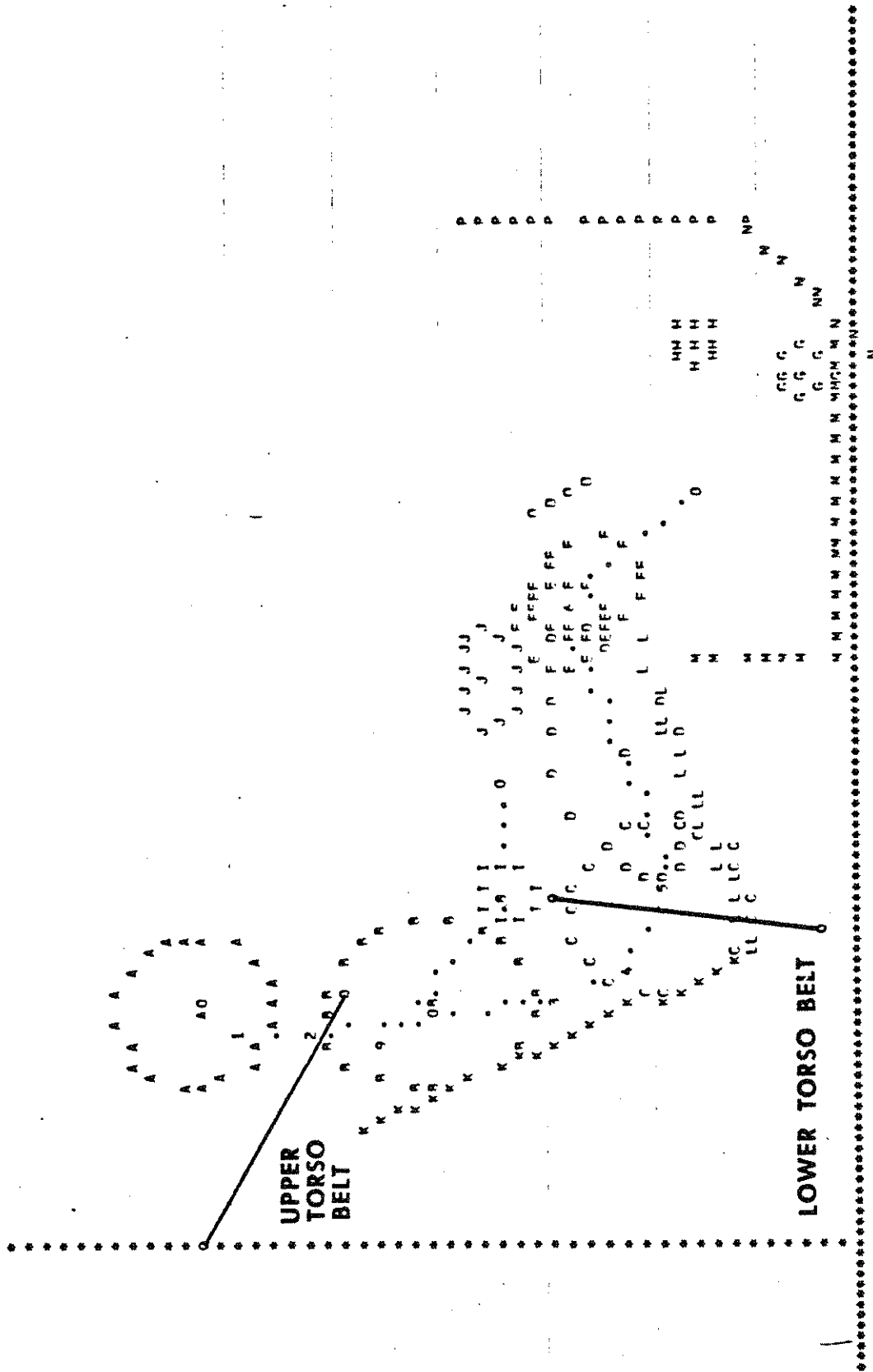
FGR	2.	.2								406
FSTAT	0.	0.								407
FSTAT	.25	100.								407
FSTAT	.5	400.								407
FSTAT	.75	1200.								407
FSTAT	1.	2400.								407
FSTAT	1.5	4000.								407
FSTAT	2.	4600.								407
FSTAT	3.	5000.								407
FSTAT	4.	5200.								407
FSTAT	6.	5400.								407
FSTAT	10.	5600.								407
FSTAT	16.	10000.								407
1.	1.	.25	.125	.125						412
1.	2.	.5								412
1.	3.	.5								412
1.	4.	.4								412
2.	2.	.8								412
3.	1.	.4								412
3.	2.	.5								412
3.	4.	.4								412
3.	5.	.67								412
3.	6.	.9								412
2.75	7.	0.	0.	0.	1.8	-1.96	14.12	-5.07		218
0.	0.	0.	0.	0.	-33.52	17.	-1.2			501
100.	0.	15.13	-.00178	6600.	6600.	10.				701
NO STRENGTH				14.04	-.00172	2.	1.			702
6% WEARING #1				6% WEBBING #2						703
6% WEARING #1	0.	0.	0.16	14.36	15.04	0.	0.			704
6% WEARING #1	5.				SBELT1	IZERO	GBELT1			705
GBELT1	0.	0.								706
GBELT1	.16	0.								706
GBELT1	1.37	.56								706
GBELT1	6.15	.95								706
GBELT1	40.	.95								706
GBELT1	0.	1.								707
GBELT1	1.37	.33								707
GBELT1	2.06	.19								707
GBELT1	6.15	.05								707
GBELT1	40.	.05								707
SBELT1	0.	0.								708
SBELT1	.533	1500.								708
SBELT1	9.91	2000.								708
SBELT1	11.28	5300.								708
SBELT1	14.36	6600.								708
SBELT1	15.04	0.								708
5% WEARING #2	0.	0.	.155	13.85	14.51	0.	0.			704
6% WEBBING #2	5.				SBELT2	IZERO	GBELT1			705
SBELT2	0.	0.								708
SBELT2	.396	1150.								708
SBELT2	9.56	1650.								708
SBELT2	10.9	5300.								708
SBELT2	13.85	6600.								708
SBELT2	14.51	0.								708
NO STRENGTH	0.	0.	0.	10.	11.	0.	0.			704
NO STRENGTH	5.				SNOSTR	IZERO	GNOSTR			705
GNOSTR	-1.	0.								706
GNOSTR	-1.	1.								707
SNOSTR	-1.	0.								708
										1000

FIGURE 13-30 Complete Data Set for Simulation Example 2 (page 4 of 5)

1, 46-48, 10-14, 21, 22, 37, 38, 49, 50, 15, 23-26, 2-5, 18-20, 33-36, 30-32, 16,								1001
27-29, 39, 17, 40, 6-9, 45								1002
0.	0.	0.	11.55	.025				1003
40.	500.	560.	0.	.85	201.	5.	5.	1004
0.	0.	-3.	62.	5.	-44.	10.	0.	1500
21.	0.	0.	1.	1.	0.	1.	0.	1501
							10.	1600

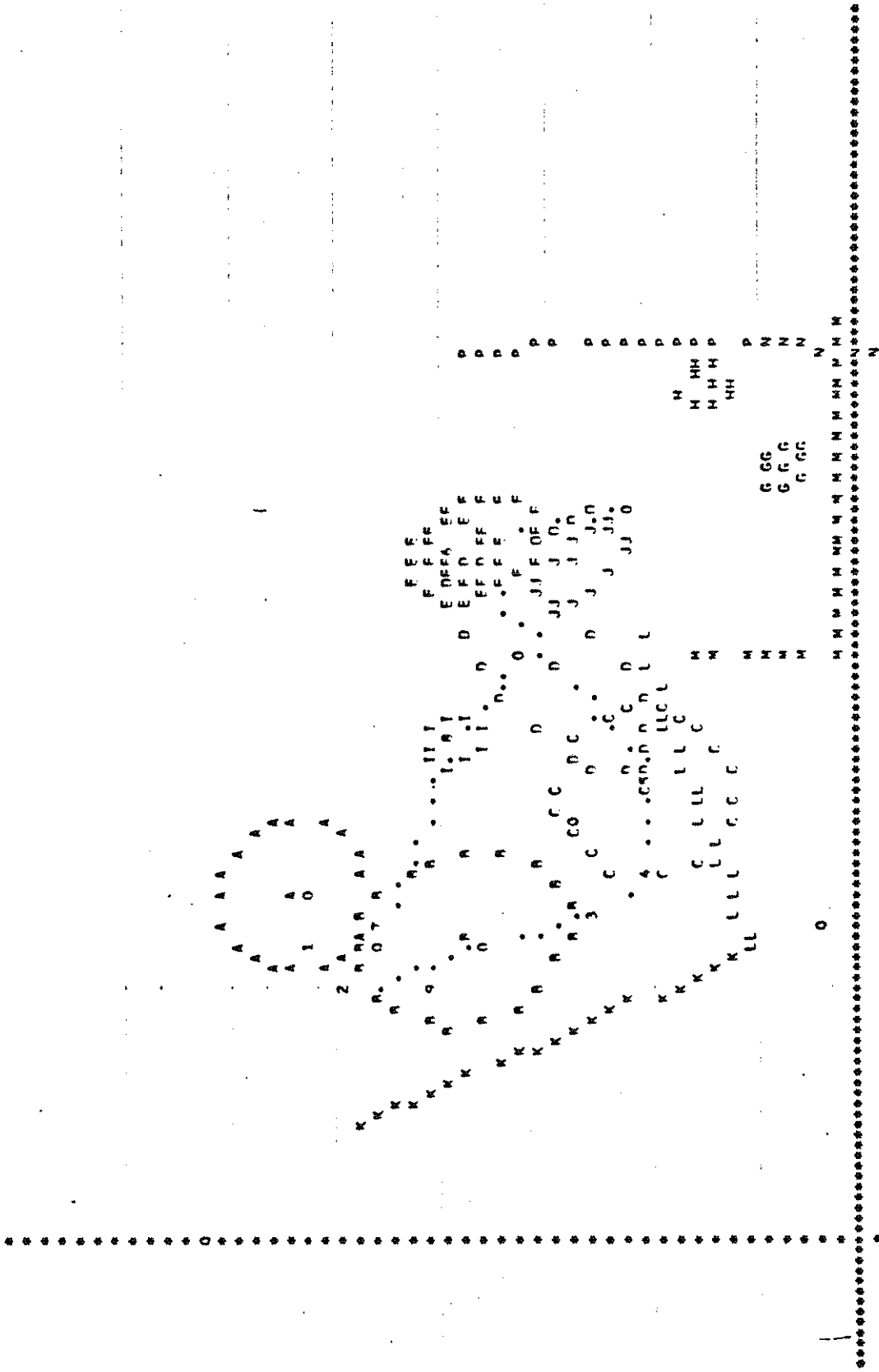
FIGURE 13-30 Complete Data Set for Simulation Example 2 (page 5 of 5)

STICK FIGURE PRINTER PLOT FRAME END TIME 0.0 MSEC.



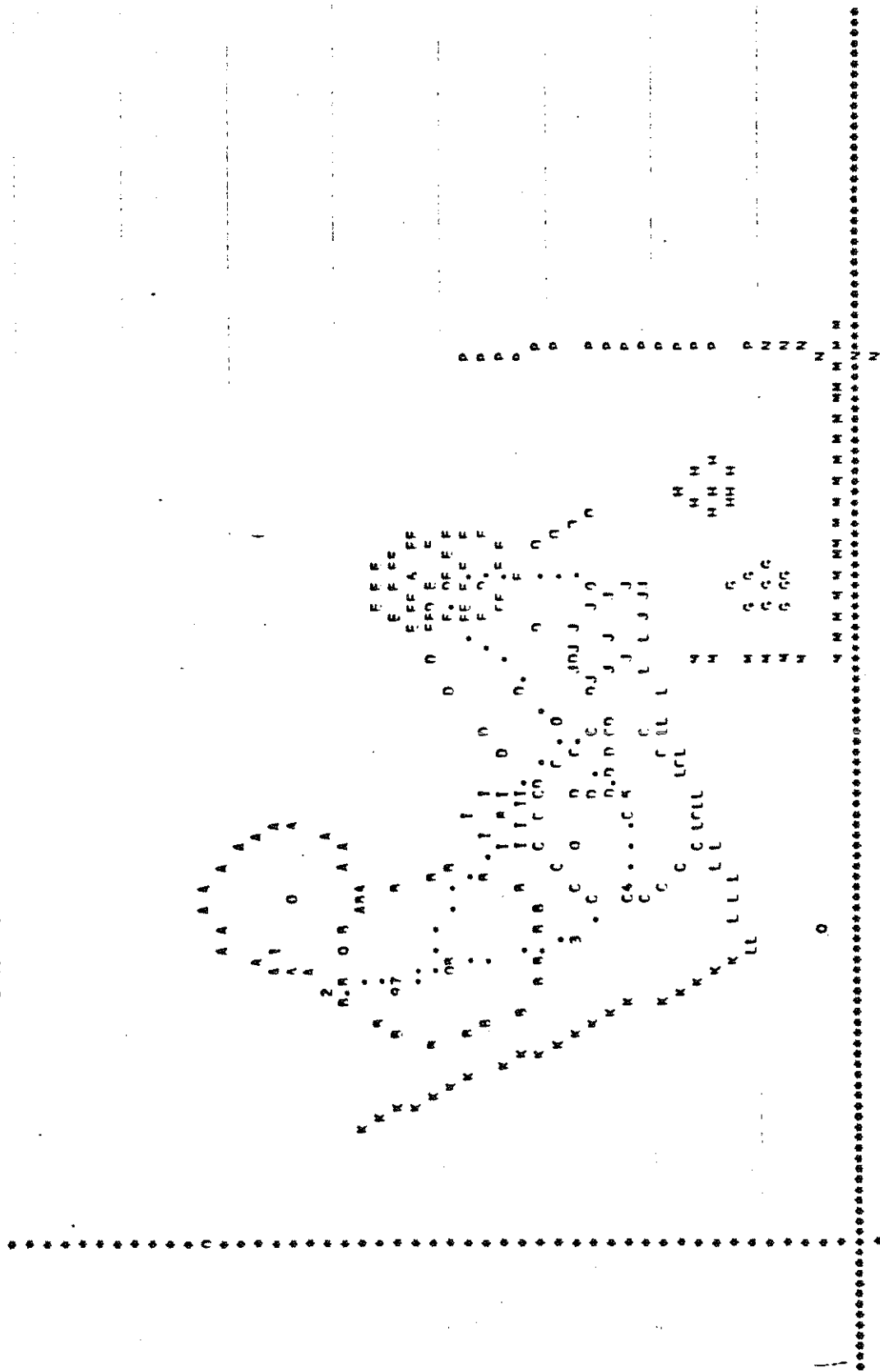
COORDINATE RANGES FOR PLOT ARE X = -6.56 (AT LEFT) TO 65.56 (AT RIGHT) AND Z = 5.00 (AT BOTTOM) TO -44.00 (AT TOP)
 SCALE FACTOR IS (IN) = 5.547 (IN) , X AND Z POINT RESOLUTION ERRORS EQUAL RESPECTIVELY 0.277 AND 0.462 (IN) IN SCALE.

FIGURE 13-31a Printer-Plot Time Sequence for Example 2 (0 ms)



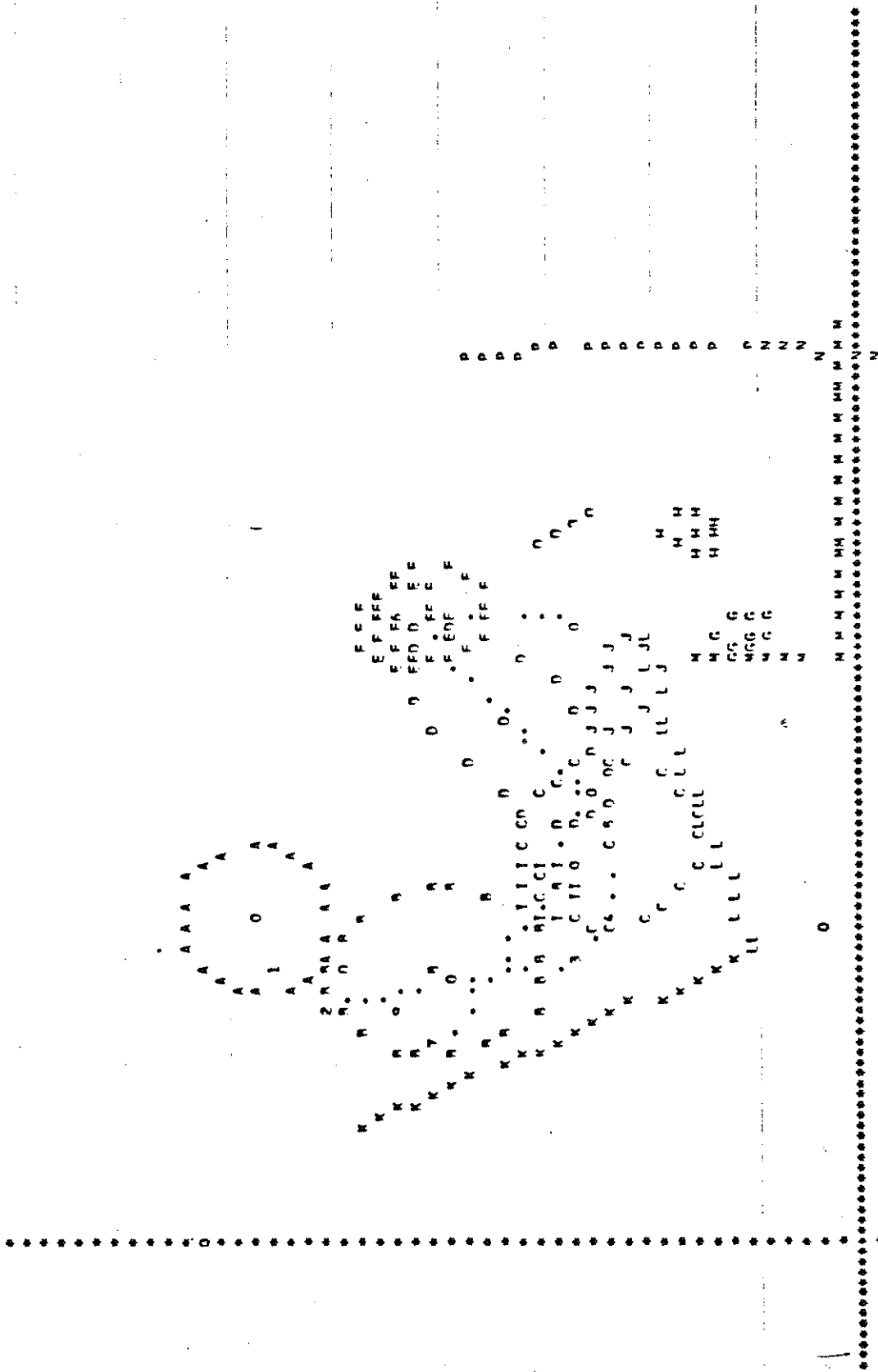
COORDINATE RANGES FOR PLOT ARE X= -6.56 (AT LEFT) TO 65.56 (AT RIGHT) AND Z= 5.00 (AT BOTTOM) TO -44.00 (AT TOP)
 SCALE FACTOR IS (IN) = 5.547 (IN) . X AND Z POINT RESOLUTION ERRORS EQUAL RESPECTIVELY 0.277 AND 0.467 (IN) IN SCALE.
 FIGURE 13-31d Printer-Plot Time Sequence for Example 2 (80 ms)

JUN 26, 1977 02:02:11
 GM WARRIN II DUMMY (PRELIMINARY DATA) KNEE BAR MVNA 2-D TUTORIAL EXAMPLE #2 PAGE 31-45
 STICK FIGURE PRINTER PLOT FRAME FOR TIME= 100.00 MSEC. NO LAP BELT



COORDINATE RANGES FOR PLOT ARE X= -4.56 (AT LEFT) TO 6.56 (AT RIGHT) AND Z= 5.00 (AT BOTTOM) TO -4.00 (AT TOP)
 SCALE FACTOR IS (IN) = 5.547 (IN) , X AND Z POINT RESOLUTION ERRORS EQUAL RESPECTIVELY 0.277 AND 0.462 (IN) IN SCALE.

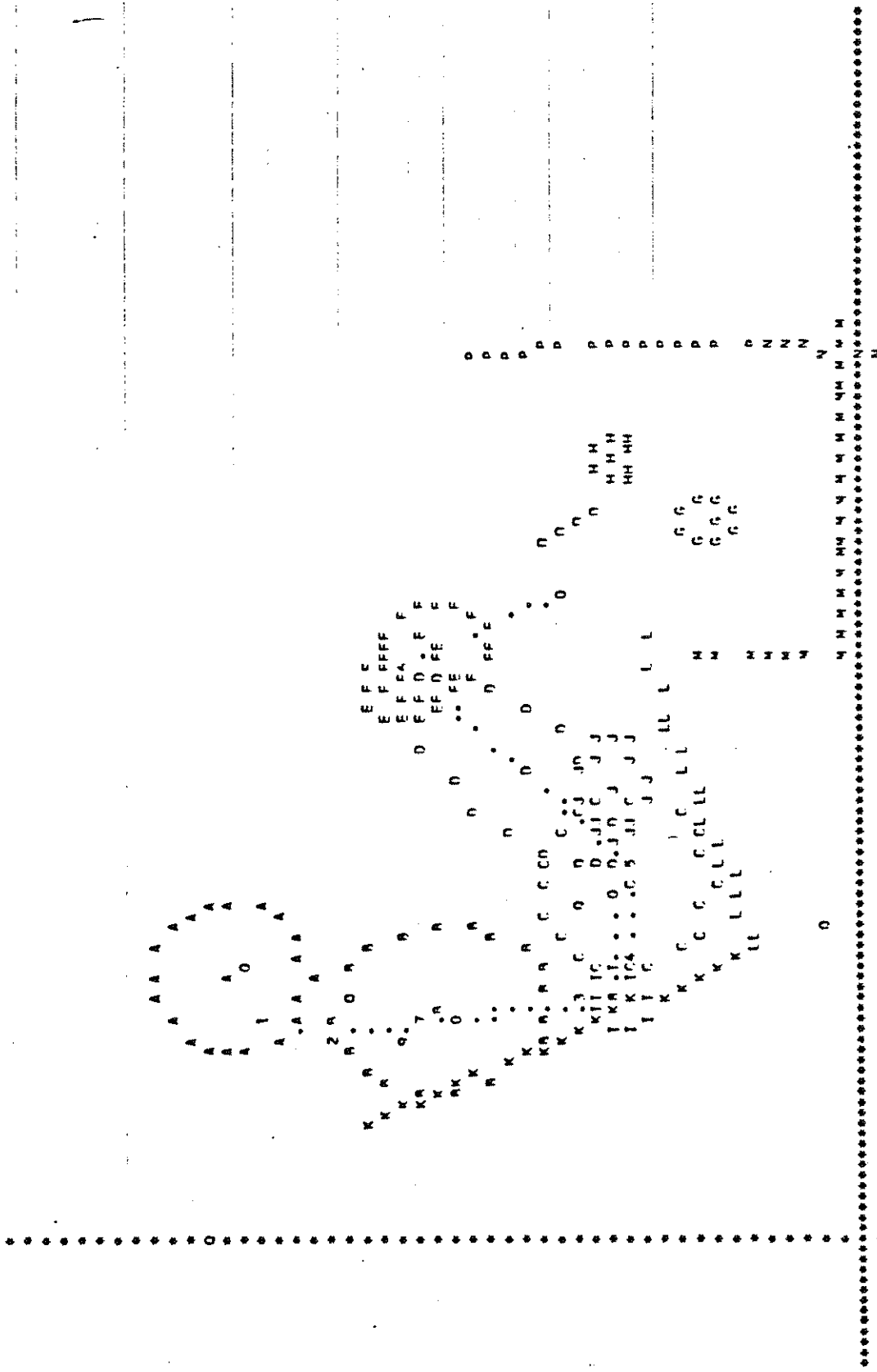
FIGURE 13-31e Printer-Plot Time Sequence for Example 2 (100 ms)



COORDINATE RANGES FOR PLOT ARE X= -4.56 (AT LEFT) TO 45.46 (AT RIGHT) AND Z= 5.00 (AT BOTTOM) TO -44.00 (AT TOP)
 SCALE FACTOR IS (IN) = 5.47 (IN) ; X AND Z POINT RESOLUTION ERRORS EQUAL RESPECTIVELY 0.277 AND 0.462 (IN) IN SCALE.

FIGURE 13-31f Printer-Plot Time Sequence for Example 2 (120 ms)

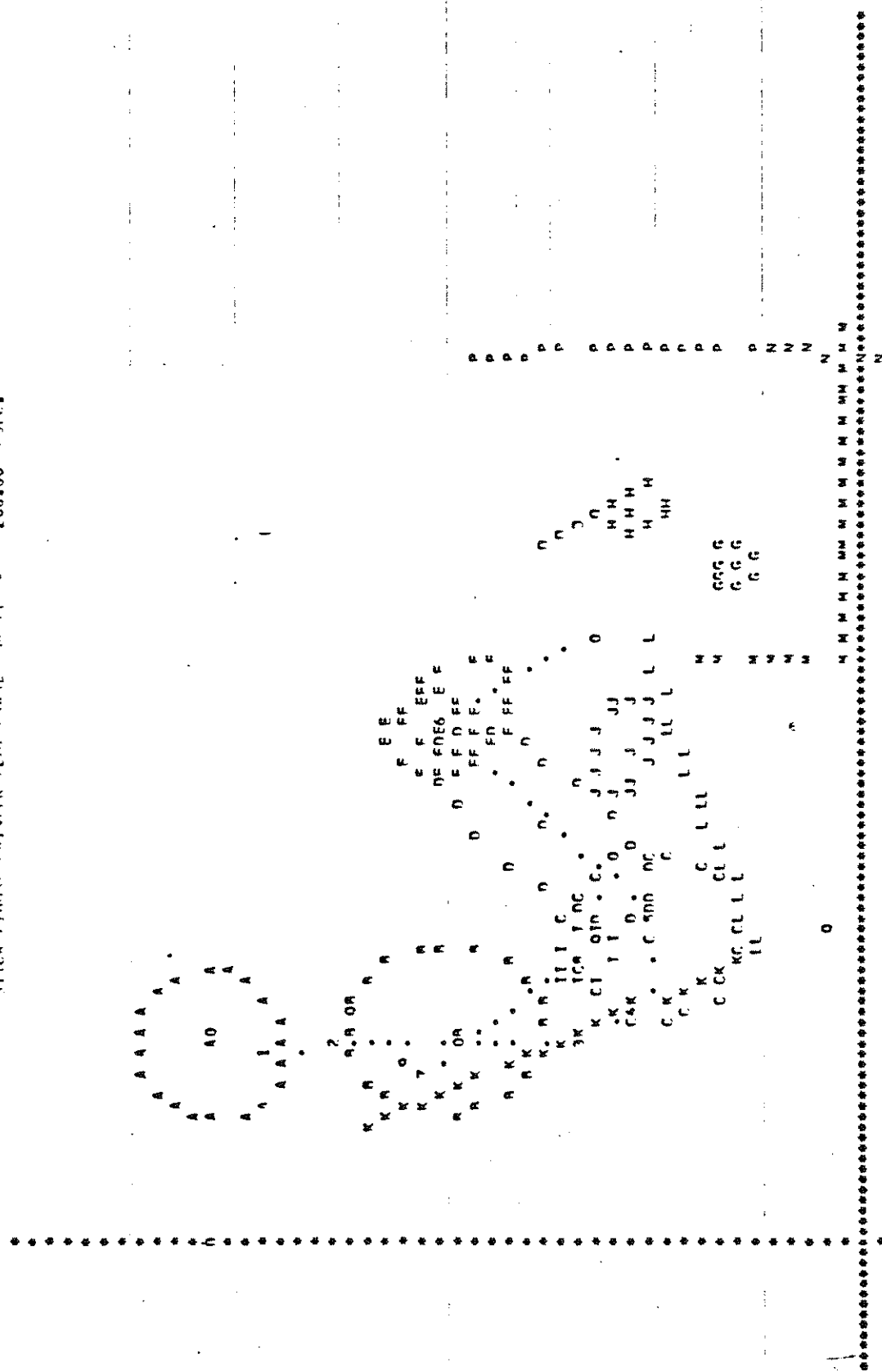
STICK FIGURE PRINTER PLOT FRAME FOR TIME= 150.00 MSEC.



COORDINATE RANGES FOR PLOT ARE X= -6.56 (AT LEFT) TO 45.56 (AT RIGHT) AND Z= 5.00 (AT BOTTOM) TO -46.00 (AT TOP)
 SCALE FACTOR IS (IN) = 9.547 (IN) . X AND Z POINT RESOLUTION ERRORS EQUAL RESPECTIVELY 0.277 AND 0.462 (IN) IN SCALE.

FIGURE 13-31g Printer-Plot Time Sequence for Example 2 (150 ms)

JUN 24, 197702102115
 NM HYABIN II DUNNY (PRELIMINARY DATA) KNFF RAP MVMA 2-0 TUTORIAL EXAMPLE #2 PAGE 61-45
 STICK FIGURE PRINTER PLOT FRAME END TIME 200.00 MSEC. NO LAP RELY



COORDINATE RANGES FOR PLOT ARE X= -4.54 (AT LEFT) TO 65.54 (AT RIGHT) AND Z= 5.00 (AT BOTTOM) TO -64.00 (AT TOP)
 SCALE FACTOR IS (IN) = 5.547 (IN) , X AND Z POINT RESOLUTION ERRORS EQUAL RESPECTIVELY 0.277 AND 0.462 (IN) IN SCALE.

FIGURE 13-31h Printer-Plot Time Sequence for Example 2 (200 ms)

CONTACT FORCES FOR UPPER TOPSO BELT MADE OF 6X WERRING #1 VS. UPPER TORSO LINK MADE OF

TIME (MSEC)	DEFLECTION (IN)	DEFLECTION RATE (IN/SEC)	RING EQUIL. TENSION (LB)	UNADJUSTED TENSION (LB)	TENSION ADJUSTMENT (LB)	RESULTANT FORCE (LB)	RESULTANT HEADING (DEGREES)	ABSORBED ENERGY (FT-LBS)
0.0	0.002	-0.0	0.0	5.009	0.0	5.009	-26.485	0.0
5.00	0.027	13.419	0.0	74.643	0.0	74.643	-26.436	0.0
10.00	0.186	38.526	0.0	523.294	0.0	523.294	-26.087	0.0
15.00	0.300	8.115	0.0	869.567	0.0	869.567	-25.743	0.0
20.00	0.340	12.848	0.0	957.781	0.0	957.781	-25.671	0.0
25.00	0.411	15.907	0.0	1157.509	0.0	1157.507	-25.816	0.0
30.00	0.467	11.172	0.0	1315.537	0.0	1315.537	-26.313	0.0
35.00	0.522	12.541	0.0	1469.501	0.0	1469.500	-27.084	0.0
40.00	0.567	2.651	0.0	1500.744	0.0	1500.743	-29.118	0.0
45.00	0.639	40.872	0.0	1505.612	0.0	1505.611	-29.259	0.0
50.00	0.664	81.385	0.0	1522.442	0.0	1522.442	-30.136	0.0
55.00	1.407	90.309	0.0	1546.586	0.0	1546.586	-30.713	0.0
60.00	1.947	116.695	0.0	1575.393	0.0	1575.393	-30.916	0.0
65.00	2.479	97.409	0.0	1603.780	0.0	1603.779	-30.774	0.0
70.00	2.810	40.056	0.0	1621.412	0.0	1621.411	-30.419	0.0
75.00	2.891	-5.706	0.0	1619.998	0.0	1619.997	-29.749	3428.47
80.00	2.847	-10.395	0.0	1518.209	0.0	1518.209	-28.483	0.0
85.00	2.751	-27.663	0.0	1300.570	0.0	1300.570	-27.187	0.0
90.00	2.584	-34.975	0.0	941.804	0.0	941.803	-26.268	0.0
95.00	2.400	-39.016	0.0	613.058	0.0	613.058	-25.720	0.0
100.00	2.102	-45.534	0.0	281.315	0.0	281.315	-25.470	0.0
105.00	1.950	-43.019	0.0	0.0	0.0	0.0	0.0	0.0
110.00	1.763	-36.056	0.0	0.0	0.0	0.0	0.0	0.0
115.00	1.502	-34.579	0.0	0.0	0.0	0.0	0.0	0.0
120.00	1.394	-47.894	0.0	0.0	0.0	0.0	0.0	0.0
125.00	1.149	-50.707	0.0	0.0	0.0	0.0	0.0	0.0
130.00	0.987	-55.345	0.0	0.0	0.0	0.0	0.0	0.0
135.00	0.621	-53.877	0.0	0.0	0.0	0.0	0.0	0.0
140.00	0.352	-55.047	0.0	0.0	0.0	0.0	0.0	0.0
145.00	0.045	-53.925	0.0	0.0	0.0	0.0	0.0	0.0
150.00	0.0	0.0	0.0	0.0	0.0	0.0	0.0	0.0
155.00	0.0	0.0	0.0	0.0	0.0	0.0	0.0	0.0
160.00	0.0	0.0	0.0	0.0	0.0	0.0	0.0	0.0
165.00	0.0	0.0	0.0	0.0	0.0	0.0	0.0	0.0
170.00	0.0	0.0	0.0	0.0	0.0	0.0	0.0	0.0
175.00	0.0	0.0	0.0	0.0	0.0	0.0	0.0	0.0
180.00	0.0	0.0	0.0	0.0	0.0	0.0	0.0	0.0
185.00	0.0	0.0	0.0	0.0	0.0	0.0	0.0	0.0
190.00	0.0	0.0	0.0	0.0	0.0	0.0	0.0	0.0
195.00	0.0	0.0	0.0	0.0	0.0	0.0	0.0	0.0
200.00	0.0	0.0	0.0	0.0	0.0	0.0	0.0	0.0

FIGURE 13-33 Belt System Response for Example 2

ACCELERATION OF BODY LINK ANGLES (DEG/SEC**2) (RELATIVE TO VEHICLE)

TIME	HEAD	NECK	UPPER TORSO	MID TORSO	LOW TORSO	UPPER LEG	LOWER LEG	SHOULDER	UPPER ARM	LOWER ARM
0.0	-0.08	2472.72	-3360.39	4187.07	4791.00	-3654.55	-532.00	-3369.38	-0.02	0.00
5.0	-3627.90	202123.63	-122074.75	511083.63	-136217.05	9182.16	-0746.21	-122074.75	30936.98	-13613.07
10.0	-60037.50	160145.50	-101421.24	535445.75	-144715.25	5840.45	-0162.04	-5850771.00	19355.12	-1235.52
15.0	-50702.54	26220.45	-130627.39	114147.81	5539.62	-3808.85	46.16	-639069.00	19995.30	-1836.06
20.0	6802.30	-132303.63	76780.39	-271422.94	90105.56	-3819.75	0780.20	-64130.02	23100.53	-2981.26
25.0	11420.43	-102145.25	59878.74	-219369.56	98105.94	-5304.78	10334.03	-105636.75	27693.31	-4512.86
30.0	9457.41	-130537.19	81464.56	-261257.63	98000.50	-5863.14	11060.36	123920.00	-23744.93	9083.46
35.0	-13472.41	-105202.64	84282.38	-251364.06	95182.56	-0042.09	11730.34	50785.32	-15507.76	6861.75
40.0	-14026.40	01897.49	-42421.32	242083.19	-53010.93	10370.45	-42745.56	-12753.38	74262.50	-20218.74
45.0	30488.34	-22120.58	43014.52	-313123.04	73345.88	107022.25	-323136.10	-354468.25	233064.31	-80275.25
50.0	7040.15	-0244.15	-3637.09	-44456.77	2248.92	80246.49	-392092.50	-96550.50	110154.31	-73141.94
55.0	-11089.00	-107795.50	31527.12	-260015.31	27702.77	10740.67	26915.59	647456.88	-325770.00	24846.93
60.0	-18656.94	-153326.25	30202.64	-295571.06	12372.99	58326.93	59442.38	549960.88	-287023.88	-13952.23
65.0	-92105.56	22540.05	-71500.88	100119.06	-7477.06	5544.13	30520.02	-6055.24	19304.21	-178778.50
70.0	-51052.16	55510.04	-01518.39	214786.13	-45751.32	-85118.31	39773.69	-72172.50	-72213.63	-180260.44
75.0	-0930.25	51974.37	-0317.07	-26902.96	-22078.02	-51734.41	-300.03	-417572.50	-4630.01	349000.56
80.0	30410.19	01340.75	-34117.00	205201.13	-44404.70	-25500.53	-1158.93	-78471.75	-32420.76	227261.44
85.0	04420.19	55627.31	14781.25	-13445.64	35007.38	-13480.38	7997.40	-107005.25	02000.56	20045.71
90.0	131200.31	29739.05	32527.42	-131744.44	67400.44	-7998.28	12310.14	-294780.56	19735.55	19071.18
95.0	115031.24	56570.52	-21263.40	117033.13	-34962.05	5434.96	11296.11	-1004787.63	11783.10	9439.92
100.0	56579.57	-7602.69	98282.15	-86393.98	-5462.32	15363.32	15246.50	-280150.00	17503.61	2179.29
105.0	31452.58	13532.64	21721.50	-103814.63	-5318.05	20480.11	17275.59	2085407.00	18358.71	4898.96
110.0	20835.14	90023.81	-43824.30	123817.69	-27117.95	-5057.83	41320.36	339520.56	3082.96	18634.95
115.0	13022.72	11480.43	-7773.85	95006.75	-39995.58	43982.23	256038.63	105292.50	-68472.13	38260.85
120.0	-13290.40	72830.13	-27225.04	140056.50	-50737.55	-2714.30	-5852.54	35314.27	-124729.00	37102.25
125.0	11307.13	70625.00	-40405.37	208307.81	-52674.27	-4571.51	-8294.20	78377.88	-110690.31	1104.51
130.0	-11356.54	135331.00	-70000.06	270748.13	-77755.98	-4979.86	-0660.11	234228.81	-45340.96	-10871.89
135.0	-0333.09	98202.06	50928.29	233828.05	-68529.69	-5035.92	-9070.35	522193.00	21784.67	-31598.70
140.0	-17581.50	101804.63	-64421.43	250533.63	-72497.38	-4572.51	-0605.40	464822.63	31040.51	-30794.24
145.0	-17372.78	100560.06	-70235.00	271788.99	-74122.13	-3770.93	-9510.38	-619088.88	41650.56	-27209.38
150.0	-12643.90	111431.88	-73031.34	275165.50	-73583.06	-2843.00	-9575.76	-569465.38	111048.31	-22023.69
155.0	-0210.14	114796.69	-75551.75	269000.81	-70734.44	221.19	-37138.03	-313556.38	209617.69	-46237.49
160.0	-27003.26	161274.24	-92843.31	286556.69	-74994.63	14863.13	-134172.44	-249063.94	217110.56	-65264.53
165.0	-6237.63	85043.50	-06732.50	212280.00	-60389.91	5576.13	-26592.73	-294225.31	22507.65	-18094.80
170.0	-28062.07	156635.56	-82738.56	262192.06	-50704.38	5495.64	-15006.77	-135756.13	-3805.79	-12194.34
175.0	1390.27	70291.00	-52604.13	171726.38	-71726.38	3945.74	-6803.27	238426.13	-33010.54	-6744.58
180.0	-15310.37	106029.04	-61733.41	195275.44	-60390.52	4750.87	-8510.39	204336.63	-53952.91	2578.55
185.0	-11496.09	36904.07	-43320.99	159204.56	-53119.63	3093.68	-0782.53	144288.13	-64538.80	9343.79
190.0	-44145.98	99959.06	-68033.63	259318.50	-63474.78	3247.14	-12222.36	85436.06	-80515.63	14715.38
195.0	-64832.52	77816.75	-69308.75	295954.69	-63156.43	1551.25	-13167.94	127607.25	-75039.69	16257.81
200.0	-57433.13	93082.38	-83737.00	365517.19	-68741.13	832.03	-13527.80	115866.56	-8261.88	-449.33

FIGURE 13-34 Body Link Angle Accelerations for Example 2

TIME	UNFILTERED ACCELERATIONS (G'S)				CHEST		RESULTANT		X		HIP		RESULTANT
	A-P	HEAD C-I	RESULTANT	A-D	S-I	RESULTANT	S-I	RESULTANT	X	Z	X	Z	
0.0	-0.100	0.080	1.000	0.509	-0.625	0.966	-0.625	0.966	-0.518	-1.623	-0.518	-1.623	1.704
5.00	2.316	-0.606	2.418	15.631	2.216	15.787	2.216	15.787	4.520	1.181	4.520	1.181	4.672
10.00	6.527	-1.005	6.604	24.832	0.574	24.838	0.574	24.838	3.780	0.245	3.780	0.245	3.788
15.00	9.050	3.715	8.966	16.501	2.630	16.897	2.630	16.897	-3.808	-3.398	-3.808	-3.398	5.104
20.00	6.651	11.978	13.553	6.086	2.497	6.578	2.497	6.578	-9.625	-1.047	-9.625	-1.047	9.682
25.00	7.532	17.871	19.393	9.752	3.024	10.512	3.024	10.512	-10.939	-1.655	-10.939	-1.655	11.063
30.00	0.025	21.209	21.132	10.614	1.414	10.708	1.414	10.708	-12.352	-2.116	-12.352	-2.116	12.532
35.00	12.569	21.906	25.255	11.606	-1.615	11.807	-1.615	11.807	-13.244	-2.890	-13.244	-2.890	13.556
40.00	14.908	21.856	26.456	22.850	2.679	22.984	2.679	22.984	-11.268	0.107	-11.268	0.107	11.269
45.00	11.017	17.527	20.702	2.205	-0.956	2.404	-0.956	2.404	-23.092	0.367	-23.092	0.367	25.756
50.00	12.242	6.461	13.842	14.756	-4.040	15.564	-4.040	15.564	-23.133	3.678	-23.133	3.678	23.423
55.00	13.067	-0.401	13.053	14.637	-16.063	22.405	-16.063	22.405	-40.477	8.136	-40.477	8.136	41.286
60.00	15.017	-2.633	15.246	17.071	-23.002	29.190	-23.002	29.190	-45.842	10.164	-45.842	10.164	47.932
65.00	23.183	5.608	23.373	38.481	-26.318	46.620	-26.318	46.620	-46.803	-7.787	-46.803	-7.787	47.647
70.00	24.224	18.616	30.551	35.913	-30.789	47.304	-30.789	47.304	-47.150	-20.374	-47.150	-20.374	51.363
75.00	24.035	26.130	35.502	1.211	-20.776	29.901	-20.776	29.901	-17.057	-19.126	-17.057	-19.126	25.627
80.00	21.007	15.624	26.381	19.642	-2.248	20.026	-2.248	20.026	-7.904	-4.788	-7.904	-4.788	10.419
85.00	18.047	18.808	26.497	14.027	3.114	14.368	3.114	14.368	-2.682	-1.165	-2.682	-1.165	8.752
90.00	12.544	10.748	23.395	6.085	4.897	8.531	4.897	8.531	-10.522	2.424	-10.522	2.424	10.797
95.00	7.346	14.438	16.252	11.571	8.349	14.280	8.349	14.280	-4.068	6.653	-4.068	6.653	7.798
100.00	4.278	8.194	9.236	1.691	2.110	2.711	2.110	2.711	-2.311	11.312	-2.311	11.312	11.546
105.00	3.151	5.133	6.023	-3.673	2.149	4.255	2.149	4.255	-0.683	13.022	-0.683	13.022	13.040
110.00	1.475	2.308	2.740	4.767	9.368	10.511	9.368	10.511	-2.424	3.424	-2.424	3.424	4.195
115.00	0.934	2.418	2.550	5.186	5.273	7.305	5.273	7.305	4.106	4.389	4.106	4.389	6.011
120.00	2.572	7.082	8.387	6.513	4.361	7.838	4.361	7.838	2.321	2.568	2.321	2.568	3.461
125.00	-0.145	10.471	10.472	7.051	5.942	9.976	5.942	9.976	2.665	1.035	2.665	1.035	2.859
130.00	0.804	9.401	9.525	8.300	7.050	10.072	7.050	10.072	3.330	0.242	3.330	0.242	3.330
135.00	-0.411	5.363	5.350	7.529	5.466	9.304	5.466	9.304	3.059	0.242	3.059	0.242	3.108
140.00	-0.364	2.139	2.228	8.852	6.274	10.849	6.274	10.849	3.654	0.009	3.654	0.009	3.654
145.00	-0.910	1.001	1.359	8.307	6.518	10.550	6.518	10.550	4.242	-0.071	4.242	-0.071	4.243
150.00	-1.082	0.003	2.178	7.383	6.534	9.850	6.534	9.850	4.752	-0.049	4.752	-0.049	4.752
155.00	-3.106	0.002	3.346	5.825	6.751	8.917	6.751	8.917	5.324	0.335	5.324	0.335	5.334
160.00	-2.302	1.082	2.544	4.647	8.053	9.209	8.053	9.209	6.954	1.624	6.954	1.624	7.141
165.00	-4.086	1.425	2.544	2.875	4.352	5.216	4.352	5.216	5.721	0.781	5.721	0.781	5.774
170.00	-3.765	-0.016	3.765	1.409	5.510	5.688	5.510	5.688	7.015	0.559	7.015	0.559	7.038
175.00	-7.416	-1.646	7.597	-1.666	0.412	1.716	0.412	1.716	7.118	0.023	7.118	0.023	7.118
180.00	-9.234	-4.779	9.521	-2.749	1.598	3.180	1.598	3.180	8.533	-0.357	8.533	-0.357	8.541
185.00	-10.048	-5.402	12.248	-2.155	-0.754	2.284	-0.754	2.284	9.406	-1.314	9.406	-1.314	8.597
190.00	-9.628	-4.738	10.757	2.174	2.710	3.481	2.710	3.481	9.937	-2.202	9.937	-2.202	10.179
195.00	-8.020	-1.540	9.061	7.527	3.451	8.281	3.451	8.281	9.756	-3.027	9.756	-3.027	10.215
200.00	-6.042	1.556	7.114	13.099	5.634	14.259	5.634	14.259	9.737	-3.220	9.737	-3.220	10.255

FIGURE 13-35 Unfiltered Head, Chest, and Hip Accelerations for Example 2

SEVERITY INDICES FOR UNFILTERED ACCELERATIONS

TIME	HIC=				HEAD				CHEST			
	3 MSEC AVE=				183.27, REG. TIME=				20.00, END TIME=			
	PEAK=				35.005 AT TIME=				3 MSEC AVE=			
	SEVERITY INDEX				35.502 AT TIME=				PEAK=			
	A-P	S-I	RESULTANT	S-I	A-P	S-I	RESULTANT	S-I	A-P	S-I	RESULTANT	S-I
0.0	0.0	0.0	0.0	0.0	0.0	0.0	0.0	0.0	0.0	0.0	0.0	0.0
5.00	0.02	0.00	0.02	0.01	0.00	0.01	0.00	0.01	3.35	0.04	3.40	0.11
10.00	0.22	0.01	0.23	0.02	0.01	0.02	0.01	0.02	12.28	0.06	12.46	0.01
15.00	1.32	0.02	1.34	0.01	0.01	0.02	0.01	0.02	28.28	0.07	28.53	0.01
20.00	2.30	0.00	2.30	0.00	0.02	0.03	0.05	0.03	31.25	0.16	31.74	0.02
25.00	3.04	5.41	9.40	0.02	0.02	0.21	0.35	0.29	32.26	0.29	32.89	0.02
30.00	4.22	14.07	20.31	0.03	0.03	0.86	1.41	0.38	34.34	0.38	35.29	0.02
35.00	6.38	24.91	34.39	0.06	0.06	1.85	3.22	0.30	36.43	0.30	37.40	0.03
40.00	10.19	34.18	52.44	0.15	0.15	2.90	5.07	0.42	43.33	0.42	48.43	0.03
45.00	13.54	45.44	67.35	0.23	0.23	3.50	7.72	0.48	55.08	0.48	55.08	0.03
50.00	15.52	48.50	73.00	0.25	0.25	3.65	7.94	0.54	55.80	0.54	57.27	0.04
55.00	18.80	48.62	76.54	0.33	0.33	3.65	8.02	0.54	60.33	0.54	66.01	0.14
60.00	22.54	48.65	80.39	0.42	0.42	3.65	8.13	0.54	65.04	0.54	80.73	0.72
65.00	30.62	51.81	88.44	1.10	1.10	3.66	8.85	0.54	83.32	0.54	134.55	3.48
70.00	43.83	51.81	107.12	2.59	2.59	5.46	12.10	0.54	129.02	0.54	208.92	9.70
75.00	57.04	44.93	139.45	4.27	4.27	5.46	21.17	0.54	140.88	0.54	255.88	17.05
80.00	60.98	75.70	165.51	5.45	5.45	6.42	27.12	0.54	141.76	0.54	266.91	27.63
85.00	73.96	81.36	184.92	6.22	6.22	6.68	29.07	0.54	149.08	0.54	274.23	28.20
90.00	84.94	90.14	201.15	6.39	6.39	7.32	32.15	0.54	150.95	0.54	275.46	28.31
95.00	86.52	96.68	210.41	6.40	6.40	7.65	32.92	0.54	151.17	0.54	277.23	28.31
100.00	86.94	98.82	213.30	6.41	6.41	7.65	32.97	0.54	151.94	0.54	278.61	28.32
105.00	87.10	98.47	214.22	6.41	6.41	7.65	32.97	0.54	152.13	0.54	279.05	28.32
110.00	87.13	99.57	214.37	6.41	6.41	7.65	32.97	0.54	152.62	0.54	280.20	28.32
115.00	87.14	99.61	214.43	6.41	6.41	7.65	32.97	0.54	152.93	0.54	280.71	28.32
120.00	87.16	101.35	214.79	6.42	6.42	7.67	32.89	0.54	153.69	0.54	291.92	28.33
125.00	87.17	103.09	218.01	6.43	6.43	7.68	32.90	0.54	154.72	0.54	293.86	28.33
130.00	87.17	103.89	218.92	6.44	6.44	7.68	32.90	0.54	155.59	0.54	295.43	28.33
135.00	87.19	104.04	219.07	6.44	6.44	7.68	32.91	0.54	156.45	0.54	295.86	28.34
140.00	87.19	104.04	219.07	6.44	6.44	7.68	32.91	0.54	157.55	0.54	298.76	28.34
145.00	87.19	104.04	219.07	6.44	6.44	7.68	32.91	0.54	158.41	0.54	299.43	28.34
150.00	87.19	104.04	219.07	6.44	6.44	7.68	32.91	0.54	159.41	0.54	299.43	28.34
155.00	87.19	104.04	219.07	6.44	6.44	7.68	32.91	0.54	160.09	0.54	291.78	28.35
160.00	87.19	104.04	219.07	6.44	6.44	7.68	32.91	0.54	160.27	0.54	292.81	28.35
165.00	87.19	104.04	219.07	6.44	6.44	7.68	32.91	0.54	160.45	0.54	293.50	28.35
170.00	87.19	104.04	219.07	6.44	6.44	7.68	32.91	0.54	160.45	0.54	293.88	28.35
175.00	87.19	104.04	219.07	6.44	6.44	7.68	32.91	0.54	160.45	0.54	293.96	28.36
180.00	87.19	104.04	219.07	6.44	6.44	7.68	32.91	0.54	160.45	0.54	294.02	28.36
185.00	87.19	104.04	219.07	6.44	6.44	7.68	32.91	0.54	160.45	0.54	294.13	28.37
190.00	87.19	104.04	219.07	6.44	6.44	7.68	32.91	0.54	160.45	0.54	295.17	28.38
195.00	87.19	104.04	219.07	6.44	6.44	7.68	32.91	0.54	160.45	0.54	297.40	28.40
200.00	87.19	104.04	219.07	6.44	6.44	7.68	32.91	0.54	162.23	0.54	297.40	28.40

FIGURE 13-36 Severity Indices for Unfiltered Accelerations for Example 2